

2019

# Natural fibre reinforced composite materials

Hernandez Michelena, Aitor

<http://hdl.handle.net/10026.1/14297>

---

<http://dx.doi.org/10.24382/782>

University of Plymouth

---

*All content in PEARL is protected by copyright law. Author manuscripts are made available in accordance with publisher policies. Please cite only the published version using the details provided on the item record or document. In the absence of an open licence (e.g. Creative Commons), permissions for further reuse of content should be sought from the publisher or author.*

*This copy of the thesis has been supplied on condition that anyone who consults it is understood to recognize that its copyright rests with its author and that no quotation from the thesis and no information derived from it may be published without the author's prior consent.*



# UNIVERSITY OF PLYMOUTH

## **NATURAL FIBRE REINFORCED COMPOSITE MATERIALS**

by

**AITOR HERNANDEZ MICHELENA**

A thesis submitted to the University of Plymouth  
in partial fulfilment for the degree of PhD

**DOCTOR OF PHILOSOPHY**

School of Engineering

June 2019

## **Acknowledgements**

Many people have greatly contributed to the development of this thesis over the years.

I want to express my most sincere thanks to the supervision team: John Summerscales (Director of Studies), Jasper Graham-Jones, Wayne Hall (latterly at Griffith University in Australia) and Mary Margaret (Miggy) Singh for their expert guidance, advice, support, and encouragement. Further the expert commentators have made valuable input: Professor M Neil James (Head of School of Marine Science & Engineering/ Associate Dean) Dr Shunqi Pan and Dr Frank Abraham.

The work was mostly conducted in the Basque Country (Euskadi) in northern Spain using facilities in the University of the Basque Country (UPV/EHU), University of Zaragoza and Acciona (latterly Nordex) Windpower in Sariguren.

Although these doctoral studies have been primarily self-funded, I am most grateful for the Santander Universities Scholarship funding which supported the experimental work in University of Zaragoza.

The author would especially like to thank Mr. Brendon Weager at Composites Evolution for reinforcement fabrics and Mr. Jaime Ferrer-Dalmau at Entropy Resins for the bio-epoxy.

I am also grateful to the anonymous referees for their respective comments on the manuscripts of the book chapter and the conference papers.

Last but not least important, I would like to thank Aurora for her unconditional love, making me believe that together nothing is impossible and giving me the strength to keep going at weakest moments. Love you Michelle for always keeping my heart happy. Aita, Ama, Xabi, Olatz, Maialen, Borja, Nora and Naia, mila esker for always believing in me and giving me the strength to continue, maite zaituztet. Thank you Iñigo for your invaluable help as I took the first steps. My Welsh family John, Irene, Lowri, Robs, Ceri, Cai, Elin, Mared and Meilyr diolch for making me feel part of the family. Max, Bea, David, Salam and Chamy, thank you for making me feel at home. Marta, Cecilia and Iker, thank you for your technical support and friendship throughout the experimental campaign. Asier, mila esker, hau posible egin dezulako. Thank you Alvaro and Elena for being good friends more than colleagues. Sorry Ion and Yeli not for attending your wedding, it was a real pity. Thank you family and friends for all your love and laughter that have made me happy every day.

Finally dedicate the work to my uncle Jose and aunty Maite who have recently passed away, thank them for making me feel proud of being part of the Mitxelena family.



### Author's declaration

At no time during the registration for the degree of Doctor of Philosophy has the author has been registered for any other University award without prior agreement of the Doctoral College Quality Sub-Committee. Work submitted for this research degree at the University of Plymouth has not formed part of any other degree either at the University of Plymouth or at another establishment. This study was partially financed with the aid of a scholarship from Santander.

### The following external institutions were visited for consultation purposes:

Green and Wood-Based Composites Pfintzal - Germany Fraunhofer ICT 30 September 2008  
CoMatComp Composites San-Sebastian - Euskadi (Spain) 06-09 September 2009  
Resin Curing Madrid - Spain TA Instruments 01-04 April 2009  
Journées Europeennes des Composites Paris - France JEC 29-31 March 2011

### Publications (or public presentation of creative research outputs):

#### Book Chapter:

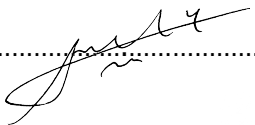
Aitor Hernandez Michelena, Jasper Graham-Jones, John Summerscales and Wayne Hall  
[Eco-friendly flax fibre/epoxy resin/composite system for surfboard production](#)  
Chapter 20 in Raul Figueiro and Sohel Rana (editors): [Natural Fibres: Advances in Science and Technology Towards Industrial Applications: From Science To Market](#),  
Springer RILEM Book Series, March 2016, (12 Part III), 267-277. ISBN 978-94-017-7513-7.  
DOI: [https://doi.org/10.1007/978-94-017-7515-1\\_20](https://doi.org/10.1007/978-94-017-7515-1_20)

#### Conference papers:

1. A Hernandez Michelena, J Graham-Jones, W Hall and J Summerscales  
[Resin transfer moulding \(RTM\) to produce surfboard fins with natural fibres](#)  
ICCST-9, Sorrento ~ ITALY, 24-26 April 2013/oral: Thursday 25 April 2013 at 15:10.  
DEStech Publications Inc, Lancaster PA, 2013. ISBN 978-1-60595-113-3, pages 577-583.
2. Aitor Hernandez Michelena, Jasper Graham-Jones, Wayne Hall and John Summerscales  
[Resin transfer moulding \(RTM\) fins production with natural fibres](#)  
1st International Conference on Natural Fibers: sustainable materials for advanced applications (ICNF2013),  
Guimarães ~ PORTUGAL, 09-11 June 2013, Session 8a, abstracts book pages 49-50.
3. Aitor Hernandez Michelena, Jasper Graham-Jones, Wayne Hall and John Summerscales  
[Ecoboard production with natural fibres](#)  
1st International Conference on Natural Fibers: sustainable materials for advanced applications (ICNF2013),  
Guimarães ~ PORTUGAL, 09-11 June 2013, poster, abstracts book pages 339-340.
4. Aitor Hernandez Michelena, Jasper Graham-Jones, Wayne Hall and John Summerscales  
[Natural fibre treatments review](#), 5th International Conference on Sustainable Materials, Polymers and Composites (EcoComp 2013), Birmingham, 03-04 July 2013.
5. A Hernandez Michelena, J Graham-Jones, J Summerscales and W Hall,  
[Resin Transfer Moulding \(RTM\) production of surfboard fins with natural fibres. Part II: experimental work and testing](#) (abstract 209)  
2nd International Conference on Natural Fibers – From Nature to Market (ICNF2015),  
São Miguel – Azores ~ PORTUGAL, 27-29 April 2015, oral presentation. CD-ROM Session 13.  
ISBN 978-989-98468-4-5. Book of Abstracts pages 265-266, ISBN 978-989-98468-5-2.
6. A Hernandez Michelena, J Graham-Jones, J Summerscales and W Hall,  
[Eco-friendly epoxy resin/flax fibre composite system as a material for surf boards production](#) (abstract 210)  
2nd International Conference on Natural Fibers – From Nature to Market (ICNF2015),  
São Miguel – Azores ~ PORTUGAL, 27-29 April 2015, oral presentation. CD-ROM Session 13.

- ISBN 978-989-98468-4-5. Book of Abstracts pages 267-268, ISBN 978-989-98468-5-2.
7. A Hernandez Michelena, J Graham-Jones, J Summerscales and W Hall [Eco-friendly epoxy resin/flax fibre composite system interface improvement with the chemical treatments of the flax surface and resin formulation](#) 2nd International Conference on Natural Fibers – From Nature to Market (ICNF2015), São Miguel – Azores ~ PORTUGAL, 27-29 April 2015, no presentation. Book of Abstracts pp 269-270. ISBN 978-989-98468-5-2.
  8. A Hernandez Michelena, J Graham-Jones, J Summerscales and W Hall. *Silane Modification of the Flax/Epoxy System Interface*. Procedia Engineering, Volume 200, 2017, Pages 448-456.  
DOI: <http://dx.doi.org/10.1016/j.proeng.2017.07.063>  
PEARL: <http://hdl.handle.net/10026.1/10050>

Word count of main body of thesis: 39479 words

Signed.......... Date..... 04/06/2019 .....

## **NATURAL FIBRE REINFORCED COMPOSITE MATERIALS**

### **Abstract**

Nowadays, due to the global warming and pollution issues, sustainable materials must be considered. Composites materials can offer excellent mechanical performance with low weight, hence saving fuel. However, most of the composites systems are based on petrochemicals, and natural materials may be a better option; for example, fibre reinforcements from plant stems (bast) and bio-based resins are becoming available commercially.

One of the major inconveniences of the NFRP is the moisture absorption in marine environments. This problem is usually solved increasing the fibre-matrix bonding. Commercially available fibre systems are chemically treated in order to tackle this issue, but those treatments produce environmental burdens. This thesis seeks to develop an environmentally-friendly, commercially competitive and easily performed treatment methodology for improving the NFRP mechanical properties.

The proposed silane-in-hardener method, adding coupling agent to the hardener, rather than direct treatment of the fibres in solvent, can eliminate solvent use, considerably reducing environmental burdens. This new proposal also reduces process time and improves the composite mechanical performance, resulting in commercial competitiveness. The primary research question in this thesis is can sensible NFRP properties be achieved with silane-in-hardener replacing prior treatment of reinforcements?

Flax fibre and epoxy resin were selected for the experimental campaign. First, flax fibre was mercerised in different immersion-time and concentrations conditions, and the resulting mechanical performance of composite systems evaluated; from the campaign the best mercerised system was selected. In a second stage, raw flax fibre and best mercerised flax fibre were silanised and resulting composite system mechanical properties evaluated. In a third stage, silane was directly added to the epoxy resin and the mechanical properties evaluated together with raw flax fibre. In the final stage, the developed silane in resin method was applied to flax/bio-epoxy system and compared with the basic system in order to evaluate its real improvement.

Additionally, water immersion tests were performed to the silanised flax fibre/epoxy resin system in order to evaluate whether the moisture resistance was increased or not.

From the experimental campaign, it was concluded that the fibre mercerisation process reduces the resulting composite mechanical performance. First, whenever the flax is immersed in the NaOH solution the fibre swells, impeding the flax fibre correct wetting, reducing as a result the composite mechanical performance. Second, because at long immersion-times and concentrations the flax fibre starts to degrade, reducing the composite performance. Similarly, when the flax was immersed in a silane solution, fibre swelling was also obtained, reducing mechanical performance. In contrast when the 1% w/w silane was added to the resin system, the swelling was avoided, and the objective interfacial properties enhanced, getting as a result static mechanical properties improvement.

However, when the enhanced and base systems moisture ingress resistance was evaluated, the values difference was not as representative as expected.

## **List of contents**

Copyright statement

Title page

Acknowledgements

Author's declaration

Publications arising from this study (Book chapter & Conference papers)

Word count

Abstract

List of contents

Index

List of Figures

List of Tables

Nomenclature (list of symbols)

## Index

CHAPTER 1:	INTRODUCTION	1
CHAPTER 2:	CONVENTIONAL COMPOSITES	
2.1.	INTRODUCTION	5
2.2.	CONTINUOUS REINFORCEMENTS: GLASS	5
2.3.	MATRICES - THERMOSET RESINS	6
2.3.1.	Epoxy resin	8
2.3.2.	Unsaturated Polyester (UP) and Vinyl ester (VE)	11
2.4.	SURFACE FINISHES ON FIBRES	13
2.5.	SHORT FIBRES AND FABRIC PRODUCTION	14
2.6.	SUMMARY	16
CHAPTER 3:	BIO-COMPOSITES	
3.1.	INTRODUCTION	17
3.2.	NATURAL FIBRE DESCRIPTION	17
3.3.	LIGNOCELLULOSIC FIBRES CLASSIFICATION AND TYPES	18
3.3.1.	Flax	20
3.4.	NATURAL FIBRES EXTRACTION TECHNIQUES	20
3.4.1.	Mechanical extraction	21
3.4.2.	Biological extraction	21
3.4.3.	Chemical extraction	22
3.5.	NATURAL FIBRES CHEMISTRY	23
3.6.	NATURAL FIBRES PROPERTIES	23
3.6.1.	Mechanical properties	23
3.6.2.	Moisture properties	24
3.7.	NATURAL FIBRE REINFORCEMENT FORMS AND FABRICS	25
3.7.1.	Slivers and yarns production	25
3.7.2.	Fabrics production	26
3.8.	NATURAL FIBRE REINFORCED POLYMERS (NFRP)	27
3.9.	BIO-POLYMERS DESCRIPTION	28
3.10.	THERMOSETS RESINS	29
3.10.1.	Bio-epoxy resins	30
3.10.2.	Bio-polyester resins	32
3.10.3.	Other bio-resins	33
3.11.	SUMMARY	33
CHAPTER 4:	THE INTERFACE IN NATURAL FIBRE COMPOSITES	
4.1.	INTRODUCTION	34
4.2.	INTERFACE/INTERPHASE	36
4.3.	COMPATIBILISERS IN THE MATRIX	39
4.3.1.	Epoxy matrix modification	40
4.4.	PHYSICAL FIBRE SURFACE TREATMENTS	41
4.5.	CHEMICAL FIBRE SURFACE TREATMENTS	42
4.5.1.	Mercerisation (NaOH) and NaCl	43
4.5.2.	Silanisation	51
4.5.3.	Other treatments	57
4.6.	COUPLING AGENTS ON THE FIBRE SURFACE	59
4.6.1.	Synthetic fibre coating	59
4.6.2.	Natural fibre coating	60
4.7.	MODELLING CHEMICAL TREATMENT	61
4.7.1.	Mercerisation (NaOH) and NaCl	61
4.7.2.	Silanisation	62
4.8.	CHARACTERISATION OF FIBRE SURFACES AND INTERFACES	62
4.8.1.	Contact angle study	62
4.8.2.	Reactive sites on fibre surface	63

4.8.3. Mechanical interface characterisation	63
4.8.3.1. Composites lamina methods	64
4.8.4. Optical qualitative analysis	64
4.9. SUMMARY AND FUTURE DIRECTION	64
CHAPTER 5: COMPOSITE DESIGN, MANUFACTURING, TESTING AND IMAGE ANALYSIS	
5.1. INTRODUCTION	67
5.2. COMPOSITE DESIGN	67
5.3. MECHANICAL TESTS	69
5.4. COMPOSITE MANUFACTURING	69
5.4.1. Resin infusion under flexible tooling (RIFT)	70
5.4.2. Flow models	71
5.5. IMAGE ANALYSIS	72
5.6. SUMMARY	73
CHAPTER 6: COMPOSITE DURABILITY IN MARINE ENVIRONMENT	
6.1. INTRODUCTION	74
6.2. COMPOSITE DURABILITY	74
6.2.1. MARINE ENVIRONMENT TEST	75
6.2.1.1. Water absorption	76
6.2.1.2. Marine immersion test	77
6.2.1.3. Composites mechanical deterioration	77
6.2.2. REFERENCE STUDIES	78
6.2.3. IN SERVICE CASE TESTING	78
6.3. SUMMARY	78
CHAPTER 7: RESEARCH METHODOLOGY	
7.1. INTRODUCTION	79
7.2. RAW MATERIAL	80
7.2.1. Flax fibre characteristics	81
7.2.1.1. Composite Evolution flax fibre	81
7.2.1.2. Lineo flax fibre	82
7.2.2. Bio-epoxy resin	83
7.2.3. Petrochemical resin	86
7.2.4. Chemical products	87
7.2.4.1. Sodium hydroxide (NaOH)	87
7.2.4.2. 3-(trimethoxysilyl) propylamine (BYK-C 8001)	88
7.2.4.3. Ethanol (Ethyl alcohol CH <sub>3</sub> CH <sub>2</sub> OH)	88
7.2.5. Infusion consumables	89
7.3. TREATMENT PROCEDURE	89
7.3.1. Mercerisation	90
7.3.2. Matrix modification	91
7.3.3. Silanisation	92
7.4. DEFINITION OF THE MANUFACTURING EQUIPMENT	92
7.4.1. Lamination table	92
7.4.2. Cutting machine	93
7.4.3. Universal testing machine	94
7.5. LAMINATE MANUFACTURE	94
7.5.1. Laminates 1 and 2	96
7.5.2. Laminates 3 and 4	98
7.5.3. Laminate 5 to 20	99
7.5.4. Laminate 21 to 24	101
7.5.5. Laminate 25 to 28	102
7.5.6. Laminate 29	103
7.5.7. Laminate 30 and 32	103
7.5.8. Laminate 31	103
7.5.9. Laminate 33 and 34	103

7.5.10. Laminate 35 and 36	104
7.6. TEST	105
7.6.1. Test standards	105
7.6.1.1. Tensile test	105
7.6.1.2. Compression test	106
7.6.1.3. In-plane shear test	106
7.6.1.4. Interlaminar shear test (ILSS)	107
7.6.1.5. Three-points bending test	107
7.7. TEST PROCEDURE	108
7.8. TEST DEVIATIONS	108
7.9. SUMMARY	110
CHAPTER 8: RESULTS	
8.1. INTRODUCTION	111
8.2. MECHANICAL TESTS	111
8.3. FLOW TESTS	114
8.4. MOISTURE TESTS	115
CHAPTER 9 DISCUSSION	
9. 1. INTRODUCTION	116
9. 2. MERCERISATION	117
9.2.1. Longitudinal tensile modulus $E_1$ ANOVA	117
9.2.2. Longitudinal strength $\sigma_1$ ANOVA	120
9.2.3. Longitudinal strain $\epsilon_1$ ANOVA	123
9.2.4. Transverse tensile modulus $E_2$ ANOVA	126
9.2.5. Transverse strength $\sigma_2$ ANOVA	129
9.2.6. Transverse strain $\epsilon_2$ ANOVA	132
9.2.7. Poisson's modulus $\nu_{21}$ ANOVA	135
9.2.8. Definitive mercerisation process selection	135
9. 3. PLATE MANUFACTURE	139
9. 4. EFFECT OF FIBRE SWELLING	139
9. 5. SILANE COUPLING AGENT	141
9. 6. BEST COMPOSITE SYSTEM	146
9. 7. VOLUME FRACTION VARIATION WITH TREATMENT	148
9. 8. VOLUME FRACTION MEASUREMENT DEVIATION	153
9. 9. PANEL MANUFACTURING HOMOGENEITY	155
9. 10. LAMINATE POSITION EFFECT	156
9. 11. METHOD SUSTAINABILITY	157
9. 12. MECHANICAL PROPERTY PREDICTION	158
9.13. WATER RESISTANCE TESTS	163
9.14. OPTIMISED SYSTEM PROPERTIES	164
9.14.1. Tensile test	165
9.14.2. Compression test	165
9.14.3. In-plane shear test	166
9.14.4. Interlaminar Shear Strength (ILSS) test	167
9.14.5. Flexural test	167
9.15. MECHANICAL TESTS UNCERTAINTY ESTIMATION	167
CHAPTER 10 CONCLUSIONS	169
CHAPTER 11: RECOMMENDATIONS AND FUTURE WORK	171
REFERENCES	172
APPENDIX A	185
APPENDIX B	194



APPENDIX C	262
APPENDIX E	265
APPENDIX F	266
APPENDIX G	304

## List of Figures

Figure 1.1: Correlation scheme of the different factors	3
Figure 2.1: Instantaneous viscosity evolution according to temperature (Courtesy of Acciona Blades)	7
Figure 2.2: Epoxy group basic structure	8
Figure 2.3: DGEBA product chart	8
Figure 2.4: UP prepolymer general synthesis reaction, where A is a chemical group	11
Figure 2.5: Prepolymer structure with the unsaturated double bond	12
Figure 2.6: General structure of organosilane where R is either vinyl or epoxy functionality [Liu, 29]	14
Figure 2.7: Fabrics types (drawn by John Summerscales and reproduced here with his permission)	16
Figure 3.1: Natural fibres classification scheme [George 34]	17
Figure 3.2: Lignocellulosic fibre internal structure scheme [George 34]	18
Figure 3.3: Flax fibre yarn roll produced by spinning technique (Courtesy of Composite Evolution)	25
Figure 3.4: Stitched flax fabric production process (Courtesy of Composite Evolution)	26
Figure 3.5: Jute woven fabrics (plain left and twill right) (Courtesy of Easy Composites)	27
Figure 4.1: Composite interface and interphase explicative scheme (Acciona Blades courtesy)	35
Figure 4.2: Transverse section of a UD NCF fibre reinforced composite (Courtesy of Acciona Blades)	35
Figure 4.3: Schematic representation of the Interphase region [Drzal, 92]	38
Figure 4.4: NF chemical treatment option scheme [Gurunathan, 104]	42
Figure 4.5: The reaction shows the surface activation by alkali treatment	43
Figure 4.6: Si-O-Si bonding scheme	51
Figure 4.7: Coupling agent performance scheme	59
Figure 4.8: Silane schematic figure	60
Figure 4.9: Classification of Mechanical interface characterisation methods [Drzal, 92]	63
Figure 5.1: Composite design, test, manufacturing and image analysis relationship chart	67
Figure 5.2: General scheme for the design of the composite [Kedward 165]	68
Figure 5.3: General flow chart of mechanical test	69
Figure 5.4: Schematic figure of RIFT manufacturing technique (Courtesy of Richard Pemberton under a Creative Commons licence)	71
Figure 5.5: SEM images of a) Sisal/PP; b) Cotton/PP resin systems [Amigó, 171]	72
Figure 7.1: Tested CE flax fibre UD roll	81
Figure 7.2: Flax-ply woven and UD fabric (Courtesy of Easy Composites)	82
Figure 7.3: Flax-ply woven and UD fabric	83
Figure 7.4: Supersap CLR/CLX system used for the panel production (Courtesy of 5TX surf)	85
Figure 7.5: 3-(trimethoxysilyl) propylamine structure	88
Figure 7.6: Lamination table controlled by thermocouples	93
Figure 7.7: Control software - (Left) Lamination table (Right) computer interface display	93
Figure 7.8: DIADISC 5200R cutting machine	93
Figure 7.9: Shimadzu AG-X PLUS 250kN Universal testing machine	94
Figure 7.10: Manufacturing process for laminates 1 and 2	97
Figure 7.11: Lamination scheme for laminates 1-2	97
Figure 7.12: manufacturing process of laminates 3 and 4	98
Figure 7.13: Lamination scheme for laminates 3 and 4	99
Figure 7.14: Manufacturing process for laminates 5 to 8	100
Figure 7.15: Lamination scheme for laminates 5 to 20	100
Figure 7.16: Manufacturing process for laminates 21-24	101
Figure 7.17: Lamination scheme for laminates 21-24	102
Figure 7.18: manufacturing process of laminates 27 and 28	103
Figure 7.19: manufacturing process of laminates 33 and 34	104

Figure 7.20: manufacturing process of laminates 35 and 36	104
Figure 7.21: UniZar longitudinal and transverse compression test samples	106
Figure 7.22: UniZar 10° shear test sample	107
Figure 7.23: Short-beam test sample	107
Figure 7.24: Short-beam test sample	108
Figure 7.25: Diamond (left) and hard steel (right) saw blades	109
Figure 7.26: Biotex UD275 fabric microscopy image	109
Figure 8.1: Tensile 0° test example (Laminate 29)	111
Figure 8.2: 90° tensile test-Laminate 1 (left) and 0° compression test-Laminate 2 (right)	112
Figure 8.3: 0° tensile test-Laminate 3 (left) and 90° tensile test-Laminate 6 (right)	112
Figure 8.4: 90° tensile test-Laminate 11 (left) and 90° tensile test-Laminate 21 (right)	112
Figure 8.5: 0° tensile test measure with strain gauges-Laminate 29	112
Figure 8.6: Laminates 5-8 (left) and laminates 21-24 right	114
Figure 8.7: Fibre diameter evolution with the mercerisation process	115
Figure 9.1. $E_1$ evolution vs. immersion time	119
Figure 9.2. $E_1$ evolution vs. concentration	119
Figure 9.3. $\sigma_1$ evolution vs. immersion time	121
Figure 9.4. $\sigma_1$ evolution vs. concentration	122
Figure 9.5. $\varepsilon_1$ evolution vs. immersion time	124
Figure 9.6. $\varepsilon_1$ evolution vs. concentration	125
Figure 9.7. $E_2$ evolution vs. immersion time	127
Figure 9.8. $E_2$ evolution vs. concentrations	128
Figure 9.9. $\sigma_2$ evolution vs. Immersion time	130
Figure 9.10. $\sigma_2$ evolution vs. concentrations	131
Figure 9.11. $\varepsilon_2$ evolution vs. immersion time	133
Figure 9.12. $\varepsilon_2$ evolution vs. concentrations	134
Figure 9.13. Longitudinal tensile properties vs concentration	137
Figure 9.14. Longitudinal tensile properties vs immersion time	137
Figure 9.15. Transverse tensile properties vs immersion time	138
Figure 9.16. Transverse tensile properties vs concentration	138
Figure 9.17: Swelling model representation graph	140
Figure 9.18. Laminates thickness values vs the chemical treatment	151
Figure 9.19. Laminates thickness increment vs the chemical treatment	152
Figure 9.20. Laminates thickness increment % vs the chemical treatment	152
Figure 9.21: Longitudinal (Blue) and transverse (Red) $V_f$ measurement CV (%)	154
Figure 9.22: Laminates 9-12 samples extraction areas	156
Figure 9.23: Figure produced based on the Hazardous Materials Identification System (HMIS)	158
Figure 9.24: Longitudinal modulus experimental and modelled properties data	160
Figure 9.25. Longitudinal strength experimental and modelled properties graph (blue is experimental data; orange line is the extended rule-of-mixture prediction)	162
Figure 9.26: Silanised (blue) and not silanised (red) systems water absorption vs time (days)	163

## List of Tables

Table 2.1: Comparative table of the E-glass and CF properties [Mallick 3]	5
Table 2.2: Physical properties of reinforcement glasses [Fecko 4]	6
Table 2.3: Different epoxy systems Tg temperatures [Varma 24]	11
Table 2.4: Epoxy resin general properties [Pham 25]	11
Table 3.1: Lignocellulosic NF classification [Pickering 33]	19
Table 3.2: NF characteristics [Pickering 33]	19
Table 3.3: Chemical composition and structural parameters of NF [Gurunathan 35]	23
Table 3.4: Physical and mechanical properties of important LF and GF [Gurunathan 35]	24
Table 3.5: NF Equilibrium Moisture Content (EMC) percentage [Pickering 33]	24
Table 3.6: Shows the NF/TS composites examples [Pickering 33]	27
Table 3.7: Shows the NF/TP composite examples [Pickering 33]	28
Table 3.8: Bio-polymers classification and examples [Reddy 55]	29
Table 3.9: Commercial bio-epoxy resins bio-content [Marrot 70]	32
Table 3.10: Commercial bio-polyester resins bio-content [Marrot 70]	32
Table 4.1: Unit cell dimensions for cellulose crystals [Wada, 109]	43
Table 4.2: Mercerisation and NaCl treatments references	45
Table 4.3: Silanisation methods references	53
Table 4.4: Flax fibre base tensile and flexural properties	55
Table 7.1: Mechanical properties of Biotex fibre (data from CE with no statistical information)	81
Table 7.2: Biotex flax fibre yarn properties (data from CE)	81
Table 7.3: Mechanical property data for composites made from Biotex UD fabrics (data from CE)	82
Table 7.4: Mechanical property data for composites made from Flax-ply UD fabric (data from Lineo)	83
Table 7.5: Supersap CLR resin system properties (Entropy Resin data)	85
Table 7.6: Supersap CLR resins manufacturing data (Entropy Resin data)	85
Table 7.7: Mechanical properties for cured Supersap resin systems (Entropy Resin data)	86
Table 7.8: Araldite LY 1569 CH/Aradur 3489 CH system properties (Huntsman LLC data)	86
Table 7.9: Typical working properties available during manufacture with Araldite LY 1569 CH/Aradur 3489 CH (Huntsman LLC data)	87
Table 7.10: Mechanical properties for cured Araldite LY 1569 CH/Aradur 3489 CH resin systems (Huntsman LLC data)	87
Table 7.11: Information from BYK-C 8001 Safety Data Sheet (MSDS)	88
Table 7.12: Different options in the Mercerisation process	91
Table 7.13: Matrix modification different options	92
Table 7.14: Different options for the silanisation process	92
Table 7.15: List of UD Laminate manufacturing tests undertaken with Biotex or Lineo flax fibra and Supersap CLR/INF or Araldite LY 1569 /Aradur 3489 epoxy matrix	96
Table 7.16: Manufacturing characteristics of laminate 1 and 2	97
Table 7.17: Manufacturing characteristics of laminate 3-4	98
Table 7.18: Manufacturing characteristics of laminate 5 to 20	99
Table 7.19: Manufacturing characteristics of laminates 21 to 24	101
Table 7.20: Longitudinal tensile test conditions	105
Table 7.21: Longitudinal compression test conditions	106
Table 7.22: 45° and 10° shear test conditions	106
Table 7.23: Short-beam test conditions	107
Table 7.24: Flexural test conditions	108
Table 8.1: Experimental campaign laminates numbering	113
Table 8.2: Laminates infusion times	114
Table 8.3: measured technical fibre diameters in mm (Appendix C)	114
Table 9.1. ANOVA analysis for the E <sub>1</sub>	118

Table 9.2. Fisher analysis of the immersion time effect in the $E_1$	118
Table 9.3. The Fisher analysis of the concentration effect in the $E_1$	119
Table 9.4. $E_1$ values variation with immersion time and concentrations	120
Table 9.5. ANOVA analysis for the $\sigma_1$	120
Table 9.6. Fisher analysis of the immersion time effect in the $\sigma_1$	121
Table 9.7. The Fisher analysis of the concentration effect in the $\sigma_1$	122
Table 9.8. $\sigma_1$ values variation with immersion time and concentrations	123
Table 9.9. ANOVA analysis for the $\varepsilon_1$	123
Table 9.10. Fisher analysis of the immersion time effect in the $\varepsilon_1$	124
Table 9.11. The Fisher analysis of the concentration effect in the $\varepsilon_1$	125
Table 9.12. $\varepsilon_1$ values variation with immersion time and concentrations	126
Table 9.13. ANOVA analysis for the $E_2$	126
Table 9.14. Fisher analysis of the immersion time effect in the $E_2$	127
Table 9.15. Fisher analysis of the concentration effect in the $E_2$	127
Table 9.16. $E_2$ values variation with immersion time and concentrations	129
Table 9.17. ANOVA analysis for the $\sigma_2$	129
Table 9.18. Fisher analysis of the immersion time effect in the $\sigma_2$	129
Table 9.19. Fisher analysis of the concentration effect in the $\sigma_2$	130
Table 9.20. $\sigma_2$ values variation with immersion time and concentrations	132
Table 9.21. ANOVA analysis for the $\varepsilon_2$	132
Table 9.22. Fisher analysis of the immersion time effect in the $\varepsilon_2$	132
Table 9.23. Fisher analysis of the concentration effect in the $\varepsilon_2$	133
Table 9.24. $\varepsilon_2$ values variation with immersion time and concentrations	134
Table 9.25: Silanisation level effect is colour coded	142
Table 9.26: Seven mechanical properties	143
Table 9.27: Seven mechanical properties <b>percentage</b>	144
Table 9.28: Mechanical properties design factor	145
Table 9.29: Seven mechanical properties <b>weighted percentage (maximum = 100, 200 or 300)</b>	146
Table 9.30: Seven mechanical properties	147
Table 9.31: Volume fraction values for laminates 1 to 28	150
Table 9.32: Volume fraction CV percentage for laminates 1 to 28	154
Table 9.33: Seven mechanical properties standard deviation for laminates 1 to 28	155
Table 9.34: Flexural properties comparison for silane and untreated systems	163
Table 9.35. Comparative table with the experimental campaign best systems	165
Table 9.36: Silanised and untreated systems compression properties comparison	166
Table 9.37: Silanised and untreated systems in-plane shear properties comparison	166
Table 9.38: Silanised and untreated systems ILSS properties comparison	167

## Nomenclature (list of symbols)

AB	Acciona Blades
ABS	Acrylonitrile/Butadiene/Styrene
AF	Aramid Fibres
Af	Fabric areal weight
AFM	Atomic Force Microscopy
A <sub>ij</sub>	Extensional stiffnesses
ANC	Acrylonitrile Copolymer
AP	Acidification Potential
Aramids	Aromatic polyamides
ASTM	American Society for Testing and Materials
ATP	Aquatic Toxicity Potential
BCM	Bulk Compression Moulding
BET-SSA	Brunauer-Emmett-Teller specific surface area
B <sub>ij</sub>	Bending-extension coupling stiffnesses
BPA	Bisphenol A
C	Specific heat
C0°	Longitudinal Compression test
C90°	Transverse Compression test
CE	Composite Evolution
CF	Carbon Fibres
CFM	Continuous Filament Mat
CFRP	Carbon Fibre Reinforced Polymer
C <sub>ij</sub>	Constant parameter
CLSM	Confocal (monochromatic) Laser Scanning Microscope
CLT	Classical Lamination Theory
cm	Centimetre
CM	Compression Moulding
CMC	Ceramic Matrix Composites
CNSL	Cashew Nut Shell Liquid
CNT	Carbon Nanotubes
CP-MAS NMR	Cross-Polarised Magic Angle Spinning Nuclear Magnetic Resonance
cPs	Centipoise
CRAG	Composite Research Advisory Group
C-RTM	Compression RTM
CSA	Cross-Sectional Area
CSM	Chopped Strand Mat
CT	Computer Tomography
CTFE	Polychlorotrifluoroethylene
CV	Coefficient of Variation
d	Diameter
D	Mass diffusivity
DCM	Dough Compression Moulding
deg	Degree
denier	g/9000m
DGEBA	Diglycidyl Ether of Bisphenol A
DIC	Digital Image Correlation
D <sub>ij</sub>	Bending stiffnesses
DIN	Deutsches Institut für Normung
DMA	Dynamic Mechanical Analysis
DMTA	Dynamic-Mechanical Thermal Analysis
dpf	Deniers per filament
DSC	Differential Scanning Calorimetry
E	Elastic modulus
E-	Electrical
E <sub>1</sub>	Elastic modulus in 1 direction

ECF	Excel Conditional Formatting
ECM	Extrusion Compression Moulding
EEW	Epoxy Equivalent Weight
$E_f$	The fibre modulus
EMC	Equilibrium Moisture Content
EP	Eutrophication Potential
$E_x$	Elastic modulus in x direction
EZP	Electrokinetic zeta-potential
F	Formaldehyde
FEA	Finite Element Analysis
FEM	Finite Element Modelling
FF	Fibre Failure
Ff	The force required to achieve debonding
fSW	Fibre Swelling ratio
FTIR	Fourier Transform InfraRed
fx	Apparent diameter
g	Gram
G	Shear modulus
GC-MS	Chromatography-Mass Spectroscopy
GF	Glass fibres
GFRP	Glass Fibre Reinforced Polymer
$G_{II}$	Mode II fracture toughness
GPa	Giga Pascals
gsm	Grams per square meter
GVI	General Visual Inspection
GWP	Global Warming Potential
h	Hour
H <sub>2</sub> O	Water
HALT	Highly Accelerated Life Testing
HDPE	High Density Polyethylene
HIPS	High Impact PS
HTP	Human Toxicity Potential
HTPB	Hydroxyl Terminated Polybutadiene Rubber
IBT	Isocyanate group back titration
ICM	Injection Compression Moulding
ICSTM	Imperial College in London
IFF	Inter Fibre Failure
IFSS	InterFacial Shear Strength
IITRI	Illinois Institute of Technology Research Institute
ILSS	Interlaminar Shear Strength
IM	Injection Moulding
IR	Infra-Red
ISO	International Organization for Standardization
Iso	Isophthalic
J	Joule
k	Kilo
K	Permeability
K	Thermal conductivity
$K_1/K_2$	Fabric characteristic constants
kg	Kilogram
kJ	KiloJoule
Kth	Layer position
L	Fibre length
Lc	Fibre critical length is defined
LCA	Life Cycle Assessment
LCM	Liquid Composite Moulding
LDPE	Low Density Polyethylene

Le	The embedded length of the fibre
LF	Lignocellulosic Fibres
LOI	Loss On Ignition
LTPT	Low Temperature Plasma Treatment
LV	Liquid/Vapour
m-	meta
m	Meter
M	Molar
MACO	Maleated Castor Oil
MAPP	Maleic Anhydride Polypropylene
MEKP	Methyl Ethyl Ketone Peroxide
min	Minute
$M_m$	Maximum moisture content
mm	Millimetre
MMC	Metal Matrix Composites
MPa	Mega Pascals
mPa.s	Milli Pascal per second
$M_t$	Moisture uptake at time t
N	Newton
N/A	Not Applicable
N6	Nylon type 6
N66	Nylon type 66
NaOH	Sodium hydroxide
NCF	Non-Crimp Fabrics
NF	Natural Fibres
NFRP	Natural Fibre Reinforced Polymer
NOL	Naval Ordnance Laboratory
NRADP	Non-Renewable/Abiotic Resource Depletion
o-	Ortho
ODP	Ozone Depletion Potential
OH	Hydroxyl
OM	Optical Microscope
Ortho	Orthophthalic
P	Page
p-	Para
P	Phenol
PAA	Poly (Acrylic Acid)
PAN	Polyacrylonitrile
PBAT	Poly(Butylene Adipate-co-Terephthalate)
PBS	Poly (Butylene Succinate)
PC	Polycarbonate
PCL	Polycaprolactone
PEI	Polyetherimide
PET	Polyethylene terephthalate
PET	Polyethylene terephthalate
$P_f$	Perimeter of the natural fibre
PF	Phenolic resin
PHB	Polyhydroxybutyrates
PLA	Poly Lactic Acid
PMC	Polymer Matrix Composite
PMMA	Poly Methyl MethAcrylate
PMMA	Polymethylmethacrylate
POCP	Photochemical Oxidants Creation Potential
POM	Acetal
PP	Polypropylene
PPS	Polyphenylene sulphide
PRC	Particle Reinforced Composites



Prepreg	Pre(im)preg(nated)
PS	Polystyrene
PTFE	Polytetrafluoro Ethylene
PU	Polyurethane
PVA	Polyvynil Acetate
PVB	Polyvinyl Butyral
PVC	Polyvinyl Chloride
Q	one-dimension volumetric flow rate
R	Radical
RH	Relative Humidity
RIFT	Infusion under Flexible Tooling
RIFT	Resin Infusion under Flexible Tooling
RRV	Resin-Rich Volumes
RT	Room Temperature
RTM	Resin Transfer Moulding
RTP	Reinforced Thermosetting Plastic
s	Second
S	Shear strength
S	Shear Test
SAN	Styrene/Acrylonitrile
SCRIMP	Seemann Composite Resin Infusion Moulding Process
SD	Standard Deviation
SEM	Scanning Electron Microscopy
SEM/TEM	Scanning/Transmission Electron Microscopes
SFFT	Single Fibre Fragmentation Test
SIE	4,4'-(1,3-dipropyl-tetramethyldisiloxane)bis-2-methoxyphenol
SL	Solid/Liquid
SMC	Sheet Moulding Compound
SV	Solid/Vapour
T	Temperature
T	Temperature
t	Time
T0°	Longitudinal Tensile test
T90°	Transverse Tensile test
TDI	Toluene Diisocyanate
tex	g/km
Tg	Glass Temperature
TGA	Thermo-Gravimetric Analysis
Tm	Melting Temperature
ToF-SIMS	Time-of-flight secondary ion mass spectrometry
TP	Thermoplastic
TS	Thermosetting
T-T	Through-Thickness
UD	Unidirectional
UP	Unsaturated Polyester resin
USA	United States of America
UT	Ultrasound Testing
UTS	Ultimate Tensile Strength
UV	UltraViolet
uε	Microstrain
v	Volume
VARTM	Vacuum-Assisted Resin Transfer Moulding
VB	Vacuum Bagging
VCXPS	X-ray Photoelectron Spectroscopy
VE	Vinyl Ester resin
Vf	fibre Volume fraction
W	Watt

w	Weight
$W_0$	Weight of dry specimen
WEEE	Waste Electrical and Electronic Equipment
wt	Weight
$W_t$	Weight of wet specimen at time t
X	Longitudinal strength
XPS	X-ray Spectroscopy
Y	Transverse strength
$\gamma$	Wenzel's contact angle
$\epsilon'$	Strain at failure
$\epsilon_x$	Strain in x direction
$\theta_Y$	Young's contact angle
$\nu$	Poisson's Ratio
$\rho_f$	Fibre density
$\sigma'$	Strength
$\sigma_1$	Tensile strength in 1 direction
$\sigma_f$	Fibre strength at the critical fibre length
$\sigma_x$	Tensile strength in x direction
$\tau$	Fibre-matrix shear strength
\$	Dollar
%	Percent
€	Euro
°	Degree
°C	Celsius degree
$\mu\text{m}$	Microns
2D	Two dimensions
3D	Three dimension
a and $\beta$	Weibull shape and scale parameters

# Chapter 1: Introduction

This thesis reports a research study on natural fibre (NF) reinforced polymer (NFRP) thermoset matrix composite materials. The low wettability and poor fibre-matrix adhesion lead to the mechanical performance of the NF/thermoset composites being lower than expected from consideration of each component characteristic. The research project sought to improve the flow and fibre/matrix interfacial properties by adding silane to the NFRP system in order to obtain the maximum, or most balanced, performance from each component, with the ultimate aim of producing a commercially competitive product that can be utilised for eco-surfboard and eco-surfboard fin production. It was therefore most important to discover how the NF/epoxy/silane composite would respond under rigorous experimental testing. In previous studies, referenced in the literature, NF surfaces have been treated directly with silanes without modifying the epoxy matrix. It is suspected that direct NF treatment leads to fibre swelling thus decreasing the NFRP performance. The present study aims to show that when silane is added directly to the matrix an enhanced NFRP is obtained. This result is a positive contribution to knowledge.

In this study, flax fibre is the principal reinforcement component. Flax is selected because it is claimed to have the best mechanical performance. In this particular study, commercially available Biotex and Lineo woven fabrics have been utilised. For the production of the NFRP Huntsman petrochemical epoxy and SuperSap bio-epoxy resins were selected, because the epoxy resin has good mechanical performance. Huntsman petrochemical resin was selected for the first stage on the basis of availability and price. The SuperSap bio-content formulation was selected for the second stage, as a potentially sustainable matrix for NFRP. The composite was manufactured using either hand-lamination or infusion techniques.

The properties of the unmodified SuperSap/flax composite system were taken as the reference case. In this investigation, flax fibre chemical treatments and epoxy resin modification were performed in

order to improve the NFRP interfacial and flow properties. Modified systems properties were compared with the reference case.

The experimental procedures were undertaken in the following order:

1. Undertake the fibre chemical treatment
2. Evaluate the flow behaviour in panel production/evaluation of mechanical properties
3. ANOVA analysis of the generated data in the mercerisation process
4. Utilise the optical microscope to establish the fibre swelling evaluation
5. Propose a flow **model** for application
6. Apply the developed knowledge in optimised system selection
7. Evaluate optimised system moisture aging properties

Mercerisation and silane treatments were selected for the flax fibre interfacial property improvement. In contrast, bio-epoxy formulations were modified with silane added directly to the epoxy hardener.

Apart from the flow properties characterisation, the mechanical properties of the different systems were evaluated. Different modifications were evaluated with the basic flax/epoxy system.

This study seeks to improve the interfacial properties of the NFRP. The improvement of the interfacial properties are directly correlated to the mechanical static, dynamic and long term performance properties. For this reason, the composite systems developed in the first part of the PhD study were tested at laboratory scale and in real use.

The main objective was to correlate the NF chemical treatment with the composite flow and mechanical properties. The following correlation scheme is proposed:

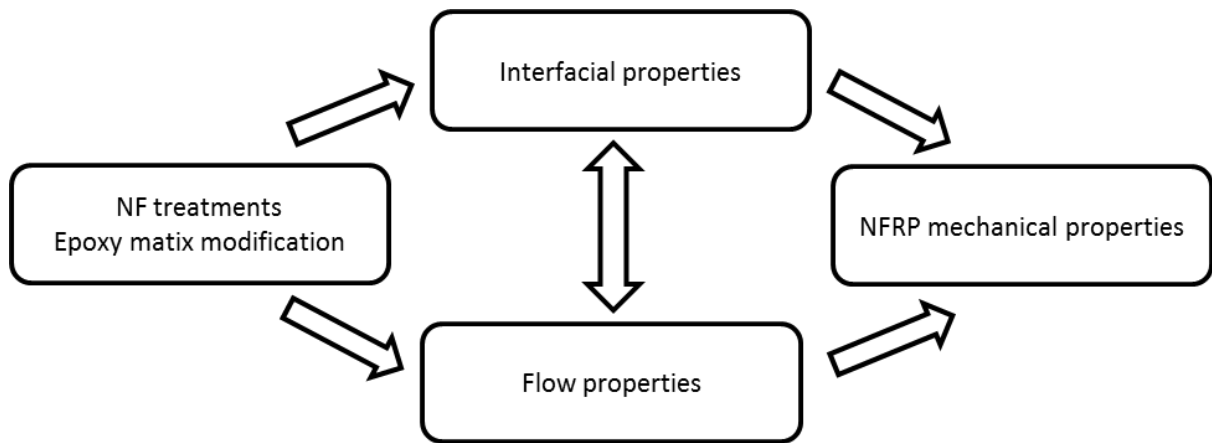


Figure 1.1: Correlation scheme of the different factors

A number of methods have been applied to optimise the fibre/matrix bond within NFRP. However, for reasons of cost, the extent of fibre processing should be limited to avoid a premium price, and for reasons of sustainability, the processes and the by-products of fibre processing should be minimised.

The research is documented in the following 11 Chapters and nine Appendices:

- **Chapter 1: Introduction** - establishes the major research question of the thesis and details the chapter contents;
  - **Chapter 2: Conventional composites** - provides an overview of the composite materials;
  - **Chapter 3: Bio-composites** - provides an overview of the composites produced with bio components, paying special attention to flax fibre and bio-epoxies;
  - **Chapter 4: The interface in natural fibre composites** – discusses the different NF treatments present in the literature focusing on mercerisation and silanisation;
  - **Chapter 5: Composite design manufacturing testing image analysis** –The present chapter reviews composite design, manufacturing, testing techniques and procedures available in the market. Image analysis for materials characterisation were shortly described;
  - **Chapter 6: Composite durability in marine environment** – discusses the addition of silane to the flax/bio-epoxy system in order to improve marine aging resistance;
  - **Chapter 7: Research methodology** – describes the fibres, resins, process materials and selected chemicals; then the selected manufacturing techniques;
  - **Chapter 8: Results** - the results of the experimental tests are presented;
  - **Chapter 9: Discussion** – the results are analysed and discussed;
  - **Chapter 10: Conclusions** – establishes the principal outcomes of the research project;
  - **Chapter 11: Future Research** - evaluates guidelines for further research interests and projects for the potential commercialisation of the product.
- 
- \* **Appendix A** collects all product technical data sheets (TDS);
  - \* **Appendix B** collects all the experimental data;
  - \* **Appendix C** shows the swelling monitoring pictures;
  - \* **Appendix D** compiles all published articles;
  - \* **Appendix E** shows all the moisture aging campaign experimental data;
  - \* **Appendix F** documents explains the procedure for the calculation of mechanical tests uncertainty;
  - \* **Appendix G** contains all the numbers used in the mechanical test results ANOVA analysis.

## 2. Conventional composites

### 2.1. INTRODUCTION

Chapter 2 describes the components in conventional composite materials and their overall characteristics. Composite reinforcements, matrix systems and surface treatments for interface optimisation are each individually described. Additional fabric reinforcement forms are also considered, specifically fabric styles (woven, knitted, stitched or random) with particular reference to fibre orientation and achievable fibre volume fraction ( $V_f$ ).

A polymer matrix composite structure is basically a matrix phase charged with a reinforcement which gives stiffness and strength to the structure. Stresses are transferred between the matrix and the reinforcement. The fibre/matrix interface is as important as the fibre and the matrix. The interface is the distinct boundary between the reinforcement and the matrix. This concept would be deeply studied in Chapter 4.

### 2.2. CONTINUOUS REINFORCEMENTS: GLASS

E-glass fibres are the principal reinforcement used in composite production, since the product is low in cost and is mechanically acceptable in both strength and stiffness (Mallick, 2010). Carbon fibre (CF) is used only in particular cases where the high elastic modulus attracts elevated price in comparison to glass fibre (GF). CF finds application in materials that require high stiffness, low thermal expansion, high thermal capacity, electrical conductivity and electromagnetic shielding properties. The comparative mechanical and physical properties of E-glass and CF are shown in Table 2.1.

Table 2.1: Comparative table of the E-glass and CF properties (Mallick, 2010)

	E-glass fibre	PAN carbon fibre
Filament diameter ( $\mu\text{m}$ )	10	7.2
Relative density (vs $\text{H}_2\text{O}$ )	2.54	1.81
Axial tensile modulus (GPa)	72.4	228
Axial tensile strength (MPa)	1725	3800
Coefficient of thermal expansion ( $10^{-6} \text{ }^\circ\text{C}^{-1}$ )	5	-0.6 (axial), 10 (radial)
Axial thermal conductivity ( $\text{W/m}\cdot^\circ\text{C}$ )	1.04	15
Axial electrical resistivity ( $\text{ohm}\cdot\text{cm}$ )	0.1	0.0017

GF is the most commonly used reinforcing inorganic fibre because of its high performance and very economical price (Khazanov, Kolesov, & Trofimov, 1995). GF is produced by melting oxides from sand together with other additives in large furnaces at very high temperatures, usually between 1000 and 1800°C (Dwight, 2000). After the melting process, this viscous glass is pushed to produce thousand-filament yarns.

In accordance to the components used in the production of each kind of glass fibre, they are denominated with a specific nomenclature. For example, the most common is designated "Electrical" E-glass, since at the beginning it was produced for electrical insulators and printed circuit boards. Other examples are A, D, S or AR glasses, all depending on the composition and manufacturing temperatures of production.

The general properties of the major GF are shown in Table 2.2.

Table 2.2: Physical properties of reinforcement glasses (Fecko, 2006)

	E-glass	R-glass	S-2 glass
Relative density ASTM 1505	2.58	2.54	2.46
Softening point ASTM C338(°C)	846	952	1056
Tensile strength 23°C (GPa)	3445	4135	4890
Tensile modulus 23°C (GPa)	72	86	87
Elongation (%)	4.8	4.8	5.7

In real production when the filament diameter measurement is not practical, the weight of a bundle of fibre per unit length is used according to units of "tex" (g/km) or "denier" (g/9000m) (Thomason, 1995).

### 2.3. MATRICES - THERMOSET RESINS

Thermosetting (TS) resins are normally oligomers (low molecular weight polymers) which are usually liquid before mixing with a second component to crosslink the different polymer chains and hence solidify the mixture. This can be achieved by either an addition or a condensation/ring-opening reaction. In some cases, heat is applied to the mixture to accelerate the process. Process temperatures are typically between ambient and 200°C.  $T_g$  (Glass transition temperature) is the temperature where segmental motion is frozen out of the



polymer chain. This is one of the greatest advantages of using the thermoset resins. The  $T_g$  normally follows the cure temperature, so it should be possible to produce creep-free composites with much lower process energies than for a TP (thermoplastic) matrix.

Resin viscosity depends directly on the molecular weight of the polymer and the temperatures used in the process. Viscosity increases with the molecular weight (Ghijssels, Groesbeek & Raadsen, 1984). The temperature increment can produce the opposite effect in the flow index of the resin; under higher temperatures the resin would flow more easily, but as cure progresses the viscosity increases. Figure 2.1 illustrates the viscosity evolution of two different epoxy formulations along the curing process. In this case, the resin curing accelerates when the system reaches 40°C, as a result the viscosity increases with progress of cure. This viscosity rise is not shown in Figure 2.1.

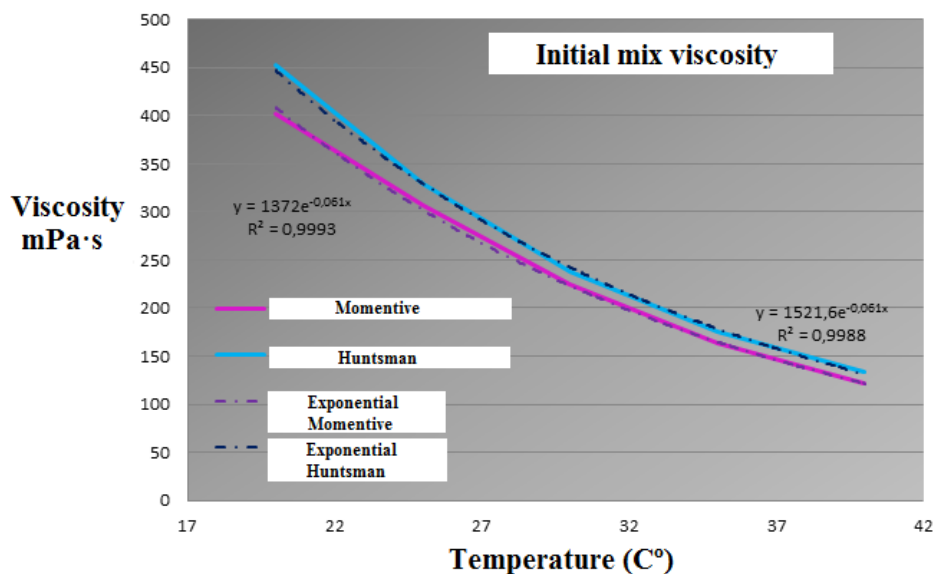


Figure 2.1: Instantaneous viscosity evolution according to temperature (Courtesy of Acciona Blades)

The most common systems would use the following formulations:

- Unsaturated Polyester resin (UP) - diluted with styrene and cured with ~ 1% catalyst
- Vinyl Ester resin (VE) - diluted with styrene and cured with ~ 1% catalyst
- Epoxy resin - cured with hardener in stoichiometric proportions – typically a 3:1 to 5:1 mix ratio

### 2.3.1. Epoxy resin

Epoxy is considered to be a high standard resin for composite material production. The cured resin has great mechanical, thermal, corrosion resistance and chemical properties. Due to its internal structure, epoxy has good electrical properties (Park et al., 2007). Finally, epoxy based adhesives are very important in the current market because of their adhesive capabilities in different substrates (Bhuniya & Maiti, 2002).

The chemistry of the epoxy resin is studied in detail in this chapter since the research project is based on a flax fibre/bio-epoxy resin composite.

The characteristic epoxy group is based on the highly-strained "epoxy ring" (Figure 2.2) a highly reactive three-member ring composed of two carbon atoms and one oxygen atom (Lee, Jang, Hong, Hwang, & Kim, 1999).

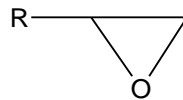


Figure 2.2: Epoxy group basic structure

The first step in the production of the epoxy resin is based on the reaction between bisphenol-A and epichlorohydrin (Wang & Zhang, 2004). Bisphenol-A is the most commonly used diol. The result of this reaction is the formation of diglycidyl ether of bisphenol A (DGEBA) a product prepolymer (Figure 2.3). There can be other options in the resin backbone production, such as the production of Bisphenol F or S.

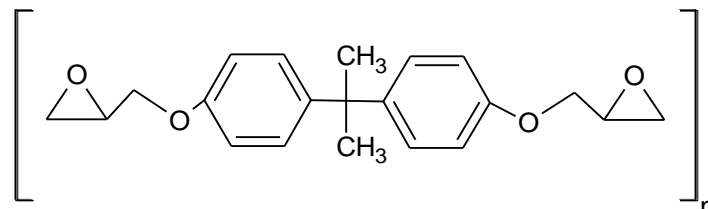


Figure 2.3: DGEBA product chart

Two great advantages in the manufacture of epoxy composites are the control of the curing cycle and low shrinkage of the resin once cured (Wan, Bu, Xu, Li, & Fan, 2011); the SuperSap resin used in the experimental part of the project shrinks by only 2% (linear shrinkage). The low shrinkage obtained in the curing of the composite part also reduces residual stresses and thus maintains dimensional stability (Nawab et al., 2012; Shah & Schubel, 2010; Li, Potter, Wisnom & Stringer, 2004).

In contrast, one disadvantage could be the elevated viscosity (800-900 mPa·s) of the epoxy prepolymer that might impede the processing and the correct fibre wetting; this disadvantage might be even higher in the flax fibre NF wetting process. Due to the elevated solid content of the epoxy formulation, its market price is also higher. Furthermore, the epoxy process is long and difficult to perform in hot and humid environments due respectively to exotherm, accelerators and side reactions, and the curing process has to be controlled (Montserrat, Flaque, Calafell, Andreu & Malek, 1995; Wan, Bu, Xu, Fan & Li, 2011; Huang et al., 2012).

The selection of the curing agent is dependent on the curing temperature, the desired Tg or the final mechanical properties. The calculation of the quantity of the curing agent depends on the concept of the Epoxy Equivalent Weight (EEW) (Ellis, 1993). This concept provides the information about the epoxy content in the resin, the number of epoxy equivalents in a kilogram of resin or number of epoxy groups grams per mole of resin.

$$EEW = \frac{\text{Epoxy Equivalent}}{1\text{kg of resin}} \text{ or } \frac{\text{Epoxy grams}}{\text{mol of resin}}$$

Elevated EEW value means that there are many available active points in the epoxy backbone, giving as a result highly reticulated epoxy. In contrast, when the EEW is low the cross-linking (reticulation) is also low. According to this number, the stoichiometry between the first component and the curing agent is determined, thus when stoichiometry is followed the maximum epoxy performance is achieved. Normally, the proportions of the first component / curing agent are 3:1 or 5:1. Occasionally, epoxy commercial systems have more than two components, and then the proportion is referred to by the first component. The epoxy system

curing agents are normally divided into two groups, the amines and the anhydrides. The SuperSap system uses a trifunctional amine for the reticulation process.

In the transformation from liquid prepolymer to infusible solid resin, the material passes through different stages. One of the most important is the "gelation" stage (Li, Li & Meng, 2012; Lin & Wang, 1994). Viscosity increment considerably decreases resin processability influencing especially on the flow process, such as in infusion or pultrusion, but not greatly influencing manual lamination. The gelation or gel-point usually occurs in the range of 55-80% of the complete process. One of the problems of gelation is that auto-acceleration of the reaction can happen suddenly, thus increasing the reaction temperature (exotherm) which can lead to final piece degradation (Jin & Park, 2012). This energy release can feed into new covalent bond production, creating in the process more free energy and advancing the reaction without much control.

In each curing process, different conversion rates (degree of cure) ( $\alpha$ ) are obtained; this value is affected by many factors such as the curing temperature and time, although the principal factors will be the type of curing agent used and the quantity that is added. In any case, the full conversion is 100% (Kim & Lee, 2002; Min, Stachurski & Hodgkin, 1993). In certain examples, for example fabric prepregs, the curing process may be halted to allow for the process to be continued later. The formulation used in this technique is referred to as a B-stage resin.

In the serial production of a composite design, it is normal for the part product to be de-moulded when the Tg of the resin has been achieved. The mould is then free to allow production to continue. The free-standing de-moulded part can then be post-cured as an extra step in the completion of the curing process in order to achieve the definitive Tg. In this PhD research project for example the panels were post-cured after the tabs had been glued, directly affecting the Tg value. In Table 2.3 some epoxy systems typical values are shown.

Table 2.3: Different epoxy systems Tg temperatures (Varma & Gupta, 2000)

Resin	Tg(°C)
DGEBA (Pure)/3,3'-DDS	184
EPN825/DDS	222
EPN828/DDS	211
EPN834/DDS	186
DGEBA (Pure)/DDM	176
DER332/DDS	190
Epon828/DDM	170

Table 2.4 presents the mechanical properties of a general amine cured epoxy system developed by using the correct resin/hardener mix rate and processed by the correct curing cycle.

Table 2.4: Epoxy resin general properties (Pham & Marks, 2000).

Properties	Values at RT (25°C)
Tensile strength (MPa)	48
Tensile modulus (GPa)	3.9
Tensile elongation (%)	1.3
Flexural strength (MPa)	127
Flexural modulus (GPa)	3.6

### 2.3.2. Unsaturated Polyester (UP) and Vinyl Ester (VE)

UP are linear poly-condensation based polymers (Mouritz, Gellert, Burchill & Challis, 2001). The poly-condensation reactions are undertaken between acids/anhydrides and diols/oxides in order to produce a prepolymer mixture. Figure 2.4 shows the general reaction between acid and diol to achieve a linear polyester molecule.

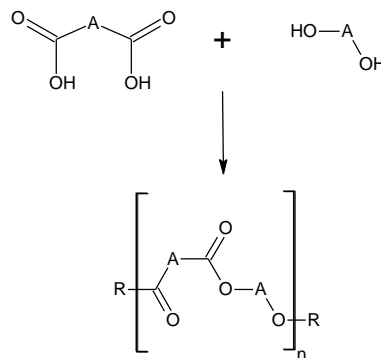


Figure 2.4: UP prepolymer general synthesis reaction, where A is a chemical group

The prepolymers are usually brittle solids or viscous liquids. When unsaturated oligomers are combined with reactive solvents, they produce UP resins. For example, the polyester prepolymer is usually formulated with a reactive diluent: styrene. This formulation is widely

used since it produces great mechanical performance at a very economical price. The formulation viscosity of these oligomers is usually between 200 and 2000 mPa·s.

The oligomers have unsaturation in the backbone that are the bonding points for the formation of 3D networks (Figure 2.5).

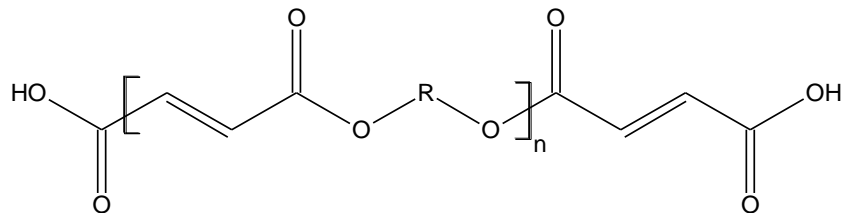


Figure 2.5: Prepolymer structure with the unsaturated double bond

UP resins have been mainly used in marine and building constructions. For example, surfboards and RTM fins are currently manufactured with UP resin reinforced with GF. The atmospheric pressure using vacuum inside a bag allows for the compacting of the different fabric layers. In addition, the resin can cure at room temperature (RT), this formulation is therefore ideal for the construction of large structures such as water tanks or ship hulls (Mouritz, Gellert, Burchill & Challis, 2001). Commercial UP formulations can vary from slow to rapid in their curing programmes according to their formulation.

Whereas UP have unsaturation distributed along the monomer backbone, VE resins have an unsaturated core molecule with terminal (chain-end) unsaturation, similar to the reaction positions in epoxy resins.

The resultant product forms a very fluid resin (200-300 mPa·s) possessing good mechanical properties and at a price that falls between the epoxy and UP resins. The low viscosity of VE is suitable for quick composite production and the process allows for the correct wetting of all the fibres. The curing process is similar to that used for conventional UP, where a free radical producer (catalyst) is added to the prepolymer to start the polymerisation of the resin at RT.

For the VE resin, the reticulation density is higher than in UP resins, resulting in the mechanical properties and chemical resistance being correspondingly higher (Banna, Shirokoff & Molgaard, 2011). Resulting from the chemical resistance of VE resins, chemical container tanks and concrete reinforcements are possible commercial products.

#### **2.4. SURFACE FINISHES ON FIBRES**

The application of a sizing medium to the reinforcement fibre surface is absolutely necessary since without coating the fabric the fibres would either break in the manufacturing process or the properties of the fabric-matrix interface would not be sufficient to withstand the appropriate use of the composite (Thomason, 1995). After fibre formation and taking into account the effect of Loss On Ignition (LOI), the commercial fibre sizing content may be between 0.2 and 2% in weight. Ideally, the sizing film should be coated over the complete filament surface. However, it has been shown by using modern surface analytical techniques that the spread of the sizing over the filament surface is heterogeneous and varying from 1nm to 10nm in thickness.

In addition to the above analytical studies, there are references to model applications that attempt to understand the fibre/matrix interface performance in the presence of the sizing (Zhuang, Burghardt & Mäder, 2010). However, few can claim 100% accuracy since it is extremely difficult to determinate the exact performance nature of the sizing agent on any specific batch of reinforcement.

In respect of the present research project, it is vitally important to understand the interfacial properties of the conventional composites as well as the surface finishes of conventional fibres; additionally, the NFRP interfacial properties are deeply studied in Chapter 4. A variety of sizing agents are normally available to coat reinforcement fibres (anti-static, binder, lubricant, film-formers, acidity/pH regulators and coupling agents). The coupling agent is utilised to create a strong interface between the fibre and the matrix. Coupling agents are usually organosilanes which bond well with most (fibre) surfaces (Liu, Thomason & Jones, 2008). A good interface can enhance stress transfer between the matrix and the reinforcement material and improve

the composite dynamic properties while minimising environmental degradation, especially in water.

In general, silanes have a different functionality at opposite ends of the molecule: the silane functional group reacts with the fibre surface while the organic moiety reacts to form covalent bonds with the matrix (Figure 2.6). The normal assumption is that the glass fibres are vinyl-sized for UP and the aramid or carbon are epoxy-sized for epoxy resins, unless it is specially stated otherwise.

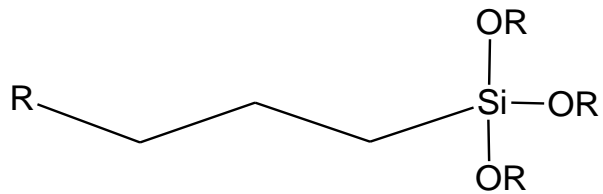


Figure 2.6: General structure of organosilane where R is either vinyl or epoxy functionality  
(Liu et al., 2008)

## 2.5. SHORT FIBRES AND FABRIC PRODUCTION

Fibres can be classified as short (less than the critical length defined by the Cox shear-lag model), long (discontinuous with length/diameter aspect ratio variously > 200-1000x) or continuous (as used e.g. in textiles/filament winding/pultrusion).

In the fibre manufacturing process, thousands of filaments will be treated and transformed into different fabric configurations. In the case of CF, once the filaments have been conveniently produced they are grouped in tows. Commercially the main sizes of CF tows contain between 3000 and 48000 filaments per tow with 6K and 12K being most popular (NOTE: although K = 1024 in computing and k = 1000 in SI units, capital K is used for thousands of filaments in designating carbon fibre tows). The heaviest tows result from a faster manufacturing process and therefore offer a price reduction; on the other hand, the finest tows are used for high performance applications particularly in the aeronautics and aerospace sector. Smaller tows, with lower areal weight fabrics, result in having smaller resin-rich volumes (RRV) and consequently have greater strength.



Woven fabrics might be easily manipulated and have excellent drapability. However, these fabrics are not usually utilised in high standard applications. Firstly, in woven fabrics the fibre orientation within the fabric is usually limited to 0° and 90° directions. This 0/90 conformation might be woven in different ways, for example, twills or satin (Gandhi & Sondhelm, 2016), surfboards are produced with GF 125g/m<sup>2</sup> and 190g/m<sup>2</sup> 0/90 twill woven fabric. Secondly, the crossovers between the tows cause mechanical properties reduction leading to fatigue and long-term strength decrease.

For high performance part production, stitched Non-Crimp Fabrics (NCF) are used. The main advantage is that the fibre can be oriented in the necessary direction depending of the external load requirements. The stitching technology gives additional through-thickness reinforcing capability to the fabric. The long-term properties of NCF are superior to woven fabrics (Adden & Horst, 2010). NCF are costly to produce and their drapability may be less suitable than in woven fabrics.

In the fabric manufacturing process, the first step is to twist the strand in order to obtain the "yarn" for short fibres, but unnecessary misorientation for continuous fibres (Clarke, 2010). Hundreds of yarns feed the loom in order to manufacture different characteristic fabrics with the aim of varying the angle, fabric weight or the weaving tension parameters.

Continuous fibres are selected for fabric production where they are usually arranged unidirectionally, randomly, cross-plyed, woven (plain weave, twill and satin), knitted or stitched interlock. Figure 2.7 shows different fabric types in schematic arrangements.

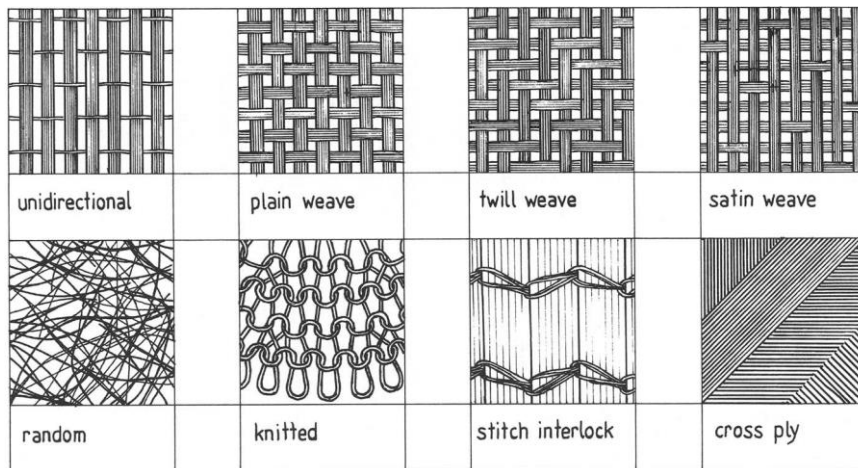


Figure 2.7: Fabrics types

(drawn by John Summerscales and reproduced here with his permission)

## 2.6. SUMMARY

In Chapter 2, the principal types of reinforcements, matrices and interfaces have been described and their utilisation summarised. For the purposes of the present research project, it is clearly necessary to have complete understanding of the conventional composite materials that can be utilised in establishing an enhanced bio-composite system which is the main target of the research.

In respect of the project, it is vitally important to understand the interfacial properties of the conventional composites as well as to establish the most suitable surface finishes that can be applied to conventional fibres, although the NFRP particular case is deeply studied in Chapter 4. The principal aim is to establish a method for NFRP properties enhancement and the sizing performance of conventional composites.

In the current study, the same organosilane was used in two different approaches (directly in the NF and dissolved in the hardener) to improve the NFRP interfacial properties.

# 3. Bio-Composites

## 3.1. INTRODUCTION

The composites produced with bio-polymers (Section 3.9) or/and NF (Natural Fibre) are commonly described as bio-composites. In the present research project, a flax fibre/bio-epoxy bio-composite was selected for detailed experimental analysis. The first part of the chapter describes NF and in the second part defines bio-polymers.

## 3.2. NATURAL FIBRE DESCRIPTION

NF are fibrous materials that may be variously sourced from plant, animal or mineral matter (Pickering, 2008). The classification of NF matter is shown in Figure 3.1. Plant fibres are the result of a photosynthesis process and are normally defined as lignocellulosic fibres (LF) because of their elevated content in both components, lignin and cellulose. Cotton is considered to be a cellulosic fibre.

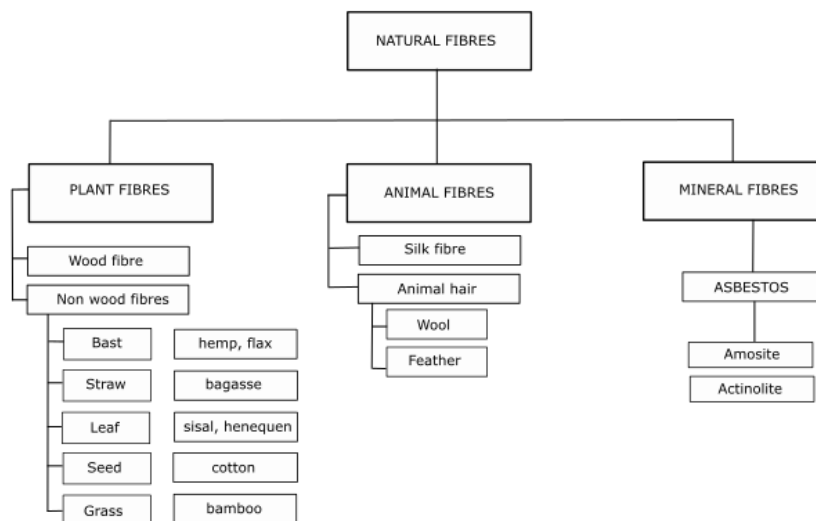


Figure 3.1: Natural fibres classification scheme (George, Chae & Bressler, 2016)

Living plants are renewable and sustainable entities, but the fibres processed from them may not be, and any claim for their green credentials should be supported by a life cycle assessment (LCA) (Gurunathan, Mohanty & Nayak, 2015), which will be further explained in Chapter 6. The environmental advantages of NF, in combination with bio-based matrices, are one of the main

reasons for their use in composite manufacturing processes. The mechanical and physical properties of NF materials are dependent on their internal structures. LF are generally formed of cellulose, hemicellulose, lignin and other components (Figure 3.2). The cellulose component gives stiffness and reinforcement strength to the structure and the lignin matrix works as a bridge transferring the load from one microfibril to the next. In recent years there has been an increase interest in microfibril isolation and its utilisation as a nano-reinforcement because of its higher mechanical property (Malainine, Mahrouz & Dufresne, 2005).

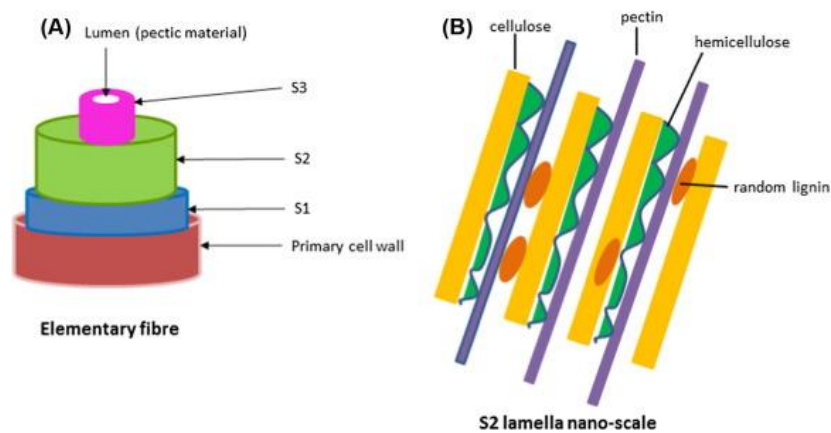


Figure 3.2: Lignocellulosic fibre internal structure scheme (George et al., 2016)

The mechanical properties of NF will vary according to their different lignocellulosic fibre composition and in the context of the present study, will directly affect the interfacial properties. Generally, in most cases where the lignocellulosic fibres have been treated to improve their interaction with the polymer matrix, the oily component from the fibre is retained. The present study will aim to eliminate this component as well as the lignin when this is also retained (Cho et al., 2007; Shanmugam & Thiruchitrambalam, 2013). The first interaction would lead to the improvement of composite rigidity, but lignin elimination would cause a drastic drop in strength. As a result mild, rather than very aggressive, treatments are usually selected.

### 3.3. LIGNOCELLULOSIC FIBRES CLASSIFICATION AND TYPES

LF originate from plant source and are classified according to their extracted parts, whether from the outer stem (bast) or the inner stem (core). Bast fibres are located around the stem and under the external bark of dicotyledons plants forming bundles or strands that run parallel to the length of the

stem. They provide structural strength and rigidity to the plant. Strands may vary in length but may attain spans of up to 1000 mm with widths of up to 1 mm. In the case of flax, ramie, hemp, kenaf and jute ultimate fibres are very long with an “aspect ratio” of 1000 (ratio of length to width).

Leaf fibres may also be long, as for example when they are extracted from sisal or pineapple leaves. Their mechanical properties are, however, lower than in the bast fibres. Reinforcing fibres may also be extracted from plant fruit, seeds, core, roots or grass, with the limitation that they are considerably shorter and therefore more suitable for use as fillers in TP composites. LF classification is shown in Table 3.1.

Table 3.1: Lignocellulosic NF classification (Pickering, 2008)

Bast	Leaf	Seed					Core	Grass/reeds	Other
		Fibres	Pod	Husk	Fruit	Hulls			
Hemp	Pineapple	Cotton	Kapok	Coir	Oil palm	Rice	Kenaf	Wheat	Wood
Ramie	Sisal		Loofah			Oat	Jute	Oat	Roots
Flax	Agava		Milk Weed			Wheat	Hemp	Barley	Galmpi
Kenaf	Henequen					Rye	Flax	Rice	
Jute	Curaua							Bamboo	
Mestra	Banana							Bagasse	
Urena	Abaca							Corn	
Roselle	Palm							Rape	
	Cabuja							Rye	
	Albardine							Esparto	
	Raphia							Sabai	
	Curauá							Canary grass	

Bast fibres are the most commonly used reinforcements in NFRP composites because of their length and mechanical properties. The characteristic properties of the most commonly utilised Natural fibres are shown in Table 3.2.

Table 3.2: NF characteristics (Pickering, 2008)

Fibre	Density (g/m <sup>3</sup> )	Length (mm)	Diameter (µm)
Cotton	1.21	15-56	12-35
Coir	-	0.3-3	7-30
Flax	1.38	10-65	5-38
Jute	1.23	0.8-6	5-25
Sisal	1.2	0.8-8	7-47
Hemp	1.35	5-55	10-51
Henequen	1.4	-	8-33
Ramie	1.44	40-250	18-80
Kenaf (bast)	1.2	1.4-11	12-36
Kenaf (core)	0.31	0.4-1.1	18-37
Pineapple	1.5	3-8	8-41
Bagasse	1.2	0.8-2.8	10-34

### **3.3.1. Flax**

Flax fibres have a particular relevance in the present research project. Flax belongs to the Linaceae family and it is one of the oldest commercial crops in the world used to produce Linen in the textile industry. The genus *Linum* has many species, and Linen flax *L. usitatissimum* is an annual plant with a plant stem diameter of 1.6-3.2mm. Flax is generally harvested after 100 days or when the base starts to turn yellow. Fibres are extracted from the plant stem and linseed/flax oil is produced from the seed. The fibres are separated from the bark by retting, and approximately 0.1-0.25 m of the stalk supply the bast fibres. Flax is grown widely in Ireland, France, China and Belarus (Heller et al., 2015).

The flax quality required for composite applications in an industrial capacity is not yet well established. Retting is one of the least well defined procedures in these applications, and is a critical parameter during flax production since it directly affects the final mechanical properties of the fibres (Martin, Mouret, Davies & Baley, 2013). Because of this problem many alternative methods have been proposed, such as radio frequency assisted retting, microwave assisted retting and enzymatic retting (Ruan, Du, Garipey & Raghavan, 2015; Nair, Rho, Yaylayan & Raghavan, 2013; Evans, Akin & Foulk, 2002).

Besides retting quality questions, a number of companies now can offer high quality flax fibre and fabrics, for example Composite Evolution based in the UK, Lineo based in Belgium or Bcomp based in Switzerland. In the current research both Composite Evolution and Lineo fibre was used for composite manufacturing.

### **3.4. NATURAL FIBRES EXTRACTION TECHNIQUES**

Lignocellulosic NF is extracted from the plant by using three main techniques - mechanical, biological and chemical - which may be applied singly or in combination depending on the quality of the fibre. The extraction techniques will directly affect the final mechanical properties of the fibre (Zeng, Mooney & Sturrock, 2015). They are described in detail below.

### **3.4.1. Mechanical extraction**

Primitive fibre separation techniques allowed the plant to rot in the field before it was gathered and beaten against a hard surface to eliminate non-essential plant tissue. Today laborious manual methods have been replaced by machinery leading to an improved extraction process and a higher yield contribution.

When machines are applied to isolate the LF from the plant, the process is denominated as decortication (Hepworth, Hobson, Bruce & Farrent, 2000). In the process the plant is passed through slotted rollers in order to separate the NF from the waste material such as the core or bark. This isolation process is applied in the extraction of LF from sugar cane (bagasse), jute, hemp or kenaf plants. Although decortication is the most commonly applied technique for most plants, in the more specific example of cotton a gin machine is used which may also be applied for the extraction of kenaf fibres.

### **3.4.2. Biological extraction**

Basically, in the biological process enzymes from micro-organisms such as moulds and bacteria are used to separate the LF from the plant. Retting or degumming is a most necessary part of the process (Shahid, Mohammad, Chen, Tang & Xing, 2016). The bast fibres are separated from the straw by retting in a slow-running river, pond or tank, typically for a 3 to 20 day period depending on the type of fibre, the humidity and temperature conditions or whether dew/ground-retting (straw left exposed in the field) or enzyme retting techniques are used. During retting the water content of the straw increases and this encourages the growth of bacteria or fungi which in turn causes the deterioration of the pectin binders that hold the cellulose fibres together in the plant stem.

It has been shown that the quality of the retting process is controlled by such factors as micro-organism diversity, water quality and pH factors, parameters that require consistent monitoring to achieve the best results. Complications arise in the thicker parts of the stem since they take longer to ret causing the thinner end stems to over-ret. As a result, it has been proven that the use of less

damaging microorganism, clean water and a controlled pH below 4.9, will considerably improve the retting process and consequently increase the quality of the extracted LF.

The requirement for high water utilisation is one of the limiting factors in the retting process. For this reason retting is undertaken directly in the field, cutting the plant after the growing season and leaving it to ret by natural biological action in the absence of humidity control and identified microorganism content (Liu et al., 2015). Under such conditions the retting process may take up to a month longer than in pond retting.

### **3.4.3. Chemical extraction**

This separation process usually involves retting by chemical action or pulping using alkaline or acid agents to extract NF from the plant.

Dew-retting is the preferred process used today since it is quicker, more efficient and creates less waste water than the water immersion methods; its disadvantage is it produces chemical pollution. A number of chemical methods have been devised to improve dew-retting. They include the use of chemical chelators (e.g. EDTA or oxalic acid) at high alkalinity or of detergents/surfactants (Adamsen, Akin & Rigsby, 2002). Chemical treatment permits a high rate of production although the quality of the fibres produced may be impaired and the cost of production may be high. Kessler has developed a flash explosion steam treatment to produce high quality natural fibres by decomposing the lignin and hemicellulose fractions at high processing temperatures (Kessler, Becker, Kohler & Goth, 1998).

Chemical "degumming" is another chemical option, whereby hot alkali solutions are used to dissolve the pectin binder and ultimately release the fibres from the bundles (Feng, Chen & Zhang, 2008). The normal reaction medium is a sodium hydroxide solution in water with sodium carbonate added for economic reasons. The process improves some characteristics of the fibres (e.g. fineness, softness and elongation-at-break) but at a cost of reducing fibre length and strength. Because of the loss of mechanical properties degumming is not normally used as a technique when fibres are required for reinforcement in composites.



### 3.5. NATURAL FIBRE CHEMISTRY

Most NF are composed of lignin, cellulose, hemicellulose and pectin with each represented by its respective component percentage, as illustrated in Table 3.3.

Table 3.3: Chemical composition and structural parameters of NF (Gurunathan et al., 2015)

Fibre	Cellulose (wt%)	Hemicellulose (wt%)	Lignin (wt%)	Pectin (wt%)	Water soluble (wt%)	Wax (wt%)	Microfibrillar angle (deg)
<b>Bark/Steam fibre</b>							
Flax	71-78	18.6-20.6	2.2	2.3	3.9-10.5	1.7	5-10
Hemp	70.2-74.4	17.9-22.4	3.7-5.7	0.9	2.10	0.8	2-6.2
Jute	61-71.5	13.6-20.4	12-13	0.2	1.2	0.5	8
Kenaf	45-57	21.5	8-13	3-5	N.S.	N.S.	N.S.
Ramie	68.6-76.2	13.1-16.7	0.6-0.7	1.9	6.1	0.3	7.5
Banana	63-64	10	5	N.S.	N.S.	N.S.	11
Nettle	86	4.0	5.4	0.6	2.1	3.1	N.S.
<b>Leaf fibre</b>							
Sisal	67-78	10-14	8-11	10	1.3	2	10-22
Curaua	73.6	9.9	7.5	N.S.	N.S.	N.S.	N.S.
Pineapple	80-83	15-20	8-12	2-4	1-3	4-7	8-15
Abaca	56-63	21.7	12-13	1.0	1.6	0.2	N.S.
Henequen	77.6	4-8	13.1	N.S.	N.S.	N.S.	N.S.
<b>Fruit/Seed fibre</b>							
Cotton	85-90	5.70	0.7-1.6	0-1	1.0	0.6	20-30
Coir	36-43	0.15-0.25	41-45	3-4	5.2-16.0	N.S.	30-49
Oil palm	65	0-22	19	N.S.	N.S.	N.S.	46
<b>Wood</b>							
Hardwood	43-47	25-35	16-24	N.S.	N.S.	N.S.	N.S.
Softwood	40-44	25-29	25-31	N.S.	N.S.	N.S.	N.S.

### 3.6. NATURAL FIBRE PROPERTIES

The mechanical and moisture properties of LF are described in the following section. Variability is one of the most complicated questions in their study arising from such factors as plant type, crop year and crop location and issues arising from the climatic cycle experienced or the extraction techniques employed. All such factors may directly influence the final chemical composition of the fibres as well as properties associated with the diameter, morphology and density of the fibres adding to the difficulty of measuring these properties accurately.

#### 3.6.1. Mechanical properties

Table 3.4 presents the general physical and mechanical properties represented in the most important LF and GF materials. The table illustrates the great variation in the test results of these properties.

**The present research project aims to optimise the mechanical properties of NFRP, limiting as many factors as possible in order to reduce the dispersion in the results.** The mechanical tests performed will be reviewed in Chapter 5 and the results summarised in Chapter 8. One of the great advantages of LF is their high specific property values. The specific property is the

evaluated property divided by the density, but since the NF density is very low in comparison with the GF density, the value obtained is accordingly elevated.

Table 3.4: Physical and mechanical properties of important LF and GF (Gurunathan et al., 2015)

Fibre	Density (g cm <sup>-3</sup> )	Length (mm)	Diameter (µm)	Strain at break (%)	Tensile strength (MPa)	Young's modulus (GPa)	Specific strength (MPa)	Specific modulus (GPa)	Moisture content (%)
Cotton	1.21	15-56	12-35	2-10	287-597	6-10	194-452	4-6.5	33-34
Jute	1.23	0.8-6	5-25	1.5-3.1	187-773	20-55	140-320	14-39	12
Flax	1.38	10-65	5-38	1.2-3	343-1035	50-70	345-620	34-48	7
Sisal	1.20	0.8-8	7-47	1.9-3	507-855	9-22	55-580	6-15	11
Ramie	1.44	40-250	18-80	2-4	400-938	61.4-128	590	29	12-17
Hemp	1.35	5-55	10-51	1.6-4.5	580-1110	30-60	210-510	20-41	8
Coir	1.2	0.3-3.0	7-30	15-25	175	6	92-152	5.2	10
Kenaf	1.2	1.4-11	12-36	2.7-6.9	295-930	22-60	246-993	18-50	6.2-12
Banana	1.35	0.9-0.4	12-30	5-6	529-914	27-32	392-677	20-24	10-11
Pineapple	1.5	3-8	8-41	1-3	170-1627	60-82	287-1130	42-57	10-13
Abaca	1.5	4.6-5.2	10-30	2.9	430-813	31.1-33.6	N.S.	N.S.	14
Bamboo	0.6-1.1	1.5-4	88-25	1.3-8	140-441	11-36	383	18	N.S.
Nettle	1.51	5.5	20-80	1.7	650	38	N.S.	N.S.	11-17
Hardwood	0.3-0.88	3.3	16	N.S.	51-120.7	5.2-15.6	N.S.	N.S.	N.S.
Softwood	0.30.59	1.0	30	4.4	45.5-11.7	3.6-14.3	N.S.	N.S.	N.S.
E-glass	2.5	N.S.	15-25	2.5	2000-3500	70-73	800-1400	29	N.S.
S-glass	2.5	N.S.	N.S.	2.8	3-3.5	63-67	1.8	34.4	N.S.

### 3.6.2. Moisture properties

LF surfaces have high levels of polar hydroxyl (-OH) groups which provides the NF with its hydrophilic property. It is therefore very important to determine the water uptake of the NFRP since moisture absorption can result in fibre/matrix interface ageing and subsequently lead to a reduction in its composite mechanical property. These properties will be examined in the experimental tests described in Chapter 6. Table 3.5 presents the equilibrium moisture content (EMC) percentages of fibres derived from the principal plant materials at 65% relative humidity and a temperature of 21°C. It is noted in this table that the fibre composite EMC for flax is 7%.

Chapter 6 describes the composite aging tests in moist environments. The experimental campaign includes comparative bio-composite systems moisture aging test in Appendix E. See Table 3.5 where different fibres EMC at 65% Relative Humidity (RH) and 21°C. According to Pickering study; 7% of EMC value is compared with the PhD experimental results.

Table 3.5: NF Equilibrium Moisture Content (EMC) percentage (Pickering, 2008)

Fibre	Sisal	Hemp	Coir	Aloe	Banana	Pineapple	Wood	Abaca	Cotton	Jute	Kapok	Ramie	Flax
EMC (%)	11	9	10	12	15	13	12	9,5	8	12	10	9	7

### 3.7. NATURAL FIBRE REINFORCEMENT FORMS AND FABRICS

In the earlier stages of producing NFRP, NF was added to the matrix in order to obtain a more economical final product without due consideration of its mechanical properties. However, following these initial stages, research in the development of NF composite materials has concentrated on introducing reinforcement tailoring into each specific final product. The matrix might be reinforced with short or continuous NF fabric depending on the final application. In composite design it would be a key factor in the selection of the correct NF, NF reinforcing form and  $V_f$ ; always considering the interface properties.

#### 3.7.1. Slivers and yarns production

With the utilisation of classical textile spinning techniques it is possible to produce sliver and fibre yarns.



Figure 3.3: Flax fibre yarn roll produced by spinning technique (Courtesy of Composite Evolution)

The first step replicates the mat production carding technique by which the fibre is opened, mixed and carded. The web obtained from the carding process is gathered into a sliver with the assistance of a can coiler and the sliver obtained from this process might be used directly in semi-finished product manufacturing, as for example in pultrusion. Additionally, if the textile requires to be produced, the slivers will have to be transformed into yarns as illustrated in Figure 3.3.

Sliver spinning strengthens the yarn to obtain a base material in fabric manufacturing which also facilitates in its handling. However, the twisting process considerably reduces the mechanical properties of the yarn because of fibre disorientation. The loss of performance has been studied in

many prediction models (Shah, Schubel & Clifford, 2013). Further, spinning is very energy intensive (Dissanayake, 2011).

### 3.7.2. Fabrics production

NF fabric manufacturing replicate the same procedures as those used in the production of GF or CF. In fabric manufacturing the first step is to twist the strand in order to obtain the yarn. This process aids the handling of the yarn in weaving the fabric. Hundreds of yarns may feed the loom in order to manufacture different fabrics, each characterised by different fibre angles, fabric weights and weaving tension parameters. In the case of NF fabrics lubricants are not applied because in comparison with synthetic fibres the wear resistance is elevated so the fibres will not be damaged. Figure 3.4 illustrates a flax fabric production method.

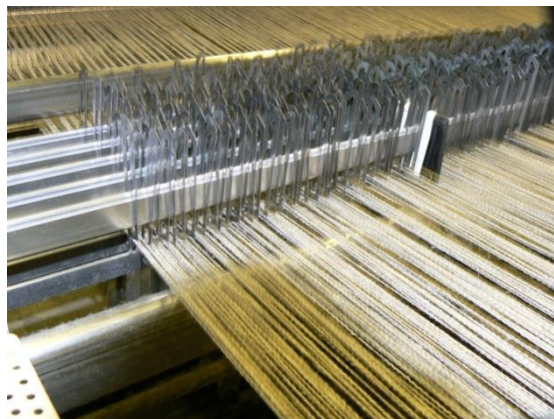


Figure 3.4: Stitched flax fabric production process (Courtesy of Composite Evolution)

Sizing has to be applied at a certain point along the manufacturing process and the various systems employed as surface treatments. Chapter 4 will discuss the different techniques for the NF fibres surface treatments used in order to improve the adhesion between fibre and matrix in the composite production.

In fabric production, the fibres are usually arranged either uni-directionally, randomly, cross-plyed, woven (plain, twill or satin weave), knitted or stitched-interlock. Figure 3.5 illustrates two different woven fabric types in schematic arrangements.

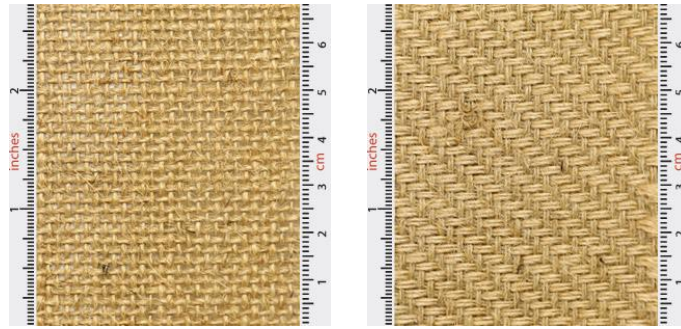


Figure 3.5: Jute woven fabrics (plain left and twill right) (Courtesy of Easy Composites)

One of the greatest advantages of NF reinforcements is their low price in relation to their reinforcing capability. This advantage is most obvious in the case of short fibres, slivers or mats, however when the fibres are transformed into fabrics production costs and embodied energy are proportionally increased to reach levels similar to GF. This phenomenon has been studied by Dissanayake (Dissanayake, 2011) using flax fibre LCA. GF has a stronger reinforcing capability than any other NF although it may lack specific rigidity. As a result, when the economic issue is a fact, NF renewable source, wear and impact properties are a positive point. Basically, this would be the only option for competing with the GF advantages.

### 3.8. NATURAL FIBRE REINFORCED POLYMERS (NFRP)

NF composites might be produced using either TP or TS matrix systems (Summerscales & Grove, 2014). The mechanical properties of NFRP systems are illustrated in Tables 3.6-3.7. Normally NF and TP or TS matrices are modified in order to improve the adhesion between fibre and matrix and will be discussed in detail in Chapter 4.

Table 3.6 captions the mechanical properties of different NF/TS composite systems. The first system is a GF/UP that may be applied as a reference and has significant comparative value. Table 3.7 captions the mechanical properties of different NF/TP composite systems

Table 3.6: Shows the NF/TS composites examples (Pickering, 2008)

Fibre/resin	Volume fraction $V_f$ (%)	Tensile strength (MPa)	Young's modulus (GPa)	Charpy impact strength (kJ/m <sup>2</sup> )	Interlaminar shear strength ILSS (MPa)
GF Chopped strand mat/polyester	30	95	8	40	25
Jute/polyester	45	60	7	29	10
Hemp/low-OH polyurethane	21	23	2	19	3
Hemp/high-OH polyurethane	19	27	3	7	3
Alkalisised Hemp/high-OH polyurethane	20	35	3	9	5

Table 3.7: Shows the NF/TP composite examples (Pickering, 2008)

Fibre/resin	Volume fraction $V_f$ (%)	Tensile strength (MPa)	Young's modulus (GPa)
GF Chopped strand mat/polyester	30	95	8
Kenaf/PLA	60	50	5
Flax/PLA	20	66	5.7
Bamboo/PP	20	16	2.5
Sugar cane/PP	20	16	6
Sisal/LDPE	20	16.5	93
Wood/PP	30	38	-
Oil palm fibre/HDPE	45	8	0.5
Hemp/starch	50	153	-

### 3.9. BIO-POLYMER DESCRIPTION

Bio-polymers can be bio-based and/or bio-degradable; the bio-based (bio-sourced) bio-polymer is derived from natural sources; bio-degradable bio-polymers can be returned to their natural origin (Reddy, Vivekanandhan, Misra, Bhatia & Mohanty, 2013). Bio-based and bio-degradable concepts are sometimes indifferently used, however this is not correct; Bio-based polymers can be totally or partially produced from renewable sources and may not be biodegradable; in contrast fossil-based polymers can be bio-degradable and may decompose and revert to nature.

Reddy has proposed grouping bio-polymers into three categories according to their production methods (Reddy, Misra & Mohanty, 2012), as illustrated in Table 3.8. They are discussed as follows -

1. **Renewable resource based biopolymers:** these products are entirely synthesised from renewable or waste resources, either from animal (e.g. chitin and chitosan, etc.) or from plant sources (e.g. starch, cellulose, lignin, etc.). The most commonly synthesised are poly(lactic acid) (PLA) and polyhydroxybutyrates (PHB) bio-plastics, although recent research has produced commodity plastics such as polyethylene (PE), polypropylene (PP) or nylon from biological sources.
2. **Petroleum-based bio-polymers:** are products synthesized from petroleum and are biodegradable with the capacity to decompose back to nature. Polycaprolactone (PCL) and poly(butylene adipate-co-terephthalate) (PBAT) are two example of these products.

3. **Bio-polymers from mixed resources:** are formed from bio-based and petroleum source monomers in combination. Bio-thermoset resins or bio-based thermoplastic blends are possible options that have been investigated in the present PhD research project.

Table 3.8: Bio-polymers classification and examples (Reddy et al., 2012)

Bio-polymer source	Type	Example
Renewable based	Poly (lactic acid) (PLA)	PDLA, PDLLA
	Polyhydroxyalkanoates (PHAs)	PHB, PHBV
	Starch plastics	Wheat, potato, corn based
	Cellulosics	Cellulose esters
	Protein-based plastics	Plant and animal proteins based
Petroleum based biodegradable	Aliphatic polyesters	PCL, PBS
	Aliphatic-Aromatic polyesters	PBT
	Poly (vinyl alcohol) (PVOH)	PVOH
Mixed resources	Polyesters	PTT
	Thermosets	Bio-based epoxy and polyurethane

The world is turning from petrochemical based products to “green chemistry” based polymers with emphasis on “end of oil” alternatives to the conventional matrix options. Dwindling fossil resources, surging energy demand and global warming are factors stimulating the growing demand for renewable polymer products with a low carbon footprint. Natural polymers, the products of biomass conversion in bio-refineries and chemical carbon dioxide fixation open new fields of research. Mülhaupt has discussed the dreams and reality of producing “green polymers” regarding their potential application (Mülhaupt, 2013), cost-effectiveness and sustainable development. This chapter refers to the current market situation concerning the application of bio-matrix materials.

When a bio-composite is produced it is normal to reinforce the matrix using NF. In this context both the matrix and the fibre are obtained from renewable sources resulting in a high bio-content product as exemplified in a starch based biodegradable bio-polymer reinforced with coconut fibre (Lomelí-Ramírez et al., 2014).

### 3.10. THERMOSET RESINS

Today many resin companies are attempting to develop bio-based TS formulations containing different “bio” constituents. The most challenging question is to maintain a petrochemical resin

performance in such bio-based formulations. As such these have been as investigated by Raquez (Raquez, Deléglise, Lacrampe & Krawczak, 2010).

In the composite industries the most widely used formulations are epoxy and UP resins. In petrochemical-based matrices the mechanical performance is very high and the interaction with the reinforcement is also excellent, resulting in a high standard composite (Oral, Guzel & Ahmetli, 2013; Yi, Um, Byun, Lee & Lee, 2013). In contrast, generally the bio-resins are not searching the required mechanical neither adjusting to a commercially competitive price. However, there are a number of products being developed to meet market requirements, and there are some resin systems that are highly competitive both for mechanical and commercial reasons.

### **3.10.1. Bio-epoxy resins**

In the Aouf study, SuperSap (PhD selected) commercial bio-epoxy system is used and other alternatives evaluated (Aouf et al., 2013). Examples of natural feedstock are itaconic acid, the cardanol (Cashew Nut Shell Liquid), seeds oil, or rosin diacid, soybean oil among other options (Ma et al., 2013; Rao & Palanisamy, 2013; Das & Karak, 2010; Huang, Zhang, Li, Xia & Zhou, 2013; Lu, Khot & Wool, 2005).

Epoxy resins are usually formed by reaction of Bisphenol A (BPA) and epichlorohydrin to formulate the prepolymer. Once the prepolymer has been formed, it is usually catalysed by an amine or anhydride. It has been proven that contact with the BPA monomer provokes an adverse human health problem and new epoxy resin formulations are being formulated from the options noted above to overcome the problem.

The isosorbide molecule is a bicyclic ring structure with chiral diols. This particular structure provides the isosorbide molecule with a monomer characteristic which is a good candidate base for epoxy, polyester or polyurethane resin formulations. This molecule can be obtained from the enzymatic hydrolysis of starch or the catalytic dehydration of sorbitol, a glucose derived material. This material



utilisation allows for a 50% bio-content resin formulation. The epichlorohydrin remains as a petrochemical based material.

Another option is epoxidised oil-based bio-epoxy resins. Triglyceride oils have been used as a base material for polymers production. In the bio-epoxy resins formulated by Entropy, triglyceride oils are extracted from pine trees (La Rosa et al., 2014). In this case the active epoxy groups are located in the middle of the aliphatic chain, impeding the correct cross-linking to form three dimensional networks. This results from steric hindrance and the autocatalysis of some of the polymer chains. The mechanical properties of bio-epoxy resins do not reach petrochemical epoxy values since the reticulation density is lower than expected.

Some epoxy systems use an amide catalyst instead of amine (Kocaman & Ahmetli, 2016). This molecule has lower reactivity than the amine to provide a lower cross-link density polymer. However, although the mechanical properties are reduced amides can be obtained from renewable resources, as from castor oil for example (Van der Steen, Bretz, Kabasci & Stevens, 2013). Unlike the aromatic amines which are toxic, the castor oils do not contain an aromatic ring thus forming a non-pollutant catalytic system. The introduction of these renewable components decreases the strength properties of the resin without significantly reducing the elastic modulus.

Some manufacturers have up-scaled their laboratory investigations into industrial production as detailed in Table 3.9 (Marrot, Bourmaud, Bono & Baley, 2014). The Sicomin (France) commercial product called Greenpoxy 55 has a bio-content determined under ASTM D6866 at 55% in weight. The epichlorohydrin is substituted by a bio component. Similarly Entropy (USA) developed the SuperSap resin system with a 51% input from renewable resources (average value dependent on the final formulation and solid content), the BPA substitution obtained from pine oil molecules and amide catalytic system bio-source. The bio-epoxy resin produced by Sandtech (France) has a bio-content grading from 55% to 85%. Part of the bio-source is again created by the substitution of the BPA molecules.

Table 3.9: Commercial bio-epoxy resins bio-content (Marrot et al., 2014)

<b>Commercial name</b>	<b>Manufacturer</b>	<b>Bio-content (%)</b>
Greenpoxy 55	Sicommin	55
Supersap	Entropy	51
L' Epoxy lin	Sandtech	55-85

### 3.10.2. Bio-polyester resins

References to sustainable UP are numerous in the research literature (Cousinet et al., 2015; Dai et al., 2015; Sadler et al., 2014; Costa et al., 2016; Gobin, Loulergue, Audic & Lemiègre, 2015). The polyester prepolymer is dissolved in styrene, a dangerous solvent to human health, and a potent environmental pollutant because of its Volatile Organic Compound (VOC) content. Research to formulate resins with a lower solvent content are ongoing and there are some formulations that are solvent free.

An alternative method to increase the UP bio-content and avoid the use of the styrene solvent would be to utilise triglyceride oil that would transform into a fatty acid monomer and form a covalent bridge in the curing process.

There is the further option of formulating UP by using the isosorbide molecule which forms the polyester prepolymer when reacting with the ethylene glycol molecule. The isosorbide is a 100% bio source material that is obtained from glucose or starch.

The laboratory conducted approaches have to be up-scaled for commercial production as shown in Table 3.10.

Table 3.10: Commercial bio-polyester resins bio-content (Marrot et al., 2014)

<b>Commercial name</b>	<b>Manufacturer</b>	<b>Bio-content (%)</b>
Enviroguard 93250	Cray Valley	53
Norsodyne G703	CCP composites	23
Eco-series products	Interplastic	5-20

### **3.10.3. Other bio-resins**

Apart from epoxy or polyester based thermoset resins, approaches have been made to utilise a range of different materials. Thermosetting resins have been produced based on cashew nut shell liquid (CNSL) used as a curing agent, or furan resins based on furfuryl alcohol (from sugar cane bagasse), or on soy oil derived polyurethanes (Kasemsiri, Neramittagapong & Chindaprasirt, 2015; Rivero, Fasce, Ceré & Manfredi, 2014; Arnold, Weager, Hoydonckx & Madsen, 2009; Luo, Mohanty & Misra, 2013). For example Transfurans is a commercialised furan based resin, and Santech is an elevated bio-content polyurethane product.

### **3.11. SUMMARY**

Chapter 3 describes natural fibres characteristics and bio-polymers available in the market; focusing on the flax fibre and bio-epoxy resin. This is in this PhD.

As mentioned in the first part of the document, flax fibre was selected as the most appropriate reinforcing NF for the PhD bio-composite production. The main reason was that the flax fabrics are commercially available in high quality product, getting as a result high standard bio-composite, consequently reducing experimental campaign variability. Both Composite Evolution and Lineo offer different types of fabrics, for example UD NCF or woven multi-axials fabrics, for easier utilisation of such components in a potential commercial product.

Similarly Entropy's SuperSap bio-epoxy resin was selected. The main reasons for its selection were the commercial availability, price, 51% bio-content and different formulations availability. For example, Entropy offers a wide range of commercial formulated resins for the infusion process, RTM or hand-lamination.

The utilisation of these two components together can result in the easy manufacture of a high quality bio-composite; both at lab-scale and scaled-up for the manufacturing of surfboards and RTM fins.

# 4. The interface in natural fibre composites

## 4.1. INTRODUCTION

The interface is the distinct boundary between the reinforcement and the matrix (Hayes, Lane & Jones, 2001; Lane, Hayes & Jones, 2001; Pukánszky, 2005). The question is that for NFRP the fibre and matrix adhesion is usually very weak, for that reason the current PhD investigation tried to solve in different ways this question. In order to select the best approximation, an extensive literature review was performed, what it is reflected in Chapter 4.

The research study is primarily involved with the analysis of the NF composites interface enhancement. The anticipated contribution to knowledge is to produce a sustainable and economical interfacial property improvement method for a particular flax fibre/bio-epoxy system. The realisation of the full mechanical performance of the reinforcement is critically dependent on the effective load transfer by shear over the "half critical length" at each fibre end, which in turn is a function of the chemical and physical bonds between the fibre and the matrix.

Instead of a distinct interface, there may be an interphase, normally considered to be a transition volume adjacent to the reinforcement component (fibres or particles) with functionally-graded properties, see Figure 4.1. The interphase may involve preferential orientation of polymer molecules, or in CMC (Ceramic Matrix Composites) and MMC (Metal Matrix Composites) may result from inter-diffusion of atoms between the two phases (Naslain, 1998; Karger-Kocsis, Mahmood & Pegoretti, 2015).

In a good (first class) interface there is strong adhesion between the fibre and the matrix, obtaining (creating) a proper load/strain/stress transfer inside the composite structure, as it might be observed in the micrograph (Figure 4.2) showing a transverse section of a

homogeneous UD composite; best practice when the system is observed with SEM. In contrast, when the interface is weak, the external load causes debonding of the reinforcement from the matrix, with no corresponding transfer of the load. When the load is correctly transferred a fibre fracture limit may be achieved with the fibres broken into segments of a critical length and developing no interface fractures.

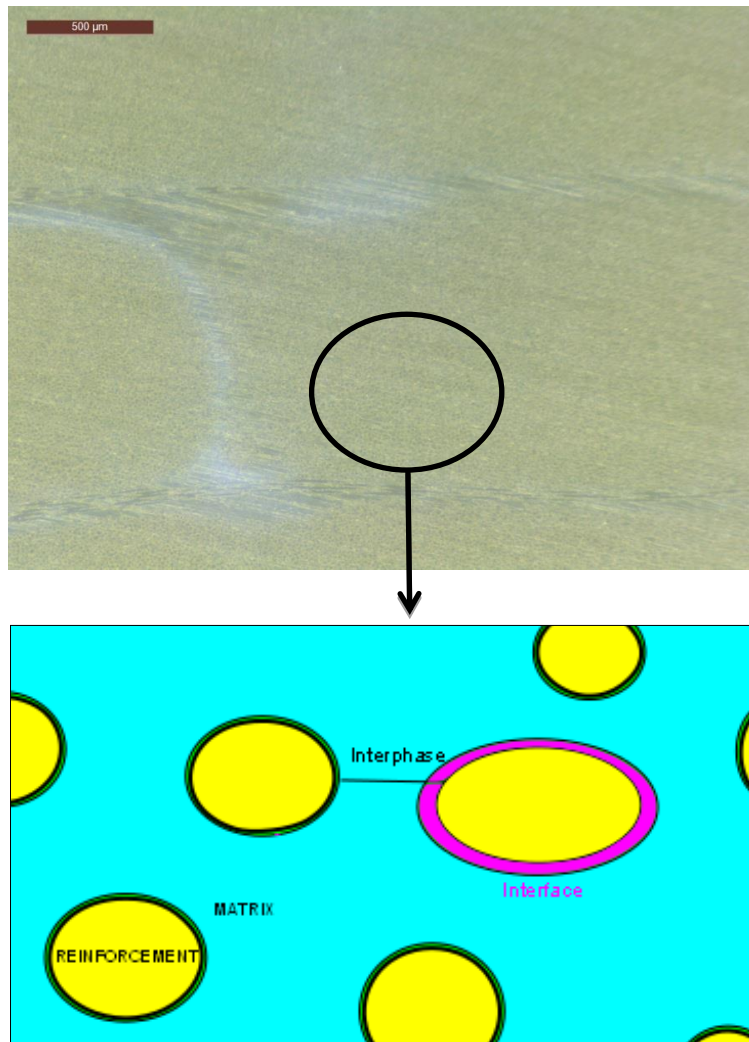


Figure 4.1: Composite interface and interphase explicative scheme (Acciona Blades courtesy)

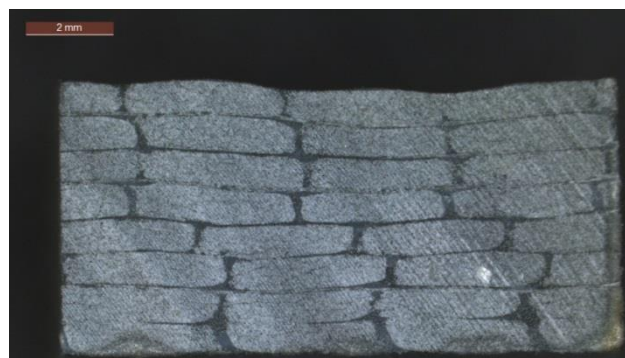


Figure 4.2: Transverse section of a UD NCF fibre reinforced composite (Courtesy of Acciona Blades)

A satisfactory interface can be achieved either by mechanical keying or by applying an appropriate chemical system, or by combining both options. The bast fibres are composed primarily of cellulose (an anhydroglucose polysaccharide) and are thus hydrophilic. The flax fibre used in this investigation is classified as bast fibre. The matrix system may be hydrophilic (e.g. polyamide or phenolic), which would increase the degree of hydrogen bonding, or it may be hydrophobic (e.g. polypropylene, unsaturated polyester or epoxy), and hence would have low compatibility and would require some treatment to achieve a good interface. The hydrophilic nature of the system makes the composite vulnerable to moist environments leading to plasticisation and possibly fungal deterioration. Decreasing the polarity of the fibre by chemical reaction could produce a more hydrophobic nature in the fibre. Bast fibre composites are targeted at low-value applications (not aerospace/defence) so it would be inappropriate to use a high cost approach to interface optimisation.

In order to maximise the interfacial properties in reinforced materials there are several possible approaches:

- Addition of compatibilisers in the matrix
- Physical modification of the fibre surface
- Chemical modification (including grafting) of the fibre surface
- Coating the fibre surface with a coupling agent

In this chapter, these four compatibility development methods are reviewed generally for NFRP. The four methods are not mutually exclusive. Specific emphasis is placed on mercerisation or silanisation as NF chemical treatment techniques, and in addition of compatibilisers (silane) to the matrix. In addition to composite mechanical characterisation tests, specific compatibility tests, as well as newly developed tests, have been studied.

#### **4.2. INTERFACE/INTERPHASE**

Fibre dominated properties, such as longitudinal tensile, compressive and flexural moduli/strength, show moderate sensitivity to interfacial properties variation, whilst off-axis properties, such as transverse tensile and flexural strength, in-plane and interlaminar shear

strength, are highly sensitive to interfacial properties variation. Using the InterFacial Shear Strength (IFSS) values, Dai, et al. demonstrated that CF treatments directly affect the IFSS properties (Dai, Shi, Zhang, Li & Zhang, 2011).

The two key factors in the mechanical properties of the fibre-matrix have been identified in the literature as the fibre-matrix adhesion level and the interphase morphology. An optimum level of fibre-matrix adhesion has been identified for each particular composite system. The best adhesion may not always result from the most adequate system. For example, when interfacial adhesion is increased normally the stiffness of the resultant composite rises considerably, producing a rigid final product (Cañigüeral, 2009). The fibre-matrix adhesion enhancement will also result in achieving higher fatigue properties (Harper & Hallett, 2010; Afaghi-Khatibi, Ye & Mai, 2001).

Many models, based on interfacial properties, have been developed in order to predict the final mechanical properties of the composite. However, these models are not accurate and have resulted in limited success. For example, Shia and Hui presented a simple interface model for the prediction of the Young's modulus of a silicate-elastomer nanocomposite system (Shia, Hui, Burnside & Giannelis, 1998). A discrepancy arose between the theoretical prediction and the experimental Young's modulus values because of the imperfect bonding between the fibre and the matrix. Kerans et al. presented a paper where the CF surface was oxidised in order to obtain the desired interface, increasing the fibre-matrix adhesion to produce composite tailored properties (Kerans, Hay, Parthasarathy & Cinibulk, 2002).

The correlation between the interfacial models and the experimental data is far from ideal, even when synthetic fibres are used. The inclusion of NF complicates the issue even further. Fotouh et al. presented a study where the TP/short NF composite system static and fatigue performance were predicted using different theoretical models (Fotouh, Wolodko & Lipsett, 2015). A number of models were presented in order to obtain the best performance prediction (micromechanical, energy method, rheology etc.), but it was concluded that models based on

empirical statistically treated values were best suited to obtain the mechanical performance prediction.

Some models are totally based on theoretical knowledge (phenomenological) whilst others are partially based on laboratory data (semi-empirical) obtained by direct methods. The lack of success of these models has resulted in a need to develop specific methods to predict multidirectional mechanical properties based on lamina methods in composites.

One of the main failings in the theoretical models is the underlying assumption that the prediction of composite mechanical and interfacial properties failure arises because the inter-relationship between fibre interface and matrix have not been considered in the models. This may mean that a wider zone than the interface is necessary for the correct understanding of the composite behaviour, and for this reason interphase understanding was added to the experimental data when the model development was being considered. The interphase was defined as the 3D space between bulk fibre and bulk matrix. This complex region is schematically explained in Figure 4.3 (Drzal, Herrera-Franco & Ho, 2000).

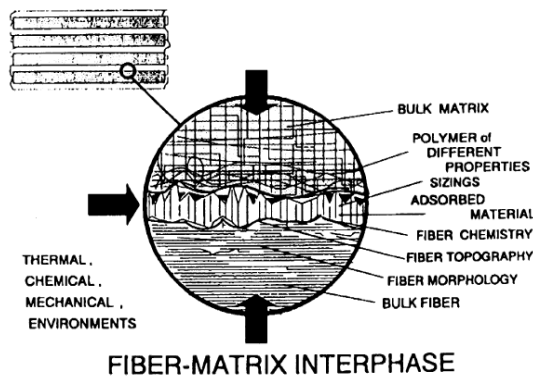


Figure 4.3: Schematic representation of the Interphase region (Drzal et al., 2000)

Interphase properties are dependent on the following factors - fibre and matrix surface energy; the mechanical bonding between fibre and matrix; the interfacial material properties in charge of giving a proper stress transfer; the resin chemical and thermal shrinkage during the curing and cooling processes. These factors are important because the residual stresses developed in the interphase region affect the final mechanical properties of the composite.



All the parameters considered above could be applied to the study of the interface/interphase in NF composites. Le Duigou, et al. studied the actual fibre surface involved in the practical adhesion of a flax/epoxy composite (Le Duigou, Kervoelen, Le Grand, Nardin & Baley, 2014). Two different flax fibre types were tested. The results showed:

- the surface chemistry studied with X-ray spectroscopy (XPS) did not affect interfacial adhesion;
- roughness observed with SEM lead to source defects which reduced composite adhesion;
- the biochemical composition of each fibre was directly related to the resin penetration, concluding that when the fibre wetting is higher the adhesion would be improved.

It is already clear that the interface/interphase concept is of vital importance in understanding the composite system. In the case of NFRP it has even greater importance to understand because:- a) reinforcing with a lignocellulosic material is very difficult in producing inhomogeneity related to the crop (Lefevre, Bourmaud, Lebrun, Morvan & Baley, 2013); b) inhomogeneity is difficult because of the transformation process in drying (Baley, Le Duigou, Bourmaud & Davies, 2012); c) the water uptake may affect the properties in the interphase region (Zhang, Milanovic, Zhang, Su & Miao, 2014; Masseteau, Michaud, Irle, Roy & Alise, 2014). All these parameters might affect the interphase property and subsequently the final performance of the composite. In order to reach interphase region performance quality and increase fibre/matrix compatibility there are different techniques which will be described in the following sections.

#### **4.3. COMPATIBILISERS IN THE MATRIX**

In the literature there are multiple matrix chemical modifications that are available for enhancing quality compatibility with NF reinforcements. For TS polymers the addition of compatibilisers might increase the fibre/matrix adhesion enhancing directly the final properties

of the composite. The most commonly referred to epoxy and TS matrix modifications will be discussed in this section.

#### **4.3.1. Epoxy matrix modification**

Generally, the epoxy resin is formulated subject to the mechanical, thermal or curing properties required in the final matrix. The main modifications in the resin formulation process may, possibly, be caused by the number of components used in prepolymer production. The number would include bisphenol, epichlorohydrin or the two in a mixed ratio, the curing agents, the reactive diluents and modifiers, the hardener selection and the selected curing cycle. Such properties will be dependent on the selection of the different mechanical, thermal, ageing, and electrical components. In the next section, the epoxy resin composite interface properties will be studied, with added reference to the most commonly used resin formulation modification techniques. The information will be classified according to the reinforcement type.

Chen, et al. (Chen et al., 2007) evaluated the newly developed T800 CF sizing technique for evaluating interface increment. The resin was reformulated in order to increase resin toughness and wetting capability. These two factors directly increase the interface properties - a tougher matrix allows this property to be transferred to the interface; increased wetting properties creates improved mechanical anchoring of the resin to the rough CF surface. If fibre sizing and resin reformulation effects are added, then the interfacial shear values might even double interface/interphase bonding. The above performance was evaluated using the NOL (Naval Ordnance Laboratory) ring innovative test method.

Since correct wetting is such an important factor in achieving a good interface many studies have been instigated to evaluate wetting methods for CF fibre. Xu (Xu et al., 2008) concluded that the utilisation of acrylic acid in the formulation of the epoxy resin substantially increases the wettability of the fibre tows and directly improves their interface properties.

The aim of any epoxy resin reformulation is to achieve a decisive performance and to increase its adhesion with the matrix. As demonstrated by Xu, the formation of chemical bonds in the

interface definitely increases the performance of the composite. For this reason, siloxane, silanes or silsequioxanes have been introduced during the epoxy resin backbone synthesis (Wang, Jiang, Zhang & Cheng, 2012; Chruściel & Leśniak, 2015), to achieve covalent chemical bonds between the resin and the fibre. The current PhD study aims to introduce silanes into the epoxy matrix formulation, differing from previously mentioned studies where the silanes were introduced into the synthesis process. In this particular case the silane will be added to the bio-epoxy resin in order to increase the adhesion between the flax fibre and the bio-epoxy resin.

Matrix modifications tend to focus on improving the static properties, but interfacial development specifically affects long term properties such as the fatigue or aging of the matrix (Koimtzoglou, Kostopoulos & Galiotis, 2001; Zafar, Bertocco, Schjødt-Thomsen & Rauhe, 2012). Damage produced by either dynamic stress or aging agents directly affects the interface. As a result, a strong interface would impede the advance of a crack through the interface debonding but would allow brittle fracture of the fibre.

#### **4.4. PHYSICAL FIBRE SURFACE TREATMENTS**

The NF surface can be modified using a wide variety of physical treatments. In general, surface roughness and composition can be changed to obtain better interfacial adhesion with the matrix. George, et al. have critically reviewed the physical and chemical treatments that improve the fibre-matrix adhesion in NFRP, identifying fibrillation and electric discharge techniques as useful NF treatments. Physical treatments by electric discharge are commonly used techniques in modifying the natural fibre surface. They can be divided into low-frequency corona treatment or high-frequency (low temperature) cold plasma treatment. In both cases, the surface roughness of the NF is increased resulting in improved mechanical adhesion in the composite. In Zheng, a tensile and impact strength increment was also applied after the electric treatment.

In both TP and TS matrices this modification is a totally physical phenomenon since the interaction forces are not dependent on the functional groups in the matrix. The interfacial shear strength values obtained are positive because of the mechanical anchoring; however, the

process is often very time consuming and cannot therefore be considered as commercially viable. For this reason, physical treatments were not undertaken in this research project.

#### 4.5. CHEMICAL FIBRE SURFACE TREATMENTS

Cellulose is a hydrophilic polar molecule while many matrix materials are hydrophobic non-polar molecules. To optimise the interface the chemical nature of one of the respective surfaces can be modified. The study of fibre treatment is basically concerned with the issue of hydrophilic/polar vs. hydrophobic/non-polar bodies. It is noted that for TP matrix composites it is unlikely that there will be a chemical reaction between the polymer and the fibre while for TS matrix composites such a reaction may occur.

The NF treatments that can be applied to secure the best NFRP interfacial properties have been compared and the following section evaluates those that have most relevance to the present research project.

The review paper by Gurunathan, et al. (Gurunathan, Mohanty & Nayak, 2015) provides a clear scheme offering different options, as shown in Figure 4.4.

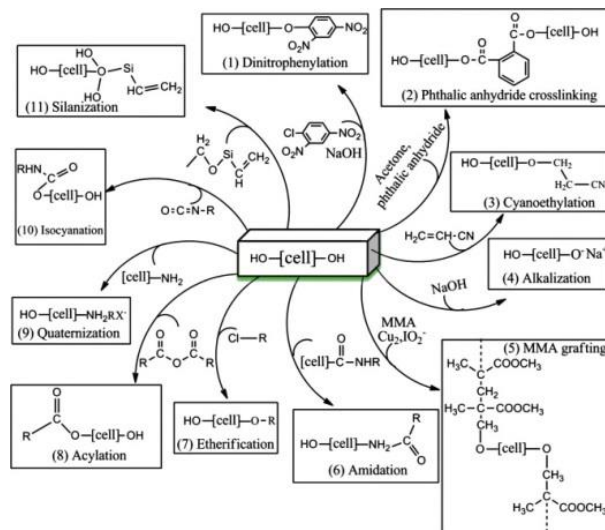


Figure 4.4: NF chemical treatment option scheme (Gurunathan et al., 2015)

#### 4.5.1. Mercerisation (NaOH) and NaCl

Chemical treatment by Mercerisation has been widely applied for the elimination of undesired substances, most especially lignin, and for subsequent NF surface activation with the polymer matrix. The Mercerisation reaction path is shown in Figure 4.5 and Table 4.2 lists the most important literature references.

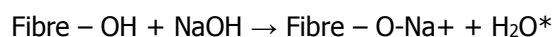


Figure 4.5: The reaction shows the surface activation by alkali treatment

Mercerisation is defined as the "treatment of cellulosic textiles in yarn or fabric form with a concentrated solution of caustic alkali [soda], whereby the fibres are swollen, the strength and dye affinity of the materials are increased, and their handle is modified. The process takes its name from its discoverer, John Mercer (1844) (Mercer, 1850). The treatment removes practically all non-cellulose components except waxes and changes the crystal structure of the cellulose. Mercerisation results in "hydrated cellulose" which is chemically identical to the precursor material but has different physical properties (Rashaduzzaman, 2013). For rapeseed straw, Paukszta (Paukszta, 2013) applied solution concentrations in the range 12.5-20% for >5 minutes to obtain optimal conditions for the process. Mercerisation converts cellulose I to 50±15% cellulose II with a consequent expansion of the crystal lattice (Table 4.1) (Guthrie, 1974).

Table 4.1: Unit cell dimensions for cellulose crystals (Wada, Nishiyama, Chanzy, Forsyth & Langan, 2008)

Cellulose	Crystal unit cell	a (nm)	b (nm)	c (nm)	α (°)	β (°)	γ (°)
I <sub>α</sub>	one-chain triclinic P1	67.17	59.62	104.0	118.08	114.80	80.37
I <sub>β</sub>	two-chain monoclinic P2 <sub>1</sub>	77.84	82.01	103.8	90	90	96.5
II	monoclinic P2 <sub>1</sub>	81.0	90.3	103.1	90	90	117.10

Chattopadhyay (Chattopadhyay & Sarkar, 1945) reviewed different methods for the determination of NF cellulose quantity. NF has been bleached with sodium chlorite (NaClO<sub>2</sub>) for many years. Sodium chloride reacts in an acid environment to produce chlorine dioxide (ClO<sub>2</sub>) molecules, which in contact with the NF removes the lignin from the structure and reacts with

the hemicellulose OH groups. Both effects will reduce the hydrophilicity of the NF structure whilst increasing its elasticity, as indicated by Li, et al. (Li, Tabil, & Panigrahi, 2007).

References to the Mercerisation process can be divided in two main groups:

- a) NF Mercerisation in isolation, and
- b) NFRP composite properties after Mercerisation.

NF were divided according to the selected fibre type, with particular reference to jute. Roy, et al. proposed a mild alkali treatment of the jute fibre for upgrading its mechanical properties (Roy et al., 2012). Different combinations were tested and it was concluded that the most satisfactory results were obtained when jute was treated with a 0.5% NaOH solution for 24h, securing an improvement of 82% tensile strength and 45% elongation at break.

Gassan and Bledzki reported an approximate increase in yarn tensile strength and modulus of 120% and 150% in jute fibre after mercerisation treatment (Gassan & Bledzki, 1999). The jute fibre was treated with 20% NaOH solution for 20 min at RT. The effect of the NaOH treatment is great. There are other references in the literature that support similar mechanical properties increments, although such increments are not as high as the data reported by Gassan and Bledzki (Ray & Sarkar, 2001; Ray, Das & Mitra, 2012).

Saha, et al. reported the mercerisation process (0.5% NaOH for 30 min) is supported by an additional alkali-steam process (under pressure 30 min alkali treatment), which is claimed to be more efficient than the conventional immersion alkali treatment (Saha et al, 2010).

Table 4.2: Mercerisation and NaCl treatments references

Fibre	Reinforcement format	Treatment	Matrix	Gain in modulus (%)	Gain in strength (%)	Other effects	Reference
Cotton and flax	Cloth	NaOH 3.25M at 15°C +neutralised with H <sub>2</sub> SO <sub>4</sub> +Wash with water	-	-	-	Improve colours in printing and dyeing	Mercer 1850
Jute	Straw	NaOH 0.25%,0.5%,1% for 0.5,1,2,4,8,16,24,36 and 48 hours +wash with distilled water	-	-	82	Reduce Hydrophilicity 50.5%, increase $\epsilon_r$ 45% and increase diameter 37%	Roy 2012
Jute	Yarn	20 min at 20°C in 25% NaOH	-	150	120	-	Gassan 1999
Jute	Straw	0.5% NaOH for 30 min + alkali-steam treatment 30 min	-	-	65	-	Saha 2010
Ramie Flax Cotton	Yarn	Pretreat 0.05% Triton QS-44 + NaOH 20% 5min+ neutralise 2%Ac-COOH	-	-	In tension Ramie 6 Flax 18 Cotton 27	$\epsilon_r$ in tension Ramie 7 Flax 20 Cotton 44	Cheek 1989a and 1989b
Ramie Flax Cotton	Yarn	Dyeing	-	-	-	Mercerisation affects the dyeing process	Cheek 1989b
Ramie	Straw	15% NaOH with applied loads of 0.049 and 0.098 N	-	decrease	4-18	Increase $\epsilon_r$ 37.5%,	Goda 2006
Flax	Pulp	Cook with sosa anthraquinone + freeze + Wash H <sub>2</sub> SO <sub>4</sub> 30 min until pH = 4	-	-	-	Increase the ISO brightness	Fillat 2010
Flax	Straw	Wash with water + dry 3h at 80°C + NaOH 5% at 55°C for 10 min + dry 7 days at 20°C + oven dry 3h at 70°C	-	-	-	Determination of the ideal mercerisation conditions = NaOH 5% at 55°C for 10 min	Aly 2012
Kenaf	Hand-made UD fabric from straw	NaOH 5% for 24h at RT + wash with water + immerse in distilled water for 24h and dry in the oven for 24h	Epoxy	-	-	Confirm the enhanced ROM	Mahjoub 2014
Kenaf	Mat and UD	NaOH 6% at RT for 48h/144h+wash with distilled water + dry RT 48h + dry in over for 6h at 100°	Epoxy	Mat 10 UD 3	Mat 26 UD 10	48h treatment improves mechanical properties while 144h damages the fibres	Fiore 2015
Kenaf	UD fabric	6% NaOH 24h + water wash + over dry at 40°C for 24 h	Epoxy	-	-	Increase flexural strength in 16%	Yousif 2012
Flax	Hand-made UD fabric from yarn	NaOH 2 min 13%	Epoxy	0.7	11	-	Van de Weyenberg 2006
Jute	Yarn	NaOH 25% for 20min at 20°C	Epoxy	150	120	-	Gassan 1999
Cotton cellulose	Yarn	NaOH 13.5% for different times at 25°,50°C and 65°C	Epoxy	-	50-70 loss	-	McKelvey 1959
Abaca	Straw	5, 10 or 15 wt.% NaOH for 2 h	Epoxy	-	-	-	Cai 2016
Flax	Yarn and biaxial weft-knitted	NaOH of 8 wt.% at 25 °C for 2 h + wash with water + neutralise with 5 wt.% Ac acid for 30 min + wash with boiled water for 30 min + wash with tap water + air dry +oven at 105 °C for 6 h	UP	5	19.8	Increase $\epsilon_r$ 29.5%	Xue 2013
Alfa fibre	Nonwoven sheet (Alfa fibre +wool +PET/PE)	NaOH+NaClO	UP	5.2	5.2	Increase the thermal properties	Triki 2013
Kenaf	Straw	NaOH 6% for 48h at 19°C + dry 5 h at 110°C	UP	-	-	Increase the flexural modulus 63%	Aziz 2005
Palmyra	Mat	NaOH 5% for 30min + neutralise HCl + dry 70°C	UP	60	37	Impact strength increment	Thiruchitrabalam

palm and jute						55%	2012
Sisal	Aligned nonwoven mats	5% NaOH for 1 h at 30°C + wash distilled water + vacuum dry	UP	-	22	43% Flexural strength and 21% impact strength	Misra 2002
Hemp	Mat	5% NaOH for 1h at RT + wash with water + neutralize with 2% ac acid to pH 6 + dry 24 at RT + vacuum dry	UP	-	34	-	Mehta 2006
Sisal	Straw	NaOH 2M at RT for 2h + washed with water + neutralised with Ac acid + dry at RT	Soy-resin	110.7	34.5	-	Kim 2010
Sisal	Straw	5% and 10% NaOH + bleached with NaClO/H <sub>2</sub> O (1:1) at 60–75 °C	Cardanol based resin	-	-	Improve the weight loss and thermal stability	Barreto 2011



Other (bast) fibres, such as ramie, may also be mercerised to modify their chemical and morphological properties. Cheek and Roussel have reported on two different mercerisation methods, namely slack and tension mercerisation (Cheek & Roussel, 1989a and 1989b). In both cases, the NF was pre-treated with 0.05% Triton QS-44 (a surfactant), followed by immersion in NaOH 20% for 5min, and finally neutralised with 2% acetic acid solution. The two treatments differ in that the slack fibres are treated directly over the fibre while tension fibres are wrapped over a steel frame in order to keep fibres equidistant. Following slack treatment, the ramie yarn strength was reduced by 45%, and for flax by 49%, while in cotton the value was increased by 26%. In contrast, using the tension method the increment for ramie was 7%, for flax 22% and for cotton 38%. The clear conclusion is that when the fibre is kept under tension the desired strength increment is achieved; in contrast when the fibres are loose the mercerisation effect may be negative. In all of the above cases, the elongation of the break property is improved. Cheek (Cheek & Roussel, 1989b) performed the NF NaOH treatment to improve the dyeing process.

Goda (Goda, Sreekala, Gomes, Kaji & Ohgi, 2006) mercerised ramie fibre under a certain tension value, obtaining an increase of up to 18% in tensile strength and 37.5% for the strain at break values.

Another option for the chemical modification treatment of the natural fibre would use *sosa*/anthraquinone in combination. This technique has been used for many years in the flax industry, particularly to bleach the flax fibres (Fillat, Pepió, Vidal & Roncero, 2010). The elimination of the lignin fraction achieves the desired aesthetic appearance of the product but contributes little to its mechanical properties since it does not directly increase the modulus and tensile strength. On the other hand, other properties are improved such as the flexural behaviour of the composite.

Aly et al. presented a study using Box–Behnken Method (Software) for the determination of the optimal mercerisation condition of flax fibre (Aly et al., 2012). The fibres were treated with a solution of NaOH 5% at 55 °C for 10 min.

NFRP references were classified according to TS matrix or TP matrix in order to facilitate comparative issues.

Mahjoub et al. have reported on a kenaf fibre/epoxy resin system using mercerisation to enhance mechanical properties (Mahjoub, Yatim, Sam & Raftari, 2014). The composite strain properties were generally increased when the kenaf fibre was treated with 5% NaOH solution for 3h, washed with water, kept in distilled water for 24h and finally dried in the oven for another 24h. Fiore et al. immersed kenaf fibres in NaOH 6% solution at RT for 48h/144h, thoroughly washed them with distilled water, dried at RT for 48h and finally dried in the oven for 6h at 100°C (Fiore, Di Bella & Valenza, 2015). For the epoxy composite three-point dynamic test, the 48h composites storage properties increased; however, in the case of 144h treatment the mechanical performance was substantially decreased because exposure to the excessive NaOH treatment caused fibre damage.

Yousif et al. presented a kenaf/epoxy system flexural properties study concluding that NaOH 6% treatment to the kenaf fibre gives 16% enhancement to the composite flexural strength (Yousif, Shalwan, Chin & Ming, 2012).

Van de Weyenberg et al. proposed a mercerisation treatment for flax fibre in which the mechanical properties were best improved when the flax fibre was immersed in a 4% NaOH solution for 45s in order to increase the flax/epoxy composite transverse strength by up to 30% (Van de Weyenberg, Truong, Vangrimde & Verpoest, 2006).

Gassan et al. proposed a similar method to improve the interfacial properties of a jute/epoxy system (Gassan & Bledzki, 1999). Resin shrinkage is a key factor in the mechanical properties

of the final composite. When jute fibre is treated with NaOH 25% solution for 20 min at 20°C the resulting mechanical properties of the composite rise considerably; the jute yarn tensile modulus and strength increase respectively by about 150% and 120%.

McKelvey et al. (McKelvey, Webre & Klein, 1959) added epoxy matrix to the cotton yarn to enhance the mechanical performance of the fibre with the fibre swelling when mercerised at different temperatures and timed immersion conditions. The conclusion was that the tensile strength of the composite was reduced by 50-70%.

Cai et al. studied the mercerisation effect in an abaca/epoxy composite system (Cai, Takagi, Nakagaito, Li & Waterhouse, 2016). The results showed that the mechanical properties developed in low concentrations at 5% to directly increase the composite performance. In contrast, higher concentrations damaged the fibre concluding, therefore, that mild mercerisation processes were more beneficial for this system.

Xue and Hu (Xue & Hu, 2013) reported mercerisation treatment in a biaxial weft-knitted flax fabric concluding that flax/UP composite tensile strength and strain at break numbers were substantially improved.

Triki et al. (Triki, Guicha, Ben Hassen & Arous, 2013) reported on improving the interfacial properties of an alfa fibre/UP composite system combining NaOH and NaClO treatments in order to improve the development of mechanical and thermal properties. Likewise, Aziz et al. (Aziz, Ansell, Clarke & Panteny, 2005) improved the interfacial properties of four different UP matrix composites that were reinforced with kenaf fibre. Each system performed differently, but in each one the mechanical and moisture resistance properties were improved following mechanical treatment of the fibre.

Shanmugam and Thiruchitrabalam (Thiruchitrabalam & Shanmugam, 2012) modified Palmyra palm leaf stalk with mercerisation using benzoylation and permanganate treatment,

which resulted in an increase in the tensile, impact and moisture absorption properties of the UP composite system.

Misra et al. (Misra, Misra, Tripathy, Nayak & Mohanty, 2002) dipped sisal fibres in a sodium chlorite solution with a liquor ratio of 25:1 at 75°C for 2h, washed with distilled water, neutralised with 2% solution of sodium sulphite ( $\text{Na}_2\text{SO}_3$ ) for 15 minutes at RT using a liquor ratio of 25:1, and finally washed and vacuum dried to obtain the bleached fibres. The impact and flexural properties of the sisal/polyester composite were raised after the bleaching process because of the elimination of the interfacial and lignin properties respectively.

Mehta (Mehta, Drzal, Mohanty & Misra, 2006), investigated the tensile strength of a hemp/UP composite system which showed an increase of 34% following alkali treatment of the hemp.

An alternative method was proposed by Kim and Netravali (Kim & Netravali, 2010) to enhance a sisal fibre/soy resin composite system. The sisal fibre was immersed in a NaOH 2M solution at RT for 2 hours, washed with water, neutralised with acetic acid and finally dried at RT. The treatment was undertaken to slack and tension fibres, the latter technique achieving better results. Compared with the reference control sample, the best results were achieved when the fibre tension was 50g/fibre, with 111% modulus and a strength increment of 34.5%.

In alternative bio-composite option sisal fibre was reinforced with a cardanol based resin (Barreto, Rosa, Fachine & Mazzetto, 2011). The alkali treatment improved the thermal and weight loss properties of the system.

In conclusion, it would appear that NFRP mechanical properties are improved in certain cases by using mild treatments whilst in other examples the treatment selected are more aggressive; also the mercerisation process is improved when the fibre has tension. For this reason, the current research project will investigate a wide range of mercerisation conditions in order to determine which may be best suited for producing a flax/bio-epoxy composite. The research

question is if the interfacial properties increment achieved by mercerisation has real impact in flax/bio-epoxy composite macro-mechanical properties; increasing macro-mechanical properties, such as transverse tensile strength.

#### 4.5.2. Silanisation

Silanisation is a chemical treatment that will increase the interfacial properties of NF composites based on obtaining covalent bonding over the NF surface (Figure 4.6). The concept is to secure a reaction between NF surface OH groups and silane OH groups. The reaction that occurs in the interface will improve the mechanical and aging properties of the NF composites.

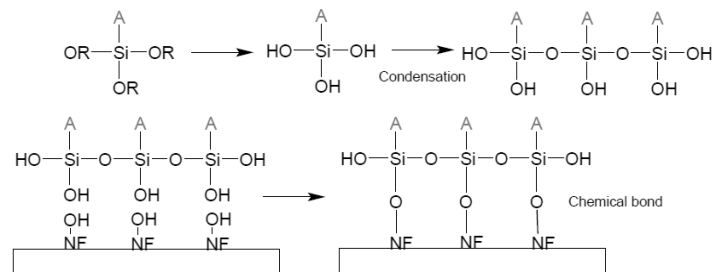


Figure 4.6: Si-O-Si bonding scheme

It is clearly understood that fibre coating and treatment are different concepts. The GF coating is normally obtained by applying a thin coating of sizing to cover the fibre surface. A similar process is followed for NF coating. In the fibre manufacturing process silane sizing is sprayed over the GF filament surface (Thomason & Adzima, 2001). The correct application of the coating and its composition will directly affect the interfacial adhesion of the composite, and consequently decide its final mechanical properties. Dey et al. (Dey, Deitzel, Gillespie & Schweiger, 2014) evaluated the performance of a GF/epoxy composite with silane sizing and clearly found that the azamide-based film former produced a 47% increase in interfacial shear strength over amino silane sizings with different film formers. The relative reactivity and wettability of the film former can enhance the chemical bond formation as well as the roughness of the fibre surface.

The most popular additive is silane. Onjun (Onjun & Pearson, 2010) reported on the importance of adding silane to the epoxy matrix into the interface area of the composite. The silane creates a bridge between the fibre and the matrix and hence enhances the long term mechanical performance of the composite. The silane increases the GF/epoxy hygrothermal resistance due to an increase in the subcritical debonding energy ( $G$ ) of the composite.

Table 4.3 compiles references to the most interesting NF silanisation literature. Many of the studies, however, involve arduous and expensive methods to reach attainment.

Table 4.3: Silanisation methods references

Fibre	Reinforcement format	Treatment	Silane	Matrix	Gain in modulus (%)	Gain in strength (%)	Other effects	Reference
Glass	-	Silane	3-aminopropyltriethoxysilane and glycidoxypropyltrimethoxysilane	Epoxy	-	-	Increase hygrothermal resistance + increase debonding energy	Onjun 2010
NF	-	Silane	General	TP/TS	-	-	Review of the literature	Xie 2010
Flax and Ramie	Straw	Silane	A-1100 and A-1120 silanes	-	-	-	Measure water contact angle	Gliesche 1995
Cellulose	Microcrystalline particles	5w/w% silane suspension in 80/20 v/v ethanol/water mixture 2 h + dry 2 days at RT + oven 2h at 120°C	$\gamma$ -Methacryloxypropyltrimethoxysilane (MPA) $\gamma$ -Aminopropyltriethoxysilane (APS) Hexadecyltrimethoxysilane (HDS) $\gamma$ -Mercaptopropyltrimethoxysilane (MRPS)	-	-	-	Silane cellulose adhesion + Enhance surface to polymer grafting	Abdelmouleh 2004
Jute	Yarn	NaOH 5% for 1.5h+washed water+UV radiation + Silane	3-(trimethoxysilyl)-propylmethacrylate	-	265	lesser water uptake and less weight loss	Increase $\epsilon_r$ 350%	Hassan 2003
Hemp	Straw	Silane 3% methyl alcohol water (60:40) + Wash in distilled water + dry at RT for 8 h + oven dry at 100°C 6h	Oligomeric siloxane	-	- 61	- 33	-	Kabir 2013
Sisal	Straw	0.2M silane 80/20 (v/v) ethanol/water mixture at RT for 72 h + wash with mix + dry RT	3-aminopropyltriethoxysilane (APS) and N-(2-aminoethyl)-3-aminopropyltrimethoxysilane (AAPTS)	-	-	-	Prove silane NF covalent bonds are formed	Zhou 2014
Flax	Straw	1-3% silane acetone and water 50/50 v/v for 2h + dry 8 h at 80 °C	3-aminopropyl trimethoxy silane	Epoxy	-	-	Flexural longitudinal modulus increased 46% and strength 4%	Van de Weyenberg 2003
Hildegardia	Fabric	NaOH + Silane (Silane/acetone sprayed over the fibre)	Silicon-based silane	Epoxy	-	-	Reduction of voids content + increase fibre-matrix bonding	Guduri 2007
Abaca	UD fabric	NaOH+ 1wt% Silane in 1:1 alcohol/water for 24 h and pH 5.3 + wash in water + oven dry for 2 h at 100°C	$\gamma$ -glycidoxypropyl-trimethoxy silane	Epoxy	-	80 transverse	-	Liu 2014
Sisal	UD fabric	NaOH + 2% silane in alcohol for 5 min at pH 5 + oven dry 2 h at 100°C	KH550 g-amine propyl triethoxysilane	Epoxy	- 1	- 16	Increase $\epsilon_r$ 47%	Rong 2001

Xie et al. (Xie, Hill, Xiao, Militz & Mai, 2010) reviewed the use of silane coupling agents in NF/polymer composites. In general, trialkoxysilanes have been selected to improve the interfacial properties of the NFRP. The silane coupling agents generic chemical structure is  $A_{(4-n)}\text{-Si}(\text{R}'\text{X})_n$  ( $n = 1,2$ ) where A is alkoxy, X represents an organofunctionality, and R' is an alkyl bridge. The alkoxy will react with the NF surface and the R' organofunctional group will react with the organic polymer matrix because of their similar polarities. Nonreactive alkyl groups in the silane increases compatibility with the matrix due to their similar polarities; however, the reactive organofunctionality may covalently bond with the polymer matrix. The organofunctional parts of the silane usually belong to amino, mercapto, glycidoxy, vinyl, or methacryloxy groups. Aminosilanes, especially  $\gamma$ -aminopropyltriethoxysilane (APS), are reported most extensively in the literature as coupling agents between natural fibres and thermoplastics or thermosets.

Gliesche and Mäder used silanes (A-1100, A-1120 from OSi-Specialties) as coupling agents in flax and ramie fibres (Gliesche & Mäder, 1995). Measurement of the contact angle of water using the capillary rise method showed no effects. Typical water contact angles for the untreated flax and ramie fibres were  $87^\circ$  and  $77^\circ$  respectively.

The silane treatment of the cellulose fibres enhances the fibre surface to produce polymer grafting and decrease its hydrophilicity (Abdelmouleh et al., 2004). The silane treatment resulted in O-Si-O and C-Si-C bridges being formed between the fibre surface and the silane groups. Fibres were treated with 5 w/o silane suspended in 80/20 v/v ethanol/water mixture stirring for two hours; the obtained fibres were dried for days at RT; and finally cured at  $120^\circ\text{C}$  for two hours in a nitrogen atmosphere.

Hassan et al. (Hassan, Islam, Shehrzade & Khan, 2003) reported improved tensile strength, elongation to break and durability in mercerised jute fibres which had been grafted with silanes and acrylamide under ultraviolet radiation. This conclusion predicts that polymer loading could be easily accepted in the future production of composites. The mercerisation might be applied to the NF under UV radiation in order to increase its effect.



Kabir et al. (Kabir, Wang, Lau & Cardona, 2013) presented a study where the hemp fibres were subjected to alkali, acetyl and silane treatments. When hemp fibre is directly treated with the silane, the mechanical properties are drastically reduced: 61% for tensile modulus and 33% for strength. In contrast, when silane is applied to a previously mercerised fibre the properties are enhanced. However, in both of these cases the mechanical properties would not reach untreated fibre composite mechanical properties.

Zhou et al. (Zhou, Cheng & Jiang, 2014) reported that when sisal fibres are treated with silane covalent bonds are formed. Van de Weyenberg (Van de Weyenberg et al., 2003) used different fibre treatments to increase the base properties of the flax fibre. Table 4.4.

Table 4.4: Flax fibre base tensile and flexural properties

	Tensile strength (MPa)	Flexural strength (MPa)	Tensile modulus (GPa)	Flexural modulus (GPa)
Longitudinal	133	218	28	17.7
Transverse	4.5	8	2.7	0.36

In all methods applying mercerisation, the first step requires the fibres to be dipped in a NaOH solution of different concentration (1, 2 or 3%) for 20 min at RT. After removal, the fibres are washed very thoroughly in cold water, then placed in acidified water (20 drops of HCl 0.1 M in 1 l of water) to remove excessive NaOH. The fibres are again rinsed in cold water and dried in an oven at 80 °C for eight hours. Silanisation is undertaken by soaking the fibres for two hours in a solution of equal volumes of acetone and water containing 3-aminopropyl trimethoxy silane with concentration of 1%. The fibres are then dried in an oven for 8 h at 80 °C. Significant improvement is achieved when the flax fibres are treated in a 1% NaOH solution and covered with 3% epoxy resin solution. Flexural longitudinal tensile modulus and strength are increased by approximately 58% and 38% respectively. Treatment by 1% silane leads to increments of 46% and 4% in longitudinal modulus and strength properties. Additionally, it is reported that with silane the transverse flexural modulus and strength properties are increased 400% and 110% respectively.

Van de Weyenberg's treatments were considered to be the most effective, the easiest to perform, are economically viable as well as being the greenest.

In certain studies, e.g. Guduri et al. (Guduri, Rajulu, & Luyt, 2007) the Hildegardia NF reinforced epoxy matrix is toughened with polycarbonate polymer. Additionally, the NF is treated in a NaOH solution for one hour and afterwards the surface is sprayed with a 1% silane coupling agent. These treatments elevate the adhesion between the fibre and the matrix but water resistance is decreased. This might be caused by the fibre surface being more polar resulting in an increase in its hydrophilicity.

Liu et al. (Liu, Zhang, Takagi, Yang & Wang, 2014) proposed a combined chemical treatment for improving the transverse mechanical properties of a unidirectional abaca fibre/epoxy system. Mercerisation formed the first step in the process by the mild immersing the fibre for five minutes in a solution of 1.0 w/o NaOH, and hard immersing the abaca for 30 minutes in a 5.0 w/o % NaOH solution. After the RT immersion both of the treated bundles were thoroughly washed with water and dried in the oven at 70°C. In the second step silane is applied to the mercerised abaca fibre. 1.0 w/o acetic acid, 1.0 w/o  $\gamma$ -glycidoxypropyl-trimethoxy silane, 49 w/o alcohol and 49 w/o water solution is prepared mixing all the components for 60 minutes in an opaque container. Next the fibre is immersed in the solution for 24h keeping the solution at 5.3 pH. The fibres are then washed with distilled water and kept at RT for 30 minutes. Finally, the abaca fibre is dried in the oven for 2h at 100°C in order to obtain covalent bonding between the fibres and the silanes. The authors concluded that thorough treatment of the fibres with silanes can increase the interfacial adhesion of the resulting composites and improve their mechanical and outdoor performance. For example, when the abaca fibre is mercerised with 5% NaOH for 30 min, followed with silane, the composite transverse tensile strength at  $V_f = 0.3$  is increased by 80%. However, the Si-O-C bonds in natural fibre composites are less stable under hydrolysis than the Si-O-Si bonds in glass fibre composites (Shokoohi, Arefazar & Khosrokhavar, 2008).

Rong et al. (Rong, Zhang, Liu, Yang & Zeng, 2001) showed that the silanisation process in a sisal/epoxy system did not produce the expected mechanical performance increment. There was, however, a 47% increment in the strain at break value, but the tensile modulus and strength values decreased.

The use of silanes will inevitably increase the proportion of silica in the ash if incineration is the chosen route for the disposal of a bast fibre composite. This ash, in the form of a respirable dust, may be a relatively harmless by-product (Normohammadi, Kakooei, Omid, Yari & Alimi, 2016).

In the above paragraph the main NF silanisation treatments were generally explained. The research question is if any of these treatments might be applied to the flax/bio-epoxy composite in order to increase their interfacial, macroscopic mechanical properties and moisture absorption properties. The silanisation is made to the untreated and mercerised flax fibre and compare their performance.

#### **4.5.3. Other treatments**

Acetylation is the process of introducing an acetyl radical into an organic molecule, and in the process the hydroxyl groups in the cellulose molecule react with the acetic acid (or anhydride) to produce cellulose acetate. The replacement of the polar hydroxyl group with the nonpolar acetyl group increases the hydrophobicity of the cellulose making it more compatible with nonpolar matrix polymers, i.e. the fibre adhesion to the non-polar polymer matrix would be raised.

Another option would be the acrylation. In the literature, references to NF treatments with acrylic acid are limited. This may arise because acrylic acid is harmful to human health producing eye irritation and pulmonary edema among other negative issues. Acrylic acid is used to increase moisture resistant properties and does not enhance interfacial properties.

Benzoyl chloride is also harmful to human health and a "short exposure could cause serious temporary or moderate residual injury" as noted in the NFPA 704 standard (Standard System for the Identification of the Hazards of Materials for Emergency Response). Basically, the method replaces

polar OH groups with non-polar benzoyl groups, it is suggested that hydrogen bridges are formed in the interface to justify mechanical and thermal property increment.

Cyanoethylation involves the reaction of alcohol groups on the cellulose molecule with 2-propenenitrile (a.k.a. acrylonitrile, cyanoethylene or vinylcyanide) to form a nitrile derivative which can be catalytically reduced to the corresponding primary amine. This amine group might form a covalent bond with the polymer matrix, subsequently enhancing the mechanical properties.

The etherification of NF is another possible treatment that can modify the final properties of composites. Functionalisation of the fibre surface commences with the activation of the hydroxyl group to increase hydrophilicity; the formation of these charged groups will attack other species compounds to form a new covalent ether bond.

Graft copolymerisation is an effective method in the modification of natural fibre surfaces to enhance fibre/matrix interaction. Graft polymerisation is based on the introduction of a new polymeric chain, polymer B, onto a principal polymeric chain, polymer A. The method will first produce activated points by which the desired synthetic branch can be attached to the main polymer chain. The new polymer branches will work as new anchoring points, or increase the similarity between the fibre surface and the composite matrix and substantially improve the interface properties.

Oxidation of NF is another useful, low cost and simple process of increasing the mechanical properties in the interface, although oxidative substances may constitute health hazards. The peroxide group tends to decompose into two radicals which interact with the hydrogen group on the NF surface transferring the radical to the fibre surface. The fibre and matrix grow more compatible with equalisation of the polarities allowing for an improvement in the tensile properties of the composite.

This process could be a useful option for improving the interface of a specific polymer/matrix system but may not be applicable in all cases. However, the isocyanate group is implicated as a cause of cancer and is not environmentally green. Isocyanate treatment of NF creates covalent bonds between

the fibre hydroxyl group and the isocyanate group (-N=C=O) producing an enhanced fibre/matrix interaction.

#### 4.6. COUPLING AGENTS ON THE FIBRE SURFACE

Fibre surface coatings (FSC) for synthetic fibres may include antistatic agents, binders for easy processing, lubricants for textile processes, and coupling agents to promote good adhesion between the fibres and the resin lubricants. For the highest quality composites, the initial surface coating may be burnt off after the fabric has been produced and the textile is then coated with a high proportion of coupling agent. This is impractical for NF as the fibres would be incinerated along with the FSC. There are a variety of surface coatings that have been used to increase the strength of the bond between fibres and the matrix. They include silanes, titanates and zirconates, maleated polyolefins, isocyanates, maleimides and triazines. These agents normally have different chemical functionality at the two opposed ends such that the molecule bonds to the two different components of the composite. Figure 4.7 illustrates a coupling agent performance scheme.



Figure 4.7: Coupling agent performance scheme

After the treatment process, the fibre structure and performance of the composite are modified while in the fibre coating only the fibre surface is altered. Coatings can be applied to synthetic and NF composites, and in both cases a reaction between fibre and silane OH groups is desired in order to achieve optimum bonding properties.

##### 4.6.1. Synthetic fibre coating

GF is one of the main reinforcements in the composite industry. The GF filaments are covered with the pertinent sizing at 0.2-0.3% of reinforcement weight. The coupling agents are the most important sizing component. The coupling agents improve the resin/fibre interaction appreciably, and enhance the mechanical properties of the composite both in the short term and after aging. Water may be one

of the most damaging agents to the interface with moisture absorption directly decreasing its mechanical properties (Plonka et al., 2004). This damage is considered to be greater in a marine environment because of the presence of  $\text{Na}^+\text{Cl}^-$  ions in the seawater (Wei, Cao & Song, 2011; Wood & Bradley, 1997; Gellert & Turley, 1999). In GF, the coupling agent is usually the silane, forming a bond between the GF surface and the pertinent matrix. Figure 4.8 presents the silane formula showing its reaction with the GF surface.

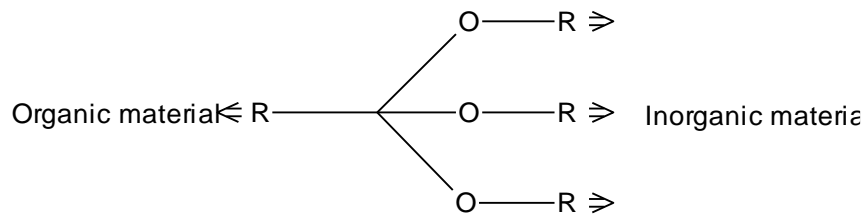


Figure 4.8: Silane schematic figure

The coating is usually applied by wetting the target fibre with a sizing emulsion but there are critical emulsion compositions and application techniques; this technique would be replicated to the NF treatment with silanes.

#### 4.6.2. Natural fibre coating

As with synthetic fibre coating, applying a polymer coating to the NF fibre surface will improve the interfacial properties of the composite. Although NF chemical or physical modifications are more popular techniques, fibre coating is also considered to be a most useful procedure. Jana and Prieto (Jana & Prieto, 2002) presented a wood fibre coating method to improve the interfacial properties. Three different coupling agents were proposed to secure the most complete adhesion of the epoxy resin coating to the wood particle surface. Once the coating had fixed the particles, the epoxy operated as a bridge between the wood layer and the thermoplastic matrix. This same concept may be applied to the flax/bio-epoxy system which is the subject of the current research project.

Xie et al. (Xie et al., 2010) reviewed the use of silane coupling agents in NF/polymer-based reinforced composites. This concept is basically replicated for the current study flax fibre treatment, in order to increment the flax/bio-epoxy adhesion.

## **4.7. MODELLING CHEMICAL TREATMENT**

### **4.7.1. Mercerisation (NaOH) and NaCl**

Bledzki (Bledzki, Fink & Specht, 2004) offered a direct model which related the mercerisation process to the final mechanical properties of a hemp fibre/epoxy resin system. For the formulation of an epoxy resin composite model, the considered parameters were listed as the alkali concentration, the temperature, and treatment time applied to the fibres and the tensile strength. In this example the model was based on the change in cellulose crystallinity from cellulose I to II under the mercerisation treatment. Similar conclusions were obtained by Borysiak (Borysiak, 2013) where the transcristalline morphology progression in a wood fibre/PP composite was studied under different treatments, concluding that a direct relationship developed between treatments and the growth of the crystalline progression.

Another model related the change in cellulose morphology with moisture absorption after mercerisation, bleaching and thermal treatments (Stana-Kleinschek, Strnad & Ribitsch, 1999). The author concluded that after the mercerisation treatment moisture absorption increased because of wax elimination and the change in cellulose crystallinity. Zou et al. (Zou, Wang, Gan & Yi, 2012) similarly concluded that in a sisal/PLA composite moisture absorption increased after the mercerisation of the fibres. It was concluded that NF treatments increase the water absorption rate although after treatment the fibre surface is cleaned and activated thus improving the interaction with the matrix and, as a consequence, reducing fibre absorption.

Jandas et al. (Jandas, Mohanty, Nayak & Srivastava, 2011) studied the interfacial properties of a banana fibre/PLA composite with different models. The banana fibre was treated with different chemical reactants modifying the surface by mercerisation which subsequently increased the mechanical performance of the composite. Mechanical prediction models, such as Hirsch's, modified Bawyer and Bader's, and Brodnyan were then applied to study the theoretical prediction process of the composite.

#### **4.7.2. Silanisation**

There are not many references in the literature where a prediction model has been applied to study the long term performance of the silanised fibres. Liu et al. (Liu, Jones, Liu & Jiang, 2014) for example, investigated the effect of air plasma and a silane coupling agent on polyurethane adhesion with human hair. The two systems were studied under immersion artificial sweat solution aging a 50°C for 24h, and micro-droplet technique was used to follow the IFSS loss in the aging. It was concluded that the air plasma technique was more efficient in maintaining the mechanical properties, performing better than the silane treated human hair.

However, the previous method evaluates the long term properties, but the model prediction is not matching correctly the experimental results. In contrast, Hidalgo-Salazar et al. matched experimental results to the Burger theoretical creep model curve (Hidalgo-Salazar, Mina & Herrera-Franco, 2013). Fique fibres were mercerised and silanised to improve their interfacial properties with recycled LDPE-Al bulk matrix. The model works best for the case of untreated and mercerised fibres composites.

#### **4.8. CHARACTERISATION OF FIBRE SURFACES AND INTERFACES**

This section describes the different techniques used to characterise fibre-matrix adhesion. All these techniques aim to quantify the fibre-matrix adhesion of a given composite system in order to predict its macroscopic performance. The characterisation techniques may be divided into the following categories:

1. contact angle study
2. reactive sites on fibre surface
3. mechanical interface characterisation
4. optical qualitative analysis.

##### **4.8.1. Contact angle study**

The technique is based on measuring the contact angle between the fibre and the composite matrix. Depending on the values achieved the fibre wettability would vary. In the NF surface treatments case, the fibre surface energy differs and is directly related to the NF wetting, related to the interfacial



properties. The Wilhelmy technique involves dipping a single fibre into a non-penetrating liquid while measuring the force on the fibre due to wetting.

#### 4.8.2. Reactive sites on fibre surface

The NF surface has many -OH reactive groups. Matrix adhesion is different depending on the treatment selected for the composite system. There are references in the literature that determine the hydroxyl number of the fibre surface, as for example in the method presented by Freire et al. (Freire, Silvestre, Neto & Rocha, 2005), where the -OH group number is determined by using a complex gas chromatography-mass spectroscopy (GC-MS) method.

#### 4.8.3. Mechanical interface characterisation

The mechanical characterisation of the interface can be divided into three main groups - direct methods, indirect methods and composite laminate methods, as explained in Figure 4.9 (Drzal et al., 2000). Direct methods have been studied in greater detail because of their relevance in the process of evaluating NF composites.

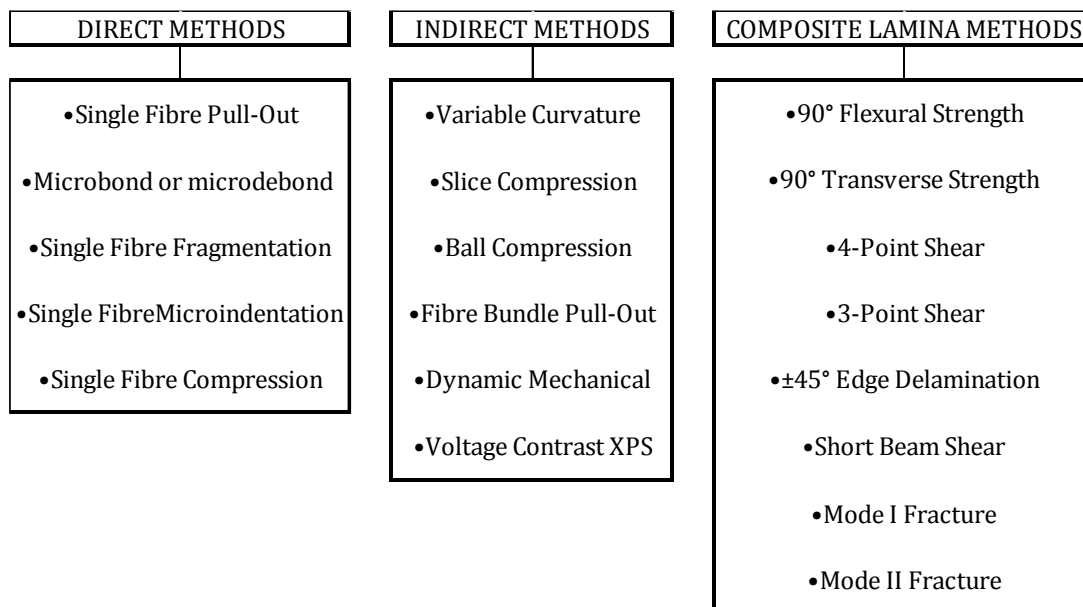


Figure 4.9: Classification of Mechanical interface characterisation methods (Drzal et al., 2000)

#### **4.8.3.1. Composite lamina methods**

Composite laminate tests are used to measure fibre-matrix adhesion. Interface dominated tests are used such as 90° tensile test; 90° flexural test; four-point shear test, short-beam shear test, Mode I/Mode II delamination tests, and in-plane 10°/45° shear test. Many of these tests are formalised by international standards such as ASTM or ISO standards. These documents are the guidelines that govern test performance, the data to be achieved and the analysis of the results.

Composite testing in general are very useful techniques for the evaluation of interfacial properties and are particularly important in the evaluation process of NFRP interfacial properties.

#### **4.8.4. Optical qualitative analysis**

These complementary techniques provide information on surface chemical and mechanical characteristics. For example, yarn swelling could be studied by optical microscopy or wetting properties determined with X-ray photoelectron spectroscopy (XPS). Other important techniques, such as IR spectroscopy, SEM fractography, Raman spectroscopy and surface energy analysis are used for the evaluation of NFRP interfacial properties.

It is of fundamental importance to characterise the NF surface in order to identify the most relevant treatment that can be applied to its surface morphology and chemistry that will subsequently have a direct effect on its mechanical and flow properties.

### **4.9. SUMMARY AND FUTURE DIRECTION**

Chapter 4 reviewed literature references to matrix and NF modifications with particular reference to composite mechanical systems and ageing property enhancement. This chapter gives the continuation to Chapter 2 where the conventional composites were revised and Chapter 3 where the natural fibres were studied.

Chapter 4 review focused on studies that enhance the understanding of interfacial properties, the application of epoxy resin silane additions, the use of NF mercerisation/silanisation treatments and

the evaluation of modified properties systems. The same silane has been selected and the amine is expected to participate in curing the epoxy matrix that has been selected for this study.

Similarly, the NF surface will be modified and the bio-epoxy resin formulation changed in order to increase the fibre matrix compatibility value. The addition of silane to the matrix and the chemical treatment of NF are the principal techniques which will be investigated. The aim is to increase the flax fibre/bio-epoxy system by tailoring the interphase region in a commercially competitive manner.

In the initial stages of the present experimental project the plan was to perform acetylation treatments on the flax fibres in order to increase their fibre-matrix adhesion properties. Acetylation was considered because it was both effective and economical to apply; however, time limitations prohibited its use. Mercerisation techniques were therefore applied which have the advantage of activating the NF surface while acetylation merely reduces fibre hydrophilicity.

The silane was added to the bio-epoxy in order to strengthen those properties impeding moisture ageing. In order to improve performance moisture tests under ASTM D5229 standards were undertaken. The aim is to discover whether or not the presence of silane in the interface will improve the moisture resistance of the composite as well as enhancing the mechanical properties.

The current study has proven that silane addition to the bio-epoxy matrix clearly improves the ILSS values by approximately 20% of the reference system. In-plane shear properties were also studied and improved; 90° tensile test and in-plane 10°/45° shear test were of particular relevance. These values can be checked in Chapter 8 which refers to the experiments undertaken in the research project.

The literature has been searched for investigations that refer to the modelling of NF treatments. The current PhD tried to set a treatment model based on the flax/bio-epoxy composites evaluation experimental results, Chapter 8; and model set in Chapter 9.

The project surface modification was not studied in detail by advanced optical analysis, such as SEM fractography, but fibre swelling after the chemical treatment was studied with the aid of optical microscopy. See result Chapter 8 and Appendix C.

Based on the collected information the mercerisation, silanisation and silane addition to the matrix and indicative conditions were identified and will be the focus of the research undertaken in this doctoral study. The research methodology is described in detail in Chapter 7. The results obtained for treated systems are presented in Chapter 8 and Appendix C. The effect of different treatment factors (e.g. treatments temperature and concentration) upon the flax/bio-epoxy composite system were evaluated with the ANOVA technique and are discussed in Chapter 9 with conclusions drawn in Chapter 10.

# 5. Composite design, manufacturing, testing and image analysis

## 5.1. INTRODUCTION

In the production process of a composite optimised design, it would follow the steps described in this Chapter; it will concentrate on the material design of the composite, its manufacture, its testing and the image analysis of the prototype. The four subjects above are directly inter-related and the processes involved in the production of the composite prototype are shown in the chart below (Figure 5.1). The input data for the design of the composite will be obtained from mechanical scale testing in the laboratory; once the designed prototype has been tested it will be manufactured; running concurrently with the manufacturing procedure will be a rigorous process of checking the quality of the product by image analysis.

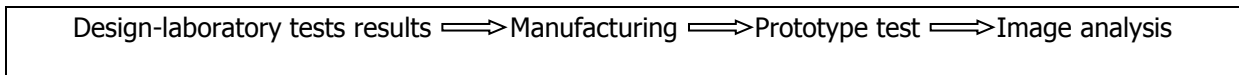


Figure 5.1: Composite design, test, manufacturing and image analysis relationship chart

All the sections would be focused on the techniques developed and used along the PhD study, such as resin infusion, development of flow models or optical microscopy.

## 5.2. COMPOSITE DESIGN

There are different approximations in the composite design process; for example Kedward (Kedward, 2000) (Figure 5.2) proposed a methodology and Potter (Potter, 1992) another. In general most of the methods are based on the same common point checklist, based on product function, geometry, environment, duty, cost issues and programme/contact issues.

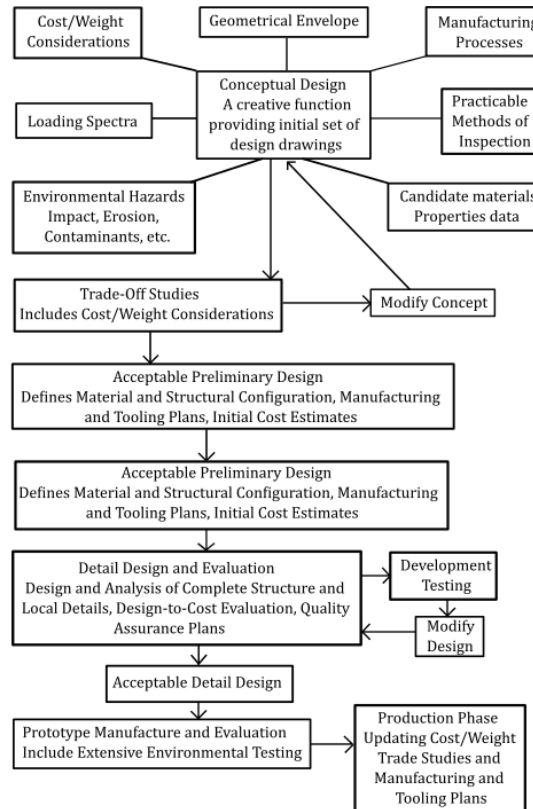


Figure 5.2: General scheme for the design of the composite (Kedward, 2000)

The starting point of any design project as proposed by Kedward is the “**conceptual design**”, which must be defined specifically and clearly to allow for the success of the project. There are a number of factors to be considered in setting the concept, and in the context of sustainable composites they can be simplified to seven main groups; <sup>1</sup>geometric envelope, <sup>2</sup>material selection, <sup>3</sup>loading conditions, <sup>4</sup>environmental conditions, <sup>5</sup>manufacturing processes, <sup>6</sup>inspection methods, <sup>7</sup>cost evaluation and life cycle assessment.

Following the “conceptual design” stage, the composite design is preliminary defined in plans and drawings and candidate material systems may also be evaluated. In a second step, referred to as “**trade-off studies**”. Trade-off involves the following procedures: first select an approximate design, check how close it matches the final requirement, and if inappropriate exchange or trade in to achieve the main goal. The outcome is the preliminary design; its structural configuration, its manufacturing definition and tooling requirement in order to achieve an accurate cost estimate.

“**Detail Design and Evaluation**” is the third step. For the study of the more detailed structural design it is imperative that secondary stresses, which usually appear in section joints or in phase transition zones, are carefully studied. Global and local FEM software models may be applied to the study of such stresses with particular reference to the angle structures of joints.

In the “**Prototype Manufacture and Evaluation**” stage the prototype is produced in accordance with the previously defined manufacturing steps. Once the prototype has been produced, it will be subjected to real scale testing to establish its correct service behaviour.

Once the prototype has been developed and evaluated the design process enters the “**production phase**”. If the prototype evaluation is accepted, then the design will then be up-scaled into an industrial product and absolute and definitive data on production costs and time will be sought.

### 5.3. MECHANICAL TESTS

The mechanical tests performed on composites are classified into two main groups; first, the characterisation of the composite system will be tested at laboratory scale to obtain the necessary data on the design (more detailed practical example in Chapter 7); second, the final composite will be tested in order to compare its theoretical performance with its real scale performance. See Figure 5.3 below.

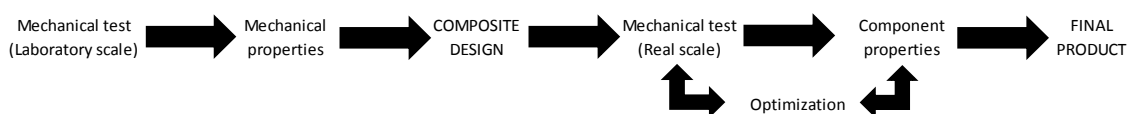


Figure 5.3: General flow chart of mechanical test

### 5.4. COMPOSITE MANUFACTURING

The main manufacturing techniques used in TS composites production are, open mould, prepregging/autoclaving, compression moulding, liquid moulding and continuous techniques.

#### 5.4.1. Resin infusion under flexible tooling (RIFT)

The resin infusion technique is a modified version of the Resin Transfer Moulding (RTM) technique. In RTM, dry fabrics are enclosed by two rigid mould parts for the subsequent wetting of the fibre and the formation of the final composite piece. In the Resin Infusion under Flexible Tooling (RIFT) technique, one of the rigid mould parts is substituted by a flexible film (Williams, 1977). The RIFT technique was selected for the manufacture of all the test plates prepared in the present research project, which will be described in detail in Chapter 7 and the results presented in Chapter 8.

In the RTM technique, the size of the final piece is controlled by the size of the mould cavity. In the RIFT technique the thickness of the product depends on the pressure applied throughout the whole manufacturing cycle. With RTM, the piece may be more strongly packed under pressure of 3 bar, whereas with RIFT the pressures are lower with typical values of 0.8-0.9 bar (and an absolute 1 bar limit). RIFT is easier to use when manufacturing pieces of different sizes, particularly when they are large. This versatility results from the flexibility of the film under vacuum whereas with RTM the contra-mould tool is rigid under internal pressure.

The RIFT technique should not be confused with the vacuum bagging technique. The principal difference is that, with RIFT, the dry fabric (not wetted fabric) is placed onto the tool and the peel-ply, release film, **flow media**, (no bleeder or breather), and vacuum bag are enclosed in the system by the sealant tape. The resin is fed directly into the vacuum system from an external source to wet the fibres. Unlike with vacuum bagging the resin is introduced into the system once the bagged dry reinforcement has been prepared. Figure 5.4 illustrates how the system is prepared and how the liquid resin progresses to wet all the fibres.



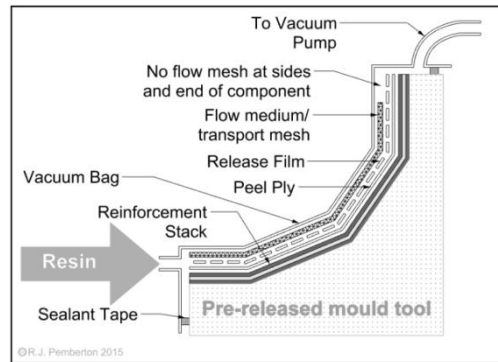


Figure 5.4: Schematic figure of RIFT manufacturing technique  
(Courtesy of Richard Pemberton under a Creative Commons licence)

### 5.4.2. Flow models

The properties of composite materials are produced by using different techniques, as, for example, by resin infusion. The flow mesh properties will vary according to the technique selected and the characteristics of the fibre/ resin. The flow properties of each particular composite system and the selected manufacturing technique will directly affect the component  $V_f$ . In the studies of Shah (Shah, 2014), the flow dynamics and mechanical properties of different plant fibre composites are related to the  $V_f$ , and the predicted absolute theoretical maximum fibre content coincides with the experimental values.

Francucci and Rodriguez (Francucci, Rodríguez & Vázquez, 2010), in a study relevant to the present research project, evaluated how each NF treatment affected the  $V_f$  of the composite and in a similar study by Cherif et al. the sorption and mechanical properties related to NF treatment was investigated.

Based on the references mentioned in the above paragraphs, the current PhD produced a simplistic prediction flow model; such model relates the laminate flow properties with the flax fibre swelling produced by different treatments. Fibre swelling data is shown in Appendix C and the model discussed in Chapter 9.

## 5.5. IMAGE ANALYSIS

Composite performance cannot be understood by mechanical property analysis alone and it is most important to discover the interface and interphase properties in the adhesion between fibre and matrix. SEM is therefore a most useful and easy to apply technique to study the above properties. Macroscopic and optical tests are complementary and best adapted techniques to study fibre-matrix adhesion. Lee, et al. (Lee, Jhan, & Chung, 2012) presented a study where the CF surface was treated to increase its roughness for better adhesion with the matrix, and subsequently to improve the shear strength of the fibre-matrix. SEM was used to relate macroscopic test values with the data from a microscopic image as exemplified in Figure 5.5.

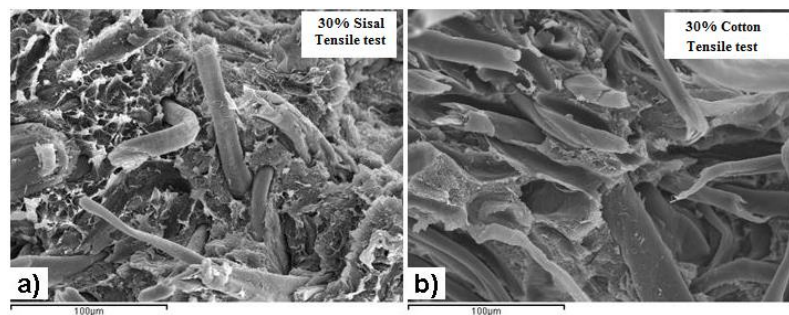


Figure 5.5: SEM images of a) Sisal/PP; b) Cotton/PP resin systems (Amigó et al., 2009)

The 2-D characterisation of fibre distribution within the image plane has been reviewed by Summerscales et al. (Summerscales, Virk & Hall, 2013). This technique can obtain similar accuracy in fibre volume fraction as can be achieved with the densities technique. Another application is the "tow structure" capacity determination which defines every yarn, tow or filament diameter, shape and spatial orientation of the fibre. Similarly, it is capable of identifying the different fibre types in a hybrid composite material reinforced with, for example, GF and carbon fibres. In the case of short-fibre reinforced composites the identification of the fibres, their spatial orientation and length can be determined by using image analysis.

However, in the current PhD study, the SEM technique was not applied. The optical microscope was used for the fibre swelling monitoring. The proposed model tried to find a relationship between the fibre swelling and the laminate  $V_f$ , with the subsequently affecting the macroscopic mechanical properties. See Appendix C for the swelling data, Chapter 8 for the macroscopic mechanical tests results and Chapter 9 to see the relationship between swelling and mechanical properties.

## **5.6. SUMMARY**

Manufacturing details are summarized in Chapter 7. The results obtained from the test campaigns (Appendix B) and from image analysis (Appendix C) are illustrated in Chapter 8 and further discussed in Chapter 9. The results from Chapter 8 and Appendix B were introduced in the proposed mechanical prediction models to check whether they were working or not. Additionally, a flow model was proposed, the proposed model tried to find a relationship between the fibre swelling and the laminate  $V_f$ . See Appendix C for the swelling data and Chapter 9 for the model discussion. The composite design, manufacturing, testing and image analysis processes that were applied to the research project are discussed in detail in Chapter 9.

# **6. Composite durability in marine environment**

## **6.1. INTRODUCTION**

In this doctoral research project, silane was added to the flax/bio-epoxy composite system in order to enhance the composite mechanical and aging properties. In this Chapter, tests to examine the durability of the composite will be briefly explained and the ageing of the composite under marine conditions will be examined.

## **6.2. COMPOSITE DURABILITY**

One of the most difficult issues to consider in the design of a bio-composite will be its mechanical properties after long term environmental exposure and hence its life prediction. The most reliable prediction would result from testing its long term performance as a case study product. However, such a programme would be long and expensive to perform and so data from accelerated ageing tests must be collated in an attempt to establish a direct correlation with the in-use composite performance.

Chapter 6 identifies the most common ageing agents in service applications and the tests performed on their respective components. The doctoral study considers the interfacial degradation of the composite in a marine environment in order to fully understand and interpret the test procedures conducted under these conditions on the NF/bio-epoxy system ageing process.

Normally after different ageing processes the mechanical properties (modulus, strength and strain-to-failure) when tested are considerably decreased. This arises as a consequence of composite chemical structural modification, characterised by matrix swelling, fibre/resin interface debonding, matrix micro-cracking, polymer chain scission and the solution of soluble components.

There are a number of options for measuring ageing processes in composite materials, but the most common procedures are -

- Chemical resistance to liquids test
- Natural weathering test
- Marine environments test

### **6.2.1. MARINE ENVIRONMENT TEST**

Marine environments may be hazardous for composite materials with water, then salt concentration, causing the main questions. It is therefore imperative to create a composite system that maintains its structural integrity in a marine environment and to discover how to overcome the most damaging factors. In the present research project, the main aim is to evaluate whether the silanisation process increases the resistance of the flax/bio-epoxy system in a marine environment (Appendix E).

GF/UP systems are selected for marine use because of their elevated corrosion resistance properties and are used in such components as marine propellers, sea water pumps, floating piers, offshore platforms, ship hulls and the strengthening of steel structures (Summerscales, 2014). Epoxy resin, CF or aramid fibre could also be used in marine applications although their utilisation would be more complicated. In the case of the marine application of a NFRP composite, the hygroscopic properties of the NF complicate its use due to moisture induced swelling and plasticisation; giving as a result mechanical performance reduction.

The eight factors of marine degradation can be listed as follows - water, salt, sand, UV radiation, marine vegetation/micro-organism attachment, marine pollutants and wave action. In each case, the harshest of these ageing agents must be identified and the experimental campaign planned in accordance. For the best test design, the composite service environment must be studied; it is not truly representative to have the composite component close to the sea, partially or totally immersed in the water; so depending on the environment the test would differ.

Based on the above facts a marine immersion test, to be discussed in the next section, and a salt spray test can be applied.; these tests are usually employed to simulate industrial and/or environmental degradation.

#### **6.2.1.1. Water absorption**

Organic resins usually absorb water, while GF and CF do not. In contrast aramid fibre and NF do absorb water leading to the swelling of the fibres. As a result laminates absorb water which is usually limited by diffusion and in turn is ruled by Fick's law (Equation 6.1) (Tsai, Bosze, Barjasteh & Nutt, 2009).

$$\frac{M_t}{M_m} = k \cdot t^n \quad \text{Equation 6.1}$$

Where  $M_t$  is the moisture uptake at time  $t$ ,  $M_m$  is its maximum moisture uptake, at equilibrium state, and  $k$  and  $n$  are the diffusion kinetic parameters. The diffusion exponent  $n$  indicates the mode of diffusion. When  $n$  is equal to 0.5, diffusion obeys Fick's law. The mechanism is non-Fickian when  $n = 1$  (or  $n > 1$ ) while the diffusion is anomalous when  $n$  shows an intermediate value, between 0.5 and 1. Moisture uptake in vegetal fibre reinforced plastics usually follows Fickian behaviour. Fick's law, in the case of a one-dimensional approach, shows that the water uptake increases linearly with the square root of time, and then gradually slows until an equilibrium plateau is reached.

Fickian diffusion process depends on density ( $\rho$ ), specific heat ( $C$ ), mass diffusivity ( $D$ ), thermal conductivity ( $K$ ) and maximum moisture content ( $M_m$ ), in addition to other factors such as the geometry and the initial condition of the samples. The application of the Fickian process may therefore be complex and may not always produce satisfactory results. For example, Fickian predictions may be invalid when there are voids in the sample, or cracks/delaminations are present, or when moisture propagates along the fibre-matrix interface.

Scida et al. (Scida, Assarar, Poilâne & Ayad, 2013) investigated a flax fibre/epoxy resin composite system with hygrothermal accelerated ageing and monitored the degradation process with Fick's law

(Equation 6.2) and water absorption uptake (Equation 6.1) and finally measuring the composite's Young's moduli and tensile strength.

$$M_t = \frac{W_t - W_0}{W_0} \times 100(\%) \quad \text{Equation 6.2}$$

Where  $W_0$  is the weight of dry specimen and  $W_t$  is the weight of wet specimen at time  $t$ . After a 38 day experimental campaign under hygrothermal ageing, the Young's modulus and tensile strength were seriously affected by the ageing process. This weight change was monitored using the formulas in ASTM D5229 standard, where liquid uptake,  $T_g$  and moisture diffusion were monitored to follow the degradation properties in the ageing process.

In the research project, the flax fibre/bio-epoxy resin composite was investigated under RT marine ageing conditions (Appendix E). Flexural samples were water age tested and their degradation monitored. Water absorption and loss of mechanical performances were evaluated in untreated and in silanised systems alike and the data compared. The test procedures are described in Chapter 7, evaluated in Chapter 8 (Appendix E) and the results discussed in Chapter 9.

#### **6.2.1.2. Marine immersion test**

In this test the samples are immersed in a saline liquid and tested for their ageing with the ASTM C581 standard. However, if a marine environment immersion is to be simulated, ASTM D1141 adds a pre-determined quantity of different ions to the water which Millero (Millero, Feistel, Wright & McDougall, 2008) has defined in detail "The composition of Standard Seawater and the definition of the Reference-Composition Salinity Scale".

#### **6.2.1.3. Composite mechanical deterioration**

The composite is aged in a marine environment to establish its destructive processes by monitoring its tensile, compression, shear and impact properties (Al-Bastaki & Al-Madani, 1995; Gu, 2009).

The flax/bio-epoxy system was subjected to the moisture test referred to above. The test records the measurement of water uptake, and evaluates the deterioration in flexural mechanical properties of the sample. This data can be compared with the deterioration data from the flexural properties tests which are presented in Appendix E.

### **6.2.2. REFERENCE STUDIES**

There are many studies in the literature which refer to the effects of marine ageing on NF reinforced composites. Le Duigou, et al. (Le Duigou, Davies & Baley, 2013) has evaluated the interfacial properties of a flax fibre/epoxy system after marine ageing, which raises similar questions to those addressed in the present research project. In the micro-droplet test conducted by the above authors, the interface debonds according to the length of time the composite has been immersed. Macromechanical and micromechanical degradation in a similar marine environment over a time period will be addressed in the research project.

### **6.2.3. IN SERVICE CASE TESTING**

Although in many studies accelerated testing can be a very useful tool, it is however better accomplished if studied under actual, authentic conditions as, for example, when US army personnel reported the different ageing properties of boats and vessel components (Fried & Graner, 1966; Cobb, 1963; Graner & Della Rocca, 1971).

### **6.3. SUMMARY**

In the first part of Chapter 6, the composite marine environment tests were described, and the procedure and standard information was collected in order to be applied to the flax/bio-epoxy system. Test procedure is described in Chapter 7 with obtained results in Appendix E, and the subsequent discussion in Chapter 9. The PhD main idea was to study whether the silane addition to the matrix achieves increment in the aging resistance, apart from upscaling to the case studies.



# 7. Research methodology

## 7.1. INTRODUCTION

The literature review in Chapter 4 identified NF treatment and matrix modification methods to improve the interfacial properties of the NFRP. Selection considered the following factors - process simplicity, procedure effectiveness, sustainability, and economic viability. The methods and procedures were applied to flax fibre/bio-epoxy and flax fibre/petrochemical resin composite systems.

Initially, all raw materials sources, their respective specifications and performance capabilities were confirmed, e.g.: "apparent" fibre diameter, modulus, strength; fabric weave style, areal weight, tows/metre in both warp and weft, crimp angle; the surface treatment of the natural fibres; and resin characteristics.

Second, the fibre modification process parameters were controlled to achieve the best NFRP performance; i.e. parameters such as the chemical treatment, solvent concentration and exposure time.

Finally, the composite infusion parameters, fibre volume fraction and fibre alignment were controlled.

In summary, consistent processes were developed to achieve quality control (QC) of the materials received and the treatment and conditioning of the fibre, to ensure the best outcome in manufacturing the composite.

After all the fibres had undergone their respective treatments and the epoxy resin system had been modified, 36 different laminates were produced which form the basis of the experimental research conducted in this project. The experiments involved a series of treatment procedures which included matrix modification, fibre mercerisation and silanisation, and most importantly the mechanical testing

of the laminate composites. These procedures are discussed in the following sections of this chapter and are summarised in (Table 7.15).

The mechanical testing of the composites was strictly aligned to the standards relating to the calibration and procedures attendant to the equipment so that the most reliable results were obtained from the mechanical tests performed. The variability of the test results undertaken on any composite material is a significant factor, a problem that is magnified in NFRP composites because of the great variation in the morphology and properties of NF. Mechanical test reliability is desired in the current PhD. Appendix F presents the test uncertainty determination process.

After the experimental study had been undertaken in the laboratory, it paved the way for the real prototype to be designed and ultimately manufactured.

This research is focused on the enhancement of NFRP interfacial properties through modification of the polymer matrix and NF surface with chemical treatments. The study was divided into different sections to fulfil the research. First, the base mechanical properties of the flax fibre/epoxy were obtained; **Laminates 1-4 and 29**, used Biotex/SuperSap bio-resin matrix in Laminates 1-2, Biotex/Huntsman in laminates 3 and 29, Lineo/Huntsman in Laminate 4. Second, the most appropriate modification methods for the specific composite were identified; **Laminates 5-29** used Huntsman petrochemical resin reinforced with Biotex fabric. Third, best modification method was applied to a bio-composite; **Laminates 30-36** used SuperSap bio-resin reinforced with Biotex fabric. Fourth, the theoretical knowledge as researched was applied to producing various bio-composite types, modifying and testing their mechanical performance under moisture conditions; **Laminates 33-34** used SuperSap bio-resin reinforced with Biotex fabric.

## **7.2. RAW MATERIAL**

The NF, bio-resin, petrochemical resin and chemical treatment characteristics as selected are described below.

### 7.2.1. Flax fibre characteristics

Two different flax fibre fabric suppliers were selected, namely Composite Evolution (CE) from Chesterfield - England and Lineo (NV) from St Martin du Tilleul - France.

#### 7.2.1.1. Composite Evolution flax fibre

CE is dedicated to the production of flax and jute yarns and fabrics under the trade name Biotex ("Natural Fibres Reinforcements", 2017). For this study, unidirectional (0° UD) 275 gsm flax fabric was supplied (See Figures 7.1 and 7.2). CE fibre properties are shown in Table 7.1 and yarn properties are shown in Table 7.2.

Table 7.1: Mechanical properties of Biotex fibre (data from CE with no statistical information)

Flax fibre average properties	
Density	1500 kg/m <sup>3</sup>
Diameter**	20 µm
Tensile modulus	50 GPa
Tensile strength	500 MPa
Strain at failure	2%

\*\* The diameter was very roughly estimated by CE\*\*

Table 7.2: Biotex flax fibre yarn properties (data from CE)

Flax yarn properties	250 tex	1000 tex
Tenacity/tensile strength	15N/tex	38N/tex
Elongation at break	15.5%	4.4%

CE also supplied data on the different tests performed on composites produced with their fabrics. The data provided one reference point for comparison with the data obtained in the present research project.



Figure 7.1: Tested CE flax fibre UD roll



Figure 7.2: Flax-ply woven and UD fabric (Courtesy of Easy Composites)

Table 7.3 presents company data for laminates made by CE from 30-33 v/o Biotex flax fabrics and unsaturated polyester resin manufactured by the vacuum infusion process. All composites were made from 250 tex Biotex flax yarn fabrics and tested at room temperature.

Table 7.3: Mechanical property data for composites made from Biotex UD fabrics (data from CE)

Property	UD flax-polyester	Biaxial flax-polyester	Woven flax-polyester	Test standard
Density	1.3 g/cm <sup>3</sup>	1.3 g/cm <sup>3</sup>	1.24 g/cm <sup>3</sup>	
Tensile modulus	18.8 GPa	8.7 GPa	7.2 GPa	ISO 527-4
Tensile strength	174 MPa	85 MPa	68.3 MPa	ISO 527-4
Tensile elongation	1.5%	1.7%	2.5%	ISO 527-4
Flexural modulus	15.1 GPa	6.8 GPa	4.0 GPa	ISO 14125
Flexural strength	196 MPa	135 MPa	97.4 MPa	ISO 14125
Charpy impact	TBC	TBC	28.0 kJ/m <sup>2</sup>	ISO 179 – 1

The technical data sheet (TDS) is included in Appendix A1.

### 7.2.1.2. Lineo flax fibre

Lineo ("Ecotechnilin", 2017) is a dedicated company producing flax and jute yarns and fabrics under the trade name Flax-ply (Figure 7.3). For this study, unidirectional (0° UD) 150 gsm flax fabric was supplied.



Figure 7.3: Flax-ply woven and UD fabric

Table 7.4 presents mechanical test results supplied by Lineo. The results are obtained for 12 layers of a 180 gsm Flax-ply UD panel. The  $V_f$  is of 60%. The selected polymer matrix was not identified in the supplier information.

Table 7.4: Mechanical property data for composites made from Flax-ply UD fabric (data from Lineo)

Property	UD Flax-ply	Test standard
Density	1.33 g/cm <sup>3</sup>	
Tensile modulus	35 GPa	ISO 527-4
Tensile strength	330 MPa	ISO 527-4
Tensile elongation	1.8 %	ISO 527-4
Flexural modulus	22 GPa	ISO 14125
Flexural strength	300 MPa	ISO 14125
Flexural Elongation	2.4 %	ISO 14125

The technical data sheet (TDS) is included in Appendix A2.

### 7.2.2. Bio-epoxy resin

The initial bio-epoxy matrix system selected was from Entropy Resins, a company established in California, USA. In 2012, Ferrer Dalmau, a Catalonian company, started production in Europe in collaboration with the parent USA Company, and this greatly facilitated the research project making the raw material more freely available.

Entropy ("Entropy Resins", 2017) offers a wide variety of formulations which were used as follows:

- Supersap CLR/INF or Supersap CLR/(CLX-INH) Infusion panels
- Supersap CPM/(CPF-CPL) RTM fins
- SuperSap ONE/ONF or SuperSap BRT/(CLX – CLF – CLS) Surfboards

Supersap CLR epoxy is a clear modified liquid bio-epoxy resin. In contrast to traditional petroleum-based resins, this formulation contains bio-renewable materials either (a) sourced as co-products from other operations, or (b) from waste streams of other industrial processes, such as wood pulp and bio-fuels production.

Supersap CLR is water-clear and UV-stabilised to avoid the yellowing of the product. It is claimed to be ideal for outdoor applications such as surfboard production. The low viscosity affords the option of producing pieces in RTM or infusion. The resin can cure at RT, or be heated in the oven. Normally post-cure is recommended.

The wettability of natural fibres is one of the most important considerations in obtaining the highest quality mechanical properties in composites. A low viscosity resin is essential for application to RTM and RIFT processes. In RTM, the resin flows long distances in comparison with other processing techniques. Rudd, et al. (Rudd, Long, Kendall & Mangin, 1997) stated that viscosity is the most significant practical limitation in the production of a suitable resin system. Low viscosity indicates a high flow rate, whilst a high viscosity indicates the opposite low flow rate. Resins with extreme low viscosity may be unsuitable for LCM processes since they may lead to high porosity or gross voidage, i.e. unwetted volumes. Resins formulated for liquid composite moulding processes typically have an initial viscosity of around 200 mPa.s (1 mPa.s = 1 centipoise). Becker (Becker, 1991), quotes an upper limit of 800 mPa.s for viscosity in RTM. The non-injection point (NIP) is defined as a viscosity of 1000 mPa.s (Pearce, Guild & Summerscales, 1998). At this viscosity level and under the low pressures applied in infusion processes the flow front is effectively stationary. For this reason,

Supersap CLR/ (CLX-INH) formulation is the most appropriate system because of its low viscosity, although Supersap CLR/INF may also be an option with its higher viscosity (See Table 7.6).

Table 7.5 illustrates the properties of the Supersap CLR resin system (Figure 7.4); Table 7.6 presents the typical working properties that are available during manufacture with Supersap CLR resins; Table 7.7 presents the mechanical properties for cured resin systems.



Figure 7.4: Supersap CLR/CLX system used for the panel production (Courtesy of 5TX surf)

Table 7.5: Supersap CLR resin system properties (Entropy Resin data)

Property	Supersap CLR
Visual appearance	White to light yellow
Gardener colour	1-2
Viscosity (cPs @ 25°C)	2000-4000
Density (SG at 25°C: water = 1)	1.17
Bio-carbon content by mass (%)	18.2-25.4
Bio-content by mass (%)	30.8-45.2

Table 7.6: Supersap CLR resins manufacturing data (Entropy Resin data)

Property	Supersap CLR/INF	Supersap CLR/ (CLX-INH)
Mix ratio by weight	100:33	100:19:19
Mix viscosity (cPs @ 25°C)	500-1000	360
System biocontent by mass	21-30%	17%
Gel-time (min, 150 g at 25°C)	45	75
Thin film set time (h @ 25°C)	4	--
Tack free time (h @ 25°C)	8	8-10
Cure cycle (25°C) before ...	7-10 days	7-10
... post-cure	2h @ 80°C	--

Table 7.7: Mechanical properties for cured Supersap resin systems (Entropy Resin data)

Property	Supersap CLR/INF/infusion fast hardener	Supersap CLR/CLX/INH
Cure cycle	24h @ 25°C the 2h @ 48°C	24h @ 25°C the 2h @ 48°C
Tg (°C)	115	56
Tensile modulus (GPa)	4.27	3.29
Tensile strength (MPa)	69	58
Elongation at break (%)	2	2.5
Flexural modulus (GPa)	3.79	3.16
Flexural strength (MPa)	110	99
Compression strength (MPa)	-	92

The values in Tables 7.5-7 were used as reference points for comparison with values obtained from the literature review and in the present research project. They were also used to inform the calculations within the different models.

The technical data sheet (TDS) is appended in Appendix A3.

### 7.2.3. Petrochemical resin

The initial experiments for NFRP production were undertaken with petrochemical epoxy resin from Huntsman LLC. (USA). Araldite LY 1569 CH/Aradur 3489 CH epoxy infusion system was selected for the production of the laminate ("Huntsman LLC", 2017).

Table 7.8: Araldite LY 1569 CH/Aradur 3489 CH system properties (Huntsman LLC data)

<b>Resin</b>	<b>Araldite LY 1569 CH</b>
Visual appearance	Clear liquid
Viscosity (ISO 12058 cPs at 25°C)	1300-1500
Density (ISO 1675 g/cm <sup>3</sup> at 25°C)	1.1-1.2
<b>Hardener</b>	<b>Aradur 3489 CH</b>
Visual appearance	Clear liquid
Viscosity (ISO 12058 cPs at 25°C)	5-20
Density (ISO 1675 g/cm <sup>3</sup> at 25°C)	0.92-0.93
<b>Mixture (100:28 by weight)</b>	<b>Araldite LY 1569 CH/Aradur 3489 CH</b>
Viscosity (ISO 12058 cPs at 25°C)	200-300



Table 7.9: Typical working properties available during manufacture with Araldite LY 1569 CH/Aradur 3489 CH (Huntsman LLC data)

<b>Property</b>	<b>Araldite LY 1569 CH/Aradur 3489 CH</b>
Mix ratio by weight	100:28
Mix viscosity (cPs @ 25°C)	200-300
Gel-time (min, at 80°C/100°C/120°C)	43-46/15-16/7-8
Tg (°C, 4h 80°C/8h 80°C)	76-79/77-80

Table 7.10: Mechanical properties for cured Araldite LY 1569 CH/Aradur 3489 CH resin systems (Huntsman LLC data)

<b>Property</b>	<b>Araldite LY 1569 CH/Aradur 3489 CH</b>
Cure cycle	8h 80°C
Tg (°C)	77-80
Tensile modulus (GPa)	2.85-3
Tensile strength (MPa)	67-71
Elongation at break (%)	4.4-5
Flexural modulus (GPa)	2.91-3
Flexural strength (MPa)	120-130
Elongation at break (%)	5.5-6.5

The values in Tables 7.8-10 were used as reference points for comparison with values obtained from the literature review and in the present research project. They were also used to inform the calculations applied to the different models.

The technical data sheet (TDS) is presented in Appendix A4.

## **7.2.4. Chemical products**

### **7.2.4.1. Sodium hydroxide (NaOH)**

CAS Number: 1310-73-2

Molecular Weight: 40

Form: granules

Supplier: Sigma-Aldrich ("Sigma-Aldrich NaOH", 2017)

### 7.2.4.2. 3-(trimethoxysilyl) propylamine (BYK-C 8001)

CAS Number: 82985-35-1

Molecular Weight: 179.29 (C<sub>6</sub>H<sub>17</sub>NO<sub>3</sub>Si)

Form: viscous liquid

Supplier/Code: BYK-Chemie GmbH / BYK-C 8001 Coupling Agent for Epoxy Composites (BYK C-8001)

Table 7.11: Information from BYK-C 8001 Safety Data Sheet (MSDS)

Chemical name	CAS-No. EC-No. Registration Number	Classification (67/548/EEC )	Classification (REGULATION (EC) No 1272/2008)	Concentration (%)
3-(trimethoxysilyl)propylamine	13822-56-5 237-511-5 01- 2119510159-45	Xi; R38 Xi; R41	Skin Irrit. 2; H315 Eye Dam. 1; H318	>= 50 - < 100
Methanol	67-56-1 200-659-6 01- 2119433307-44	F; R11 T; R23/24/25- R39/23/24/25	Flam. Liq. 2; H225 Acute Tox. 3; H331 Acute Tox. 3; H311 Acute Tox. 3; H301 STOT SE 1; H370	>= 1 - < 3

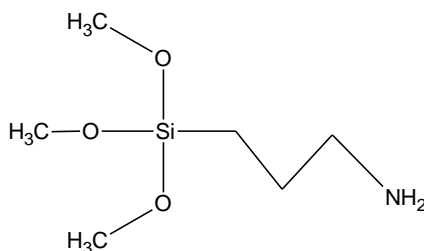


Figure 7.5: 3-(trimethoxysilyl) propylamine structure

### 7.2.4.3. Ethanol (Ethyl alcohol CH<sub>3</sub>CH<sub>2</sub>OH)

CAS Number: 64-17-5

Molecular Weight: 46.07

Form: thin clear liquid

Supplier: Sigma-Aldrich ("Sigma-Aldrich Ethanol", 2017)

### **7.2.5. Infusion consumables** (“Easy Composites”, 2017)

Vacuum bag: AeroFilm® VB160

Peel-ply: AeroFilm® PP230

Flow mesh: AeroFilm® FM105

Pipes: 1/2" I.D. Wire Reinforced Vacuum Hose

Spiral: Resin Infusion Spiral Medium Flow 10m Coil

VAP membrane: AB production material (commercially sensitive data not released for this thesis)

Tacky tape: Vacuum Bagging Gum Sealant Tape 15m

### **7.3. TREATMENT PROCEDURE**

Experimental procedures for modifying the matrix, and the chemical treatment for the NF were selected from the options in the literature review in Chapter 4. The most appropriate method was selected for each procedure with emphasis upon the economic viability, the operational validity and the effectiveness of each selection.

In the Laminates from 1 to 29, for each fibre/matrix combination, one laminate was produced and two sets of samples are extracted: (i) for the evaluation of longitudinal tensile properties; and (ii) for the evaluation of transverse tensile properties. Laminates 1, 2, 3, 4 and 29 were tested in order to get the base properties, **untreated systems mechanical properties**, in longitudinal and transverse directions. For the **modified systems**, from Laminate 5 to 28, the longitudinal test was used to check if the fibre had been damaged during the test, and the transverse test to check the evolution of the fibre/matrix interface.

After undertaking the following processes – treatment of the fibres, production of the laminate, and the cutting and testing of the samples - the data recorded was used to determine which treatments had the greatest value/effectiveness to undertake the research. Once this process was completed, the

know-how information was applied to **Supersap CLR-INF/ Biotex UD composite system**; Laminates 30 to 36 were manufactured and tested to complete the characterisation process.

The laminate samples were investigated for the following procedures - mercerisation, matrix modification and silanisation

### **7.3.1. Mercerisation**

In the research Project, a similar method to that proposed by Kim and Netravali (KN) [194] to increase the sisal fibre/soy resin in the composite system was applied (See Chapter 4 section 4.1). The KN sisal fibre was immersed in 2M NaOH solution for 2 hours at RT, washed with water, neutralised with acetic acid and finally dried at RT. This method was selected because of its low energy consumption, its effectiveness in the improvement of mechanical properties and its potential for a low pollutant product. In the KN study, in comparison with the reference control sample, the highest quality results were achieved when the fibre tension was at 50g/fibre, reaching strength of 35% and showing a modulus increase of 111%.

The method developed for treating the NF had the following major procedures:

- The fibres were immersed in five different solutions, **0.25M, 0.5M, 1M, 1.5M** and **2M** solutions, to avoid damaging the mechanical performance of the fibres since it is implied in the literature that the application of a 2M solution might be damaging, although Kim and Netravali [194] have stated otherwise.
- An alternative option was to increase the concentration of the solution and reduce the immersion time; however, the intention was to proceed in the opposite direction, by extending the immersion time and maintaining or reducing the solution concentration. This procedure was undertaken to minimise/eliminate the production of pollutant substances. Based on this strategy the fibres were immersed for **2h, 4h, 12h** and **24h**; -the fibres were

**dried for 24h at RT;** the fibres were **not washed with water, but neutralised with acetic acid** and **dried in the oven**. The objective was to minimise both pollutant production and the consumption of energy.

Based on the procedures above, twenty (20) different options were defined for the mercerisation of the NF as presented in Table 7.12.

Table 7.12: Different options in the Mercerisation process

Mercerisation	<b>1h</b>	<b>3h</b>	<b>12h</b>	<b>24h</b>
<b>0.25M</b>	Laminate 5	Laminate 6	Laminate 7	Laminate 8
<b>0.5M</b>	Laminate 9	Laminate 10	Laminate 11	Laminate 12
<b>1M</b>	Laminate 13	Laminate 14	Laminate 15	Laminate 16
<b>1.5M</b>	Laminate 17	Laminate 18	Laminate 19	Laminate 20
<b>2M</b>	Laminate 21	Laminate 22	Laminate 23	Laminate 24

### 7.3.2. Matrix modification

The matrix was modified with **1%** (in resin/hardener system weight) of 3-(trimethoxysilyl) propylamine. The silane was added directly to the epoxy system hardener and stirred; once it had been fully mixed it was added to the epoxy base resin. This procedure has been described as "Epoxy matrix modification" in Chapter 4, section 3.1.1. Of equal relevance the studies presented by Wang, et al. and Chruściel et al. suggested that the interfacial properties of the composite fibre/matrix might be improved by adding silanes to the petrochemical matrix for use with synthetic fibres. To evaluate this matrix modification method in this PhD, two laminates were manufactured; Laminate 25 and Laminate 26. From the Laminate 5-24 tests, the best mercerisation treatment was identified: **1M NaOH for 3h**, the results from **Laminate 14**. *Laminate 25* was manufactured with untreated flax fibre/ 1% silane modified epoxy matrix and *Laminate 26* was manufactured with 1M NaOH for 3h mercerised flax fibre/ 1% silane modified epoxy matrix (Table 7.13).

Table 7.13: Matrix modification different options

<b>Epoxy system</b>	<b>Untreated</b>	<b>1M NaOH 3h</b>
<b>Modified (1%)</b>	Laminate 25	Laminate 26

### 7.3.3. Silanisation

The silanisation process was undertaken by combining the most relevant factors identified in the literature review (Chapter 4, section 5.2) with due reference to sustainable issues. The methodology adopted the following procedure – the NF laminates were immersed in a 1-5% silane solution in water/solvent, washed with water and dried in the oven for some hours at 80-100°C. However, the Van de Weyenberg [160] treatments were considered to be the most effective, the easiest to perform, economically viable, and were deemed to be the greenest; additionally, silanisation is performed once the NF has been mercerized. One change from the Van de Weyenberg treatment was that the drying was at RT for 48 h, thus reducing energy consumption.

The previously activated, mercerised and aligned fibres were immersed in **1%** (in solution weight) 3-(trimethoxysilyl) propylamine solution (**50%/50% by volume of ethanol/water**) then **dried at RT for 48h**. Laminate 27 was produced with 1% silanised flax fibre and epoxy resin but was not mercerised; laminate 28 was produced with both mercerised (1M NaOH 3h) and silanised flax fibre and epoxy resin. See Table 7.14.

Table 7.14: Different options for the silanisation process

<b>Solution</b>	<b>Untreated</b>	<b>1M NaOH 3h</b>
<b>1% Silanised</b>	Laminate 27	Laminate 28

## 7.4. DEFINITION OF THE MANUFACTURING EQUIPMENT

### 7.4.1. Lamination table

Laminates 1 and 2 were produced at UniZar. The laminates were formed on a steel plate then cured in an oven preheated for 30min before introducing the laminates for cure at 80°C for 2h. In contrast, laminates 3 to 36 were produced in AB, and manufactured on an AMOND lamination table (Figure

7.6). The process was monitored with AB in-house software and cured on an electrically heated mould tool (Figure 7.7).

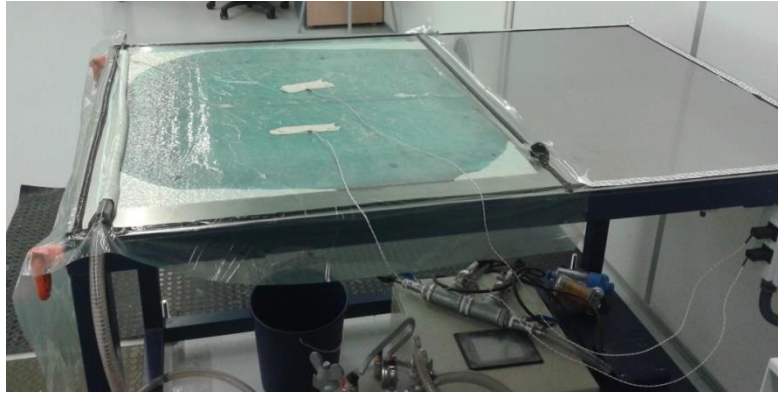


Figure 7.6: Lamination table controlled by thermocouples



Figure 7.7: Control software - (Left) Lamination table (Right) computer interface display

#### 7.4.2. Cutting machine

The AB Mutronic DIADISC 5200R was selected for ease of sample manufacturing (Figure 7.8).

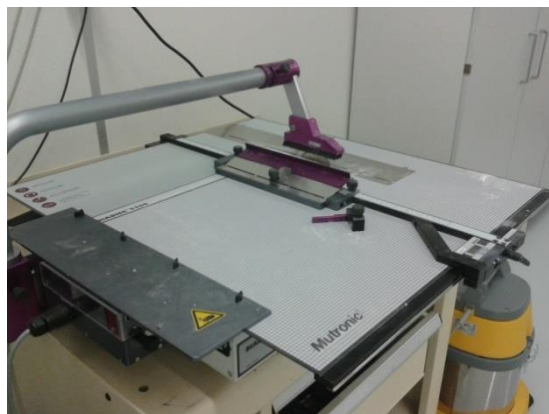


Figure 7.8: DIADISC 5200R cutting machine

### 7.4.3. Universal testing machine

Two Universal machines were used as follows:

- Unizar: Universal testing machine Ibertest STIB 200 W, computer coupled, accuracy class 1 according to UNE-EN-ISO-7500-1:2006, load cell 200kN.
- AB: Universal testing machine Shimadzu AG-X PLUS 250kN, computer coupled, TRAPEZIUM X software, accuracy class 0.5 according to UNE-EN-ISO-7500-1:2006, load cell 100kN (Figure 7.9).



Figure 7.9: Shimadzu AG-X PLUS 250kN Universal testing machine

## 7.5. LAMINATE MANUFACTURE

Laminate manufacturing was divided in three different blocks, Laminates 1, 2, 3, 4 and 29 to acquire base properties, Laminates 5 to 28 for the best treatment selection, Laminates 30 to 36 for optimised system complete mechanical characterisation. Table 7.15 summarises all the manufactured laminates.

To obtain reference properties, Supersap CLR-INF/ Biotex UD composite system was completely characterised. For this aim two different laminates were manufactured: (i) laminate 1 for longitudinal tensile test ( $T0^\circ$ ), transverse tensile ( $T90^\circ$ ),  $10^\circ$  in-plane shear test ( $S10^\circ$ ); and (ii) laminate 2 for the longitudinal compression ( $C0^\circ$ ) and transverse compression ( $C90^\circ$ ) tests. The standards used for testing are given in §7.5.1 below.



The Laminate 3 samples were produced and tested at AB laboratory to obtain longitudinal and transverse reference properties for Huntsman/Biotex UD composite system. Additionally, Laminate 29 was manufactured using VAP membrane in the process, this was done to establish any effect of the membrane.

The Laminate 4 samples were produced and tested at AB laboratory to obtain longitudinal and transverse reference properties for Lineo/ Biotex UD composite system. Lineo commercially available fabric is already pre-treated with a patented treatment method to enhance the fibre/matrix interfacial properties.

For Laminates 5-28, the fibres were treated in the 5'TX" surf workshop and subsequent panel manufacturing and testing were undertaken at AB. Optimised system Laminates 30 to 36 were manufactured and tested in AB.

Note that Laminates 3-29 used petrochemical **Araldite LY 1569 CH/Aradur 3489 CH** Huntsman epoxy resin, because it is (i) more readily available, (ii) relatively inexpensive and (iii) the formulation manufacturing parameters are well-known.

Flax fabric wettability was modified by the treatments, so it proved necessary to modify the infusion strategy as the experimental campaign progressed.

All the experimental tests undertaken on the laminates in the project are summarised in Table 7.15.

Table 7.15: List of UD Laminate manufacturing tests undertaken with Biotex or Lineo flax fibra and Supersap CLR/INF or Araldite LY 1569 /Aradur 3489 epoxy matrix

ID	Matrix	Fibre	Layers	Treatment			Method	Where
				None	NaOH	Silane		
1	Supersap CLR/INF	Biotex	4	✓	*	*	No	Unizar
2	Supersap CLR/INF	Biotex	8	✓	*	*	No	Unizar
3	LY 1569 / 3489	Biotex	4	✓	*	*	No	AB
4	LY 1569 / 3489	Lineo	8	✓	*	*	No	AB
5	LY 1569 / 3489	Biotex	4	*	✓	*	0.25M/1h	5'TX''/AB
6	LY 1569 / 3489	Biotex	4	*	✓	*	0.25M/3h	5'TX''/AB
7	LY 1569 / 3489	Biotex	4	*	✓	*	0.25M/12h	5'TX''/AB
8	LY 1569 / 3489	Biotex	4	*	✓	*	0.25M/24h	5'TX''/AB
9	LY 1569 / 3489	Biotex	4	*	✓	*	0.5M/1h	5'TX''/AB
10	LY 1569 / 3489	Biotex	4	*	✓	*	0.5M/3h	5'TX''/AB
11	LY 1569 / 3489	Biotex	4	*	✓	*	0.5M/12h	5'TX''/AB
12	LY 1569 / 3489	Biotex	4	*	✓	*	0.5M/24h	5'TX''/AB
13	LY 1569 / 3489	Biotex	4	*	✓	*	1M/1h	5'TX''/AB
14	LY 1569 / 3489	Biotex	4	*	✓	*	1M/3h	5'TX''/AB
15	LY 1569 / 3489	Biotex	4	*	✓	*	1M/12h	5'TX''/AB
16	LY 1569 / 3489	Biotex	4	*	✓	*	1M/24h	5'TX''/AB
17	LY 1569 / 3489	Biotex	4	*	✓	*	1.5M/1h	5'TX''/AB
18	LY 1569 / 3489	Biotex	4	*	✓	*	1.5M/3h	5'TX''/AB
19	LY 1569 / 3489	Biotex	4	*	✓	*	1.5M/12h	5'TX''/AB
20	LY 1569 / 3489	Biotex	4	*	✓	*	1.5M/24h	5'TX''/AB
21	LY 1569 / 3489	Biotex	4	*	✓	*	2M/1h	5'TX''/AB
22	LY 1569 / 3489	Biotex	4	*	✓	*	2M/3h	5'TX''/AB
23	LY 1569 / 3489	Biotex	4	*	✓	*	2M/12h	5'TX''/AB
24	LY 1569 / 3489	Biotex	4	*	✓	*	2M/24h	5'TX''/AB
25	LY 1569 / 3489	Biotex	4	*	*	✓	1% hardener	AB
26	LY 1569 / 3489	Biotex	4	*	✓	✓	1M/3h+1% hardener	5'TX''/AB
27	LY 1569 / 3489	Biotex	4	*	*	✓	1% fibre	AB
28	LY 1569 / 3489	Biotex	4	*	✓	✓	1M/3h+1% fibre	5'TX''/AB
29	LY 1569 / 3489	Biotex	4	✓	*	*	No	AB
30	Supersap CLR/INF	Biotex	8	✓	*	*	No	AB
31	Supersap CLR/INF	Biotex	4	*	*	✓	1% hardener	AB
32	Supersap CLR/INF	Biotex	8	*	*	✓	1% hardener	AB
33	Supersap CLR/INF	Biotex	4	*	*	✓	1% hardener	AB
34	Supersap CLR/INF	Biotex	4	✓	*	*	No	AB
35	Supersap CLR/INF	Biotex	4	*	*	✓	1% hardener	AB
36	Supersap CLR/INF	Biotex	4	✓	*	*	No	AB

### 7.5.1 Laminates 1 and 2

The manufacturing parameters of the UniZar reference laminates 1 and 2 are summarised in Table 7.16. The infusion process is illustrated in Figure 7.10 and the lamination scheme for the two laminates is shown in Figure 7.11.

Table 7.16: Manufacturing characteristics of laminate 1 and 2

	<b>Laminate 1</b>	<b>Laminate 2</b>
Test samples	T0°, T90°, Sh10°	C0°, C90°
Reinforcement	4 layers of fabric	8 layers of fabric
Fabric weight (gsm)	275	275
Fabric dimensions	450mm x 330 mm	450mm x 330 mm
Mass of fabric (g)	163.35	326.70
Resin used (g)	177	354.7
Resin preheat	40°C for 30 min	40°C for 30 min
Infusion vacuum (atm gauge)	0.9	0.9
Infusion time (minutes)	17	23
Cure cycle	5min RT + 2h @ 80°C	2h @ 80°C



Figure 7.10: Manufacturing process for laminates 1 and 2

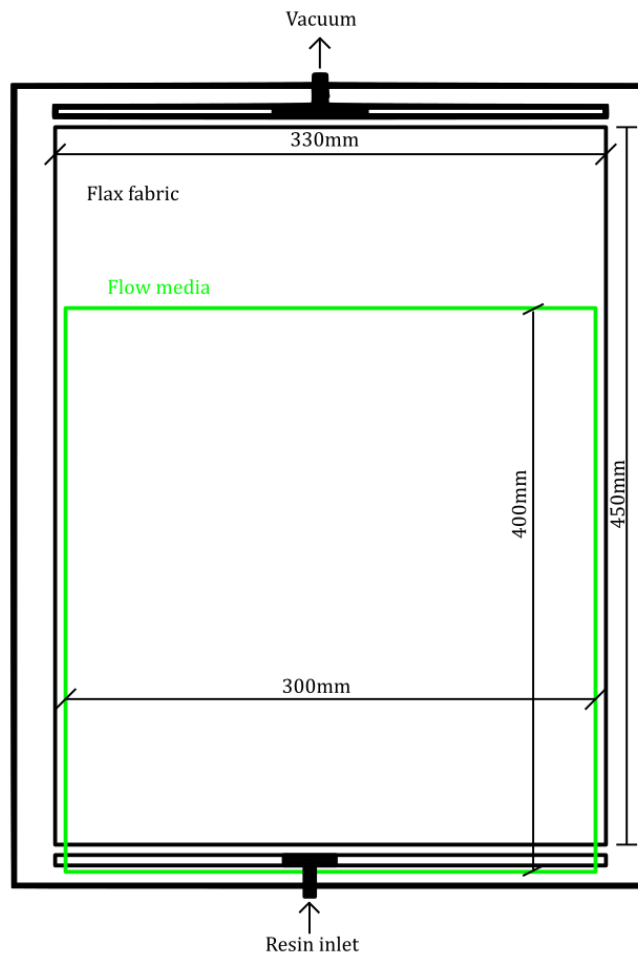


Figure 7.11: Lamination scheme for laminates 1-2

### 7.5.2. Laminates 3 and 4

The manufacturing parameters of the AB reference laminates, 3 Biotex and 4 Lineo, are summarised in Table 7.17. Both laminates were infused in one shot under the same infusion strategy as illustrated in Figure 7.12. Figure 7.13 shows the lamination scheme for laminates 3 and 4.

Table 7.17: Manufacturing characteristics of laminate 3-4

	<b>Laminate 3</b>	<b>Laminate 4</b>
Test samples	T0°, T90°	T0°, T90°
Reinforcement	4 layers of fabric	8 layers of fabric
Fabric weight (gsm)	275	150
Fabric dimensions	600mm x 330 mm	600mm x 330 mm
Mass of fabric (g)	218	120
Resin used (g)	1000	1000
Infusion temperature (°C)	40	40°C for 30 min
Infusion vacuum (atm gauge)	0.93	0.93
Infusion time (minutes)	12	12
Cure cycle	2h @ 65°C + 1h @ 80°C + 1h @ 100°C	2h @ 65°C + 1h @ 80°C + 1h @ 100°C
Tg (°C)	65	65

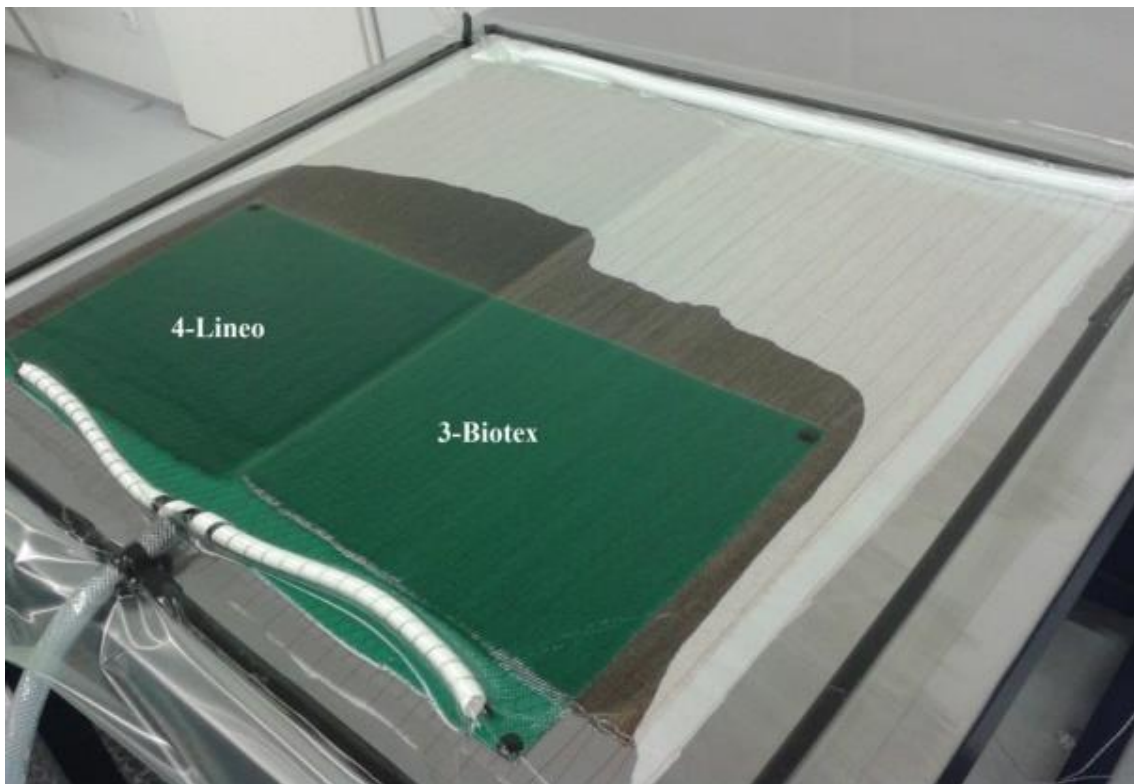


Figure 7.12: manufacturing process of laminates 3 and 4

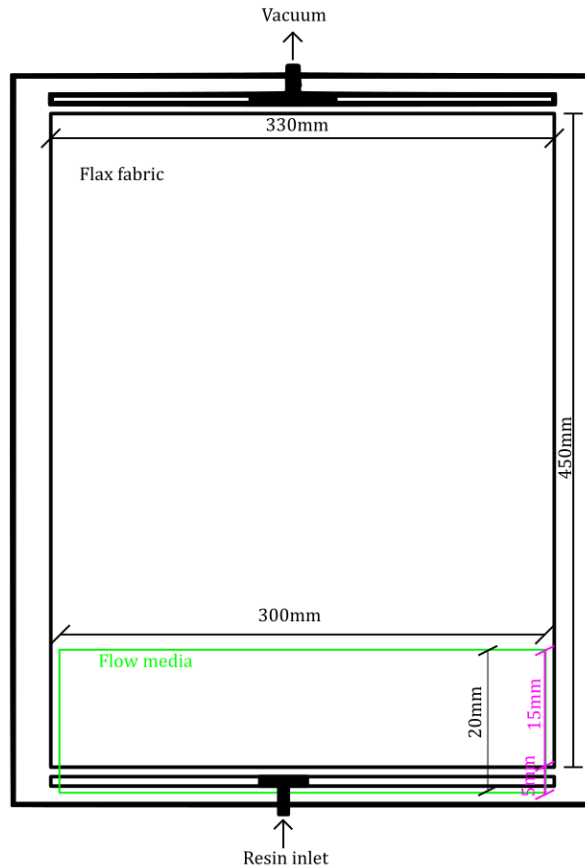


Figure 7.13: Lamination scheme for laminates 3 and 4

### 7.5.3. Laminate 5 to 20

Once the base properties were clear, a different mercerisation treatments were applied to the Biotex/Huntsman composites system. Four laminates were manufactured at one shot as it is shown in Figure 7.14. The laminates manufacturing parameters are summarised in Table 7.18. Figure 7.15 shows the scheme for each of laminate 5 to 20 characteristics.

Table 7.18: Manufacturing characteristics of laminate 5 to 20

	<b>Laminate 5 to 20</b>
Test samples	T0°, T90°
Reinforcement	4 layers of fabric
Fabric weight (gsm)	275
Fabric dimensions	600mm x 330 mm
Mass of fabric (g)	218
Resin used (g)	1000
Resin preheat	40°C for 30 min
Infusion vacuum (atm gauge)	0.93-5
Infusion time (minutes)	12-52
Cure cycle	2h @ 65°C + 1h @ 80°C + 1h @ 100°C
Tg (°C)	65

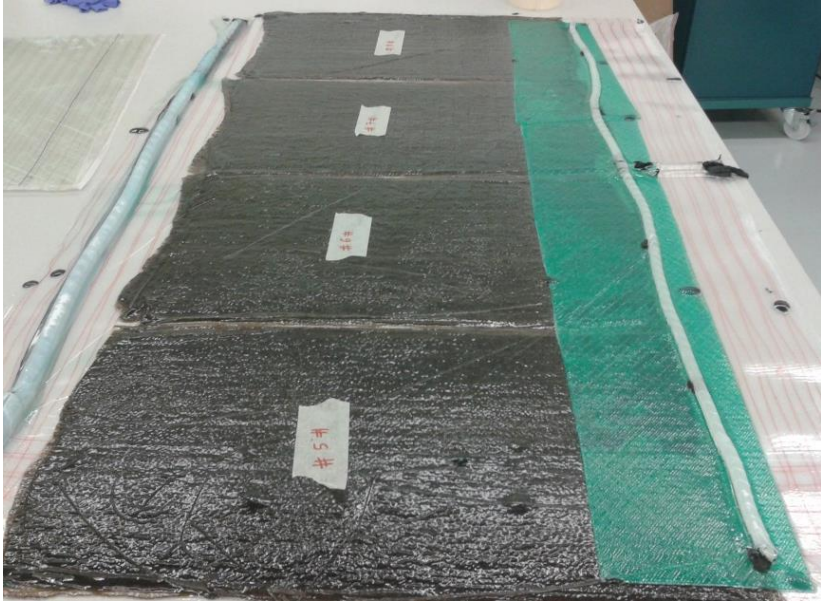


Figure 7.14: Manufacturing process for laminates 5 to 8

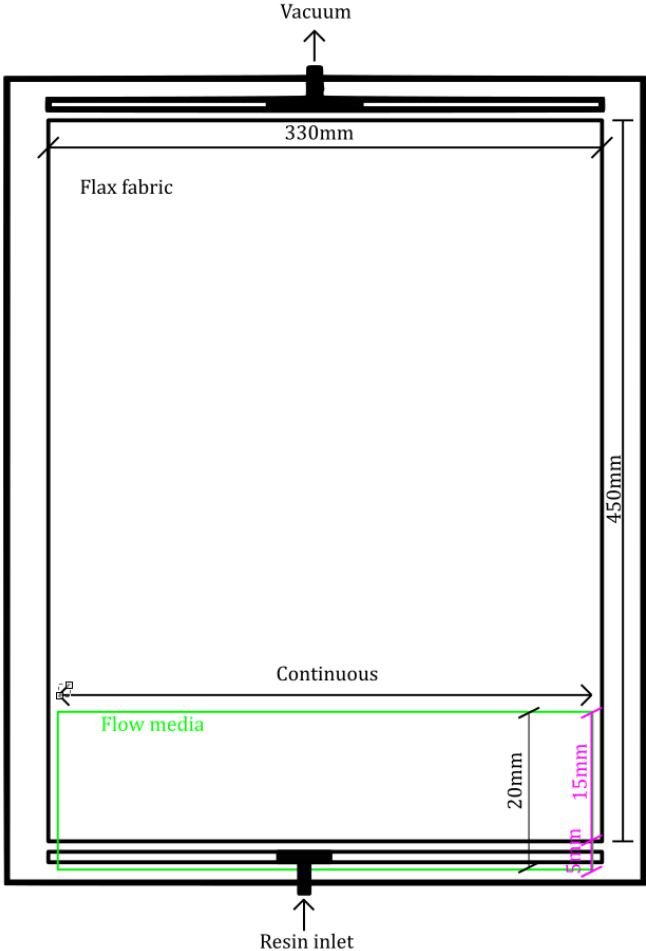


Figure 7.15: Lamination scheme for laminates 5 to 20

#### 7.5.4. Laminate 21 to 24

Once the base properties were clear, different mercerisation treatments were applied to Biotex/Huntsman composites system. Four laminates were manufactured at one shot (Figure 7.16). On this occasion, flow media was placed covering all the laminate surface and VAP membrane introduced to the laminate scheme (Figure 7.17). The infusion strategy was modified since the mercerisation treatment provoked fibre swelling (as previously observed by other researchers [Francucci 13, Masoodi 14 and Nguyen 15]) with the consequent flow reduction in the infusion process. The laminate manufacturing parameters are summarised in Table 7.19. Figure 7.17 shows the scheme for a single laminate with 21 to 24 laminates characteristics.

Table 7.19: Manufacturing characteristics of laminates 21 to 24

	<b>Laminate 21 to 24</b>
Test samples	T0°, T90°
Reinforcement	4 layers of fabric
Fabric weight (gsm)	275
Fabric dimensions	600mm x 330 mm
Mass of fabric (g)	218
Resin used (g)	1000
Resin preheat	40°C for 30 min
Infusion vacuum (atm gauge)	0.93-5
Infusion time (minutes)	-
Cure cycle	2h @ 65°C + 1h @ 80°C + 1h @ 100°C
Tg (°C)	65



Figure 7.16: Manufacturing process for laminates 21-24

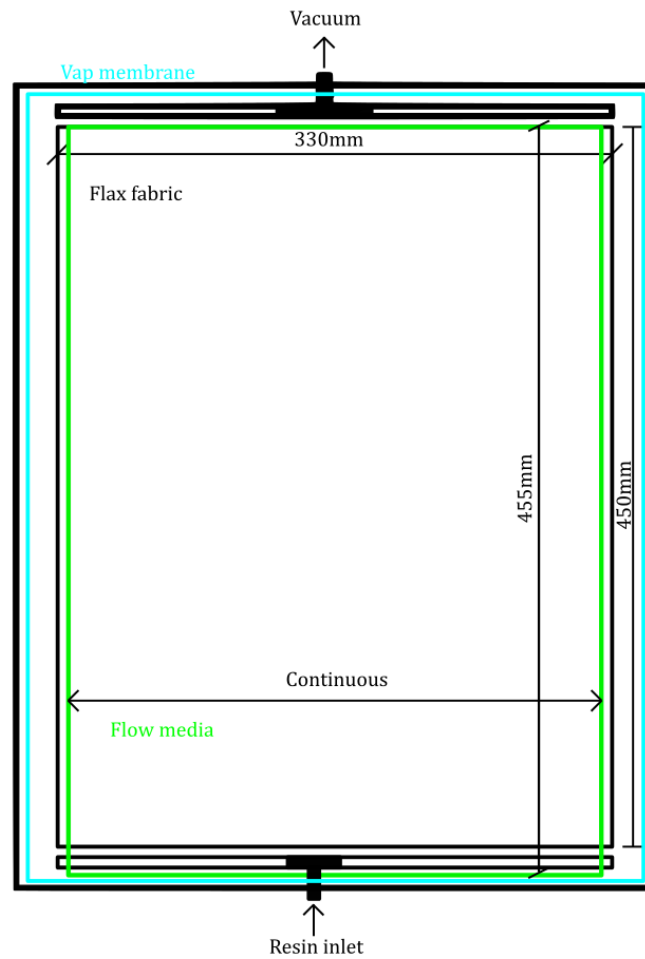


Figure 7.17: Lamination scheme for laminates 21-24

For laminates 25-36, the flow medium was placed covering all the laminate surface and VAP membrane introduced to the laminate scheme.

### 7.5.5. Laminate 25 to 28

Once the best mercerisation treatment was selected, silanisation process was performed on the Biotex flax UD fabric. For laminates 25-26, the resin system was modified. For laminates 27-28, the fibre was modified. For all of these cases, the manufacturing characteristics (Table 7.19) and lamination scheme (Figure 7.17) were common. On this occasion, two laminates were manufactured at one shot (Figure 7.18).



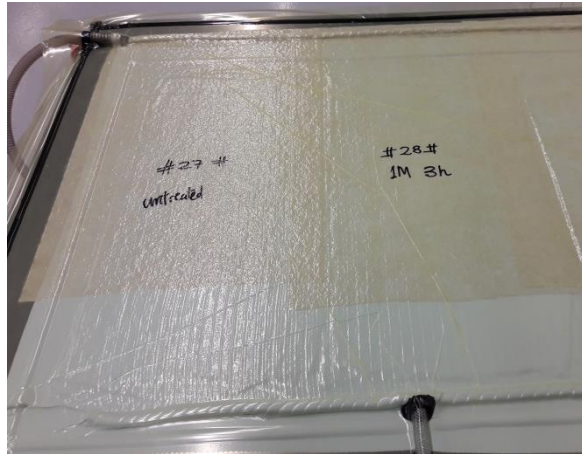


Figure 7.18: manufacturing process of laminates 27 and 28

#### **7.5.6. Laminate 29**

Laminate 29 was manufactured to determine whether the mechanical properties differ from Laminate 3 properties when the manufacturing conditions were modified; both were manufactured with Biotex/Huntsman combination. The manufacturing characteristics were described in Table 7.19 and lamination scheme in Figure 7.17.

#### **7.5.7. Laminate 30 and 32**

Laminates 30 and 32 were manufactured to evaluate the silane addition to the matrix in compression and interlaminar shear properties. Both laminates were manufactured with Biotex/SuperSap composite system, and in the Laminate 32 production 1% silane was added to the matrix. The manufacturing characteristics were described in Table 7.19 and lamination scheme in Figure 7.17.

#### **7.5.8. Laminate 31**

Laminate 31 was manufactured in order to get optimised system mechanical properties. The samples were tested using strain gauges in order to get the more accurate mechanical properties. The manufacturing characteristics were described in Table 7.19 and lamination scheme in Figure 7.17.

#### **7.5.9. Laminate 33 and 34**

Laminates 33 and 34 were manufactured in order to evaluate the silane addition to the matrix in flexural properties. Both laminates were manufactured with Biotex/SuperSap composite system, and

in the Laminate 33 production 1% silane was added to the matrix. The manufacturing characteristics were described in Table 7.19 and lamination scheme in Figure 7.17. In this occasion two laminates were manufactured at one shot (Figure 7.19).



Figure 7.19: manufacturing process of laminates 33 and 34

#### 7.5.10. Laminate 35 and 36

Laminates 35 and 36 were manufactured in order to evaluate the silane addition to the matrix in in-plane shear properties. Both laminates were manufactured with Biotex/SuperSap composite system, and in the Laminate 35 production 1% silane was added to the matrix. The manufacturing characteristics were described in Table 7.19 and lamination scheme in Figure 7.17. In this occasion two laminates were manufactured at one shot (Figure 7.20).

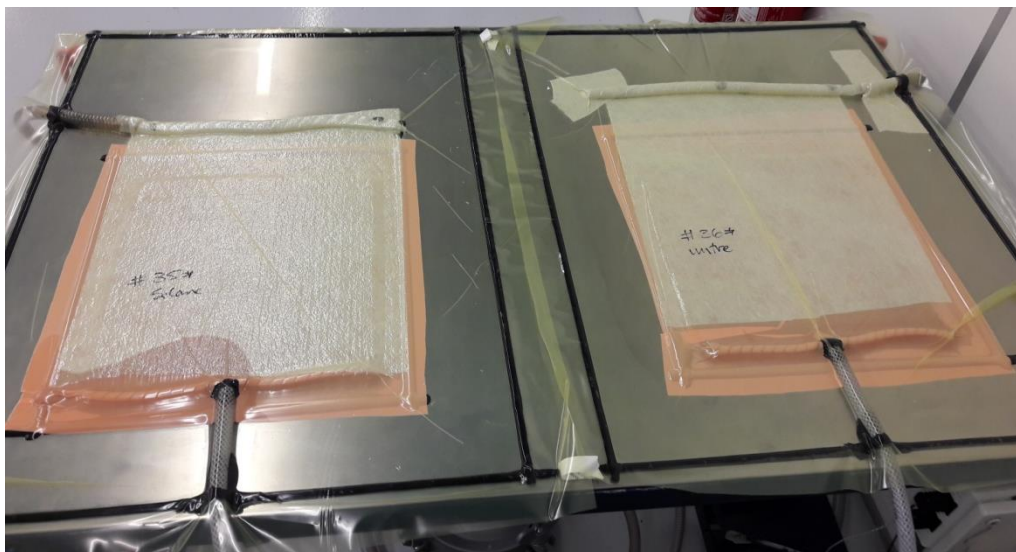


Figure 7.20: manufacturing process of laminates 35 and 36

## 7.6. TEST

In the research process, between six and ten samples were tested for each laminate in every specified type of test. The procedures were defined by international (ISO) standards indicated below.

### 7.6.1. Test standards

The following standard tests were conducted:

- Tension (ISO527-5 for unidirectional or ISO527-4 for multiaxial composites)
- Compression (ISO 14126:1999)
- In-plane shear 10° off-axis
- In-plane shear  $\pm 45^\circ$  (BS EN ISO 14129:1998) for unidirectional composites
- ILSS (ASTM D2344)
- Flexural test (ASTM D 790-03)

In all the tests performed, the thickness measurement was the arithmetic mean from three different positions. Test data for the standards included - stress-strain curves, maximum load, Young's modulus, stress at break (strength), and strain at break.

#### 7.6.1.1. Tensile test

For the **ISO 527-4/-5** tensile test standard, longitudinal and transverse tests were performed on the samples as shown in Table 7.20.

Table 7.20: Longitudinal tensile test conditions

	<b>ISO 527-4/-5 longitudinal tensile test conditions</b>	<b>ISO 527-4/-5 Transverse tensile test conditions</b>
Number of specimens	10	10
Specimen dimensions	250mm x 15mm x a(mm)	250mm x 25mm x a(mm)
Tabs type	Double bonded GF/epoxy $\pm 45^\circ$ tabs	Double bonded GF/epoxy $\pm 45^\circ$ tabs
Tabs dimensions	50mm x 15mm x a(mm)	50mm x 25mm x a(mm)
Free length between tabs	150mm	150mm
Test speed	2mm/min	2mm/min
Strain measurement	Video extensometers	Video extensometers
Test climate	ISO291 class 2	ISO291 class 2

### 7.6.1.2. Compression test

For the **ISO 14126** compression test standard, longitudinal and transverse tests were performed on the samples as shown in Table 7.21:

Table 7.21: Longitudinal compression test conditions

	<b>ISO 14126 longitudinal compression test conditions</b>	<b>ISO 14126 Transverse compression test conditions</b>
Number of specimens	10	10
Specimen dimensions	110mm x 10mm x a(mm)	110mm x 25mm x a(mm)
Tabs type	Double bonded GF/epoxy $\pm 45^\circ$ tabs	Double bonded GF/epoxy $\pm 45^\circ$ tabs
Tabs dimensions	50mm x 10mm x a(mm)	50mm x 25mm x a(mm)
Free length between tabs	10mm	10mm
Test speed	2mm/min	2mm/min
Strain measurement	Strain Gauges	Strain Gauges
Test climate	ISO291 class 2	ISO291 class 2

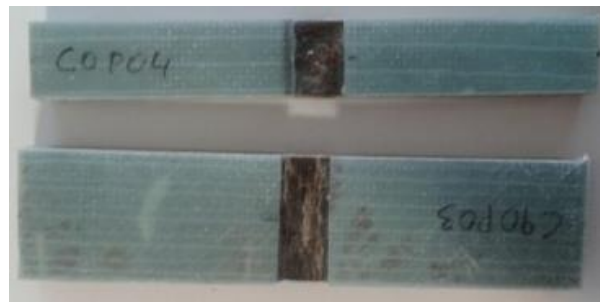


Figure 7.21: UniZar longitudinal and transverse compression test samples

### 7.6.1.3. In-plane shear test

For the in-plane shear properties, both  $45^\circ$  (**ISO 14129** standard) and  $10^\circ$  (no International standard) shear tests were adopted. Samples and test characteristics were identical except for the  $45^\circ$  or  $10^\circ$  angle between the reinforcement and the test axis (Table 7.22).

Table 7.22:  $45^\circ$  and  $10^\circ$  shear test conditions

<b><math>45^\circ</math> (ISO 14129) and <math>10^\circ</math> in-plane shear test conditions</b>	
Number of specimens	10
Specimen dimensions	250mm x 25mm x a(mm)
Tabs type	Double bonded GF/epoxy $\pm 45^\circ$ tabs
Tabs dimensions	50mm x 25mm x a(mm)
Free length between tabs	150mm
Test speed	2mm/min
Strain measurement	Video extensometers
Test climate	ISO291 class 2

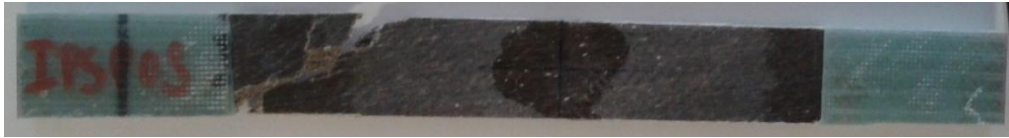


Figure 7.22: UniZar 10° shear test sample

#### 7.6.1.4. Interlaminar shear test (ILSS)

The composite interlaminar shear properties were tested under **ASTM D2344** standard, "*Short-Beam Strength of Polymer Matrix Composite Materials and Their Laminates*". The samples were tested in three-point bending with a short span to promote interlaminar delamination rather than invalid tension, compression or flexure failure modes. Tests conditions are shown in Table 7.23 and test example in Figure 7.23.

Table 7.23: Short-beam test conditions

	<b>ASTM D2344 short-beam test conditions</b>
Number of specimens	10
Specimen dimensions	6 a x 2 a x a (thickness, mm)
Tabs type	No tabs
Span	4 a
Test speed	1mm/min
Test climate	ASTM D 5229



Figure 7.23: Short-beam test sample

#### 7.6.1.5. Three-points bending test

The composite flexural properties were tested under **UN EN ISO14125** standard, "*Fibre-reinforced plastic composites -- Determination of flexural properties*". The samples were tested in three-point bending with a long span designed to get flexural failure. Tests conditions are shown in Table 7.24 and an example tested sample in Figure 7.24.

Table 7.24: Flexural test conditions

<b>UN EN ISO14125 flexural test conditions</b>	
Number of specimens	10
Specimen dimensions	100mm x 15mm x 2(mm)
Span	80mm
Tabs type	No tabs
Test speed	2mm/min
Strain measurement	Bridge movement
Test climate	ISO291 class 2

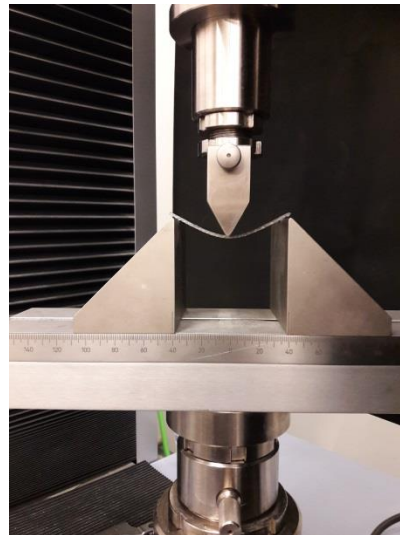


Figure 7.24: Short-beam test sample

### **7.7. TEST PROCEDURE**

Tests performed by AB were undertaken under DNV-GL accredited procedures. The reliability study is attached in Appendix F to show such tests high quality.

### **7.8. TEST DEVIATIONS**

There were three major inconveniences during the testing campaign:

First, in the cutting process the diamond saw blade was burning the surface of the flax/ epoxy composite panels. The cut was precise and clean but friction from the saw was igniting the dust released in the process. To overcome this problem hard steel saw blades were substituted for the diamond blades and they produced equally precise cuts, without burning (Figure 7.25).



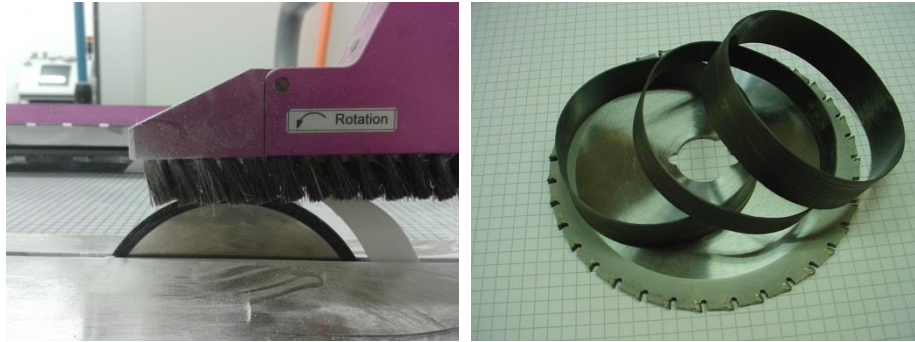


Figure 7.25: Diamond (left) and hard steel (right) saw blades

Second, the material supply times were unreliable. A further constraint was that CE stopped the production of the Biotex UD275 format fabric. This was substituted for a new Biotex UD150 product. In the construction of the Biotex UD275 fabric the longitudinal flax rovings are wrapped by a polyester yarn in order to provide stability to the fabric (Figure 7.26). The wrapping reduces the mechanical properties of the fabric. For this reason, CE has commercialised the Biotex UD150 alternative where the rovings are kept aligned with a binder. Any future work would be limited to use the new Biotex UD150 or any sensible alternative

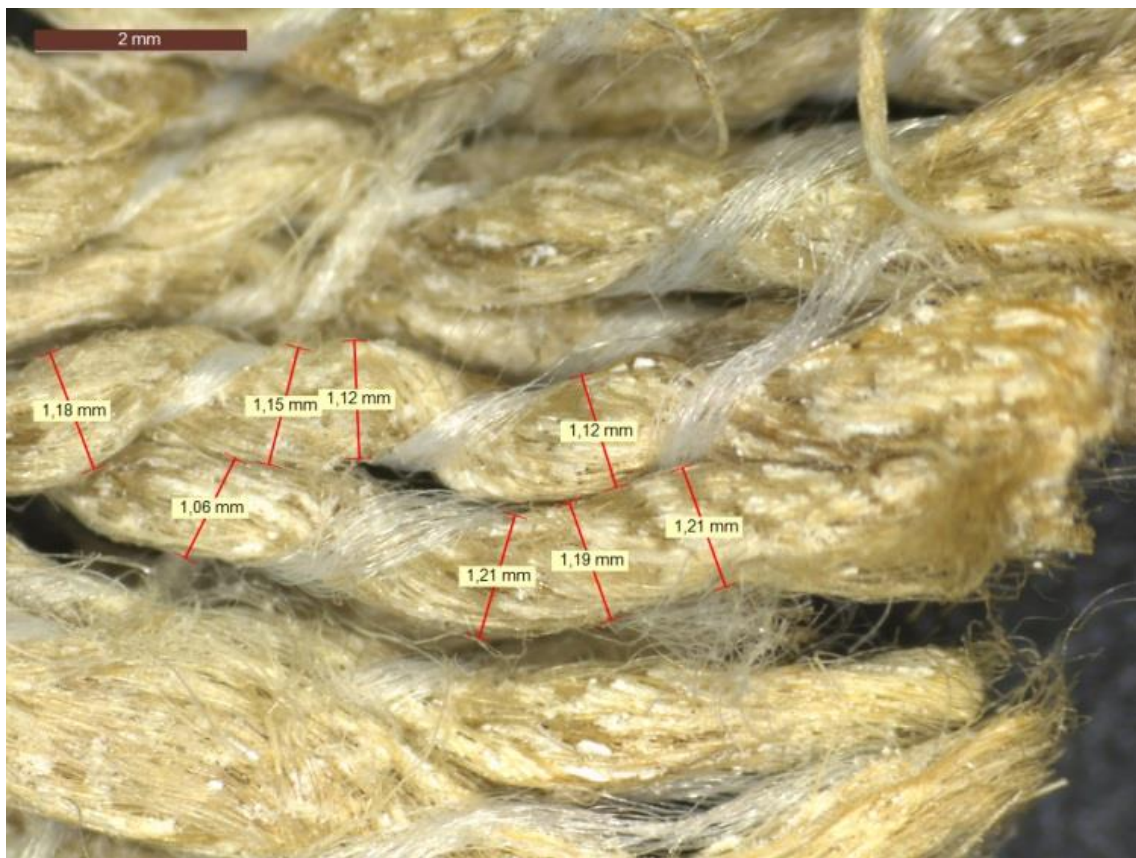


Figure 7.26: Biotex UD275 fabric microscopy image

Third, 2M NaOH produced flax fibre swelling impeding the complete panel infusion. A new trial infusion strategy incorporating VAP was devised to produce laminates 21 to 24 with minimal defects.

## **7.9. SUMMARY**

In Chapter 7 the materials and the equipment used to undertake the research project have been stated and described. The definition of the flax fibre treatment procedures has been reviewed in detail and the selection of the most appropriate procedures addressed based upon the appraisal conducted in Chapter 4.



# 8. Results

## 8.1. INTRODUCTION

Chapter 8 presents the data obtained from the experimental campaign.

## 8.2. MECHANICAL TESTS

Table 8.1 summarises the treatment of the respective laminates. The mechanical testing data is contained in Appendix B, and the page number as indicated in the final column of the Table 8.1. The experimental campaign covers different mechanical tests and all of them give as a result stress-strain curves; an example is shown in Figure 8.1.

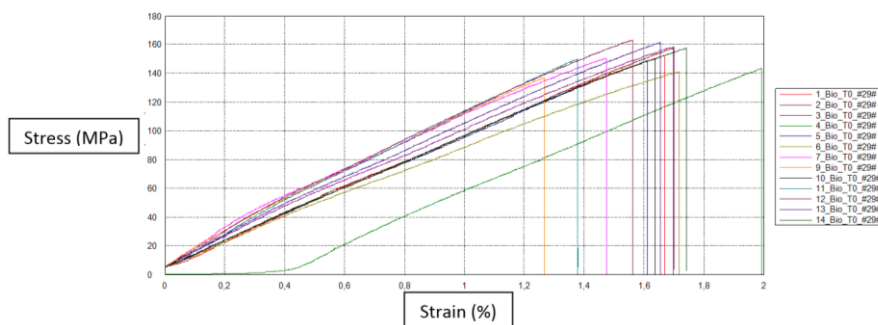


Figure 8.1: Tensile 0° test example (Laminate 29)

During the experimental campaign there are some deviations from the expected data from mechanical tests. In the following point those deviations would be clarified.

1. For transverse tensile test usually some noise is always detected in the deformation signal, this happens because of the interfibre cracking; example **Laminate 1 Tensile 90° test** (Figure 8.2. left) or **Laminate 25 Tensile 90° test**
2. Depending on the software configuration, the negative strains might be plot as negative or positive; example **Laminate 2 Compression 0° test** (Figure 8.2. right)
3. Along all the experimental testing campaign it was seen that sometimes the deformation signal initially goes negative and next it changes to positive, e.g. **Laminate 3 Tensile 0° test** (Figure 8.3. left). This happens because of two factors, initial coupon angle and video-extensometry. The testing coupons have got initial curvature, that angle provokes initial negative deformation record by the extensometers. This phenomenon might be solved using more accurate data acquisition camera or testing with strain gauges. **Laminate 6 Tensile 90° test** (Figure 8.3. right) example is very exaggerated case, where the laminate initial bending provokes negative records
4. Sometimes the video-extensometry stickers release from the testing coupons, getting as a result strange records like in **Laminate 11 Tensile 90° test, samples 6 and 8.** (Figure 8.4. left)
5. When the camera lens is not correctly adjusted the signal line tends to be thicker, example **Laminate 21 Tensile 90° test** (Figure 8.4. right)

6. Some laminates have been tested with strain gauges in order to obtain more accurate modulus and strain values, example **Laminate 29 Tensile 0° test** (Figure 8.5)

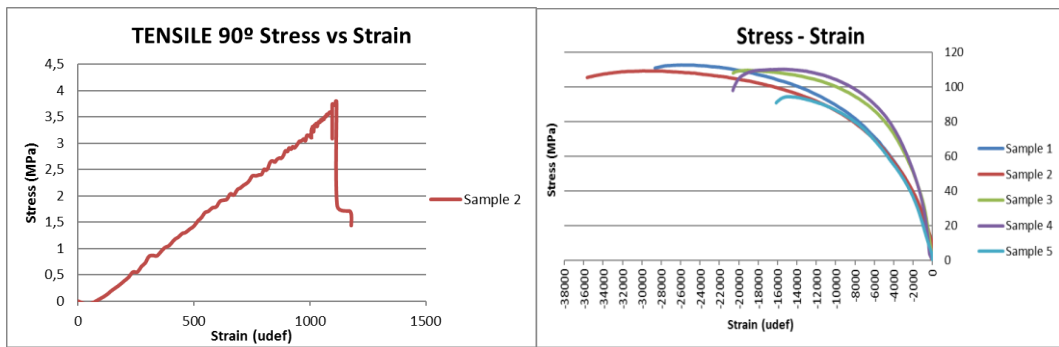


Figure 8.2: 90° tensile test-Laminate 1 (left) and 0° compression test-Laminate 2 (right)

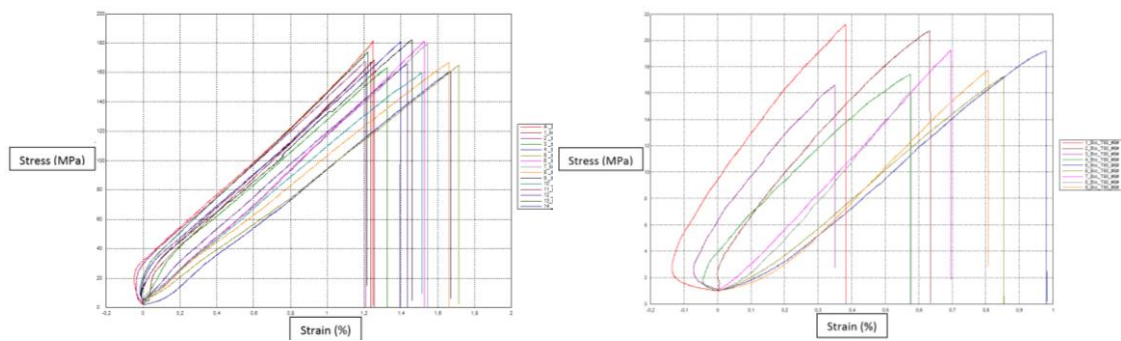


Figure 8.3: 0° tensile test-Laminate 3 (left) and 90° tensile test-Laminate 6 (right)

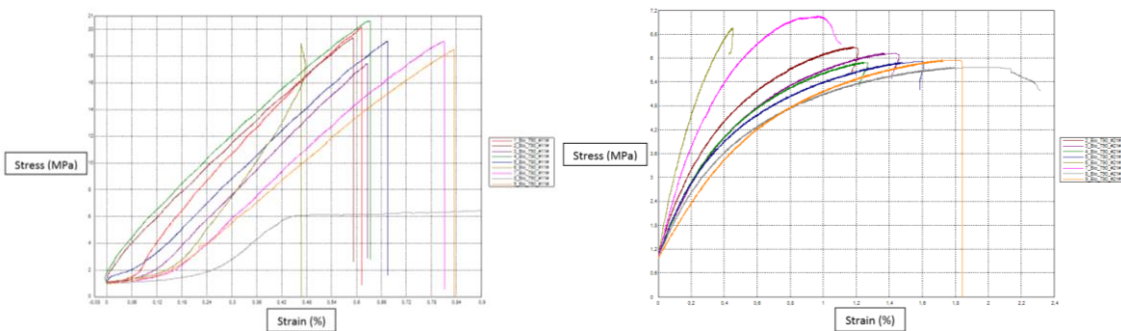


Figure 8.4: 90° tensile test-Laminate 11 (left) and 90° tensile test-Laminate 21 (right)

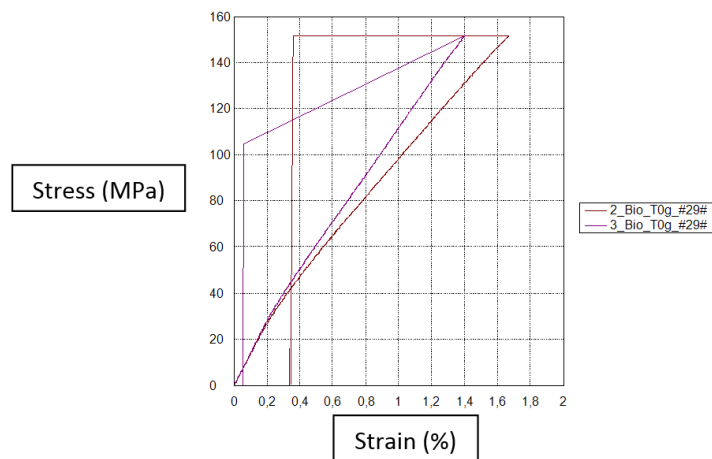


Figure 8.5: 0° tensile test measure with strain gauges-Laminate 29

Table 8.1: Experimental campaign laminates numbering

ID	Matrix	Fibre	Layers	Treatment	Method	Where	APPENDIX C
1	Supersap CLR/INF	Biotex UD	4	No	No	Unizar	Pages 190-191
2	Supersap CLR/INF	Biotex UD	8	No	No	Unizar	Pages 192-193
3	Araldite LY 1569 /Aradur 3489	Biotex UD	4	No	No	AB	Pages 194-195
4	Araldite LY 1569 /Aradur 3489	Lineo UD	8	No	No	AB	Pages 196-197
5	Araldite LY 1569 /Aradur 3489	Biotex UD	4	NaOH	0.25M/1h	5'TX"/AB	Pages 198-199
6	Araldite LY 1569 /Aradur 3489	Biotex UD	4	NaOH	0.25M/3h	5'TX"/AB	Pages 200-201
7	Araldite LY 1569 /Aradur 3489	Biotex UD	4	NaOH	0.25M/12h	5'TX"/AB	Pages 202-203
8	Araldite LY 1569 /Aradur 3489	Biotex UD	4	NaOH	0.25M/24h	5'TX"/AB	Pages 204-205
9	Araldite LY 1569 /Aradur 3489	Biotex UD	4	NaOH	0.5M/1h	5'TX"/AB	Pages 206-207
10	Araldite LY 1569 /Aradur 3489	Biotex UD	4	NaOH	0.5M/3h	5'TX"/AB	Pages 208-209
11	Araldite LY 1569 /Aradur 3489	Biotex UD	4	NaOH	0.5M/12h	5'TX"/AB	Pages 210-211
12	Araldite LY 1569 /Aradur 3489	Biotex UD	4	NaOH	0.5M/24h	5'TX"/AB	Pages 212-213
13	Araldite LY 1569 /Aradur 3489	Biotex UD	4	NaOH	1M/1h	5'TX"/AB	Pages 214-215
14	Araldite LY 1569 /Aradur 3489	Biotex UD	4	NaOH	1M/3h	5'TX"/AB	Pages 216-217
15	Araldite LY 1569 /Aradur 3489	Biotex UD	4	NaOH	1M/12h	5'TX"/AB	Pages 218-219
16	Araldite LY 1569 /Aradur 3489	Biotex UD	4	NaOH	1M/24h	5'TX"/AB	Pages 220-221
17	Araldite LY 1569 /Aradur 3489	Biotex UD	4	NaOH	1.5M/1h	5'TX"/AB	Pages 222-223
18	Araldite LY 1569 /Aradur 3489	Biotex UD	4	NaOH	1.5M/3h	5'TX"/AB	Pages 224-225
19	Araldite LY 1569 /Aradur 3489	Biotex UD	4	NaOH	1.5M/12h	5'TX"/AB	Pages 226-227
20	Araldite LY 1569 /Aradur 3489	Biotex UD	4	NaOH	1.5M/24h	5'TX"/AB	Pages 228-229
21	Araldite LY 1569 /Aradur 3489	Biotex UD	4	NaOH	2M/1h	5'TX"/AB	Pages 230-231
22	Araldite LY 1569 /Aradur 3489	Biotex UD	4	NaOH	2M/3h	5'TX"/AB	Pages 232-233
23	Araldite LY 1569 /Aradur 3489	Biotex UD	4	NaOH	2M/12h	5'TX"/AB	Pages 234-235
24	Araldite LY 1569 /Aradur 3489	Biotex UD	4	NaOH	2M/24h	5'TX"/AB	Pages 236-237
25	Araldite LY 1569 /Aradur 3489	Biotex UD	4	Silane	1% hardener	5'TX"/AB	Pages 238-239
26	Araldite LY 1569 /Aradur 3489	Biotex UD	4	NaOH+Silane	1M/3h+1% hardener	5'TX"/AB	Pages 240-241
27	Araldite LY 1569 /Aradur 3489	Biotex UD	4	Silane	1% fibre	5'TX"/AB	Pages 242-243
28	Araldite LY 1569 /Aradur 3489	Biotex UD	4	Silane	1M/3h+1% fibre	5'TX"/AB	Pages 244-245
29	Araldite LY 1569 /Aradur 3489	Biotex UD	4	No	No	5'TX"/AB	Pages 246-247
30	SuperSap CLR/INF	Biotex UD	8	No	No	5'TX"/AB	Pages 248-250
31	SuperSap CLR/INF	Biotex UD	4	Silane	1% hardener	5'TX"/AB	Pages 251-252
32	SuperSap CLR/INF	Biotex UD	8	Silane	1% hardener	5'TX"/AB	Pages 253-255
33	SuperSap CLR/INF	Biotex UD	4	Silane	1% hardener	5'TX"/AB	Pages 255
34	SuperSap CLR/INF	Biotex UD	4	No	No	5'TX"/AB	Pages 255
35	SuperSap CLR/INF	Biotex UD	4	Silane	1% hardener	5'TX"/AB	Pages 256
36	SuperSap CLR/INF	Biotex UD	4	No	No	5'TX"/AB	Pages 256

### 8.3. FLOW TESTS

In the panels production process different flow properties were observed. Laminates infusion times have been monitored and the results are shown in Table 8.2 and Figure 8.6. In Figure 8.6. it is clearly appreciated a change in the fibre colour, suggesting a degradation of the flax apart from the swelling process.

Table 8.2: Laminates infusion times

Laminates	Concentration (M)	Infusion t (min)
5-8	0.25	14
9-12	0.50	13
13-16	1.00	12
17-20	1.50	52
21-24	2.00	None



Figure 8.6: Laminates 5-8 (left) and laminates 21-24 right

Additionally, three different fibres swelling were studied. Table 8.3 shows fibre diameter measurement results obtained for Untreated, 1M NaOH 3h treated and 2M NaOH 72h treated systems. In the Figure 8.7 technical fibre (> 40  $\mu\text{m}$ ) diameter evolution with the mercerisation process was graph. X-axis lists the measurement points (Appendix C) and Y-axis gives the diameter values in mm.

Table 8.3: measured technical fibre diameters in mm (Appendix C)

Number	Untreated	1M NaOH 3h	2M NaOH 72h
1			0,69
2			0,71
3			0,9
4			0,92
5			0,94
6			1,04
7		0,56	1,05
8	0,67	0,71	1,06
9	0,82	0,73	1,06
10	0,84	0,74	1,06
11	0,85	0,76	1,07
12	0,85	0,78	1,12
13	0,89	0,78	1,12
14	0,9	0,79	1,12
15	0,91	0,83	1,13
16	0,93	0,89	1,13
17	0,93	0,91	1,14
18	0,93	0,93	1,15
19	0,97	0,94	1,15
20	1,01	0,97	1,16
21	1,04	1	1,18
22	1,24	1,01	1,19
23		1,04	1,21
24		1,27	1,21
25		1,28	1,22
26			1,22
27			1,23
28			1,24
29			1,27
30			1,4
Average (mm)	0,92	0,91	1,17

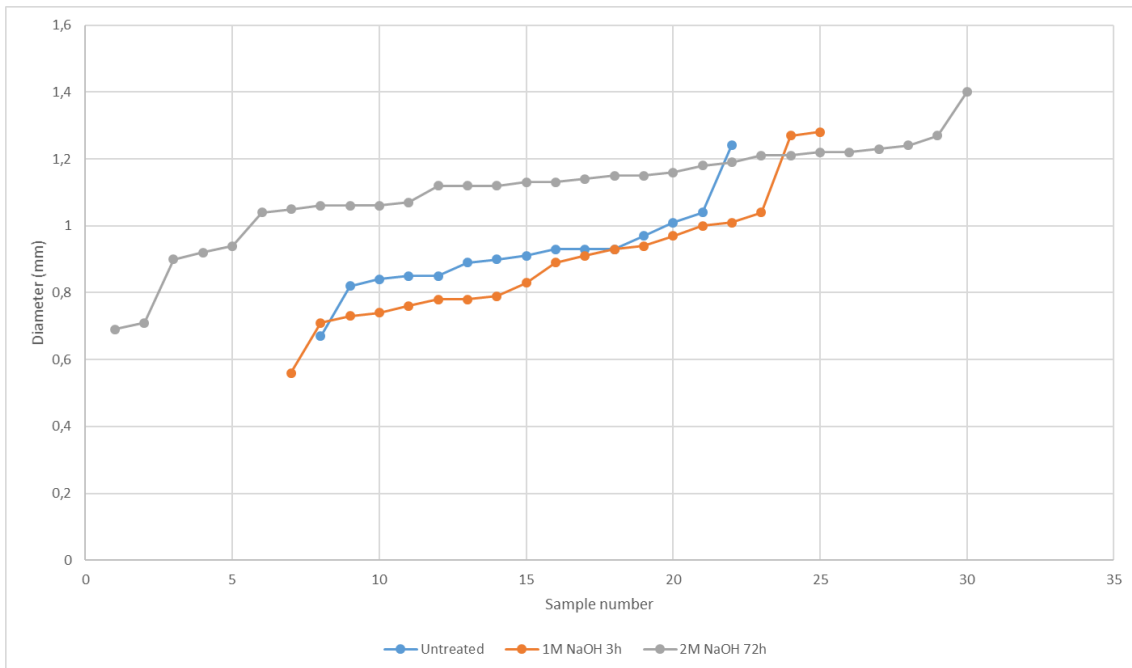


Figure 8.7: Fibre diameter evolution with the mercerisation process

#### 8.4. MOISTURE TESTS

Two different samples were immersed in tap water for a certain days in order to monitor those coupons moisture absorption percentage. The idea was to compare the water uptake percentage for 33 system with silane in the hardener and 34 base system. The sample aging was performed under ASTM D5229 standard. The resulting data after the flexural test was shown in Appendix E.

# Chapter 9: Discussion

## 9.1. INTRODUCTION

The main issue when NFRP are manufactured is the poor adhesion between the NF and the polymer matrix. For that reason many methods have been proposed to improve the NFRP interfacial properties; and the most important methods were reviewed in Chapter 4. The review process identified that mercerisation and silanisation were the most promising methods, given their (i) interfacial properties improvement, (ii) ease of implementation, (iii) sustainability, and (iv) cost effectiveness.

The following sections aim to prove that the selected methods enhance the selected flax/bio-resin composite system interfacial properties in a simple, sustainable and economical way; and thus address the key research question posed for this doctoral study.

Interfacial properties improvement is also believed to enhance the moisture resistance and fatigue properties. Moisture resistance tests were performed in the current study, but fatigue tests were outside the scope and timescale of the current study.

A series of 36 panels were manufactured as described in Chapter 7. Samples were extracted for mechanical testing as described in Chapter 8. The results of individual tests are presented in Appendix B. The panels were divided to have different characteristics:

- 35 with Biotex and 1 with Lineo flax fabric
- 26 with synthetic resin and 10 with bio-based resin
- 13 with untreated, 21 with mercerised fabric, 1 with silanised fabric and 1 with combined mercerisation/silanisation treatment
- 30 with untreated resin system and 6 with coupling agent in the resin hardener

Samples were extracted from the panels for laminate characterisation and mechanical testing, including:

- Plate thickness, fibre volume and mass fraction for every panel

- Longitudinal tension (modulus, strengths, strains at break and Poisson's ratios)
- Transverse tension (modulus and strengths, strains at break and Poisson's ratios)
- Longitudinal compression (modulus, strengths and strains at break)
- Transverse compression (modulus, strengths and strains at break)
- In-plane shear test (modulus, strengths and strains at break)
- ILSS (strength and displacement)
- Flexural tests (displacement, modulus and strength)

A total of 746 laminate thickness measurements, 73 volume fraction determinations, and 746 mechanical tests were conducted.

Additionally, ANOVA (Analysis of Variance) statistical method was applied to the mercerisation data in order to get clearer conclusion from the set of results. ANOVA is a method for testing the hypothesis that there is no difference between two or more population means. The ANOVA analysis process data is shown in Appendix G and the graphs obtained in the §9.2. MERCERISATION.

## **9.2. MERCERISATION**

In this subsection it is studied whether mercerisation process increases flax/epoxy composite interfacial properties, as a part of the PhD research question. In order to make data strong and scientific analysis, ANOVA method was selected. ANOVA method was then applied to the mercerisation data. In the following subsections, ANOVA analysis was complemented with different properties plots for better understanding of the property evolution through the mercerisation process; two plots are obtained, first the property vs. immersion time and second the property vs. concentration. Each property was individually studied and conclusions were obtained in §9.2.8. **"Definitive mercerisation process selection"**.

### **9.2.1. Longitudinal tensile modulus $E_1$ ANOVA**

In this particular case there are three hypotheses to prove. For the null hypothesis, it must be checked whether the mean values of all groups are equal under immersion time, concentration and combinative effect.

For the case of the longitudinal modulus, the **ANOVA analysis confirms that there is significant effect due to immersion time, concentration or combination of both factors**; this was confirmed because after the data analysis the **p-value** is lower than the  $\alpha = 0.05$  for the 95% level of significance, see Table 9.1.

Table 9.1. ANOVA analysis for the  $E_1$

Source	SS	df	MS	F <sub>0</sub>	p-value
Effect A: Immersion time	40975430,507	3	13658476,836	16,076	0,000000002653552740
Effect B: Concentration	1126725565,783	4	281681391,446	331,538	0,000000000000000000
Effect AB: Combined	110512596,819	12	9209383,068	10,839	0,0000000000000000450
Error	152931675,247	180	849620,418		
Total	1431145268,356	199			

The posterior Fisher's analysis says that when the box is red, the difference between mean values is significant, and when the box is unaltered the difference is not significant. The value is significant when the difference is higher than the calculated **LSD (Least Significant Difference)**, in this case **813.402**. See the Fisher's analysis in Tables 9.2 and 9.3.

Table 9.2. Fisher analysis of the immersion time effect in the  $E_1$

0.25M		0.5M		1M		1.5M		2M	
	Value		Value		Value		Value		Value
0.25M 1h - 0.25M 3h	320,29	0.5M 1h - 0.5M 3h	831,79	1M 1h - 1M 3h	78,20	1.5M 1h - 1.5M 3h	2316,65	2M 1h - 2M 3h	1004,57
0.25M 1h - 0.25M 12h	71,28	0.5M 1h - 0.5M 12h	77,80	1M 1h - 1M 12h	2303,38	1.5M 1h - 1.5M 12h	2696,26	2M 1h - 2M 12h	889,64
0.25M 1h - 0.25M 24h	540,21	0.5M 1h - 0.5M 24h	1516,87	1M 1h - 1M 24h	1387,82	1.5M 1h - 1.5M 24h	821,33	2M 1h - 2M 24h	789,56
0.25M 3h - 0.25M 12h	249,01	0.5M 3h - 0.5M 12h	753,99	1M 3h - 1M 12h	2225,18	1.5M 3h - 1.5M 12h	379,61	2M 3h - 2M 12h	114,93
0.25M 3h - 0.25M 24h	860,50	0.5M 3h - 0.5M 24h	685,09	1M 3h - 1M 24h	1309,61	1.5M 3h - 1.5M 24h	3137,98	2M 3h - 2M 24h	215,01
0.25M 12h - 0.25M 24h	611,49	0.5M 12h - 0.5M 24h	1439,07	1M 12h - 1M 24h	915,57	1.5M 12h - 1.5M 24h	3517,59	2M 12h - 2M 24h	100,08

Table 9.2 studies the immersion time effect in the  $E_1$  values. It is initially observed that for the lowest concentration of 0.25M the mean values difference in the set of measurements it is not significant, except for the difference between 3h and 24h. With increasing concentration, the difference between the mean values becomes more significant; for 0.5M the difference is lower than for 1M and 1.5M cases. For the case of 2M concentration, the set of values looks to be homogeneous, except at short immersion times.

Figure 9.1 plots the  $E_1$  variation vs. the immersion time. This graph supports Fisher's analysis in the paragraph above. The variations for 0.25M and 2M concentrations tends to be a line with no fluctuations; for 0.5M the variations is bigger; when for the case of 1M and 1.5M the values variation is more pronounced.



In comparison to the untreated fibre, the mercerisation process provokes an increment of the  $E_1$  value, above the basic system, except for the case of the 2M solution case. For longer immersion times, the difference is lower.

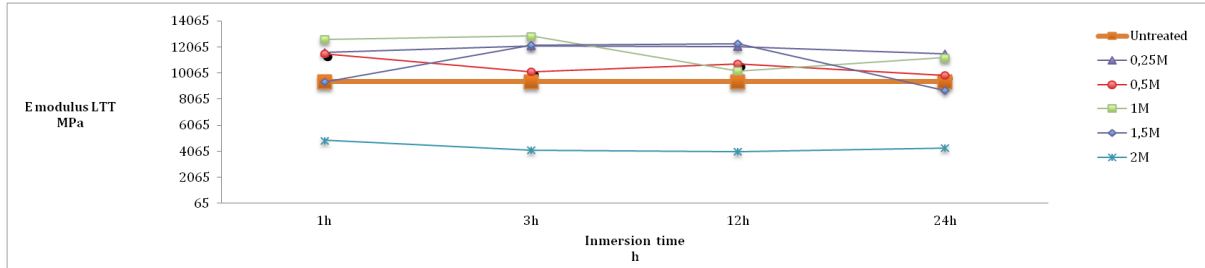


Figure 9.1.  $E_1$  evolution vs. immersion time

Table 9.3. The Fisher analysis of the concentration effect in the  $E_1$

1h		Value	3h		Value	12h		Value	24h		Value
0.25M 1h -	0.5M 1h	405,72	0.25M 3h -	0.5M 3h	746,35	0.25M 12h -	0.5M 12h	256,65	0.25M 24h -	0.5M 24h	570,94
0.25M 1h -	1M 1h	41,96	0.25M 3h -	1M 3h	356,53	0.25M 12h -	1M 12h	2332,70	0.25M 24h -	1M 24h	805,65
0.25M 1h -	1.5M 1h	2484,39	0.25M 3h -	1.5M 3h	488,03	0.25M 12h -	1.5M 12h	140,59	0.25M 24h -	1.5M 24h	2765,52
0.25M 1h -	2M 1h	5772,55	0.25M 3h -	2M 3h	7097,41	0.25M 12h -	2M 12h	6733,47	0.25M 24h -	2M 24h	6021,90
0.5M 1h -	1M 1h	363,77	0.5M 3h -	1M 3h	389,82	0.5M 12h -	1M 12h	2589,35	0.5M 24h -	1M 24h	234,71
0.5M 1h -	1.5M 1h	2890,12	0.5M 3h -	1.5M 3h	258,32	0.5M 12h -	1.5M 12h	116,06	0.5M 24h -	1.5M 24h	2194,58
0.5M 1h -	2M 1h	6178,27	0.5M 3h -	2M 3h	6351,06	0.5M 12h -	2M 12h	6990,12	0.5M 24h -	2M 24h	5450,96
1M 1h -	1.5M 1h	2526,35	1M 3h -	1.5M 3h	131,50	1M 12h -	1.5M 12h	2473,29	1M 24h -	1.5M 24h	1959,87
1M 1h -	2M 1h	5814,51	1M 3h -	2M 3h	6740,87	1M 12h -	2M 12h	4400,77	1M 24h -	2M 24h	5216,25
1.5M 1h -	2M 1h	3288,16	1.5M 3h -	2M 3h	6609,38	1.5M 12h -	2M 12h	6874,06	1.5M 24h -	2M 24h	3256,38

Table 9.3 studies the concentration effect in the  $E_1$  values. In general, the  $E_1$  values are not greatly affected by low concentration variation. In contrast, for higher solution concentrations, the  $E_1$  value differences tend to be higher. This analysis is supported by the Figure 9.2, where a plateau tendency at lower concentration values, and higher variance for **1M** in advance.

The  $E_1$  values for 0.25M, 0.5M and 1M concentrations are higher than those for the untreated system. For 1.5M concentration, the treated systems mechanical performance starts to decrease, and for 2M concentration there is a definite great loss of properties.

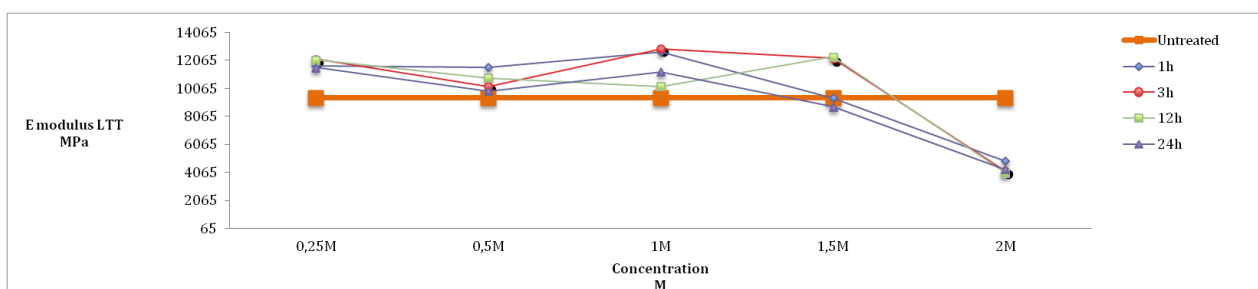


Figure 9.2.  $E_1$  evolution vs. concentration

Summarising the analysis above and the absolute numbers in Table 9.4, the following conclusions are drawn:

- **The ANOVA analysis confirms that there is significant effect due to immersion time, concentration or combination of both factors**
- Fisher's analysis, that studied the data variation between individual set of values, confirms that  $E_1$  values observed for 0.25M and 2M are more similar than for the rest of concentrations along different immersion times, although the  $E_1$  value drop is substantial at 2M concentration. In addition, when the concentration effect is studied for a specific immersion time, the data variation is less significant for low concentrations
- Table 9.4 suggests that long immersion times (24h) and high concentrations (2M) reduce the flax/epoxy composite performance. The 1h to 12h immersion times and 1.0M to 1.5M concentrations appear to be the most convenient combinations

Table 9.4.  $E_1$  values variation with immersion time and concentrations

CORRECTED $E_1$ modulus (MPa)	B: Concentration				
A: Immersion time	0,25M	0,5M	1M	1,5M	2M
1h	11675,83	11563,63	12669,16	9378,23	4884,59
3h	12147,91	10176,85	12897,66	12195,89	4141,23
12h	12091,61	10791,98	10217,37	12311,32	4027,48
24h	11538,00	9865,64	11238,33	8747,22	4292,35

\*NOTE: The longitudinal properties are corrected to  $V_f=0.3$  according to CLT

### 9.2.2. Longitudinal strength $\sigma_1$ ANOVA

There are three hypotheses to prove here. For the case of the null hypothesis, it must be checked whether the means values of all groups are equal under immersion time, concentration and combinative effect. For the case of the longitudinal strength, **the ANOVA analysis confirms that there is significant effect due to immersion time, concentration or combination of both factors**; this was confirmed because after the data analysis the **p-value** is lower than the  $\alpha = 0.05$  for the 95% level of significance, see Table 9.5.

Table 9.5. ANOVA analysis for the  $\sigma_1$

Source	SS	df	MS	F <sub>0</sub>	p-value
Effect A: Immersion time	2077,831	3	692,610	16,649	0,00014149319847
Effect B: Concentration	84579,465	4	21144,866	508,285	0,000000000000028
Effect AB: Combined	3740,495	12	311,708	7,493	0,00072518551999
Error	7488,078	180	41,600		
Total	97885,868	199			

When the box is red in the posterior Fisher's analysis, the difference between mean values is significant, and when the box is unaltered the difference is not significant. The value is significant when the difference is higher than the calculated **LSD**, in this case **5.692**. See the Fisher's analysis in Tables 9.6 and 9.7.

Table 9.6. Fisher analysis of the immersion time effect in the  $\sigma_1$

0.25M		Value	0.5M		Value	1M		Value	1.5M		Value	2M		Value
0.25M 1h - 0.25M 3h	1,15		0.5M 1h - 0.5M 3h	7,85		1M 1h - 1M 3h	8,71		1.5M 1h - 1.5M 3h	9,96		2M 1h - 2M 3h	14,13	
0.25M 1h - 0.25M 12h	5,61		0.5M 1h - 0.5M 12h	10,26		1M 1h - 1M 12h	0,25		1.5M 1h - 1.5M 12h	16,51		2M 1h - 2M 12h	8,52	
0.25M 1h - 0.25M 24h	11,60		0.5M 1h - 0.5M 24h	13,04		1M 1h - 1M 24h	3,00		1.5M 1h - 1.5M 24h	1,60		2M 1h - 2M 24h	13,88	
0.25M 3h - 0.25M 12h	6,76		0.5M 3h - 0.5M 12h	2,41		1M 3h - 1M 12h	8,46		1.5M 3h - 1.5M 12h	6,55		2M 3h - 2M 12h	5,60	
0.25M 3h - 0.25M 24h	12,75		0.5M 3h - 0.5M 24h	5,19		1M 3h - 1M 24h	11,71		1.5M 3h - 1.5M 24h	8,36		2M 3h - 2M 24h	0,24	
0.25M 12h - 0.25M 24h	5,99		0.5M 12h - 0.5M 24h	2,78		1M 12h - 1M 24h	3,25		1.5M 12h - 1.5M 24h	14,90		2M 12h - 2M 24h	5,36	

Table 9.6 studies the immersion time effect in the  $\sigma_1$  values. Excepting for the 0.25M concentration, there is a great change of properties from 1h immersion time to 3h. For the 1M and 1.5M cases the strength rises. From the Fisher's analysis, it might be assumed that after the initial peak, the strength values get to a plateau, where the properties tend to be lower but not drastically. This tendency is clearly supported by the Table data, for the 0.5M and 2M cases.

Figure 9.3 plots the  $\sigma_1$  variation vs. the immersion time. This graph supports the Fisher's analysis above. After the initial fluctuation, the data tends to vary less with the time evolution.

In comparison to the untreated system, most of the treated systems longitudinal strengths are lower, excepting for the case of 0.25M 1h and 1M 3h systems. The mercerisation process appears to decrease the system longitudinal strength properties.

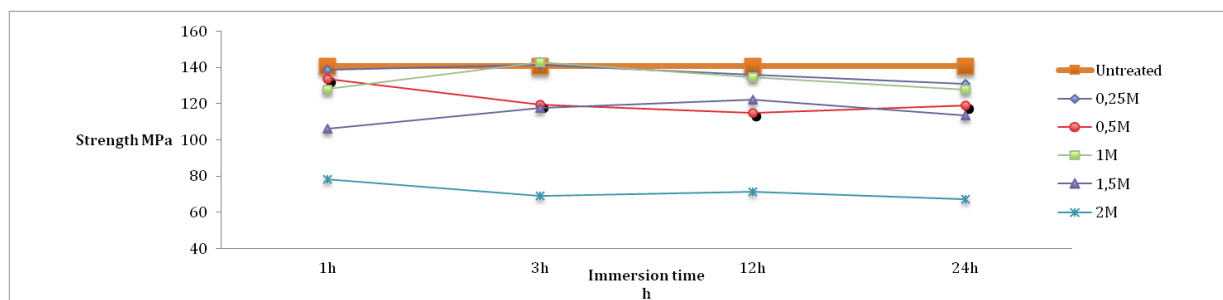


Figure 9.3.  $\sigma_1$  evolution vs. immersion time

Table 9.7. The Fisher analysis of the concentration effect in the  $\sigma_1$

1h		Value	3h		Value	12h		Value	24h		Value
0.25M 1h -	0.5M 1h	1,22	0.25M 3h -	0.5M 3h	7,79	0.25M 12h -	0.5M 12h	3,44	0.25M 24h -	0.5M 24h	0,23
0.25M 1h -	1M 1h	17,37	0.25M 3h -	1M 3h	9,81	0.25M 12h -	1M 12h	11,51	0.25M 24h -	1M 24h	8,77
0.25M 1h -	1.5M 1h	33,79	0.25M 3h -	1.5M 3h	24,98	0.25M 12h -	1.5M 12h	11,68	0.25M 24h -	1.5M 24h	20,58
0.25M 1h -	2M 1h	51,54	0.25M 3h -	2M 3h	66,82	0.25M 12h -	2M 12h	54,46	0.25M 24h -	2M 24h	53,83
0.5M 1h -	1M 1h	18,59	0.5M 3h -	1M 3h	2,02	0.5M 12h -	1M 12h	8,07	0.5M 24h -	1M 24h	8,55
0.5M 1h -	1.5M 1h	35,00	0.5M 3h -	1.5M 3h	17,19	0.5M 12h -	1.5M 12h	8,24	0.5M 24h -	1.5M 24h	20,36
0.5M 1h -	2M 1h	52,76	0.5M 3h -	2M 3h	59,03	0.5M 12h -	2M 12h	51,02	0.5M 24h -	2M 24h	53,60
1M 1h -	1.5M 1h	16,42	1M 3h -	1.5M 3h	15,17	1M 12h -	1.5M 12h	0,16	1M 24h -	1.5M 24h	11,81
1M 1h -	2M 1h	34,17	1M 3h -	2M 3h	57,01	1M 12h -	2M 12h	42,95	1M 24h -	2M 24h	45,05
1.5M 1h -	2M 1h	17,75	1.5M 3h -	2M 3h	41,84	1.5M 12h -	2M 12h	42,78	1.5M 24h -	2M 24h	33,24

Table 9.7 studies the concentration effect in the  $\sigma_1$  values. In line with the conclusions obtained from the previous analysis (Table 9.6), the maximum mean value fluctuations in different concentrations are obtained for the 3h and 12h immersion times. For the case of the 24h, the values also fluctuate but in a lower proportion. Finally, for the 1h immersion time the concentration produces a progressive loss of strength properties; in the first row of Table 9.7 the difference between the mean values follows a progressive evolution.

This analysis is supported by the Figure 9.4, where there is a clear difference between mean values for 3h and 12h with a lower difference for the 24h case; and the 1h case has progressive loss of properties.

In comparison to the untreated system, the properties are generally lower because of the mercerisation effect, independent of the concentration; being the higher difference for 1.5M and 2M concentrations.

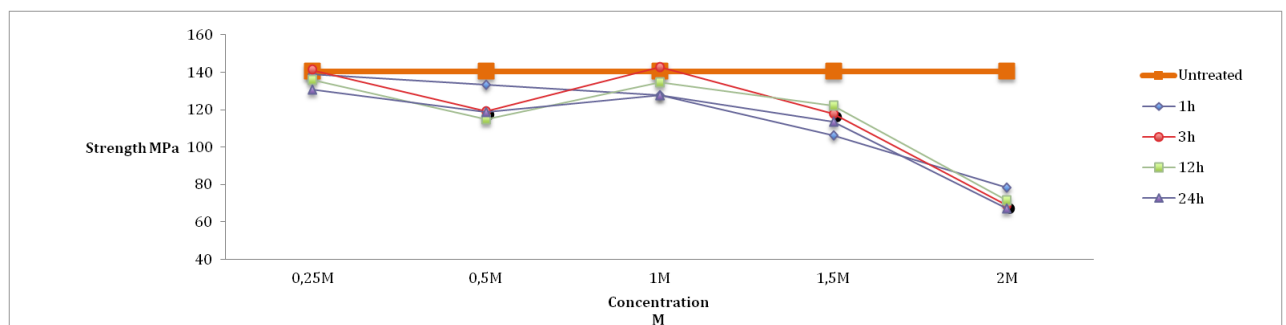


Figure 9.4.  $\sigma_1$  evolution vs. concentration

Summarising the analysis above and the absolute numbers in Table 9.8, the following conclusions are drawn:

- **The ANOVA analysis confirms that there is significant effect due to immersion time, concentration or combination of both factors**
- Fisher's analysis, that studied the data variation between individual set of values, suggests that  $\sigma_1$  values considerably fluctuates from 1h immersion time to 3h, staying similar for the rest of times. In regards to the concentrations, there are values fluctuation from 0.25M to 1M, getting highest values for 1M 3h case. Above 1M the mechanical performance decreased
- Table 9.8 suggests that long immersion times (24h) and high concentrations (2M) reduce the flax/epoxy composite performance. In addition, suggesting 1-12h 0.25M and 3h 1.0M combinations give best mechanical performance

Table 9.8.  $\sigma_1$  values variation with immersion time and concentrations

CORRECTED $\sigma_1$ strength (MPa)	B: Concentration				
A: Immersion time	0,25M	0,5M	1M	1,5M	2M
1h	138,81	133,44	127,91	106,14	78,18
3h	141,27	119,31	142,61	117,70	68,85
12h	135,95	114,68	134,50	122,32	71,51
24h	130,81	118,84	127,89	113,40	67,11

\*NOTE: The longitudinal properties are corrected to  $V_f=0.3$  according to CLT

### 9.2.3. Longitudinal strain $\epsilon_1$ ANOVA

There are three hypotheses to prove. For the case of the null hypothesis it must be checked whether the mean values of all groups are equal under immersion time, concentration and combinative effect. For the case of the longitudinal strain, the **ANOVA analysis confirms that there is significant effect due to immersion time, concentration or combination of both factors**; this was confirmed because after the data analysis the **p-value** is lower than the  $\alpha = 0.05$  for the 95% level of significance, see Table 9.9.

Table 9.9. ANOVA analysis for the  $\epsilon_1$

Source	SS	df	MS	F0	p-value
Effect A: Immersion time	1,864	3	0,621	8,805	0,00233067302800
Effect B: Concentration	228,586	4	57,146	809,802	0,000000000000002
Effect AB: Combined	7,828	12	0,652	9,244	0,00025871237142
Error	12,702	180	0,071		
Total	250,980	199			

When the box is red, the posterior Fisher's analysis says the difference between mean values is significant, and when the box is unaltered the difference is not significant. The value is significant

when the difference is higher than the calculated **LSD**, in this case **0.234**. See the Fisher's analysis in Tables 9.10 and 9.11.

Table 9.10. Fisher analysis of the immersion time effect in the  $\epsilon_1$

0.25M		Value	0.5M		Value	1M		Value	1.5M		Value	2M		Value
0.25M 1h - 0.25M 3h	0,09	0.25M 1h - 0.5M 3h	0,03	1M 1h - 1M 3h	0,08	1.5M 1h - 1.5M 3h	0,08	2M 1h - 2M 3h	0,37					
0.25M 1h - 0.25M 12h	0,03	0.5M 1h - 0.5M 12h	0,12	1M 1h - 1M 12h	0,26	1.5M 1h - 1.5M 12h	0,13	2M 1h - 2M 12h	1,24					
0.25M 1h - 0.25M 24h	0,15	0.5M 1h - 0.5M 24h	0,04	1M 1h - 1M 24h	0,36	1.5M 1h - 1.5M 24h	0,11	2M 1h - 2M 24h	0,72					
0.25M 3h - 0.25M 12h	0,07	0.5M 3h - 0.5M 12h	0,09	1M 3h - 1M 12h	0,18	1.5M 3h - 1.5M 12h	0,21	2M 3h - 2M 12h	0,87					
0.25M 3h - 0.25M 24h	0,06	0.5M 3h - 0.5M 24h	0,01	1M 3h - 1M 24h	0,28	1.5M 3h - 1.5M 24h	0,03	2M 3h - 2M 24h	0,35					
0.25M 12h - 0.25M 24h	0,13	0.5M 12h - 0.5M 24h	0,07	1M 12h - 1M 24h	0,10	1.5M 12h - 1.5M 24h	0,24	2M 12h - 2M 24h	0,52					

The Table 9.10 studies the immersion time effect in the  $\epsilon_1$  values. According to the table above, most of the differences are below the LSD value, in this case 0.234. There are some red values for 1M and 1.5M columns, however it is considered that there is no significant fluctuation in the number since they are close to LSD number. In contrast, for 2M case there is a great fluctuation between all the values from the same set; according to all red boxes in Fisher.

The Figure 9.5 plots the  $\epsilon_1$  variation vs. the immersion time. This graph supports what confirmed in the paragraph above, Fisher's analysis. 0.25M and 0.5M lines are practically unchanged; 1M and 1.5M lines slightly fluctuate; and the 2M values considerably vary with the concentration effect.

In most cases, the longitudinal strain values are higher than the untreated system, and there is a great increment for the case of the 2M concentration.

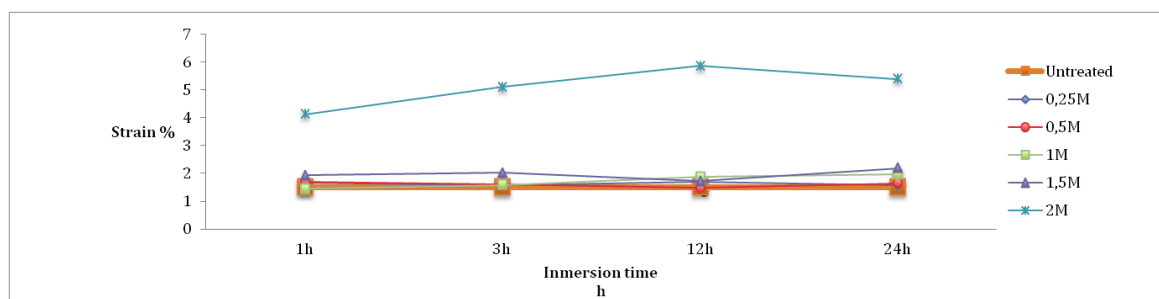


Figure 9.5.  $\epsilon_1$  evolution vs. immersion time

Table 9.11. The Fisher analysis of the concentration effect in the  $\epsilon_1$

1h		Value	3h		Value	12h		Value	24h		Value
0.25M 1h -	0.5M 1h	0,10	0.25M 3h -	0.5M 3h	0,16	0.25M 12h -	0.5M 12h	0,00	0.25M 24h -	0.5M 24h	0,20
0.25M 1h -	1M 1h	0,28	0.25M 3h -	1M 3h	0,11	0.25M 12h -	1M 12h	0,00	0.25M 24h -	1M 24h	0,23
0.25M 1h -	1.5M 1h	0,12	0.25M 3h -	1.5M 3h	0,30	0.25M 12h -	1.5M 12h	0,02	0.25M 24h -	1.5M 24h	0,39
0.25M 1h -	2M 1h	2,09	0.25M 3h -	2M 3h	2,55	0.25M 12h -	2M 12h	3,35	0.25M 24h -	2M 24h	2,95
0.5M 1h -	1M 1h	0,38	0.5M 3h -	1M 3h	0,27	0.5M 12h -	1M 12h	0,00	0.5M 24h -	1M 24h	0,03
0.5M 1h -	1.5M 1h	0,03	0.5M 3h -	1.5M 3h	0,14	0.5M 12h -	1.5M 12h	0,02	0.5M 24h -	1.5M 24h	0,19
0.5M 1h -	2M 1h	1,99	0.5M 3h -	2M 3h	2,39	0.5M 12h -	2M 12h	3,34	0.5M 24h -	2M 24h	2,75
1M 1h -	1.5M 1h	0,40	1M 3h -	1.5M 3h	0,41	1M 12h -	1.5M 12h	0,02	1M 24h -	1.5M 24h	0,16
1M 1h -	2M 1h	2,37	1M 3h -	2M 3h	2,66	1M 12h -	2M 12h	3,34	1M 24h -	2M 24h	2,72
1.5M 1h -	2M 1h	1,96	1.5M 3h -	2M 3h	2,25	1.5M 12h -	2M 12h	3,33	1.5M 24h -	2M 24h	2,57

The Table 9.11 studies the concentration effect in the  $\epsilon_1$  values. The clearest conclusion obtained from Fisher's analysis is that the boxes are in red when compared with 2M data, much higher than the rest of the data population. In a lower scale, something similar happens for the 1.5M concentration, but the difference is not significant for all the cases. This behaviour is common for all the immersion times.

This analysis is supported by the Figure 9.6, where a clear rise in the values for 2M concentration is observed, and in a lower scale for the 1.5M concentration.

The strain values suffer a great increment for 2M case in comparison to the untreated system, and for the rest of concentrations the values are similar.

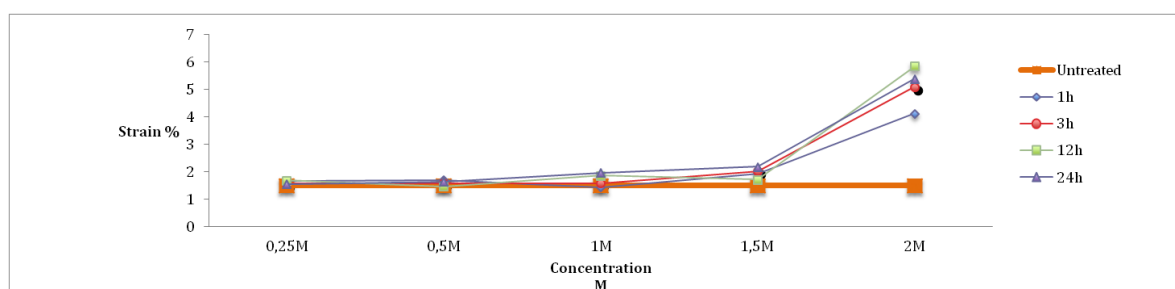


Figure 9.6.  $\epsilon_1$  evolution vs. concentration

Summarising the analysis above and the absolute numbers in Table 9.12, the following conclusions are drawn:

- **The ANOVA analysis confirms that there is significant effect due to immersion time, concentration or combination of both factors**
- In regards to the immersion times, the 2M values are the ones fluctuating most. Fisher's analysis, that studied the data variation between individual set of values, suggests that  $\epsilon_1$

values considerably rise when the concentration increases, a little for 1.5M and drastically for 2M

- Table 9.12 suggests that long immersion times from 1h to 12h and high concentrations (2M) increase the strain values. In addition, 24h immersion time and 2M concentration suggest that the fibre was degraded during the treatment because of the low values

Table 9.12.  $\epsilon_1$  values variation with immersion time and concentrations

CORRECTED $\epsilon_1$ strain (%)	B: Concentration				
A: Immersion time	0,25M	0,5M	1M	1,5M	2M
1h	1,67	1,70	1,45	1,94	4,13
3h	1,58	1,59	1,59	2,03	5,10
12h	1,69	1,47	1,87	1,72	5,86
24h	1,56	1,65	1,97	2,19	5,39

\*NOTE: The longitudinal properties are corrected to  $V_f=0.3$  according to CLT

#### 9.2.4. Transverse tensile modulus $E_2$ ANOVA

There are three hypotheses to prove. For the case of the null hypothesis it must be checked whether the mean values of all groups are equal under immersion time, concentration and combinative effect. For the case of the transverse modulus, the **ANOVA analysis confirms that there is significant effect due to immersion time, concentration or combination of both factors**; this was confirmed because after the data analysis the **p-value** is lower than the  $\alpha = 0.05$  for the 95% level of significance, see Table 9.13.

Table 9.13. ANOVA analysis for the  $E_2$

Source	SS	df	MS	F0	p-value
Effect A: Immersion time	3724535,905	3	1241511,968	8,286	0,00003709505623
Effect B: Concentration	191631888,940	4	47907972,235	319,736	0,000000000000000
Effect AB: Combined	14084428,872	12	1173702,406	7,833	0,00000000002225
Error	23973742,731	160	149835,892		
Total	233414596,448	179			

When the box is red, the posterior Fisher's analysis says the difference between mean values is significant, and when the box is unaltered the difference is not significant. The value is significant when the difference is higher than the calculated **LSD**, in this case **341.876**. See the data in Tables 9.14 and 9.15 where Fisher's analysis was done.



Table 9.14. Fisher analysis of the immersion time effect in the E<sub>2</sub>

0.25M		Value	0.5M		Value	1M		Value	1.5M		Value	2M		Value
0.25M 1h - 0.25M 3h	294,38	0.5M 1h - 0.5M 3h	259,11	1M 1h - 1M 3h	192,68	1.5M 1h - 1.5M 3h	532,83	2M 1h - 2M 3h	8,33					
0.25M 1h - 0.25M 12h	723,53	0.5M 1h - 0.5M 12h	367,20	1M 1h - 1M 12h	440,43	1.5M 1h - 1.5M 12h	544,25	2M 1h - 2M 12h	218,00					
0.25M 1h - 0.25M 24h	294,16	0.5M 1h - 0.5M 24h	87,03	1M 1h - 1M 24h	1,78	1.5M 1h - 1.5M 24h	711,47	2M 1h - 2M 24h	78,04					
0.25M 3h - 0.25M 12h	429,15	0.5M 3h - 0.5M 12h	626,31	1M 3h - 1M 12h	247,75	1.5M 3h - 1.5M 12h	1077,07	2M 3h - 2M 12h	226,33					
0.25M 3h - 0.25M 24h	0,23	0.5M 3h - 0.5M 24h	346,14	1M 3h - 1M 24h	194,46	1.5M 3h - 1.5M 24h	1244,30	2M 3h - 2M 24h	69,72					
0.25M 12h - 0.25M 24h	429,38	0.5M 12h - 0.5M 24h	280,18	1M 12h - 1M 24h	442,21	1.5M 12h - 1.5M 24h	167,23	2M 12h - 2M 24h	296,04					

Table 9.14 studies the immersion time effect in the E<sub>2</sub> values according to Fisher analysis. For the first three concentrations, 0.25M, 0.5M and 1M, the immersion time effect for 1h and 24h values is the same, getting similar values for both cases; for middle way immersion times, 3h and 12h, the E<sub>2</sub> values are fluctuating. For the 1.5M concentration, the values are varying excepting from 12h to 24h that the values are keeping stable. Finally for the case of the 2M concentration, the value difference is lower than the **LSD=341.876** for all immersion times.

The Figure 9.7 plots the E<sub>2</sub> variation vs. the immersion time. This graph supports Fisher's analysis above. The lowest variation was obtained for 2M case, followed by the 0.25M, 0.5M and 1M cases, being 1.5M data the set of results fluctuating the most.

Transverse modulus properties are higher than the untreated system, excepting for the case of the 2M concentration. Independently from the immersion time.

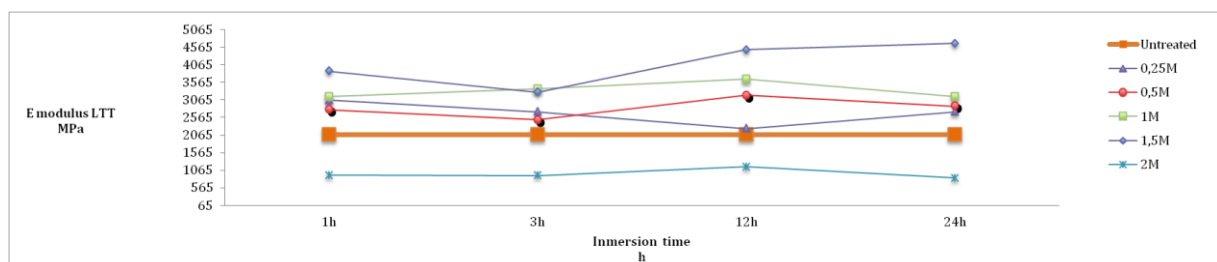


Figure 9.7. E<sub>2</sub> evolution vs. immersion time

Table 9.15. Fisher analysis of the concentration effect in the E<sub>2</sub>

1h		Value	3h		Value	12h		Value	24h		Value
0.25M 1h - 0.5M 1h	241,07	0.25M 3h - 0.5M 3h	205,80	0.25M 12h - 0.5M 12h	849,66	0.25M 24h - 0.5M 24h	140,11				
0.25M 1h - 1M 1h	95,01	0.25M 3h - 1M 3h	582,07	0.25M 12h - 1M 12h	1258,97	0.25M 24h - 1M 24h	387,38				
0.25M 1h - 1.5M 1h	742,31	0.25M 3h - 1.5M 3h	503,87	0.25M 12h - 1.5M 12h	2010,09	0.25M 24h - 1.5M 24h	1747,94				
0.25M 1h - 2M 1h	1918,00	0.25M 3h - 2M 3h	1631,95	0.25M 12h - 2M 12h	976,47	0.25M 24h - 2M 24h	1701,89				
0.5M 1h - 1M 1h	336,08	0.5M 3h - 1M 3h	787,87	0.5M 12h - 1M 12h	409,31	0.5M 24h - 1M 24h	247,27				
0.5M 1h - 1.5M 1h	983,38	0.5M 3h - 1.5M 3h	709,66	0.5M 12h - 1.5M 12h	1160,42	0.5M 24h - 1.5M 24h	1607,82				
0.5M 1h - 2M 1h	1676,93	0.5M 3h - 2M 3h	1426,15	0.5M 12h - 2M 12h	1826,13	0.5M 24h - 2M 24h	1842,00				
1M 1h - 1.5M 1h	647,30	1M 3h - 1.5M 3h	78,21	1M 12h - 1.5M 12h	751,11	1M 24h - 1.5M 24h	1360,55				
1M 1h - 2M 1h	2013,01	1M 3h - 2M 3h	2214,02	1M 12h - 2M 12h	2235,44	1M 24h - 2M 24h	2089,27				
1.5M 1h - 2M 1h	2660,31	1.5M 3h - 2M 3h	2135,81	1.5M 12h - 2M 12h	2986,56	1.5M 24h - 2M 24h	3449,82				

The Table 9.15 studies the concentration effect in the  $E_2$  values. The clearest conclusion obtained in the Fisher analysis is shown by the last line of the table. The value drop is huge when increasing the solution concentration from 1.5M to 2M. Similarly, when the concentration is increased from 1M to 1.5M the properties increment is significant, excepting for the case of the 3h immersion time. Finally confirm that the value fluctuation looks to be proportional to the immersion time, highest fluctuation was obtained for the longest immersion times.

Figure 9.8 confirms that highest fluctuation was obtained for immersion times between 1M and 2M concentrations.

The transverse modulus drastically drops to values lower than the untreated systems, when the treatment concentration is 2M.

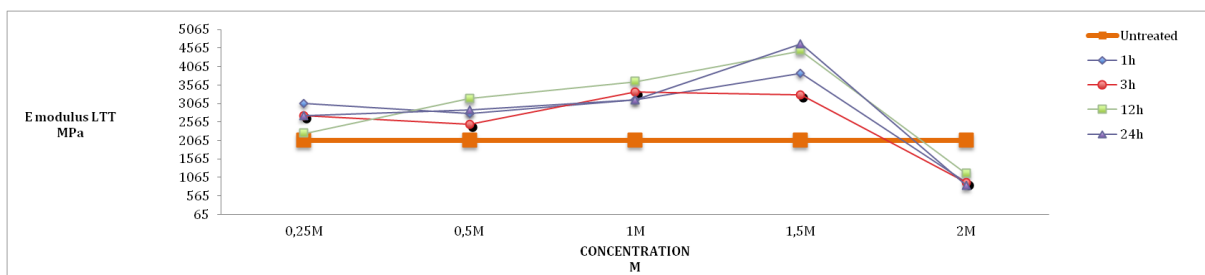


Figure 9.8.  $E_2$  evolution vs. concentrations

Summarising the analysis above and the absolute numbers in Table 9.16, the following conclusions are drawn:

- **The ANOVA analysis confirms that there is significant effect due to immersion time, concentration or combination of both factors**
- In regards to the immersion times, it looks like in general for 12h the  $E_2$  values are increasing, and 24h immersion time is too long, excepting for the 1.5M concentration.  
In regards to the concentrations it looks like the  $E_2$  values are increasing for 1M and 1.5M cases. However, for 2M there is a dramatic loss of properties
- Table 9.16 suggests that 2M concentration is clearly damaging the fibre/matrix interface, getting a drastic decrease in the mechanical properties. Similarly, it looks like the 24h long

immersion times are generally reducing the E<sub>2</sub> value, excepting for the 1.5M case where optimised 4.67 MPa value is obtained.

Table 9.16. E<sub>2</sub> values variation with immersion time and concentrations

E2 modulus (MPa)	B: Concentration				
A: Immersion time	0,25M	0,5M	1M	1,5M	2M
1h	3058,53	2790,68	3164,10	3883,32	927,42
3h	2731,44	2502,78	3378,19	3291,29	918,17
12h	2254,61	3198,68	3653,47	4488,04	1169,64
24h	2731,69	2887,37	3162,12	4673,84	840,71

### 9.2.5. Transverse strength $\sigma_2$ ANOVA

There are three hypotheses to prove. For the case of the null hypothesis, it must be checked whether the means values of all groups are equal under immersion time, concentration and combinative effect. For the case of the transverse strength, the **ANOVA analysis confirms that there is significant effect due to immersion time, concentration or combination of both factors;** this was confirmed because after the data analysis the **p-value** is lower than the  $\alpha = 0.05$  for the 95% level of significance, see Table 9.17.

Table 9.17. ANOVA analysis for the  $\sigma_2$

Source	SS	df	MS	Fo	p-value
Effect A: Immersion time	75,379	3	25,126	8,005	0,00005269874953
Effect B: Concentration	5678,963	4	1419,741	452,340	0,0000000000000000
Effect AB: Combined	290,418	12	24,202	7,711	0,00000000003374
Error	502,185	160	3,139		
Total	6546,946	179			

When the box is red, the posterior Fisher's analysis says the difference between mean values is significant, and when the box is unaltered the difference is not significant enough. The value is significant when the difference is higher than the calculated **LSD**, in this case **1.565**. See the data in Tables 9.18 and 9.19 where Fisher's analysis was done.

Table 9.18. Fisher analysis of the immersion time effect in the  $\sigma_2$

0.25M	Value	0.5M	Value	1M	Value	1.5M	Value	2M	Value
0.25M 1h - 0.25M 3h	1,22	0.5M 1h - 0.5M 3h	1,22	1M 1h - 1M 3h	1,64	1.5M 1h - 1.5M 3h	3,98	2M 1h - 2M 3h	1,28
0.25M 1h - 0.25M 12h	1,94	0.5M 1h - 0.5M 12h	0,52	1M 1h - 1M 12h	1,33	1.5M 1h - 1.5M 12h	0,84	2M 1h - 2M 12h	1,70
0.25M 1h - 0.25M 24h	0,59	0.5M 1h - 0.5M 24h	2,95	1M 1h - 1M 24h	1,78	1.5M 1h - 1.5M 24h	1,04	2M 1h - 2M 24h	0,07
0.25M 3h - 0.25M 12h	3,16	0.5M 3h - 0.5M 12h	0,70	1M 3h - 1M 12h	0,30	1.5M 3h - 1.5M 12h	4,83	2M 3h - 2M 12h	0,42
0.25M 3h - 0.25M 24h	1,81	0.5M 3h - 0.5M 24h	1,73	1M 3h - 1M 24h	3,42	1.5M 3h - 1.5M 24h	2,95	2M 3h - 2M 24h	1,21
0.25M 12h - 0.25M 24h	1,35	0.5M 12h - 0.5M 24h	2,43	1M 12h - 1M 24h	3,11	1.5M 12h - 1.5M 24h	1,88	2M 12h - 2M 24h	1,63

Table 9.18 studies the immersion time effect in the  $\sigma_2$  values according to Fisher analysis. For the concentrations from 0.25M and 0.5M, the  $\sigma_2$  values fluctuate along the four immersion times; the 1M and 1.5M fluctuate more according to Fisher; finally the 2M measurements tend to be more stable.

Figure 9.9 plots the  $\sigma_2$  variation vs. the immersion time. This graph supports Fisher's analysis above. The lowest variation was obtained for 2M case, followed by the 0.25M and 0.5M, being 1M and 1.5M cases the set of results fluctuating the most.

Transverse strength values are higher and lower than the untreated system depending on the immersion times, excepting for the case of the 2M concentration that there is a great drop of properties.

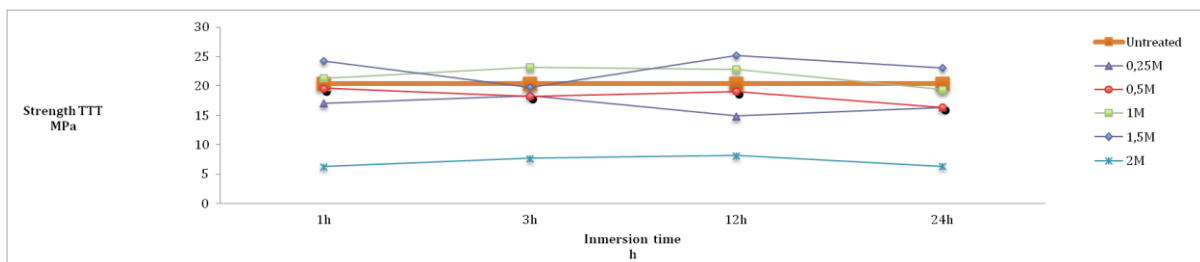


Figure 9.9.  $\sigma_2$  evolution vs. Immersion time

Table 9.19. Fisher analysis of the concentration effect in the  $\sigma_2$

1h		Value	3h		Value	12h		Value	24h		Value
0.25M 1h -	0.5M 1h	2,31	0.25M 3h -	0.5M 3h	0,13	0.25M 12h -	0.5M 12h	3,73	0.25M 24h -	0.5M 24h	0,05
0.25M 1h -	1M 1h	3,89	0.25M 3h -	1M 3h	4,30	0.25M 12h -	1M 12h	7,16	0.25M 24h -	1M 24h	2,69
0.25M 1h -	1.5M 1h	6,47	0.25M 3h -	1.5M 3h	1,27	0.25M 12h -	1.5M 12h	9,26	0.25M 24h -	1.5M 24h	6,02
0.25M 1h -	2M 1h	9,70	0.25M 3h -	2M 3h	9,64	0.25M 12h -	2M 12h	6,06	0.25M 24h -	2M 24h	9,04
0.5M 1h -	1M 1h	1,58	0.5M 3h -	1M 3h	4,43	0.5M 12h -	1M 12h	3,43	0.5M 24h -	1M 24h	2,75
0.5M 1h -	1.5M 1h	4,16	0.5M 3h -	1.5M 3h	1,40	0.5M 12h -	1.5M 12h	5,53	0.5M 24h -	1.5M 24h	6,08
0.5M 1h -	2M 1h	12,01	0.5M 3h -	2M 3h	9,51	0.5M 12h -	2M 12h	9,79	0.5M 24h -	2M 24h	8,99
1M 1h -	1.5M 1h	2,59	1M 3h -	1.5M 3h	3,03	1M 12h -	1.5M 12h	2,10	1M 24h -	1.5M 24h	3,33
1M 1h -	2M 1h	13,58	1M 3h -	2M 3h	13,94	1M 12h -	2M 12h	13,21	1M 24h -	2M 24h	11,73
1.5M 1h -	2M 1h	16,17	1.5M 3h -	2M 3h	10,91	1.5M 12h -	2M 12h	15,31	1.5M 24h -	2M 24h	15,07

Table 9.19 studies the concentration effect in the  $\sigma_2$  values. The clearest conclusion obtained in the Fisher analysis is shown by the last line of the table. The value drop is huge when increasing the solution concentration from 1.5M to 2M. For 1h, 12h and 24h cases, there is a clear strength improvement with along the concentration, until 1.5M concentration is reached with the highest value and drop is obtained for 2M. 3h case is the exception, where the property drop happens from 1M to 2M concentrations.

Figure 9.10 confirms that 2M concentration is too elevated and provokes a drop in the mechanical performance of the flax/epoxy composite. At the same way, 1M and 1.5M would be the most optimum concentrations.

According to the Figure 9.10, the properties are lower than the untreated system for 0.25M, 0.50M systems and higher for 1M, 1.5M systems. For the case of 2M the documents are much lower than the basic system.

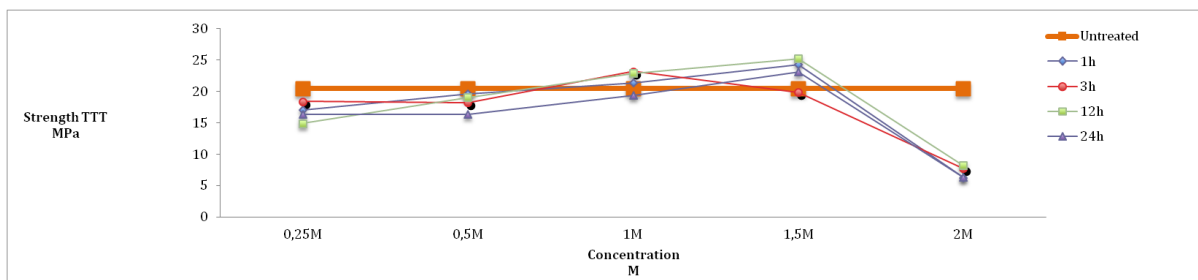


Figure 9.10.  $\sigma_2$  evolution vs. concentrations

Summarising the analysis above and the absolute numbers in Table 9.20, the following conclusions are drawn:

- **The ANOVA analysis confirms that there is significant effect due to immersion time, concentration or combination of both factors**
- It is confirmed that 24h immersion time and 2M concentration are too long/high respectively and the properties are clearly reduced. Fluctuation was obtained for immersion times between 1M and 2M concentrations, but 1M and 1.5M might be considered the optimum concentrations.
- Table 9.20 suggests that 2M concentration is clearly damaging the flax fibre, getting a drastic decrease in the mechanical properties. Similarly it looks like the 24h long immersion times are generally reducing the  $E_2$  value, excepting for the 1.5M case where the severity is lower. According to the table 1.5M concentration is working better in all immersion times.

Table 9.20.  $\sigma_2$  values variation with immersion time and concentrations

s2 Strength(MPa)	B: Concentration				
A: Immersion time	0,25M	0,5M	1M	1,5M	2M
1h	17,03	19,60	21,35	24,23	6,26
3h	18,39	18,25	23,17	19,80	7,68
12h	14,88	19,02	22,83	25,16	8,15
24h	16,38	16,32	19,37	23,07	6,33

### 9.2.6. Transverse strain $\epsilon_2$ ANOVA

There are three hypotheses to prove. For the case of the null hypothesis it must be checked whether the means values of all groups are equal under immersion time, concentration and combinative effect. For the case of the duration ANOVA analysis confirms that **there is NO main effect due to immersion time**, since the **p-value** is higher than the  $\alpha = 0.05$  for the 95%, 0.059. For the concentration or combination of both factors; ANOVA analysis confirms that **there is main effect due to concentration or combination of both factors**, since the **p-value** is lower than the  $\alpha = 0.05$  for the 95% level of significance, see Table 9.21.

Table 9.21. ANOVA analysis for the  $\epsilon_2$

Source	SS	df	MS	$F_0$	p-value
Effect A: Immersion time	0,331	3	0,110	2,527	0,05940115382354
Effect B: Concentration	14,118	4	3,529	80,740	0,0000000000000000
Effect AB: Combined	1,184	12	0,099	2,256	0,01152343425999
Error	6,994	160	0,044		
Total	22,627	179			

When the box is red, the posterior Fisher's analysis says the difference between mean values is significant, and when the box is unaltered the difference is not significant. The value is significant when the difference is higher than the calculated **LSD**, in this case **0.185**. The Fisher's analysis data is presented in Tables 9.22 and 9.23.

Table 9.22. Fisher analysis of the immersion time effect in the  $\epsilon_2$

0.25M	Value	0.5M	Value	1M	Value	1.5M	Value	2M	Value
0.25M 1h - 0.25M 3h	0,06	0.5M 1h - 0.5M 3h	0,09	1M 1h - 1M 3h	0,08	1.5M 1h - 1.5M 3h	0,01	2M 1h - 2M 3h	0,00
0.25M 1h - 0.25M 12h	0,05	0.5M 1h - 0.5M 12h	0,05	1M 1h - 1M 12h	0,08	1.5M 1h - 1.5M 12h	0,01	2M 1h - 2M 12h	0,27
0.25M 1h - 0.25M 24h	0,01	0.5M 1h - 0.5M 24h	0,13	1M 1h - 1M 24h	0,25	1.5M 1h - 1.5M 24h	0,04	2M 1h - 2M 24h	0,10
0.25M 3h - 0.25M 12h	0,01	0.5M 3h - 0.5M 12h	0,14	1M 3h - 1M 12h	0,00	1.5M 3h - 1.5M 12h	0,02	2M 3h - 2M 12h	0,27
0.25M 3h - 0.25M 24h	0,05	0.5M 3h - 0.5M 24h	0,23	1M 3h - 1M 24h	0,17	1.5M 3h - 1.5M 24h	0,05	2M 3h - 2M 24h	0,09
0.25M 12h - 0.25M 24h	0,04	0.5M 12h - 0.5M 24h	0,09	1M 12h - 1M 24h	0,17	1.5M 12h - 1.5M 24h	0,02	2M 12h - 2M 24h	0,36

The Table 9.22 studies the immersion time effect in the  $\epsilon_2$  values according to Fisher analysis. Excepting for the 2M concentration, the transverse strain values are not changing significantly with the immersion time variation. In contrast, for the 2M data it is seen that the values are fluctuating, more in detail for the 12h immersion time test, where the value is lower in comparison to the rest of the set.

The analysis in the paragraph above it is supported by the Figure 9.11, where it is clearly seen that 2M data set is fluctuating most along the immersion times.

The transverse strain in general is slightly higher than the untreated systems for most of the cases, excepting the 2M case that obtains much higher values.

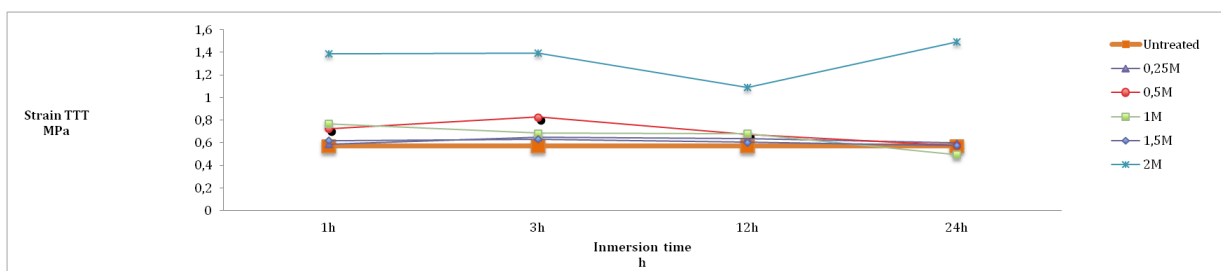


Figure 9.11.  $\epsilon_2$  evolution vs. immersion time

Table 9.23. Fisher analysis of the concentration effect in the  $\epsilon_2$

1h	Value	3h	Value	12h	Value	24h	Value
0.25M 1h - 0.5M 1h	0,13	0.25M 3h - 0.5M 3h	0,16	0.25M 12h - 0.5M 12h	0,03	0.25M 24h - 0.5M 24h	0,02
0.25M 1h - 1M 1h	0,16	0.25M 3h - 1M 3h	0,03	0.25M 12h - 1M 12h	0,04	0.25M 24h - 1M 24h	0,09
0.25M 1h - 1.5M 1h	0,03	0.25M 3h - 1.5M 3h	0,02	0.25M 12h - 1.5M 12h	0,03	0.25M 24h - 1.5M 24h	0,02
0.25M 1h - 2M 1h	0,72	0.25M 3h - 2M 3h	0,67	0.25M 12h - 2M 12h	0,41	0.25M 24h - 2M 24h	0,81
0.5M 1h - 1M 1h	0,04	0.5M 3h - 1M 3h	0,13	0.5M 12h - 1M 12h	0,01	0.5M 24h - 1M 24h	0,07
0.5M 1h - 1.5M 1h	0,10	0.5M 3h - 1.5M 3h	0,18	0.5M 12h - 1.5M 12h	0,06	0.5M 24h - 1.5M 24h	0,00
0.5M 1h - 2M 1h	0,60	0.5M 3h - 2M 3h	0,51	0.5M 12h - 2M 12h	0,37	0.5M 24h - 2M 24h	0,83
1M 1h - 1.5M 1h	0,13	1M 3h - 1.5M 3h	0,05	1M 12h - 1.5M 12h	0,07	1M 24h - 1.5M 24h	0,08
1M 1h - 2M 1h	0,56	1M 3h - 2M 3h	0,64	1M 12h - 2M 12h	0,37	1M 24h - 2M 24h	0,90
1.5M 1h - 2M 1h	0,69	1.5M 3h - 2M 3h	0,69	1.5M 12h - 2M 12h	0,44	1.5M 24h - 2M 24h	0,82

Table 9.23 studies the concentration effect in the  $\epsilon_2$  values. According to the table above it is seen same tendency for all the four immersion times: the transverse strain is almost a plateau between 0.25M and 1.5M concentration, however the strain values drastically raise from 1.5M to 2M concentrations.

Figure 9.12 supports what is described in the paragraph above. The transverse strain values drastically increase for 2M concentration.

The great difference happens for 2M system in comparison to the untreated system, where the transverse strain values increment is visible.

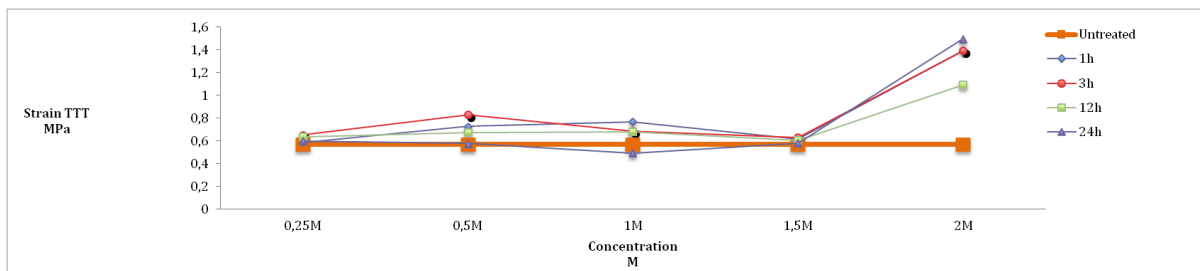


Figure 9.12.  $\epsilon_2$  evolution vs. concentrations

Summarising the analysis above and the absolute numbers in Table 9.24, the following conclusions are drawn:

- **The ANOVA analysis confirms that there is NO significant effect due to immersion time, there is significant effect due to concentration or combination of both factors**
- It is confirmed that only for 2M set of values the concentrations are affecting the strain values. Similarly, when the fibres are treated at 2M the strain values suffer a great value rise
- Table 9.24 suggests that 2M concentration is clearly affecting the composite performance, getting a drastic increase in the strain values. It is suspected that the aggressive treatment might be damaging the fibre/matrix interface

Table 9.24.  $\epsilon_2$  values variation with immersion time and concentrations

$\epsilon_2$ Strain (%)	B: Concentration				
	0,25M	0,5M	1M	1,5M	2M
A: Immersion time					
1h	0,59	0,73	0,77	0,62	1,39
3h	0,65	0,83	0,68	0,63	1,39
12h	0,64	0,68	0,68	0,60	1,09
24h	0,60	0,58	0,49	0,58	1,49



### 9.2.7. Poisson's ratio $\nu_{21}$ ANOVA

The Poisson's ratio was not evaluated by ANOVA for two reasons.

- First, low signal-to-noise ratio of the video-extensometer camera resolution means the system is not able to resolve small deformations. This problem might be solved either by measuring the deformations with strain gauges or by increasing the video-extensometer camera resolution. The greater longitudinal strain is sensibly resolved by the video extensometer. However, the Poisson's ratio data generated is not reliable because of the uncertainty in the measured transverse strain.
- Second, it is not clear what the optimum magnitude should be for Poisson's ratio. Normally, each fabric has got its own natural value; Craig and Summerscales (Craig & Summerscales, 1988) studied two glass-fibre laminates (unidirectional and bidirectional) experimentally and presented a full set of axial moduli and Poisson's ratios for the three orthogonal planes in the respective composites. The values obtained were shown to satisfy Lempriere's criteria (Lempriere, 1968) which impose a thermodynamic constraint. A full study of this characteristic for the materials in the doctoral study is beyond the scope and duration of the project given that available systems cannot resolve the data.

In this case the UD fabric value must be around 0.25 and 0.35. Away from this range it might be confirmed that the immersion time and the concentration is affecting the Poisson's ratio, but no more conclusion might be obtained from ANOVA analysis

### 9.2.8. Definitive mercerisation process selection

Based on all the properties obtained from the mercerisation process and the ANOVA study, an optimum mercerisation process was selected. ANOVA analysis was performed in §9.2.1-9.2.6; with the mechanical data plotted in Figures from 9.13 to 9.16:

- Figure 9.13. Longitudinal tensile properties vs concentration
- Figure 9.14. Longitudinal tensile properties vs immersion time
- Figure 9.15. Transverse tensile properties vs immersion time
- Figure 9.16. Transverse tensile properties vs concentration

The main conclusions obtained from the analysis were:

- The ANOVA analysis confirms that for most of the properties **there is significant effect due to immersion time and concentration or combination of both factors**. Excepting for the transverse strain values where **there is NO significant** effect due to immersion time and **there is significant** effect due to concentration or combination of both factors  
The posterior Fisher's analysis studied the data variations between individual set of values and confirms their variations in different tables and plots
- Table 9.2 presents that analysis. For a sensible balance of these four properties ( $E_1$ ,  $E_2$ ,  $\sigma'_1$  and  $\sigma'_2$ ), the caustic soda concentration is in the range 0.5M to 1.5M with treatment times of 3h or 12h giving the best balance of mechanical properties. In regards to the longitudinal properties, 3h immersion time in a 1M concentration was the optimised combination. Additionally, making the **balance between the transverse modulus and strength**, the best system selected would be the **12h immersion time in a 1.5M concentration**. For **best longitudinal properties** while maintaining sensible transverse properties, the **3h and 1M combination was selected**. Appropriate transverse properties means that there is a great locking between fibre and matrix after the treatment. The idea is to get even better transverse properties after the silane addition to the interface
- It is certainly clear that 2.0M NaOH is not realising the potential of the reinforcement fibres. Clearly 2.0M NaOH is not the appropriate choice given the high proportion of red cells for  $E_1$ ,  $E_2$ ,  $\sigma'_1$  and  $\sigma'_2$ . **24h immersion time and 2M concentration** is damaging to the composite system, reducing drastically its performance

From the paragraph above it is concluded that the 1M/3h combination would be obtaining the best mechanical performance from all the options; however, the immersion produced during the mercerisation process looks to be decreasing the mechanical performance in comparison to the untreated system. **The reply to the research question would be that the mercerisation process is decreasing the flax/epoxy system mechanical performance.**

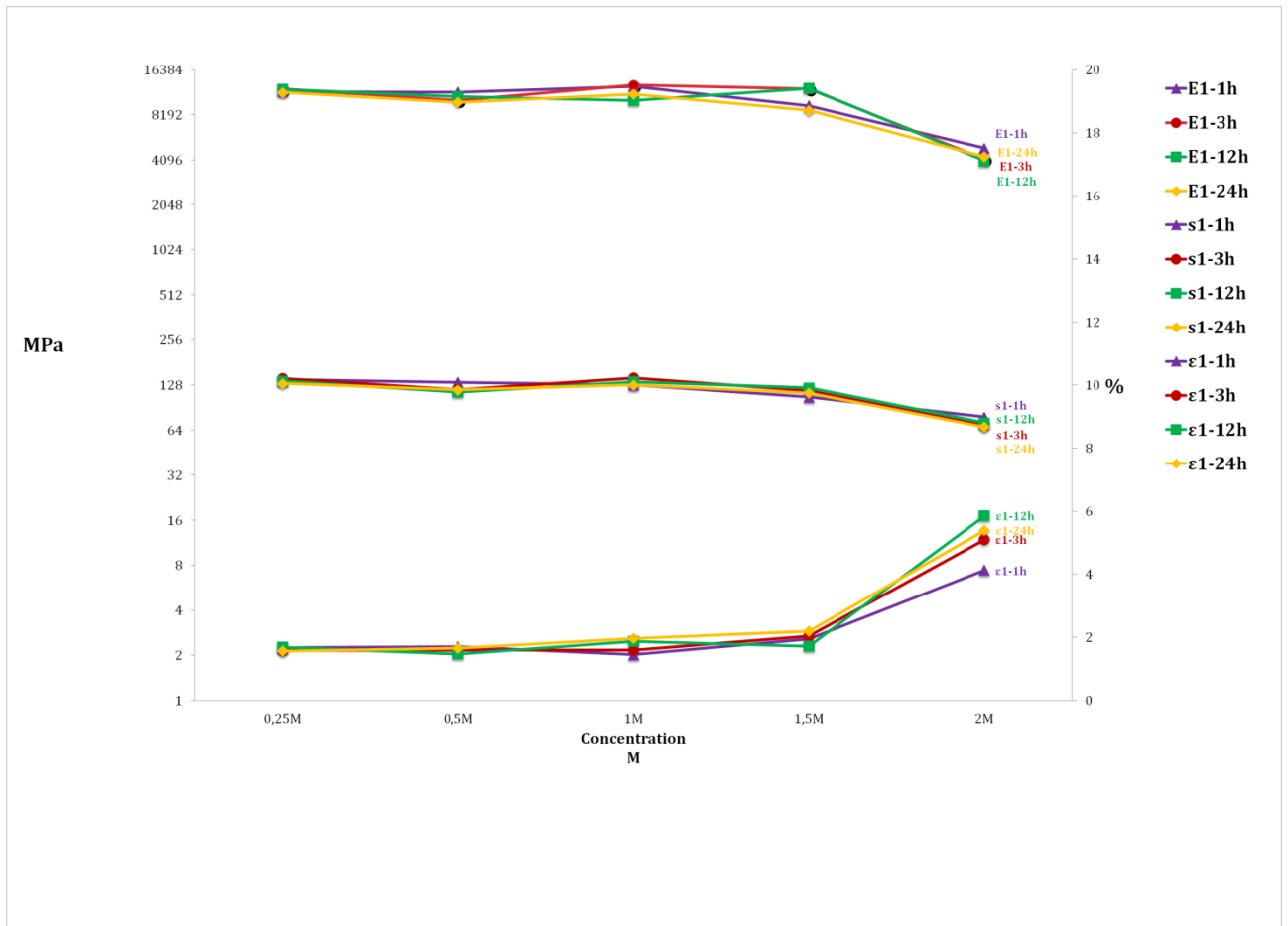


Figure 9.13. Longitudinal tensile properties vs concentration

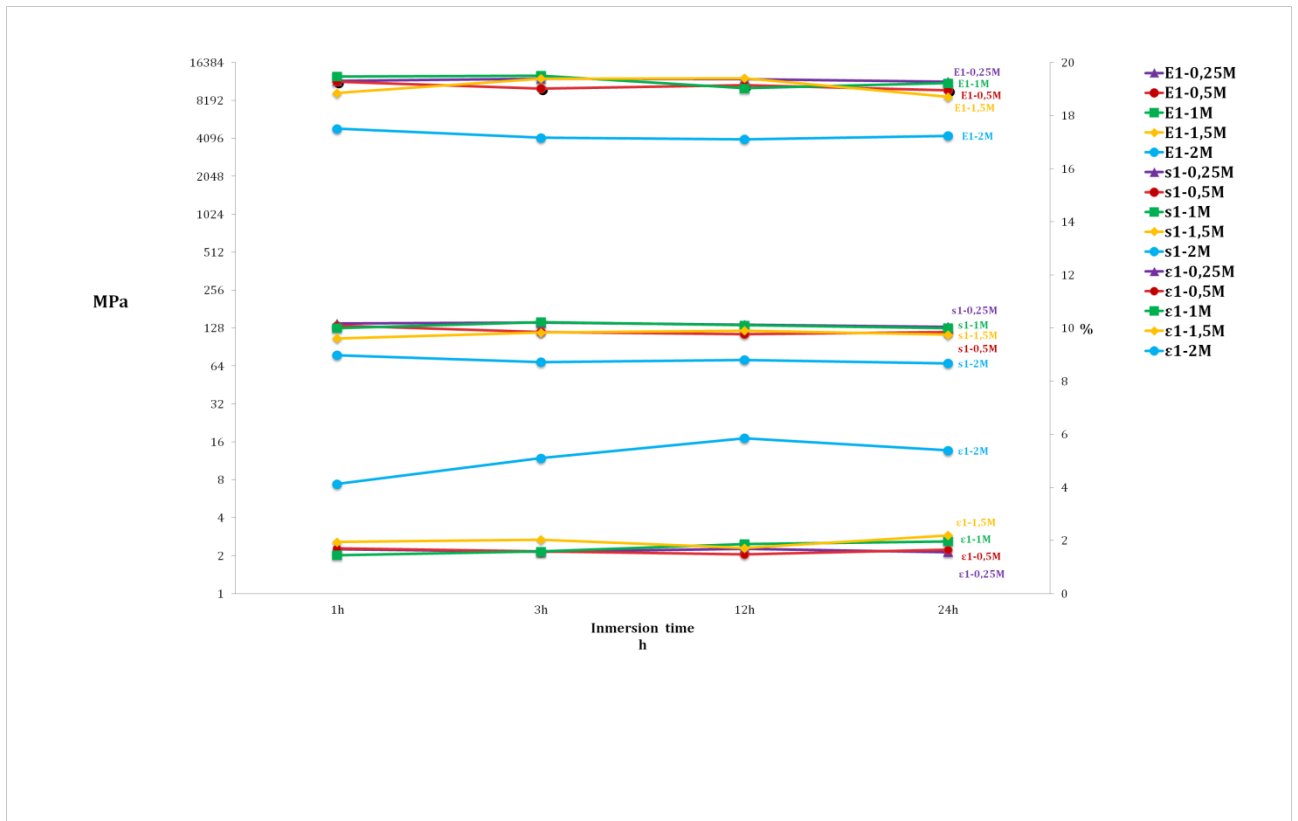


Figure 9.14. Longitudinal tensile properties vs immersion time

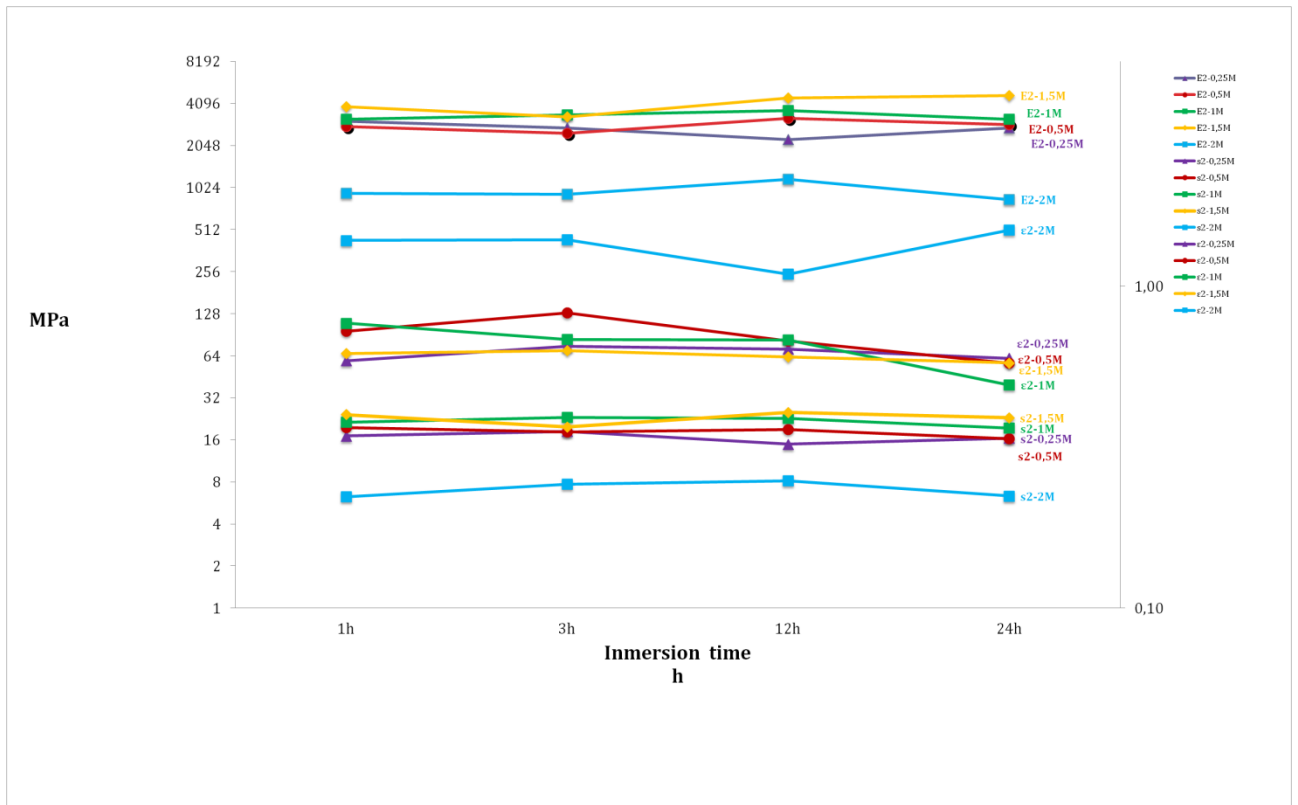


Figure 9.15. Transverse tensile properties vs immersion time

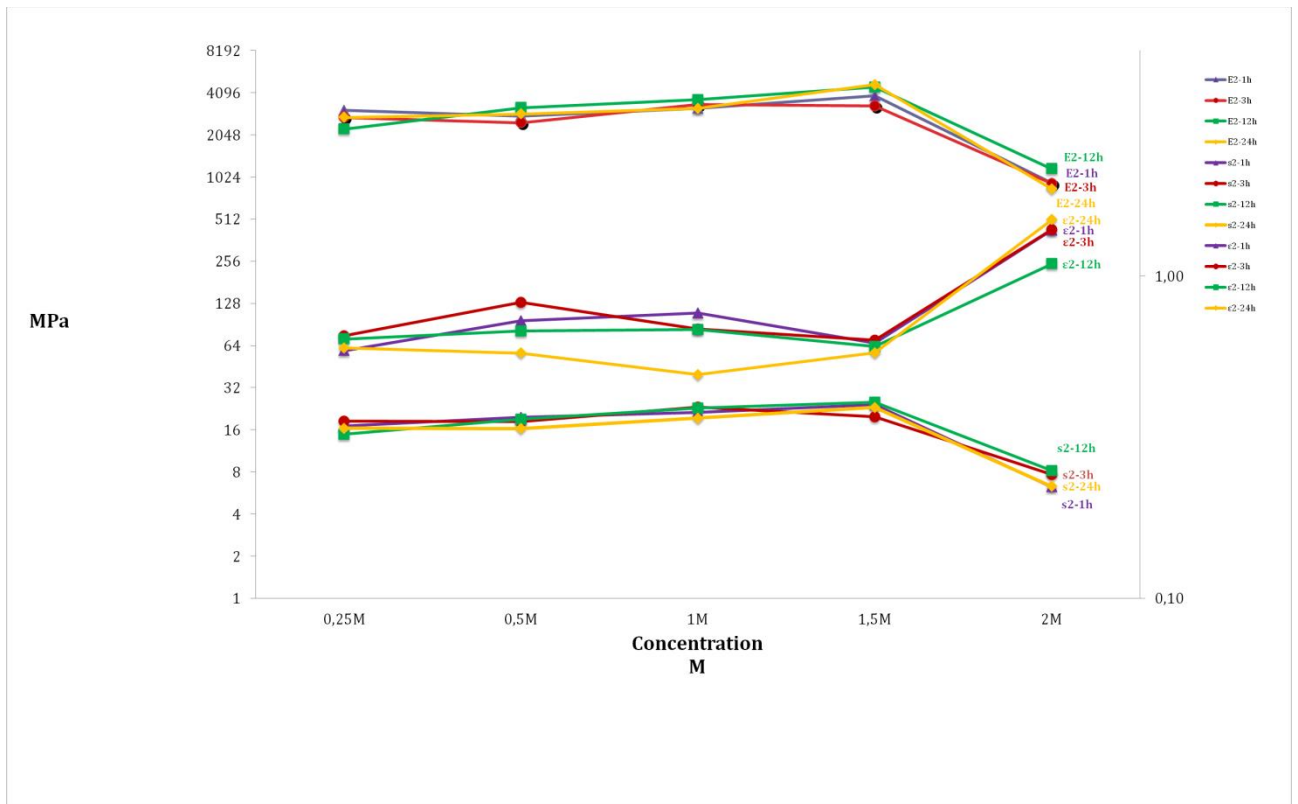


Figure 9.16. Transverse tensile properties vs concentration

### **9.3. PLATE MANUFACTURE**

A series of 600 x 330 mm composite plates were manufactured by resin infusion under flexible tooling with a flow medium (RIFT II). The flow direction was parallel to the long axis of the plates with the flow medium covering the first quarter (150 mm) of the length. Up to 1.0M NaOH treatment, the reinforcement pack filled in ~10-12 minutes. The 1.5M NaOH panel took ~30 minutes to fill. The 2.0M NaOH treated reinforcement did not fill until the flow medium was extended to within 50 mm of the downstream edge. The selected 3h and 1M combination treatment (§9.2) is thus compatible with short process times.

In the plate manufacturing it was detected that the fibre degradation (§9.2) and swelling (§9.3) due to the mercerisation process, was affecting the plate manufacturing. For that reason different solutions were developed along the research project.

### **9.4. EFFECT OF FIBRE SWELLING**

The mercerisation process provokes the fibre swelling, directly affecting the composite mechanical and flow properties. This phenomenon is studied in this subsection as a part of the overall research question.

The fibre swelling may provoke two effects: the resin may be delayed if the flow front constrains liquid moving forwards or may have a favourable effect by forcing resin forwards. These two effects must be included in the mass conservation equation using sink and source terms. As a result, the permeability value may be varied with the exposure time and position. Nguyen applied this variation in his models, varying permeability (mass source/sink terms) which led to better agreement with the experimental flow measurements than the constant permeability model. Mass sink became higher when the fibre volume increased.

Optical microscopy to determine the apparent fibre diameter revealed that fibres exposed to mercerisation were swollen up to 20% linearly (i.e. change in the diameter, Table 8.3) during the most aggressive treatments. The lignocellulosic material thus occupies a greater volume for the same areal weight of reinforcement fabric. Cripps et al. proposed that the dependence of permeability on

fibre volume fraction (assuming no contact between the individual filaments) would be (Cripps, Searle & Summerscales, 2000):

$$K \propto (1 - V_f)^3 / V_f^2 \quad \text{or} \quad \varepsilon^3 / (1 - \varepsilon)^2 \quad \text{Equation 9.1}$$

Where the porosity is  $\varepsilon = 1 - V_f$

For a reduction of permeability of one third for over-treated fibres relative to untreated fibres (1.5 M vs 1.0M NaOH), the above proportionality can be recalculated; because the swollen fibre would increase the cavity size as the flow progresses during RIFT process. Using the volume fraction of the swollen fibre derived from the apparent diameters (assuming circular fibre cross-section), the equation becomes  $V_{ft} = \phi_t^2 V_{fu} / \phi_u^2$ , where  $\phi_x$  is the apparent diameter of the treated (subscript t) or untreated (subscript u) fibre. Subject to the foregoing assumptions, we might expect the new permeability to be predicted by Equation 9.1a:

$$\frac{K_t}{K_u} = \frac{1}{3} = \frac{(1 - V_{ft})^3}{(1 - V_{fu})^3} \frac{V_{fu}^2}{V_{ft}^2} \quad \text{Equation 9.1a}$$

While appropriate quantitative data for permeability is not available due to the complex deformation history during the fabric compression and flow stages of resin infusion (and the limited monitoring capability in the manufacturing laboratory), the qualitative data are consistent with the expectations of the Cripps et al proportionality. See Figure 9.17:

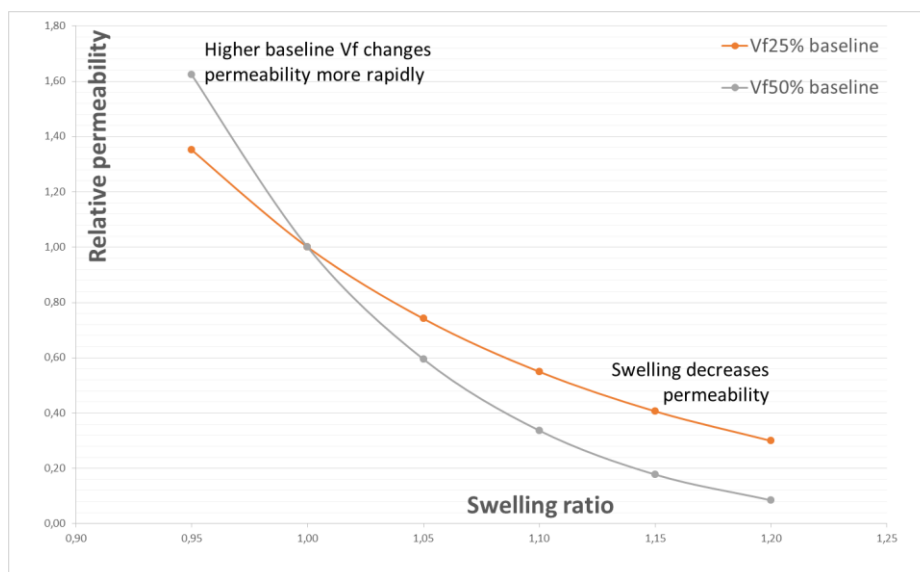


Figure 9.17: Swelling model representation graph

Further, Francucci et al. (Francucci, Rodríguez & Vázquez, 2010) and Masoodi et al. (Masoodi, Pillai, Grahl & Tan, 2012) have studied the absorption, and consequent swelling, of natural fibre reinforcements by permeant fluids. The increased fibre diameter was indicated to be the principal reason for inconsistencies in permeability measurements for these reinforcements. In a study by Nguyen et al. on the influence of liquid absorption and fibre swelling during RTM resin impregnation of flax fibre reinforcements, the authors suggested a relationship between fibre swelling and permeability as given by Equation 9.2 (Nguyen, Lagardère, Cosson & Park, 2014):

$$K = (1 - f_{sw}^2 V_f)^{n+1} / A (f_{sw}^2 V_f)^n \quad \text{Equation 9.2}$$

where K is the permeability,  $f_{sw}$  is the fibre swelling ratio (wet diameter/dry diameter),  $V_f$  is the fibre volume fraction and A and n are empirically derived constants. Note that Equation 9.2 has a similar format to Equation 9.1, now with exponent n (instead of 2) and a new parameter,  $f_{sw}$ .

## 9.5. SILANE COUPLING AGENT

Having established that 1.0M NaOH treatment for 3 hours (See §9.2.8.) should provide a sensible balance of mechanical properties without extended treatment and resin infusion times, this combination was used for the **definitive tests** to confirm or refute the hypothesis that silane treatment would enhance the properties and might be achieved by adding the silane to the resin hardener rather than extending fibre treatment times by further processing the reinforcement before composites manufacture.

The silane molecule (coupling agent) is normally an oleophilic (aliphatic) chain with an oleophobic reactive entity (e.g. silane) as a terminal group. To minimise the chemical energy of the system, the oleophobic entity should be expelled from the liquid resin to the surfaces, or in bulk systems to any available interface where it may react, dependent on compatibility of the reactive entity with the reinforcement fibre. Mixing the coupling agent into the resin system hardener will eliminate the need for fibre/fabric treatment prior to composite manufacture. Should this approach be demonstrated to work, then the laminate manufacture will be more "sustainable": the solvents used for fabric

treatments are eliminated (the hardener becomes the necessary solvent) with benefits to the environment and to worker health.

A series of panels were manufactured as described in Chapter 7 with samples extracted for mechanical testing as described in Chapter 8. The results of individual tests are presented in Appendix C. In Table 9.25, four different treatments results are shown (by reference to the relative heights of the bar graphs in the above Appendix using three colours: white = low, orange = middle and green = high). In Table 9.26, the data are grouped according to the seven mechanical properties ( $E_1$ ,  $E_2$ ,  $\sigma'_1$ ,  $\sigma'_2$ ,  $\epsilon'_1$ ,  $\epsilon'_2$ ,  $\nu_{12}$ ).

The selected four systems using Biotex flax fibre and Huntsman epoxy resin have got the following characteristics:

- **25-untreated fibre/ resin + 1% silane in the hardener**
- **26- fibre treatment in 1M NaOH solution for 3h immersion time/ resin + 1% silane in the hardener**
- **27- fibre treatment in 1% silane solution / resin**
- **28- fibre treatment in 1M NaOH solution for 3h immersion time + 1%silane solution/ resin**

Table 9.25: Silanisation level effect is colour coded

	25 Biotex/Huntsman Silane in hardener	26 Biotex 3h 1M NaOH fibre treatment/Huntsnan- Silane in Hardener	27 Biotex 1% silane fibre treatment/Huntsman	28 Biotex 3h 1M NaOH + 1% silane fibre treatment/Huntsman
E1 p57	H	M	M	M
E2 p60	L	H	M	M
S1 p58	H	L	M	L
S2 p61	M	L	M	H
$\epsilon_1$ p58	L	H	M	L
$\epsilon_2$ p61	L	L	H	H
$\nu_{12}$ p59	M	H	L	H



Table 9.26: Seven mechanical properties

	<b>25</b> <b>Biotex/Huntsman</b> <b>Silane in hardener</b>	<b>26</b> <b>Biotex 3h 1M NaOH</b> <b>fibre</b> <b>treatment/Huntsman-</b> <b>Silane in Hardener</b>	<b>27</b> <b>Biotex 1% silane</b> <b>fibre</b> <b>treatment/Huntsman</b>	<b>28</b> <b>Biotex 3h 1M NaOH</b> <b>+ 1% silane fibre</b> <b>treatment/Huntsman</b>
<b>E1 p57</b>	13,08	10,08	10,05	10,88
<b>E2 p60</b>	3,66	4,08	3,72	3,87
<b>S1 p58</b>	136,46	105,24	120,50	95,49
<b>S2 p61</b>	16,65	14,11	17,53	19,28
<b>ε1 p58</b>	1,29	1,92	1,57	1,44
<b>ε2 p61</b>	0,36	0,33	0,44	0,50
<b>ν12 p59</b>	0,52	0,73	0,31	0,68

Note that  $\nu_{12}$  data is included in the table but is not considered in the evaluation since Poisson's ratio(s) is (are) not considered to be a "performance" parameter in the same way as the other six properties.

Table 9.25 has

- 2 green cells for 1% silane in the hardener,
- 3 green cells for 1M NaOH+1% silane in the hardener,
- 3 green cells for 1M NaOH+1% silane in the fibre,
- 5 orange cells for 1% silane in the fibre, and
- 2 orange cells for 1% silane in the hardener and for 1M NaOH+1% silane in the fibre.

Panels 25, 26 and 27 had the greatest proportion of white (low) cells, indicating this case as a non-optimal treatment.

The analysis in Table 9.25 considers only relative values of the respective mechanical properties. Table 9.26 presents the analysis for absolute properties. In regards to the interfacial properties, the 1M NaOH mercerisation followed by 1% silane treatment increases the transverse strength  $\sigma_2$  and strain  $\epsilon_2$ , keeping the modulus  $E_2$  in an acceptable value. In contrast, the longitudinal properties  $E_1$ ,  $\sigma'_1$ ,  $\epsilon'_1$  are clearly damaged by the chemical treatment. Similarly, when the fibres were treated with 1% silane, the longitudinal properties  $E_1$ ,  $\sigma'_1$ ,  $\epsilon'_1$ , were also reduced, but at lower scale; while the transverse properties  $E_2$ ,  $\sigma'_2$ ,  $\epsilon'_2$ , were slightly improved. These two systems comparison suggests that flax fibre silane treatment reduces the longitudinal properties while the 1M NaOH 3h + 1% silane treatments works to increase fibre-matrix adhesion.

When 1% **silane was added to the hardener, the highest  $E_1$  and  $\sigma'_1$  values** were achieved. In contrast,  $E_2$ ,  $\sigma'_2$ ,  $\varepsilon'_2$  values were reduced in comparison with the flax fibre direct silane treatment. When the fibre was mercerised and silane added to the hardener, longitudinal and transverse properties clearly decreased. This decrement suggested that the mercerisation process reduced the longitudinal properties; and the silane was not reacting with the mercerised flax surface when dissolved in the hardener.

In Table 9.27, all the values have been converted to percentages relative to the highest value achieved on each row (**hence one of the four values must be 100%**). The final row of the table gives the sum of the values in each column to identify the treatment with the best performance. This initial analysis indicates that the performance of each of the systems is broadly identical. For this reason, a new classification scheme was introduced to give weight to the importance of each property according to its relevance to composite design.

Table 9.27: Seven mechanical properties **percentage**

Percentage (%)	25 Biotex/Huntsman Silane in hardener	26 Biotex 3h 1M NaOH fibre treatment/Huntsman- Silane in Hardener	27 Biotex 1% silane fibre treatment/Huntsman	28 Biotex 3h 1M NaOH + 1% silane fibre treatment/Huntsman
<b>E1 p57</b>	100,00	77,04	76,80	83,14
<b>E2 p60</b>	89,71	100,00	91,27	94,92
<b>S1 p58</b>	100,00	77,12	88,30	69,98
<b>S2 p61</b>	86,34	84,77	90,92	100,00
<b><math>\varepsilon_1</math> p58</b>	67,13	100,00	81,68	74,93
<b><math>\varepsilon_2</math> p61</b>	71,85	65,44	87,83	100,00
<b><math>\nu_{12}</math> p59*</b>	71,75	100,00	43,03	93,66
<b>Total</b>	<b>515,03</b>	<b>504,38</b>	<b>516,81</b>	<b>522,96</b>

\*  $\nu_{12}$  is not considered in the subtotal value

Note:  $\nu_{12}$  was not considered in the subtotal value because the highest value was not considered as the best.

For orthotropic materials, elastic moduli values ( $E_1$ ,  $E_2$  and  $\nu_{12}$ ) are fundamental in the design process based in the rigidity matrix (Equation 9.3).

$$\begin{Bmatrix} \varepsilon_1 \\ \varepsilon_2 \\ \gamma_{12} \end{Bmatrix} = \begin{bmatrix} \frac{1}{E_1} & -\frac{\nu_{12}}{E_2} & 0 \\ -\frac{\nu_{12}}{E_2} & \frac{1}{E_2} & 0 \\ 0 & 0 & \frac{1}{G_{12}} \end{bmatrix} \begin{Bmatrix} \sigma_1 \\ \sigma_2 \\ \sigma_3 \end{Bmatrix}$$

**Equation 9.3**

Additionally there are different composite failure criteria. Puck says that the laminate can fail because of Fibre Failure (FF) and Inter Fibre Failure (IFF). The criteria distinguish between FF and IFF; and in the IFF there are three modes of failure, giving the angle of the crack in reference to the laminate plane. Depending on the IFF mode, the failure might be critical or acceptable for the design of the composite.

Puck bases the FF criteria on the fact that the fibre failure of a UD lamina under particular tensile conditions will occur when the tensile stress in the fibre  $\sigma_{1f}$  reaches the same level of a uniaxial tensile strength  $\sigma_{1t}$  or uniaxial compression strength  $\sigma_{1c}$ . The criteria are shown in the Equation 9.4:

$$f_{E,FF} = \frac{1}{\pm R_{II}^{\epsilon,c}} \left[ \sigma_1 - \left( v_{\perp\parallel} - v_{\perp\parallel f} m_{\sigma f} \frac{E_{\parallel}}{E_{\parallel f}} \right) (\sigma_2 + \sigma_3) \right] \quad \text{Equation 9.4}$$

$$R_{II}^t \text{ for } [...] \geq 0$$

$$-R_{II}^c \text{ for } [...] < 0$$

Finally, since the design idea would be based in the strength values and not in the strain values, the strain would be considered as the weakest factor.

Based on the justification above, the next **design factors** are considered in Table 9.17:

Table 9.28: Mechanical properties design factor

Property	Design factor
$E_1, E_2, \nu_{12}$	3
$\sigma_1, \sigma_2$	2
$\epsilon_1, \epsilon_2$	1

Based in the values in Table 9.28, Table 9.29 was produced. Table 9.27 percentage values were multiplied with the design factors in Table 9.28 in order to get Table 9.29.

Table 9.29: Seven mechanical properties **weighted percentage (maximum = 100, 200 or 300)**

Percentage (%)	25 Biotex/Huntsman Silane in hardener	26 Biotex 3h 1M NaOH fibre treatment/Huntsman- Silane in Hardener	27 Biotex 1% silane fibre treatment/Huntsman	28 Biotex 3h 1M NaOH + 1% silane fibre treatment/Huntsman	Design factors
E1 p57	300,00	231,12	230,41	249,43	3
E2 p60	269,12	300,00	273,81	284,75	3
S1 p58	200,00	154,24	176,60	139,95	2
S2 p61	172,69	169,55	181,84	200,00	2
ε1 p58	67,13	100,00	81,68	74,93	1
ε2 p61	71,85	65,44	87,83	100,00	1
v12 p59*	215,25	300,00	129,09	280,97	3
<b>Total</b>	<b>1080,78</b>	<b>1020,36</b>	<b>1032,18</b>	<b>1049,06</b>	

\* v<sub>12</sub> is not considered in the subtotal value

Table 9.29 quantifies different laminate modification effectiveness for the measured mechanical properties; supporting the idea that the **laminates 25 was performing the best**.

In conclusion, for the silane in hardener series of tests, the mechanical properties conclusions were:

- **Silane-in-hardener without mercerisation achieves the best composite system**, this would be one clear answer for the PhD research question
- The silane reacts with the mercerised surface only when the fibre is directly treated with the silane but not when the silane is added to the hardener
- Mercerisation clearly reduce the composite longitudinal properties
- Fibre silane treatment slightly reduce the composite mechanical properties
- All the assumptions were supported with simplistic method in Table 9.29

## 9.6. BEST COMPOSITE SYSTEM

In Table 9.30, the data are grouped according to the seven mechanical properties ( $E_1$ ,  $E_2$ ,  $\sigma'_1$ ,  $\sigma'_2$ ,  $\varepsilon'_1$ ,  $\varepsilon'_2$ ,  $v_{12}$ ). In order to determine the best system from the experimental campaign, the following four combinations were selected:

- **1-Untreated Biotex flax fibre/SuperSap bio-epoxy resin**
- **3-Untreated Biotex flax fibre/Huntsman epoxy resin**
- **4-Commercially treated Lineo flax fibre/Huntsman epoxy resin**
- **25-Untreated Biotex flax fibre/Huntsman epoxy resin + 1% silane in the hardener**

Table 9.30: Seven mechanical properties

	<b>1</b> <b>Biotex/SuperSap</b>	<b>3</b> <b>Biotex/Huntsman</b>	<b>4</b> <b>Lineo/Huntsman</b>	<b>25</b> <b>Biotex/Huntsman Silane in hardener</b>
<b>E1 p57</b>	15,62	10,21	8,49	14,18
<b>E2 p60</b>	3,37	2,57	3,21	3,66
<b>S1 p58</b>	175,04	136,66	168,02	147,88
<b>S2 p61</b>	3,80	16,22	29,15	16,65
<b><math>\epsilon_1</math> p58</b>	1,36	0,96	1,52	1,40
<b><math>\epsilon_2</math> p61</b>	0,11	0,53	0,88	0,36
<b><math>\nu_{12}</math> p59</b>	0,44	0,17	0,25	0,56

Note that  $\nu_{12}$  data is included in the table, but is not considered in the evaluation since Poisson's ratio(s) is (are) not considered to be a "performance" parameter in the same way as the other six properties.

Table 9.30 shows the results for the four best laminates of the experimental campaign. When comparing the 3<sup>rd</sup> and 25<sup>th</sup> laminates, untreated flax and 1% silane in the hardener system respectively, it was clearly shown that six mechanical properties out of seven were improved. This supports the utilisation of the silane in the hardener for the enhancement of flax/epoxy composites.

When comparing the Biotex enhanced Laminate 25 system with the Lineo reinforced composite, panel 4, these were the conclusions: The Biotex panel longitudinal rigidity was higher comparing the  $E_1$  and  $\epsilon'_1$  values, being very low  $E_1$  value for Lineo system. In contrast longitudinal strength value was higher for Lineo, suggesting a better fibre-matrix adhesion. In regards to the transverse properties,  $E_2$  and  $\epsilon'_2$  values suggest that the Biotex interface was more rigid/brittle than the Lineo. Additionally,  $\sigma'_2$  confirms that the Lineo system had stronger fibre-matrix adhesion than the Biotex system. It is true that the patented Lineo fibre treatment is properly increasing the fibre matrix adhesion, however the longitudinal rigidity loss is too pronounced in regards to design issues; for that reason the enhanced Biotex/Huntsman 25<sup>th</sup> system is preferred at this occasion.

Finally, the 1<sup>st</sup> laminate manufactured with Biotex and SuperSap resin confirms that high quality composite system can be produced with a Bio-epoxy system. The data suggests that although high quality longitudinal properties are obtained, the fibre/matrix adhesion is too low.

Resuming:

- **1% addition to the hardener clearly improved the unmercerised Biotex system transverse mechanical properties, suggesting a great improvement of the fibre/matrix adhesion.** This would be one clear answers for the PhD research question
- Lineo system still has better fibre-matrix interfacial properties than the enhanced Biotex, however longitudinal rigidity properties are drastically reduced with the Lineo's patented chemical treatment
- SuperSap bio-epoxy may be used for high standard composite manufacturing. The PhD experimental campaign was completed with the mechanical characterisation of the **Biotex/SuperSap + 1% silane in the hardener optimised system** in §9.14

## 9.7. VOLUME FRACTION VARIATION WITH TREATMENT

In previous sections, the relation between the flax chemical treatment with the fibre swelling and with the  $V_f$  variation was evaluated.  $V_f$  measurement was determined by CRAG 1000 "Density measurement" method; for all cases, the untreated fabric areal weight was considered, because it did not vary with the chemical treatments. A model was proposed in §9.4 for the mercerisation process and a tendency described for the silane treatment in the §9.5, in order to give an answer to the research question.

However, it was not mentioned that each treatment changed the laminate  $V_f$ ; i.e. each laminate has a characteristic  $V_f$  depending on the received chemical treatment. Although, in this doctoral study, the longitudinal properties were corrected for the best comparison, in the case studies and real manufacturing processes, higher volume fractions are preferred. As a result, ideally good mechanical properties balance must be accompanied with high  $V_f$  value. In Table 9.31, the  $V_f$  data are shown.

From the experimental campaign, the main conclusion obtained was that the fibre chemical treatment provokes  $V_f$  values decrement; the chemical treatment provokes fibre swelling and subsequent laminate thickness increment. Panels from 1 to 3 were manufactured with untreated fibres getting as a result the highest  $V_f$  values. When instead of treating fibres the **silane was added to the**

**hardener, the  $V_f$  reduction was not observed**, supporting with another the panel 25 enhanced method.

In section §9.4 the fibre swelling was related to the panel manufacturing flow properties. The fibre swelling must be directly correlated to the laminate thickness, for that reason Figure 9.18 represents the laminate thickness variation with the treatment and compare to the unswollen laminate thickness (Lamina #3#).

Table 9.31: Volume fraction values for laminates 1 to 28

Laminate	Vf longitudinal	Vf transverse
1-Biotex/SuperSap	0,300	0,300
3-Biotex/Huntsman	0,340	0,350
4-Lineo/Huntsman	0,369	0,352
5-Biotex 1h 0.25M NaOH treatment/Huntsman	0,255	0,266
6-Biotex 3h 0.25M NaOH treatment/Huntsman	0,252	0,241
7-Biotex 12h 0.25M NaOH treatment/Huntsman	0,248	0,251
8-Biotex 24h 0.25M NaOH treatment/Huntsman	0,244	0,246
9-Biotex 1h 0.50M NaOH treatment/Huntsman	0,268	0,266
10-Biotex 3h 0.50M NaOH treatment/Huntsman	0,280	0,277
11-Biotex 12h 0.50M NaOH treatment/Huntsman	0,285	0,273
12-Biotex 24h 0.50M NaOH treatment/Huntsman	0,272	0,259
13-Biotex 1h 1.00M NaOH treatment/Huntsman	0,236	0,233
14-Biotex 3h 1.00M NaOH treatment/Huntsman	0,230	0,230
15-Biotex 12h 1.00M NaOH treatment/Huntsman	0,226	0,242
16-Biotex 24h 1.00M NaOH treatment/Huntsman	0,229	0,224
17-Biotex 1h 1.50M NaOH treatment/Huntsman	0,238	0,245
18-Biotex 3h 1.50M NaOH treatment/Huntsman	0,259	0,250
19-Biotex 12h 1.50M NaOH treatment/Huntsman	0,247	0,238
20-Biotex 24h 1.50M NaOH treatment/Huntsman	0,227	0,219
21-Biotex 1h 2.00M NaOH treatment/Huntsman	0,255	0,251
22-Biotex 3h 2.00M NaOH treatment/Huntsman	0,228	0,235
23-Biotex 12h 2.00M NaOH treatment/Huntsman	0,243	0,243
24-Biotex 24h 2.00M NaOH treatment/Huntsman	0,235	0,244
25-Biotex/Huntsman 1% silane in hardener	0,325	0,316
26-Biotex 3h 1.00M NaOH treatment/Huntsman 1% silane in hardener	0,234	0,221
27-Biotex 1% silane fibre treatment/Huntsman	0,276	0,269
28-Biotex 3h 1M NaOH + 1% silane fibre treatment/Huntsman	0,251	0,230



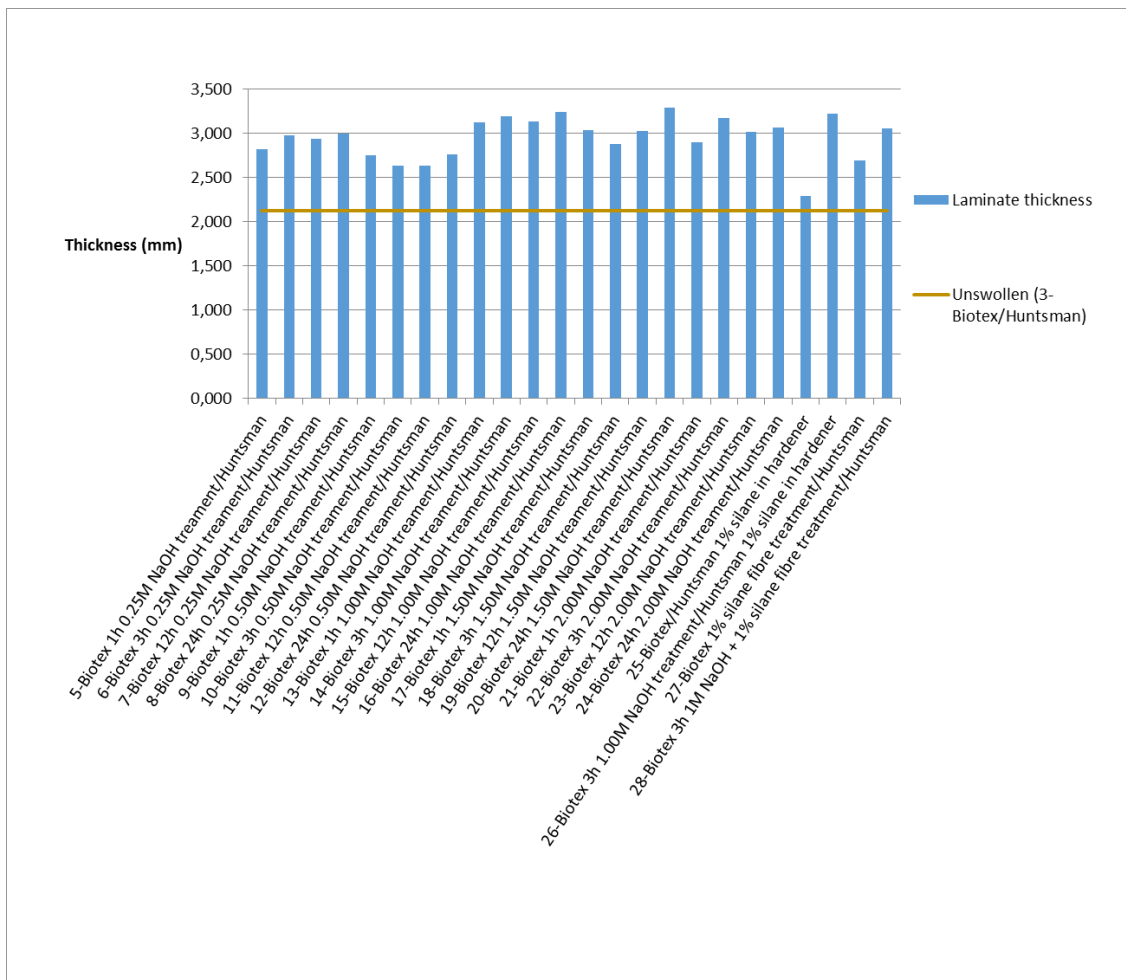


Figure 9.18. Laminates thickness values vs the chemical treatment

\*NOTE: The values are the average numbers from longitudinal and transverse plates

According to the Figure 9.18, the chemical treatment is provoking a swelling of the fibres and as a result an increment in the laminate thickness. Chapter 8 Table 8.3, shows data for the fibre swelling, however this data is insufficient for a quality analysis. An easy prediction method to determinate the laminate thickness increment and  $V_f$  decrement after any treatment, might be to measure the fibre swelling variation.

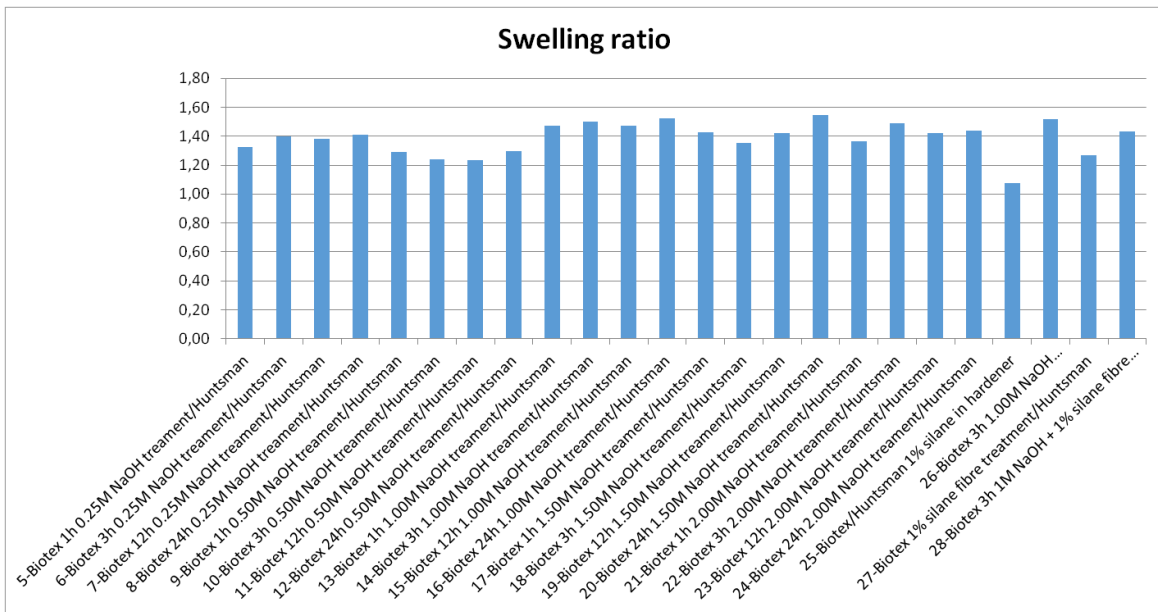


Figure 9.19. Laminates thickness increment vs the chemical treatment

Additionally Figure 9.19 represents different panels thickness differences in comparison to the unswollen system. For the case of the mercerisation process the values can reach values of 1.55, with the lowest values for the addition of the silane to the hardener and untreated fibres composite system.

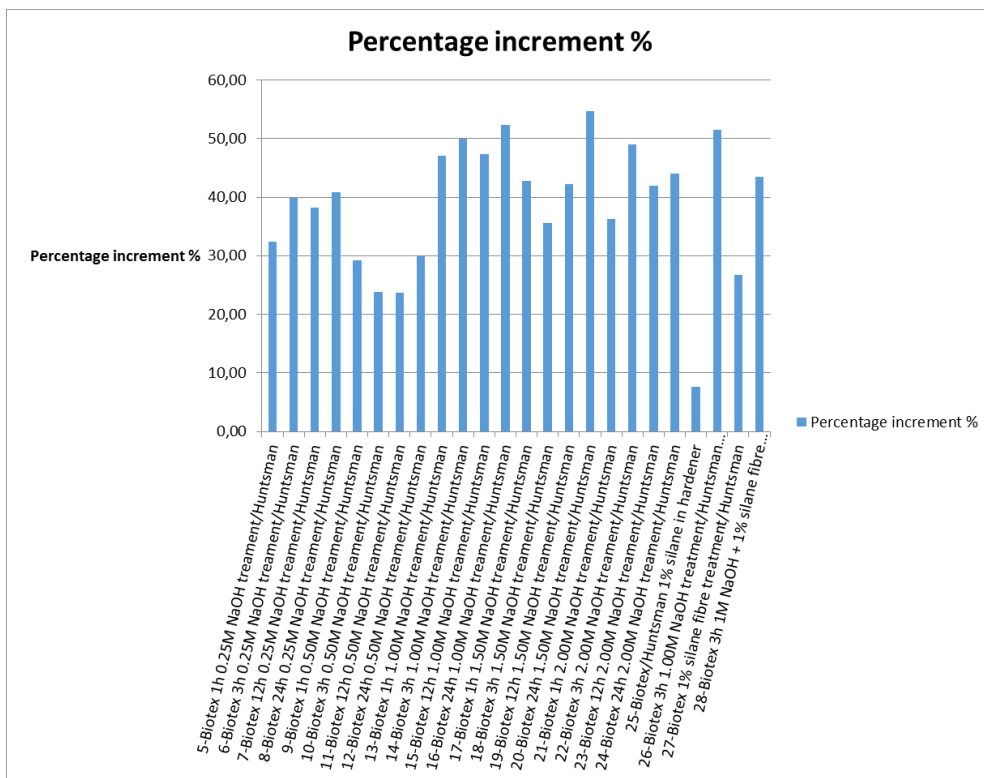


Figure 9.20. Laminates thickness increment % vs the chemical treatment

When the data is represented the treatment vs. the percentage improvement, see Figure 9.20. This representation shows more definitive results. For the best of the cases just 7% is incremented the laminate thickness, and for the worse of the cases 55%, elevated value.

The reflection is that the fibre quantity (weight or volume) introduced in the system is the same, however the resin amount is varying from one sample to another. The first supposition is that fibre treatment provokes fibre swelling, getting as a result increased laminate thickness, resulting in a lower  $V_f$  value.

For the untreated fibre with silane in the hardener, the time for the fibre to swell in the liquid matrix will be limited by the cure time of the resin during plate manufacture, and hence shorter than the swelling duration during optimal mercerisation (albeit that the different liquids may also influence swelling).

### **9.8. VOLUME FRACTION MEASUREMENT DEVIATION**

It was reported in Chapter 8 that the flax fibre swells after chemical treatment. The swelling altered the fabric homogeneity, giving as a result thickness variation along the laminate, subsequently increasing the deviation in the  $V_f$  measurement.

In Table 9.32, the  $V_f$  data Coefficient of Variation (CV) across all samples are represented, this was done in order to evaluate panel homogeneity.

Table 9.32: Volume fraction CV percentage for laminates 1 to 28

Laminate	CV (%) Vf Longitudinal	CV (%) Vf Transverse
3-Biotex/Huntsman	3,82	3,43
4-Lineo/Huntsman	2,71	1,99
5-Biotex 1h 0.25M NaOH treatment/Huntsman	2,75	2,63
6-Biotex 3h 0.25M NaOH treatment/Huntsman	4,37	2,07
7-Biotex 12h 0.25M NaOH treatment/Huntsman	4,03	2,79
8-Biotex 24h 0.25M NaOH treatment/Huntsman	4,10	4,47
9-Biotex 1h 0.50M NaOH treatment/Huntsman	2,24	3,01
10-Biotex 3h 0.50M NaOH treatment/Huntsman	3,21	3,61
11-Biotex 12h 0.50M NaOH treatment/Huntsman	4,91	3,66
12-Biotex 24h 0.50M NaOH treatment/Huntsman	6,62	3,86
13-Biotex 1h 1.00M NaOH treatment/Huntsman	4,24	4,77
14-Biotex 3h 1.00M NaOH treatment/Huntsman	4,35	3,48
15-Biotex 12h 1.00M NaOH treatment/Huntsman	3,98	3,72
16-Biotex 24h 1.00M NaOH treatment/Huntsman	5,68	4,46
17-Biotex 1h 1.50M NaOH treatment/Huntsman	5,04	2,86
18-Biotex 3h 1.50M NaOH treatment/Huntsman	5,79	5,60
19-Biotex 12h 1.50M NaOH treatment/Huntsman	3,24	4,20
20-Biotex 24h 1.50M NaOH treatment/Huntsman	4,41	4,11
21-Biotex 1h 2.00M NaOH treatment/Huntsman	4,31	2,79
22-Biotex 3h 2.00M NaOH treatment/Huntsman	6,14	5,11
23-Biotex 12h 2.00M NaOH treatment/Huntsman	4,53	4,53
24-Biotex 24h 2.00M NaOH treatment/Huntsman	4,26	3,69
25-Biotex/Huntsman 1% silane in hardener	3,08	1,58
26-Biotex 3h 1.00M NaOH treatment/Huntsman 1% silane in hardener	4,70	2,71
27-Biotex 1% silane fibre treatment/Huntsman	3,26	3,72
28-Biotex 3h 1M NaOH + 1% silane fibre treatment/Huntsman	5,58	2,61

Although the results are not as clear as in the other Chapter 9 sections, there may be a tendency for lower  $V_f$  CV deviations for untreated/low treated fibre systems (from 3 to 9 laminates) and panels manufactured with whole flow mesh plus VAP membrane infusion strategy (from 25 to 28 laminates).

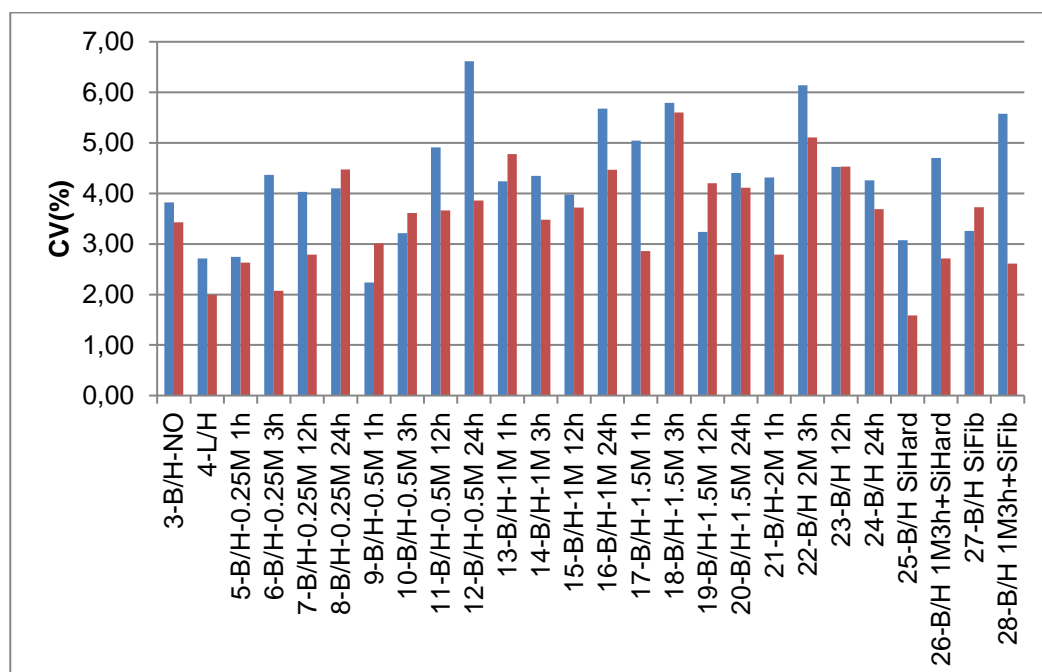


Figure 9.21: Longitudinal (Blue) and transverse (Red)  $V_f$  measurement CV (%)

Additionally Figure 9.21 graphically represents the CV variation, and compares the values difference between longitudinal and transverse panels data. The bar graphs confirms that in 20 out of 26 (three-quarters) cases, the CV values for the longitudinal (Blue) measurements are higher than for the transverse (Red); this phenomenon suggests that transverse panels are more homogeneous than the longitudinal, supporting the “laminare position effect” studied in §9.10.

### 9.9. PANEL MANUFACTURING HOMOGENEITY

Table 9.33 resumes mechanical test standard deviations grouped according to the seven mechanical properties ( $E_1$ ,  $E_2$ ,  $\sigma_1$ ,  $\sigma_2$ ,  $\epsilon_1$ ,  $\epsilon_2$ ,  $\nu_{12}$ ).

Table 9.33: Seven mechanical properties standard deviation for laminates 1 to 28

SD	F <sub>1</sub> (kN)	E <sub>1</sub> (GPa)	$\sigma_1$ (MPa)	$\epsilon_1$ (%)	$\nu_{12}$	F <sub>2</sub> (kN)	E <sub>2</sub> (GPa)	$\sigma_2$ (MPa)	$\epsilon_2$ (%)
3-Biotex/Huntsman	0,45	0,59	7,76	0,15	0,02	0,05	0,19	0,84	0,08
4-Lineo/Huntsman	0,20	0,32	8,37	0,08	0,07	0,06	0,23	1,01	0,08
5-Biotex 1h 0.25M NaOH treatment/Huntsman	0,23	0,83	6,20	0,13	0,08	0,16	0,38	2,62	0,08
6-Biotex 3h 0.25M NaOH treatment/Huntsman	0,38	0,93	6,82	0,12	0,04	0,13	0,45	1,80	0,21
7-Biotex 12h 0.25M NaOH treatment/Huntsman	0,18	0,82	5,07	0,09	0,08	0,21	0,34	3,23	0,06
8-Biotex 24h 0.25M NaOH treatment/Huntsman	0,39	0,89	7,46	0,12	0,09	0,19	0,33	3,11	0,14
9-Biotex 1h 0.50M NaOH treatment/Huntsman	0,23	1,17	8,01	0,07	0,06	0,06	0,39	1,11	0,22
10-Biotex 3h 0.50M NaOH treatment/Huntsman	0,35	0,64	9,68	0,13	0,04	0,10	0,08	1,98	0,14
11-Biotex 12h 0.50M NaOH treatment/Huntsman	0,37	0,89	10,30	0,16	0,08	0,07	0,58	0,97	0,12
12-Biotex 24h 0.50M NaOH treatment/Huntsman	0,30	1,12	7,46	0,13	0,08	0,07	0,29	1,11	0,06
13-Biotex 1h 1.00M NaOH treatment/Huntsman	0,37	0,70	9,27	0,11	0,07	0,13	0,35	2,01	0,12
14-Biotex 3h 1.00M NaOH treatment/Huntsman	0,35	1,46	5,57	0,12	0,04	0,11	0,47	1,74	0,20
15-Biotex 12h 1.00M NaOH treatment/Huntsman	0,45	1,98	5,58	0,14	0,06	0,22	0,74	2,59	0,13
16-Biotex 24h 1.00M NaOH treatment/Huntsman	0,39	1,23	6,74	0,30	0,05	0,15	0,19	2,13	0,05
17-Biotex 1h 1.50M NaOH treatment/Huntsman	0,17	1,18	5,89	0,16	0,17	0,05	0,39	1,18	0,14
18-Biotex 3h 1.50M NaOH treatment/Huntsman	0,17	1,20	5,25	0,17	0,06	0,28	0,47	1,20	0,11
19-Biotex 12h 1.50M NaOH treatment/Huntsman	0,17	1,06	2,78	0,11	0,06	0,11	0,55	1,64	0,10
20-Biotex 24h 1.50M NaOH treatment/Huntsman	0,22	0,87	6,12	0,27	0,05	0,18	0,43	2,27	0,11
21-Biotex 1h 2.00M NaOH treatment/Huntsman	0,11	0,32	3,43	0,41	0,06	0,03	0,29	0,44	0,55
22-Biotex 3h 2.00M NaOH treatment/Huntsman	0,14	0,24	3,03	0,71	0,08	0,05	0,16	0,66	0,38
23-Biotex 12h 2.00M NaOH treatment/Huntsman	0,08	0,23	2,64	0,44	0,16	0,06	0,27	0,74	0,32
24-Biotex 24h 2.00M NaOH treatment/Huntsman	0,11	0,29	3,02	0,61	0,16	0,04	0,09	0,66	0,24
25-Biotex/Huntsman 1% silane in hardener	0,17	2,04	4,66	0,07	0,17	0,04	0,51	0,74	0,09
26-Biotex 3h 1.00M NaOH treatment/Huntsman 1% silane in hardener	0,15	1,19	1,88	0,12	0,14	0,07	0,45	1,08	0,05
27-Biotex 1% silane fibre treatment/Huntsman	0,15	0,68	2,74	0,08	0,07	0,08	0,54	1,58	0,07
28-Biotex 3h 1M NaOH + 1% silane fibre treatment/Huntsman	0,19	0,81	5,50	0,17	0,15	0,09	0,30	1,35	0,07

Laminates 3 and 4 have low deviations because the fibres were untreated, resulting in a more homogeneous reinforcement. In the panels from 5 to 20, there were more red and orange cells because the chemical treatment provoked fibre swelling and inhomogeneous reinforcement. Panels from 21 to 24 were also deeply treated, however since the infusion strategy was modified covering whole panel surface with the flow media, the panel quality subsequently improved, contributing in the green cells achievement.

Finally, 25-28 group panels were manufactured with whole flow media and VAP membrane. This group general tendency was to obtain low CV measurement, especially for the strain values; however, there were slight differences depending on the treatment. It may be assumed that the laminates 25

and 26 where the silane was added to the hardener had more homogeneous values. In contrast, for laminate 27 and 28 where the fibre were directly treated with the silane the CV was higher; getting for the 28<sup>th</sup> laminate the highest deviation because of the sum of silanisation and mercerisation treatments.

### 9.10. LAMINATE POSITION EFFECT

In all the laminates, the longitudinal and transverse coupons were obtained from the areas shown in Figure 9.22.

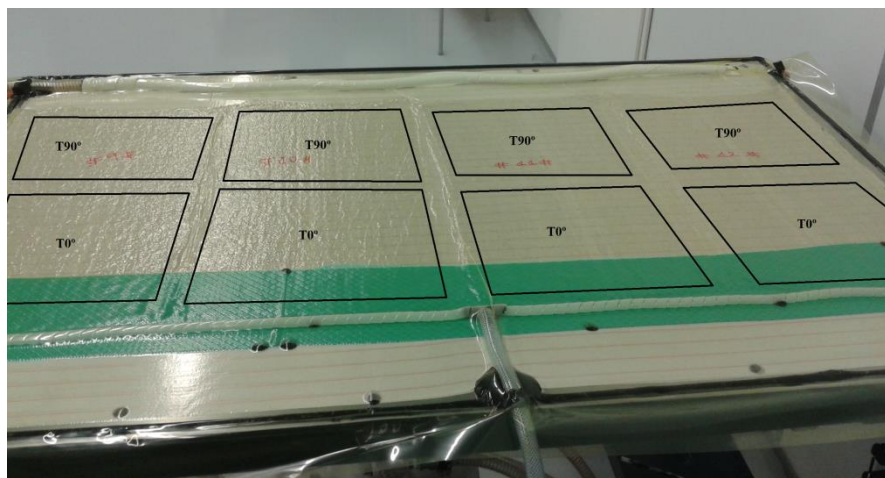


Figure 9.22: Laminates 9-12 samples extraction areas

Based in the Table 9.32,  $V_f$  CV values and Figure 9.22, it was assumed that the laminates produced for transverse ( $T90^\circ$ ) tests were more homogeneous panels; obtaining lower CV values in general. Additionally this homogeneity effect is supported with lower CV in the mechanical tests results (Table 9.33).

It is believed that this effect happens because of these two factors.

- The resin inlet area is always "resin richer" than the rest of the panel, increasing the laminate thickness. This effect led to lower  $V_f$  in the first part of the  $T0^\circ$  panel, getting as a result inhomogeneous panel
- The panel under the flow mesh and the rest of the panel have different  $V_f$  values

This effect was not solved even using the VAP membrane; the general panel homogeneity was increased, however the difference between the T0° and T90° was still obvious.

### **9.11. METHOD SUSTAINABILITY**

The current study has used experimental measurements of a range of mechanical properties to consider the effect of mercerisation in combination with fibre or in-hardener matrix silanisation. In Chapter 4, different literature references and methods have been studied for the execution of the treatments. The main idea was to develop the most sustainable method keeping at the same time the treatment effectiveness while not compromising mechanical performance. These were the sustainable steps in the treatment:

- All the fibres were dried at RT
- The treatments were all applied at RT
- The fibres were not washed after the treatment (the washing was proved not to have an effect)
- Acid neutralisation was avoided
- In the case of the silane addition to the hardener, all solvent consumption was avoided

It was concluded that most of the chemical treatments proposed in Chapter 4 review are neither environmentally nor healthy treatments, at least in regards to the materials selected, see Figure 9.23. However, among all the treatments it is suggested that the mercerisation and silanisation are one of the less hazardous treatments.

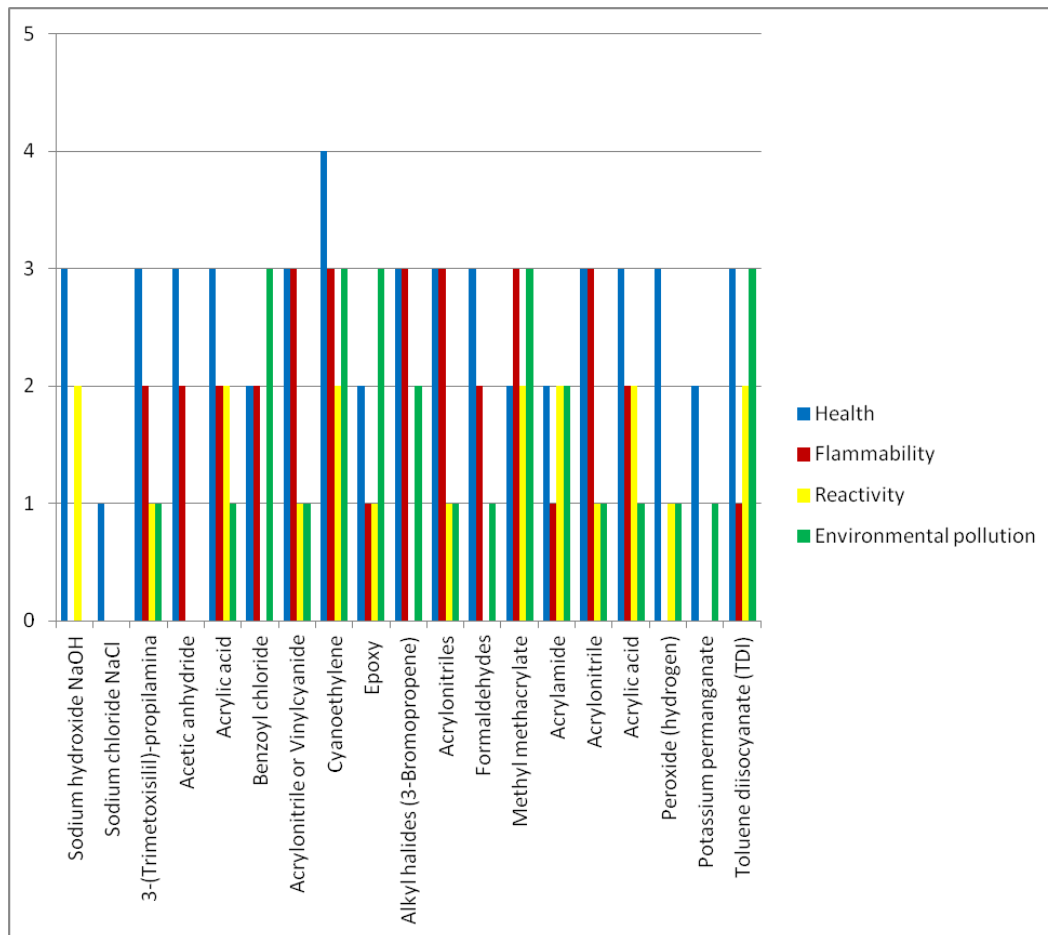


Figure 9.23: Figure produced based on the Hazardous Materials Identification System (HMIS)

The data from the experimental campaign suggest that **optimum mechanical performance can be obtained using unmercerised fibre with silane-in-hardener**. The elimination of both the mercerisation and pre-manufacture silanisation processes obviously reduces environmental burdens by not generating pollutant wastes.

## 9.12. MECHANICAL PROPERTY PREDICTION

The values obtained for the longitudinal modulus and strength should correspond to the predictions from the rules-of-mixture presented by Virk et al. (Virk, Hall & Summerscales, 2012) (Equations 9.5, 9.6):

$$E_c = \kappa \eta_d \eta_l \eta_o V_f E_f + V_m E_m \quad \text{Equation 9.5}$$

$$\sigma'_c = \kappa \sigma'_f V_f + \sigma_m^* (1 - V_f) \quad \text{Equation 9.6}$$



Equation 9.6 is only valid for the axial strength of unidirectional composites although Potter has suggested that, for small misalignments, a correction factor can be included such that the first term of the equation becomes:

$$\sigma'_c = \kappa \sigma'_f V_f \sec^2\theta \quad \text{Equation 9.7}$$

In the above Equations, the nomenclature and data appropriate to each parameter are:

- $E_x$  is the Young's modulus,
- $\sigma'_x$  is the strength,  
 $\sigma'_f = 500 \text{ MPa}$  from Composite Evolution data
- $\sigma_{m^*}$  is the stress in the matrix at the failure strain of the fibre,  
 $\sigma_{m^*} = 17 \text{ MPa}$  from Huntsman data
- $V_x$  is the component volume fraction ( $V_f + V_m + V_v = 1$ ):  
 derived from laminate measurements using CRAG 1000 thickness method
- $\kappa$  is the fibre area correction factor:  
 for flax,  $\kappa = 1.12$  (Brierley ultimates) (Brierley, 2014),  $\kappa = 2.55$  (Thomason et al. technical fibres) (Thomason, Carruthers, Kelly & Johnson, 2011) or  $\kappa = 2.70$  (Soatthiyanon technical fibres) (Soatthiyanon, 2014). The boundary between fibre scales may be ultimate fibre "apparent diameter"  $< 40 \mu\text{m}$  or technical fibre "apparent diameter"  $> 40 \mu\text{m}$ .
- $\eta_d$  is the fibre diameter distribution factor,
- $\eta_l$  is the fibre length distribution factor,
- $\eta_o$  is the fibre orientation distribution factor, and
- subscript  $x$  being  $c$ ,  $f$ ,  $m$  or  $v$  for composite, fibre, matrix or void respectively.

Data for the mechanical properties of fibre or resin were obtained from the reinforcement supplier, Composites Evolution, or the resin supplier, Huntsman, respectively.

Equation 9.5 was used to compare the predicted values for the composite Young's modulus and real values obtained from the investigation.

- $E_c$  is the composite Young's modulus, calculated  **$E_c = 17100 \text{ MPa} = 17,1 \text{ GPa}$**

- $E_f$  is the fibre Young's modulus from Composite Evolution,  $E_f=50000\text{MPa}=50\text{GPa}$
- $E_m$  is the matrix Young's modulus from Huntsman,  $E_m=3000\text{MPa}$
- $V_f=0.3$
- $V_m=0.7$
- $\kappa$  assumed 1
- $\eta_d$  assumed 1
- $\eta_l$  assumed 1
- $\eta_o$  assumed 1

Figure 9.24 shows the results for longitudinal modulus properties.

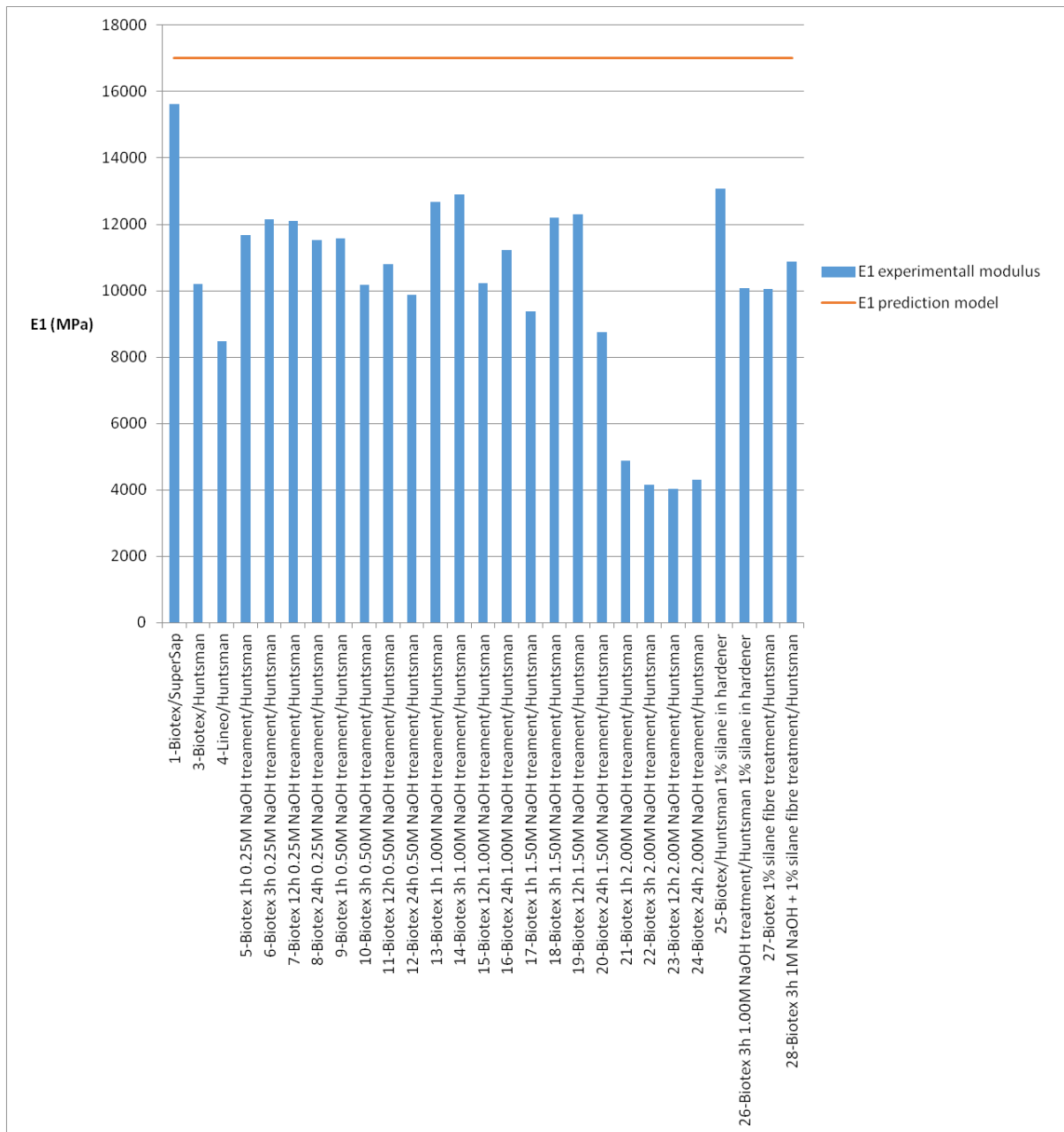


Figure 9.24: Longitudinal modulus experimental and modelled properties data

Experimental modulus (Figure 9.24) is not expected to exceed theoretical predictions. In order to justify the behaviour, the key assumptions include:

- Supplier data for fibre and matrix properties is optimistic
- Orthotropic, macroscopically homogeneous, linearly elastic materials
- Both the fibre and the matrix are free of voids
- Each lamina has uniform thickness across the layer
- Poisson's strains are neglected
- Fibres are continuous with uniform cross-section (but these are polygonal natural fibres)
- Fibres lie parallel to each other
- Fibres are actually spun at  $\sim 30^\circ$  maximum angle to yarn axis ( $\eta_0 = \cos^4\theta = 0.5625$ )
- Perfect bonding between the fibre and the matrix and hence Cox shear-lag theory applies

The strength (Figure 9.25) was predicted with the Equation 9.6, using:

- $\sigma'_c$  is the composite strength,  **$\sigma'_c = 158.75 \text{ MPa}$**
- $\sigma'_f$  is the fibre strength,  $\sigma'_f = 500 \text{ MPa}$  from Composite Evolution data
- $\sigma_{m^*}$  is the stress in the matrix at the failure strain of the fibre. The fibre strain at failure is  $\epsilon'_f = 1.25\%$  and for the matrix  $\epsilon'_m = 5.0\%$ . For that reason, the 50MPa strength of the matrix is recalculated to **12.5MPa** at strain of fibre failure.
- $V_f = 0.3$
- $V_m = 0.7$
- $\kappa$  assumed 1

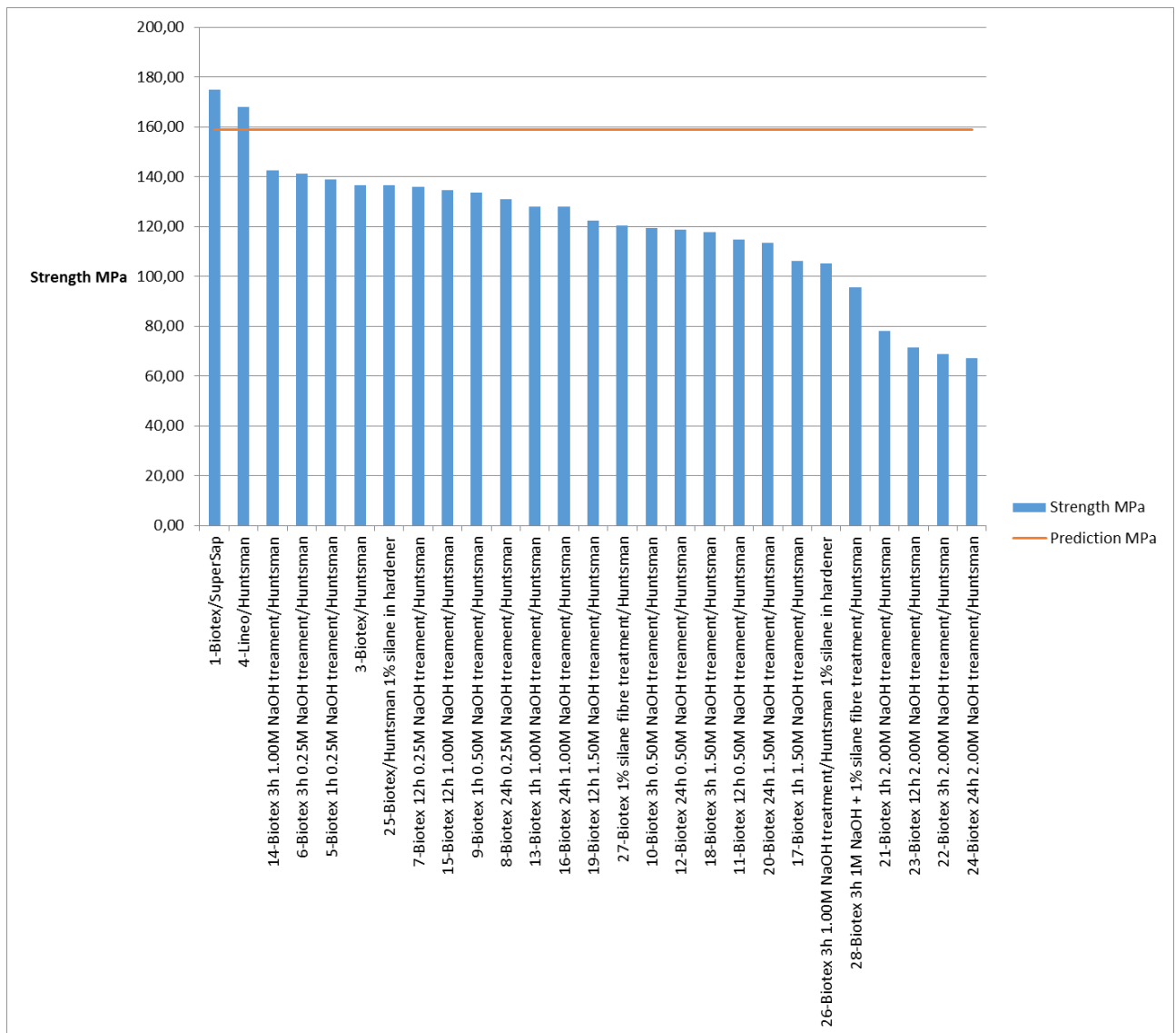


Figure 9.25. Longitudinal strength experimental and modelled properties graph (blue is experimental data; orange line is the extended rule-of-mixture prediction)

Experimental strengths are not expected to exceed theoretical predictions

- Fibre volume fractions are not consistent at 30%
- Virk (Virk et al., 2012) reported ~100 MPa for jute quasi-unidirectional NFRP, but jute is normally considered to be weaker than flax
- Virk (Virk et al., 2012) jute fibre composite strengths with CV 40%

Failure to achieve the predicted strength may arise from:

- Poor fibre-matrix adhesion
- Defects and voids in composite
- Fibre misalignment

### 9.13. WATER RESISTANCE TESTS

The #33 system was produced with the optimised combination, silanisation process adding silane to the hardener in the composite production. The silanised system was compared to the basic unmodified system, #34. Both composite systems were aged in water at same conditions. Figure 9.26 shows the water absorption percentage evolution against time in days. The samples were degraded for **81 days** under the same conditions, and the conclusions obtained from the study were that there is no great different between the two systems. However, when the samples were dried at RT during 19 days, the conclusion was that the silanised system (33) had absorbed marginally less than the base system (34).

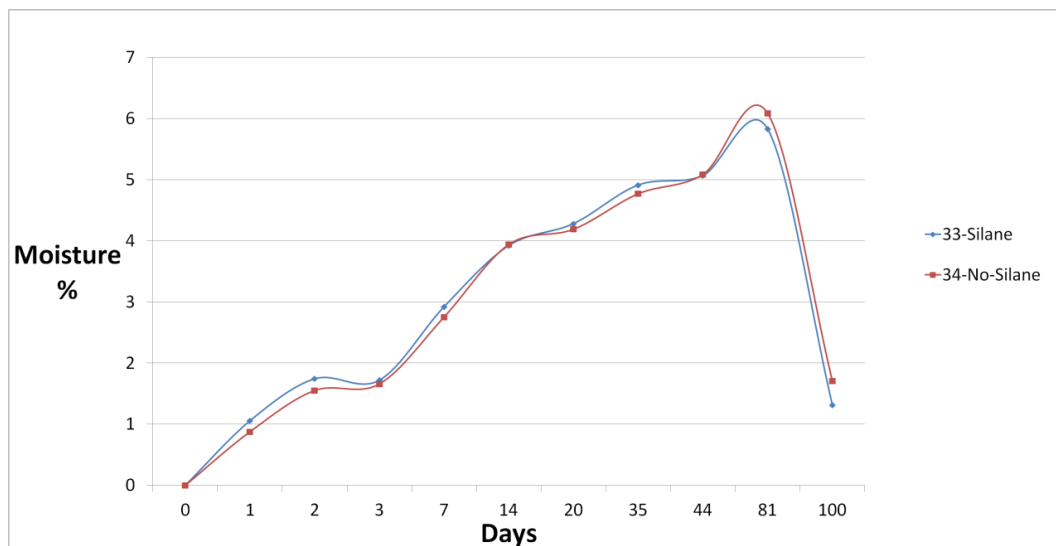


Figure 9.26: Silanised (blue) and not silanised (red) systems water absorption vs time (days)

Although the longitudinal flexural test is not the most representative for the interfacial properties evaluation; this test was selected because the samples were prepared and available to be degraded in the immersion test; additionally as was observed for the tensile or compression tests, the silane is improving the composite longitudinal properties. For that reason, to complete the study, transverse flexural samples were degraded for **ten days** in water at RT then tested. The resulting data is shown in Table 9.34.

Table 9.34: Flexural properties comparison for silane and untreated systems

		Initial flexural properties		Degraded flexural properties		Percentage	
		Force (N)	Modulus (N/mm <sup>2</sup> )	Force (N)	Modulus (N/mm <sup>2</sup> )	Force (%)	Modulus (%)
Logitudinal	Silane in hardener	103,12	18900	65,77	7877	36,22	58,32
	No treated	84,47	16222	62,28	12483	26,27	23,05
Transverse	Silane in hardener	23,00	5720	15,03	3700	34,65	35,31
	No treated	21,70	5620	12,10	2985	44,24	46,89

For the case of the longitudinal tests, it was observed that the silanised system flexural initial performance is greater, in both, force at failure and modulus. However, when degraded it appears that the silanised system is performing worse than the basic system; especially for the modulus data, degrading up to 58,32%. In contrast, when comparing the transverse properties, the silanised system is performing better than the basic one.

The silanised system interfacial properties look to be stronger than the untreated system. However, in the mechanical properties comparison they are not as strong as expected. The selected flexural test is not the most appropriate; the transverse tensile test would be a better alternative.

Apart from this, it is believed that the silane addition to the system will improve the fatigue properties, but this was outside the scope and duration of the PhD study.

#### **9.14. OPTIMISED SYSTEM PROPERTIES**

It was determined that an optimised system (balance of mechanical properties, composite manufacture times and minimisation of environmental burdens) treatment would be to add 1% silane to the hardener and use untreated fibres. To work with the most sustainable combination, **Biotex/SuperSap + 1% silane in the hardener optimised system was selected**. The selected system was consciously studied in order to obtain the most reliable design properties from the mechanical tests; for example the optimum laminates were manufactured with VAP membrane and the strain values during the test were measured with strain gauges. For the complete characterisation of the composite systems, the following tests were performed:

- Tensile test with gauges
- Compression with gauges
- Shear with gauges
- Flexural test

The mechanical properties were obtained in order to perform the case studies design in §9.16.1, and in order to make a comparative study with the basic system, described in the following lines.

From all the tests it was concluded that the silanised system is performing better than the untreated system, suggesting an interfacial properties improvement between the fibre and the resin. This might be possible because the silane migration to the interfacial region and creation of new bond between the fibre surface and epoxy active groups.

#### 9.14.1. Tensile test

Two laminates were manufactured in order to get the most reliable properties measurements:

- **29-Biotex fabric/Huntsman resin**
- **31-Biotex fabric/SuperSap bio-epoxy resin + 1% silane added to the hardener**

Laminate 29 was manufactured in order to get reliable base properties for the best comparison to the enhanced system, Laminate 31 (VAP membrane, and silane added to the bio-epoxy system hardener). Both systems were characterised with strain gauges. Results are shown in Table 9.35.

Table 9.35. Comparative table with the experimental campaign best systems

System	1 Biotex/SuperSap No treated	3 Biotex/Huntsman No treated	29 Biotex/Huntsman No treated+VAP	31 Biote/SuperSap Silane in hardener+VAP	4 Lineo/Huntsman No treated	25 Biotex/Huntsman Silane in hardener
E <sub>1</sub>	15,62	10,21	10,95	13,82	8,49	14,18
E <sub>2</sub>	3,37	2,57	2,07	2,94	3,21	3,66
S <sub>1</sub>	175,04	136,66	152,25	153,46	168,02	147,88
S <sub>2</sub>	3,80	16,22	20,41	18,54	29,15	16,65
ε <sub>1</sub>	1,36	0,96	1,59	1,51	1,52	1,40
ε <sub>2</sub>	0,11	0,53	0,53	0,47	0,88	0,36
ν <sub>12</sub>	0,44	0,17	0,40	0,52	0,25	0,56

Apart from the 29 and 31 systems data, the balance of the data was added in order to have overall view of the whole experimental campaign. The main conclusions were listed in the following points:

- **New VAP** has been used for the manufacturing
- Silane generally has better strength values
- SuperSap generally better than Huntsman
- Slight penalisation in moduli values

#### 9.14.2. Compression test

Both systems compression properties were tested using strain gauges, and the obtained properties were compared in Table 9.36.

- **31-Biotex fabric/SuperSap bio-epoxy resin + 1% silane added to the hardener**
- **30-Biotex fabric/ SuperSap bio-epoxy resin**

Table 9.36: Silanised and untreated systems compression properties comparison

System	31 Biotex/SuperSap Silane in hardener+VAP	30 Biotex/SuperSap No treated+VAP
$E_{c1}$	11,50	10,50
$E_{c2}$	2,60	3,10
$S_{c1}$	110,00	107,00
$S_{c2}$	91,00	86,00
$\epsilon_{c1}$	4,30	3,50
$\epsilon_{c2}$	4,20	4,35

The conclusion was that the mechanical properties are generally improved adding silane to the hardener. The exception was that the transverse modulus was higher for the case of the untreated system; however in regards to design question strength values are more important than modulus values, especially for the case of the transverse properties. Similarly, the transverse strain properties difference is not considered as substantial.

### 9.14.3. In-plane shear test

Both systems in-plane shear properties were tested using strain gauges, and the obtained properties were compared in Table 9.37.

- **35-Biotex fabric/SuperSap bio-epoxy resin + 1% silane added to the hardener**
- **36-Biotex fabric/ SuperSap bio-epoxy resin**

Table 9.37: Silanised and untreated systems in-plane shear properties comparison

System	35 Biotex/SuperSap Silane in hardener+VAP	36 Biotex/SuperSap No treated+VAP
$G_{12}$	1,64	1,54
$\tau_{12}$	25,60	24,90
$\gamma_{12}$	2,90	3,80



The conclusion is that the silane addition to the hardener is increasing NFRP in-plane shear properties in regards to modulus and strength. It was also seen the in-plane shear properties were decreased.

#### 9.14.4. Interlaminar Shear Strength (ILSS) test

Both systems ILSS properties were tested, and the obtained properties were compared in Table 9.38.

- **31-Biotex fabric/SuperSap bio-epoxy resin + 1% silane added to the hardener**
- **30-Biotex fabric/ SuperSap bio-epoxy resin**

Table 9.38: Silanised and untreated systems ILSS properties comparison

System	31 Biotex/SuperSap Silane in hardener+VAP	30 Biotex/SuperSap No treated+VAP
G <sub>12</sub>	992,00	964,00

It was proved that the adhesion of the silane to the hardener increases the laminate ILSS values considerably, in this occasion almost 50MPa.

#### 9.14.5. Optimised system flexural test

For tensile, compression, flexural, in-plane and interlaminar shear tests, the silanised system mechanical properties were better than the untreated system. In contrast, according to the §9.13, the interfacial properties against the moisture absorption are not increasing as much as expected.

### 9. 15. MECHANICAL TESTS UNCERTAINTY ESTIMATION

Every mechanical test has got its own level of uncertainty: it is vital to determine every test uncertainty level in order to determine the **test quality** or reliability. In the Appendix H, mechanical tests uncertainty levels were calculated.

This point has got special importance for the case of the NFRP mechanical properties determination process since the NF inhomogeneity produces a great impact in the tests variability. The question is that the literature is full of NF composites characterisation documents and data, however in general they are not mentioning any quality standard for the test campaign. For that reason, the current PhD

obtained reliable mechanical properties for flax/bio-epoxy system, enabling consistent design process with truthful mechanical properties.

# Chapter 10: Conclusions

Flax fibre has been mercerised at different immersion times and concentrations conditions, and it was concluded that 3h 1M combination produces the best mechanical performance (§ 9.2). Apart from that, it was concluded that 2M concentrations damage the flax fibre and consequently also decreased the composite performance.

The mercerisation treatment concentration drastically affects the infusion speed, while 0.25M and 0.5M concentrations are not affected, 1M starts to change speed, at 1.5M concentration effect is higher and 2M impedes the infusion process. (§ 9.3). The infusion speed mentioned can be related to the fibre swelling and  $V_f$  with a flow model (§ 9.4).

When silane is introduced in the composite system, either in the fibre or in the resin (§ 9.5); Silane-in-hardener 1% without mercerisation achieves the best composite system; and the silane reacts with the mercerised surface only when the fibre is directly treated with the silane but not when the silane is added to the hardener

Although optimised system was obtained, Lineo system still has better fibre-matrix interfacial properties than the enhanced Biotex, however longitudinal rigidity properties are drastically reduced with the Lineo's patented chemical treatment, supporting as a result the idea that SuperSap bio-epoxy may be used for high standard composite manufacturing.

In regards to the treatments sustainability, according to the chemical products MSDS (Material Safety Data Sheet) of the products, it was concluded that the Mercerisation and silanisation treatments are less polluting than the other treatments reviewed in Chapter 4. (§ 9.11)

In the literature, there are many references where the NFRP systems are mechanically characterised, but most of the tests quality is usually very poor with elevated CV values. One of the current PhD's objectives was to get reliable design properties, and the conclusion is that high quality mechanical properties can be achieved if the process is performed under controlled parameters. (§ 9.15)

As a summary the following three conclusions might be assumed as the most important PhD's outcoming conclusions:

- Mercerisation process may work in order to increase flax/epoxy interfacial properties in particular immersion time/concentration combinations, however; mercerisation would definitely reduce NFRP general mechanical performance
- Addition of silane in 1% concentration to the epoxy system would substantially increment flax/epoxy system static mechanical properties, although not as much as expected the moisture resistance properties
- Finally say that it may be manufactured a high standard flax/bio-epoxy composite with the contribution to knowledge developed along the PhD, in regards to process, mechanical testing and fibre treatments developed

# Chapter 11: Recommendations and future work

The insights gained during this doctoral study have identified a sensible route to manufacture composites with low environmental burdens yet a reasonable balance of static mechanical properties. Because of lack of time, some experimental work was not completed. For that reason, it would be very interesting to complete the following work in next steps.

The optimised eco-composite system has been developed, mechanically tested and immersion properties studied; however, the immersion tests results were not as definitive as expected, see §9.13. For that reason, it would be very interesting to age again some samples and tests the interfacial evolution using different test couple, for example making **transverse tensile test to the aged samples**. From this test is expected to get more information about the interfacial properties.

Increasing the interfacial properties, it is also expected that the **fatigue resistance properties** would be improved. There are many references in the literature where the fatigue property enhancement is reported for NFRP.

Completing these two experiments the mechanical properties improvement would be confirmed.

Related to the system optimization (§9.14), it would be interesting to test different silanes to be added to the hardener to get most from the selected flax/bio-epoxy. **Different silanes structures** might perform differently an increase the composite interfacial properties due to the increment of the covalent bonds.

Apart from the laboratory scale tests it would be very interesting to scale up the knowledge achieved at laboratory scale into the real production.

## REFERENCES

- Abdelmouleh, M., Boufi, S., Belgacem, M. N., Duarte, A. P., Salah, A. B., & Gandini, A. (2004). Modification of cellulosic fibres with functionalised silanes: development of surface properties. *International Journal of Adhesion and Adhesives*, 24(1), 43-54.
- Adamsen, A. P. S., Akin, D. E., & Rigsby, L. L. (2002). Chemical retting of flax straw under alkaline conditions. *Textile research journal*, 72(9), 789-794.
- Adden, S., & Horst, P. (2010). Stiffness degradation under fatigue in multiaxially loaded non-crimped-fabrics. *International journal of fatigue*, 32(1), 108-122.
- Afaghi-Khatibi, A., Ye, L., & Mai, Y. W. (2001). An experimental study of the influence of fibre-matrix interface on fatigue tensile strength of notched composite laminates. *Composites Part B: Engineering*, 32(4), 371-377.
- Al-Bastaki, N. M. S., & Al-Madani, H. M. N. (1995). Effect of local atmospheric conditions in Bahrain on the mechanical properties of GRP. *Polymer testing*, 14(3), 263-272.
- Aly, M., Hashmi, M. S. J., Olabi, A. G., Benyounis, K. Y., Messeiry, M., Hussain, A. I., & Abadir, E. F. (2012). Optimization of alkaline treatment conditions of flax fiber using Box-Behnken method. *Journal of natural fibers*, 9(4), 256-276.
- Amigó, V., Salvador, M. D., Sahuquillo, O., Llorens, R., & Martí, F. (2009). Aprovechamiento de residuos de fibras naturales como elementos de refuerzo de materiales poliméricos. *Instituto de Tecnología de Materiales Universidad Politécnica de Valencia, España*.
- Aouf, C., Nouailhas, H., Fache, M., Caillol, S., Boutevin, B., & Fulcrand, H. (2013). Multi-functionalization of gallic acid. Synthesis of a novel bio-based epoxy resin. *European Polymer Journal*, 49(6), 1185-1195.
- Arnold, E. L., Weager, B. M., Hoydonckx, H. E., & Madsen, B. (2009, July). Next generation sustainable composites: Development and processing of furan-flax biocomposites. In *17th international conference on composite materials* (pp. 27-31). British Composites Society.
- Aziz, S. H., Ansell, M. P., Clarke, S. J., & Panteny, S. R. (2005). Modified polyester resins for natural fibre composites. *Composites Science and Technology*, 65(3-4), 525-535.
- Baley, C., Le Duigou, A., Bourmaud, A., & Davies, P. (2012). Influence of drying on the mechanical behaviour of flax fibres and their unidirectional composites. *Composites Part A: Applied Science and Manufacturing*, 43(8), 1226-1233.
- Banna, M. H., Shirokoff, J., & Molgaard, J. (2011). Effects of two aqueous acidic solutions on polyester and bisphenol A epoxy vinyl ester resins. *Materials Science and Engineering: A*, 528(4-5), 2137-2142.
- Barreto, A. C. H., Rosa, D. S., Fachine, P. B. A., & Mazzetto, S. E. (2011). Properties of sisal fibers treated by alkali solution and their application into cardanol-based biocomposites. *Composites Part A: Applied Science and Manufacturing*, 42(5), 492-500.
- Becker, D. W. (1991). Tooling for resin transfer moulding. *Wichita State University, Wichita Kansas, no date*.
- Bhuniya, S. P., & Maiti, S. (2002). Phosphorus based epoxy terminated structural adhesive 2. Curing, adhesive strength and thermal stability. *European polymer journal*, 38(1), 195-201.

- Bledzki, A. K., Fink, H. P., & Specht, K. (2004). Unidirectional hemp and flax EP-and PP-composites: Influence of defined fiber treatments. *Journal of Applied Polymer Science*, *93*(5), 2150-2156.
- Borysiak, S. (2013). Fundamental studies on lignocellulose/polypropylene composites: effects of wood treatment on the transcrystalline morphology and mechanical properties. *Journal of Applied Polymer Science*, *127*(2), 1309-1322.
- Brierley, M. (2014). Fibre area correction factor for flax fibre reinforcements. *Plymouth University BEng (honours) Mechanical Engineering with Composites final year project, in collaboration with Composites Evolution Limited*.
- BYK C-8001. (2017). Retrieved January 26, 2017, from <https://www.byk.com/en/additives/additives-by-name/byk-c-8001.php>
- Cai, M., Takagi, H., Nakagaito, A. N., Li, Y., & Waterhouse, G. I. (2016). Effect of alkali treatment on interfacial bonding in abaca fiber-reinforced composites. *Composites Part A: Applied Science and Manufacturing*, *90*, 589-597.
- Cañigueral, N., Vilaseca, F., Méndez, J. A., López, J. P., Barberà, L., Puig, J., ... & Mutjé, P. (2009). Behavior of biocomposite materials from flax strands and starch-based biopolymer. *Chemical Engineering Science*, *64*(11), 2651-2658.
- Chattopadhyay, H., & Sarkar, P. B. (1945). *A new method for the estimation of cellulose* (Doctoral dissertation, Dacca University).
- Cheek, L., & Roussel, L. (1989). Mercerization of ramie: Comparisons with flax and cotton: Part I: Effects on physical, mechanical, and accessibility characteristics. *Textile Research Journal*, *59*(8), 478-483.
- Cheek, L., & Roussel, L. (1989). Mercerization of Ramie: Comparisons with Flax and Cotton: Part II: Effects on Dyeing and Behavior. *Textile Research Journal*, *59*(9), 541-546.
- Chen, W., Yu, Y., Li, P., Wang, C., Zhou, T., & Yang, X. (2007). Effect of new epoxy matrix for T800 carbon fiber/epoxy filament wound composites. *Composites Science and Technology*, *67*(11-12), 2261-2270.
- Cho, D., Seo, J. M., Lee, H. S., Cho, C. W., Han, S. O., & Park, W. H. (2007). Property improvement of natural fiber-reinforced green composites by water treatment. *Advanced Composite Materials*, *16*(4), 299-314.
- Chruściel, J. J., & Leśniak, E. (2015). Modification of epoxy resins with functional silanes, polysiloxanes, silsesquioxanes, silica and silicates. *Progress in Polymer Science*, *41*, 67-121.
- Clarke, R. C. (2010). Traditional Fiber Hemp (Cannabis) Production, Processing, Yarn Making, and Weaving Strategies—Functional Constraints and Regional Responses. Part 1. *Journal of Natural Fibers*, *7*(2), 118-153.
- Cobb, B. (1963). Long-term durability of resinglass boats. *Ship and Boat Builder*.
- Costa, C. S., Fonseca, A. C., Moniz, J., Godinho, M., Serra, A. C., & Coelho, J. F. (2016). Soybean and coconut oil based unsaturated polyester resins: Thermomechanical characterization. *Industrial Crops and Products*, *85*, 403-411.
- Cousinet, S., Ghadban, A., Fleury, E., Lortie, F., Pascault, J. P., & Portinha, D. (2015). Toward replacement of styrene by bio-based methacrylates in unsaturated polyester resins. *European Polymer Journal*, *67*, 539-550.

- Craig, P. D., & Summerscales, J. (1988). Poisson's ratios in glass fibre reinforced plastics. *Composite structures*, 9(3), 173-188.
- Cripps, D., Searle, T. J., & Summerscales, J. (2000). Open mold techniques for thermoset composites.
- Dai, J., Ma, S., Liu, X., Han, L., Wu, Y., Dai, X., & Zhu, J. (2015). Synthesis of bio-based unsaturated polyester resins and their application in waterborne UV-curable coatings. *Progress in Organic Coatings*, 78, 49-54.
- Dai, Z., Shi, F., Zhang, B., Li, M., & Zhang, Z. (2011). Effect of sizing on carbon fiber surface properties and fibers/epoxy interfacial adhesion. *Applied Surface Science*, 257(15), 6980-6985.
- Das, G., & Karak, N. (2010). Thermostable and flame retardant Mesua ferrea L. seed oil based non-halogenated epoxy resin/clay nanocomposites. *Progress in Organic Coatings*, 69(4), 495-503.
- Dey, M., Deitzel, J. M., Gillespie Jr, J. W., & Schweiger, S. (2014). Influence of sizing formulations on glass/epoxy interphase properties. *Composites Part A: Applied Science and Manufacturing*, 63, 59-67.
- Dissanayake, N. P. (2011). LIFE CYCLE ASSESSMENT OF FLAX FIBRES.
- Drzal, L. T., Herrera-Franco, P. J., & Ho, H. (2000). Fiber–matrix interface tests.
- Dwight, D. W. (2000). Glass fiber reinforcements.
- Easy Composites Process Materials. (2017). Retrieved January 27, 2017, from <http://www.easycomposites.co.uk/#/>
- Ecotechnilin. (2017). Retrieved January 27, 2017, from <http://www.lineo.eu/#!products/vstc3=flaxply>
- Ellis, B. (Ed.). (1993). *Chemistry and technology of epoxy resins* (1st ed., pp. 42-43). London: Blackie Academic & Professional.
- Entropy Resins. (2017). Retrieved January 27, 2017, from <http://entropyresins.eu/store/supersap-clr-clx-clf-clf/>
- Evans, J. D., Akin, D. E., & Foulk, J. A. (2002). Flax-retting by polygalacturonase-containing enzyme mixtures and effects on fiber properties. *Journal of Biotechnology*, 97(3), 223-231.
- Fecko, D. (2006). High strength glass reinforcements still being discovered. *Reinforced Plastics*, 50(4), 40-44.
- Feng, X. X., Chen, J. Y., & Zhang, H. P. (2008). Effect of high temperature alkali cooking on the constituents, structure and thermal degradation of hemp fiber. *Journal of applied polymer science*, 108(6), 4058-4064.
- Fillat, U., Pepió, M., Vidal, T., & Roncero, M. B. (2010). Flax fibers as a raw material: How to bleach efficiently a non-woody plant to obtain high-quality pulp. *Biomass and bioenergy*, 34(12), 1896-1905.
- Fiore, V., Di Bella, G., & Valenza, A. (2015). The effect of alkaline treatment on mechanical properties of kenaf fibers and their epoxy composites. *Composites Part B: Engineering*, 68, 14-21.



- Fotouh, A., Wolodko, J. D., & Lipsett, M. G. (2015). A review of aspects affecting performance and modeling of short-natural-fiber-reinforced polymers under monotonic and cyclic loading conditions. *Polymer Composites*, *36*(3), 397-409.
- Francucci, G., Rodríguez, E. S., & Vázquez, A. (2010). Study of saturated and unsaturated permeability in natural fiber fabrics. *Composites Part A: Applied Science and Manufacturing*, *41*(1), 16-21.
- Francucci, G., Rodríguez, E. S., & Vázquez, A. (2010). Study of saturated and unsaturated permeability in natural fiber fabrics. *Composites Part A: Applied Science and Manufacturing*, *41*(1), 16-21.
- Freire, C. S. R., Silvestre, A. J. D., Neto, C. P., & Rocha, R. M. A. (2005). An efficient method for determination of the degree of substitution of cellulose esters of long chain aliphatic acids. *Cellulose*, *12*(5), 449-458.
- Fried, N., & Graner, W. R. (1966). Durability of Reinforced Plastic Structural Materials in Marine Service. *Marine Technology*, *3*(3).
- Gandhi, K. L., & Sondhelm, W. S. (2016). Technical fabric structures—1. Woven fabrics. In *Handbook of Technical Textiles* (pp. 63-106). Woodhead Publishing.
- Gassan, J., & Bledzki, A. K. (1999). Alkali treatment of jute fibers: relationship between structure and mechanical properties. *Journal of Applied Polymer Science*, *71*(4), 623-629.
- Gassan, J., & Bledzki, A. K. (1999). Possibilities for improving the mechanical properties of jute/epoxy composites by alkali treatment of fibres. *Composites Science and Technology*, *59*(9), 1303-1309.
- Gellert, E. P., & Turley, D. M. (1999). Seawater immersion ageing of glass-fibre reinforced polymer laminates for marine applications. *Composites Part A: Applied Science and Manufacturing*, *30*(11), 1259-1265.
- George, M., Chae, M., & Bressler, D. C. (2016). Composite materials with bast fibres: structural, technical, and environmental properties. *Progress in Materials Science*, *83*, 1-23.
- Ghijssels, A., Groesbeek, N., & Raadsen, J. (1984). Temperature dependence of the zero-shear melt viscosity of oligomeric epoxy resins. *Polymer*, *25*(4), 463-466.
- Gliesche, K., & Mäder, E. (1995). Langfaserverstärkte Kunststoffe auf der Basis von Naturfasern. In *Proceedings of 7th international techtextil symposium, Frankfurt, Germany*.
- Gobin, M., Loulergue, P., Audic, J. L., & Lemiègre, L. (2015). Synthesis and characterisation of bio-based polyester materials from vegetable oil and short to long chain dicarboxylic acids. *Industrial Crops and Products*, *70*, 213-220.
- Goda, K., Sreekala, M. S., Gomes, A., Kaji, T., & Ohgi, J. (2006). Improvement of plant based natural fibers for toughening green composites—Effect of load application during mercerization of ramie fibers. *Composites Part A: Applied science and manufacturing*, *37*(12), 2213-2220.
- Graner, W. R., & Della Rocca, R. J. (1971). *Evaluation of US Navy GRP Boats for Material Durability*. Owens-Corning Fiberglass Corporation.
- Gu, H. (2009). Behaviours of glass fibre/unsaturated polyester composites under seawater environment. *Materials & Design*, *30*(4), 1337-1340.

- Guduri, B. R., Rajulu, A. V., & Luyt, A. S. (2007). Chemical resistance, void contents, and morphological properties of Hildegardia fabric/polycarbonate-toughened epoxy composites. *Journal of applied polymer science*, *106*(6), 3945-3951.
- Gurunathan, T., Mohanty, S., & Nayak, S. K. (2015). A review of the recent developments in biocomposites based on natural fibres and their application perspectives. *Composites Part A: Applied Science and Manufacturing*, *77*, 1-25.
- Gurunathan, T., Mohanty, S., & Nayak, S. K. (2015). A review of the recent developments in biocomposites based on natural fibres and their application perspectives. *Composites Part A: Applied Science and Manufacturing*, *77*, 1-25.
- Guthrie, R. D. (1974). *Guthrie and Honeyman's introduction to carbohydrate chemistry*. Oxford: Clarendon Press.
- Harper, P. W., & Hallett, S. R. (2010). A fatigue degradation law for cohesive interface elements—development and application to composite materials. *International Journal of Fatigue*, *32*(11), 1774-1787.
- Hassan, M. M., Islam, M. R., Shehrzade, S., & Khan, M. A. (2003). Influence of Mercerization Along with Ultraviolet (UV) and Gamma Radiation on Physical and Mechanical Properties of Jute Yarn by Grafting with 3-(Trimethoxysilyl) Propylmethacrylate (Silane) and Acrylamide Under UV Radiation. *Polymer-Plastics Technology and Engineering*, *42*(4), 515-531.
- Hayes, S. A., Lane, R., & Jones, F. R. (2001). Fibre/matrix stress transfer through a discrete interphase. Part 1: single-fibre model composites. *Composites Part A: applied science and manufacturing*, *32*(3-4), 379-389.
- Heller, K., Sheng, Q. C., Guan, F., Alexopoulou, E., Hua, L. S., Wu, G. W., ... & Fu, W. Y. (2015). A comparative study between Europe and China in crop management of two types of flax: linseed and fibre flax. *Industrial Crops and Products*, *68*, 24-31.
- Hepworth, D. G., Hobson, R. N., Bruce, D. M., & Farrent, J. W. (2000). The use of unretted hemp fibre in composite manufacture. *Composites part A: applied science and manufacturing*, *31*(11), 1279-1283.
- Hidalgo-Salazar, M. A., Mina, J. H., & Herrera-Franco, P. J. (2013). The effect of interfacial adhesion on the creep behaviour of LDPE–Al–Fique composite materials. *Composites Part B: Engineering*, *55*, 345-351.
- Huang, K., Zhang, J., Li, M., Xia, J., & Zhou, Y. (2013). Exploration of the complementary properties of biobased epoxies derived from rosin diacid and dimer fatty acid for balanced performance. *Industrial crops and products*, *49*, 497-506.
- Huang, K., Zhang, Y., Li, M., Lian, J., Yang, X., & Xia, J. (2012). Preparation of a light color cardanol-based curing agent and epoxy resin composite: Cure-induced phase separation and its effect on properties. *Progress in organic coatings*, *74*(1), 240-247.
- Huntsman International LLC. (2017). Retrieved January 1, 2017, from [http://www.huntsman.com/advanced\\_materials/Search](http://www.huntsman.com/advanced_materials/Search)
- Jana, S. C., & Prieto, A. (2002). Natural fiber composites of high-temperature thermoplastic polymers: Effects of coupling agents. *Journal of applied polymer science*, *86*(9), 2168-2173.
- Jandas, P. J., Mohanty, S., Nayak, S. K., & Srivastava, H. (2011). Effect of surface treatments of banana fiber on mechanical, thermal, and biodegradability properties of PLA/banana fiber biocomposites. *Polymer Composites*, *32*(11), 1689-1700.

- Jin, F. L., & Park, S. J. (2012). Thermal properties of epoxy resin/filler hybrid composites. *Polymer degradation and stability*, *97*(11), 2148-2153.
- Kabir, M. M., Wang, H., Lau, K. T., & Cardona, F. (2013). Tensile properties of chemically treated hemp fibres as reinforcement for composites. *Composites Part B: Engineering*, *53*, 362-368.
- Karger-Kocsis, J., Mahmood, H., & Pegoretti, A. (2015). Recent advances in fiber/matrix interphase engineering for polymer composites. *Progress in Materials Science*, *73*, 1-43.
- Kasemsiri, P., Neramittagapong, A., & Chindapasirt, P. (2015). Curing kinetic, thermal and adhesive properties of epoxy resin cured with cashew nut shell liquid. *Thermochimica acta*, *600*, 20-27.
- Kedward, K. T. (2000). Generic Approaches and Issues for Structural Composite Design and Application.
- Kerans, R. J., Hay, R. S., Parthasarathy, T. A., & Cinibulk, M. K. (2002). Interface design for oxidation-resistant ceramic composites. *Journal of the American Ceramic Society*, *85*(11), 2599-2632.
- Kessler, R. W., Becker, U., Kohler, R., & Goth, B. (1998). Steam explosion of flax—a superior technique for upgrading fibre value. *Biomass and Bioenergy*, *14*(3), 237-249.
- Khazanov, V. E., Kolesov, Y. I., & Trofimov, N. N. (1995). Glass fibres. In *Fibre science and technology* (pp. 15-230). Springer, Dordrecht.
- Kim, J. T., & Netravali, A. N. (2010). Mercerization of sisal fibers: Effect of tension on mechanical properties of sisal fiber and fiber-reinforced composites. *Composites Part A: Applied science and manufacturing*, *41*(9), 1245-1252.
- Kim, J. T., & Netravali, A. N. (2010). Mercerization of sisal fibers: Effect of tension on mechanical properties of sisal fiber and fiber-reinforced composites. *Composites Part A: Applied science and manufacturing*, *41*(9), 1245-1252.
- Kim, W. G., & Lee, J. Y. (2002). Contributions of the network structure to the cure kinetics of epoxy resin systems according to the change of hardeners. *Polymer*, *43*(21), 5713-5722.
- Kocaman, S., & Ahmetli, G. (2016). A study of coating properties of biobased modified epoxy resin with different hardeners. *Progress in Organic Coatings*, *97*, 53-64.
- Koimtzoglou, C., Kostopoulos, V., & Galiotis, C. (2001). Micromechanics of reinforcement and damage initiation in carbon fibre/epoxy composites under fatigue loading. *Composites Part A: Applied Science and Manufacturing*, *32*(3-4), 457-471.
- La Rosa, A. D., Recca, G., Summerscales, J., Latteri, A., Cozzo, G., & Cicala, G. (2014). Bio-based versus traditional polymer composites. A life cycle assessment perspective. *Journal of cleaner production*, *74*, 135-144.
- Lane, R., Hayes, S. A., & Jones, F. R. (2001). Fibre/matrix stress transfer through a discrete interphase: 2. High volume fraction systems. *Composites science and technology*, *61*(4), 565-578.
- Le Duigou, A., Davies, P., & Baley, C. (2013). Exploring durability of interfaces in flax fibre/epoxy micro-composites. *Composites Part A: Applied science and manufacturing*, *48*, 121-128.

- Le Duigou, A., Kervoelen, A., Le Grand, A., Nardin, M., & Baley, C. (2014). Interfacial properties of flax fibre–epoxy resin systems: existence of a complex interphase. *Composites Science and Technology*, *100*, 152-157.
- Lee, J. Y., Jang, J., Hong, S. M., Hwang, S. S., & Kim, K. U. (1999). Relationship between the structure of the bridging group and curing of liquid crystalline epoxy resins. *Polymer*, *40*(11), 3197-3202.
- Lee, Y. J., Jhan, Y. T., & Chung, C. H. (2012). Fluid–structure interaction of FRP wind turbine blades under aerodynamic effect. *Composites Part B: Engineering*, *43*(5), 2180-2191.
- Lefeuvre, A., Bourmaud, A., Lebrun, L., Morvan, C., & Baley, C. (2013). A study of the yearly reproducibility of flax fiber tensile properties. *Industrial crops and products*, *50*, 400-407.
- Lempriere, B. M. (1968). Poisson's ratio in orthotropic materials. *AIAA Journal*, *6*(11), 2226-2227.
- Li, C., Potter, K., Wisnom, M. R., & Stringer, G. (2004). In-situ measurement of chemical shrinkage of MY750 epoxy resin by a novel gravimetric method. *Composites Science and Technology*, *64*(1), 55-64.
- Li, Q., Li, X., & Meng, Y. (2012). Curing of DGEBA epoxy using a phenol-terminated hyperbranched curing agent: cure kinetics, gelation, and the TTT cure diagram. *Thermochimica acta*, *549*, 69-80.
- Li, X., Tabil, L. G., & Panigrahi, S. (2007). Chemical treatments of natural fiber for use in natural fiber-reinforced composites: a review. *Journal of Polymers and the Environment*, *15*(1), 25-33.
- Lin, K. F., & Wang, F. W. (1994). Fluorescence monitoring of polarity change and gelation during epoxy cure. *Polymer*, *35*(4), 687-691.
- Liu, K., Zhang, X., Takagi, H., Yang, Z., & Wang, D. (2014). Effect of chemical treatments on transverse thermal conductivity of unidirectional abaca fiber/epoxy composite. *Composites Part A: Applied Science and Manufacturing*, *66*, 227-236.
- Liu, M., Fernando, D., Daniel, G., Madsen, B., Meyer, A. S., Ale, M. T., & Thygesen, A. (2015). Effect of harvest time and field retting duration on the chemical composition, morphology and mechanical properties of hemp fibers. *Industrial Crops and Products*, *69*, 29-39.
- Liu, X., Thomason, J. L., & Jones, F. R. (2008). XPS and AFM study of interaction of organosilane and sizing with E-glass fibre surface. *The Journal of Adhesion*, *84*(4), 322-338.
- Liu, Z., Jones, F. R., Liu, Y., & Jiang, B. (2014). Adhesion of aqueous polyurethane adhesive to human hair. *International Journal of Adhesion and Adhesives*, *48*, 14-19.
- Lomelí-Ramírez, M. G., Kestur, S. G., Manríquez-González, R., Iwakiri, S., de Muniz, G. B., & Flores-Sahagun, T. S. (2014). Bio-composites of cassava starch-green coconut fiber: Part II—Structure and properties. *Carbohydrate polymers*, *102*, 576-583.
- Lu, J., Khot, S., & Wool, R. P. (2005). New sheet molding compound resins from soybean oil. I. Synthesis and characterization. *Polymer*, *46*(1), 71-80.
- Luo, X., Mohanty, A., & Misra, M. (2013). Lignin as a reactive reinforcing filler for water-blown rigid biofoam composites from soy oil-based polyurethane. *Industrial Crops and Products*, *47*, 13-19.
- Ma, S., Liu, X., Jiang, Y., Tang, Z., Zhang, C., & Zhu, J. (2013). Bio-based epoxy resin from itaconic acid and its thermosets cured with anhydride and comonomers. *Green Chemistry*, *15*(1), 245-254.

- Mahjoub, R., Yatim, J. M., Sam, A. R. M., & Raftari, M. (2014). Characteristics of continuous unidirectional kenaf fiber reinforced epoxy composites. *Materials & Design*, *64*, 640-649.
- Malainine, M. E., Mahrouz, M., & Dufresne, A. (2005). Thermoplastic nanocomposites based on cellulose microfibrils from *Opuntia ficus-indica* parenchyma cell. *Composites Science and Technology*, *65*(10), 1520-1526.
- Mallick, P. K. (2000). Particulate and short fiber reinforced polymer composites.
- Marrot, L., Bourmaud, A., Bono, P., & Baley, C. (2014). Multi-scale study of the adhesion between flax fibers and biobased thermoset matrices. *Materials & Design (1980-2015)*, *62*, 47-56.
- Martin, N., Mouret, N., Davies, P., & Baley, C. (2013). Influence of the degree of retting of flax fibers on the tensile properties of single fibers and short fiber/polypropylene composites. *Industrial crops and products*, *49*, 755-767.
- Masoodi, R., Pillai, K. M., Grahl, N., & Tan, H. (2012). Numerical simulation of LCM mold-filling during the manufacture of natural fiber composites. *Journal of Reinforced Plastics and Composites*, *31*(6), 363-378.
- Massetau, B., Michaud, F., Irle, M., Roy, A., & Alise, G. (2014). An evaluation of the effects of moisture content on the modulus of elasticity of a unidirectional flax fiber composite. *Composites Part A: Applied Science and Manufacturing*, *60*, 32-37.
- McKelvey, J. B., Webre, B. G., & Klein, E. (1959). Reaction of epoxides with cotton cellulose in the presence of sodium hydroxide. *Textile Research Journal*, *29*(11), 918-925.
- Mehta, G., Drzal, L. T., Mohanty, A. K., & Misra, M. (2006). Effect of fiber surface treatment on the properties of biocomposites from nonwoven industrial hemp fiber mats and unsaturated polyester resin. *Journal of applied polymer science*, *99*(3), 1055-1068.
- Mercer, J. (1850). Improvements in the preparation of cotton and other fabrics and other fibrous materials. *British Patent*, *13*, 1850.
- Millero, F. J., Feistel, R., Wright, D. G., & McDougall, T. J. (2008). The composition of Standard Seawater and the definition of the Reference-Composition Salinity Scale. *Deep Sea Research Part I: Oceanographic Research Papers*, *55*(1), 50-72.
- Min, B. G., Stachurski, Z. H., & Hodgkin, J. H. (1993). Cure kinetics of elementary reactions of a diglycidyl ether of bisphenol A/diaminodiphenylsulfone epoxy resin: 2. Conversion versus time. *Polymer*, *34*(21), 4488-4495.
- Misra, S., Misra, M., Tripathy, S. S., Nayak, S. K., & Mohanty, A. K. (2002). The influence of chemical surface modification on the performance of sisal-polyester biocomposites. *Polymer Composites*, *23*(2), 164-170.
- Montserrat, S., Flaque, C., Calafell, M., Andreu, G., & Malek, J. (1995). Influence of the accelerator concentration on the curing reaction of an epoxy-anhydride system. *Thermochimica Acta*, *269*, 213-229.
- Mouritz, A. P., Gellert, E., Burchill, P., & Challis, K. (2001). Review of advanced composite structures for naval ships and submarines. *Composite structures*, *53*(1), 21-42.
- Mülhaupt, R. (2013). Green polymer chemistry and bio-based plastics: dreams and reality. *Macromolecular Chemistry and Physics*, *214*(2), 159-174.
- Nair, G. R., Rho, D., Yaylayan, V., & Raghavan, V. (2013). Microwave assisted retting—A novel method of processing of flax stems. *Biosystems engineering*, *116*(4), 427-435.

- Naslain, R. R. (1998). The design of the fibre-matrix interfacial zone in ceramic matrix composites. *Composites Part A: Applied Science and Manufacturing*, 29(9-10), 1145-1155.
- Natural Fibres Reinforcements. (2017). Retrieved January 1, 2017, from <http://compositesevolution.com/biotex/>
- Nawab, Y., Tardif, X., Boyard, N., Sobotka, V., Casari, P., & Jacquemin, F. (2012). Determination and modelling of the cure shrinkage of epoxy vinylester resin and associated composites by considering thermal gradients. *Composites Science and Technology*, 73, 81-87.
- Nguyen, V., Lagardère, M., Cosson, B., & Park, C. H. (2014, July). Experimental analysis of flow behavior in the flax fiber reinforcement with double scale porosity. In *12th international conference on flow processing in composite materials (FPCM 12), Enschede*.
- Normohammadi, M., Kakooei, H., Omid, L., Yari, S., & Alimi, R. (2016). Risk assessment of exposure to silica dust in building demolition sites. *Safety and health at work*, 7(3), 251-255.
- Onjun, O., & Pearson, R. A. (2010). Effect of silane adhesion promoters on subcritical debonding of epoxy/glass interfaces after hygrothermal aging. *The Journal of Adhesion*, 86(12), 1178-1202.
- Oral, I., Guzel, H., & Ahmetli, G. (2013). Determining the mechanical properties of epoxy resin (DGEBA) composites by ultrasonic velocity measurement. *Journal of Applied Polymer Science*, 127(3), 1667-1675.
- Park, J. M., Kim, D. S., Kim, S. J., Kim, P. G., Yoon, D. J., & DeVries, K. L. (2007). Inherent sensing and interfacial evaluation of carbon nanofiber and nanotube/epoxy composites using electrical resistance measurement and micromechanical technique. *Composites Part B: Engineering*, 38(7-8), 847-861.
- Paukszta, D. (2013). Mercerisation of rapeseed straw investigated with the use of WAXS method. *Fibres & Textiles in Eastern Europe*.
- Pearce, N. R. L., Guild, F. J., & Summerscales, J. (1998). An investigation into the effects of fabric architecture on the processing and properties of fibre reinforced composites produced by resin transfer moulding. *Composites Part A: Applied Science and Manufacturing*, 29(1-2), 19-27.
- Pham, H. Q., & Marks, M. J. (2000). Epoxy resins. *Ullmann's Encyclopedia of Industrial Chemistry*.
- Pickering, K. (Ed.). (2008). *Properties and performance of natural-fibre composites*. Elsevier.
- Plonka, R., Mäder, E., Gao, S. L., Bellmann, C., Dutschk, V., & Zhandarov, S. (2004). Adhesion of epoxy/glass fibre composites influenced by aging effects on sizings. *Composites Part A: Applied science and manufacturing*, 35(10), 1207-1216.
- Potter, K. (1992). Design of composite products—a personal viewpoint. *Composites Manufacturing*, 3(3), 173-182.
- Pukánszky, B. (2005). Interfaces and interphases in multicomponent materials: past, present, future. *European polymer journal*, 41(4), 645-662.
- Rao, B. S., & Palanisamy, A. (2013). Synthesis of bio based low temperature curable liquid epoxy, benzoxazine monomer system from cardanol: Thermal and viscoelastic properties. *European Polymer Journal*, 49(8), 2365-2376.

- Raquez, J. M., Deléglise, M., Lacrampe, M. F., & Krawczak, P. (2010). Thermosetting (bio) materials derived from renewable resources: a critical review. *Progress in polymer science*, 35(4), 487-509.
- Rashaduzzaman, M. (2013). Mercerizing cellulosic fibres & its effects. [*Bangladesh*] *Textile Today*.
- Ray, D., & Sarkar, B. K. (2001). Characterization of alkali-treated jute fibers for physical and mechanical properties. *Journal of Applied Polymer Science*, 80(7), 1013-1020.
- Ray, D., Das, M., & Mitra, D. (2012). A comparative study of the stress-relaxation behavior of untreated and alkali-treated jute fibers. *Journal of Applied Polymer Science*, 123(3), 1348-1358.
- Reddy, M. M., Misra, M., & Mohanty, A. K. (2012). Bio-based materials in the new bio-economy. *Chemical Engineering Progress*, 108(5), 37-42.
- Reddy, M. M., Vivekanandhan, S., Misra, M., Bhatia, S. K., & Mohanty, A. K. (2013). Biobased plastics and bionanocomposites: Current status and future opportunities. *Progress in polymer Science*, 38(10-11), 1653-1689.
- Rivero, G., Fasce, L. A., Ceré, S. M., & Manfredi, L. B. (2014). Furan resins as replacement of phenolic protective coatings: Structural, mechanical and functional characterization. *Progress in Organic Coatings*, 77(1), 247-256.
- Rong, M. Z., Zhang, M. Q., Liu, Y., Yang, G. C., & Zeng, H. M. (2001). The effect of fiber treatment on the mechanical properties of unidirectional sisal-reinforced epoxy composites. *Composites Science and technology*, 61(10), 1437-1447.
- Roy, A., Chakraborty, S., Kundu, S. P., Basak, R. K., Majumder, S. B., & Adhikari, B. (2012). Improvement in mechanical properties of jute fibres through mild alkali treatment as demonstrated by utilisation of the Weibull distribution model. *Bioresource technology*, 107, 222-228.
- Ruan, P., Du, J., Garipey, Y., & Raghavan, V. (2015). Characterization of radio frequency assisted water retting and flax fibers obtained. *Industrial Crops and Products*, 69, 228-237.
- Rudd, C. D., Long, A. C., Kendall, K. N., & Mangin, C. (1997). *Liquid moulding technologies: Resin transfer moulding, structural reaction injection moulding and related processing techniques*. Elsevier.
- Sadler, J. M., Toulan, F. R., Nguyen, A. P. T., Kayea III, R. V., Ziaee, S., Palmese, G. R., & La Scala, J. J. (2014). Isosorbide as the structural component of bio-based unsaturated polyesters for use as thermosetting resins. *Carbohydrate polymers*, 100, 97-106.
- Saha, P., Manna, S., Chowdhury, S. R., Sen, R., Roy, D., & Adhikari, B. (2010). Enhancement of tensile strength of lignocellulosic jute fibers by alkali-steam treatment. *Bioresource technology*, 101(9), 3182-3187.
- Scida, D., Assarar, M., Poilâne, C., & Ayad, R. (2013). Influence of hygrothermal ageing on the damage mechanisms of flax-fibre reinforced epoxy composite. *Composites Part B: Engineering*, 48, 51-58.
- Shah, D. U. (2014). Natural fibre composites: Comprehensive Ashby-type materials selection charts. *Materials & Design (1980-2015)*, 62, 21-31.
- Shah, D. U., & Schubel, P. J. (2010). Evaluation of cure shrinkage measurement techniques for thermosetting resins. *Polymer Testing*, 29(6), 629-639.

- Shah, D. U., Schubel, P. J., & Clifford, M. J. (2013). Modelling the effect of yarn twist on the tensile strength of unidirectional plant fibre yarn composites. *Journal of Composite Materials*, 47(4), 425-436.
- Shahid, M., Mohammad, F., Chen, G., Tang, R. C., & Xing, T. (2016). Enzymatic processing of natural fibres: white biotechnology for sustainable development. *Green Chemistry*, 18(8), 2256-2281.
- Shanmugam, D., & Thiruchitrambalam, M. (2013). Static and dynamic mechanical properties of alkali treated unidirectional continuous Palmyra Palm Leaf Stalk Fiber/jute fiber reinforced hybrid polyester composites. *Materials & Design*, 50, 533-542.
- Shia, D., Hui, C. Y., Burnside, S. D., & Giannelis, E. P. (1998). An interface model for the prediction of Young's modulus of layered silicate-elastomer nanocomposites. *Polymer Composites*, 19(5), 608-617.
- Shokoohi, S., Arefazar, A., & Khosrokhavar, R. (2008). Silane coupling agents in polymer-based reinforced composites: a review. *Journal of Reinforced Plastics and Composites*, 27(5), 473-485.
- Sigma-Aldrich Ethanol. (2017). Retrieved January 26, 2017, from <http://www.sigmaaldrich.com/catalog/search?term=ethanol&interface=All&N=0&mode=match%20partialmax&lang=es&region=ES&focus=product>
- Sigma-Aldrich NaOH. (2017). Retrieved January 26, 2017, from <http://www.sigmaaldrich.com/catalog/search?term=1310-73-2&interface=CAS%20No.&N=0&mode=match%20partialmax&lang=es&region=ES&focus=product>
- Soatthiyanon, N. (2014). Separation and characterisation of elementary kenaf fibres as reinforcement in high-density polyethylene-matrix composites and tensile behaviour of flax fibres as reinforcement in vinyl ester-matrix composites. <http://handle.unsw.edu.au/1959.4/53585>
- Stana-Kleinschek, K., Strnad, S., & Ribitsch, V. (1999). Surface characterization and adsorption abilities of cellulose fibers. *Polymer Engineering & Science*, 39(8), 1412-1424.
- Summerscales, J. (2014). Durability of composites in the marine environment. In *Durability of Composites in a Marine Environment* (pp. 1-13). Springer, Dordrecht.
- Summerscales, J., & Grove, S. (2014). Manufacturing methods for natural fibre composites. In *Natural Fibre Composites* (pp. 176-215). Woodhead Publishing.
- Summerscales, J., Virk, A., & Hall, W. (2013). A review of bast fibres and their composites: Part 3—Modelling. *Composites Part A: Applied Science and Manufacturing*, 44, 132-139.
- Thiruchitrambalam, M., & Shanmugam, D. (2012). Influence of pre-treatments on the mechanical properties of palmyra palm leaf stalk fiber–polyester composites. *Journal of Reinforced Plastics and Composites*, 31(20), 1400-1414.
- Thomason, J. L. (1995). The interface region in glass fibre-reinforced epoxy resin composites: 3. Characterization of fibre surface coatings and the interphase. *Composites*, 26(7), 487-498.
- Thomason, J. L., & Adzima, L. J. (2001). Sizing up the interphase: an insider's guide to the science of sizing. *Composites Part A: Applied Science and Manufacturing*, 32(3-4), 313-321.
- Thomason, J. L., Carruthers, J., Kelly, J., & Johnson, G. (2011). Fibre cross-section determination and variability in sisal and flax and its effects on fibre performance characterisation. *Composites Science and Technology*, 71(7), 1008-1015.



- Triki, A., Guicha, M., Ben Hassen, M., & Arous, M. (2013). Comparative study of the dielectric properties of natural-fiber–matrix composites and E-glass–matrix composites. *Journal of Applied Polymer Science*, *129*(1), 487-498.
- Tsai, Y. I., Bosze, E. J., Barjasteh, E., & Nutt, S. R. (2009). Influence of hygrothermal environment on thermal and mechanical properties of carbon fiber/fiberglass hybrid composites. *Composites Science and Technology*, *69*(3-4), 432-437.
- Van de Weyenberg, I., Ivens, J., De Coster, A., Kino, B., Baetens, E., & Verpoest, I. (2003). Influence of processing and chemical treatment of flax fibres on their composites. *Composites science and technology*, *63*(9), 1241-1246.
- Van de Weyenberg, I., Truong, T. C., Vangrimde, B., & Verpoest, I. (2006). Improving the properties of UD flax fibre reinforced composites by applying an alkaline fibre treatment. *Composites Part A: Applied Science and Manufacturing*, *37*(9), 1368-1376.
- Van der Steen, M., Bretz, I., Kabasci, S., & Stevens, C. V. (2013). Synthesis of biobased multivalent cross-linkers from a castor oil-derived C22-acyloin. *Industrial crops and products*, *46*, 238-245.
- Varma, I. K., & Gupta, V. B. (2000). Thermosetting resin—properties.
- Virk, A. S., Hall, W., & Summerscales, J. (2012). Modulus and strength prediction for natural fibre composites. *Materials Science and Technology*, *28*(7), 864-871.
- Wada, M., Nishiyama, Y., Chanzy, H., Forsyth, T., & Langan, P. (2008). The structure of celluloses. *Powder Diffraction*, *23*(2), 92-95.
- Wan, J., Bu, Z. Y., Xu, C. J., Fan, H., & Li, B. G. (2011). Model-fitting and model-free nonisothermal curing kinetics of epoxy resin with a low-volatile five-armed starlike aliphatic polyamine. *Thermochimica acta*, *525*(1-2), 31-39.
- Wan, J., Bu, Z. Y., Xu, C. J., Li, B. G., & Fan, H. (2011). Preparation, curing kinetics, and properties of a novel low-volatile starlike aliphatic-polyamine curing agent for epoxy resins. *Chemical Engineering Journal*, *171*(1), 357-367.
- Wang, X., & Zhang, Q. (2004). Synthesis, characterization, and cure properties of phosphorus-containing epoxy resins for flame retardance. *European Polymer Journal*, *40*(2), 385-395.
- Wang, Z., Jiang, J., Zhang, D., & Cheng, R. (2012). Synthesis and characterization of high-performance epoxy resin based on disiloxane and 4, 4'-oxybis (benzoic acid) ester. *Journal of Applied Polymer Science*, *123*(4), 2485-2491.
- Wei, B., Cao, H., & Song, S. (2011). Degradation of basalt fibre and glass fibre/epoxy resin composites in seawater. *Corrosion Science*, *53*(1), 426-431.
- Williams, J. G. (1977). The effects of tropical weathering on glass-reinforced epoxy resins. *Composites*, *8*(3), 157-160.
- Wood, C. A., & Bradley, W. L. (1997). Determination of the effect of seawater on the interfacial strength of an interlayer E-glass/graphite/epoxy composite by in situ observation of transverse cracking in an environmental SEM. *Composites science and Technology*, *57*(8), 1033-1043.
- Xie, Y., Hill, C. A., Xiao, Z., Militz, H., & Mai, C. (2010). Silane coupling agents used for natural fiber/polymer composites: A review. *Composites Part A: Applied Science and Manufacturing*, *41*(7), 806-819.

- Xu, Z., Chen, L., Huang, Y., Li, J., Wu, X., Li, X., & Jiao, Y. (2008). Wettability of carbon fibers modified by acrylic acid and interface properties of carbon fiber/epoxy. *European polymer journal*, 44(2), 494-503.
- Xue, D., & Hu, H. (2013). Mechanical properties of biaxial weft-knitted flax composites. *Materials & Design*, 46, 264-269.
- Yi, J. W., Um, M. K., Byun, J. H., Lee, S. B., & Lee, S. K. (2013). Development of high Tg epoxy resin and mechanical properties of its fiber-reinforced composites. *Journal of Applied Polymer Science*, 127(6), 4328-4333.
- Yousif, B. F., Shalwan, A., Chin, C. W., & Ming, K. C. (2012). Flexural properties of treated and untreated kenaf/epoxy composites. *Materials & Design*, 40, 378-385.
- Zafar, A., Bertocco, F., Schjødt-Thomsen, J., & Rauhe, J. C. (2012). Investigation of the long term effects of moisture on carbon fibre and epoxy matrix composites. *Composites Science and Technology*, 72(6), 656-666.
- Zeng, X., Mooney, S. J., & Sturrock, C. J. (2015). Assessing the effect of fibre extraction processes on the strength of flax fibre reinforcement. *Composites Part A: Applied Science and Manufacturing*, 70, 1-7.
- Zhang, D., Milanovic, N. R., Zhang, Y., Su, F., & Miao, M. (2014). Effects of humidity conditions at fabrication on the interfacial shear strength of flax/unsaturated polyester composites. *Composites Part B: Engineering*, 60, 186-192.
- Zhou, F., Cheng, G., & Jiang, B. (2014). Effect of silane treatment on microstructure of sisal fibers. *Applied Surface Science*, 292, 806-812.
- Zhuang, R. C., Burghardt, T., & Mäder, E. (2010). Study on interfacial adhesion strength of single glass fibre/polypropylene model composites by altering the nature of the surface of sized glass fibres. *Composites Science and Technology*, 70(10), 1523-1529.
- Zou, H., Wang, L., Gan, H., & Yi, C. (2012). Effect of fiber surface treatments on the properties of short sisal fiber/poly (lactic acid) biocomposites. *Polymer composites*, 33(10), 1659-1666.

# Appendix A

## APPENDIX A1



### Biotex Flax Yarn Technical Data Sheet March 2012

#### Introduction

Biotex Flax Yarn is a continuous reinforcement yarn based on natural flax fibre and designed for fibre-reinforced polymer composite applications. The yarn can be used directly in processes include filament winding and pultrusion or can be converted into woven or non-woven textiles. The yarn can be processed in a similar way to glass or carbon fibre.

Biotex natural reinforcements and intermediates provide the high performance and easy processing normally associated with glass fibre composites but with lower weight and environmental impact. They are suitable for semi-structural and decorative applications in sectors such as automotive, construction, marine, sports and consumer goods. Biotex uses a unique Twistless Technology to ensure a high degree of fibre alignment, impregnation and performance.

#### Linear Density

250tex            Standard  
250-2000tex    On request

#### Fibre Properties

Typical average properties for flax fibres:

Flax fibre properties*	
Density	1.5g/cm <sup>3</sup>
Diameter**	20µm
Tensile modulus	50GPa
Tensile strength	500MPa
Strain	2%

\*Flax fibre is a natural product and a certain amount of variation should be expected.

\*\*Flax fibre has a non-circular cross-section.

#### Yarn Properties

Flax yarn properties	250tex	1000tex
Tenacity/tensile strength	15N	38N
Elongation at break	15.5%	4.4%



Composites Evolution Ltd, 4A Broom Business Park, Bridge Way, Chesterfield, S41 9QG, UK  
■ Tel: +44(0)1246 266248 ■ Fax: +44(0)1246 266249 ■ Email: info@compositeevolution.com ■ www.compositeevolution.com  
Company Registration No: 07024132

### Composite Properties

Property	UD flax-polyester laminate (0 dir)	Biaxial flax-polyester laminate (0 dir)	Woven flax-polyester laminate (0 dir)	Test Method
Density	1.30g/cm <sup>3</sup>	1.30g/cm <sup>3</sup>	1.24g/cm <sup>3</sup>	
Tensile modulus	18.8GPa	8.7GPa	7.2GPa	ISO 527-4
Tensile strength	174MPa	85MPa	68.3MPa	ISO 527-4
Tensile elongation	1.5%	1.7%	2.5%	ISO 527-4
Flexural modulus	15.1GPa	6.8GPa	4.0GPa	ISO 14125
Flexural strength	196MPa	135MPa	97.4MPa	ISO 14125
Charpy impact	TBC	TBC	28.0kJ/m <sup>2</sup>	ISO 179-1 U

Data for laminates made from 30-33vol% Biotex flax fabrics and unsaturated polyester resin by the vacuum infusion process and tested at ambient temperature. All fabrics made from 250tex Biotex flax yarn.

### Sizing

Biotex Flax Yarn is supplied unsized as standard. Sizings are possible on request.

### Packaging

Standard package options are shown in the table. Other packaging is possible on request. Packages are typically wrapped in plastic and delivered in cardboard cartons.

Package type	Length (mm)	Internal diameter (mm)	Base (mm)	Tip (mm)	Standard weight (kg)	Possible weight range (kg)
Cardboard cone	228	N/A	62	25	5	1 - 6
Cardboard tube	228	76	N/A	N/A	5	1 - 6

### Storage

Biotex Flax yarn should be stored in a cool dry place away from direct sunlight. Flax fibre can absorb moisture from the atmosphere so drying may be required before use, especially if exposed to excessive humidity.

### Safety

Flax fibre is a naturally occurring, non-hazardous material, but typical precautions should be taken when handling the material including using appropriate PPE and adequate ventilation. See MSDS for details.

### Disclaimer

The information provided here is believed to be accurate but should be considered indicative only. It is the responsibility of the customer to check the suitability of the product for their specific application prior to use.



Composites Evolution Ltd, 4A Broom Business Park, Bridge Way, Chesterfield, S41 9QG, UK

■ Tel: +44(0)1246 266248 ■ Fax: +44(0)1246 266249 ■ Email: [info@compositesevolution.com](mailto:info@compositesevolution.com) ■ [www.compositesevolution.com](http://www.compositesevolution.com)  
Company Registration No: 07024132



TECHNICAL DATA SHEET - FLAXTAPE™

**Products:**

FlaxTape™ is the brand used for our patented tapes of unidirectional flax fibers. FlaxTape™ is ready to be used for all conventional processes (infusion, RTM, film stacking, prepreg...)



Pictures of FlaxTape™ production

Name	Description	Weight	Width
FLAXTAPE™ 50	Tapes of unidirectional flax fibers	50gr of flax/m <sup>2</sup>	40 cm
FLAXTAPE™ 70		70gr of flax/m <sup>2</sup>	40 cm
FLAXTAPE™ 110		110gr of flax/m <sup>2</sup>	40 cm
FLAXTAPE™ 200		200gr of flax/m <sup>2</sup>	40 cm

**Main markets:**

		Advantages
Sport and leisure	rackets, bicycle frames, skis, boards, ...	Dampening properties
Transportation	Already used in aeronautic, automotive, boat manufacturing, railway.	Weight reduction, Mechanical & Acoustic properties, Bio-based material

**Mechanical properties:**

Composite made with 12 layers of "FlaxTape™ 110" and an epoxy resin processed by RTM:

RATE OF FIBRES	By Volume	50%
TRACTION (ISO 527)	Modulus	35 GPa
	Tensile strength	365 MPa
	Failure Strain	1,35 %
FLEXION (ISO 14 125)	Modulus	31 GPa
	Max Strength	294 MPa
	Failure Strain	2,6 %
THEORIC DENSITY		1.31gr/cm <sup>3</sup>

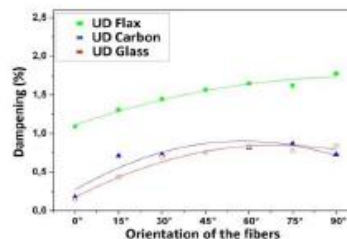
Composite made with 12 layers of "FlaxTape™ 110" and 20 PP films by film stacking and compression moulding:

RATE OF FIBRES	By Volume	43%
TRACTION (ISO 527)	Modulus	33 GPa
	Tensile strength	275 MPa
	Failure Strain	1,22%
FLEXION (ISO 14 125)	Modulus	23 GPa
	Max Strength	210 MPa
	Failure Strain	2,1 %
THEORIC DENSITY		1.13gr/cm <sup>3</sup>

**Dampening properties:**

Low frequency dampening (flexion/mode 2):

Product	Dampening ratio
UD Flax	1.47%
UD Carbon	0.18%
UD Glass	0.15%



Contact: François Vanfleteren – [sales@lineo.eu](mailto:sales@lineo.eu) - +33.232.43.13.67

TDS FlaxTape™

APPENDIX A3



# Technical Data Sheet

**SUPER SAP® CLR System**  
 Clear, UV Stable Epoxy Resin for high color work laminations, coatings and marine epoxy applications.

**Product Overview**

SUPER SAP® CLR Epoxy Resin is our flagship, high-performance clear coating epoxy resin system. The CLR System is a water clear, UV stabilized epoxy system for applications that require a low color, low yellowing epoxy resin such as high color applications. This system features a quick air-release and a world-class UV resistance package. SUPER SAP® CLR works with multiple hardeners to match your working parameters. It has an ideal viscosity for a wide range of applications that use hand layup techniques with fast room temperature cures. Super Sap – Make Things Better.

**CLX**  
EXTRA FAST

**CLF**  
FAST

**CLS**  
SLOW

MECHANICAL DATA	CLX	CLF	CLS
<b>Tensile Modulus (ASTM D638)</b>	450,000 psi (3.1 GPa)	440,000 psi (3.0 GPa)	468,000 psi (3.2 GPa)
<b>Tensile Strength (ASTM D638)</b>	9,500 psi (65.5 MPa)	9,500 psi (65.5 MPa)	9,800 psi (67.6 MPa)
<b>Elongation (ASTM D638)</b>	6%	5%	6%
<b>Flexural Modulus (ASTM D790)</b>	440,000 psi (3. GPa)	440,000 psi (3. GPa)	430,000 psi (3. GPa)
<b>Flexural Strength (ASTM D790)</b>	14,000 psi (96.5 MPa)	13,500 psi (93.1 MPa)	14,580 psi (100.5 MPa)
<b>Compression Strength (ASTM D695)</b>	11,330 psi (78.1 MPa)	11,330 psi (78.1 MPa)	12,520 psi (86.3 MPa)
<b>Tg Ultimate (DSC, midpoint)</b>	170°F/62°C	149°F/51°C	171°F/63°C
<b>Hardness (Shore D)</b>	70-80	70-80	70-80

PROCESSING DATA	CLX	CLF	CLS
<b>Mix Ratio (by volume)</b>	2:1	2:1	2:1
<b>Mix Ratio (by weight)</b>	100:47	100:47	100:47
<b>Viscosity (A/B/Mixed @ 77°F/25°C)</b>	1850/100/580	1850/265/725	1850/500/800
<b>Component Density (specific density @ 77°F/25°C)</b>	1.12 (epoxy), 1.02 (hardener)	1.12 (epoxy), 1.01 (hardener)	1.12 (epoxy), 0.98 (hardener)
<b>Mixed Density (specific density @ 77°F/25°C)</b>	1.09	1.08	1.08
<b>Pot Life (@ 77°F/25°C)</b>	18 min	21 min	43 min
<b>Tack Free Time (@ 95°F/35°C)</b>	2 hrs	4 hrs	8 hrs
<b>Recommended Full Cure</b>	7 days @ 77°F/25°C	7 days @ 77°F/25°C	7 days @ 77°F/25°C, Post cure recommended

ENVIRONMENT DATA	CLX	CLF	CLS
<b>VOC Content (ASTM D2369)</b>	0.16 lbs/gal (19.5 g/L)	0.26 lbs/gal (31.5 g/L)	0.13 lbs/gal (16.1 g/L)
<b>Biobased Carbon Content (ASTM D6866)</b>	21%	21%	29%

All technical information is provided in good faith and is based on Entropy Resins, Inc. best knowledge. Entropy Resins, Inc. does not guarantee any of this data nor the misuse of its products or the consequences because of conditions that are beyond their control. © Copyright Entropy Resins Inc. 2015

<p>AMERICAS                  ENTROPY RESINS, INC.                  info@entropyresins.com                  877.882.2120</p>	<p>EU/AFRICA                  FERRER-DALMAU                  info@entropyresins.eu                  +34.93.4874015                  entropyresin.eu</p>	<p>ASIA                  COMPOSITE CREATIONS CO., LTD.                  info@entropyresins.com                  877.882.2120</p>	<p>30621 San Antonio St. Hayward, CA 94544                  www.entropyresins.com</p>
---	---	--	---

24/7 Emergency Hotline: (760) 476-3962  
 Global Response Access Code: 333178





Advanced Materials

**Araldite® LY 1568 CH\***  
**Aradur® 3489 CH\***

STRUCTURAL COMPOSITES

Technical Data Sheet

<b>APPLICATIONS</b>	Industrial composites		
<b>PROPERTIES</b>	Laminating system with low viscosity. The long pot life of the system facilitates the production of very large industrial parts.		
<b>PROCESSING</b>	<ul style="list-style-type: none"> <li>• Infusion</li> <li>• Resin Transfer Moulding</li> <li>• Wet lay-up</li> <li>• Filament Winding</li> </ul>		
<b>KEY DATA</b>	<b>Resin Araldite® LY 1568 CH</b>		
	Aspect (visual)	clear liquid	
	Viscosity at 25 °C (ISO 12058-1)	1300 - 1500	[mPa.s]
	Density at 25 °C (ISO 1675)	1.1-1.2	[g/cm <sup>3</sup> ]
	Storage temperature (see expiry date on original container)	2 - 40	[°C]
	<b>Hardener Aradur® 3489 CH</b>		
	Aspect (visual)	clear liquid	
	Viscosity at 25 °C (ISO 12058-1)	5 - 20	[mPa.s]
	Density at 25 °C (ISO 1675)	0.92-0.93	[g/cm <sup>3</sup> ]
	Storage temperature (see expiry date on original container)	2 - 40	[°C]
<b>STORAGE</b>	<p>Provided that Araldite® LY 1568 CH and Aradur® 3489 CH are stored in a dry place in their original, properly closed containers at the above mentioned storage temperatures they will have the shelf lives indicated on the labels.</p> <p>Partly emptied containers should be closed immediately after use.</p>		

\* In addition to the brand name product denomination may show different appendices, which allows us to differentiate between our production sites: e.g. BD = Germany, US = United States, IN = India, CI = China, etc.. These appendices are in use on packaging, transport and invoicing documents. Generally the same specifications apply for all versions. Please address any additional need for clarification to the appropriate Huntsman contact.

## PROCESSING DATA

MIX RATIO	Components	Parts by weight	Parts by volume
	Araldite® LY 1568 CH	100	100
	Aradur® 3489 CH	28	35

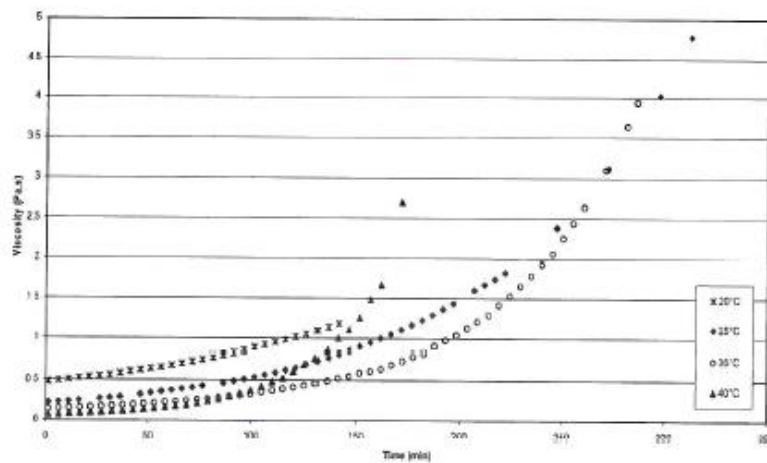
We recommend that the components are weighed with an accurate balance to prevent mixing inaccuracies which can affect the properties of the matrix system. The components should be mixed thoroughly to ensure homogeneity. It is important that the side and the bottom of the vessel are incorporated into the mixing process.

When processing large quantities of mixture the pot life will decrease due to exothermic reaction. It is advisable to divide large mixes into several smaller containers.

INITIAL MIX VISCOSITY (ISO 12058-1)		[°C]	[mPa s]
	Araldite® LY 1568 CH/Aradur® 3489 CH	at 25	200 - 300

## VISCOSITY BUILT UP

(Rheometer AGR2,  
plate/plate 25 mm,  
100 rpm)



POT LIFE (Tecam, 23°C, 65 % RH)		[s]	[min]
	Araldite® LY 1568 CH/Aradur® 3489 CH	100	850 - 950

GEL TIME (Hot plate)		[°C]	[min]
	Araldite® LY 1568 CH/Aradur® 3489 CH	at 80	43-46
		at 100	15-10
		at 120	7-8

The values shown are for small amounts of pure resin/hardener mix. In composite structures the gel time can differ significantly from the given values depending on the fibre content and the laminate thickness.



<b>PROPERTIES OF THE CURED, NEAT FORMULATION</b>			
<b>GLASS TRANSITION TEMPERATURE (<math>T_g</math>)</b> (IEC 1006, 10 K/min)	<i>Cure:</i> 15 h 50 °C 6 h 70 °C 4 h 80 °C 8 h 80°C 5 h 100°C	$T_g$ [°C]	Araldite® LY 1568 CH/Aradur® 3489 CH  61-65 75-78 76-79 77-80 79-83
<b>TENSILE TEST</b> (ISO 527)		<i>Cure:</i>	8 h 80 °C
	Tensile strength	[MPa]	67-71
	Elongation at tensile strength	[%]	4.4-5.0
	Ultimate strength	[MPa]	54-58
	Ultimate elongation	[%]	10.5-11
	Tensile modulus	[MPa]	2850-3000
<b>FLEXURAL TEST</b> (ISO 178)		<i>Cure:</i>	8 h 80 °C
	Flexural strength	[MPa]	120-130
	Elongation at flexural strength	[%]	5.5-6.5
	Ultimate strength	[MPa]	100-115
	Ultimate elongation	[%]	9-10
	Flexural modulus	[MPa]	2910-3010
<b>FRACTURE PROPERTIES</b>		<i>Cure:</i>	8 h 80 °C
<b>BEND NOTCH TEST</b> (PM 258-0/90)	Fracture toughness $K_{1C}$	[MPa√m]	0.7 – 0.8
	Fracture energy $G_{1C}$	[J/m <sup>2</sup> ]	170 - 210

**HANDLING  
PRECAUTIONS****Personal hygiene***Safety precautions at workplace*

protective clothing	yes
gloves	essential
arm protectors	recommended when skin contact likely
<u>goggles/safety glasses</u>	<u>yes</u>

*Skin protection*

before starting work	Apply barrier cream to exposed skin
<u>after washing</u>	<u>Apply barrier or nourishing cream</u>

*Cleansing of contaminated skin*

Dab off with absorbent paper, wash with warm water and alkali-free soap, then dry with disposable towels.  
Do not use solvents

*Disposal of spillage*

Soak up with sawdust or cotton waste and deposit in plastic-lined bin

*Ventilation*

of workshop	Renew air 3 to 5 times an hour
of workplaces	Exhaust fans. Operatives should avoid inhaling vapours

**FIRST AID**

Contamination of the *eyes* by resin, hardener or mix should be treated immediately by flushing with clean, running water for 10 to 15 minutes. A doctor should then be consulted.

Material smeared or splashed on the *skin* should be dabbed off, and the contaminated area then washed and treated with a cleansing cream (see above). A doctor should be consulted in the event of severe irritation or burns. Contaminated clothing should be changed immediately.

Anyone taken ill after *inhaling* vapours should be moved out of doors immediately.

In all cases of doubt call for medical assistance.

**Huntsman Advanced Materials**  
(Switzerland) GmbH  
Klybeckstrasse 200  
4057 Basel  
Switzerland

Tel: +41 (0)61 299 11 11  
Fax: +41 (0)61 299 11 12

[www.huntsman.com/advanced\\_materials](http://www.huntsman.com/advanced_materials)  
Email: [advanced\\_materials@huntsman.com](mailto:advanced_materials@huntsman.com)



Huntsman Advanced Materials warrants only that its products meet the specifications agreed with the buyer. Typical properties, where stated, are to be considered as representative of current production and should not be treated as specifications.

The manufacture of materials is the subject of granted patents and patent applications; freedom to operate patented processes is not implied by this publication.

While all the information and recommendations in this publication are, to the best of our knowledge, information and belief, accurate at the date of publication, NOTHING HEREIN IS TO BE CONSTRUED AS A WARRANTY, EXPRESS OR OTHERWISE.

IN ALL CASES, IT IS THE RESPONSIBILITY OF THE USER TO DETERMINE THE APPLICABILITY OF SUCH INFORMATION AND RECOMMENDATIONS AND THE SUITABILITY OF ANY PRODUCT FOR ITS OWN PARTICULAR PURPOSE.

The behaviour of the products referred to in this publication in manufacturing processes and their suitability in any given end-use environment are dependent upon various conditions such as chemical compatibility, temperature, and other variables, which are not known to Huntsman Advanced Materials. It is the responsibility of the user to evaluate the manufacturing circumstances and the final product under actual end-use requirements and to adequately advise and warn purchasers and users thereof.

Products may be toxic and require special precautions in handling. The user should obtain Safety Data Sheets from Huntsman Advanced Materials containing detailed information on toxicity, together with proper shipping, handling and storage procedures, and should comply with all applicable safety and environmental standards.

Hazards, toxicity and behaviour of the products may differ when used with other materials and are dependent on manufacturing circumstances or other processes. Such hazards, toxicity and behaviour should be determined by the user and made known to handlers, processors and end users.

Except where explicitly agreed otherwise, the sale of products referred to in this publication is subject to the general terms and conditions of sale of Huntsman Advanced Materials LLC or of its affiliated companies including without limitation, Huntsman Advanced Materials (Europe) BVBA, Huntsman Advanced Materials Americas, Inc., and Huntsman Advanced Materials (Hong Kong) Ltd. Huntsman Advanced Materials is an international business as well of Huntsman Corporation. Huntsman Advanced Materials trades through Huntsman affiliated companies in different countries including but not limited to Huntsman Advanced Materials LLC in the USA and Huntsman Advanced Materials (Europe) BVBA in Europe.

Copyright © 2009 Huntsman Corporation or an affiliate thereof. All rights reserved.

# APPENDIX B

## 1. TEST DEVIATIONS

During the experimental campaign there are some deviations from the expected data from mechanical tests. In the following point those deviations would be clarified.

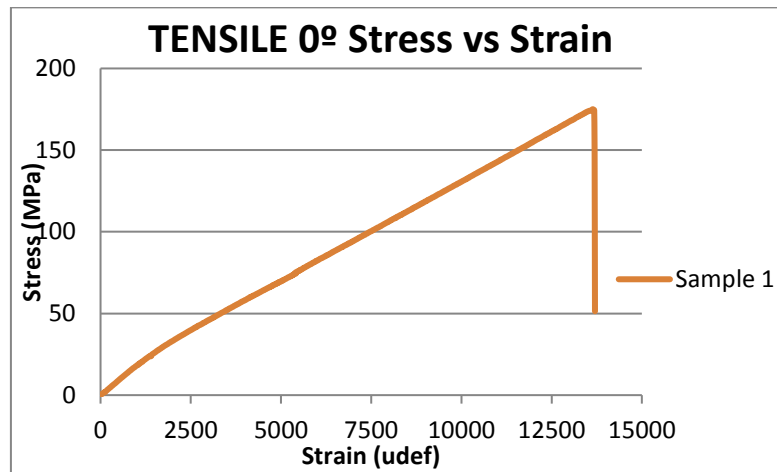
1. For transverse tensile test usually some noise is always detected in the deformation signal, this happens because of the interfibre cracking; example **Laminate 1 Tensile 90° test** or **Laminate 25 Tensile 90° test**
2. Depending on the software configuration, the negative strains might be plotted as negative or positive; example **Laminate 2 Compression 0° test**
3. Along all the experimental testing campaign it was seen that sometimes the deformation signal initially goes negative and next it changes to positive, e.g. **Laminate 3 Tensile 0° test**. This happens because of two factors, initial coupon angle and video-extensometry. The testing coupons have an initial curvature, that angle provokes an initial negative deformation record by the extensometers. This phenomenon might be solved using more accurate data acquisition camera or testing with strain gauges. **Laminate 6 Tensile 90° test** example is a very exaggerated case, where the laminate initial bending provokes negative records
4. Sometimes the video-extensometry stickers release from the testing coupons, getting as a result strange records like in **Laminate 11 Tensile 90° test, samples 6 and 8**.
5. When the camera lens is not correctly adjusted the signal line tends to be thicker, example **Laminate 21 Tensile 90° test**
6. Some laminates have been tested with strain gauges in order to obtain more accurate modulus and strain values, example **Laminate 29 Tensile 0° test**

## 2. MECHANICAL TESTS DATA

### Laminates 1 and 2\_Supersap CLR/INF-Biotex UD-No treatment

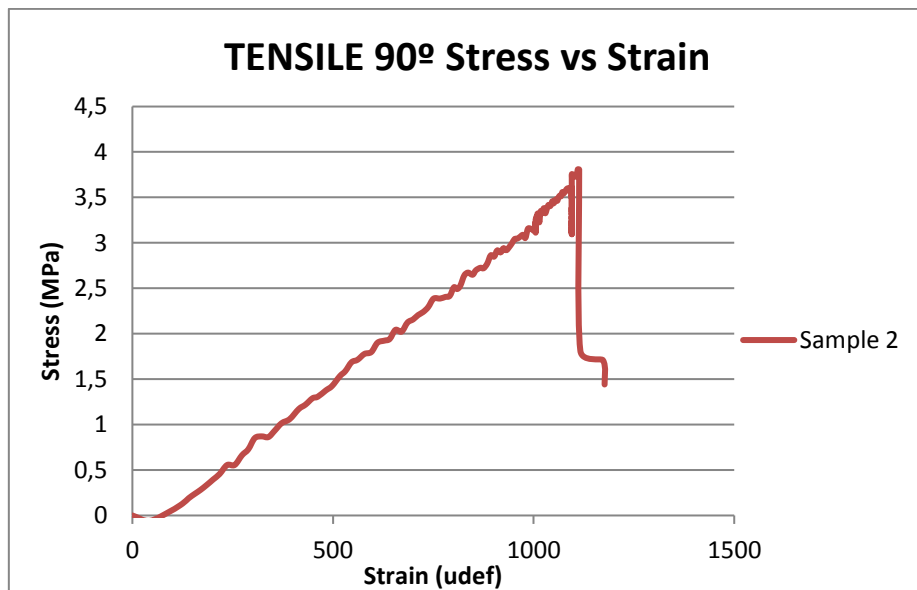
#### Laminate 1 Tensile 0° test

Sample	Width	Thickness	Tensile load	Tensile strength	Tensile modulus (Extensometry)	Tensile modulus (Gauges)	Failure elongation	Poisson coefficient
	a	e	F	$\sigma_{xt}$	$E_{xt}$	$E_{xt}$	$\epsilon_{xt}$	$\nu_{xy}$
	mm	mm	kN	MPa	GPa	GPa	def (%)	
LINO_T0°_P01	15,05	2,03	5,358	175,039	15,617	15,203	1,36	0,436



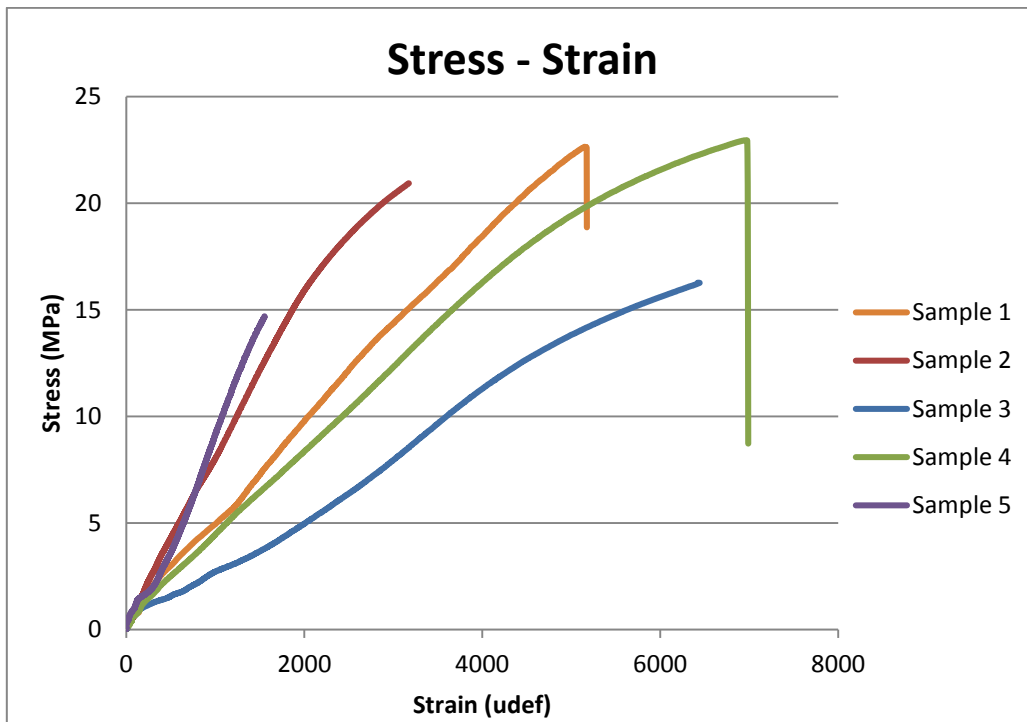
#### Laminate 1 Tensile 90° test

Sample	Width	Thickness	Tensile load	Tensile strength	Tensile modulus (Extensometry)	Tensile modulus (Gauges)	Failure elongation	Poisson coefficient
	a	e	F	$\sigma_{xt}$	$E_{xt}$	$E_{xt}$	$\epsilon_{xt}$	$\nu_{xy}$
	mm	mm	kN	MPa	GPa	GPa	def (%)	
LINO_T90°_P01	25,13	2,01	0,192	3,809	3,37	Lectura nula por ruido	0,11	-



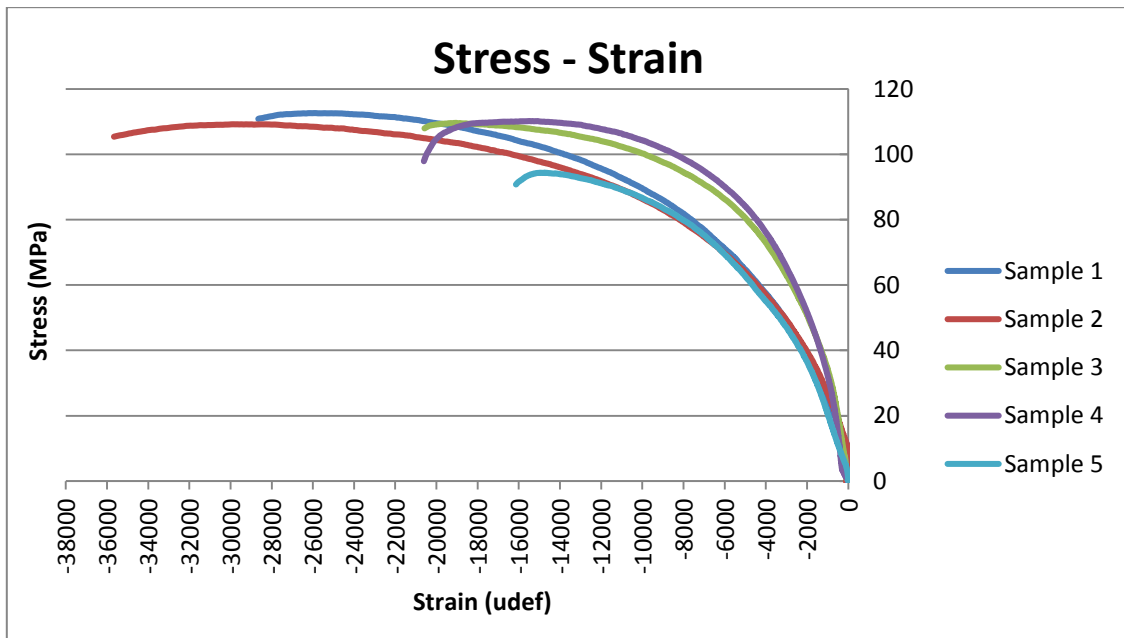
### Laminate 1 In-plane shear 10° test

Sample	Width	Thickness	In plane shear	In plane shear modulus	Maximum shear elongation
	a	e	IPS	G	$\gamma$
	mm	mm	MPa	GPa	%
E-IPSP01	25,81	3,78	22,650	4,409	0,51
E-IPSP02	25,28	3,96	21,952	6,572	Gage failure
E-IPSP03	25,95	3,90	23,306	2,973	Gage failure
E-IPSP04	25,01	3,89	22,957	3,861	0,28
E-IPSP05	25,79	3,87	21,514	10,406	Gage failure
<b>Average</b>	<b>25,57</b>	<b>3,88</b>	<b>22,48</b>	<b>5,64</b>	<b>0,39</b>
Standard deviation	0,40	0,06	0,73	2,97	0,17
cv (%)	1,57%	1,63%	3,26%	52,69%	42,34%
Characteristic value			20,888	-0,795	0,03



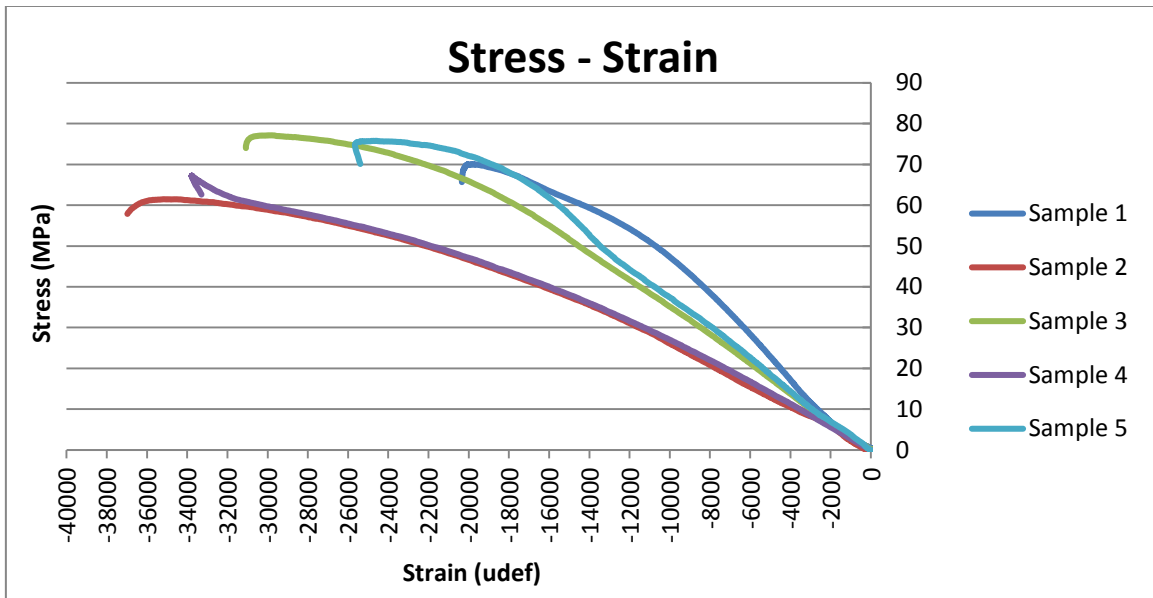
### Laminate 2 Compression 0° test

Sample	Width	Thickness	Failure load	Compression strength	Compression modulus	Failure elongation
	a	e	F	$\sigma_{xc}$	$E_{xc}$	$\epsilon_{xc}$
	mm	mm	kN	MPa	GPa	def (%)
COP01	14,77	3,89	6,471	112,647	13,716	-2,59
COP02	14,77	3,86	6,231	109,223	13,002	-2,84
COP03	14,80	3,82	6,192	109,649	18,293	-1,90
COP04	15,13	3,85	6,416	110,210	22,017	-3,01
COP05	14,67	3,79	5,253	94,401	16,024	-1,47
Average	<b>14,83</b>	<b>3,84</b>	<b>6,11</b>	<b>107,226</b>	<b>16,610</b>	<b>-2,36</b>
Standard deviation	0,18	0,04	0,49	7,29	3,67	0,65
cv (%)	1,20%	0,99%	8,09%	6,80%	22,08%	-27,68%
Characteristic value				89,868	7,879	-0,947



### Laminate 2 Compression 90° test

Sample	Width	Thickness	Failure load	Compression strength	Compression modulus	Failure elongation
	a	e	F	$\sigma_{yc}$	$E_{yc}$	$\epsilon_{yc}$
	mm	mm	kN	MPa	GPa	def (%)
E-C90P01	25,95	3,96	7,201	70,029	4,010	-1,99
E-C90P02	25,90	3,92	6,240	61,450	3,600	-3,51
E-C90P03	25,76	3,95	7,841	77,115	3,124	-2,97
E-C90P04	25,68	3,93	6,789	67,220	2,834	-3,32
E-C90P05	25,67	3,96	7,694	75,771	3,265	-2,53
<b>Average</b>	<b>25,79</b>	<b>3,94</b>	<b>7,15</b>	<b>70,317</b>	<b>3,367</b>	<b>-2,86</b>
Standard deviation	0,13	0,02	0,66	6,41	0,45	0,61
cv (%)	0,50%	0,44%	9,21%	9,11%	13,46%	-21,47%
Characteristic value				55,061	2,288	-1,533

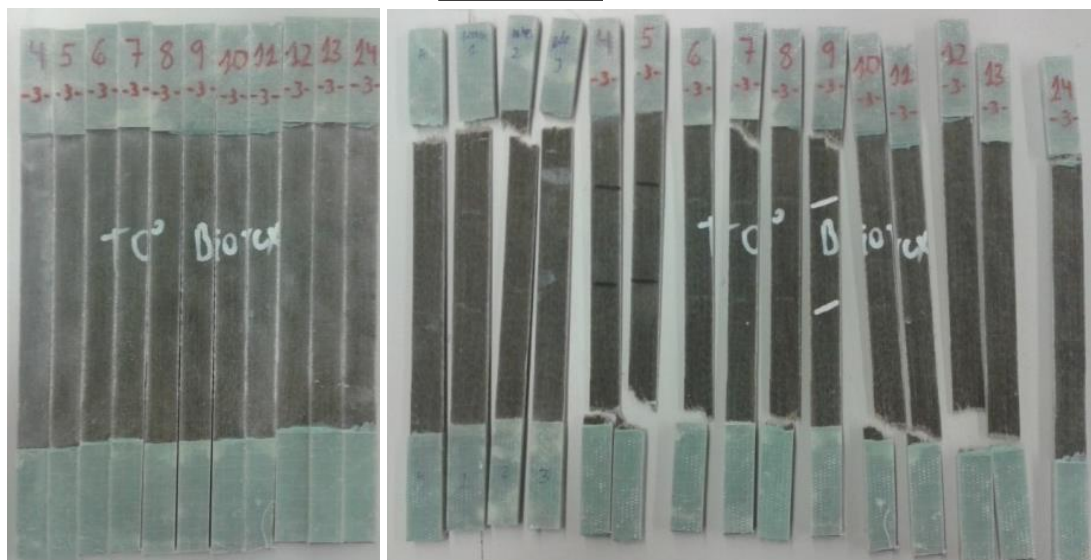
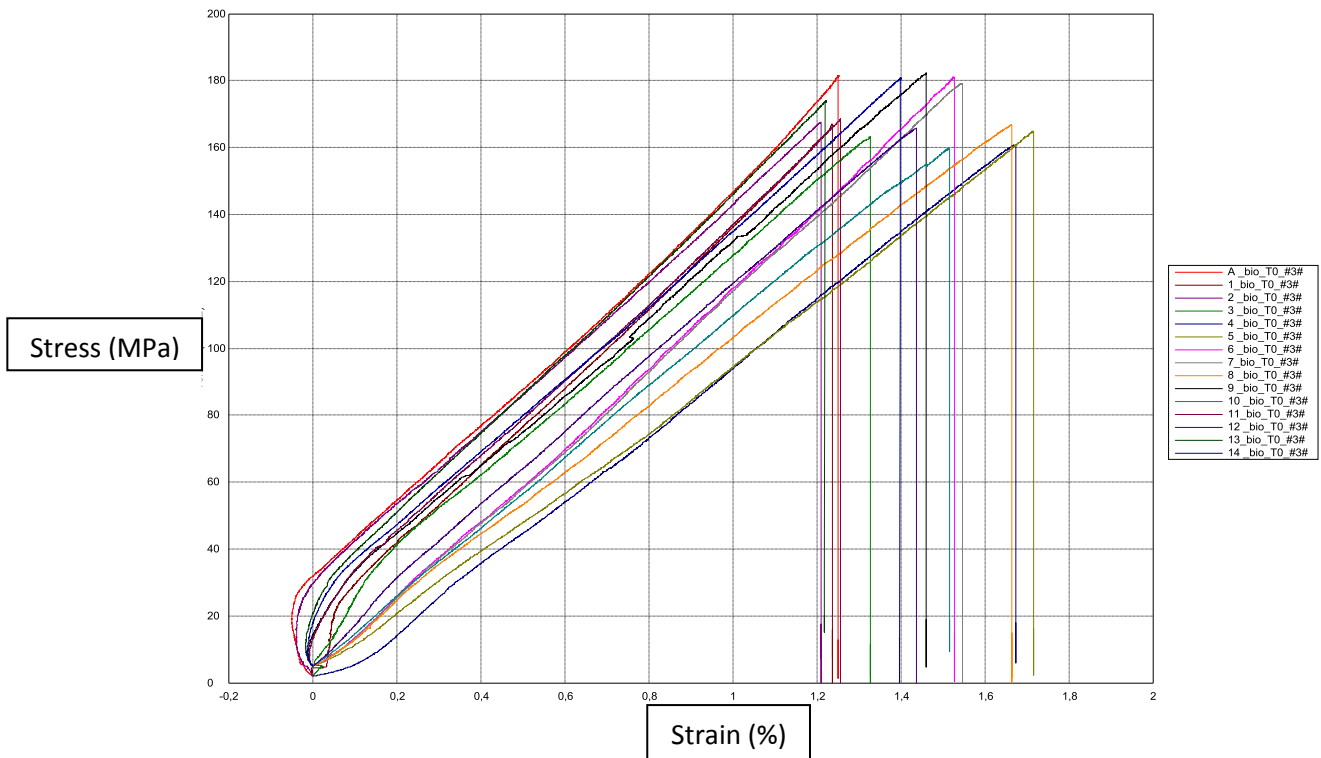




## Laminate 3\_Araldite LY 1569 /Aradur 3489-Biotex UD-No treatment

### Laminate 3 Tensile 0° test

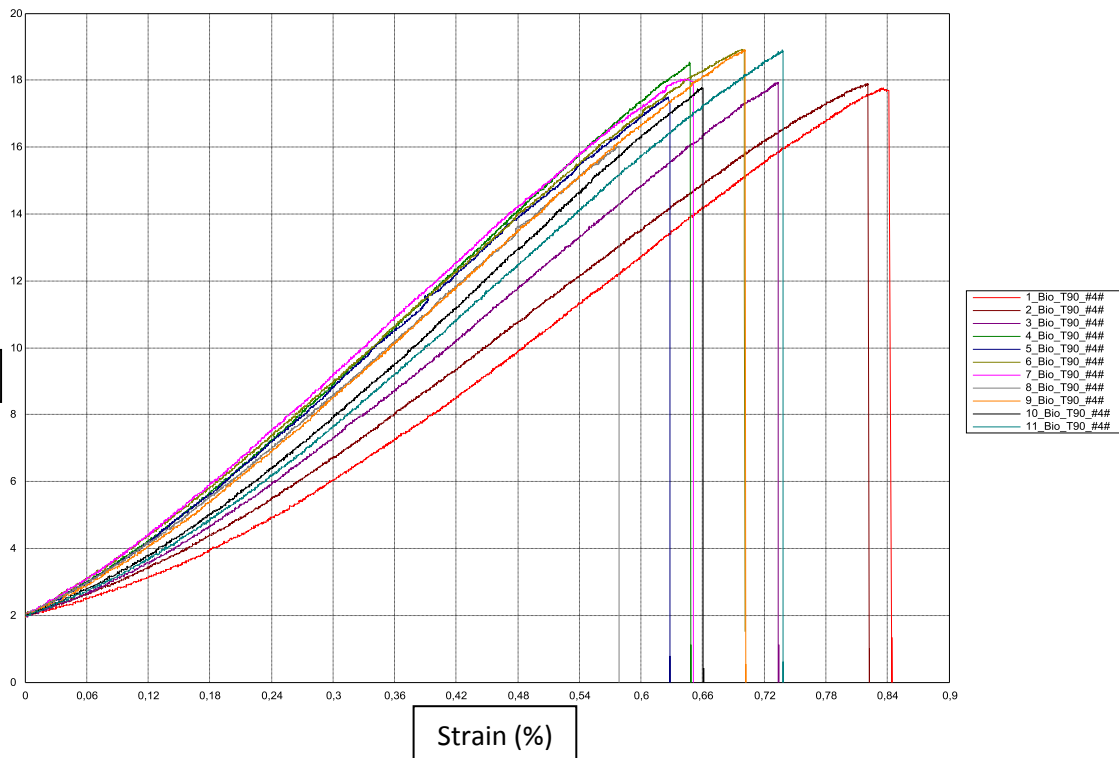
Sample	ID	Longitudinal tensile test							Failure mode	Vf	Mf
		a mm	b mm	F kN	Ext Mpa	σxt Mpa	ext %	vxy		(%)	(%)
1	1 Bio_TO_#3#	2,24	17,90	6,70	12087,10	167,11	1,24	0,21	Top	34	41,3
2	2 Bio_TO_#3#	2,16	14,54	5,26	11129,20	167,63	1,21	0,22	Top		
3	3 Bio_TO_#3#	2,2	15,54	5,58	10662,60	163,23	1,33	0,18	Top		
4	6 Bio_TO_#3#	2,1	14,35	5,46	12128,80	181,13	1,53	0,16	Bottom	Parameters	Value
5	7 Bio_TO_#3#	2,04	14,74	5,38	11776,20	179,08	1,55	0,20	Top		
6	8 Bio_TO_#3#	2,04	14,95	5,09	11373,50	166,86	1,66	0,18	Bottom	Testing speed (mm/min)	2
7	9 Bio_TO_#3#	2,06	15,13	5,68	11902,40	182,16	1,46	0,19	Top	Extensometry	Video
8	10 Bio_TO_#3#	2,29	14,88	5,44	11177,10	159,69	1,52	0,18	Bottom	Reference points	Stickers
9	11 Bio_TO_#3#	2,08	14,65	5,14	12559,20	168,54	1,26	0,17	Bottom	Norma	EN ISO527-5
10	12 Bio_TO_#3#	2,19	15,40	5,59	11067,10	165,71	1,44	0,19	Bottom	Precharge (kN)	5
11	13 Bio_TO_#3#	2,22	15,33	5,92	12065,70	173,98	1,22	0,22	Bottom	Modulus (ε %)	0,05-0,25
12	14 Bio_TO_#3#	2,17	15,43	6,05	10974,30	180,81	1,40	0,17	Top		
Average value		2,15	15,24	5,61	11575,27	171,33	1,40	0,19			
Standard deviation				0,45	585,82	7,76	0,15	0,02			
CV(%)				0,08	0,05	0,05	0,11	0,10			
Characteristic value					10333,41	154,88	1,08	0,15			



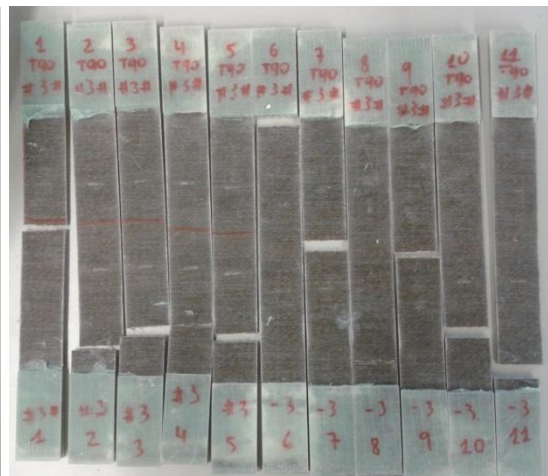
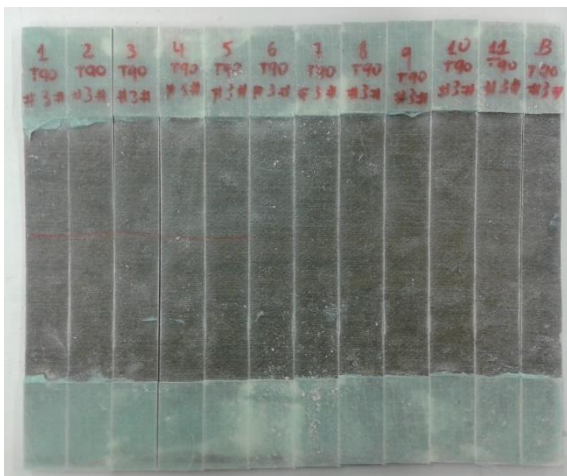
### Laminate 3 Tensile 90° test

Sample	ID	Transverse tensile test						Failure mode	Vf (%)	Mf (%)
		a mm	b mm	F kN	Eyt Mpa	oyt Mpa	eyt %			
1	1_Bio_T90_#3#	2,07	25,17	0,93	2286,66	17,78	0,84	35	42,3	
2	2_Bio_T90_#3#	2,17	25,38	0,99	2185,75	17,90	0,82			
3	3_Bio_T90_#3#	2,16	25,56	0,99	2442,16	17,92	0,73			
4	4_Bio_T90_#3#	2,06	25,25	0,96	2809,75	18,53	0,65			
5	5_Bio_T90_#3#	2,22	25,31	0,98	2732,02	17,50	0,63			
6	6_Bio_T90_#3#	2,16	25,32	1,03	2563,81	18,92	0,70			
7	7_Bio_T90_#3#	2,06	25,28	0,94	2709,21	18,04	0,65			
8	8_Bio_T90_#3#	2,11	25,42	0,86	2620,94	16,02	0,58			
9	9_Bio_T90_#3#	2,03	25,5	0,98	2675,14	18,91	0,70			
10	10_Bio_T90_#3#	1,98	25,34	0,89	2693,45	17,77	0,66			
11	11_Bio_T90_#3#	2,00	25,22	0,95	2634,65	18,89	0,74			
Average value		2,09	25,34	0,95	<b>2577,59</b>	18,02	0,70			
Standard deviation				0,05	194,90	0,84	0,08			
CV(%)				0,05	0,08	0,05	0,11			
Characteristic value					2160,32	<b>16,22</b>	<b>0,53</b>			

Stress (MPa)



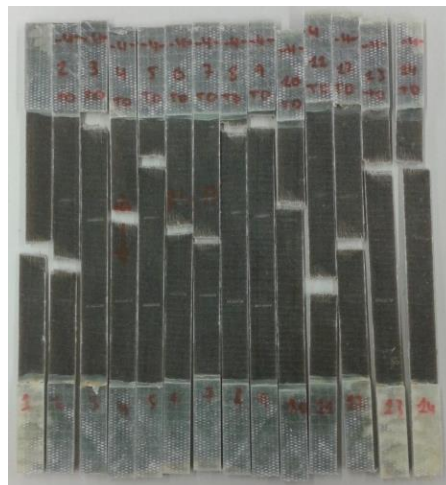
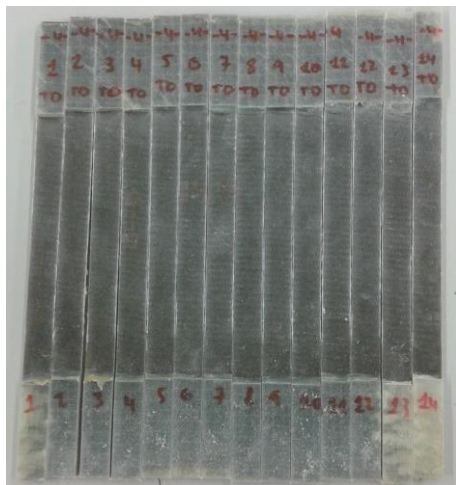
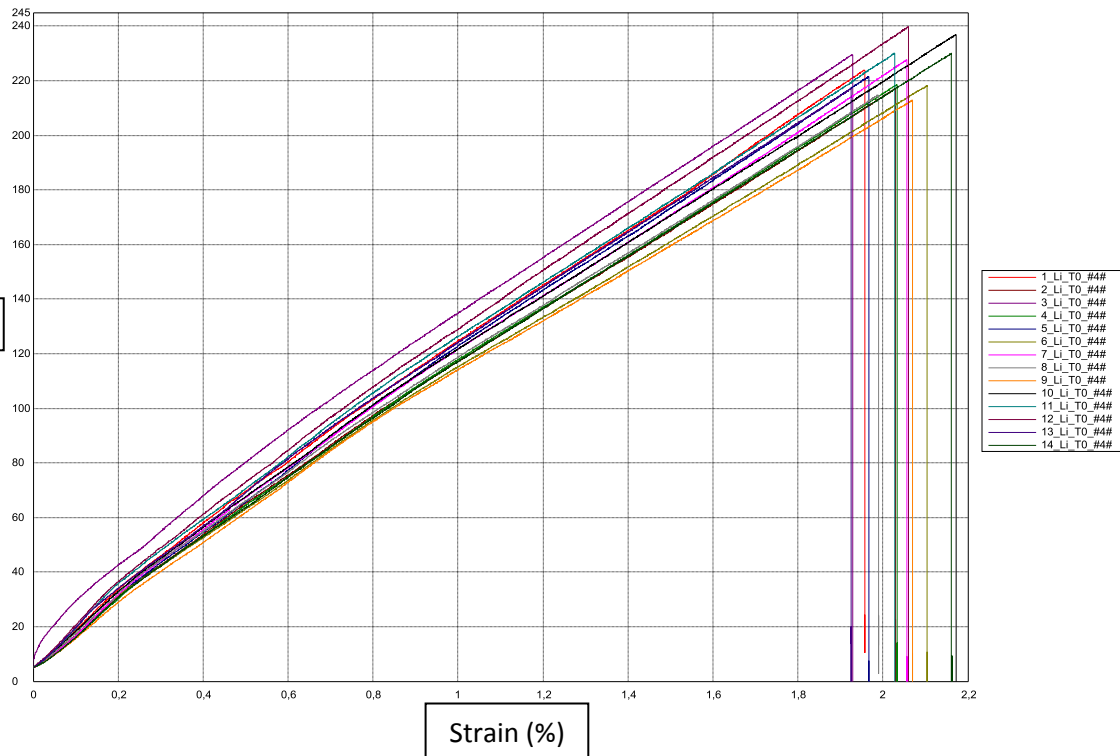
- 1\_Bio\_T90\_#4#
- 2\_Bio\_T90\_#4#
- 3\_Bio\_T90\_#4#
- 4\_Bio\_T90\_#4#
- 5\_Bio\_T90\_#4#
- 6\_Bio\_T90\_#4#
- 7\_Bio\_T90\_#4#
- 8\_Bio\_T90\_#4#
- 9\_Bio\_T90\_#4#
- 10\_Bio\_T90\_#4#
- 11\_Bio\_T90\_#4#



# Laminate 4\_Araldite LY 1569 /Aradur 3489-Lineo UD-No treatment

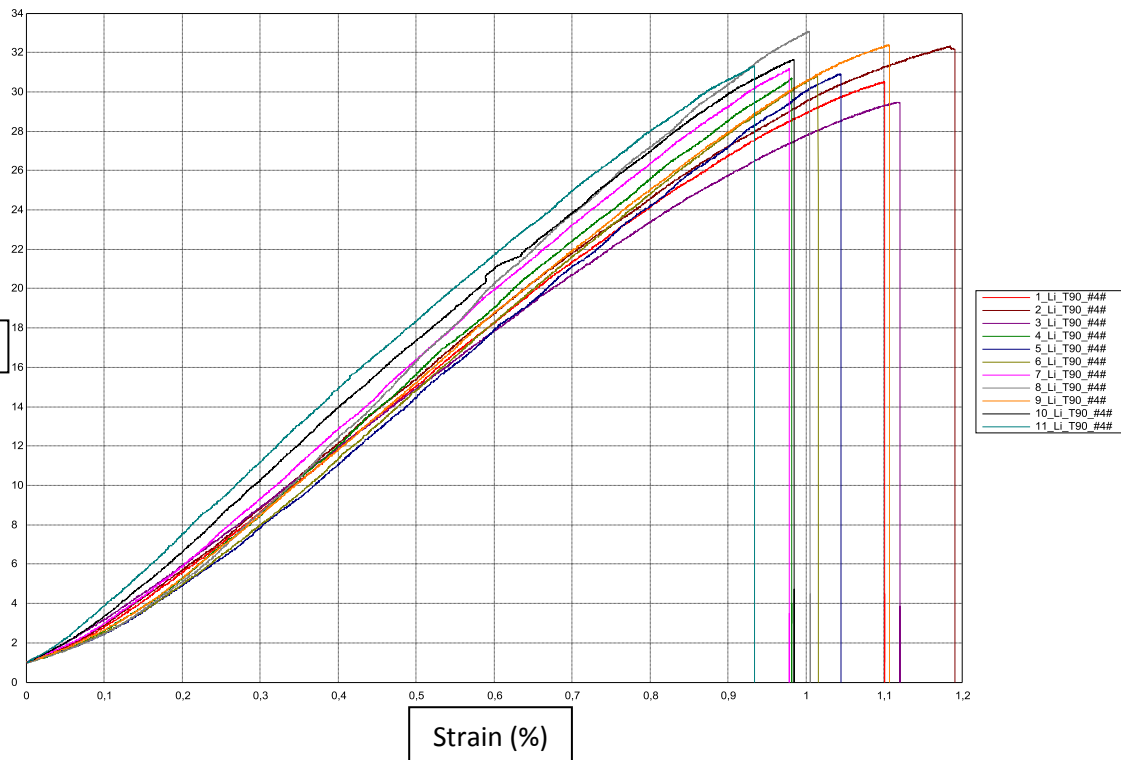
## Laminate 4 Tensile 0° test

Sample	ID	Longitudinal tensile test							Failure mode	Vf	Mf
		a mm	b mm	F kN	Ext Mpa	oxt Mpa	ext %	vxy		(%)	(%)
1	1 Li_TO_#4#	1,93	15,07	6,51	10829,00	223,94	1,96	0,33	Middle	34	38,4
2	2 Li_TO_#4#	1,98	15,11	6,50	10224,60	217,12	2,03		Middle		
3	3 Li_TO_#4#	2,00	15,24	7,00	10989,20	229,56	1,93		Tab	Parameters	Value
4	4 Li_TO_#4#	2,03	15,24	6,76	10238,80	218,53	2,03	0,36	Middle		
5	5 Li_TO_#4#	1,94	15,19	6,53	10725,90	221,49	1,97	0,30	Top	Testing speed (mm/min)	2
6	6 Li_TO_#4#	2,13	15,21	7,07	9922,72	218,13	2,10	0,35	Middle		
7	7 Li_TO_#4#	1,97	15,15	6,79	10520,90	227,57	2,06		Middle	Extensometry	Video
8	8 Li_TO_#4#	2,02	15,18	6,58	10347,50	214,73	1,99		Tab	Reference points	Stickers
9	9 Li_TO_#4#	2,07	15,26	6,72	9995,89	212,78	2,07	0,19	Tab	Norma	EN ISO527-5
10	10 Li_TO_#4#	1,95	15,16	7,01	10314,60	236,96	2,17	0,35	Middle	Precharge (kN)	5
11	11 Li_TO_#4#	1,97	15,21	6,90	10699,50	230,15	2,03	0,37	Middle	Modulus (ε %)	0,05-0,25
12	12 Li_TO_#4#	1,92	15,17	6,98	10634,90	239,75	2,06		Middle		
13	13 Li_TO_#4#	2,02	15,29	6,70	10611,20	216,99	1,92	0,20	Top		
14	14 Li_TO_#4#	1,94	15,08	6,73	10187,30	229,91	2,16		Top		
Average value		1,99	15,18	6,77	10445,86	224,12	2,03	0,31			
Standard deviation				0,20	318,07	8,37	0,08	0,07			
CV(%)				0,03	0,03	0,04	0,04	0,23			
Characteristic value					9782,79	206,66	1,87	0,15			



### Laminate 4 Tensile 90° test

Sample	ID	Transverse tensile test						Failure mode	Vf (%)	Mf (%)
		a (mm)	b (mm)	F (kN)	Eyt (Mpa)	oyt (Mpa)	eyt (%)			
1	1_Li_T90_#4#	2,04	24,4	1,52	2978,59	30,51	1,10	Tab	32,5	36,8
2	2_Li_T90_#4#	2,04	25,4	1,67	3092,73	32,32	1,19	Middle		
3	3_Li_T90_#4#	2,08	25,2	1,55	2880,90	29,48	1,12	Middle		
4	4_Li_T90_#4#	2,06	25,3	1,60	3159,33	30,70	0,98	Tab	Parameters	Value
5	5_Li_T90_#4#	2,11	24,81	1,62	3117,08	30,92	1,05	Tab		
6	6_Li_T90_#4#	2,06	24,97	1,59	3114,91	30,83	1,02	Tab	Testing speed (mm/min)	2
7	7_Li_T90_#4#	2,12	24,94	1,65	3296,60	31,17	0,98	Tab	Extensometry	Video
8	8_Li_T90_#4#	2,02	24,84	1,66	3636,07	33,08	1,01	Tab	Reference points	Stickers
9	9_Li_T90_#4#	2,11	24,9	1,70	3206,99	32,39	1,11	Middle	Norma	EN ISO527-5
10	10_Li_T90_#4#	2,15	25,02	1,70	3274,36	31,66	0,98	Tab	Precharge (kN)	1
11	11_Li_T90_#4#	2,13	24,96	1,66	3614,16	31,31	0,93	Tab	Modulus (ε %)	0,05-0,25
Average value		2,08	24,98	1,63	<b>3215,61</b>	31,31	1,04			
Standard deviation				0,06	234,96	1,01	0,08			
CV(%)				0,04	0,07	0,03	0,07			
Characteristic value					2712,58	<b>29,15</b>	<b>0,88</b>			

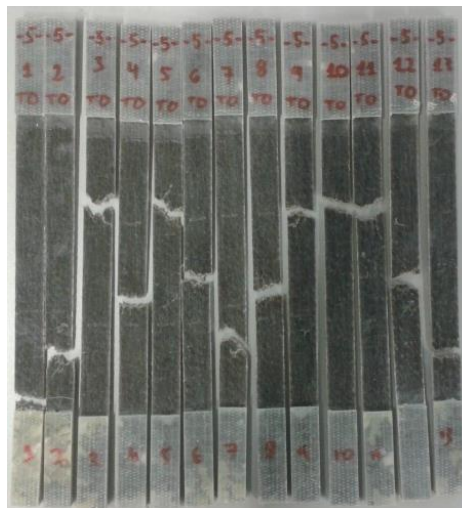
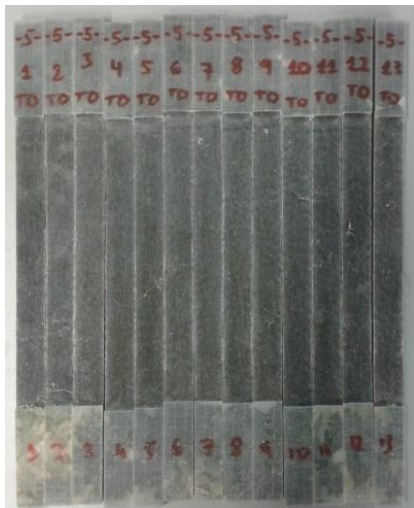
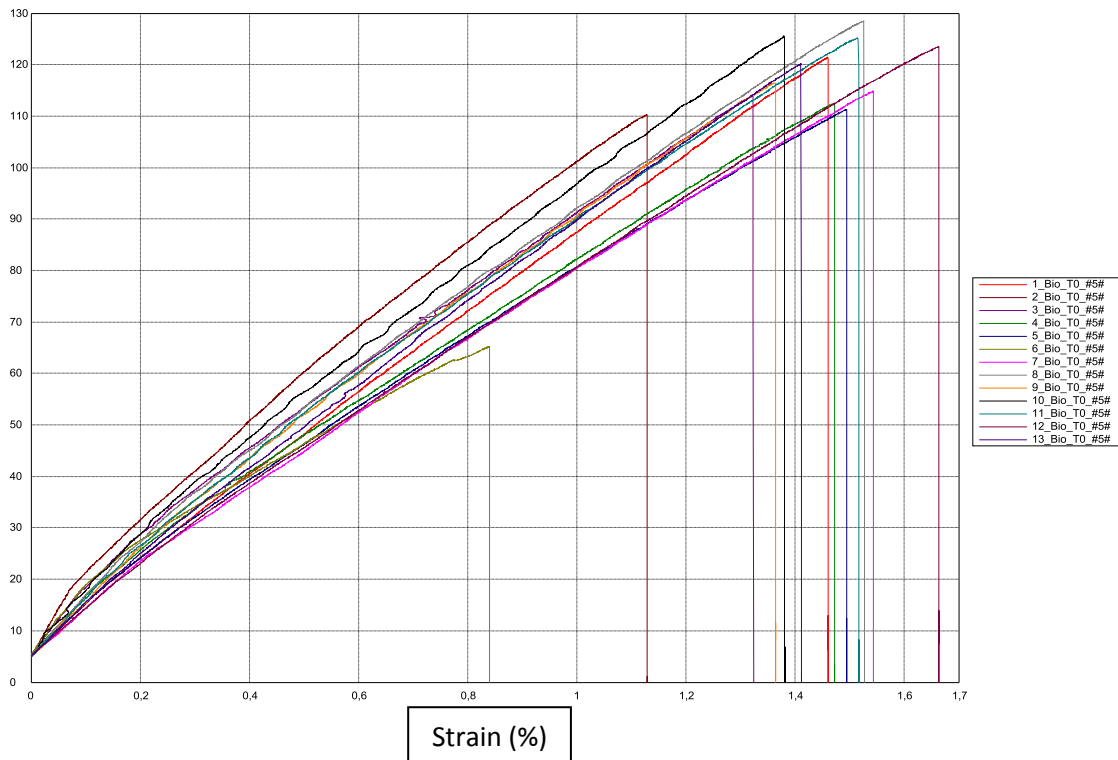




# Laminate 5\_Araldite LY 1569 /Aradur 3489-Biotex UD-NaOH 0,25M\_1h

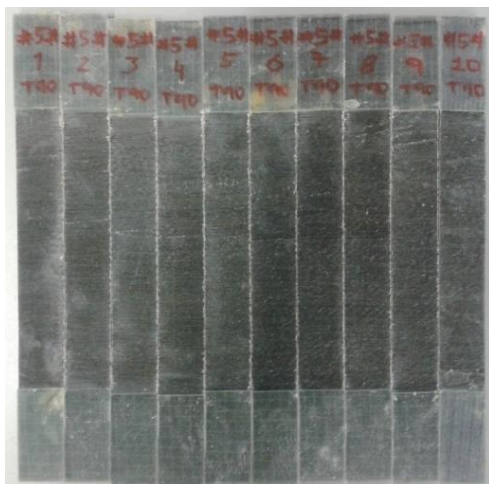
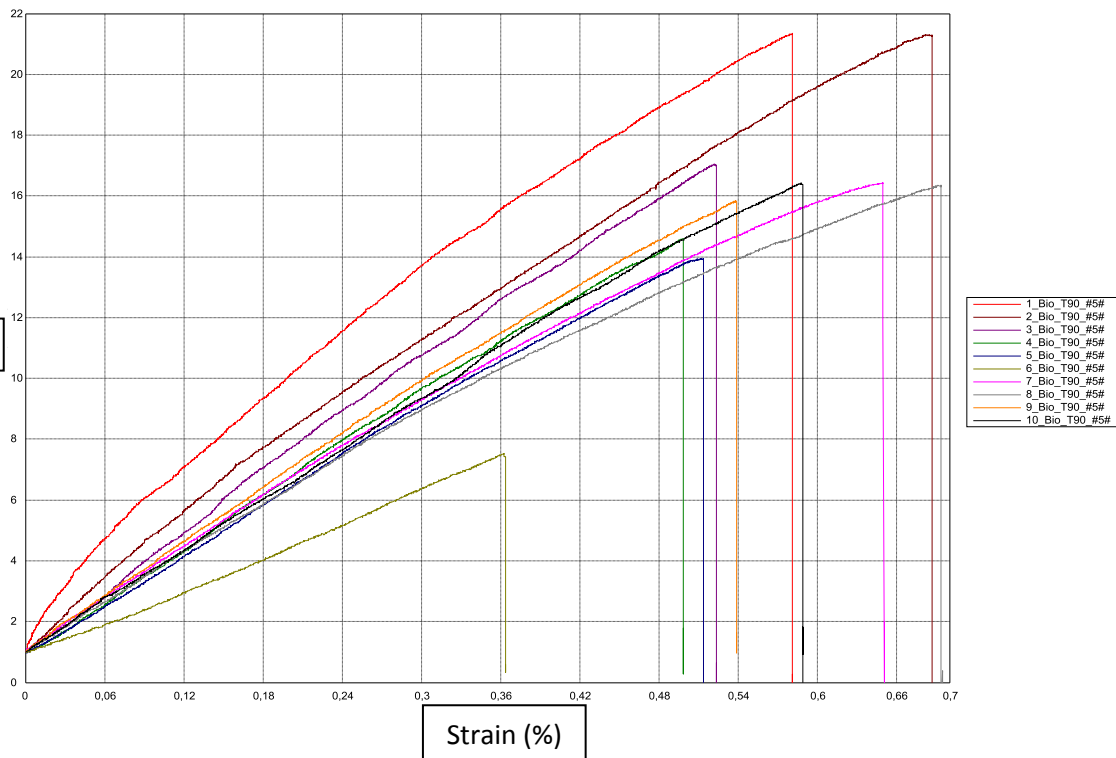
## Laminate 5 Tensile 0° test

Sample	ID	Longitudinal tensile test							Failure mode	Vf (%)	Mf (%)
		a mm	b mm	F kN	Ext Mpa	oxt Mpa	ext %	vxy			
1	1 Bio_TO_#5#	2,88	15,12	5,29	8961,39	121,40	1,46		Tab	25,5	31,8
2	2 Bio_TO_#5#	2,91	14,68	4,71	10620,20	110,26	1,13		Bottom		
3	3 Bio_TO_#5#	2,94	15,24	5,11	10279,60	114,07	1,32	0,49	Middle		
4	4 Bio_TO_#5#	2,86	15,25	4,91	9291,24	112,47	1,47		Middle	Parameters	Value
5	5 Bio_TO_#5#	2,97	15,23	5,03	8935,08	111,26	1,49	0,41	Middle		
6	7 Bio_TO_#5#	2,77	15,15	4,82	9014,91	114,85	1,54	0,41	Bottom	Testing speed (mm/min)	2
7	8 Bio_TO_#5#	2,75	14,95	5,28	10648,80	128,46	1,53	0,35	Middle	Extensometry	Video
8	9 Bio_TO_#5#	2,93	15,15	5,17	10253,10	116,44	1,36	0,47	Middle	Reference points	Stickers
9	10 Bio_TO_#5#	2,76	15,23	5,28	11093,50	125,57	1,38	0,29	Middle	Norma	EN ISO527-5
10	11 Bio_TO_#5#	2,84	15,23	5,41	10146,70	125,13	1,52	0,47	Middle	Precharge (kN)	5
11	12 Bio_TO_#5#	2,81	15,32	5,32	8726,02	123,52	1,66		Middle	Modulus (ε %)	0,05-0,25
12	13 Bio_TO_#5#	2,97	15,16	5,41	9057,59	120,15	1,41		Bottom		
Average value		2,87	15,14	5,14	<b>9752,34</b>	118,63	1,44	<b>0,41</b>			
Standard deviation				0,23	832,62	6,20	0,13	0,08			
CV(%)				0,05	0,09	0,05	0,09	0,18			
Characteristic value					7987,30	<b>105,48</b>	<b>1,16</b>	0,24			



### Laminate 5 Tensile 90° test

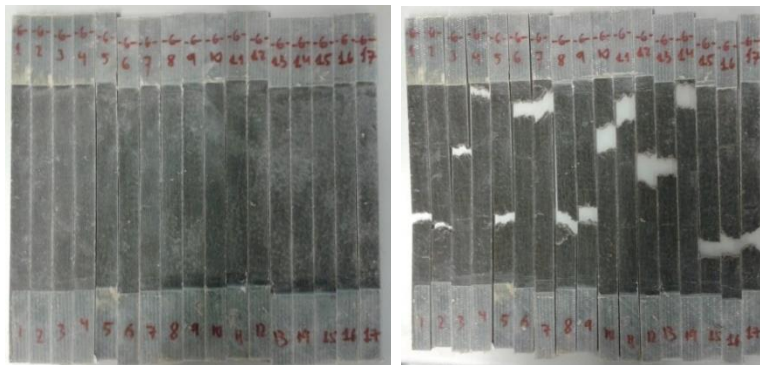
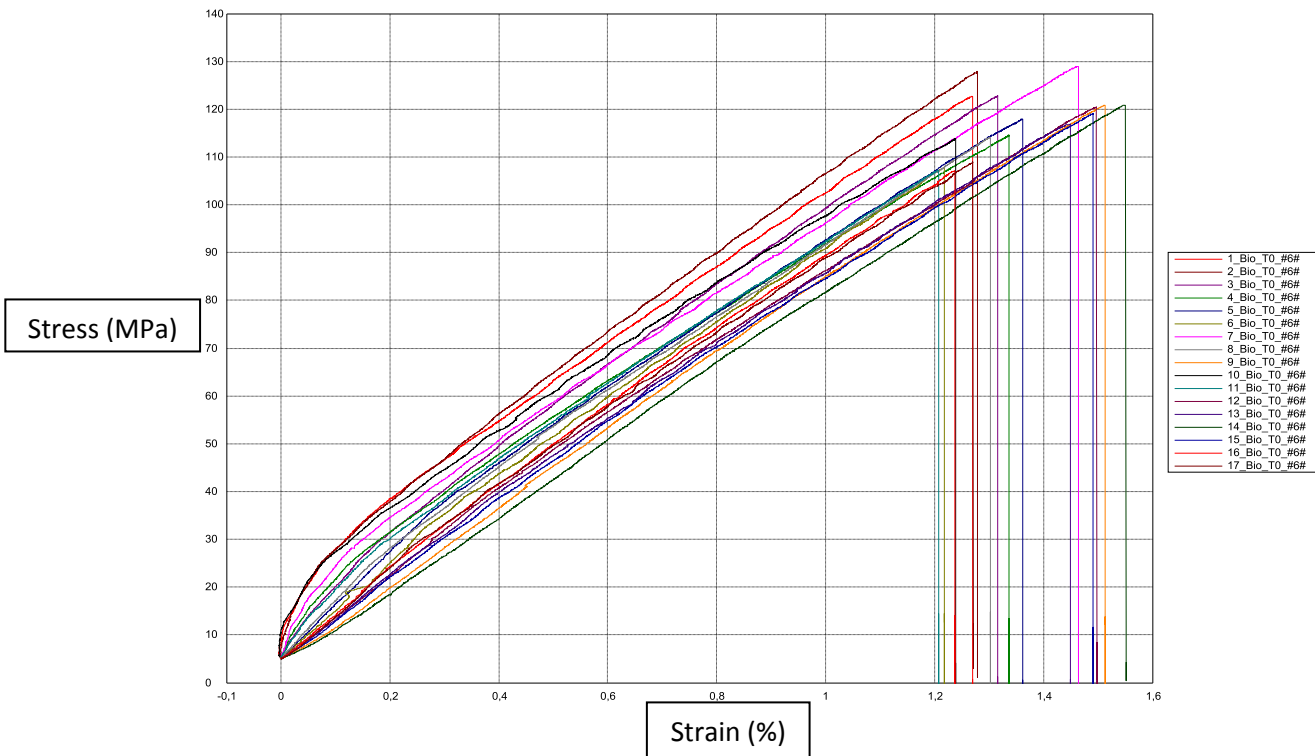
Sample	ID	Transverse tensile test						Failure mode	Vf	Mf
		a	b	F	Eyt	oyt	eyt		(%)	(%)
		mm	mm	kN	Mpa	Mpa	%			
1	1_Bio_T90_#5#	2,60	24,86	1,38	3759,37	21,34	0,58	Middle	26,6	33,1
2	2_Bio_T90_#5#	2,77	24,80	1,46	3381,06	21,31	0,69	Top	Parameters	Value
3	3_Bio_T90_#5#	2,76	25,03	1,18	3409,10	17,05	0,52	Bottom		
4	4_Bio_T90_#5#	2,81	25,04	1,03	3016,79	14,59	0,50	Top	Testing speed (mm/min)	2
5	5_Bio_T90_#5#	2,77	25,02	0,97	2810,50	13,95	0,51	Middle	Extensometry	Video
6	7_Bio_T90_#5#	2,85	25,07	1,17	2785,04	16,44	0,65	Bottom	Reference points	Stickers
7	8_Bio_T90_#5#	2,73	25,01	1,12	2652,43	16,34	0,69	Middle	Norma	EN ISO527-5
8	9_Bio_T90_#5#	2,69	25,03	1,07	2984,97	15,85	0,54	Middle	Precharge (kN)	1
9	10_Bio_T90_#5#	2,79	24,95	1,14	2727,53	16,42	0,59	Bottom	Modulus (ε %)	0,05-0,25
Average value		2,75	24,98	1,17	<b>3058,53</b>	17,03	0,59			
Standard deviation				0,16	376,84	2,62	0,08			
CV(%)				0,14	0,12	0,15	0,13			
Characteristic value					2232,00	<b>11,29</b>	<b>0,42</b>			



# Laminate 6\_Araldite LY 1569 /Aradur 3489-Biotex UD-NaOH 0,25M\_3h

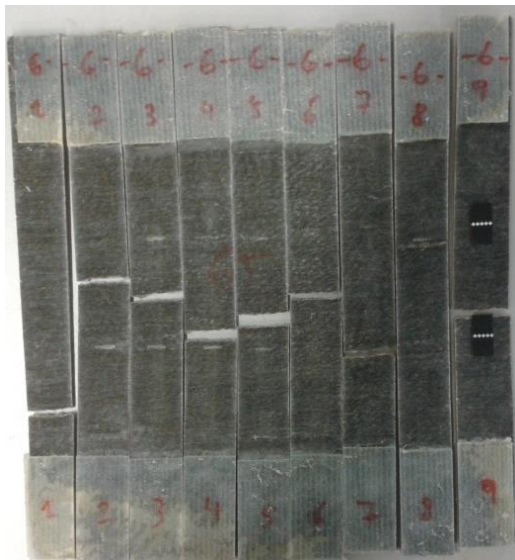
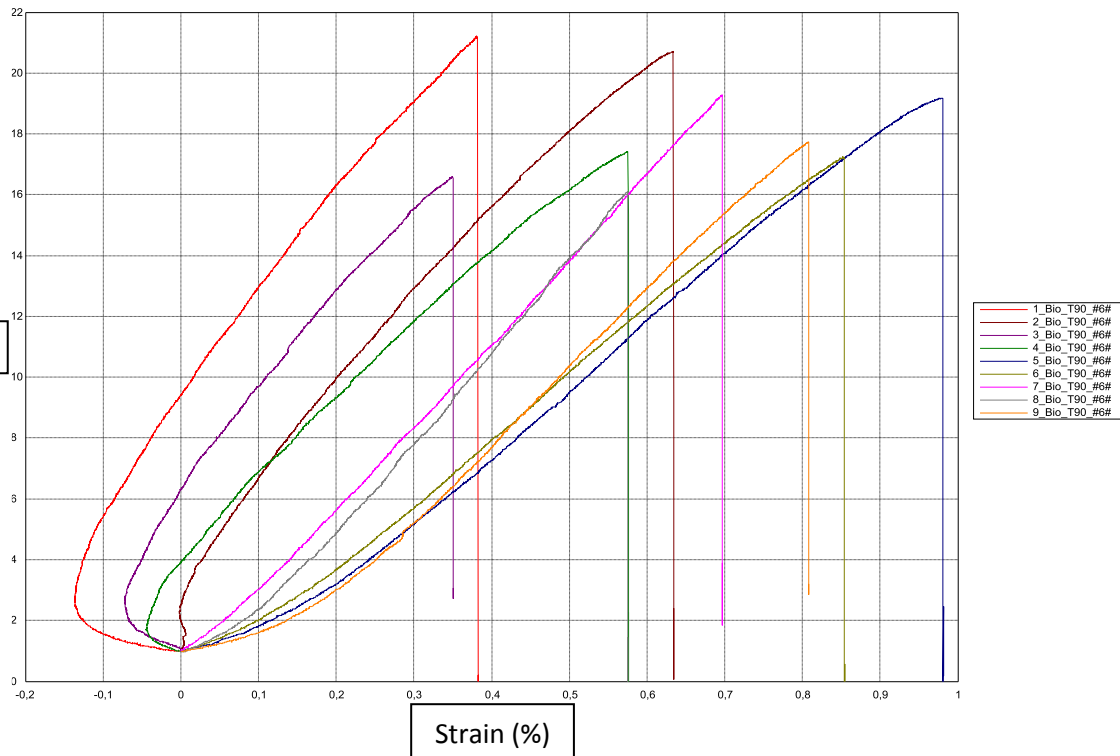
## Laminate 6 Tensile 0° test

Sample	ID	Longitudinal tensile test							Failure mode	Vf (%)	Mf (%)		
		a mm	b mm	F kN	Ext Mpa	oxt Mpa	ext %	vxy					
1	1 Bio_TO_#6#	2,63	14,12	4,56	10779,70	122,72	1,27		Middle	25,2	31,5		
2	2 Bio_TO_#6#	2,84	15,38	5,58	10384,90	127,86	1,28	0,33					
3	3 Bio_TO_#6#	2,96	15,13	5,50	11157,30	122,85	1,32		Top	Parameters	Value		
4	4 Bio_TO_#6#	3,07	15,28	5,37	10047,80	114,51	1,34		Tab				
5	5 Bio_TO_#6#	2,87	15,08	5,11	11115,40	117,99	1,36	0,30	Middle				
6	6 Bio_TO_#6#	2,82	14,86	4,51	10032,20	107,70	1,22	0,28	Top				
7	7 Bio_TO_#6#	2,86	15,09	5,57	10414,00	129,00	1,46		Top				
8	8 Bio_TO_#6#	3	15,39	5,27	10754,10	114,10	1,30	0,28	Middle				
9	9 Bio_TO_#6#	3,03	15,29	5,60	8479,27	120,83	1,51	0,30	Middle				
10	10 Bio_TO_#6#	2,85	15,25	4,95	9282,72	113,87	1,24	0,30	Top				
11	11 Bio_TO_#6#	2,71	15,06	4,38	10610,30	107,22	1,21	0,33	Top				
12	12 Bio_TO_#6#	2,89	14,98	5,21	9436,29	120,39	1,50	0,26	Middle				
13	13 Bio_TO_#6#	2,9	15,13	5,13	9311,83	116,84	1,45		Middle				
14	14 Bio_TO_#6#	2,9	15,17	5,32	7856,78	120,89	1,55	0,22	Tab				
15	15 Bio_TO_#6#	2,98	15,23	5,40	8939,67	119,05	1,49	0,27	Bottom				
16	16 Bio_TO_#6#	3,03	15,14	4,92	9797,01	107,15	1,24	0,21	Bottom				
17	17 Bio_TO_#6#	3,06	15,26	5,09	10317,90	108,92	1,27	0,21	bottom				
Average value		2,91	15,11	5,14	<b>9924,54</b>	117,17	1,35	<b>0,27</b>				Testing speed (mm/min)	2
Standard deviation				0,38	929,95	6,82	0,12	0,04				Extensometry	Video
CV(%)				0,07	0,09	0,06	0,09	0,16		Reference points	Stickers		
Characteristic value					8023,74	<b>103,23</b>	<b>1,12</b>	0,18		Standard	EN ISO527-5		
										Precharge (kN)	5		
										Modulus (ε %)	0,05-0,25		



## Laminate 6 Tensile 90° test

Sample	ID	Transverse tensile test						Failure mode	Vf	Mf
		a	b	F	Eyt	oyt	eyt		(%)	(%)
		mm	mm	kN	Mpa	Mpa	%			
1	1_Bio_T90_#6#	3,02	22,94	1,47	3299,92	21,21	0,38	Bottom	24,1	30,2
2	2_Bio_T90_#6#	3,14	25,26	1,64	3261,10	20,72	0,63	Middle	Parameters	Value
3	3_Bio_T90_#6#	3,04	25,34	1,28	3116,33	16,60	0,35	Middle		
4	4_Bio_T90_#6#	3,06	25,30	1,35	2531,06	17,42	0,58	Middle	Testing speed (mm/min)	2
5	5_Bio_T90_#6#	2,98	25,98	1,48	2155,53	19,18	0,98	Middle	Extensometry	Video
6	6_Bio_T90_#6#	3,08	25,35	1,35	2096,07	17,24	0,85	Middle	Reference points	Stickers
7	7_Bio_T90_#6#	2,96	25,41	1,45	2685,28	19,28	0,70	Bottom	Norma	EN ISO527-5
8	8_Bio_T90_#6#	2,95	25,36	1,20	2949,79	16,10	0,58	Middle	Precharge (kN)	1
9	9_Bio_T90_#6#	3,12	26,92	1,49	2487,90	17,74	0,81	Middle	Modulus (ε %)	0,05-0,25
Average value		3,04	25,32	1,41	<b>2731,44</b>	18,39	0,65			
Standard deviation				0,13	452,28	1,80	0,21			
CV(%)				0,09	0,17	0,10	0,32			
Characteristic value					1739,43	<b>14,44</b>	<b>0,19</b>			

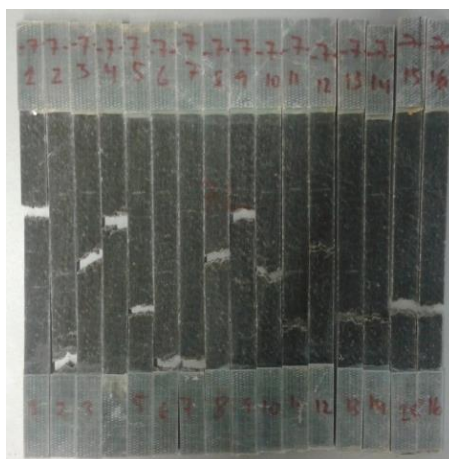
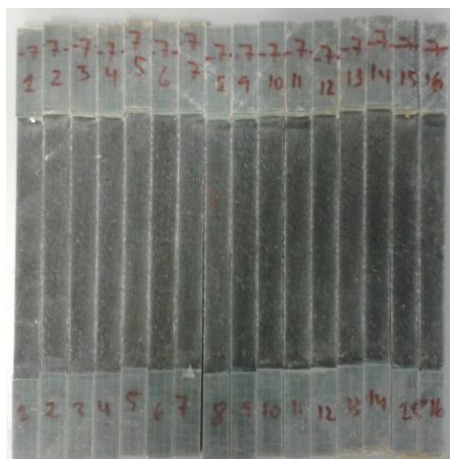
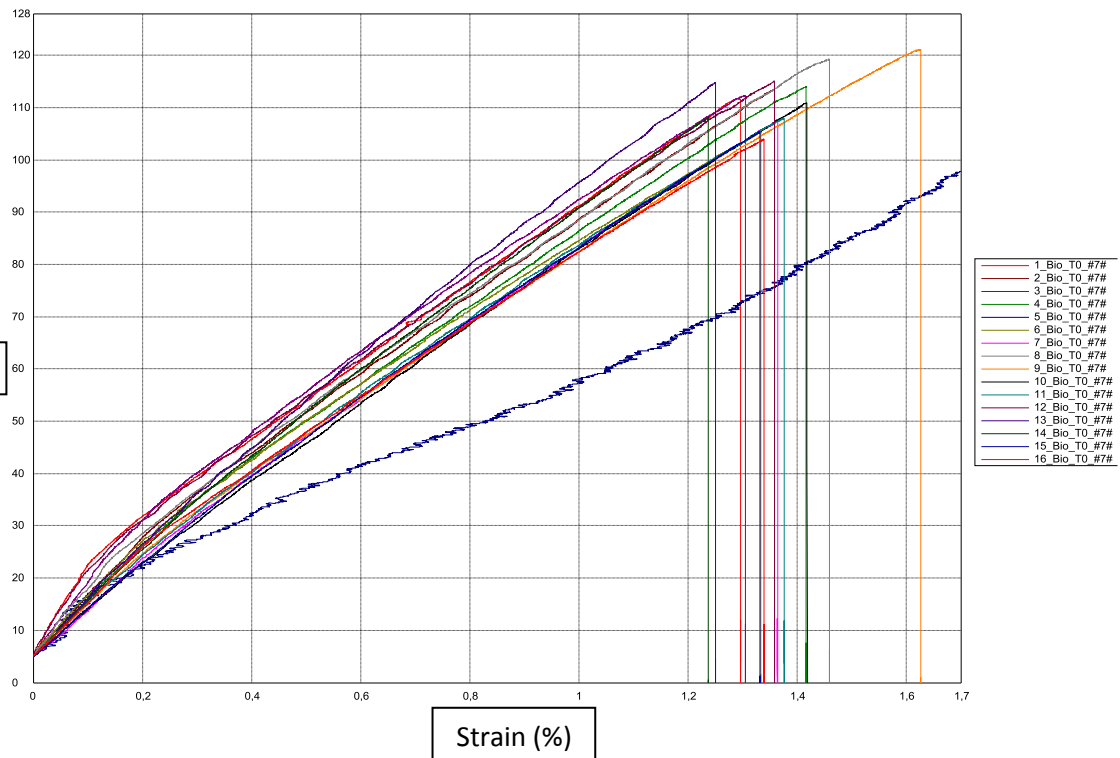




# Laminate 7\_Araldite LY 1569 /Aradur 3489-Biotex UD-NaOH 0,25M\_12h

## Laminate 7 Tensile 0° test

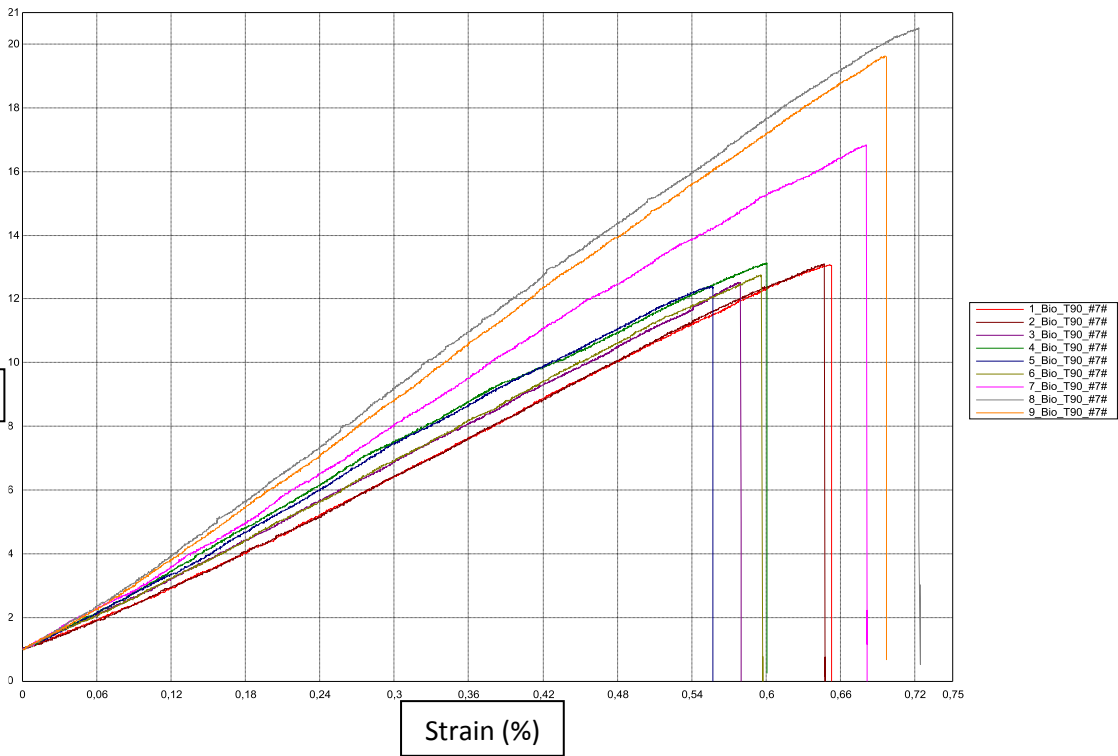
Sample	ID	Longitudinal tensile test							Failure mode	Vf	Mf		
		a mm	b mm	F kN	Ext Mpa	oxt Mpa	ext %	vxy		(%)	(%)		
1	1_Bio_TO_#7#	2,88	15,04	4,84	10291,10	111,78	1,30	0,34	Middle	24,8	31		
2	2_Bio_TO_#7#	3	15,05	5,12	10888,00	113,39	1,36	0,46	Tab				
3	3_Bio_TO_#7#	2,9	15,08	4,91	11765,40	112,32	1,31	0,31	Middle	Parameters	Value		
4	4_Bio_TO_#7#	2,97	15,04	5,09	10101,10	114,03	1,42	0,23	Middle				
5	6_Bio_TO_#7#	3,08	15,07	4,89	10025,30	105,34	1,33	0,31	Tab				
6	7_Bio_TO_#7#	2,75	15,15	4,48	9638,86	107,64	1,36		Tab				
7	8_Bio_TO_#7#	2,79	14,92	4,96	10185,40	119,26	1,46	0,23	Middle				
8	9_Bio_TO_#7#	2,84	14,94	5,14	9465,76	121,12	1,63	0,29	Middle				
9	10_Bio_TO_#7#	2,91	15,23	4,92	8618,24	110,93	1,42		Middle				
10	11_Bio_TO_#7#	2,94	15,23	4,84	8978,15	108,04	1,38		Bottom				
11	12_Bio_TO_#7#	3,03	14,98	5,22	10197,90	115,11	1,36	0,33	Middle				
12	13_Bio_TO_#7#	2,91	15,2	5,08	10290,30	114,79	1,25		Bottom				
13	14_Bio_TO_#7#	3,03	14,98	4,91	9830,44	108,11	1,24	0,43	Bottom				
14	15_Bio_TO_#7#	3,09	15,08	4,91	8688,57	105,30	1,33	0,20	Bottom				
15	16_Bio_TO_#7#	3,15	14,99	4,91	10292,50	103,92	1,34	0,37	Bottom				
Average value		2,95	15,07	4,95	9950,47	111,41	1,37	0,32				Testing speed (mm/min)	2
Standard deviation				0,18	816,14	5,07	0,09	0,08				Extensometry	Video
CV(%)				0,04	0,08	0,05	0,07	0,25				Reference points	Stickers
Characteristic value					8261,27	100,91	1,17	0,15		Standard	EN ISO527-5		
										Precharge (kN)	5		
										Modulus (ε %)	0,05-0,25		



### Laminate 7 Tensile 90° test

Sample	ID	Transverse tensile test						Failure mode	Vf	Mf
		a mm	b mm	F kN	Eyt Mpa	oyt Mpa	eyt %		(%)	(%)
1	1_Bio_T90_#7#	3,06	23,71	0,95	1965,90	13,07	0,65	Middle	25,1	31,4
2	2_Bio_T90_#7#	2,94	24,89	0,96	1954,17	13,10	0,65	Bottom	Parameters	Value
3	3_Bio_T90_#7#	2,90	24,88	0,90	1995,96	12,51	0,58	Bottom		
4	4_Bio_T90_#7#	2,89	24,78	0,94	2244,50	13,13	0,60	Middle	Testing speed (mm/min)	2
5	5_Bio_T90_#7#	2,97	24,92	0,92	2157,22	12,39	0,56	Middle	Extensometry	Video
6	6_Bio_T90_#7#	2,97	24,75	0,94	2003,56	12,75	0,60	Middle	Reference points	Stickers
7	7_Bio_T90_#7#	2,85	24,84	1,19	2391,17	16,83	0,68	Middle	Norma	EN ISO527-5
8	8_Bio_T90_#7#	2,77	24,90	1,41	2819,02	20,50	0,72	Middle	Precharge (kN)	1
9	9_Bio_T90_#7#	2,93	24,69	1,42	2759,98	19,63	0,70	Middle	Modulus (ε %)	0,05-0,25
Average value		2,92	24,71	1,07	<b>2254,61</b>	14,88	0,64			
Standard deviation				0,21	336,48	3,23	0,06			
CV(%)				0,20	0,15	0,22	0,09			
Characteristic value					1516,60	<b>7,78</b>	<b>0,51</b>			

Stress (MPa)



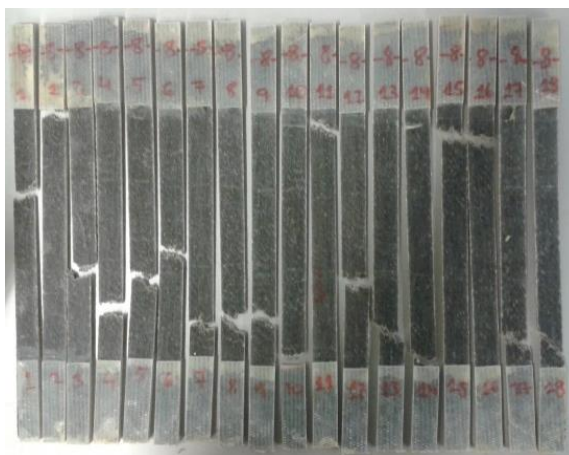
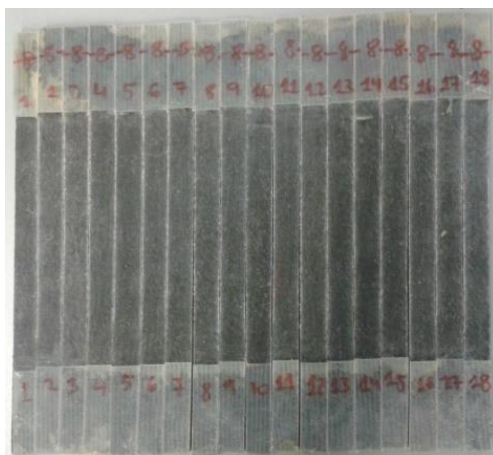
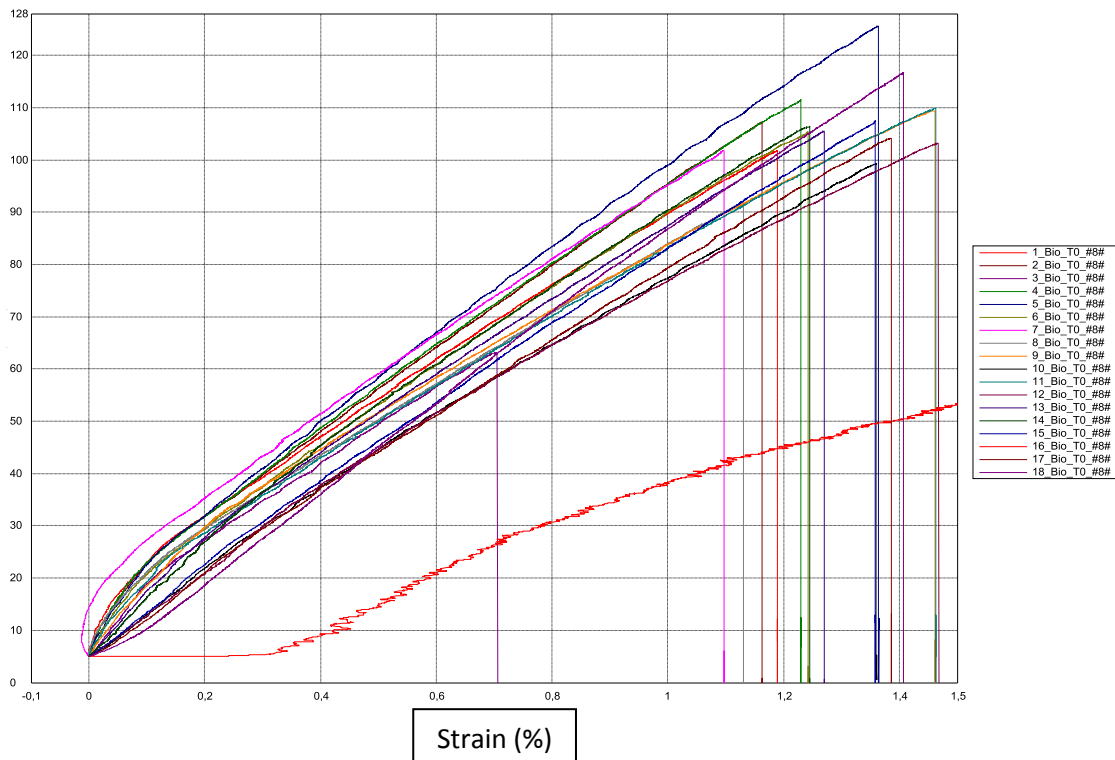
Strain (%)



# Laminate 8\_Araldite LY 1569 /Aradur 3489-Biotex UD-NaOH 0,25M\_24h

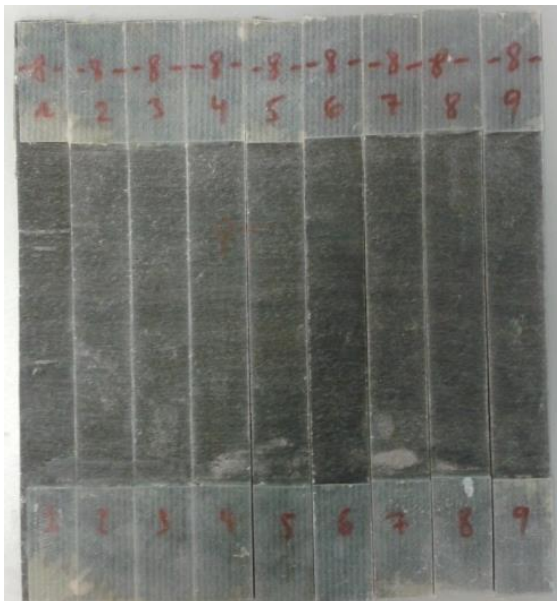
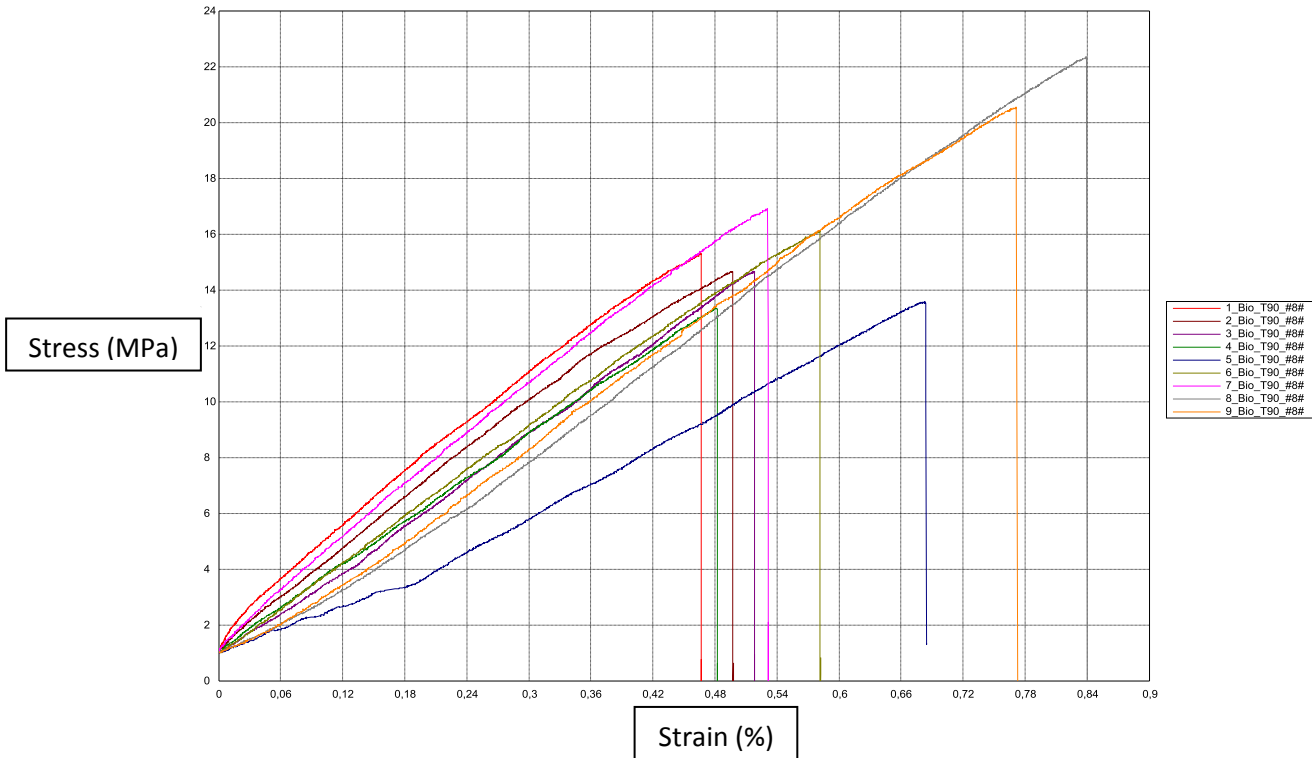
## Laminate 8 Tensile 0° test

Sample	ID	Longitudinal tensile test							Failure mode	Vf	Mf
		a mm	b mm	F kN	Ext Mpa	oxt Mpa	ext %	vxy		(%)	(%)
1	1 Bio_TO_#8#	2,85	13,61	3,95	9253,32	101,75	1,19		Middle	24,4	30,6
2	2 Bio_TO_#8#	3,00	14,69	4,72	9626,97	107,18	1,16	0,35	Tab		
3	4 Bio_TO_#8#	3,09	14,70	5,06	9581,84	111,47	1,23	0,26	Middle	Parameters	Value
4	5 Bio_TO_#8#	2,80	15,95	5,61	10214,9	125,58	1,36	0,26	Bottom		
5	6 Bio_TO_#8#	3,14	14,34	4,75	9309,13	105,38	1,24	0,40	Middle		
6	7 Bio_TO_#8#	2,96	15,11	4,55	8310,75	101,82	1,10	0,32	Bottom		
7	8 Bio_TO_#8#	3,05	14,88	4,18	8564,69	92,07	1,13	0,32	Bottom		
8	9 Bio_TO_#8#	2,95	14,79	4,78	10950,6	109,45	1,46	0,49	Bottom		
9	10 Bio_TO_#8#	2,91	15,06	4,35	8826,16	99,31	1,36		Tab		
10	11 Bio_TO_#8#	2,99	14,86	4,88	9204,06	109,91	1,46	0,25	Top		
11	12 Bio_TO_#8#	2,98	15,04	4,63	8028,1	103,25	1,47	0,40	Middle		
12	13 Bio_TO_#8#	3,22	15,22	5,17	10543,2	105,51	1,27	0,52	Bottom		
13	14 Bio_TO_#8#	3,18	14,88	5,03	10772,5	106,37	1,24	0,35	Tab		
14	15 Bio_TO_#8#	2,94	15,05	4,75	9221,03	107,44	1,36	0,31	Top		
15	17 Bio_TO_#8#	3,08	15,02	4,82	8883,35	104,15	1,39	0,26	Bottom		
16	18 Bio_TO_#8#	2,88	14,32	4,81	8337,81	116,63	1,41	0,24	Bottom		
Average value		3,00	14,85	4,75	<b>9351,78</b>	106,70	1,30	<b>0,34</b>		Testing speed (mm/min)	2
Standard deviation				0,39	890,60	7,46	0,12	0,09		Extensometry	Video
CV(%)				0,08	0,10	0,07	0,09	0,26		Reference points	Stickers
Characteristic value					7520,49	<b>91,36</b>	<b>1,05</b>	0,16		Standard	EN ISO527-5
										Precharge (kN)	5
										Modulus (ε %)	0,05-0,25



### Laminate 8 Tensile 90° test

Sample	ID	Transverse tensile test						Failure mode	Vf	Mf
		a	b	F	Eyt	oyt	eyt		(%)	(%)
		mm	mm	kN	Mpa	Mpa	%			
1	1_Bio_T90_#8#	2,97	23,64	1,07	3163,61	15,31	0,47	Top	24,6	30,8
2	2_Bio_T90_#8#	3,15	24,94	1,15	3004,76	14,66	0,50	Top	Parameters	Value
3	3_Bio_T90_#8#	3,08	24,93	1,12	2681,53	14,65	0,52	Top		
4	4_Bio_T90_#8#	3,11	25,10	1,04	2561,01	13,34	0,48	Top	Testing speed (mm/min)	2
5	5_Bio_T90_#8#	3,07	24,92	1,04	2116,07	13,58	0,68	Top	Extensometry	Video
6	6_Bio_T90_#8#	2,82	24,88	1,13	2779,44	16,10	0,58	Bottom	Reference points	Stickers
7	7_Bio_T90_#8#	2,90	24,84	1,22	3120,60	16,91	0,53	Bottom	Norma	EN ISO527-5
8	8_Bio_T90_#8#	2,78	24,83	1,54	2604,24	22,33	0,84	Bottom	Precharge (kN)	1
9	9_Bio_T90_#8#	2,90	24,87	1,48	2553,98	20,54	0,77	Middle	Modulus (ε %)	0,05-0,25
Average value		2,98	24,77	1,20	<b>2731,69</b>	16,38	0,60			
Standard deviation				0,19	330,36	3,11	0,14			
CV(%)				0,15	0,12	0,19	0,23			
Characteristic value					2007,10	<b>9,56</b>	<b>0,30</b>			

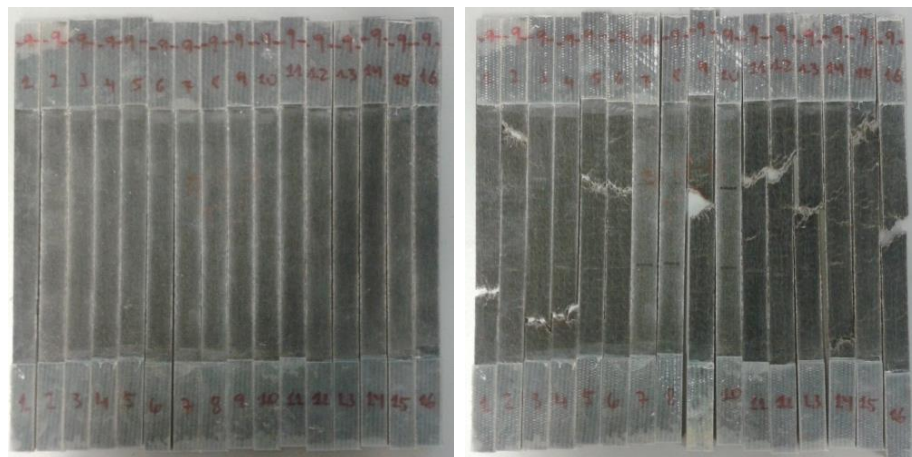
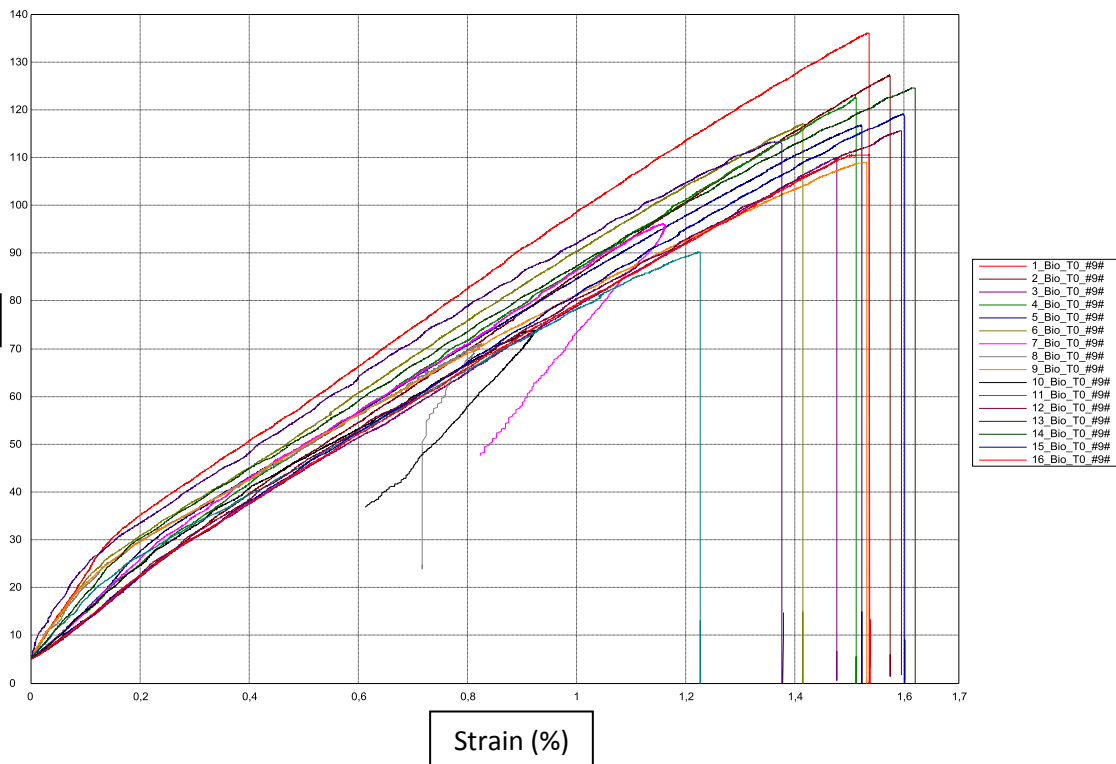




# Laminate 9\_Araldite LY 1569 /Aradur 3489-Biotex UD-NaOH 0,5M\_1h

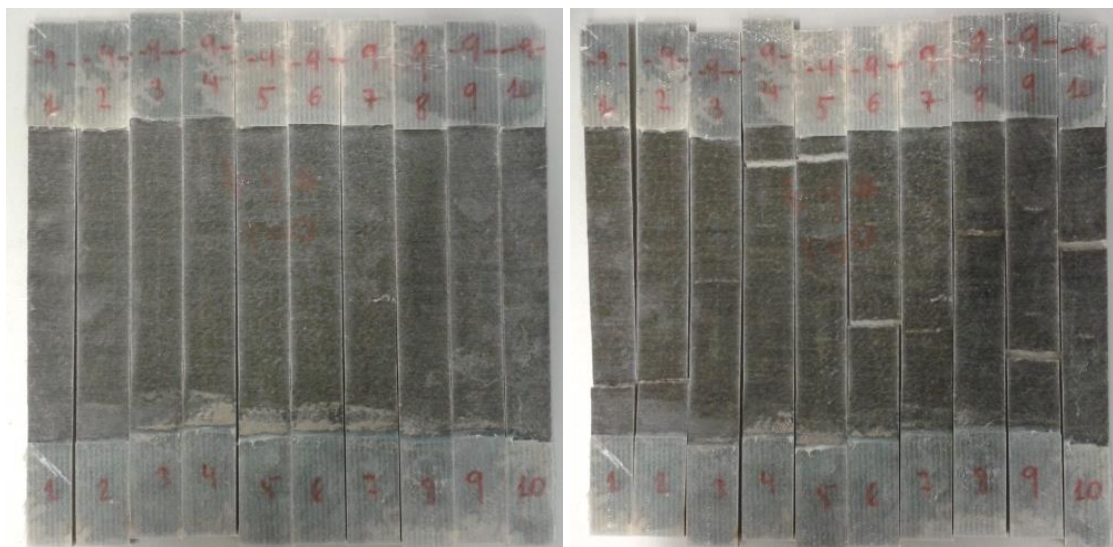
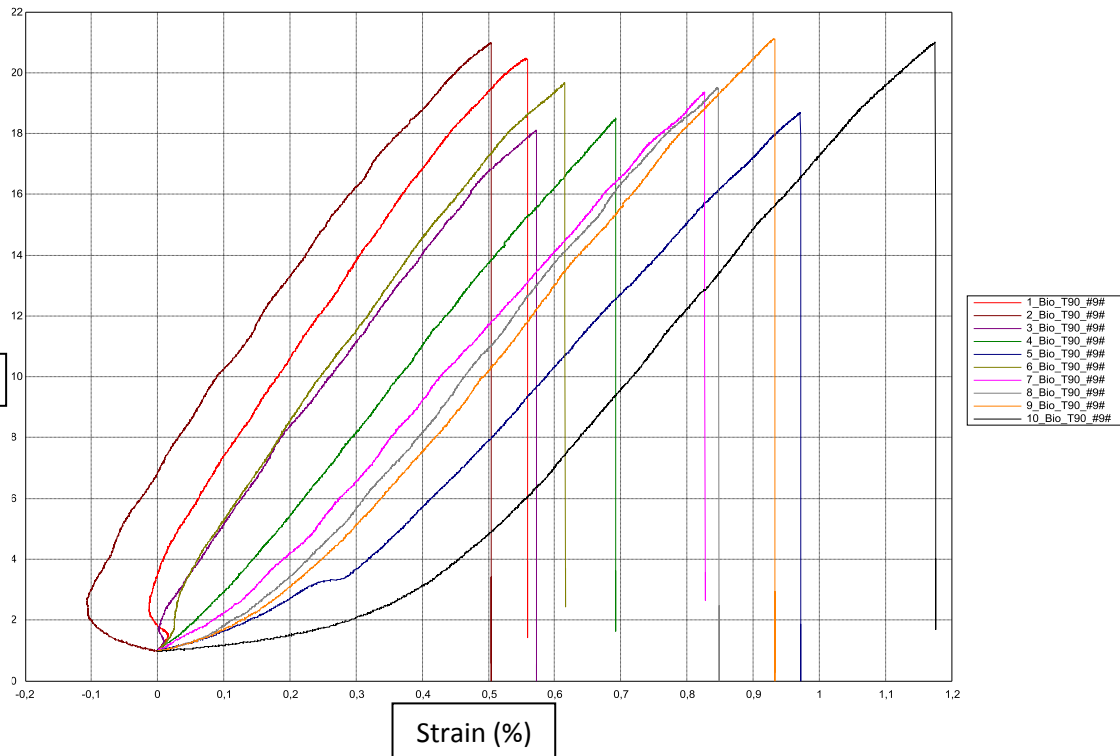
## Laminate 9 Tensile 0° test

Sample	ID	Longitudinal tensile test							Failure mode	Vf	Mf
		a mm	b mm	F kN	Ext Mpa	σxt Mpa	ext %	vxy		(%)	(%)
1	1_Bio_TO_#9#	2,62	14,20	5,06	12602,70	136,10	1,54		Middle	26,8	33,3
2	2_Bio_TO_#9#	2,75	15,05	5,26	9259,02	127,18	1,58	0,38			
3	3_Bio_TO_#9#	2,77	14,97	4,56	9191,33	109,97	1,48	0,35	Bottom	Parameters	Value
4	4_Bio_TO_#9#	2,67	15,01	4,91	10096,00	122,63	1,51	0,23	Bottom		
5	5_Bio_TO_#9#	2,75	15,20	4,88	11667,90	116,70	1,52	0,36	Middle		
6	6_Bio_TO_#9#	2,70	15,26	4,82	10190,30	117,02	1,42	0,43	Middle		
7	9_Bio_TO_#9#	2,80	15,08	4,60	9419,04	108,99	1,53	0,38	Middle	Testing speed (mm/min)	2
8	12_Bio_TO_#9#	2,70	15,00	4,68	9579,96	115,61	1,60	0,23	Middle	Extensometry	Video
9	13_Bio_TO_#9#	2,80	14,87	4,72	9905,71	113,29	1,38	0,33	Middle	Reference points	Stickers
10	14_Bio_TO_#9#	2,70	14,81	4,98	11389,80	124,59	1,62	0,33	Bottom	Standard	EN ISO527-5
11	15_Bio_TO_#9#	2,78	14,80	4,90	8913,33	119,06	1,60	0,38	Top	Precharge (kN)	5
12	16_Bio_TO_#9#	2,70	14,86	4,44	9069,00	110,58	1,54		Middle	Modulus (ε %)	0,05-0,25
Average value		2,73	14,93	4,82	10107,01	118,48	1,53	0,34			
Standard deviation				0,23	1174,31	8,01	0,07	0,06			
CV(%)				0,05	0,12	0,07	0,05	0,19			
Characteristic value					7617,63	101,49	1,37	0,20			



### Laminate 9 Tensile 90° test

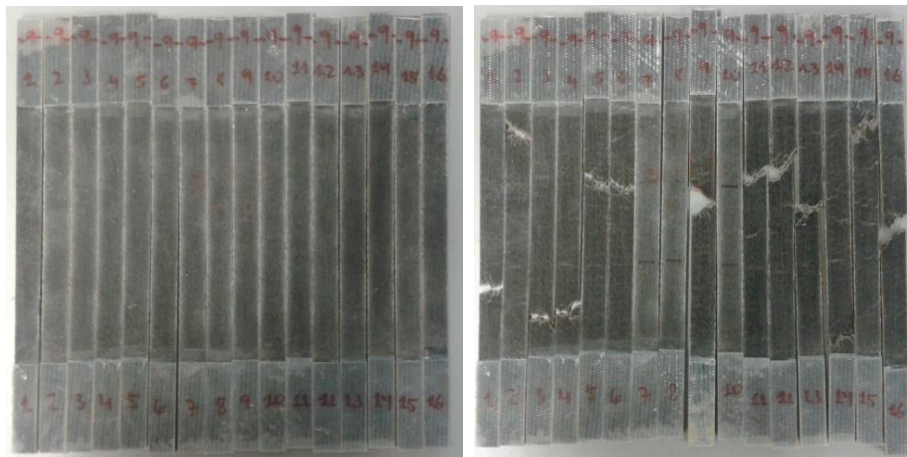
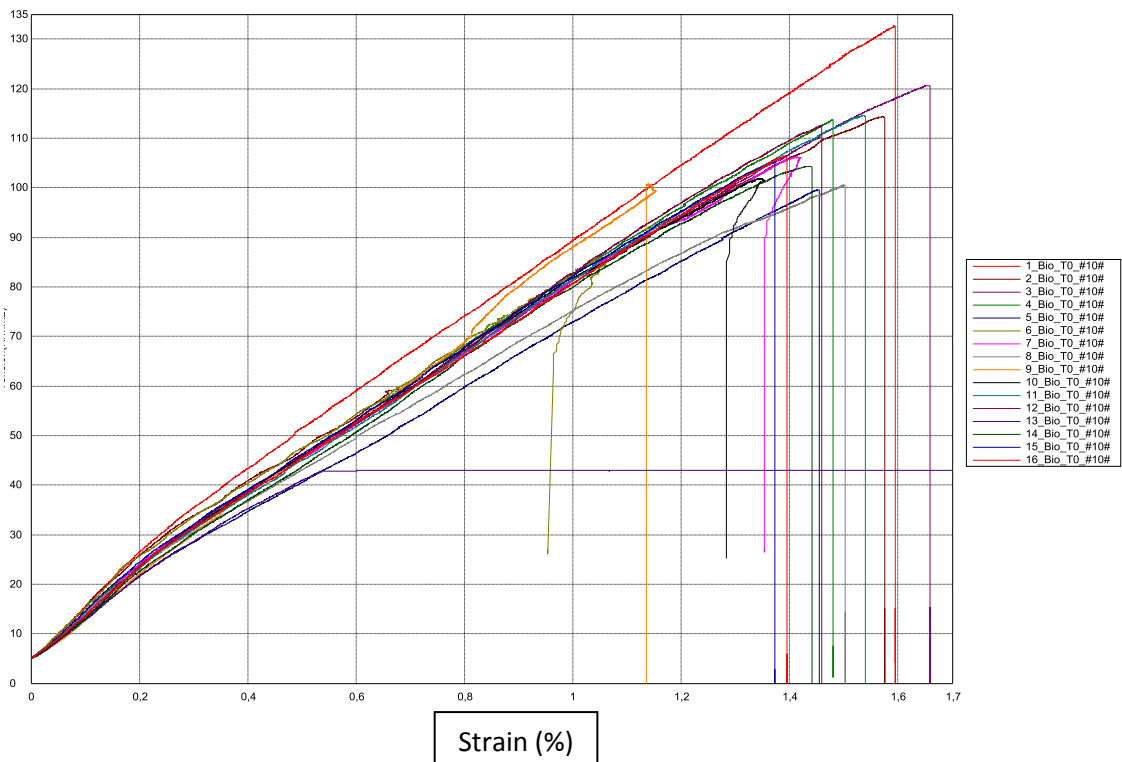
Sample	ID	Transverse tensile test						Failure mode	Vf	Mf
		a mm	b mm	F kN	Eyt Mpa	oyt Mpa	eyt %		(%)	(%)
1	1_Bio_T90_#9#	2,74	22,17	1,24	3290,28	20,48	0,56	Bottom	26,6	33,1
2	2_Bio_T90_#9#	2,68	25,14	1,41	3091,16	20,98	0,50	Bottom		
3	3_Bio_T90_#9#	2,77	25,07	1,26	3124,89	18,09	0,57	Middle	Parameters	Value
4	4_Bio_T90_#9#	2,92	25,12	1,36	2667,47	18,50	0,69	Top		
5	5_Bio_T90_#9#	2,86	25,12	1,34	2242,68	18,70	0,97	Top	Testing speed (mm/min)	2
6	6_Bio_T90_#9#	2,65	25,06	1,31	3252,59	19,68	0,62	Middle	Extensometry	Video
7	7_Bio_T90_#9#	2,71	25,15	1,32	2396,06	19,35	0,83	Middle	Reference points	Stickers
8	8_Bio_T90_#9#	2,70	24,96	1,32	2507,79	19,52	0,85	Middle	Norma	EN ISO527-5
9	9_Bio_T90_#9#	2,70	24,87	1,42	2543,20	21,11	0,93	Bottom	Precharge (kN)	1
10	10_Bio_T90_#9#	2,77	22,66	1,32	2435,95	21,01	1,18	Middle	Modulus (ε %)	0,05-0,25
Average value		2,75	24,53	1,33	2755,21	19,74	0,77			
Standard deviation				0,06	393,09	1,11	0,22			
CV(%)				0,04	0,14	0,06	0,28			
Characteristic value					1904,09	17,33	0,30			



# Laminate 10\_Araldite LY 1569 /Aradur 3489-Biotex UD-NaOH 0,5M\_3h

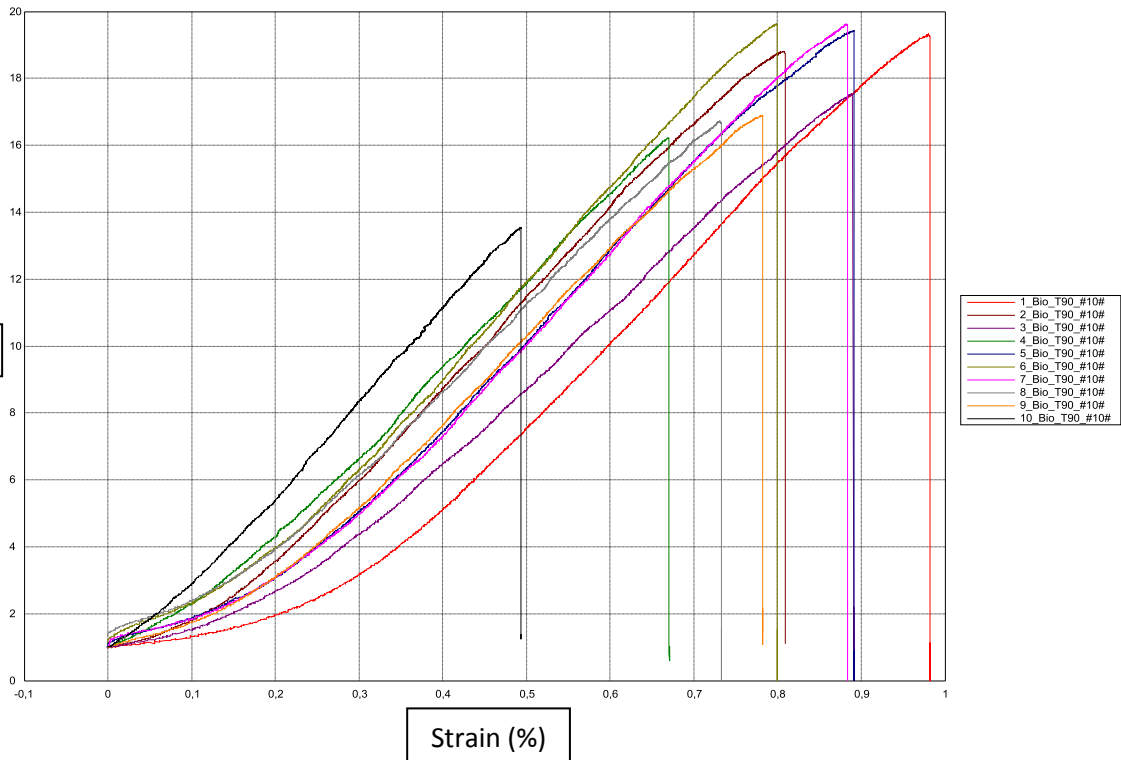
## Laminate 10 Tensile 0° test

Sample	ID	Longitudinal tensile test							Failure mode	Vf (%)	Mf (%)
		a mm	b mm	F kN	Ext Mpa	σxt Mpa	ext %	vxy			
1	1 Bio_TO_#10#	2,52	14,40	4,81	10783,80	132,61	1,59		Top	28	34,7
2	2 Bio_TO_#10#	2,68	15,03	4,61	10264,30	114,36	1,58		Middle		
3	3 Bio_TO_#10#	2,73	14,35	4,73	9367,06	120,63	1,66	0,29	Middle		
4	4 Bio_TO_#10#	2,67	15,13	4,59	9371,11	113,70	1,48	0,38	Tab	Parameters	Value
5	5 Bio_TO_#10#	2,70	15,05	4,05	8288,80	99,62	1,45	0,40	Top		
6	8 Bio_TO_#10#	2,61	14,96	3,93	8990,58	100,56	1,50	0,34	Bottom		
7	9 Bio_TO_#10#	2,58	14,94	3,88	9164,77	100,67	1,15	0,29	Top	Testing speed (mm/min)	2
8	11 Bio_TO_#10#	2,66	14,92	4,55	9529,20	114,57	1,54	0,33	Bottom	Extensometry	Video
9	12 Bio_TO_#10#	2,45	15,02	4,14	10042,40	112,50	1,46	0,30	Bottom	Reference points	Stickers
10	14 Bio_TO_#10#	2,58	14,88	4,01	9181,88	104,33	1,44		Middle	Standard	EN ISO527-5
11	15 Bio_TO_#10#	2,58	15,03	4,09	9730,35	105,44	1,37	0,33	Bottom	Precharge (kN)	5
12	16 Bio_TO_#10#	2,53	14,74	3,97	9578,73	106,42	1,39	0,41	Bottom	Modulus (ε %)	0,05-0,25
Average value		2,61	14,87	4,28	<b>9524,42</b>	110,45	1,47	<b>0,34</b>			
Standard deviation				0,35	643,42	9,68	0,13	0,04			
CV(%)				0,08	0,07	0,09	0,09	0,13			
Characteristic value					8160,46	<b>89,92</b>	<b>1,19</b>	0,24			



# Laminate 10 Tensile 90° test

Sample	ID	Transverse tensile test						Failure mode	Vf	Mf
		a mm	b mm	F kN	Eyt Mpa	oyt Mpa	eyt %		(%)	(%)
1	1_Bio_T90_#10#	2,54	24,10	1,18	2431,92	19,33	0,98	Bottom	27,7	34,3
2	2_Bio_T90_#10#	2,61	25,08	1,23	2524,89	18,82	0,81	Middle	Parameters	Value
3	3_Bio_T90_#10#	2,58	25,19	1,14	2385,04	17,55	0,89	Top		
4	4_Bio_T90_#10#	2,61	25,03	1,06	2483,01	16,23	0,67	Middle	Testing speed (mm/min)	2
5	5_Bio_T90_#10#	2,63	25,00	1,28	2578,59	19,42	0,89	Top	Extensometry	Video
6	6_Bio_T90_#10#	2,51	25,13	1,24	2661,60	19,64	0,80	Middle	Reference points	Stickers
7	7_Bio_T90_#10#	2,60	25,10	1,28	2533,97	19,62	0,88	Top	Norma	EN ISO527-5
8	8_Bio_T90_#10#	2,70	25,19	1,14	2418,49	16,72	0,73	Middle	Precharge (kN)	1
9	9_Bio_T90_#10#	2,80	25,11	1,19	2507,49	16,89	0,78	Bottom	Modulus (ε %)	0,05-0,25
10	10_Bio_T90_#10#	2,80	24,86	0,94	2542,77	13,53	0,49	Bottom		
Average value		2,64	24,98	1,17	2506,78	17,78	0,79			
Standard deviation				0,10	81,84	1,98	0,14			
CV(%)				0,09	0,03	0,11	0,17			
Characteristic value					2329,59	13,48	0,49			

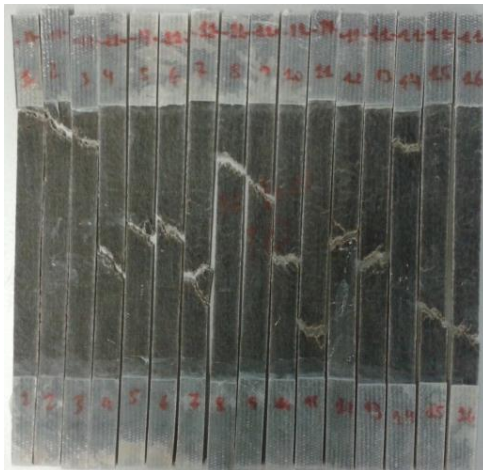
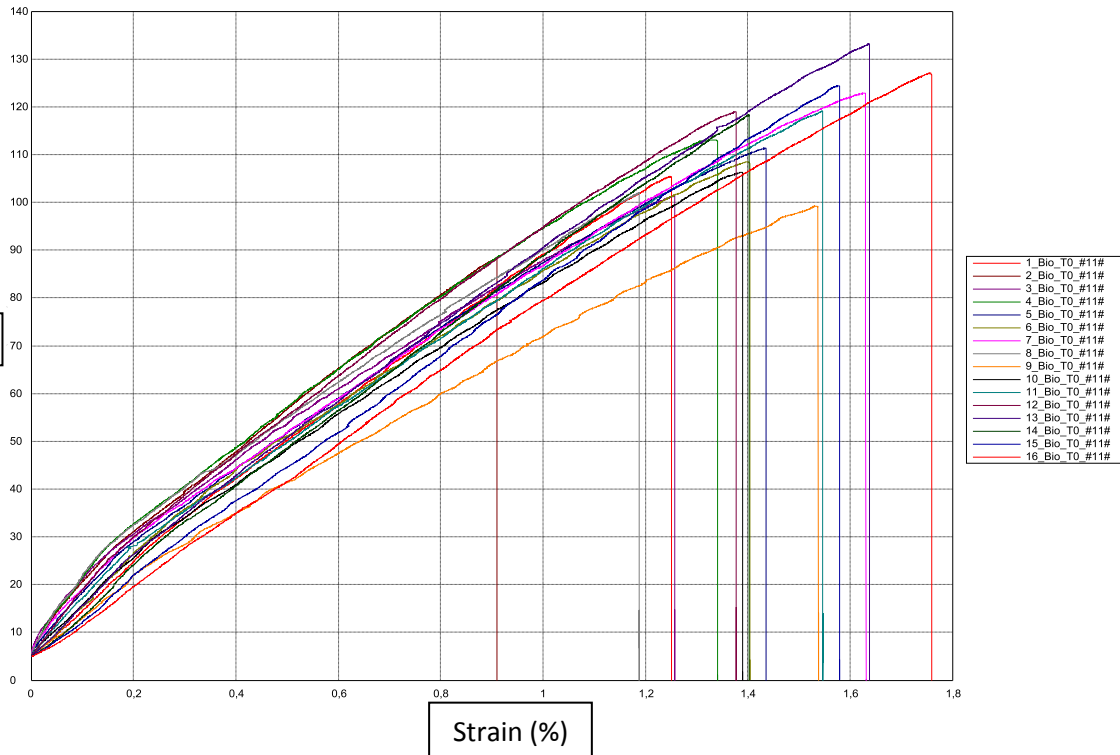




# Laminate 11\_Araldite LY 1569 /Aradur 3489-Biotex UD-NaOH 0,5M\_12h

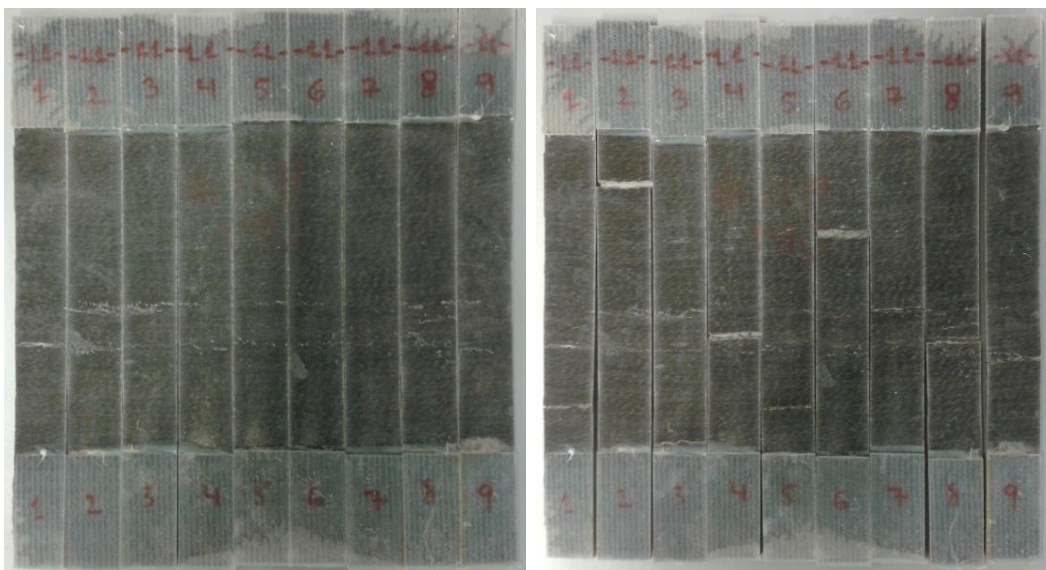
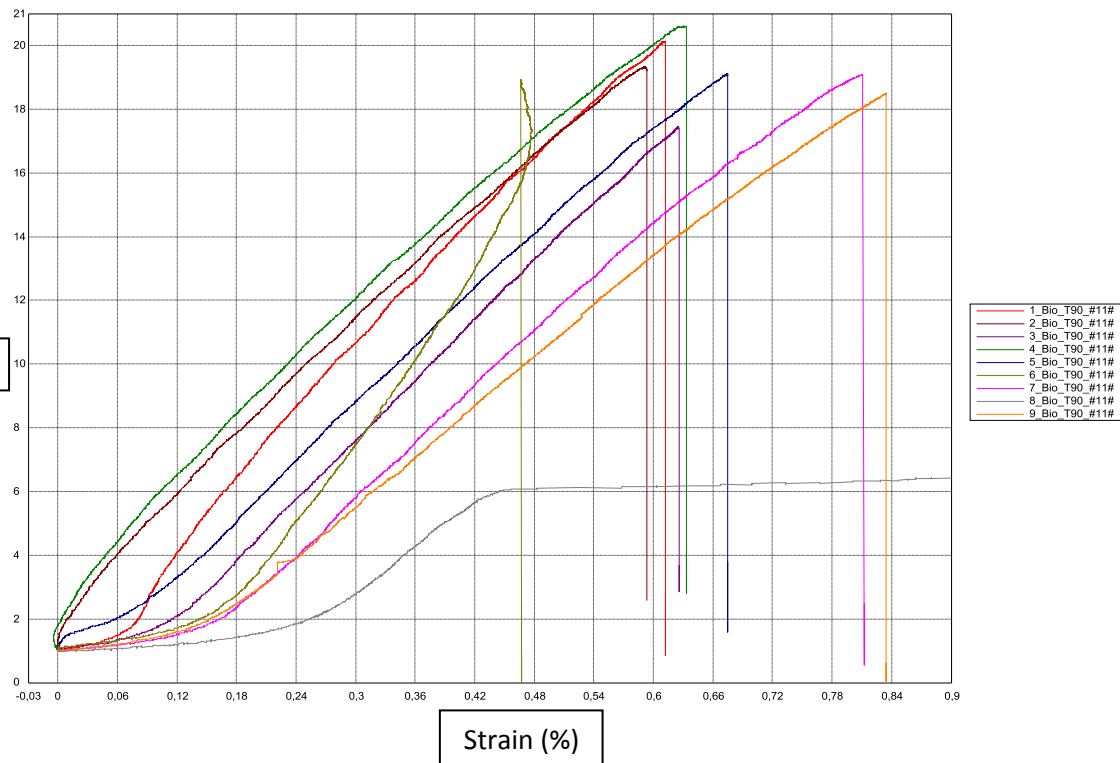
## Laminate 11 Tensile 0° test

Sample	ID	Longitudinal tensile test							Failure mode	Vf	Mf
		a mm	b mm	F kN	Ext Mpa	oxt Mpa	ext %	vxy		(%)	(%)
1	1 Bio_TO_#11#	2,55	14,33	3,85	10250,70	105,43	1,25		Tab	28,5	35,2
2	3 Bio_TO_#11#	2,69	14,69	4,00	9672,13	101,35	1,26	0,40	Top		
3	4 Bio_TO_#11#	2,53	14,71	4,21	11265,80	113,10	1,34	0,46	Middle		
4	5 Bio_TO_#11#	2,66	14,85	4,40	10422,60	111,41	1,44	0,32	Middle	Parameters	Value
5	6 Bio_TO_#11#	2,44	14,76	3,91	10827,80	108,51	1,40	0,46	Middle		
6	7 Bio_TO_#11#	2,44	14,38	4,31	10288,10	122,91	1,63		Middle		
7	8 Bio_TO_#11#	2,74	14,86	4,15	10740,00	102,02	1,19	0,52	Middle		
8	9 Bio_TO_#11#	2,84	14,92	4,21	8572,76	99,26	1,54	0,32	Middle		
9	10 Bio_TO_#11#	2,42	14,92	3,84	10059,60	106,35	1,39	0,39	Middle		
10	11 Bio_TO_#11#	2,60	14,97	4,64	10424,30	119,14	1,55	0,39	Bottom		
11	12 Bio_TO_#11#	2,60	15,01	4,64	11127,50	118,98	1,38	0,51	Middle		
12	13 Bio_TO_#11#	2,45	15,07	4,91	10554,80	133,12	1,64	0,53	Middle		
13	14 Bio_TO_#11#	2,47	14,92	4,36	10595,80	118,26	1,40	0,31	Top		
14	15 Bio_TO_#11#	2,45	14,94	4,55	9320,68	124,39	1,58	0,33	Middle		
15	16 Bio_TO_#11#	2,62	15,12	5,04	8130,86	127,11	1,76		Bottom		
Average value		2,57	14,83	4,34	<b>10150,23</b>	114,09	1,45	<b>0,41</b>		Testing speed (mm/min)	2
Standard deviation				0,37	887,95	10,30	0,16	0,08		Extensometry	Video
CV(%)				0,08	0,09	0,09	0,11	0,20		Reference points	Stickers
Characteristic value					8312,41	<b>92,78</b>	<b>1,11</b>	0,24		Standard	EN ISO527-5
										Precharge (kN)	5
										Modulus (ε %)	0,05-0,25



### Laminate 11 Tensile 90° test

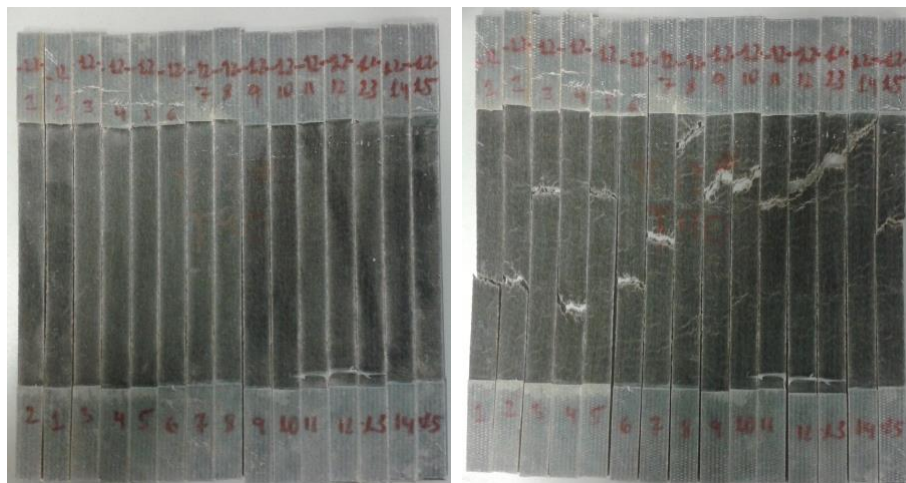
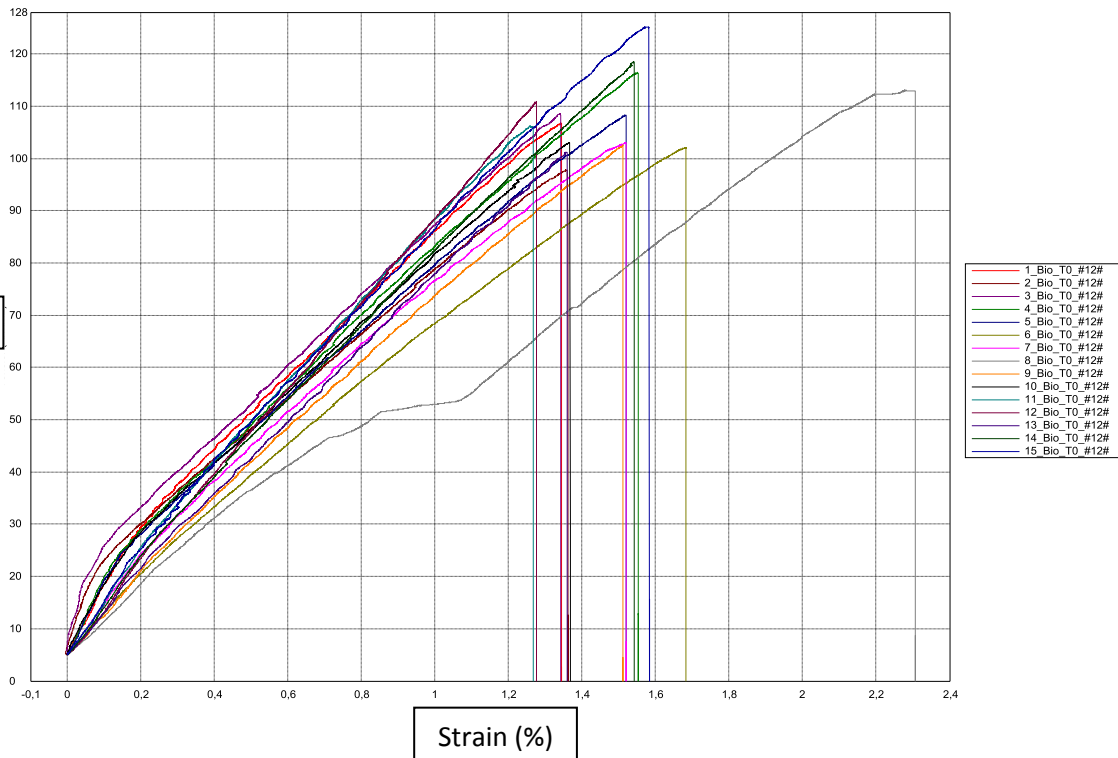
Sample	ID	Transverse tensile test						Failure mode	Vf	Mf
		a mm	b mm	F kN	Eyt Mpa	oyt Mpa	eyt %		(%)	(%)
1	1_Bio_T90_#11#	2,66	23,74	1,27	4100,54	20,13	0,61	Bottom	27,3	33,9
2	2_Bio_T90_#11#	2,69	25,06	1,30	3132,84	19,34	0,59	Top	Parameters	Value
3	3_Bio_T90_#11#	2,61	25,12	1,14	2919,23	17,44	0,63	Middle		
4	4_Bio_T90_#11#	2,60	25,11	1,35	3215,11	20,61	0,63	Middle	Testing speed (mm/min)	2
5	5_Bio_T90_#11#	2,69	25,06	1,29	2956,44	19,12	0,68	Bottom	Extensometry	Video
6	6_Bio_T90_#11#	2,72	25,00	1,29	4109,66	18,92	0,48	Middle	Reference points	Stickers
7	7_Bio_T90_#11#	2,64	25,14	1,27	2942,66	19,08	0,81	Middle	Norma	EN ISO527-5
8	8_Bio_T90_#11#	2,66	25,17	1,21		18,09		Middle	Precharge (kN)	1
9	9_Bio_T90_#11#	2,94	25,15	1,37	2468,98	18,49	0,83	Middle	Modulus (ε %)	0,05-0,25
Average value		2,69	24,95	1,28	<b>3230,68</b>	19,02	0,66			
Standard deviation				0,07	582,41	0,97	0,12			
CV(%)				0,05	0,18	0,05	0,18			
Characteristic value					1933,89	<b>16,89</b>	<b>0,40</b>			



# Laminate 12\_Araldite LY 1569 /Aradur 3489-Biotex UD-NaOH 0,5M\_24h

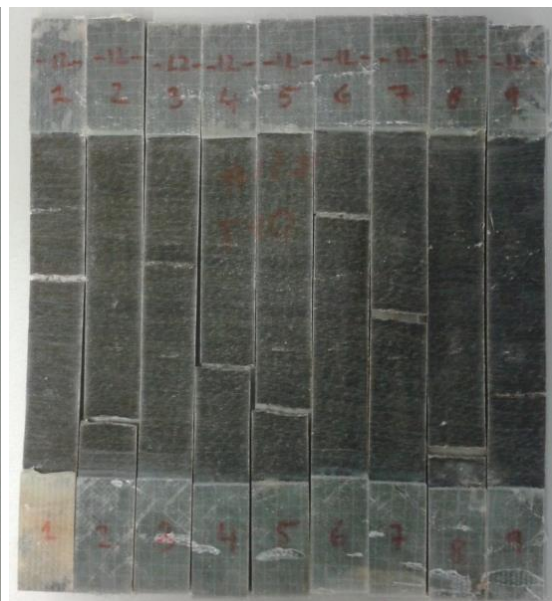
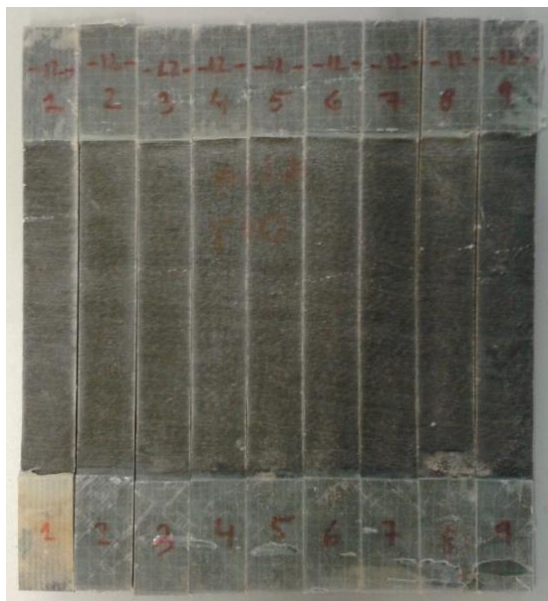
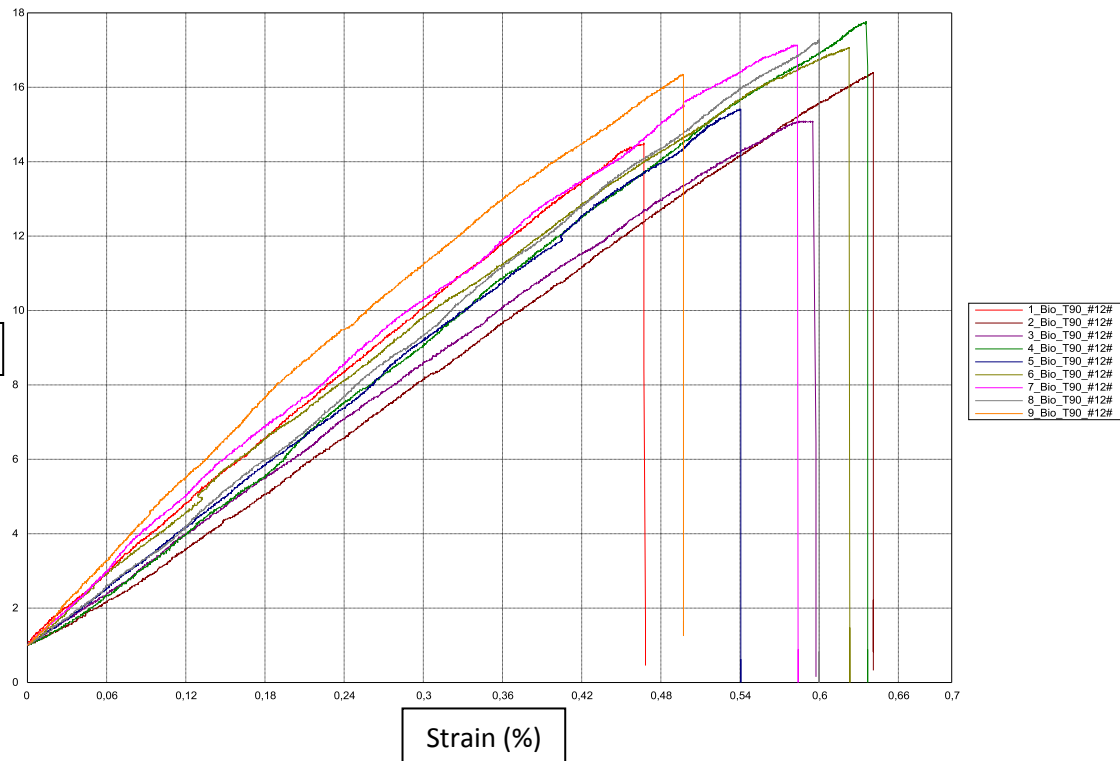
## Laminate 12 Tensile 0° test

Sample	ID	Longitudinal tensile test							Failure mode	Vf	Mf
		a mm	b mm	F kN	Ext Mpa	oxt Mpa	ext %	vxy		(%)	(%)
1	1 Bio_TO #12#	2,83	14,53	4,39	10926,90	106,72	1,34		Middle	26,8	33,3
2	2 Bio_TO #12#	3,07	14,74	4,43	7605,88	97,84	1,36	0,30	Middle		
3	3 Bio_TO #12#	2,68	15,15	4,41	8214,20	108,54	1,34	0,35	Middle		
4	4 Bio_TO #12#	2,63	15,95	4,88	9690,30	116,41	1,55	0,28	Middle	Parameters	Value
5	5 Bio_TO #12#	2,82	15,23	4,65	9522,93	108,33	1,52	0,33	Middle		
6	6 Bio_TO #12#	2,88	15,23	4,48	7544,60	102,05	1,68	0,45	Middle		
7	7 Bio_TO #12#	2,88	15,19	4,51	9181,14	103,05	1,52	0,25	Middle		
8	8 Bio_TO #12#	2,83	15,19	4,86	7259,32	113,14		0,25	Top		
9	9 Bio_TO #12#	2,61	15,16	4,06	8229,67	102,50	1,51	0,28	Middle		
10	10 Bio_TO #12#	2,56	15,3	4,04	9958,11	103,08	1,37	0,28	Middle		
11	11 Bio_TO #12#	2,44	15,23	3,95	10321,30	106,21	1,27	0,39	Middle		
12	12 Bio_TO #12#	2,47	15,29	4,19	9955,19	110,88	1,28	0,24	Middle		
13	13 Bio_TO #12#	2,78	15,23	4,29	8691,46	101,23	1,36	0,24	Top		
14	14 Bio_TO #12#	2,54	15,13	4,55	9697,92	118,50	1,54	0,27	Top		
15	15 Bio_TO #12#	2,54	15,28	4,86	9905,67	125,21	1,58	0,49	Middle		
Average value		2,70	15,19	4,44	<b>9113,64</b>	108,25	1,45	<b>0,31</b>			
Standard deviation				0,30	1120,69	7,46	0,13	0,08			
CV(%)				0,07	0,12	0,07	0,09	0,25			
Characteristic value					6794,10	<b>92,80</b>	<b>1,18</b>	0,15			
									Testing speed (mm/min)	2	
									Extensometry	Video	
									Reference points	Stickers	
									Standard	EN ISO527-5	
									Precharge (kN)	5	
									Modulus (ε %)	0,05-0,25	



### Laminate 12 Tensile 90° test

Sample	ID	Transverse tensile test						Failure mode	Vf	Mf
		a mm	b mm	F kN	Eyt Mpa	oyt Mpa	eyt %		(%)	(%)
1	1_Bio_T90_#12#	2,88	24,3	1,01	2986,58	14,48	0,47	Bottom	25,9	32,3
2	2_Bio_T90_#12#	3	25,46	1,25	2483,84	16,37	0,64	Top	Parameters	Value
3	3_Bio_T90_#12#	2,96	24,2	1,08	2589,97	15,09	0,60	Middle		
4	4_Bio_T90_#12#	2,7	24,7	1,18	2879,95	17,74	0,64	Middle	Testing speed (mm/min)	2
5	5_Bio_T90_#12#	2,89	24,96	1,11	2717,42	15,41	0,54	Bottom	Extensometry	Video
6	6_Bio_T90_#12#	2,82	24,95	1,20	2945,75	17,05	0,62	Middle	Reference points	Stickers
7	7_Bio_T90_#12#	2,68	24,96	1,15	3036,87	17,13	0,58	Middle	Norma	EN ISO527-5
8	8_Bio_T90_#12#	2,77	25,04	1,20	2855,23	17,26	0,60	Middle	Precharge (kN)	1
9	9_Bio_T90_#12#	2,79	25,43	1,16	3490,76	16,35	0,50	Middle	Modulus (ε %)	0,05-0,25
Average value		2,83	24,89	1,15	<b>2887,37</b>	16,32	0,58			
Standard deviation					0,07	291,75	1,11	0,06		
CV(%)					0,06	0,10	0,07	0,11		
Characteristic value					2247,47	<b>13,89</b>	<b>0,44</b>			

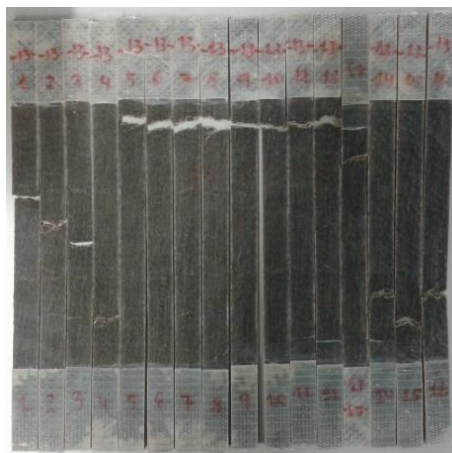
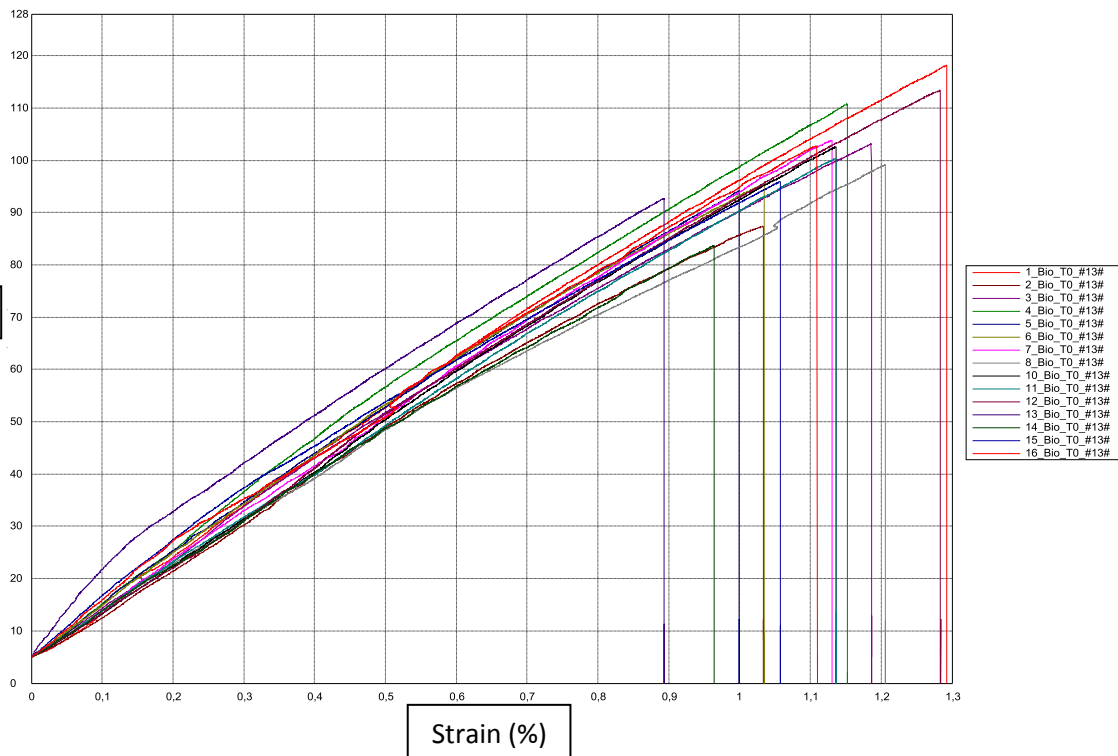




# Laminate 13\_Araldite LY 1569 /Aradur 3489-Biotex UD-NaOH 1M\_1h

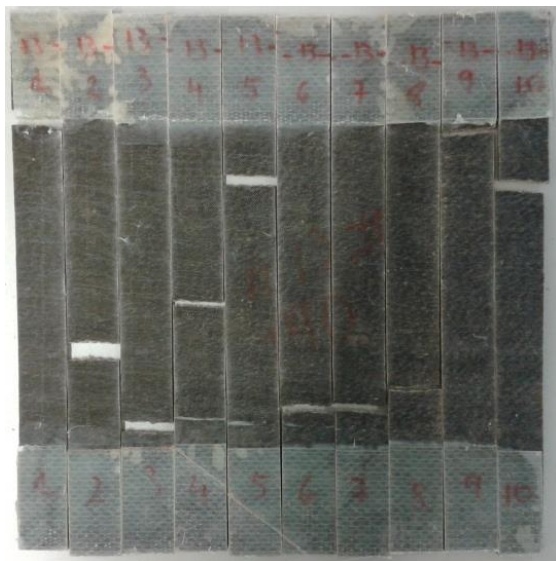
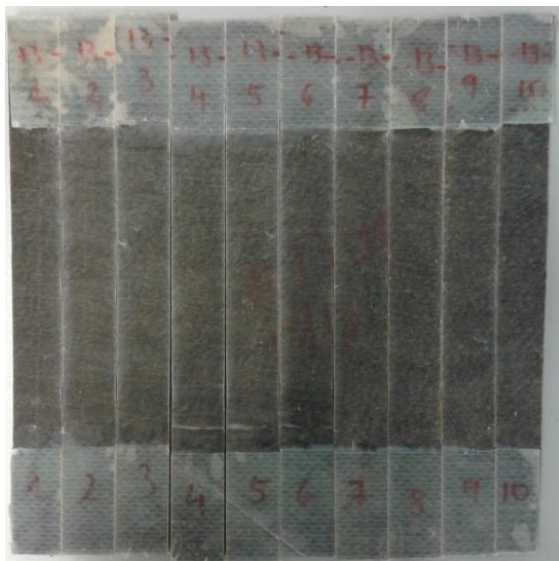
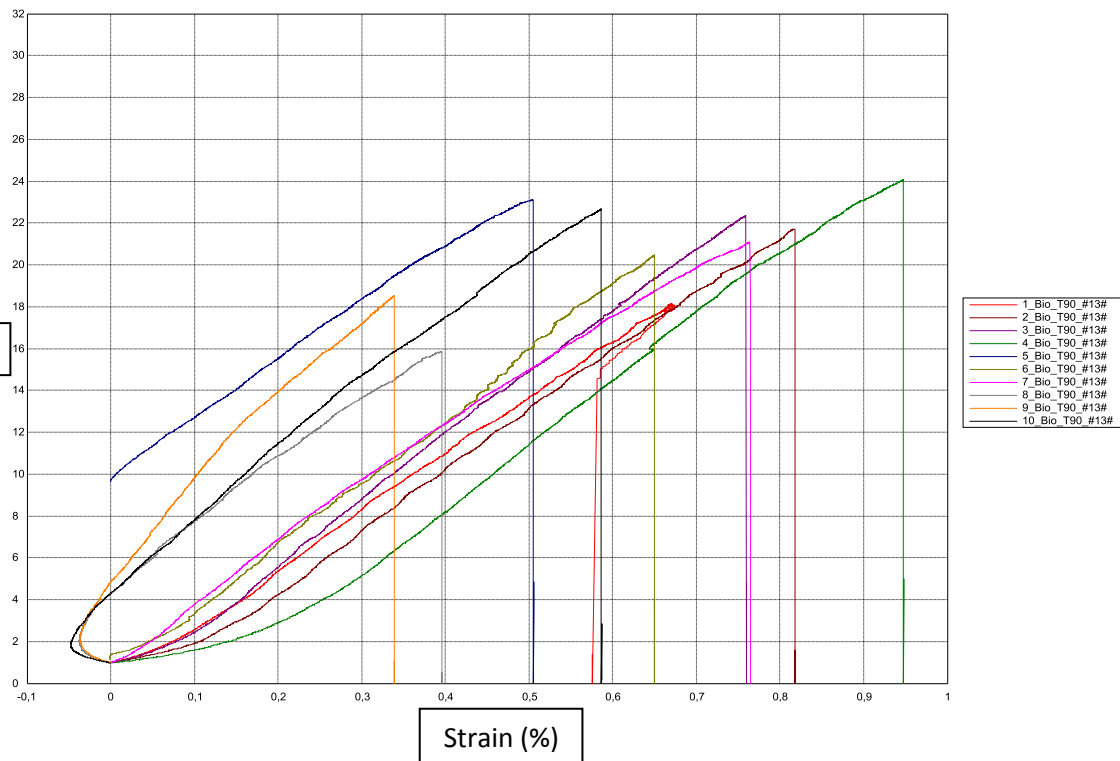
## Laminate 13 Tensile 0° test

Sample	ID	Longitudinal tensile test							Failure mode	Vf (%)	Mf (%)
		a mm	b mm	F kN	Ext Mpa	oxt Mpa	ext %	vxy			
1	1 Bio_TO_#13#	3,00	15,30	5,42	10581,00	118,18	1,29		Middle	23,6	29,6
2	2 Bio_TO_#13#	3,43	15,20	4,55	9275,18	87,36	1,03	0,42			
3	3 Bio_TO_#13#	3,16	15,26	4,97	10005,20	103,14	1,19		Middle		
4	4 Bio_TO_#13#	2,98	15,34	5,07	10949,40	110,84	1,15				
5	5 Bio_TO_#13#	3,15	15,40	4,57	10150,70	94,16	1,00	0,37	Bottom		
6	6 Bio_TO_#13#	3,20	15,25	4,66	9962,64	95,55	1,04				
7	7 Bio_TO_#13#	2,95	15,60	4,78	9741,82	103,80	1,13	0,27	Top		
8	8 Bio_TO_#13#	3,04	15,70	4,73	8906,97	99,12	1,21	0,29			
9	9 Bio_TO_#13#	3,29	15,66	4,71	10578,00	91,43		0,39	Top		
10	10 Bio_TO_#13#	2,96	15,23	4,63	9513,18	102,64	1,14				
11	11 Bio_TO_#13#	2,98	15,18	4,54	9249,89	100,33	1,14		Top		
12	12 Bio_TO_#13#	3,07	15,09	5,25	9534,47	113,40	1,28				
13	13 Bio_TO_#13#	2,98	15,20	4,20	10837,20	92,70	0,89		Top		
14	14 Bio_TO_#13#	3,08	15,12	3,90	8964,78	83,67	0,96	0,46			
15	15 Bio_TO_#13#	3,24	15,13	4,71	10791,90	95,98	1,06		Bottom		
16	16 Bio_TO_#13#	3,18	15,10	4,94	10767,50	102,79	1,11				
Average value		3,11	15,30	4,73	<b>9988,11</b>	99,69	1,11	<b>0,37</b>			
Standard deviation				0,37	701,75	9,27	0,11	0,07			
CV(%)				0,08	0,07	0,09	0,10	0,20			
Characteristic value					8545,15	<b>80,63</b>	<b>0,88</b>	0,20			
									Testing speed (mm/min)	2	
									Extensometry	Video	
									Reference points	Stickers	
									Standard	EN ISO527-5	
									Precharge (kN)	5	
									Modulus (ε %)	0,05-0,25	



### Laminate 13 Tensile 90° test

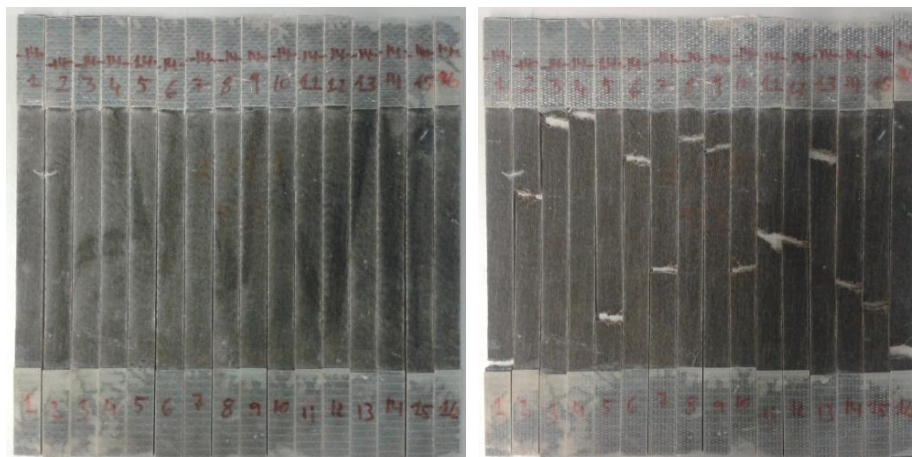
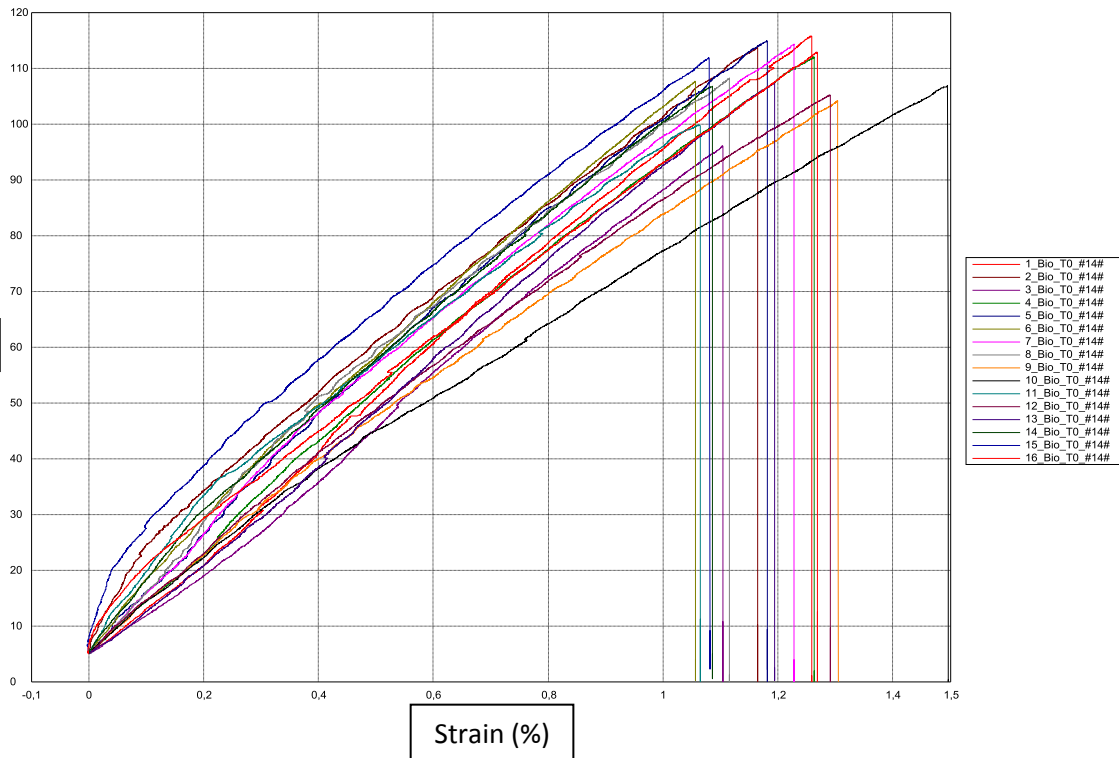
Sample	ID	Transverse tensile test						Failure mode	Vf	Mf
		a mm	b mm	F kN	Eyt Mpa	oyt Mpa	eyt %		(%)	(%)
1	1_Bio_T90_#13#	3,72	22,86	1,54	2839,04	18,16	0,67	Tab	22,3	28,1
2	2_Bio_T90_#13#	3,20	25,07	1,74	2833,20	21,72	0,82	Middle	Parameters	Value
3	3_Bio_T90_#13#	3,30	24,92	1,84	3059,49	22,35	0,76	Bottom		
4	4_Bio_T90_#13#	3,06	25,11	1,85	3067,19	24,06	0,95	Middle	Testing speed (mm/min)	2
5	5_Bio_T90_#13#	3,24	24,94	1,87	2826,85	23,13		Top	Extensometry	Video
6	6_Bio_T90_#13#	3,28	25,12	1,69	3263,50	20,45	0,65	Bottom	Reference points	Stickers
7	7_Bio_T90_#13#	3,40	25,14	1,80	3178,15	21,10	0,76	Bottom	Norma	EN ISO527-5
8	9_Bio_T90_#13#	3,25	24,98	1,51	3874,40	18,55		Tab	Precharge (kN)	1
9	10_Bio_T90_#13#	3,18	22,82	1,64	3535,07	22,65	0,58	Top	Modulus (ε %)	0,05-0,25
Average value		3,29	24,55	1,72	<b>3164,10</b>	21,35	0,74			
Standard deviation				0,13	353,81	2,01	0,12			
CV(%)				0,08	0,11	0,09	0,16			
Characteristic value					2388,07	<b>16,95</b>	<b>0,47</b>			



# Laminate 14\_Araldite LY 1569 /Aradur 3489-Biotex UD-NaOH 1M\_3h

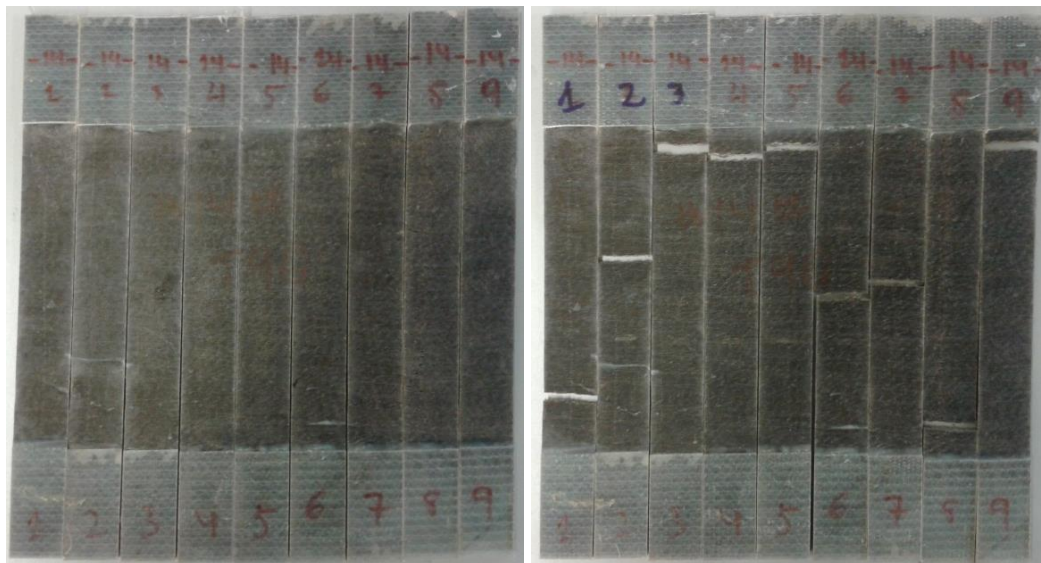
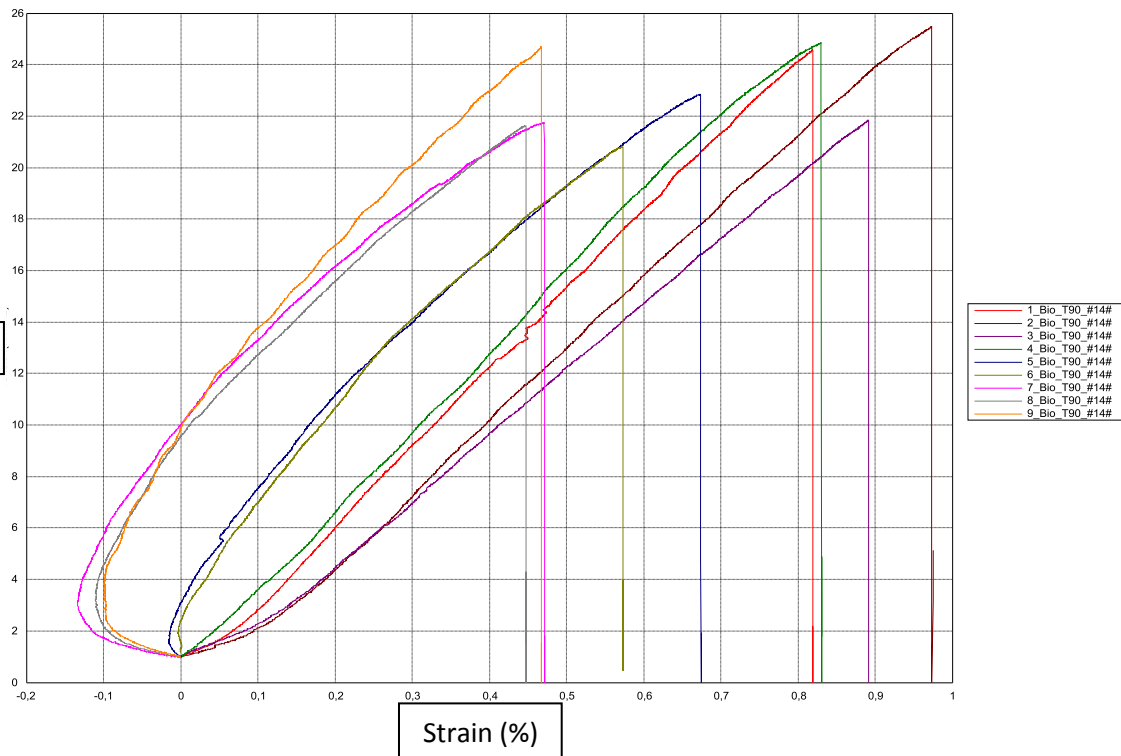
## Laminate 14 Tensile 0° test

Sample	ID	Longitudinal tensile test							Failure mode	Vf (%)	Mf (%)
		a mm	b mm	F kN	Ext Mpa	oxt Mpa	ext %	vxy			
1	1 Bio_TO_#14#	3,28	15,22	5,78	8303,93	115,72	1,26	0,34	Tab	23	28,9
2	2 Bio_TO_#14#	3,35	15,05	5,73	10729,10	113,74	1,16	0,32	Middle		
3	3 Bio_TO_#14#	3,38	15,33	4,98	8399,13	96,03	1,10	0,25	Top		
4	4 Bio_TO_#14#	3,21	15,36	5,52	9561,48	111,97	1,26	0,33	Tab		
5	5 Bio_TO_#14#	3,26	15,38	5,76	10529,80	114,86	1,18	0,35	Middle		
6	6 Bio_TO_#14#	3,00	15,37	4,96	11246,10	107,64	1,06		Middle		
7	7 Bio_TO_#14#	3,18	15,38	5,59	10906,70	114,26	1,23		Middle		
8	8 Bio_TO_#14#	3,05	15,01	4,95	12360,80	108,19	1,12	0,28	Top		
9	9 Bio_TO_#14#	2,91	15,12	4,58	8577,66	104,11	1,30	0,26	Top		
10	10 Bio_TO_#14#	3,24	14,98	5,18	8267,36	106,81	1,50	0,32	Middle		
11	11 Bio_TO_#14#	3,38	15,22	5,13		99,82	1,06	0,28	Middle		
12	12 Bio_TO_#14#	3,26	15,28	5,24	8681,31	105,16	1,29		Middle		
13	13 Bio_TO_#14#	3,06	15,10	4,96	8718,33	107,34	1,19		Top		
14	14 Bio_TO_#14#	3,15	15,12	5,08	12140,20	106,67	1,09		Middle		
15	15 Bio_TO_#14#	3,18	15,08	5,36	11116,50	111,85	1,08	0,33	Middle		
16	16 Bio_TO_#14#	3,11	14,93	5,24	8792,14	112,85	1,27		Bottom		
Average value		3,19	15,18	5,25	<b>9888,70</b>	108,56	1,20	<b>0,30</b>			
Standard deviation				0,35	1461,39	5,57	0,12	0,04			
CV(%)				0,07	0,15	0,05	0,10	0,12			
Characteristic value					6864,02	<b>97,12</b>	<b>0,96</b>	0,23			



### Laminate 14 Tensile 90° test

Sample	ID	Transverse tensile test						Failure mode	Vf	Mf
		a mm	b mm	F kN	Eyt Mpa	oyt Mpa	eyt %		(%)	(%)
1	1_Bio_T90_#14#	3,25	25,03	2,00	3143,40	24,56	0,82	Bottom	23	28,9
2	2_Bio_T90_#14#	3,00	24,68	1,89	2824,21	25,49	0,97	Middle	Parameters	Value
3	3_Bio_T90_#14#	3,30	24,96	1,80	2596,01	21,85	0,89	Top		
4	4_Bio_T90_#14#	3,15	25,05	1,96	3093,05	24,84	0,83	Top	Testing speed (mm/min)	2
5	5_Bio_T90_#14#	3,28	25,11	1,88	3606,11	22,86	0,68	Top	Extensometry	Video
6	6_Bio_T90_#14#	3,26	24,97	1,69	3695,65	20,82	0,57	Middle	Reference points	Stickers
7	7_Bio_T90_#14#	3,08	25,00	1,67	3791,45	21,75	0,47	Middle	Norma	EN ISO527-5
8	8_Bio_T90_#14#	3,26	24,99	1,76	3844,45	21,64	0,45	Bottom	Precharge (kN)	1
9	9_Bio_T90_#14#	3,11	24,77	1,90	3809,36	24,71	0,47	Top	Modulus (ε %)	0,05-0,25
Average value		3,19	24,95	1,84	<b>3378,19</b>	23,17	0,68			
Standard deviation				0,11	471,96	1,74	0,20			
CV(%)				0,06	0,14	0,08	0,30			
Characteristic value					2343,03	<b>19,35</b>	<b>0,22</b>			

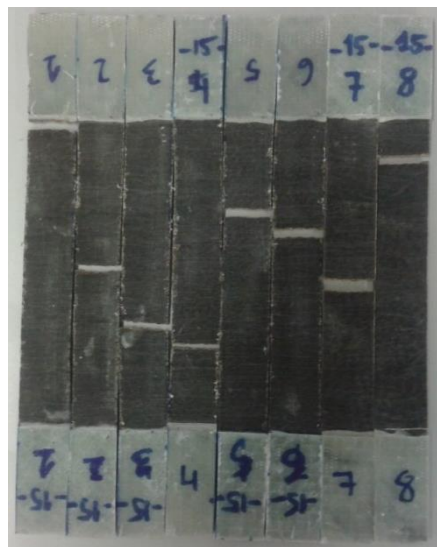
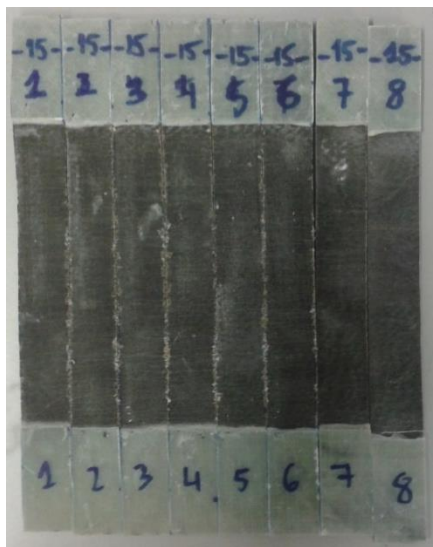
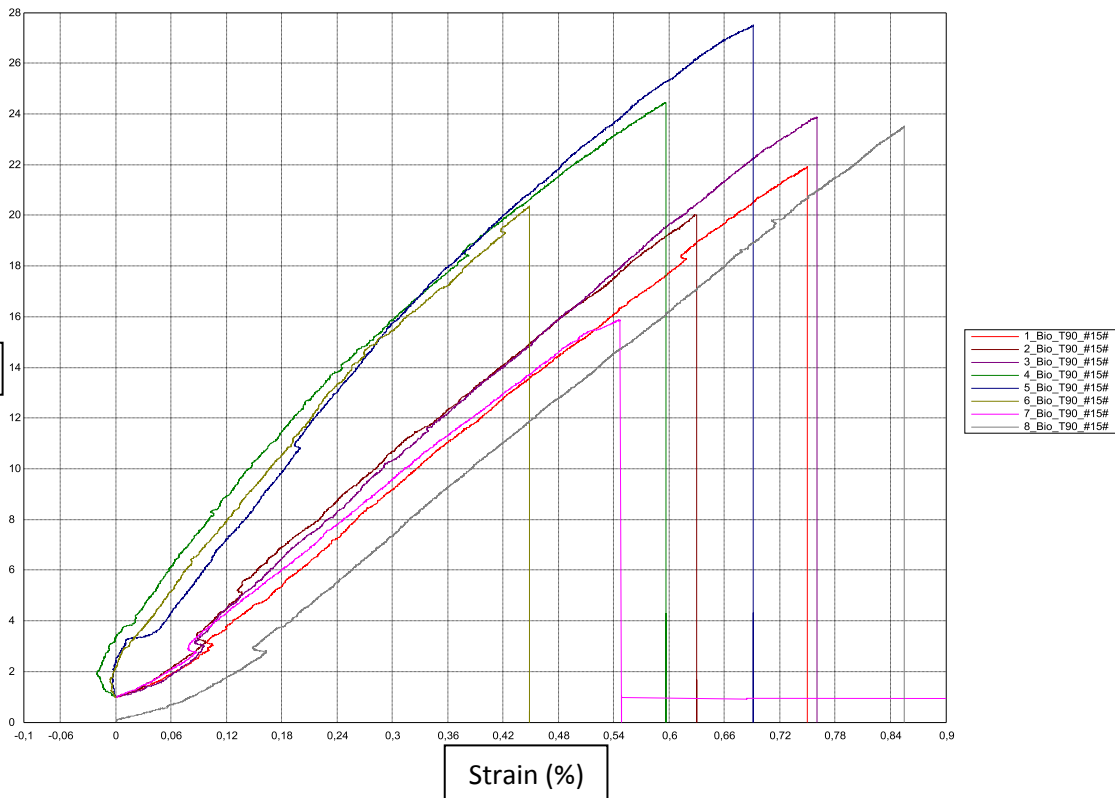






### Laminate 15 Tensile 90° test

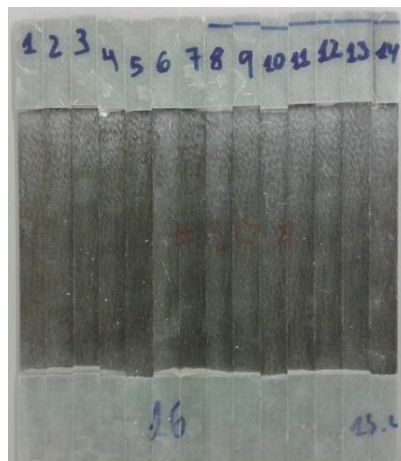
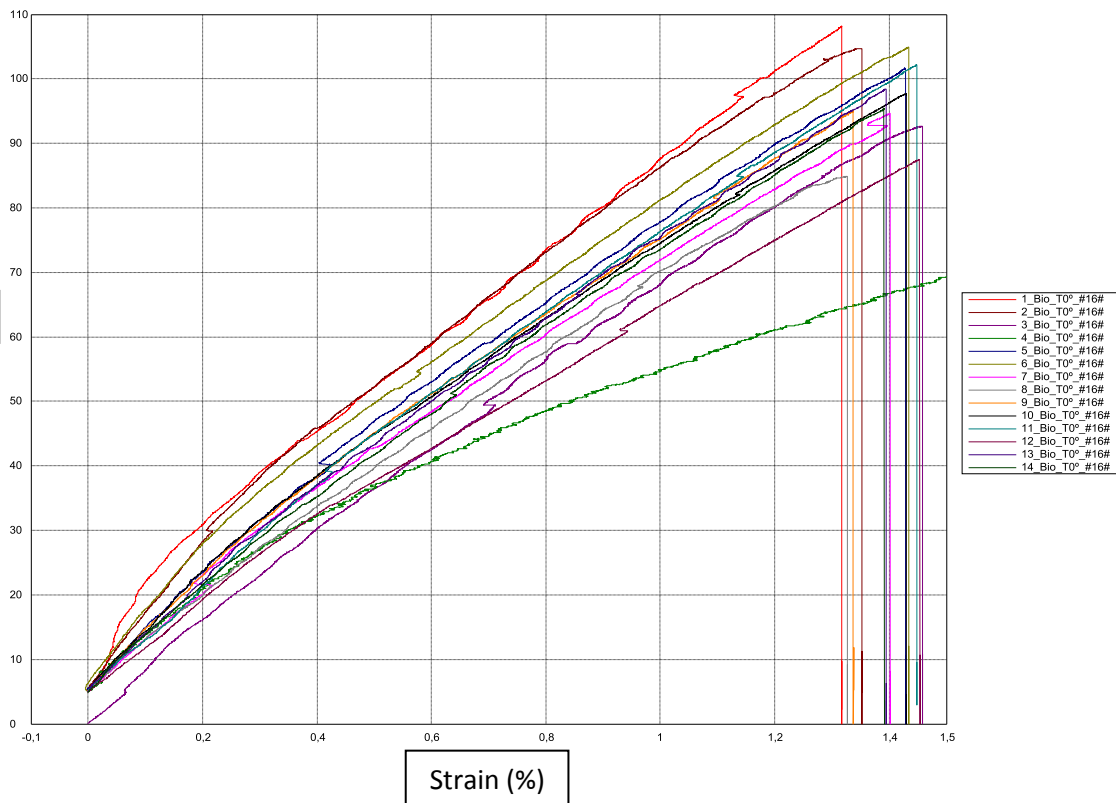
Sample	ID	Transverse tensile test						Failure mode	Vf	Mf
		a mm	b mm	F kN	Eyt Mpa	oyt Mpa	eyt %		(%)	(%)
1	1_Bio_T90_#15#	3,15	24,81	1,71	3007,81	21,91	0,75	Tab	24,2	30,3
2	2_Bio_T90_#15#	3,02	22,59	1,37	3736,34	20,03	0,63	Middle	Parameters	Value
3	3_Bio_T90_#15#	3,07	23,77	1,74	3600,49	23,88	0,76	Middle		
4	4_Bio_T90_#15#	2,97	24,05	1,75	4319,40	24,44	0,60	Middle	Testing speed (mm/min)	2
5	5_Bio_T90_#15#	2,82	23,72	1,84	4869,34	27,49	0,69	Middle	Extensometry	Video
6	6_Bio_T90_#15#	3,02	24,46	1,50	4466,06	20,36	0,45	Middle	Reference points	Stickers
7	7_Bio_T90_#15#	3,13	24,84	1,23	3104,42		0,55	Middle	Norma	EN ISO527-5
8	8_Bio_T90_#15#	3,08	25,03	1,81	2888,68	23,51	0,86	Top	Precharge (kN)	1
Average value		3,03	24,16	1,62	<b>3749,07</b>	23,09	0,66		Modulus (ε %)	0,05-0,25
Standard deviation				0,22	738,91	2,59	0,13			
CV(%)				0,14		0,11	0,20			
Characteristic value					2103,82	<b>17,22</b>	<b>0,37</b>			



# Laminate 16\_Araldite LY 1569 /Aradur 3489-Biotex UD-NaOH 1M\_24h

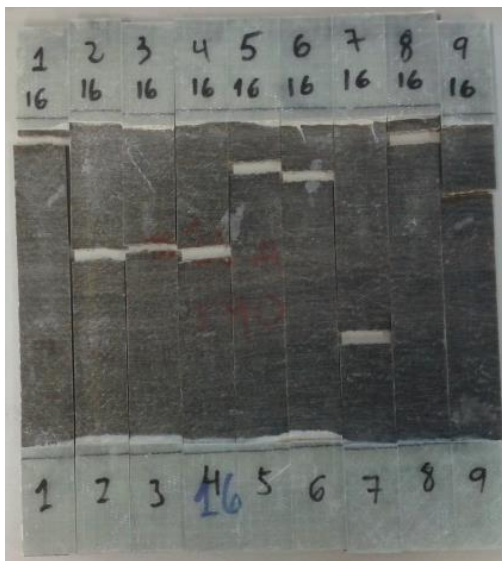
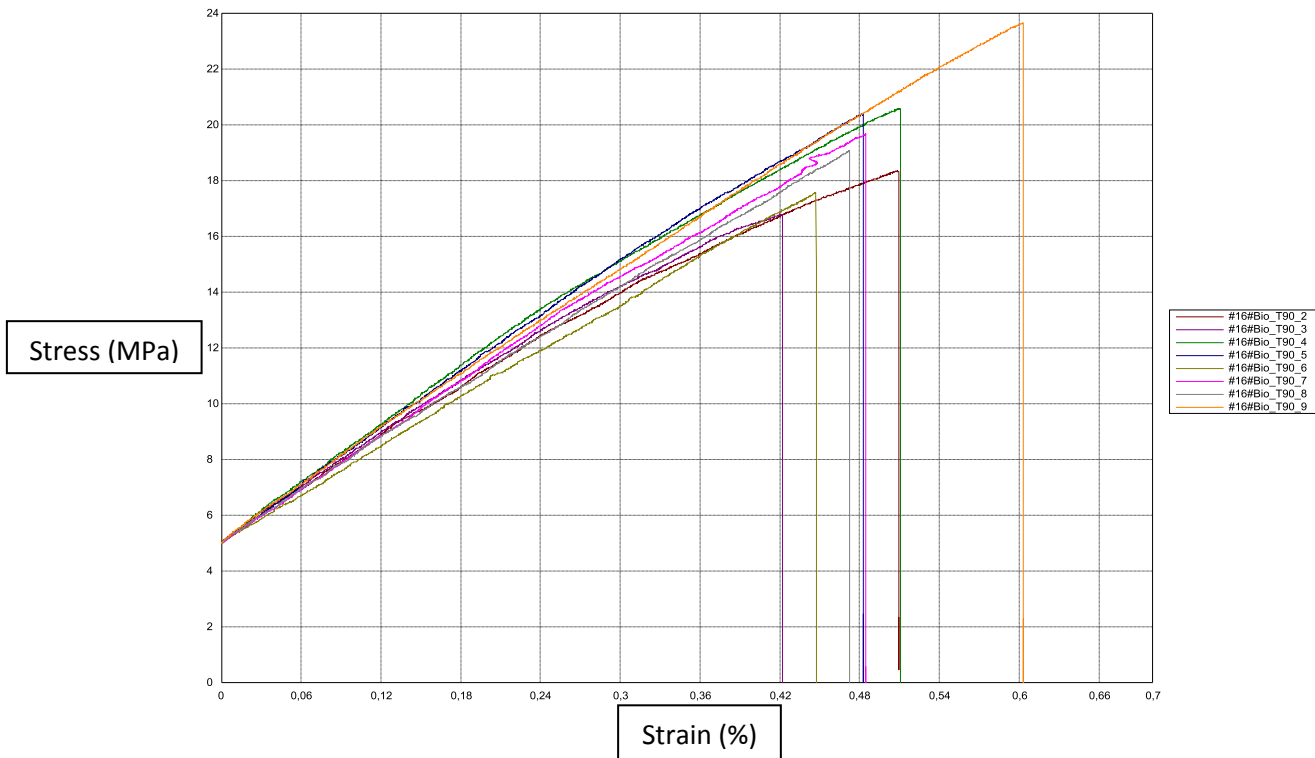
## Laminate 16 Tensile 0° test

Sample	ID	Longitudinal tensile test							Failure mode	Vf (%)	Mf (%)
		a (mm)	b (mm)	F (kN)	Ext (Mpa)	oxt (Mpa)	ext (%)	vxy			
1	1_Bio_TO° #16#	3,08	15,43	5,14	7060,92	108,13	1,32		Bottom	22,9	28,8
2	2_Bio_TO° #16#	3,10	15,46	5,02	11306,20	104,73	1,35	0,39	Bottom		
3	3_Bio_TO° #16#	3,19	14,98	4,43	8023,67	92,67	1,46	0,36	Middle		
4	4_Bio_TO° #16#	3,17	14,95	4,35	7021,02	91,88	2,52		Bottom		
5	5_Bio_TO° #16#	3,19	14,95	4,85	8917,43	101,63	1,43	0,40	Middle		
6	6_Bio_TO° #16#	2,99	15,05	4,72	10047,90	104,97	1,43		Middle		
7	7_Bio_TO° #16#	3,25	14,94	4,60	8815,23	94,67	1,40		Bottom		
8	8_Bio_TO° #16#	3,13	15,03	3,99	6907,00	84,89	1,33		Bottom		
9	9_Bio_TO° #16#	2,89	14,94	4,10	8611,93	95,01	1,34		Middle		
10	10_Bio_TO° #16#	3,00	15,10	4,42	9074,64	97,63	1,43	0,26	Bottom		
11	11_Bio_TO° #16#	3,46	15,00	5,30	8156,06	102,21	1,45	0,34	Middle		
12	12_Bio_TO° #16#	3,50	15,10	4,63	7410,13	87,54	1,45		Top		
13	13_Bio_TO° #16#	3,40	15,05	5,04	8309,74	98,45	1,39	0,36	Middle		
14	14_Bio_TO° #16#	3,40	14,97	4,85	7655,30	95,38	1,39	0,39	Middle		
Average value		3,20	15,07	4,67	8379,80	97,13	1,48	0,36		Testing speed (mm/min)	2
Standard deviation				0,39	1232,99	6,74	0,30	0,05		Extensometry	Video
CV(%)				0,08	0,15	0,07	0,21	0,14		Reference points	Stickers
Characteristic value					5809,45	83,07	0,85	0,24		Standard	EN ISO527-5
										Precharge (kN)	5
										Modulus (ε %)	0,05-0,25



### Laminate 16 Tensile 90° test

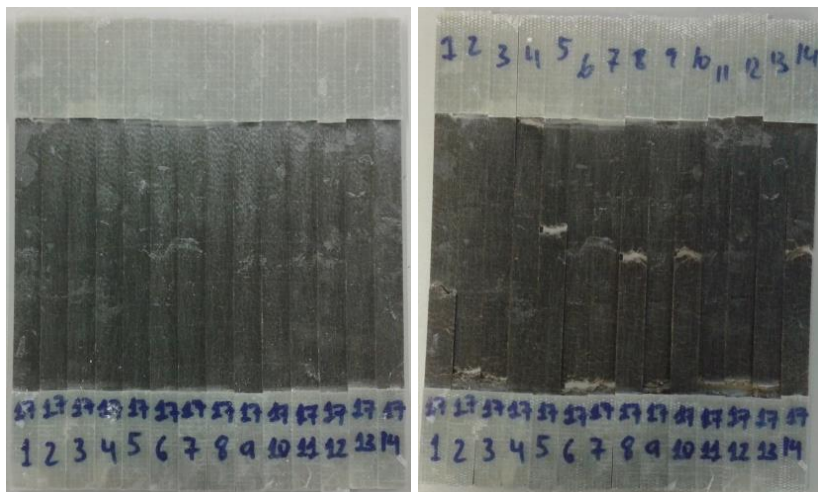
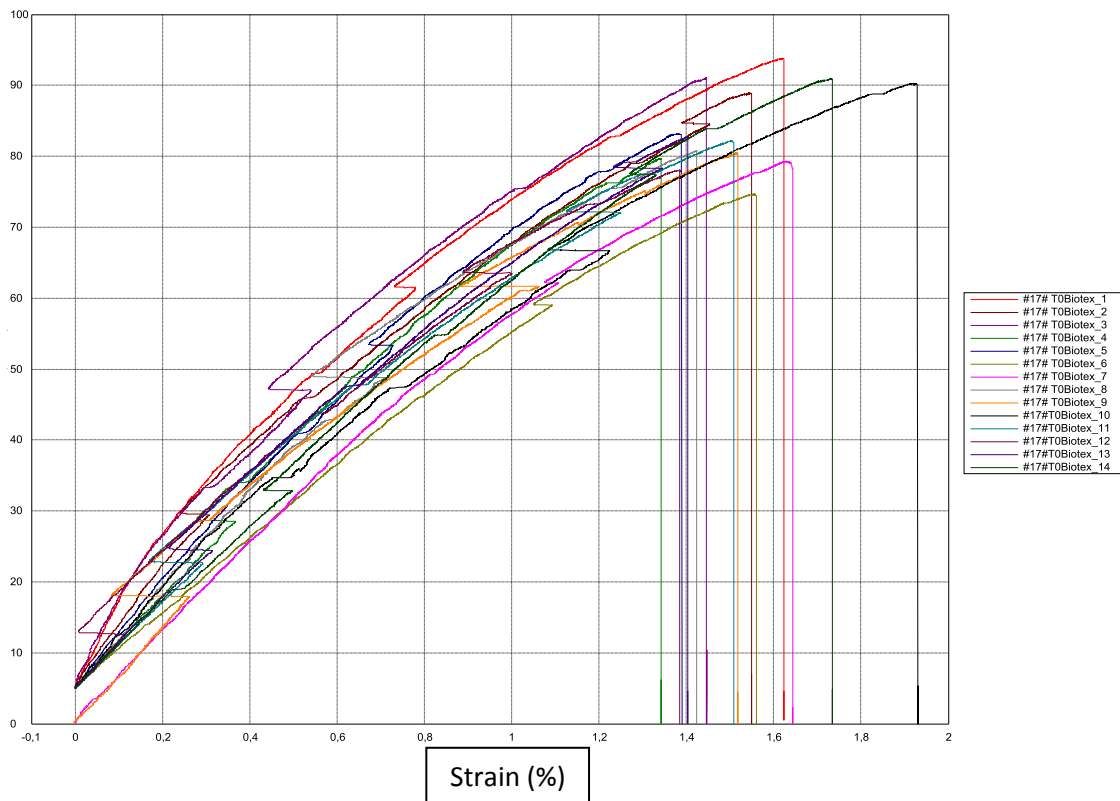
Sample	ID	Transverse tensile test						Failure mode	Vf	Mf
		a mm	b mm	F kN	Eyt Mpa	oyt Mpa	eyt %		(%)	(%)
1	1_Bio_T90_#16#	3,10	25,26					Top	22,6	28,5
2	2_Bio_T90_#16#	3,19	25,26	1,48	3015,66	18,34	0,51	Middle	Parameters	Value
3	3_Bio_T90_#16#	3,20	25,24	1,36	3090,58	16,78	0,42	Middle		
4	4_Bio_T90_#16#	3,25	25,30	1,69	3462,95	20,56	0,51	Middle	Testing speed (mm/min)	2
5	5_Bio_T90_#16#	3,14	25,32	1,62	3384,38	20,40	0,48	Top	Extensometry	Video
6	6_Bio_T90_#16#	3,60	25,30	1,60	2914,80	17,55	0,45	Top	Reference points	Stickers
7	7_Bio_T90_#16#	3,37	25,44	1,69	3282,63	19,66	0,48	Down	Norma	EN ISO527-5
8	8_Bio_T90_#16#	3,25	25,20	1,56	3035,85	19,05	0,47	Top	Precharge (kN)	1
9	9_Bio_T90_#16#	3,15	25,16	1,87	3256,58	23,65	0,60	Middle	Modulus (ε %)	0,05-0,25
Average value		3,25	25,28	1,61	<b>3180,43</b>	19,50	0,49			
Standard deviation				0,15	194,33	2,13	0,05			
CV(%)				0,10	0,06	0,11	0,11			
Characteristic value					2747,74	<b>14,75</b>	<b>0,37</b>			



# Laminate 17\_Araldite LY 1569 /Aradur 3489-Biotex UD-NaOH 1.5M\_1h

## Laminate 17 Tensile 0° test

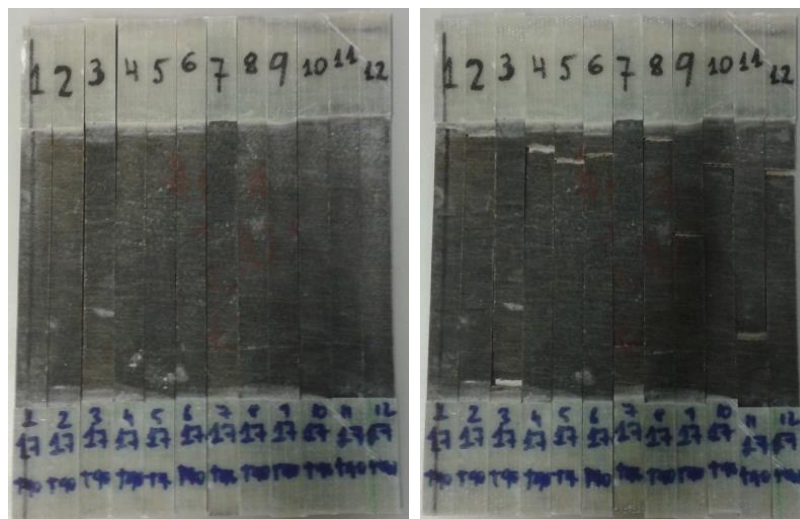
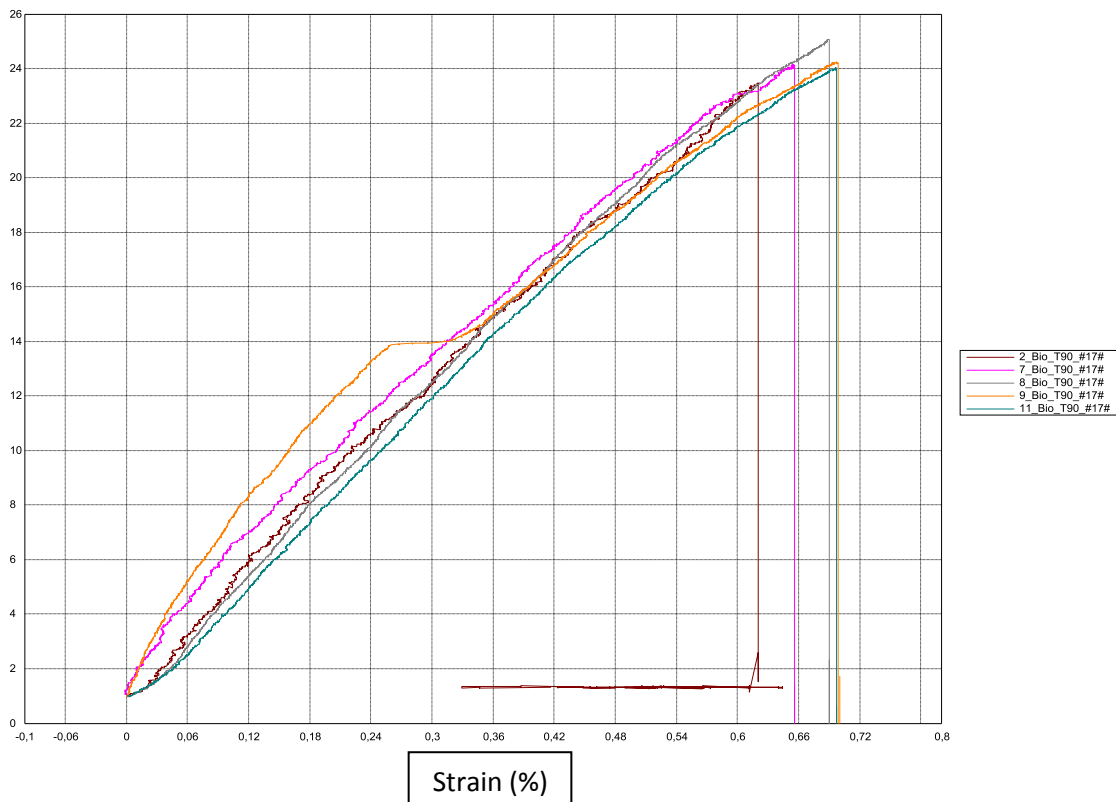
Sample	ID	Longitudinal tensile test							Failure mode	Vf	Mf		
		a mm	b mm	F kN	Ext Mpa	oxt Mpa	ext %	vxy		(%)	(%)		
1	1 Bio_TO_#17#	2,90	14,98	4,08	9685,35	93,84	1,62	0,58	Middle	23,8	29,9		
2	2 Bio_TO_#17#	3,00	15,07	4,02	8122,03	88,90	1,55	0,32	Bottom				
3	3 Bio_TO_#17#	2,94	15,08	4,04	9049,65	91,05	1,45	0,33	Bottom	Parameters	Value		
4	4 Bio_TO_#17#	3,05	15,00	3,64	6278,69	79,67	1,34		Top				
5	5 Bio_TO_#17#	2,90	14,96	3,61	7453,10	83,17	1,39		Middle				
6	6 Bio_TO_#17#	3,40	15,05	3,82		74,63	1,56	0,13	Bottom				
7	7 Bio_TO_#17#	3,17	15,04	3,78	6385,00	79,29	1,64		Bottom				
8	8 Bio_TO_#17#	3,16	15,00	3,83	7358,69	80,78	1,42	0,15	Middle				
9	9 Bio_TO_#17#	3,30	15,01	3,98	7011,46	80,45	1,52	0,31	Bottom				
10	10 Bio_TO_#17#	3,07	15,02	4,16	7054,89	90,26	1,93	0,19	Bottom				
11	11 Bio_TO_#17#	3,10	14,82	3,77	6001,73	82,13	1,51	0,23	Bottom				
12	12 Bio_TO_#17#	3,18	15,02	3,73	8385,84	78,02	1,39	0,54	Bottom				
13	13 Bio_TO_#17#	2,96	15,08	3,69	6221,25	82,70	1,40	0,35	Bottom				
14	14 Bio_TO_#17#	2,91	14,96	3,96	6170,84	90,92	1,73	x	Middle				
Average value		3,07	15,01	3,86	<b>7321,42</b>	83,99	1,53	<b>0,31</b>				Testing speed (mm/min)	2
Standard deviation				0,17	1182,33	5,89	0,16	0,17				Extensometry	Video
CV(%)				0,04		0,07	0,10	0,55		Reference points	Stickers		
Characteristic value					4837,07	<b>71,71</b>	<b>1,20</b>	-0,06		Standard	EN ISO527-5		
										Precharge (kN)	5		
										Modulus (ε %)	0,05-0,25		





### Laminate 17 Tensile 90° test

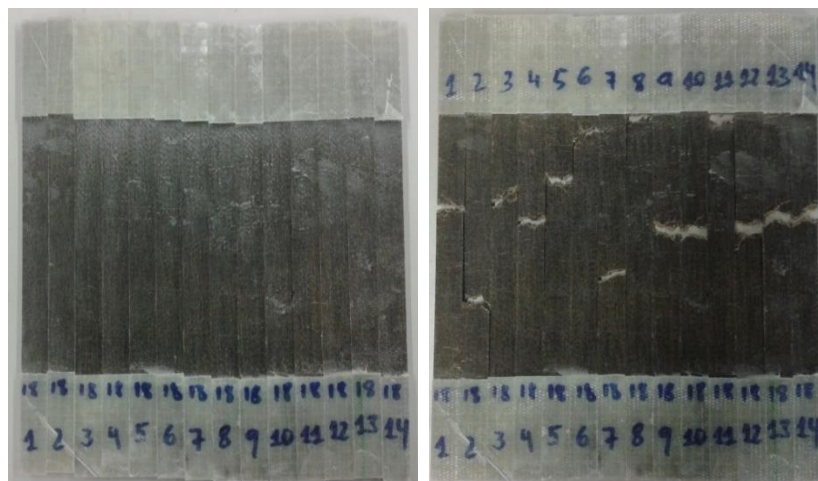
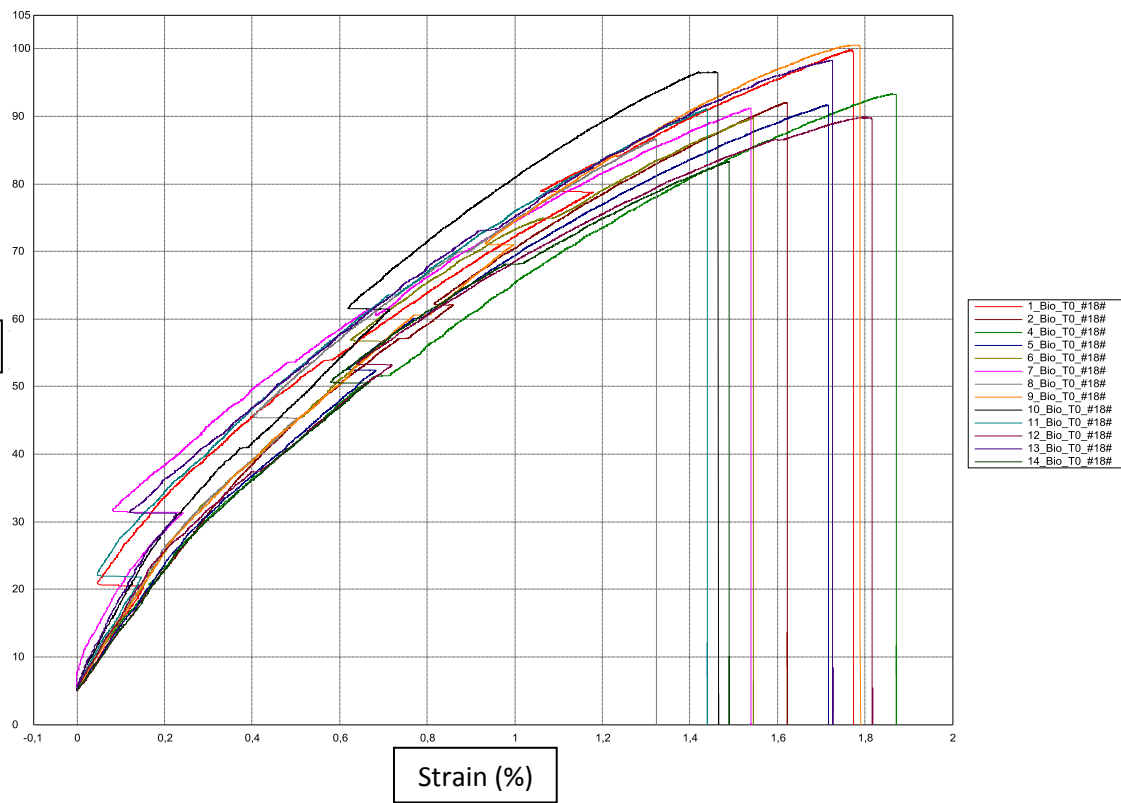
Sample	ID	Transverse tensile test						Failure mode	Vf	Mf
		a mm	b mm	F kN	Eyt Mpa	oyt Mpa	eyt %		(%)	(%)
1	1_Bio_T90_#17#	3,02	16,00	1,15	3284,11	23,87	0,34	Tab	24,5	30,7
2	2_Bio_T90_#17#	2,96	15,93	1,11	4181,58	23,46	0,62	Top	Parameters	Value
3	3_Bio_T90_#17#	2,96	15,44	1,12	3938,83	24,42	0,39	Bottom		
4	4_Bio_T90_#17#	3,09	15,20	1,11	3697,35	23,59	0,68	Top	Testing speed (mm/min)	2
5	5_Bio_T90_#17#	3,06	15,27	1,13	3889,78	24,20	0,69	Top	Extensometry	Video
6	6_Bio_T90_#17#	3,02	15,18	1,15	3563,20	25,08	0,81	Top	Reference points	Stickers
7	7_Bio_T90_#17#	3,07	15,33	1,14	3805,91	24,14	0,65	Middle	Norma	EN ISO527-5
8	8_Bio_T90_#17#	2,93	15,24	1,12	4102,67	25,06	0,69	Top	Precharge (kN)	1
9	9_Bio_T90_#17#	3,00	15,40	1,12	4486,46	24,23	0,70	Middle	Modulus (ε %)	0,05-0,25
10	10_Bio_T90_#17#	3,10	15,70	1,00		20,59		Top		
11	11_Bio_T90_#17#	2,85	15,70	1,08	3974,35	24,04	0,70	Middle		
12	12_Bio_T90_#17#	2,85	15,35	1,00	3168,79	22,91	0,75	Top		
Average value		2,99	15,48	1,10	<b>3826,64</b>	23,80	0,64			
Standard deviation				0,05	385,95	1,18	0,14			
CV(%)				0,05	0,10	0,05	0,23			
Characteristic value					3000,32	<b>21,29</b>	<b>0,33</b>			



# Laminate 18\_Araldite LY 1569 /Aradur 3489-Biotex UD-NaOH 1.5M\_3h

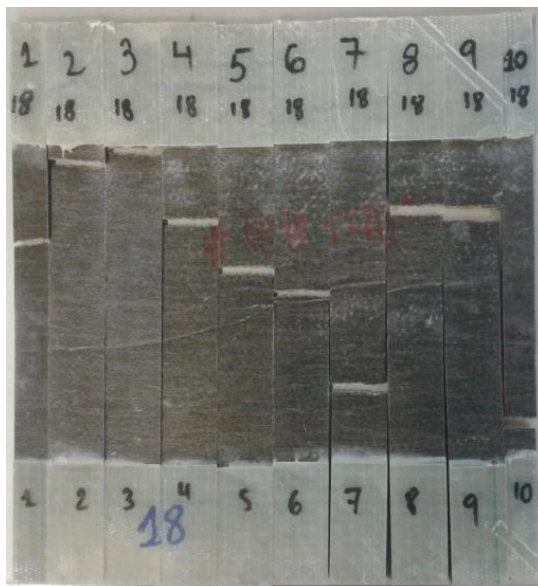
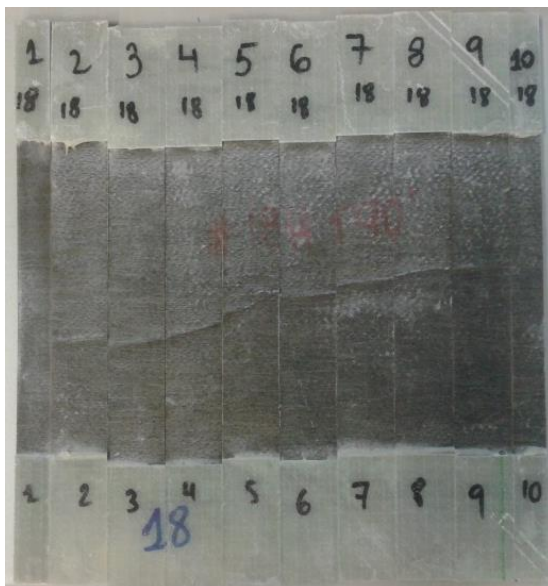
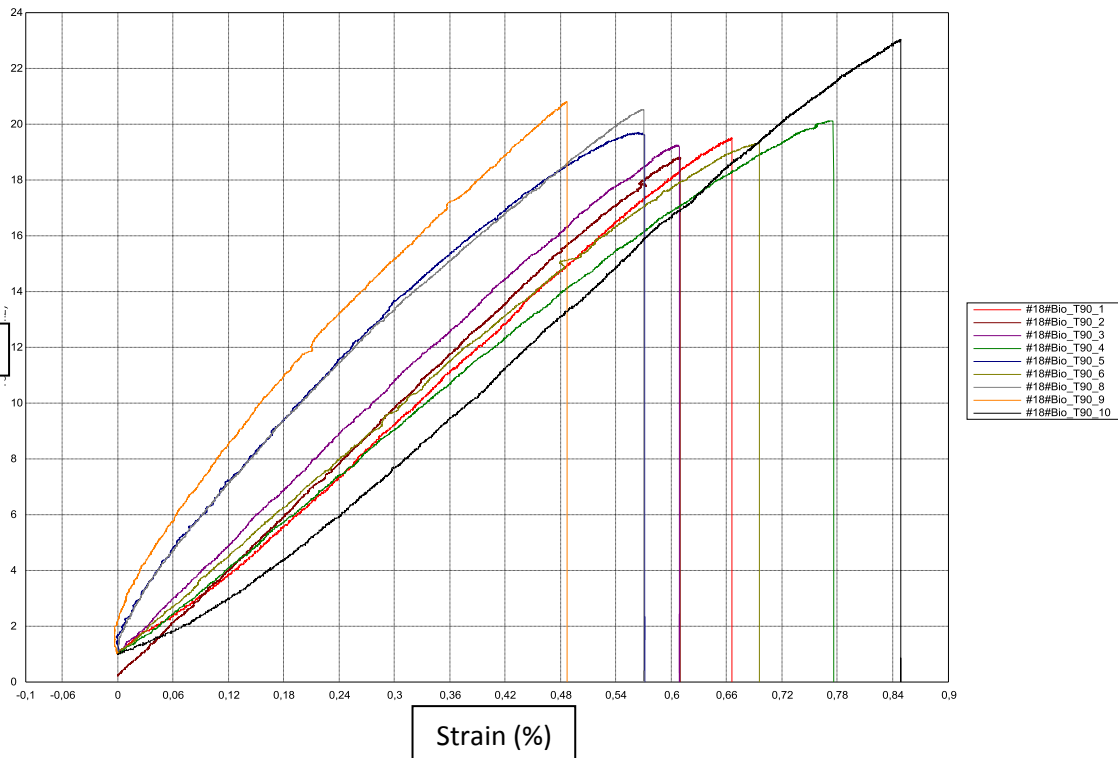
## Laminate 18 Tensile 0° test

Sample	ID	Longitudinal tensile test							Failure mode	Vf (%)	Mf (%)
		a mm	b mm	F kN	Ext Mpa	σxt Mpa	Ext %	vxy			
1	1 Bio_TO_#18#	2,67	15,00	4,00	11739,10	99,84	1,77		Middle	24	30,1
2	2 Bio_TO_#18#	2,62	14,97	3,61	8705,80	92,07	1,62	0,38	Middle		
3	3 Bio_TO_#18#	2,52	14,98	3,78	10617,80	100,05			Middle		
4	4 Bio_TO_#18#	2,82	15,02	3,95	8261,29	93,31	1,87	0,39	Middle		
5	5 Bio_TO_#18#	2,87	14,96	3,94	9030,97	91,66	1,72		Middle		
6	6 Bio_TO_#18#	2,89	15,04	3,90	9712,83	89,72	1,55	0,37	Top		
7	7 Bio_TO_#18#	2,95	14,95	4,02	9803,28	91,21	1,54		Middle		
8	8 Bio_TO_#18#	2,96	14,99	3,84	9587,87	86,64	1,32		Tab		
9	9 Bio_TO_#18#	2,80	15,05	4,24	9708,06	100,56	1,79	0,33	Middle		
10	10 Bio_TO_#18#	2,75	15,02	3,99	10400,10	96,57	1,47		Middle		
11	11 Bio_TO_#18#	2,96	15,08	4,06	10929,60	91,03	1,44	0,28	Tab		
12	12 Bio_TO_#18#	3,07	15,11	4,17	9126,67	89,84	1,82	0,43	Middle		
13	13 Bio_TO_#18#	2,80	15,19	4,18	12500,00	98,30	1,73	0,27	Middle		
14	14 Bio_TO_#18#	3,05	15,00	3,81	8832,65	83,31	1,49		Middle		
Average value		2,84	15,03	3,96	<b>9925,43</b>	93,15	1,62	<b>0,35</b>			
Standard deviation				0,17	1200,68	5,25	0,17	0,06			
CV(%)				0,04	0,12	0,06	0,10	0,17			
Characteristic value					7402,51	<b>82,20</b>	<b>1,27</b>	0,22			
									Testing speed (mm/min)	2	
									Extensometry	Video	
									Reference points	Stickers	
									Standard	EN ISO527-5	
									Precharge (kN)	5	
									Modulus (ε %)	0,05-0,25	



### Laminate 18 Tensile 90° test

Sample	ID	Transverse tensile test						Failure mode	Vf	Mf
		a mm	b mm	F kN	Eyt Mpa	oyt Mpa	eyt %		(%)	(%)
1	1_Bio_T90_#18#	2,66	15,61	0,81	2962,27	19,48	0,67	Middle	25,0	31,3
2	2_Bio_T90_#18#	2,72	25,32	1,30	3204,95	18,80	0,61	Top	Parameters	Value
3	3_Bio_T90_#18#	2,88	25,50	1,41	3284,36	19,24	0,61	Middle		
4	4_Bio_T90_#18#	2,89	25,42	1,48	2758,34	20,11	0,78	Middle	Testing speed (mm/min)	2
5	5_Bio_T90_#18#	3,00	25,44	1,50	3754,58	19,68	0,57	Middle	Extensometry	Video
6	6_Bio_T90_#18#	3,18	25,45	1,56	2923,68	19,29	0,70	Middle	Reference points	Stickers
7	7_Bio_T90_#18#	2,93	25,44	1,51	2881,12	20,24		Middle	Norma	EN ISO527-5
8	8_Bio_T90_#18#	3,12	25,42	1,63	3738,90	20,52	0,57	Middle	Precharge (kN)	1
9	9_Bio_T90_#18#	3,07	25,53	1,63	4113,44	20,81	0,49	Middle	Modulus (ε %)	0,05-0,25
10	10_Bio_T90_#18#	2,88	14,40	0,95	2854,45	23,02	0,85	Down		
Average value		2,93	23,35	1,38	3247,61	20,12	0,65			
Standard deviation				0,28	467,36	1,20	0,11			
CV(%)				0,20	0,14	0,06	0,17			
Characteristic value					2235,68	17,53	0,40			

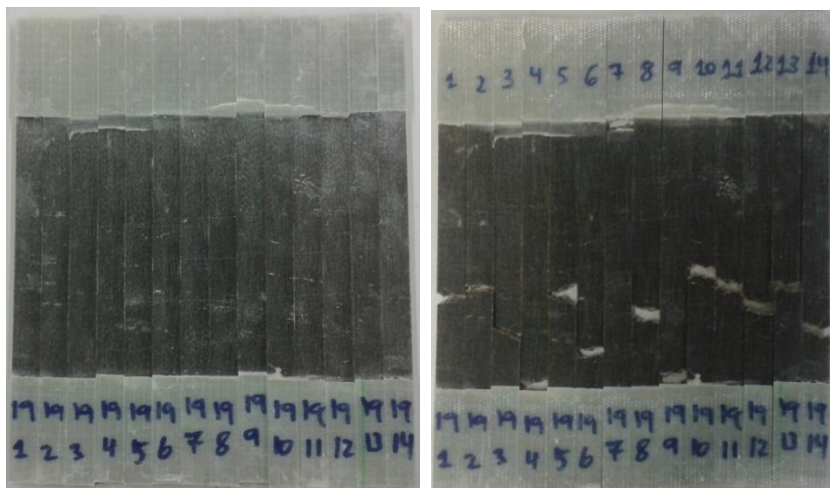
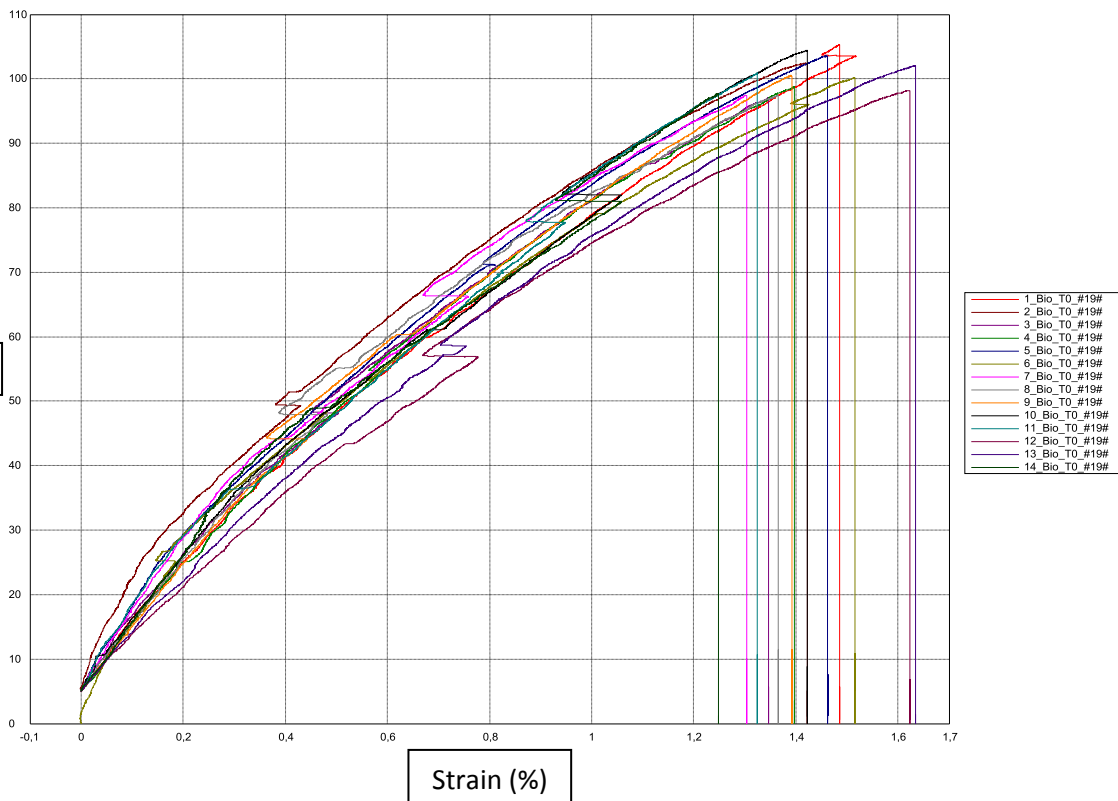




# Laminate 19\_Araldite LY 1569 /Aradur 3489-Biotex UD-NaOH 1.5M\_12h

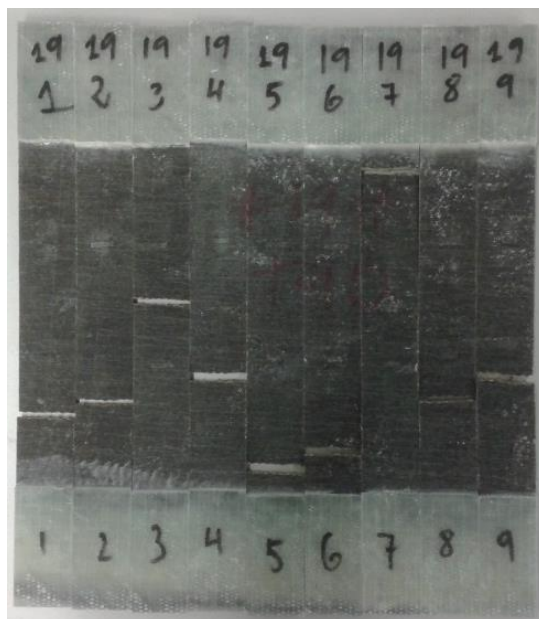
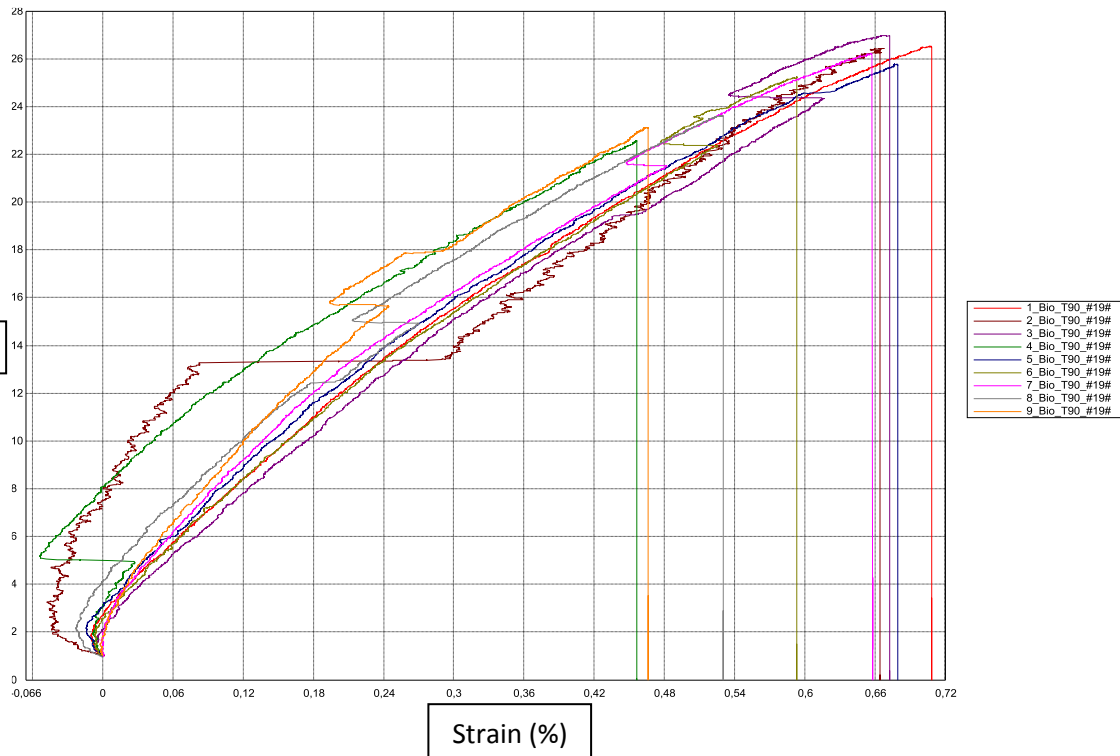
## Laminate 19 Tensile 0° test

Sample	ID	Longitudinal tensile test							Failure mode	Vf	Mf
		a mm	b mm	F kN	Ext Mpa	σxt Mpa	Ext %	vxy		(%)	(%)
1	1_Bio_TO_#19#	2,96	15,02	4,68	9015,98	105,28	1,52		Middle	24,7	30,9
2	2_Bio_TO_#19#	3,02	14,92	4,62	10591,10	102,43	1,42				
3	3_Bio_TO_#19#	3,04	14,90	4,39	9423,22	97,03	1,35				
4	4_Bio_TO_#19#	3,05	14,83	4,47	8872,58	98,82	1,40				
5	5_Bio_TO_#19#	2,98	15,01	4,63	10723,90	103,56	1,46				
6	6_Bio_TO_#19#	3,10	15,05	4,67	12220,00	100,18	1,52				
7	7_Bio_TO_#19#	2,98	14,99	4,35	11125,00	97,46	1,30	Down			
8	8_Bio_TO_#19#	3,02	14,95	4,40	9709,50	97,40	1,37	Top			
9	9_Bio_TO_#19#	3,03	15,00	4,57	9747,39	100,53	1,39	Middle			
10	10_Bio_TO_#19#	2,80	14,88	4,35	9934,53	104,40	1,42	Down			
11	11_Bio_TO_#19#	2,82	14,98	4,26	10601,80	100,90	1,33	Middle			
12	12_Bio_TO_#19#	3,03	15,00	4,46		98,21	1,62	0,53			
13	13_Bio_TO_#19#	2,90	14,93	4,42	8427,49	102,04	1,64	0,39			
14	14_Bio_TO_#19#	2,80	14,98	4,10	11065,00	97,65	1,25	0,43			
Average value		2,97	14,96	4,46	<b>10112,11</b>	100,42	1,43	<b>0,44</b>	Testing speed (mm/min)	2	
Standard deviation				0,17	1064,49	2,78	0,11	0,06	Extensometry	Video	
CV(%)				0,04	0,11	0,03	0,08	0,15	Reference points	Stickers	
Characteristic value					7875,36	<b>94,62</b>	<b>1,19</b>	0,29	Standard	EN ISO527-5	
									Precharge (kN)	5	
									Modulus (ε %)	0,05-0,25	



### Laminate 19 Tensile 90° test

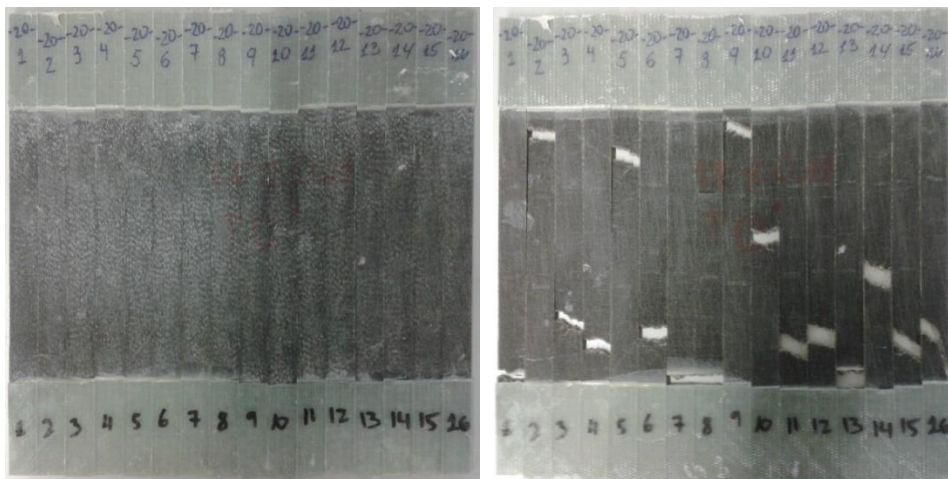
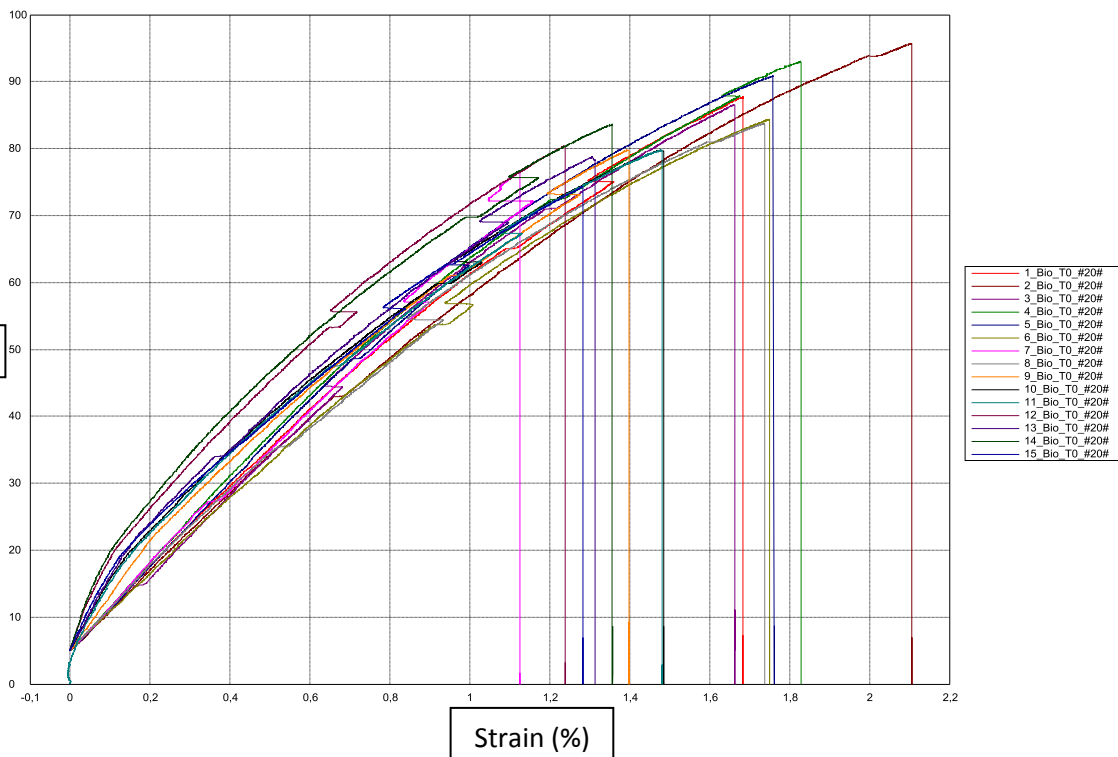
Sample	ID	Transverse tensile test						Failure mode	Vf	Mf
		a mm	b mm	F kN	Eyt Mpa	oyt Mpa	eyt %		(%)	(%)
1	1_Bio_T90_#19#	3,05	24,80	2,01	4303,16	26,51	0,71	Middle	23,8	29,9
2	2_Bio_T90_#19#	3,03	24,87	1,99		26,44	0,67	Middle	Parameters	Value
3	3_Bio_T90_#19#	3,00	24,89	2,01	4208,54	26,98	0,67	Middle		
4	4_Bio_T90_#19#	3,40	24,85	1,91		22,58	0,46	Middle	Testing speed (mm/min)	2
5	5_Bio_T90_#19#	3,07	24,90	1,97	4337,65	25,79	0,68	Bottom	Extensometry	Video
6	6_Bio_T90_#19#	3,11	24,88	1,95	4241,07	25,23	0,59	Bottom	Reference points	Stickers
7	7_Bio_T90_#19#	3,02	24,87	1,97	4576,94	26,21	0,66	Top	Norma	EN ISO527-5
8	8_Bio_T90_#19#	3,13	24,71	1,83		23,61	0,53	Middle	Precharge (kN)	1
9	9_Bio_T90_#19#	2,90	24,93	1,67	5636,35	23,12	0,47	Middle	Modulus (ε %)	0,05-0,25
Average value		3,08	24,86	1,92	<b>4550,62</b>	25,16	0,60			
Standard deviation				0,11	547,53	1,64	0,10			
CV(%)				0,06	0,12	0,07	0,16			
Characteristic value					3282,23	<b>21,57</b>	<b>0,39</b>			



# Laminate 20\_Araldite LY 1569 /Aradur 3489-Biotex UD-NaOH 1.5M\_24h

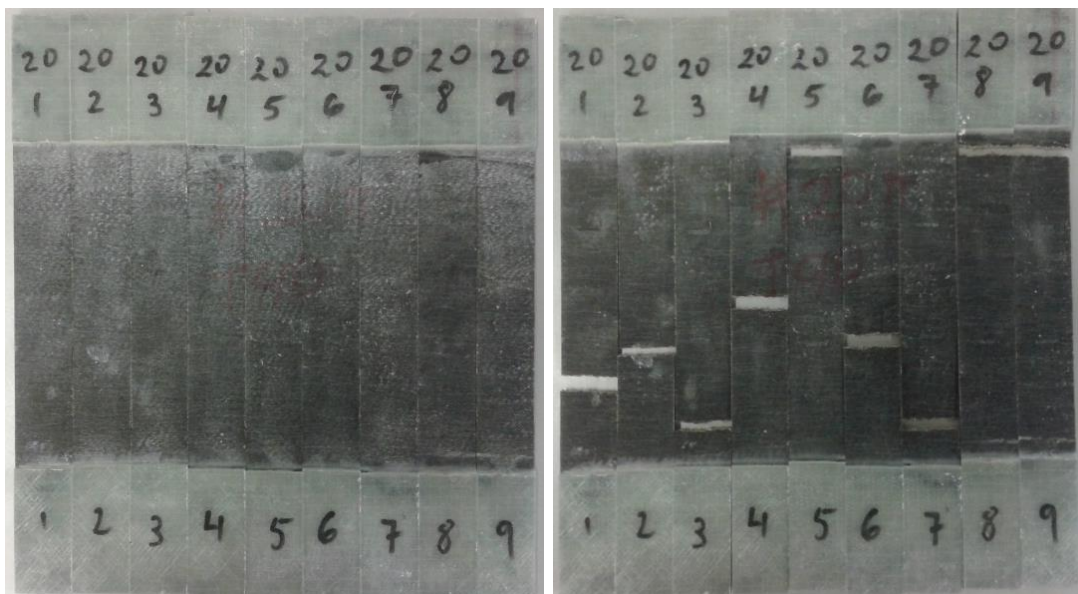
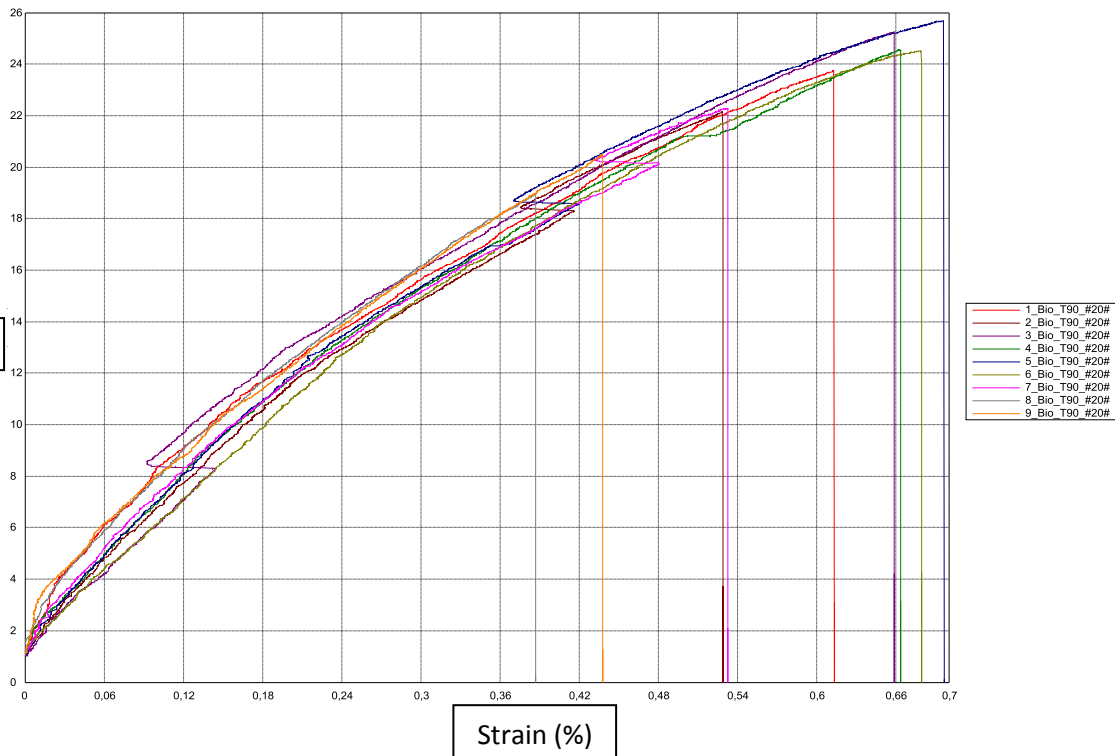
## Laminate 20 Tensile 0° test

Sample	ID	Longitudinal tensile test							Failure mode	Vf (%)	Mf (%)
		a mm	b mm	F kN	Ext Mpa	oxt Mpa	Ext %	vxy %			
1	1 Bio_TO_#20#	3,10	15,59	4,24	6513,80	87,73	1,68	0,33	Tab	22,7	28,6
2	2 Bio_TO_#20#	3,02	15,56	4,50	6126,86	95,68	2,11	0,23	Top		
3	3 Bio_TO_#20#	3,13	15,60	4,23	6093,36	86,58	1,66	0,28	Bottom	Parameters	Value
4	4 Bio_TO_#20#	3,04	15,57	4,40	6647,37	93,00	1,83	0,38	Bottom		
5	5 Bio_TO_#20#	3,22	15,59	4,56	6416,69	90,83	1,76	0,24	Top		
6	6 Bio_TO_#20#	3,25	15,70	4,31	5666,63	84,40	1,75	0,35	Bottom		
7	7 Bio_TO_#20#	3,20	15,64	3,83	6736,91	76,62	1,16	0,29	Tab		
8	8 Bio_TO_#20#	3,33	15,69	4,37	6385,00	83,73	1,74		Tab		
9	9 Bio_TO_#20#	3,46	15,67	4,33	8007,56	79,81	1,40	0,39	Top		
10	10 Bio_TO_#20#	3,49	15,63	4,35	7593,09	79,69	1,49	0,39	Middle		
11	11 Bio_TO_#20#	3,37	15,66	4,21	7754,43	79,81	1,48	0,30	Bottom		
12	12 Bio_TO_#20#	3,20	15,72	4,04	8032,32	80,40	1,24	0,36	Bottom		
13	13 Bio_TO_#20#	3,30	15,60	4,06	8214,09	78,78	1,31	0,33	Tab		
14	14 Bio_TO_#20#	3,14	15,70	4,12	8244,93	83,59	1,36	0,36	Middle		
15	15 Bio_TO_#20#	3,26	15,77	3,82	7477,96	74,37	1,28		Bottom		
Average value		3,23	15,65	4,22	<b>7060,73</b>	83,67	1,55	<b>0,33</b>			
Standard deviation				0,22	874,62	6,12	0,27	0,05			
CV(%)				0,05		0,07	0,17	0,16			
Characteristic value					5250,50	<b>71,00</b>	<b>0,99</b>	0,21			



### Laminate 20 Tensile 90° test

Sample	ID	Transverse tensile test						Failure mode	Vf	Mf
		a mm	b mm	F kN	Eyt Mpa	oyt Mpa	eyt %		(%)	(%)
1	1_Bio_T90_#20#	3,50	24,87	2,07	4342,90	23,76	0,61	Middle	21,9	27,7
2	2_Bio_T90_#20#	3,53	24,86	1,94	4632,38	22,16	0,53	Middle	Parameters	Value
3	3_Bio_T90_#20#	3,30	24,81	2,07	5727,21	25,25	0,66	Bottom		
4	4_Bio_T90_#20#	3,16	24,81	1,93	4682,86	24,56	0,66	Middle	Testing speed (mm/min)	2
5	5_Bio_T90_#20#	3,24	24,66	2,05	4787,59	25,69	0,70	Top	Extensometry	Video
6	6_Bio_T90_#20#	3,36	25,00	2,06	4658,65	24,50	0,68	Middle	Reference points	Stickers
7	7_Bio_T90_#20#	3,50	24,81	1,93	4453,18	22,28	0,53	Bottom	Norma	EN ISO527-5
8	8_Bio_T90_#20#	3,32	25,01	1,58	4503,68	18,98	0,39	Top	Precharge (kN)	1
9	9_Bio_T90_#20#	3,24	24,86	1,65	4276,15	20,49	0,44	Top	Modulus (ε %)	0,05-0,25
Average value		3,35	24,85	1,92	<b>4673,84</b>	23,07	0,58			
Standard deviation				0,18	428,64	2,27	0,11			
CV(%)				0,10	0,09	0,10	0,19			
Characteristic value					3733,69	<b>18,10</b>	<b>0,33</b>			

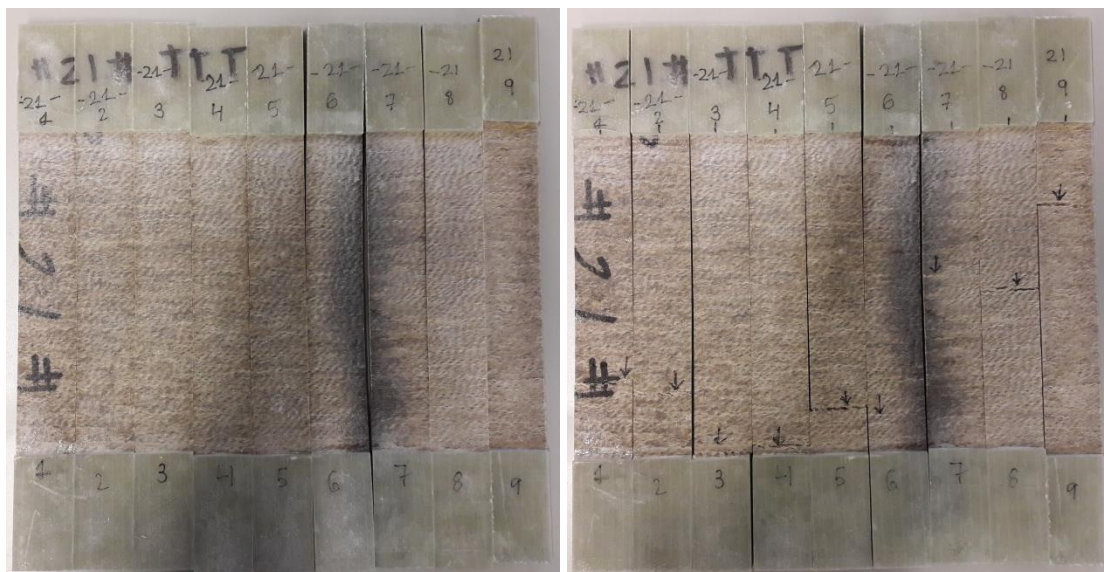
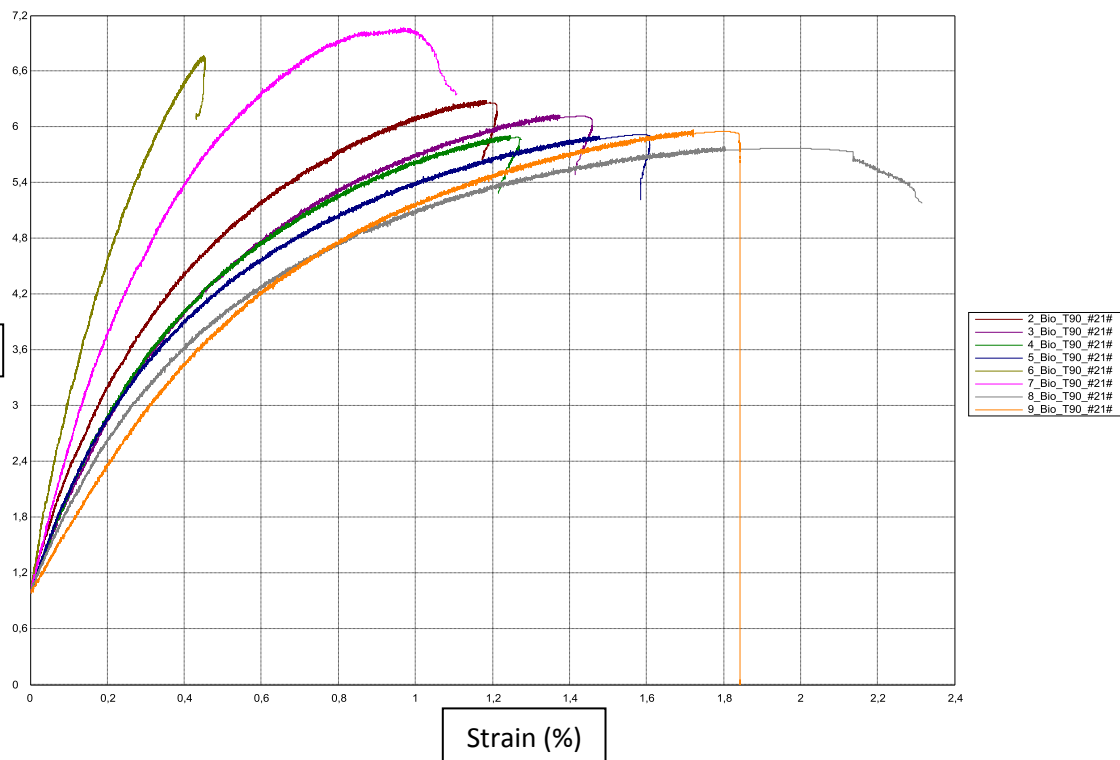






## Laminate 21 Tensile 90° test

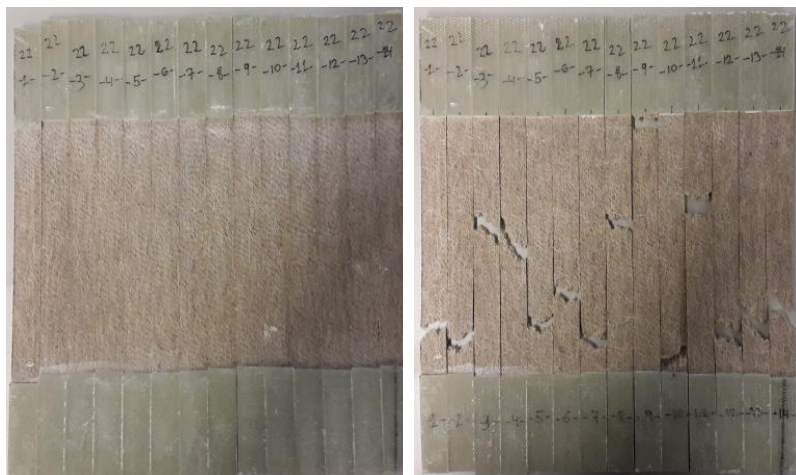
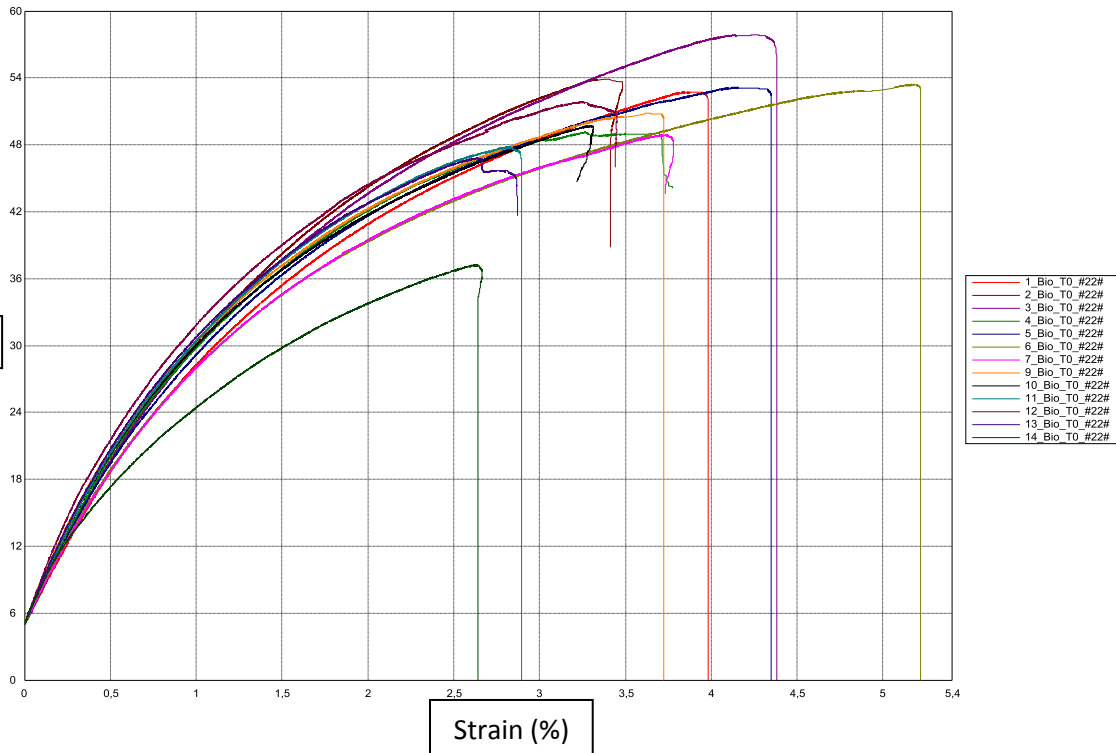
Sample	ID	Transverse tensile test						Failure mode	Vf	Mf
		a	b	F	Eyt	oyt	eyt		(%)	(%)
		mm	mm	kN	Mpa	Mpa	%			
1	1_Bio_T90_#21#	3,06	25,10	0,498		6,490		Middle	25,12	30,4
2	2_Bio_T90_#21#	2,96	25,12	0,467	903,744	6,285	1,212	Bottom	Parameters	Value
3	3_Bio_T90_#21#	2,97	25,08	0,457	820,166	6,132	1,459	Tab		
4	4_Bio_T90_#21#	2,94	25,24	0,439	826,064	5,912	1,274	Bottom	Testing speed (mm/min)	2
5	5_Bio_T90_#21#	2,92	25,03	0,432	791,317	5,917	1,610	Bottom	Extensometry	Video
6	6_Bio_T90_#21#	2,80	24,87	0,471	1500,500	6,767	0,454	Bottom	Reference points	Stickers
7	7_Bio_T90_#21#	2,84	24,74	0,496	1224,410	7,063	1,109	Middle	Norma	EN ISO527-5
8	8_Bio_T90_#21#	2,90	24,88	0,418	717,076	5,787	2,315	Middle	Precharge (kN)	1
9	9_Bio_T90_#21#	2,88	24,64	0,424	659,774	5,971	1,843	Middle	Modulus (ε %)	0,05-0,25
Average value		2,92	24,97	0,46	930,38	6,26	1,41			
Standard deviation				0,03	286,18	0,44	0,55			
CV(%)				0,07	0,31	0,07	0,39			
Characteristic value					293,17	5,30	0,19			



# Laminate 22\_Araldite LY 1569 /Aradur 3489-Biotex UD-NaOH 2M\_3h

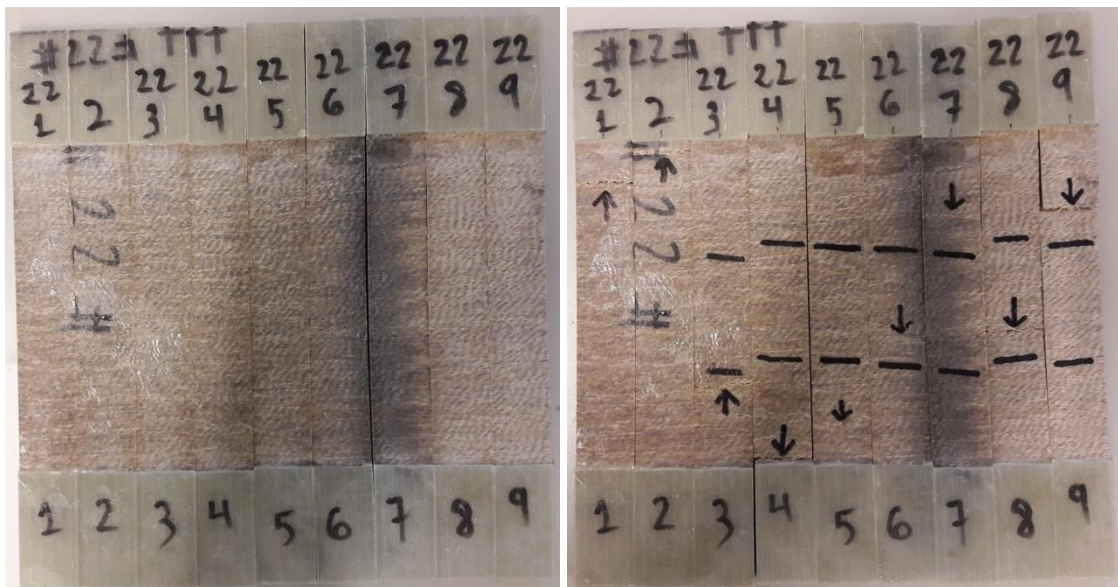
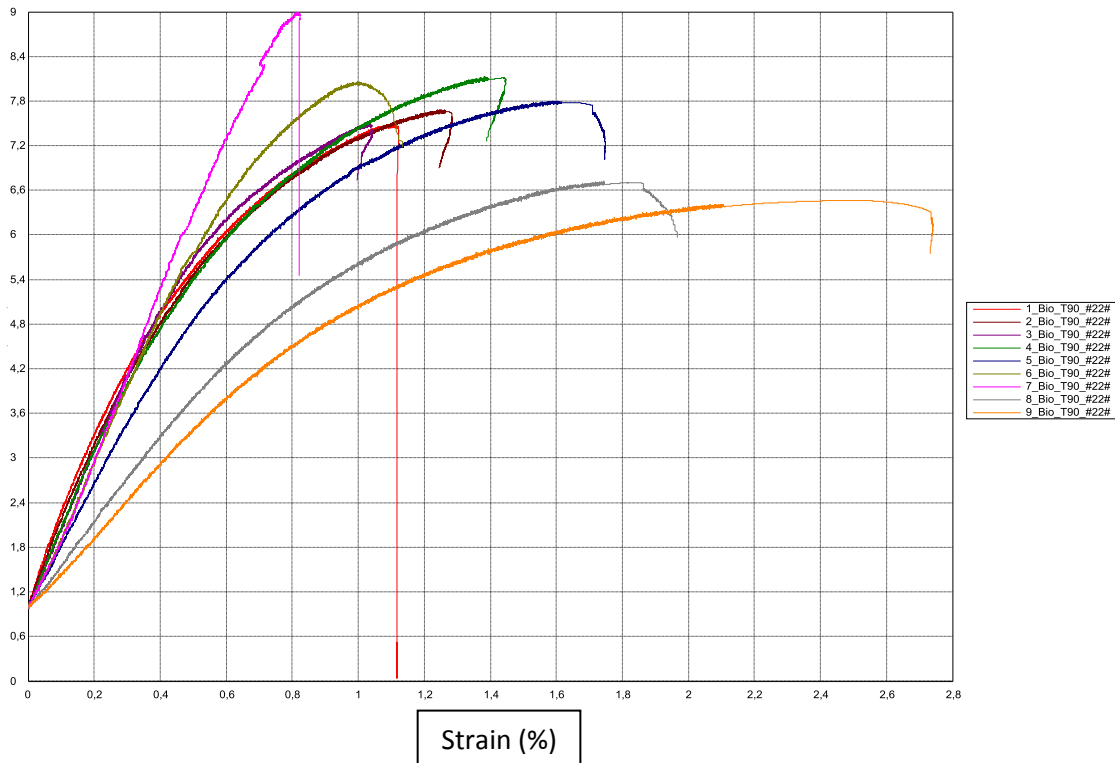
## Laminate 22 Tensile 0° test

Sample	ID	Longitudinal tensile test							Failure mode	Vf	Mf
		a mm	b mm	F kN	Ext Mpa	oxt Mpa	Ext %	vxy		(%)	(%)
1	1 Bio_TO_#22#	3,12	14,80	2,44	2886,18	52,75	3,84		Bottom	22,8	28,7
2	2 Bio_TO_#22#	3,00	14,85	2,40	3130,49	53,89	3,48	0,30	Bottom		
3	3 Bio_TO_#22#	2,98	14,89	2,57	3176,77	57,85	4,26	0,37	Middle		
4	4 Bio_TO_#22#	3,16	14,94	2,32	3257,43	49,14	3,27	0,39	Middle		
5	5 Bio_TO_#22#	3,16	15,03	2,52	3166,17	53,14	4,15	0,32	Bottom		
6	6 Bio_TO_#22#	3,27	15,06	2,63	3026,69	53,41	5,17	0,49	Bottom		
7	7 Bio_TO_#22#	3,29	15,14	2,44	2974,85	48,90	3,78	0,44	Bottom		
8	8 Bio_TO_#22#	3,28	15,17	2,67	3119,62	53,63		0,37	Middle		
9	9 Bio_TO_#22#	3,29	15,30	2,56	3442,36	50,81	3,72	0,37	Top		
10	10 Bio_TO_#22#	3,29	15,24	2,49	3292,76	49,71	3,31	0,29	Bottom		
11	11 Bio_TO_#22#	3,13	15,30	2,29	3359,96	47,82	2,83	0,28	Middle		
12	12 Bio_TO_#22#	3,08	15,30	2,44	3738,25	51,85	3,24	0,44	Bottom		
13	13 Bio_TO_#22#	3,12	15,35	2,24	3453,87	46,81	2,64	0,40	Bottom		
14	14 Bio_TO_#22#	3,94	15,30	2,24	2856,48		2,67	0,54	Bottom		
Average value		3,22	15,12	2,45	<b>3205,85</b>	51,52	3,57	<b>0,38</b>			
Standard deviation				0,14	241,81	3,03	0,71	0,08			
CV(%)				0,06	0,08	0,06	0,20	0,20			
Characteristic value					2701,77	<b>45,15</b>	<b>2,08</b>	0,22			
									Testing speed (mm/min)	2	
									Extensometry	Video	
									Reference points	Stickers	
									Standard	EN ISO527-5	
									Precharge (kN)	5	
									Modulus (ε %)	0,05-0,25	



### Laminate 22 Tensile 90° test

Sample	ID	Transverse tensile test						Failure mode	Vf	Mf
		a mm	b mm	F kN	Eyt Mpa	oyt Mpa	eyt %		(%)	(%)
1	1_Bio_T90_#22#	3,26	24,89	0,608	1040,470	7,489	1,123	Top	23,55	28,7
2	2_Bio_T90_#22#	3,28	24,92	0,628	1009,840	7,684	1,284	Top	Parameters	Value
3	3_Bio_T90_#22#	3,33	24,90	0,622	1045,030	7,497	1,043	Bottom		
4	4_Bio_T90_#22#	3,05	24,84	0,615	1027,430	8,124	1,449	Tab	Testing speed (mm/min)	2
5	5_Bio_T90_#22#	3,17	25,00	0,618	844,426	7,795	1,748	Bottom	Extensometry	Video
6	6_Bio_T90_#22#	3,07	24,88	0,616	1028,200	8,061	1,133	Middle	Reference points	Stickers
7	7_Bio_T90_#22#	3,00	24,78	0,670	1066,150	9,010	0,823	Middle	Norma	EN ISO527-5
8	8_Bio_T90_#22#	3,01	25,03	0,506	600,986	6,718	1,966	Middle	Precharge (kN)	1
9	9_Bio_T90_#22#	2,85	24,72					Middle	Modulus (ε %)	0,05-0,25
Average value		3,11	24,88	0,61	957,82	7,80	1,32			
Standard deviation				0,05	159,85	0,66	0,38			
CV(%)				0,08	0,17	0,08	0,29			
Characteristic value					601,89	6,34	0,47			

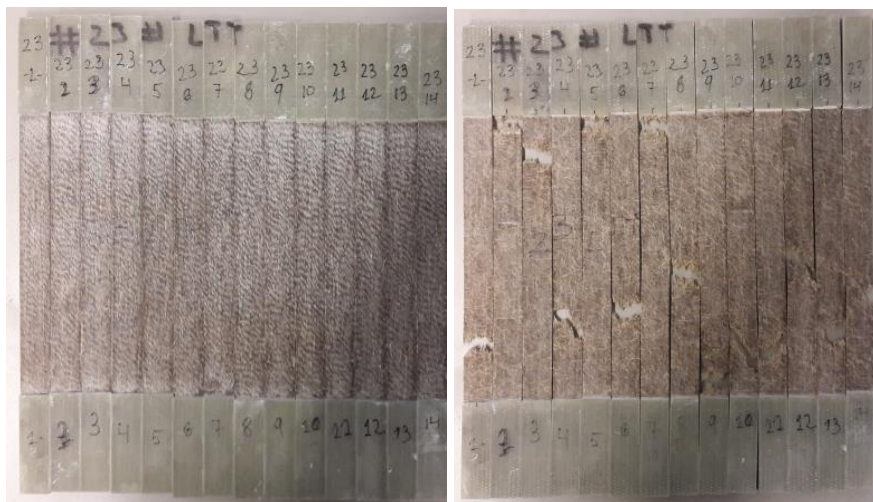
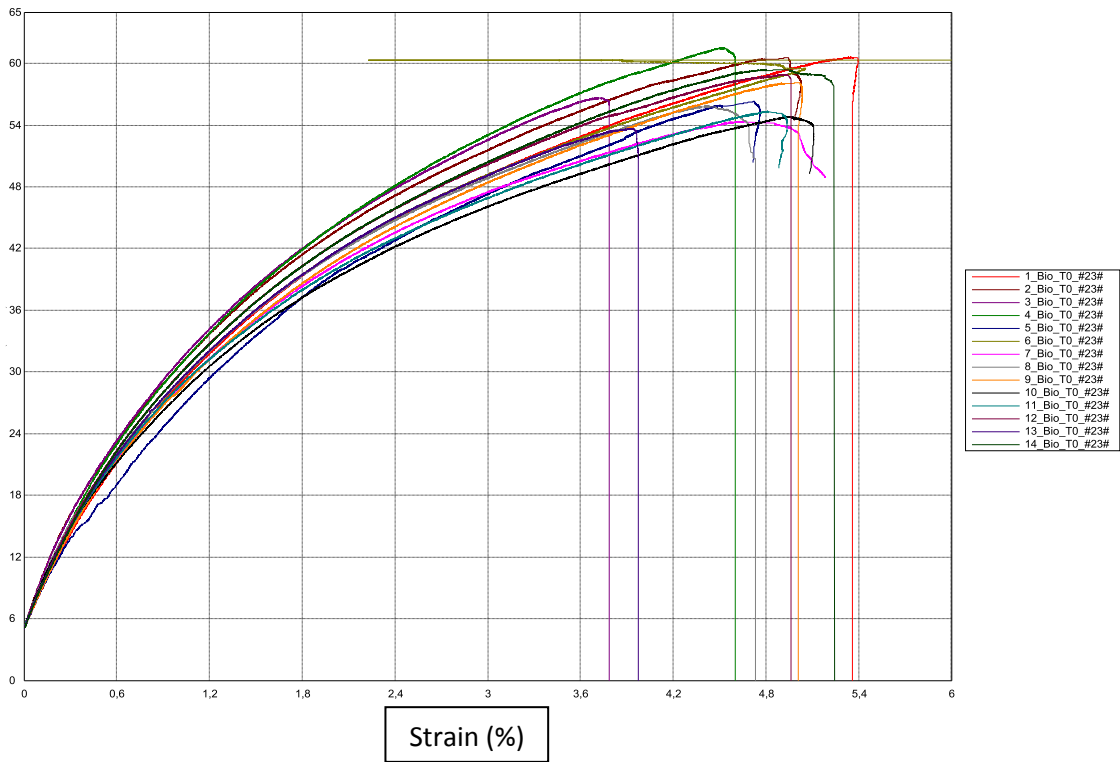




# Laminate 23\_Araldite LY 1569 /Aradur 3489-Biotex UD-NaOH 2M\_12h

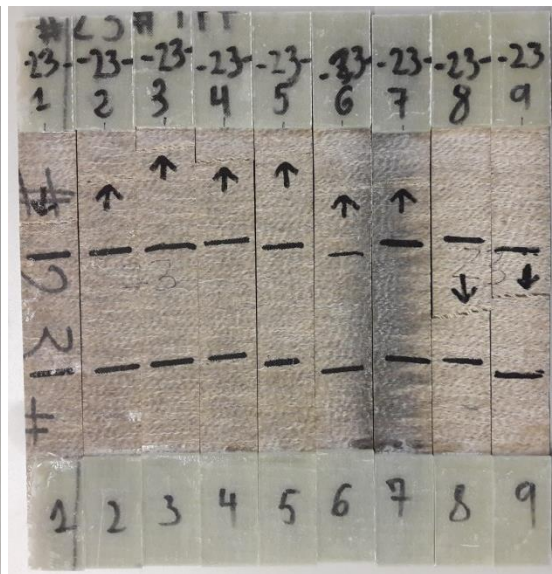
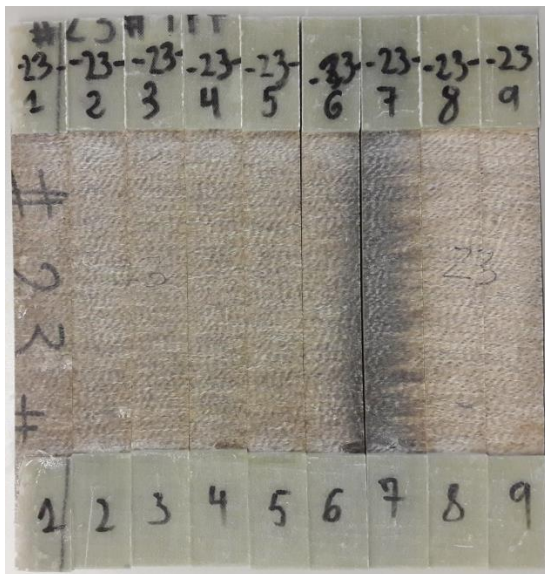
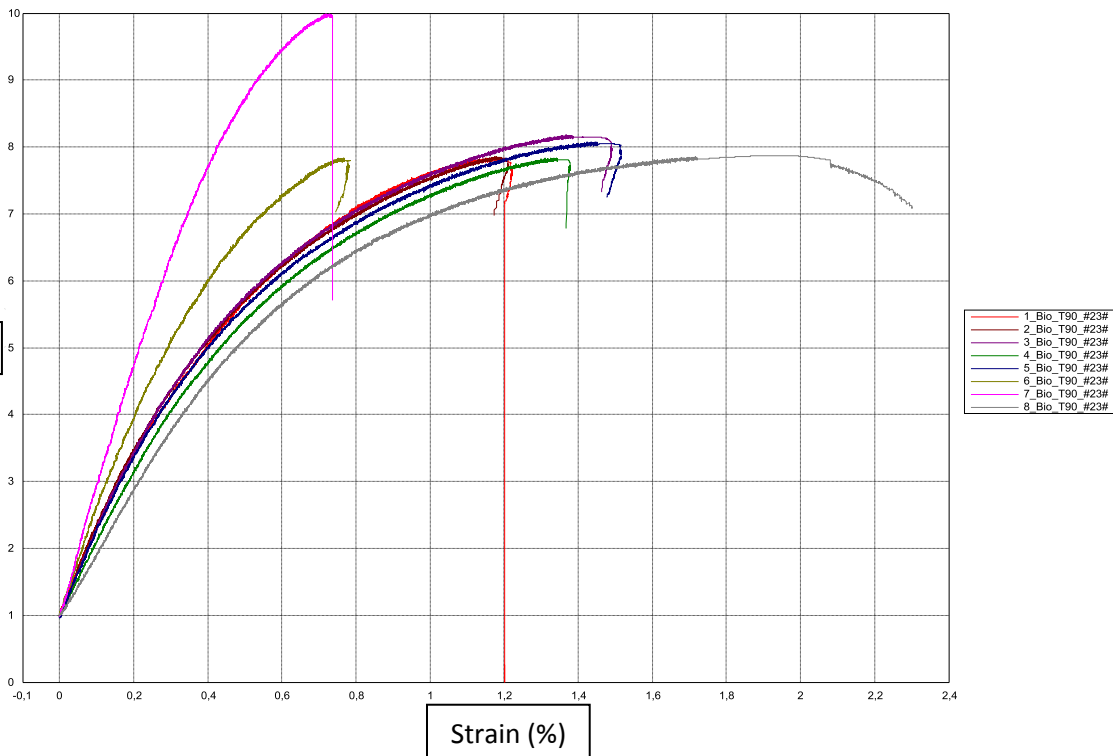
## Laminate 23 Tensile 0° test

Sample	ID	Longitudinal tensile test							Failure mode	Vf (%)	Mf (%)
		a mm	b mm	F kN	Ext Mpa	$\sigma_{xt}$ Mpa	Ext %	$v_{xy}$			
1	1_Bio_TO_#23#	2,81	15,08	2,57	3063,85	60,63	5,40	0,25	Bottom	24,3	30,4
2	2_Bio_TO_#23#	2,81	15,07	2,56	3692,20	60,56	5,03	0,40	Top		
3	3_Bio_TO_#23#	2,93	15,11	2,51	3641,65	56,68	3,79	0,47	Bottom		
4	4_Bio_TO_#23#	2,90	15,11	2,70	3450,86	61,51	4,51	0,31	Middle		
5	5_Bio_TO_#23#	2,99	15,08	2,54	2888,33	56,30	4,72	0,39	Top		
6	6_Bio_TO_#23#	3,00	15,15	2,74	3102,64	60,39	4,98	0,50	Middle		
7	7_Bio_TO_#23#	3,15	15,23	2,61	3065,34	54,37	4,65	0,76	Top		
8	8_Bio_TO_#23#	3,12	15,18	2,65	3391,70	55,87	4,41	0,64	Middle		
9	9_Bio_TO_#23#	3,08	15,26	2,73	3111,82	58,11	5,00		Bottom		
10	10_Bio_TO_#23#	3,20	15,12	2,65	3214,21	54,86	4,95	0,55	Bottom		
11	11_Bio_TO_#23#	3,20	15,26	2,70	3167,68	55,35	4,81	0,51	Bottom		
12	12_Bio_TO_#23#	3,01	15,14	2,69	3330,50	58,93	4,92	0,46	Middle		
13	13_Bio_TO_#23#	3,13	14,80	2,49	3276,22	53,68	3,92	0,64	Bottom		
14	14_Bio_TO_#23#	2,97	15,11	2,67	3194,82	59,42	4,93	0,23	Middle		
Average value		3,02	15,12	2,63	<b>3256,56</b>	57,62	4,72	<b>0,47</b>			
Standard deviation				0,08	226,58	2,64	0,44	0,16			
CV(%)				0,03	0,07	0,05	0,09	0,33			
Characteristic value					2784,22	<b>52,08</b>	<b>3,80</b>	0,14			
									Testing speed (mm/min)	2	
									Extensometry	Video	
									Reference points	Stickers	
									Standard	EN ISO527-5	
									Precharge (kN)	5	
									Modulus (ε %)	0,05-0,25	



### Laminate 23 Tensile 90° test

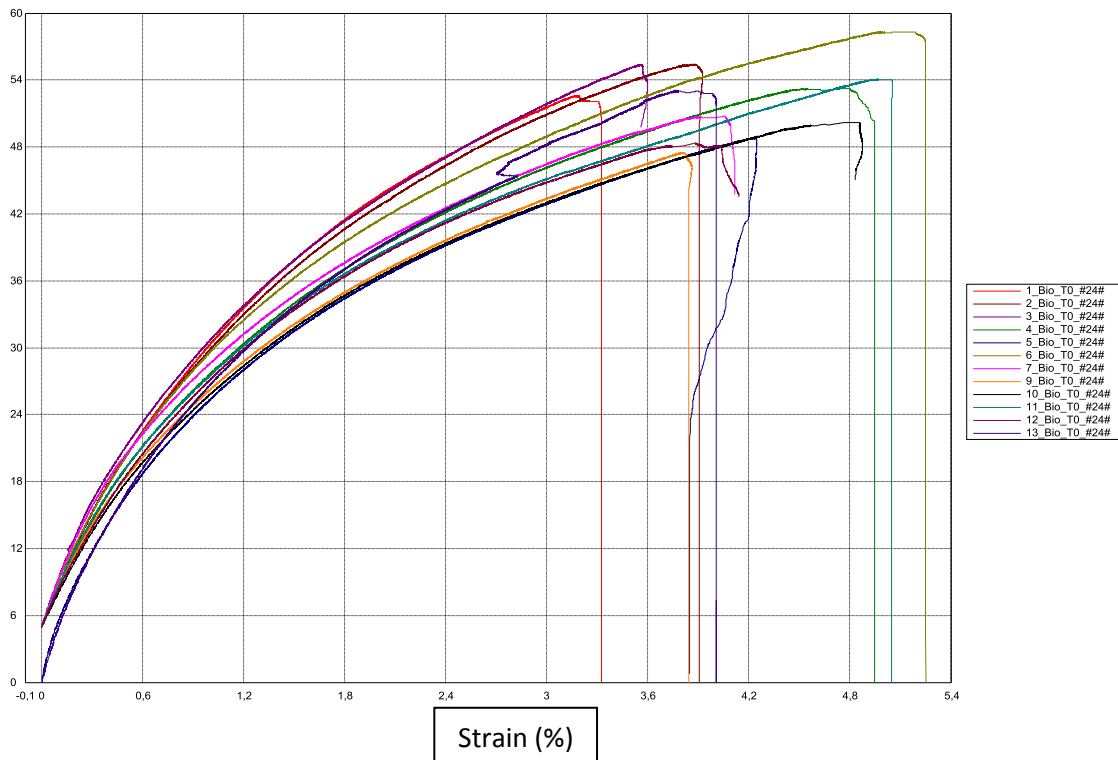
Sample	ID	Transverse tensile test						Failure mode	Vf	Mf
		a mm	b mm	F kN	Eyt Mpa	oyt Mpa	eyt %		(%)	(%)
1	1_Bio_T90_#23#	3,17	24,71	0,613	1069,300	7,828	1,221	Top	24,29	29,5
2	2_Bio_T90_#23#	3,08	24,80	0,600	1115,820	7,852	1,211	Top	Parameters	Value
3	3_Bio_T90_#23#	3,00	24,78	0,609	1135,650	8,186	1,490	Top		
4	4_Bio_T90_#23#	3,19	24,72	0,618	1032,370	7,837	1,379	Top	Testing speed (mm/min)	2
5	5_Bio_T90_#23#	3,04	24,71	0,606	1102,800	8,071	1,516	Top	Extensometry	Video
6	6_Bio_T90_#23#	3,01	24,68	0,582	1357,830	7,831	0,785	Top	Reference points	Stickers
7	7_Bio_T90_#23#	3,04	24,80	0,753	1796,980	9,994	0,737	Top	Norma	EN ISO527-5
8	8_Bio_T90_#23#	2,80	24,82	0,547	958,025	7,873		Middle	Precharge (kN)	1
9	9_Bio_T90_#23#	2,84	24,67					Middle	Modulus (ε %)	0,05-0,25
Average value		3,02	24,74	0,62	<b>1196,10</b>	8,18	1,19			
Standard deviation				0,06	268,75	0,74	0,32			
CV(%)				0,10	0,22	0,09	0,27			
Characteristic value					597,70	<b>6,53</b>	<b>0,49</b>			



# Laminate 24 Araldite LY 1569 /Aradur 3489-Biotex UD-NaOH 2M\_24h

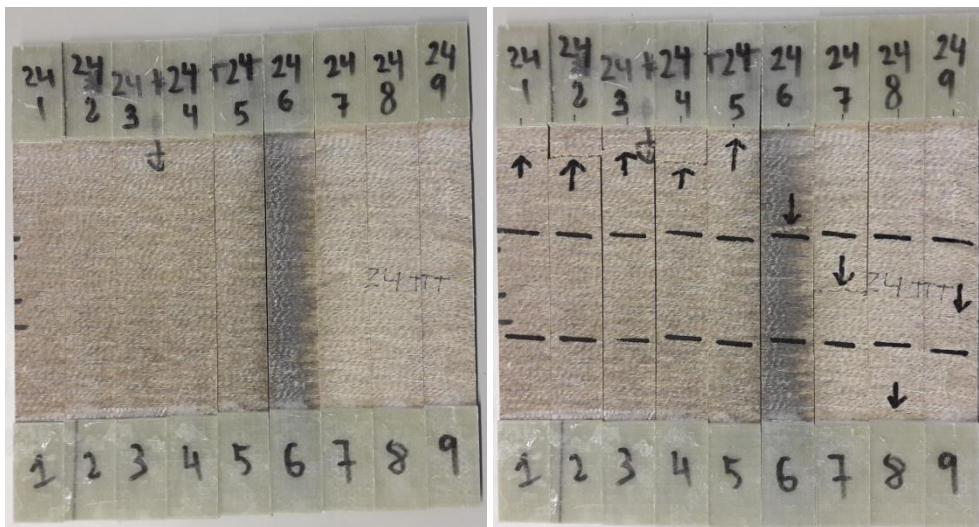
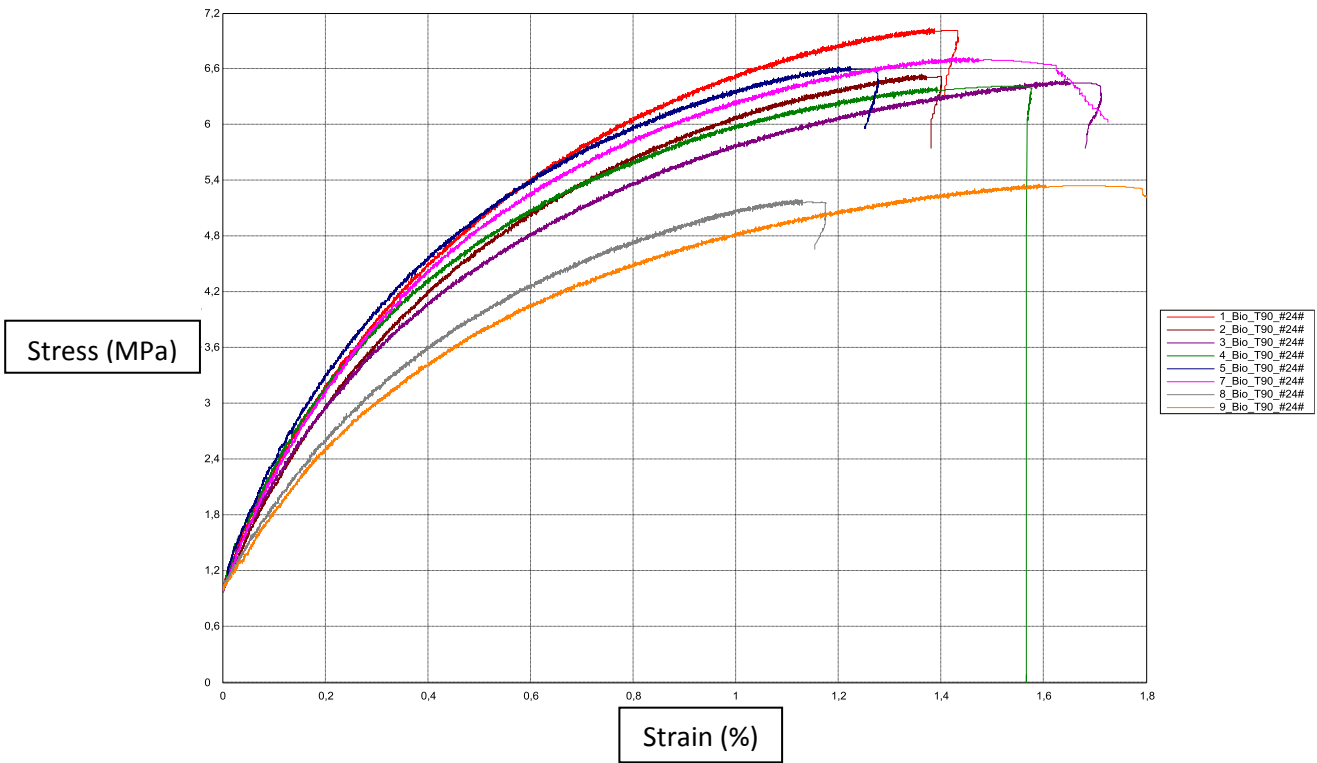
## Laminate 24 Tensile 0° test

Sample	ID	Longitudinal tensile test							Failure mode	Vf	Mf
		a mm	b mm	F kN	Ext Mpa	oxt Mpa	ext %	vxy		(%)	(%)
1	1_Bio_TO_#24#	3,18	14,96	2,50	3516,76	52,58	3,32	0,30	Parameters	Value	
2	2_Bio_TO_#24#	3,12	15,04	2,60	3483,83	55,41	3,92	0,51			
3	3_Bio_TO_#24#	2,94	15,11	2,46	3762,92	55,39	3,60	0,51			
4	4_Bio_TO_#24#	3,25	14,99	2,59	3143,20	53,23	4,94	0,29			
5	5_Bio_TO_#24#	3,25	15,12	2,40	3457,43	48,85	4,25	0,15			
6	6_Bio_TO_#24#	2,95	15,16	2,61	3328,32	58,32	5,25	0,15			
7	7_Bio_TO_#24#	3,03	15,14	2,33	3559,90	50,73	4,11	0,54			
8	8_Bio_TO_#24#	3,05	15,10	2,46	3456,91	53,46		0,62			
9	9_Bio_TO_#24#	3,30	15,15	2,37	3066,12	47,48	3,86	0,46			
10	10_Bio_TO_#24#	3,22	15,12	2,44	2848,04	50,21	4,88				
11	11_Bio_TO_#24#	3,20	15,15	2,62	3215,93	54,06	5,05	0,69			
12	12_Bio_TO_#24#	3,20	15,14	2,34	2863,37	48,38	4,14	0,24			
13	13_Bio_TO_#24#	2,96	15,11	2,37	3708,65	53,05	4,01	0,32			
14	14_Bio_TO_#24#	3,01	15,07	2,36	3053,43	52,02		0,34			
Average value		3,12	15,10	2,46	<b>3318,92</b>	52,37	4,28	<b>0,41</b>	Testing speed (mm/min)	2	
Standard deviation				0,11	293,11	3,02	0,61	0,16	Extensometry	Video	
CV(%)				0,04	0,09	0,06	0,14	0,40	Reference points	Stickers	
Characteristic value					2707,88	<b>46,07</b>	<b>2,98</b>	0,07	Standard	EN ISO527-5	
									Precharge (kN)	5	
									Modulus (ε %)	0,05-0,25	



### Laminate 24 Tensile 90° test

Sample	ID	Transverse tensile test						Failure mode	Vf	Mf
		a mm	b mm	F kN	Eyt Mpa	oyt Mpa	eyt %		(%)	(%)
1	1_Bio_T90_#24#	2,92	24,80	0,509	905,295	7,035	1,433	Top	24,39	29,6
2	2_Bio_T90_#24#	2,92	24,84	0,475	855,473	6,543	1,401	Top	Parameters	Value
3	3_Bio_T90_#24#	2,98	24,84	0,480	804,154	6,480	1,713	Top		
4	4_Bio_T90_#24#	3,04	24,87	0,485	867,100	6,414	1,577	Top	Testing speed (mm/min)	2
5	5_Bio_T90_#24#	3,04	24,85	0,500	924,193	6,623	1,277	Top	Extensometry	Video
6	6_Bio_T90_#24#	2,98	24,77					Middle	Reference points	Stickers
7	7_Bio_T90_#24#	2,88	24,95	0,483	906,686	6,723	1,726	Middle	Norma	EN ISO527-5
8	8_Bio_T90_#24#	3,04	24,87	0,393	699,823	5,198	1,176	Bottom	Precharge (kN)	1
9	9_Bio_T90_#24#	3,25	24,80	0,432	679,443	5,358	1,866	Middle	Modulus (ε %)	0,05-0,25
Average value		3,01	24,84	0,47	<b>830,27</b>	6,30	1,52			
Standard deviation				0,04	94,66	0,66	0,24			
CV(%)				0,08	0,11	0,10	0,16			
Characteristic value					619,49	<b>4,83</b>	<b>0,99</b>			

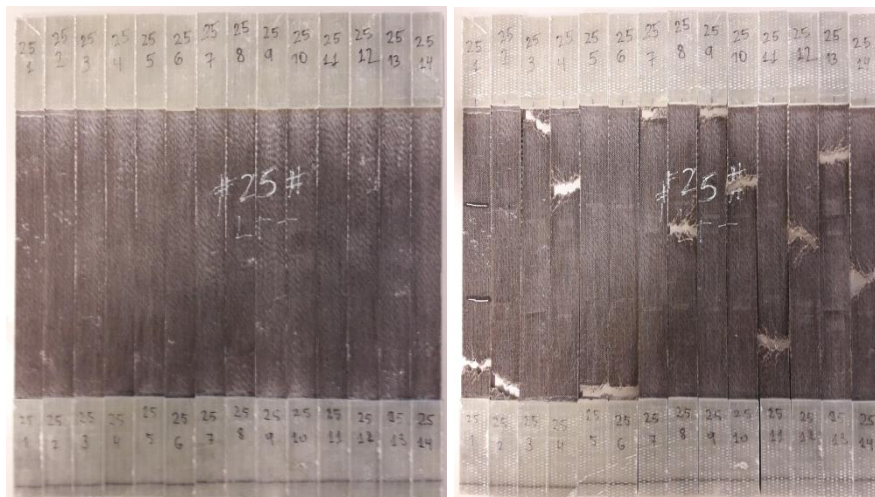
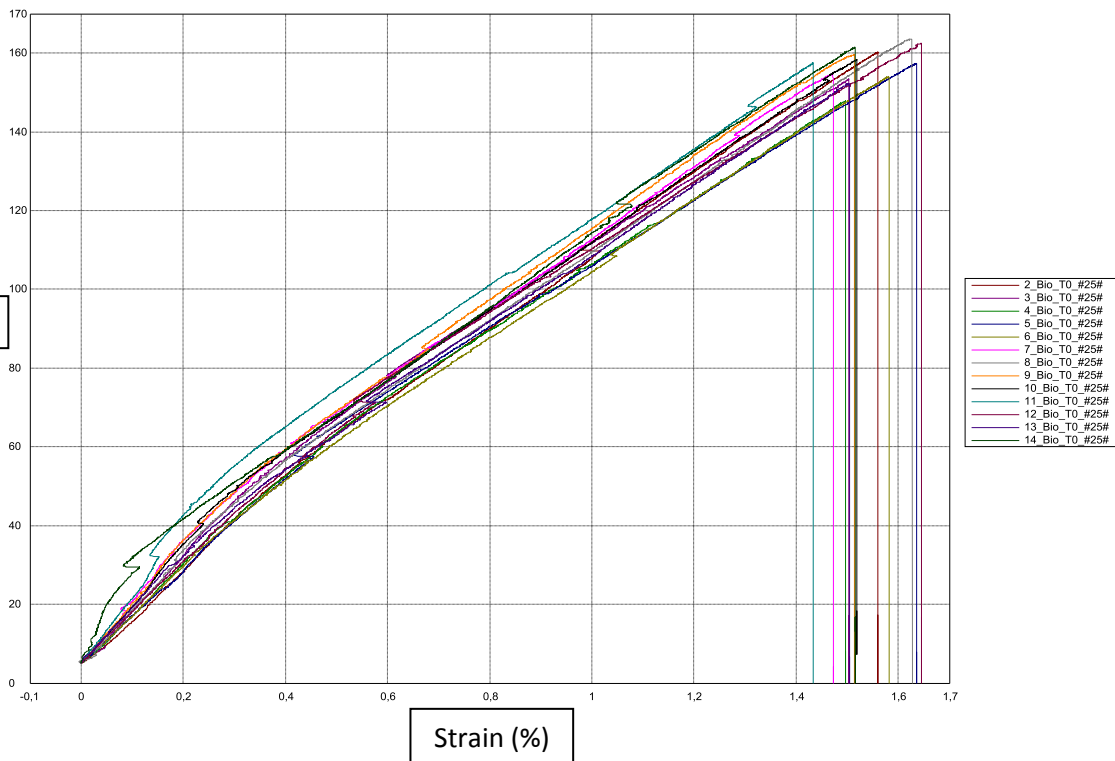




# Laminate 25 Araldite LY 1569 /Aradur 3489 (1% silane)-Biotex UD-Untreated

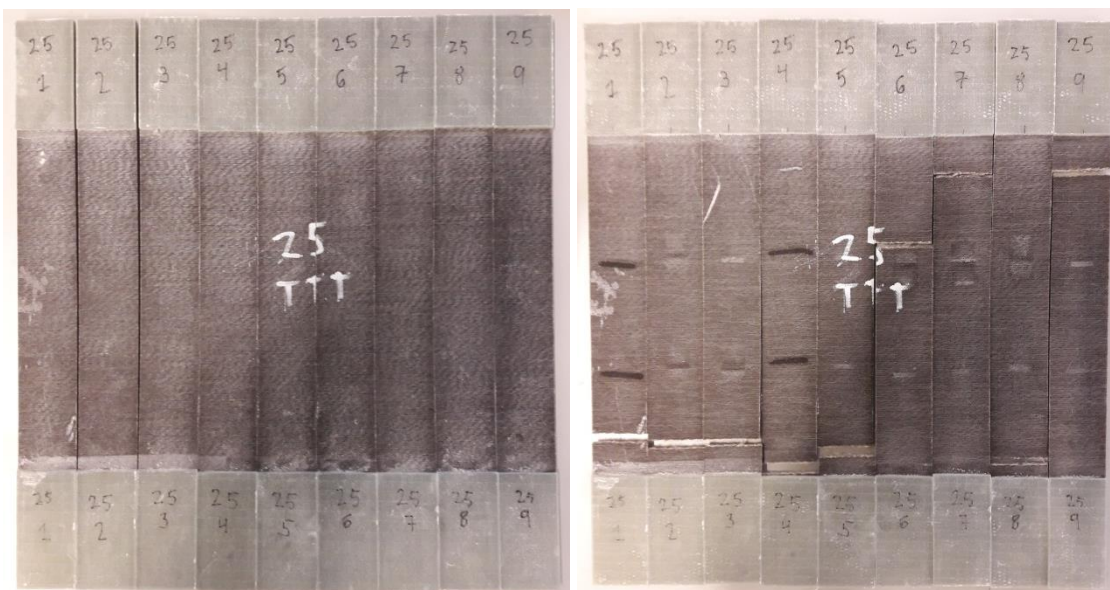
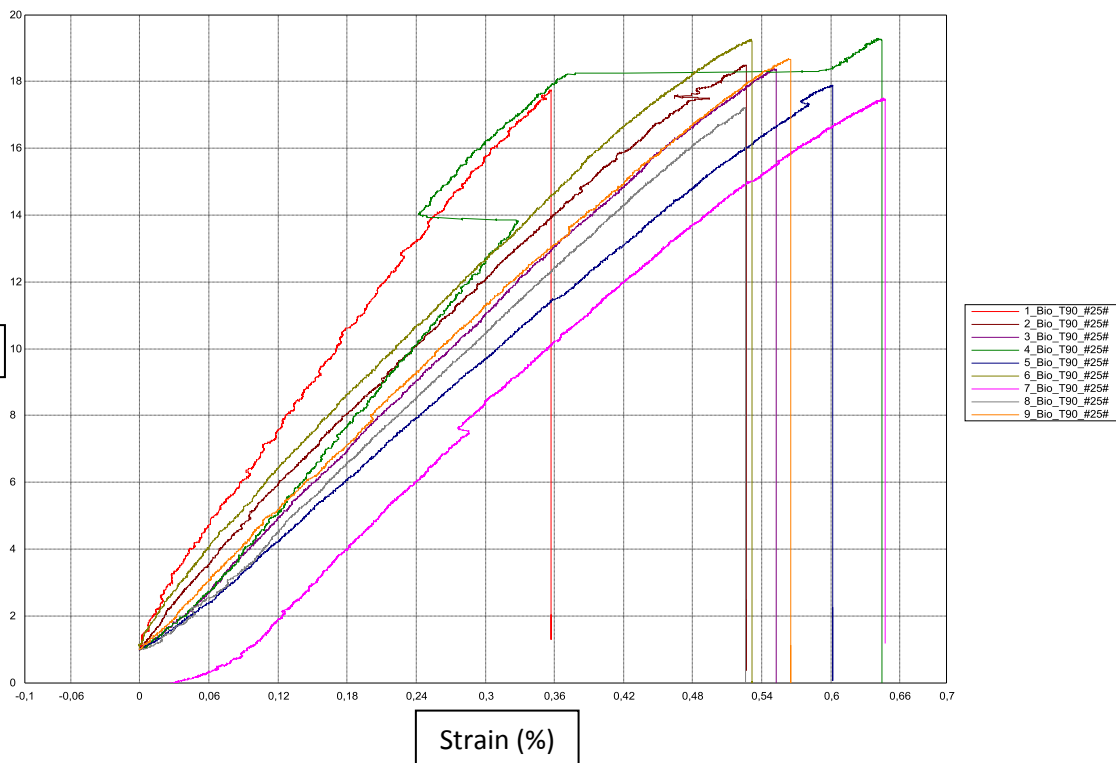
## Laminate 25 Tensile 0° test

Sample	ID	Longitudinal tensile test							Failure mode	Vf (%)	Mf (%)
		a mm	b mm	F kN	Ext Mpa	oxt Mpa	Ext %	vxy			
1	1 Bio_TO_#25#	2,11	15,57	5,36		163,18					
2	2 Bio_TO_#25#	2,18	15,55	5,43	12847,20	160,24	1,56	0,36	Bottom	32,51	38,6
3	3 Bio_TO_#25#	2,20	15,50	5,23	14424,10	153,37	1,50	0,82	Bottom		
4	4 Bio_TO_#25#	2,30	15,55	5,29	13308,80	147,84	1,50	0,61	Top		
5	5 Bio_TO_#25#	2,33	15,48	5,68	11934,60	157,44	1,64	0,59	Middle		
6	6 Bio_TO_#25#	2,30	15,48	5,48	12670,00	153,99	1,58	0,55	Bottom		
7	7 Bio_TO_#25#	2,34	15,52	5,62	15429,90	154,67	1,47	0,64	Bottom		
8	8 Bio_TO_#25#	2,30	15,51	5,84	14620,90	163,62	1,63	0,77	Top		
9	9 Bio_TO_#25#	2,30	15,52	5,70	15631,40	159,58	1,51	0,43	Middle		
10	10 Bio_TO_#25#	2,30	15,53	5,66	15729,90	158,33	1,52	0,79	Top		
11	11 Bio_TO_#25#	2,22	15,53	5,43	19412,60	157,51	1,43	0,66	Bottom		
12	12 Bio_TO_#25#	2,22	15,47	5,58	12504,90	162,55	1,65	0,40	Middle		
13	13 Bio_TO_#25#	2,30	15,52	5,44	13247,60	152,28	1,51	0,42	Top		
14	14 Bio_TO_#25#	2,18	15,50	5,46	12541,40	161,53	1,52	0,30	Middle		
Average value		2,26	15,52	5,51	<b>14177,18</b>	157,58	1,54	<b>0,56</b>			
Standard deviation				0,17	2039,66	4,66	0,07	0,17		Standard	EN ISO527-5
CV(%)				0,03	0,14	0,03	0,04	0,30		Precharge (kN)	5
Characteristic value					9891,36	<b>147,88</b>	<b>1,40</b>	0,20		Reference points	Stickers
										Testing speed (mm/min)	2
										Extensometry	Video
										Modulus (ε %)	0,05-0,25



## Laminate 25 Tensile 90° test

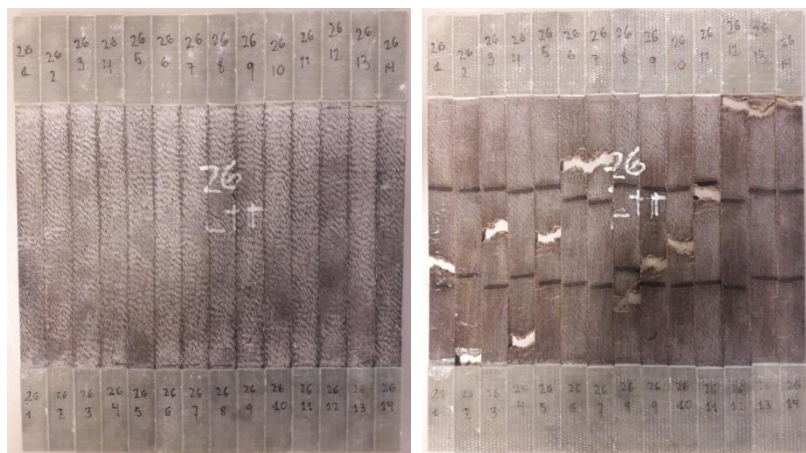
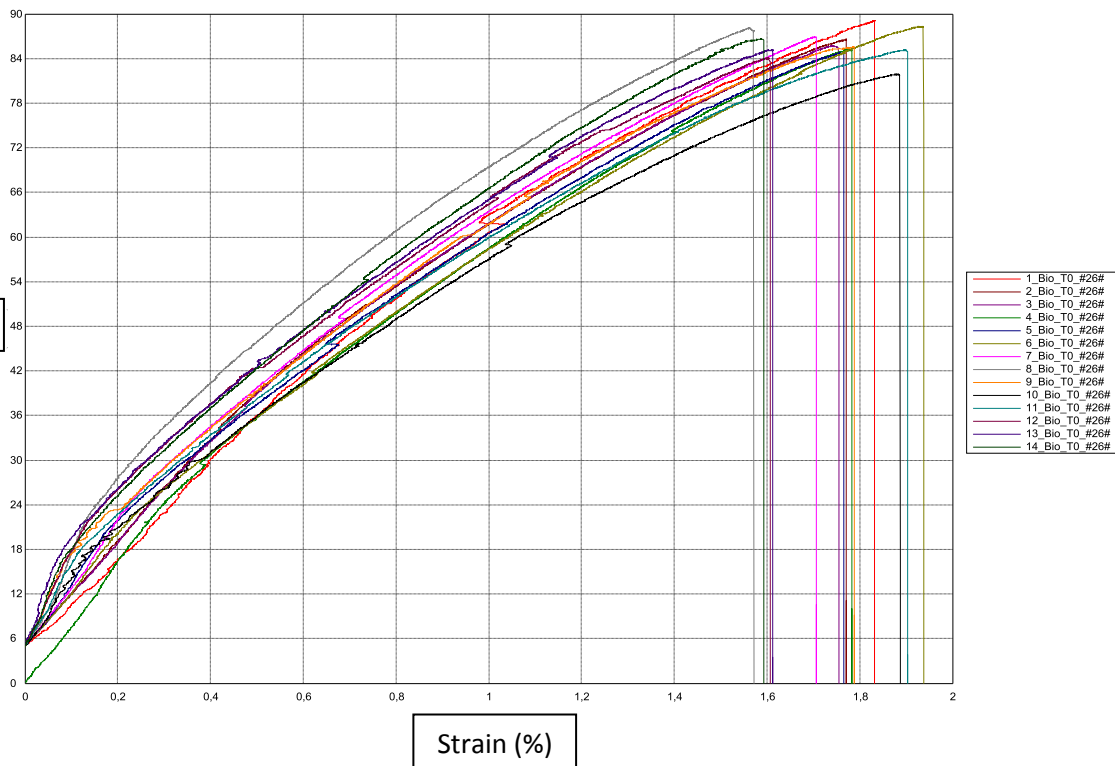
Sample	ID	Transverse tensile test						Failure mode	Vf	Mf
		a mm	b mm	F kN	Eyt Mpa	oyt Mpa	eyt %		(%)	(%)
1	1_Bio_T90_#25#	2,30	25,53	1,04	4766,93	17,74	0,36	Bottom	31,59	37,6
2	2_Bio_T90_#25#	2,33	25,51	1,10	3587,89	18,49	0,53	Bottom	Parameters	Value
3	3_Bio_T90_#25#	2,30	25,61	1,08	3497,29	18,36	0,55	Bottom		
4	4_Bio_T90_#25#	2,31	25,58	1,14	4147,54	19,29	0,64	Bottom	Testing speed (mm/min)	2
5	5_Bio_T90_#25#	2,32	25,64	1,06	3078,15	17,89	0,60	Bottom	Extensometry	Video
6	6_Bio_T90_#25#	2,31	25,60	1,14	3662,66	19,26	0,53	Middle	Reference points	Stickers
7	7_Bio_T90_#25#	2,42	25,60	1,08	3364,95	17,49	0,65	Top	Norma	EN ISO527-5
8	8_Bio_T90_#25#	2,31	25,60	1,02	3393,12	17,22	0,53	Bottom	Precharge (kN)	1
9	9_Bio_T90_#25#	2,29	25,56	1,09	3435,42	18,68	0,57	Top	Modulus (ε %)	0,05-0,25
Average value		2,32	25,58	1,08	<b>3659,33</b>	18,27	0,55			
Standard deviation				0,04	505,21	0,74	0,09			
CV(%)				0,04	0,14	0,04	0,16			
Characteristic value					2551,22	<b>16,65</b>	<b>0,36</b>			



# Laminate 26 Araldite LY 1569 /Aradur 3489 (1% silane)-Biotex UD-NaOH 1M\_3h

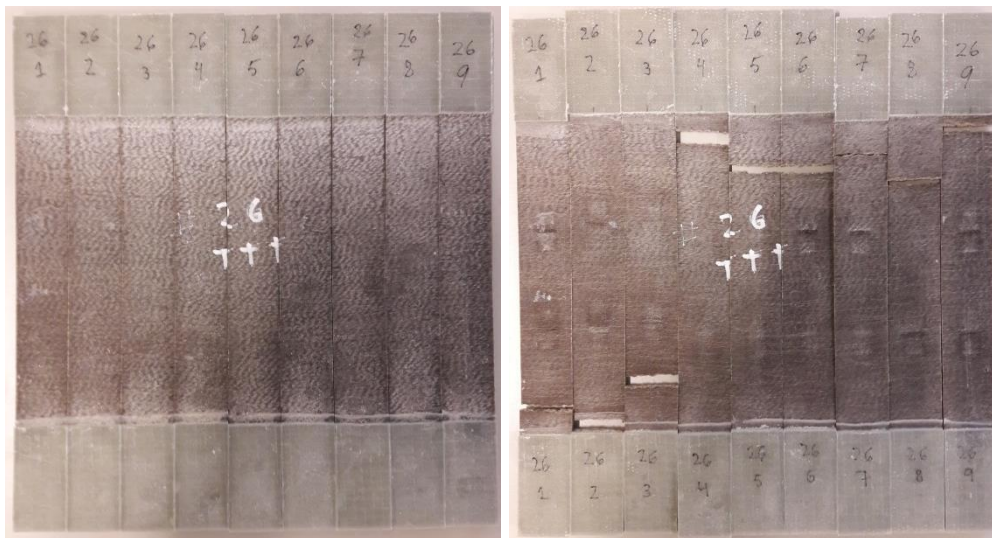
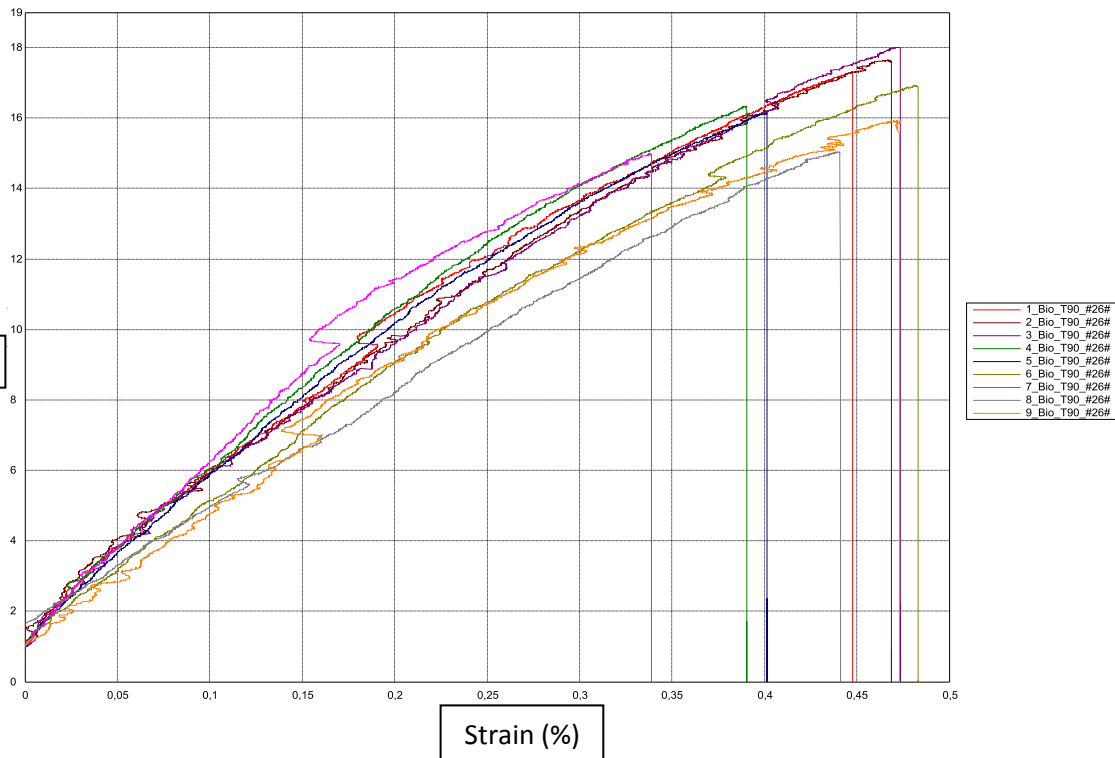
## Laminate 26 Tensile 0° test

Sample	ID	Longitudinal tensile test							Failure mode	Vf (%)	Mf (%)
		a mm	b mm	F kN	Ext Mpa	σxt Mpa	Ext %	vxy			
1	1 Bio_TO_#26#	2,90	15,48	4,00	6062,39	89,11	1,83		Middle	23,38	28,5
2	2 Bio_TO_#26#	3,00	15,47	4,02	7073,04	86,56	1,77	0,41	Bottom		
3	3 Bio_TO_#26#	2,95	15,44	3,90	7001,18	85,68	1,76	0,41	Middle		
4	4 Bio_TO_#26#	3,10	15,50	4,09	8640,83	85,17	1,78	0,79	Bottom		
5	5 Bio_TO_#26#	3,27	15,50	4,30	8518,94	84,77	1,77	0,66	Middle		
6	6 Bio_TO_#26#	3,12	15,50	4,27	7792,02	88,30	1,94	0,76	Middle		
7	7 Bio_TO_#26#	3,15	15,49	4,24	8918,14	86,93	1,71	0,53	Middle		
8	8 Bio_TO_#26#	3,09	15,52	4,23	10799,70	88,12	1,57		Middle		
9	9 Bio_TO_#26#	3,29	15,51	4,37	6805,29	85,60	1,79	0,65	Middle		
10	10 Bio_TO_#26#	3,42	15,44	4,32	7096,19	81,87	1,89	0,59	Middle		
11	11 Bio_TO_#26#	3,26	15,51	4,30	7448,78	85,12	1,90	0,47	Middle		
12	12 Bio_TO_#26#	3,08	15,53	4,02	8731,97	84,05	1,61	0,66	Top		
13	13 Bio_TO_#26#	3,21	15,46	4,23	7373,47	85,15	1,61	0,48	Top		
14	14 Bio_TO_#26#	3,06	15,40	4,08	7707,10	86,63	1,59	0,37	Top		
Average value		3,14	15,48	4,17	<b>7854,93</b>	85,93	1,75	<b>0,57</b>			
Standard deviation				0,15	1185,92	1,88	0,12	0,14			
CV(%)				0,04	0,15	0,02	0,07	0,25			
Characteristic value					5382,71	<b>82,02</b>	<b>1,50</b>	0,27			
									Testing speed (mm/min)	2	
									Extensometry	Video	
									Reference points	Stickers	
									Standard	EN ISO527-5	
									Precharge (kN)	5	
									Modulus (ε %)	0,05-0,25	



# Laminate 26 Tensile 90° test

Sample	ID	Transverse tensile test						Failure mode	Vf	Mf
		a mm	b mm	F kN	Eyt Mpa	oyt Mpa	eyt %		(%)	(%)
1	1_Bio_T90_#26#	3,17	25,53	1,40	4253,69	17,32	0,45	Bottom	22,14	27,1
2	2_Bio_T90_#26#	3,21	25,64	1,45	3825,74	17,66	0,47	Bottom	Parameters	Value
3	3_Bio_T90_#26#	3,23	25,76	1,50	3803,26	18,01	0,47	Bottom		
4	4_Bio_T90_#26#	3,38	25,79	1,42	4379,05	16,34	0,39	Top	Testing speed (mm/min)	2
5	5_Bio_T90_#26#	3,33	25,44	1,37	4261,18	16,13	0,40	Top	Extensometry	Video
6	6_Bio_T90_#26#	3,42	25,63	1,48	3870,56	16,92	0,48	Top	Reference points	Stickers
7	7_Bio_T90_#26#	3,39	25,72	1,31	4879,11	14,99	0,34	Top	Norma	EN ISO527-5
8	8_Bio_T90_#26#	3,40	25,75	1,32	3293,20	15,04	0,44	Top	Precharge (kN)	1
9	9_Bio_T90_#26#	3,28	25,60	1,34	4146,95	15,93	0,47	Top	Modulus (ε %)	0,05-0,25
Average value		3,31	25,65	1,40	<b>4079,19</b>	16,48	0,44			
Standard deviation				0,07	447,16	1,08	0,05			
CV(%)				0,05	0,11	0,07	0,11			
Characteristic value					3098,42	<b>14,11</b>	<b>0,33</b>			

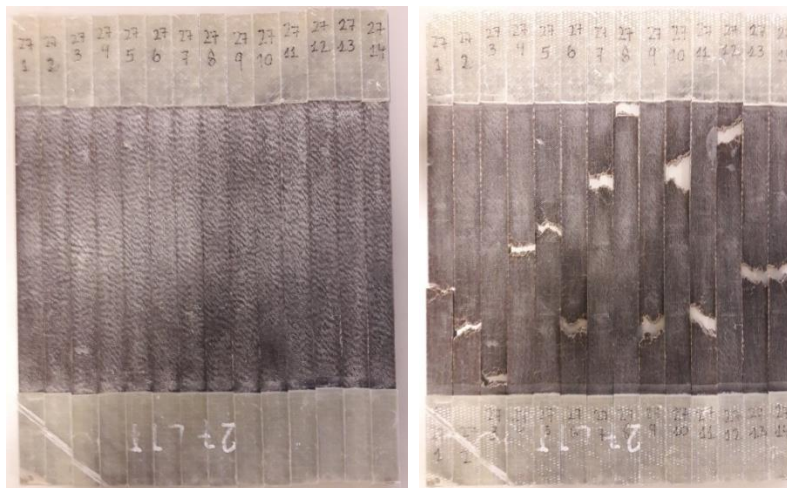
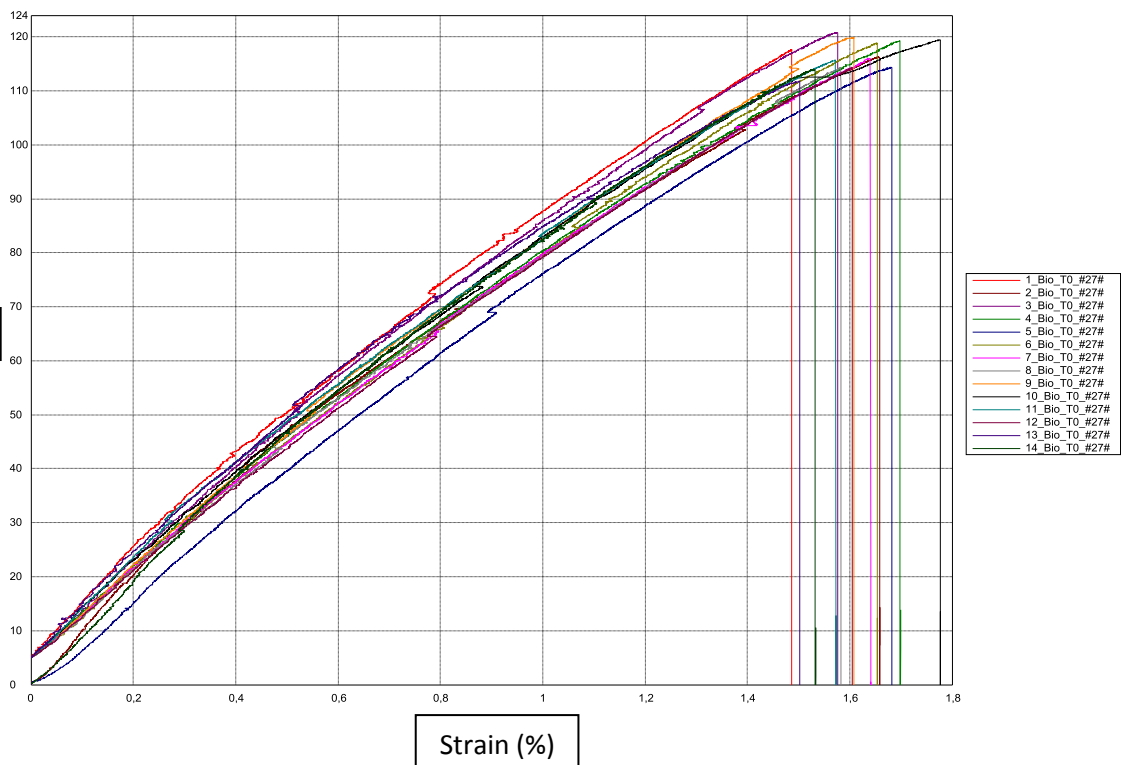




## Laminate 27 Araldite LY 1569 /Aradur 3489-Biotex UD-1% silane

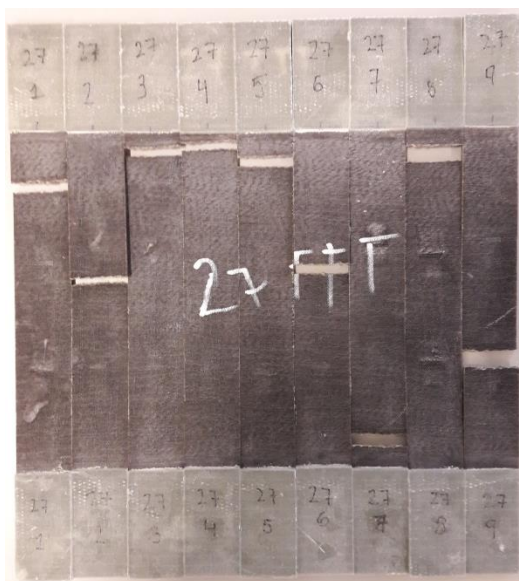
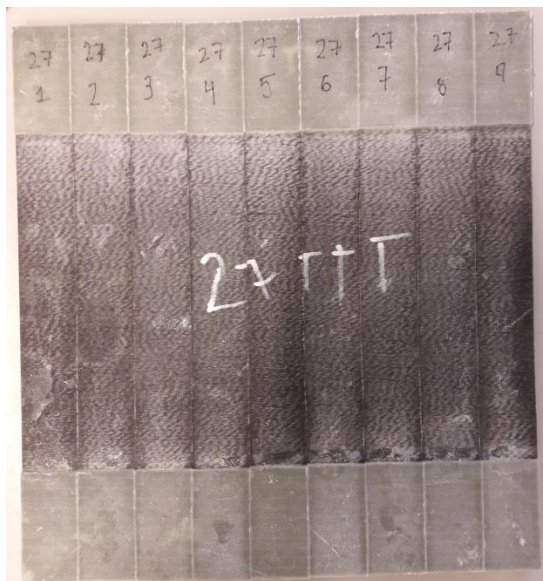
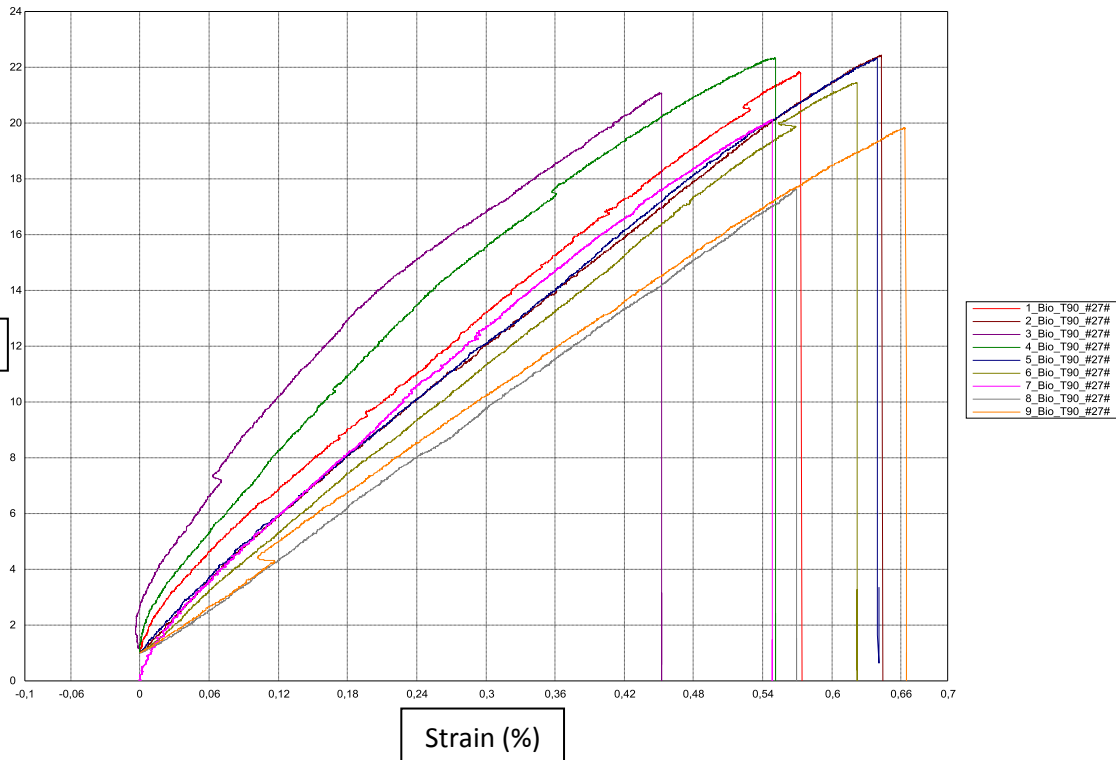
### Laminate 27 Tensile 0° test

Sample	ID	Longitudinal tensile test							Failure mode	Vf (%)	Mf (%)		
		a mm	b mm	F kN	Ext Mpa	$\sigma_{xt}$ Mpa	Ext %	vxy %					
1	1_Bio_TO_#27#	2,48	14,72	4,29	10169,90	117,61	1,49	0,25	Middle	27,61	33,2		
2	2_Bio_TO_#27#	2,55	14,80	4,39	10569,80	116,31	1,66	0,26				Bottom	
3	3_Bio_TO_#27#	2,63	14,73	4,68	9293,36	120,85	1,58		Bottom	Parameters	Value		
4	4_Bio_TO_#27#	2,58	14,78	4,55	8555,02	119,28	1,70		Middle				
5	5_Bio_TO_#27#	2,78	14,76	4,69	8870,52	114,40	1,68		Middle				
6	6_Bio_TO_#27#	2,73	14,78	4,80	8834,74	118,84	1,65		Bottom				
7	7_Bio_TO_#27#	2,66	14,78	4,56	8732,16	116,06	1,64	0,32	Middle				
8	8_Bio_TO_#27#	2,68	14,73	4,51	8787,60	114,27	1,58	0,21	Tab				
9	9_Bio_TO_#27#	2,64	14,62	4,63	8925,52	119,86	1,61	0,22	Bottom				
10	10_Bio_TO_#27#	2,65	14,66	4,64	8908,91	119,50	1,78	0,29	Top				
11	11_Bio_TO_#27#	2,77	14,73	4,72	9523,20	115,62	1,57	0,30	Bottom				
12	12_Bio_TO_#27#	2,69	14,73	4,53	8454,35	114,35	1,61	0,24	Top				
13	13_Bio_TO_#27#	2,70	14,69	4,43	9509,66	111,75	1,50	0,36	Middle				
14	14_Bio_TO_#27#	2,64	14,59	4,39	10329,10	113,92	1,53	0,42	Middle				
Average value		2,66	14,72	4,56	<b>9247,42</b>	116,62	1,61	<b>0,29</b>				Testing speed (mm/min)	2
Standard deviation				0,15	681,20	2,74	0,08	0,07				Extensometry	Video
CV(%)				0,03	0,07	0,02	0,05	0,23		Reference points	Stickers		
Characteristic value					7827,35	<b>110,90</b>	<b>1,45</b>	0,14		Standard	EN ISO527-5		
										Precharge (kN)	5		
										Modulus (ε %)	0,05-0,25		



## Laminate 27 Tensile 90° test

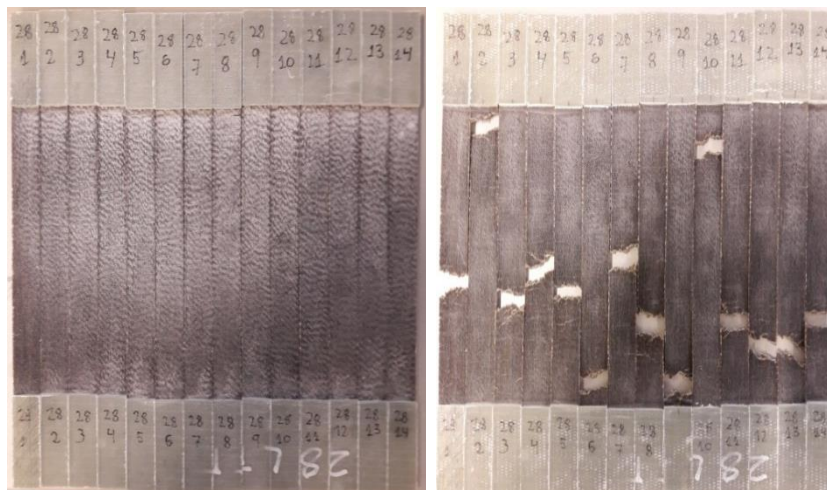
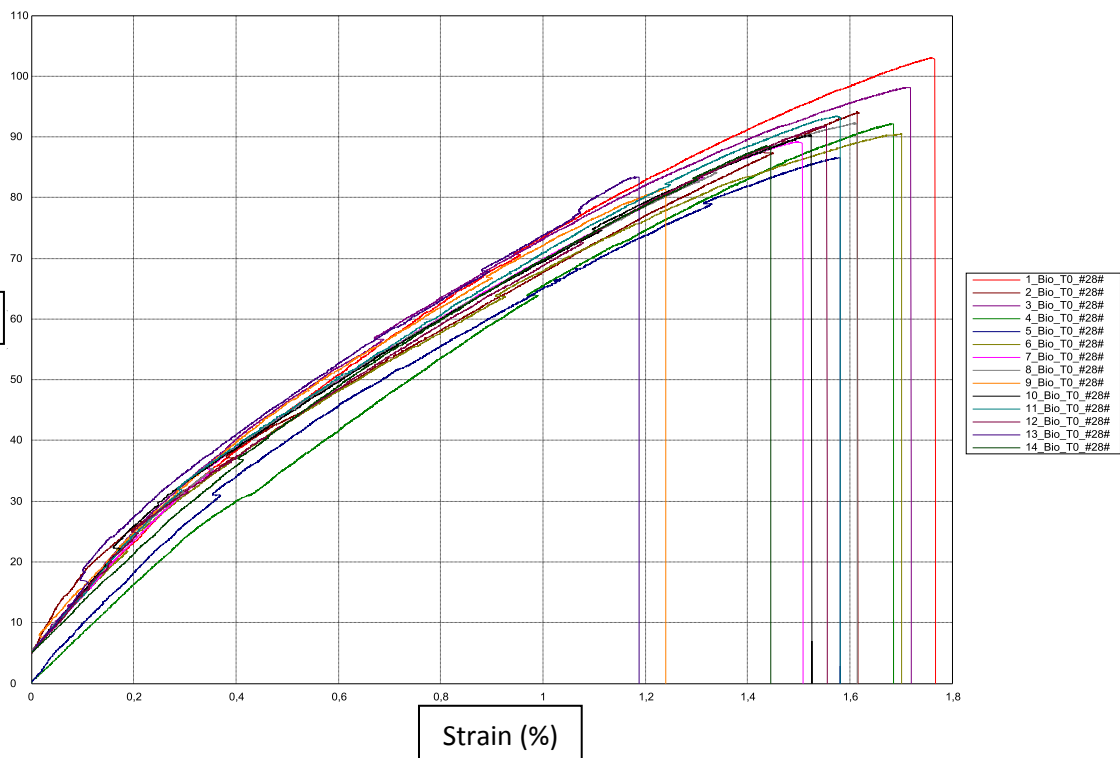
Sample	ID	Transverse tensile test						Failure mode	Vf	Mf
		a mm	b mm	F kN	Eyt Mpa	oyt Mpa	eyt %		(%)	(%)
1	1_Bio_T90_#27#	2,70	25,29	1,49	3536,19	21,83	0,57	Top	26,85	32,4
2	2_Bio_T90_#27#	2,62	25,33	1,49	3588,87	22,41	0,64	Middle	Parameters	Value
3	3_Bio_T90_#27#	2,64	25,27	1,41	4675,62	21,07	0,45	Top		
4	4_Bio_T90_#27#	2,64	25,20	1,49	4542,67	22,33	0,55	Top	Testing speed (mm/min)	2
5	5_Bio_T90_#27#	2,66	25,18	1,49	3533,98	22,32	0,64	Top	Extensometry	Video
6	6_Bio_T90_#27#	2,80	25,30	1,52	3409,44	21,44	0,62	Middle	Reference points	Stickers
7	7_Bio_T90_#27#	2,83	25,33	1,44	3815,34	20,11	0,55	Bottom	Norma	EN ISO527-5
8	8_Bio_T90_#27#	2,82	25,21	1,25	3086,32	17,62	0,57	Top	Precharge (kN)	1
9	9_Bio_T90_#27#	2,87	25,07	1,43	3319,30	19,82	0,66	Middle	Modulus (ε %)	0,05-0,25
Average value		2,73	25,24	1,44	<b>3723,08</b>	20,99	0,59			
Standard deviation				0,08	541,20	1,58	0,07			
CV(%)				0,06	0,15	0,08	0,11			
Characteristic value					2536,06	<b>17,53</b>	<b>0,44</b>			



# Laminate 28 Araldite LY 1569 /Aradur 3489-Biotex UD-1% silane + NaOH 1M\_3h

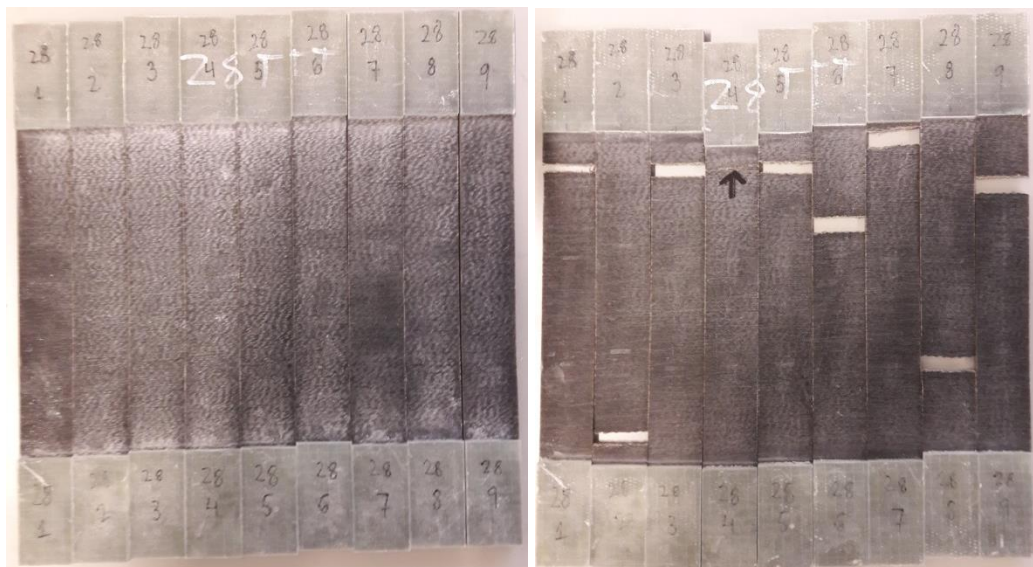
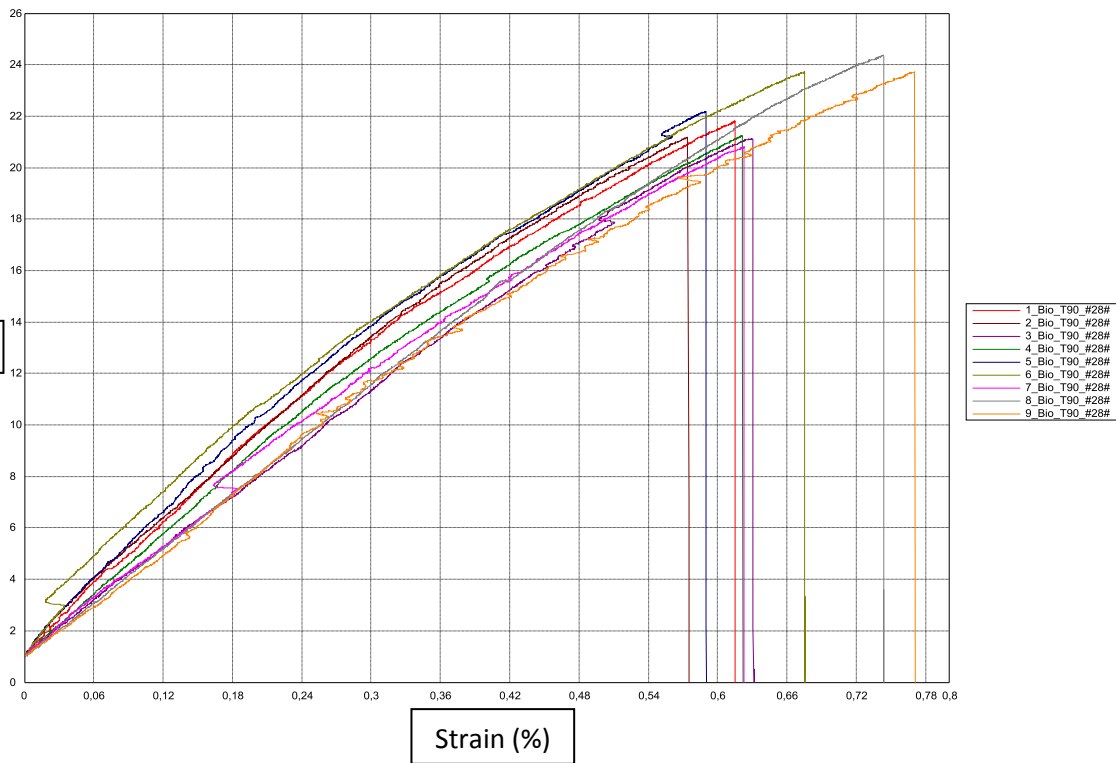
## Laminate 28 Tensile 0° test

Sample	ID	Longitudinal tensile test							Failure mode	Vf	Mf
		a mm	b mm	F kN	Ext Mpa	σxt Mpa	Ext %	vxy		(%)	(%)
1	1 Bio_TO_#28#	2,57	14,72	3,90	8676,80	103,01	1,77	0,40	Middle	25,06	31
2	2 Bio_TO_#28#	2,71	14,73	3,76	7925,24	94,07	1,62	0,44	Top		
3	3 Bio_TO_#28#	2,88	14,67	4,15	9637,17	98,17	1,72	0,60	Middle		
4	4 Bio_TO_#28#	2,77	14,73	3,76	7984,33	92,17	1,69		Middle		
5	5 Bio_TO_#28#	2,94	14,73	3,75	8501,73	86,57	1,58	0,71	Middle		
6	6 Bio_TO_#28#	3,10	14,77	4,14	9227,89	90,50	1,70	0,79	Bottom		
7	7 Bio_TO_#28#	3,01	14,68	3,94	8970,15	89,20	1,51	0,34	Middle		
8	8 Bio_TO_#28#	3,04	14,68	4,12	9219,70	92,23	1,62	0,47	Middle		
9	9 Bio_TO_#28#	2,97	14,63	3,54	8802,18	81,42	1,24	0,51	Bottom		
10	10 Bio_TO_#28#	3,07	14,52	4,02	10280,20	90,25	1,53	0,88	Top		
11	11 Bio_TO_#28#	3,04	14,66	4,16	9498,57	93,41	1,58	0,63	Middle		
12	12 Bio_TO_#28#	2,88	14,71	3,89	9677,50	91,74	1,56	0,56	Bottom		
13	13 Bio_TO_#28#	3,05	14,61	3,72	10502,90	83,39	1,19	0,56	Bottom		
14	14 Bio_TO_#28#	2,93	14,65	3,80	7998,83	88,52	1,45	0,47	Middle		
Average value		2,93	14,68	3,90	9064,51	91,05	1,55	0,57		Testing speed (mm/min)	2
Standard deviation				0,19	815,00	5,50	0,17	0,15		Extensometry	Video
CV(%)				0,05	0,09	0,06	0,11	0,27		Reference points	Stickers
Characteristic value					7365,53	79,57	1,20	0,23		Standard	EN ISO527-5
										Precharge (kN)	5
										Modulus (ε %)	0,05-0,25



### Laminate 28 Tensile 90° test

Sample	ID	Transverse tensile test						Failure mode	Vf	Mf
		a mm	b mm	F kN	Eyt Mpa	oyt Mpa	eyt %		(%)	(%)
1	1_Bio_T90_#28#	3,17	24,85	1,72	4120,74	21,80	0,62	Top	22,98	28
2	2_Bio_T90_#28#	3,14	25,36	1,69	3956,53	21,17	0,57	Bottom	Parameters	Value
3	3_Bio_T90_#28#	3,21	25,27	1,71	3325,78	21,13	0,63	Top		
4	4_Bio_T90_#28#	3,21	25,31	1,73	3984,09	21,26	0,62	Top	Testing speed (mm/min)	2
5	5_Bio_T90_#28#	3,18	25,28	1,78	4300,32	22,19	0,59	Top	Extensometry	Video
6	6_Bio_T90_#28#	3,12	25,20	1,86	3960,75	23,72	0,68	Middle	Reference points	Stickers
7	7_Bio_T90_#28#	3,33	25,17	1,74	3943,17	20,79	0,62	Top	Norma	EN ISO527-5
8	8_Bio_T90_#28#	3,05	25,16	1,87	3536,83	24,37	0,74	Bottom	Precharge (kN)	1
9	9_Bio_T90_#28#	3,30	24,85	1,94	3718,65	23,72	0,77	Top	Modulus (ε %)	0,05-0,25
Average value		3,19	25,16	1,78	<b>3871,87</b>	22,24	0,65			
Standard deviation				0,09	298,37	1,35	0,07			
CV(%)				0,05	0,08	0,06	0,10			
Characteristic value					3217,45	<b>19,28</b>	<b>0,50</b>			

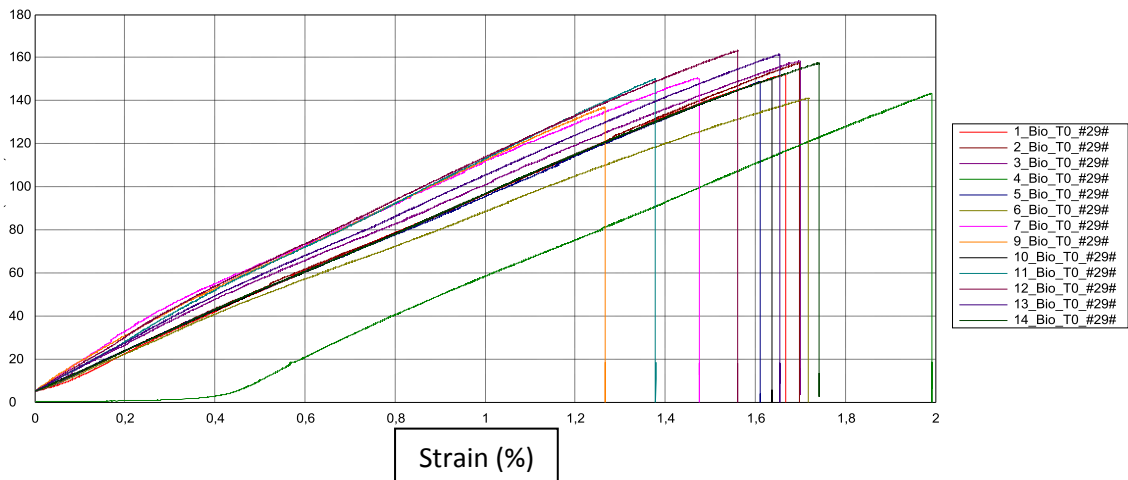




## Laminate 29 Araldite LY 1569 /Aradur 3489-Biotex UD

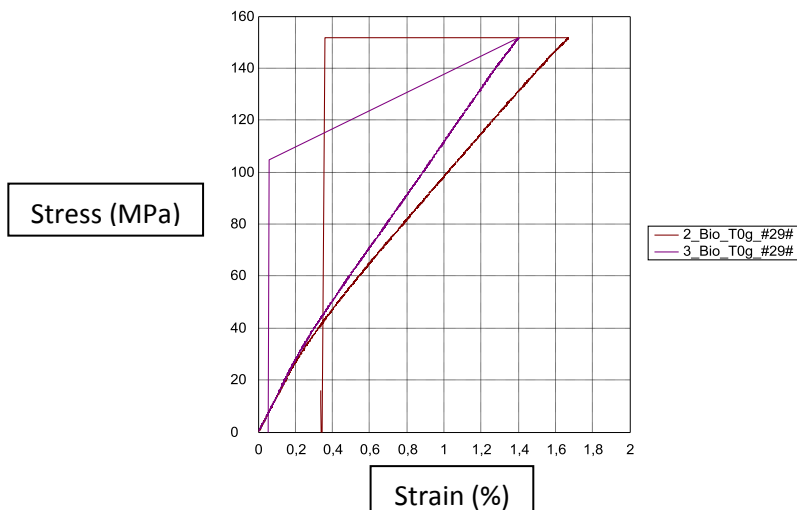
### Laminate 29 Tensile 0° test

Sample	ID	Longitudinal tensile test						Vf (%)	Mf (%)
		a (mm)	b (mm)	F (kN)	Ext (Mpa)	oxt (Mpa)	ext (%)		
1	1_Bio_TO_#29#	2,19	14,50	4,831	10295,900	152,147	1,669	32	45
2	2_Bio_TO_#29#	2,14	15,48	5,212	10016,500	157,342	1,699		
3	3_Bio_TO_#29#	2,18	15,38	5,311	11051,100	158,391	1,701		
4	4_Bio_TO_#29#	2,19	14,67	4,610	263,631	143,484	1,992	Parameters	Value
5	5_Bio_TO_#29#	2,24	14,85	4,947	10041,100	148,707	1,611		
6	6_Bio_TO_#29#	2,54	15,05	5,395	9186,350	141,131	1,719		
7	7_Bio_TO_#29#	2,27	15,00	5,122	13848,200	150,425	1,476		
8	8_Bio_TO_#29#	2,26	14,96					Testing speed (mm/min)	2
9	9_Bio_TO_#29#	2,26	14,98	4,635	11985,800	136,902	1,268	Extensometry	Video
10	10_Bio_TO_#29#	2,37	14,72	5,232	9601,120	149,960	1,636	Reference points	Stickers
11	11_Bio_TO_#29#	2,31	14,93	5,174	11847,500	150,012	1,379	Norma	EN ISO527-5
12	12_Bio_TO_#29#	2,27	14,93	5,533	12799,600	163,252	1,561	Precharge (kN)	5
13	13_Bio_TO_#29#	2,22	14,97	5,365	11239,800	161,426	1,655	Modulus (ε %)	0,05-0,25
14	14_Bio_TO_#29#	2,31	15,00	5,450	9524,930	157,292	1,742		
Average value		2,27	14,96	5,14	<b>10130,89</b>	151,57	1,62		
Standard deviation		0,10	0,25	0,30	3270,52	7,91	0,18		
CV(%)				0,06	0,32	0,05	0,11		
Characteristic value					3197,81	<b>134,81</b>	<b>1,24</b>		



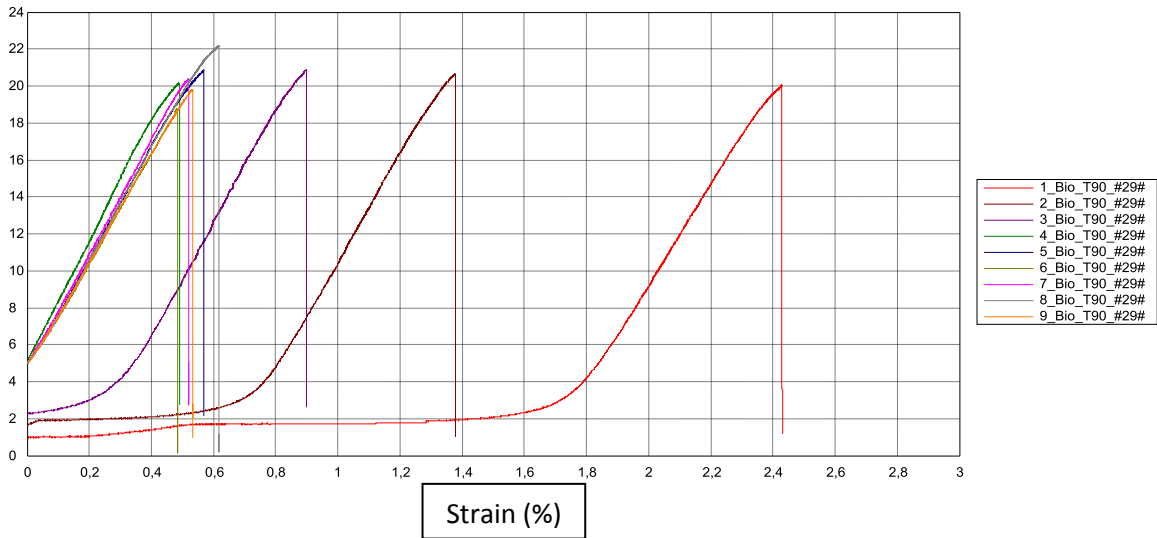
### Laminate 29 Tensile 0° test –gauges

Sample	ID	Longitudinal tensile test							Vf (%)	Mf (%)
		a (mm)	b (mm)	F (kN)	Ext (Mpa)	oxt (Mpa)	ext (%)	vxy		
1	1_Bio_TOg_#29#	2,13	14,88	5,00		158,00			33,4	46,5
2	2_Bio_TOg_#29#	2,26	14,62	5,01	13100,00	152,00	1,70	0,43	Parameters	Value
3	3_Bio_TOg_#29#	2,10	14,95	4,76	13800,00	152,00	1,40	0,49		
Average value		2,16	14,82	4,92	13450,00	154,00	1,55	0,46		
Standard deviation				0,14	494,97	3,46	0,21	0,04		
CV(%)				0,03	0,04	0,02	0,14	0,09		
Characteristic value					12364,36	<b>146,40</b>	<b>1,08</b>	<b>0,37</b>		



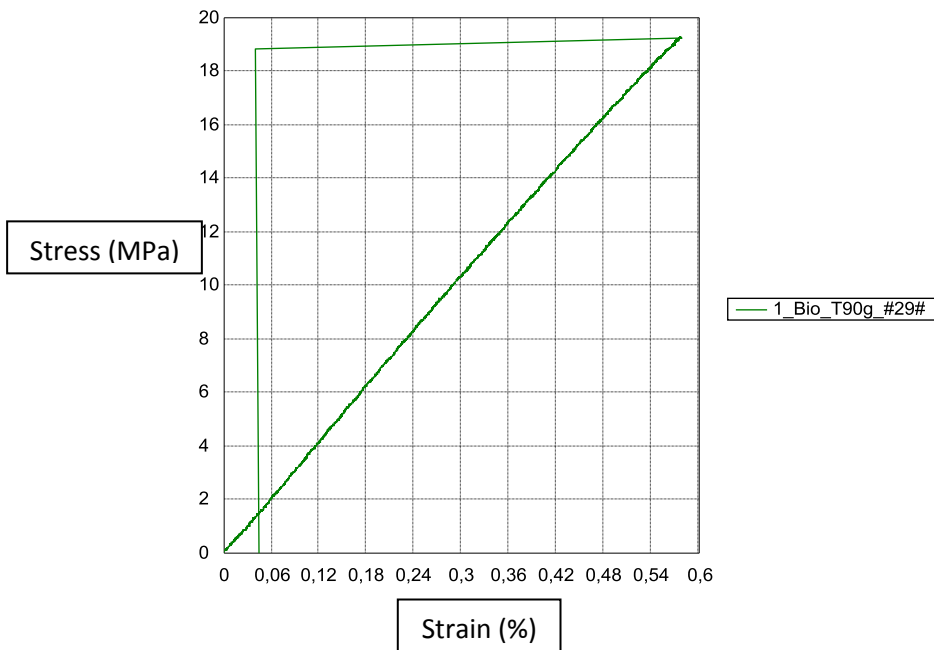
### Laminate 29 Tensile 90° test

ID	Transverse tensile test						Vf	Mf
	a mm	b mm	F kN	Eyt Mpa	oyt Mpa	eyt %	(%)	(%)
1_Bio_T90_#29#	2,41	25,33	1,22	45,35	20,05	0,73	31,1	27
2_Bio_T90_#29#	2,34	25,35	1,22	42,74	20,64	0,60	Parameters	Value
3_Bio_T90_#29#	2,33	25,4	1,24	534,24	20,89	0,63		
4_Bio_T90_#29#	2,43	25,06	1,23	3233,71	20,14	0,49	Testing speed (mm/min)	2
5_Bio_T90_#29#	2,36	25,36	1,25	2991,92	20,84	0,57	Extensometry	Video
6_Bio_T90_#29#	2,46	25,36	1,17	2861,46	18,76	0,48	Reference points	Stickers
7_Bio_T90_#29#	2,31	25,38	1,20	3047,46	20,40	0,52	Norma	EN ISO527-5
8_Bio_T90_#29#	2,22	25,36	1,25	3018,23	22,16	0,62	Precharge (kN)	1
9_Bio_T90_#29#	2,37	25,38	1,19	2867,93	19,81	0,53	Modulus (ε %)	0,05-0,25
	2,36	25,33	1,22	<b>2071,45</b>	20,41	0,57		
			0,03	1409,31	0,93	0,08		
			0,02	0,68	0,05	0,14		
				-1019,65	<b>18,38</b>	<b>0,40</b>		



### Laminate 29 Tensile 90° test

Sample	ID	Transverse tensile test							Vf	Mf
		a mm	b mm	F kN	Eyt Mpa	oyt Mpa	eyt %	vyx	(%)	(%)
1	1_Bio_T90g_#29#	2,3	24,9	1,1	3510	19,3	0,73	0,11	33,4	46,5

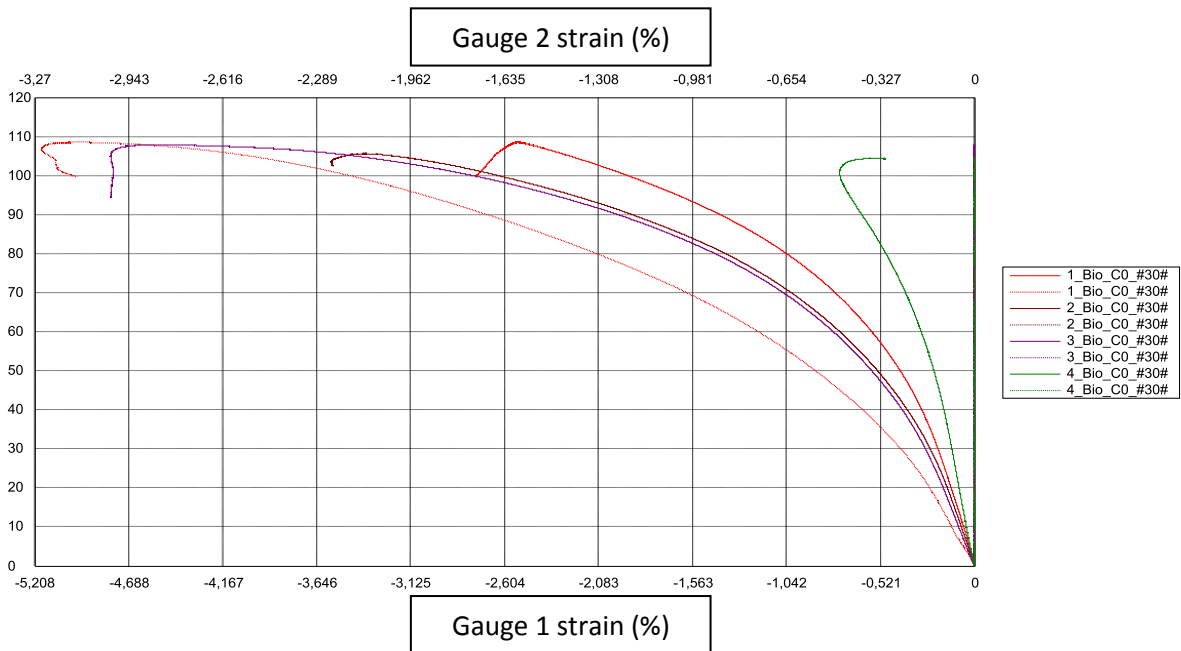


# Laminate 30 SuperSap CLR/INF-Biotex UD

## Laminate 30 Compression 0° test

Sample	ID	Longitudinal compression test						Vf (%)	Mf (%)
		a (mm)	b (mm)	F (kN)	Exc (MPa)	σxc (MPa)	exc (%)		
1	1_Bio_CO_#30#	3,62	24,79	9730,00	11512,75	108,00	2,80	0,31	43,8
2	2_Bio_CO_#30#	3,66	24,84	9600,00	10575,00	106,00	3,60		
3	3_Bio_CO_#30#	3,40	24,90	9130,00	10436,00	108,00	4,80		
4	4_Bio_CO_#30#	3,40	25,07	8890,00		104,00			
5	5_Bio_CO_#30#	3,51	25,29	9700,00	10183,50	109,00	3,90		
Average value		3,52	24,98	9410,00	<b>10676,81</b>	107,00	3,78	Parameters	Value
Standard deviation		0,12	0,20	377,96	580,37	2,00	0,83		
CV(%)				0,04	0,05	0,02	0,22		
Characteristic value					9446,49	<b>102,76</b>	<b>2,02</b>		

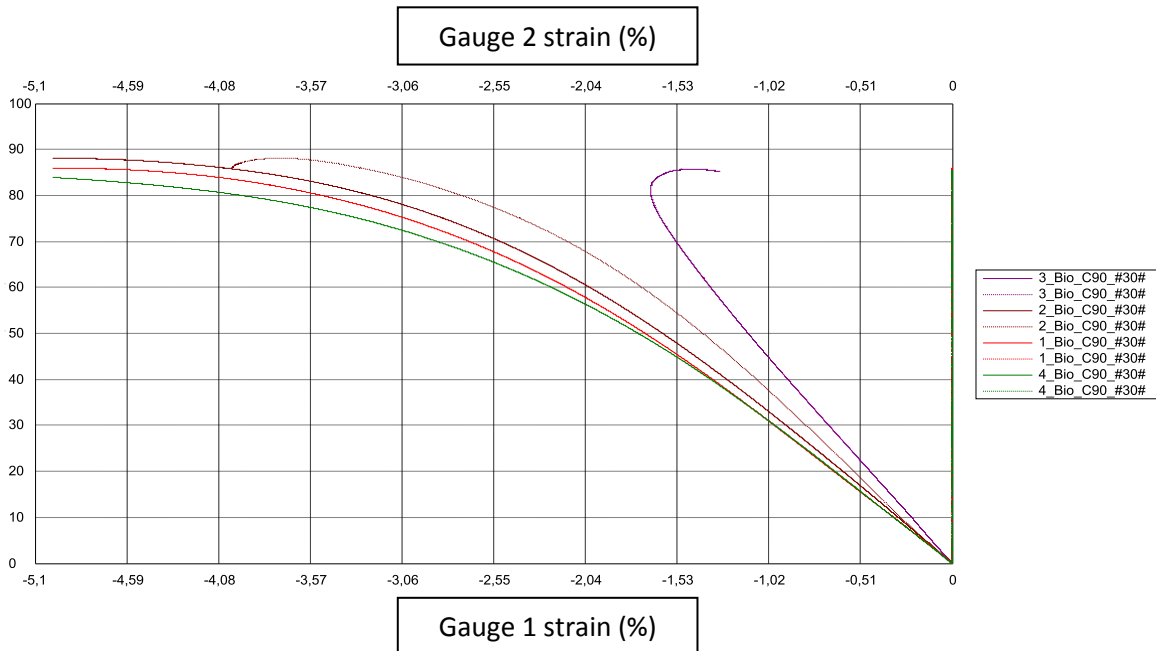
Module	Exc	Exc1	Gauge 1		Exc2	Gauge 2	
			σxc 0,1	σxc 0,3		σxc 0,1	σxc 0,3
1_Bio_CO_#30#	11512,75	12570,50	15,67	40,81	10455,00	12,81	33,72
2_Bio_CO_#30#	10575,00	10575,00	13,61	34,76	0,00		
3_Bio_CO_#30#	10436,00	10436,00	11,53	32,40	0,00		
4_Bio_CO_#30#	0,00	0,00			0,00		
5_Bio_CO_#30#	10183,50	9791,50	13,34	32,92	10575,50	14,13	35,28



### Laminate 30 Compression 90° test

Sample	ID	Transverse compression test						Vf	Mf
		a	b	F	E <sub>yc</sub>	σ <sub>yc</sub>	ε <sub>yc</sub>	(%)	(%)
		mm	mm	kN	MPa	MPa	%		
1	1_Bio_C90_#30#	3,60	24,93	7720	2980,00	86,00		0,31	43,8
2	2_Bio_C90_#30#	3,48	24,98	7660	3315,00	88,10	4,35		
3	3_Bio_C90_#30#	3,52	24,91	7520	4475,00	85,70			
4	4_Bio_C90_#30#	3,65	25,27	7870	2884,00	85,30	5,00		
Average value		3,56	25,02	7692,50	<b>3413,50</b>	86,28	4,68	Parameters	Value
Standard deviation		0,08	0,17	145,00	731,39	1,25	0,46		
CV(%)				0,02	0,21	0,01	0,10		
Characteristic value					1863,06	<b>83,63</b>	<b>3,70</b>		

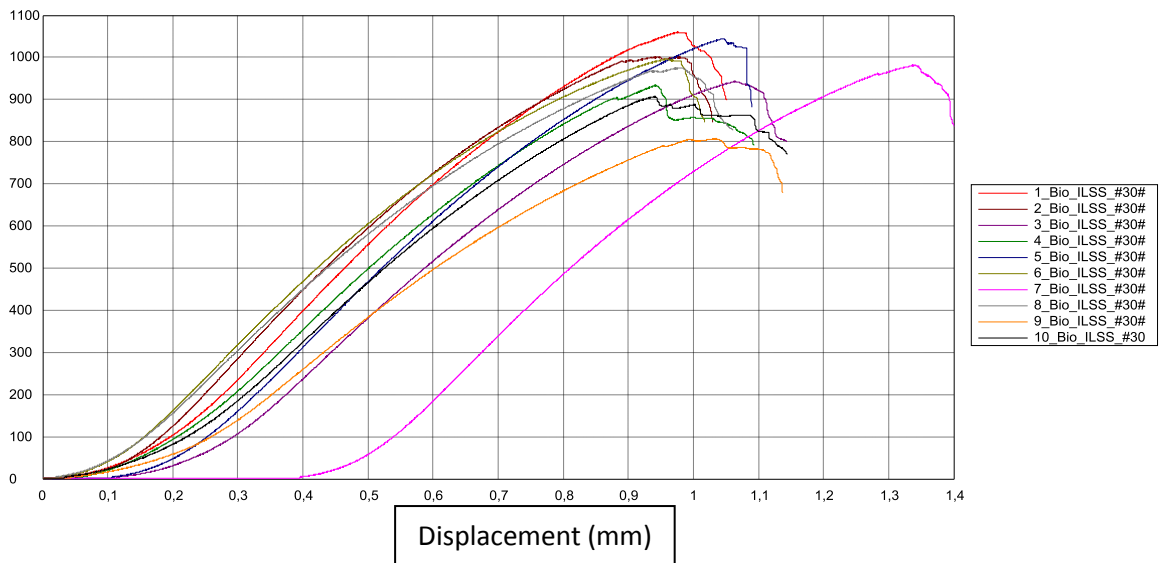
Module	Gauge 1		Gauge 2	
	Exc	Exc1	σ <sub>xc</sub> 0,1	σ <sub>xc</sub> 0,3
1_Bio_C90_#30#	<b>2980,00</b>	<b>2980,00</b>	3,40	9,36
2_Bio_C90_#30#	<b>3315,00</b>	<b>3315,00</b>	3,40	10,03
3_Bio_C90_#30#	<b>4475,00</b>	<b>4475,00</b>	4,30	13,25
4_Bio_C90_#30#	<b>2884,00</b>	<b>2884,00</b>	3,35	9,12





### Laminate 30 ILSS test

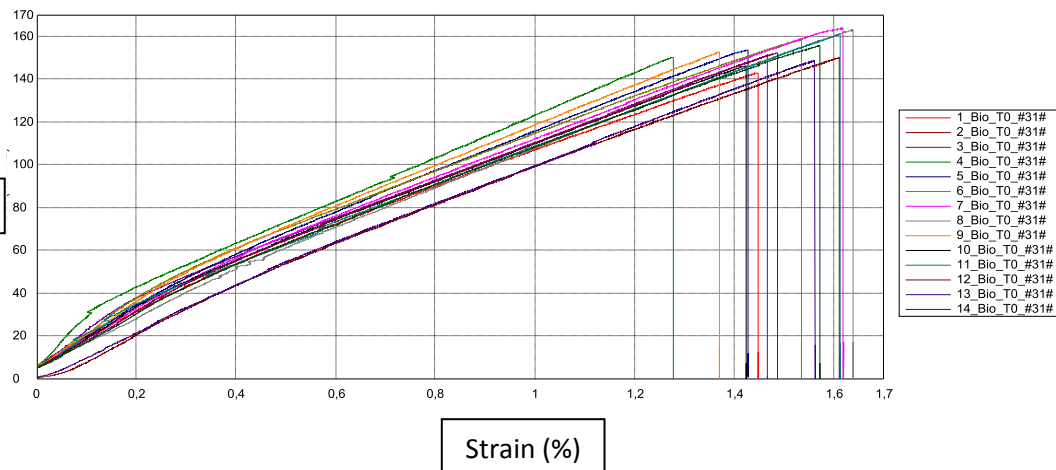
ILSS Sample	Fmax N	Short-beam Stregth N/mm2	Max strength N/mm2	Max displacement mm
1_Bio_ILSS_#30#	1750	18,52	1060,00	0,98
2_Bio_ILSS_#30#	1860	18,65	1000,00	0,94
3_Bio_ILSS_#30#	1920	18,42	943,00	1,10
4_Bio_ILSS_#30#	1970	18,49	933,00	0,94
5_Bio_ILSS_#30#	2020	19,84	1040,00	1,00
6_Bio_ILSS_#30#	2150	19,99	996,00	0,96
7_Bio_ILSS_#30#	1710	17,71	982,00	1,30
8_Bio_ILSS_#30#	1820	18,19	975,00	0,98
9_Bio_ILSS_#30#	1740	16,18	807,00	1,00
10_Bio_ILSS_#30	1840	17,66	907,00	0,94
Average	1880	18,3631	964	1,00
SD	138,71	1,09	72,31	0,11
Max	2150,00	19,99	1060,00	1,30
Min	1710,00	16,18	807,00	0,94
CV	0,07	0,06	0,07	0,11



## Laminate 31 SuperSap CLR/INF (1% silane in hardener)-Biotex UD

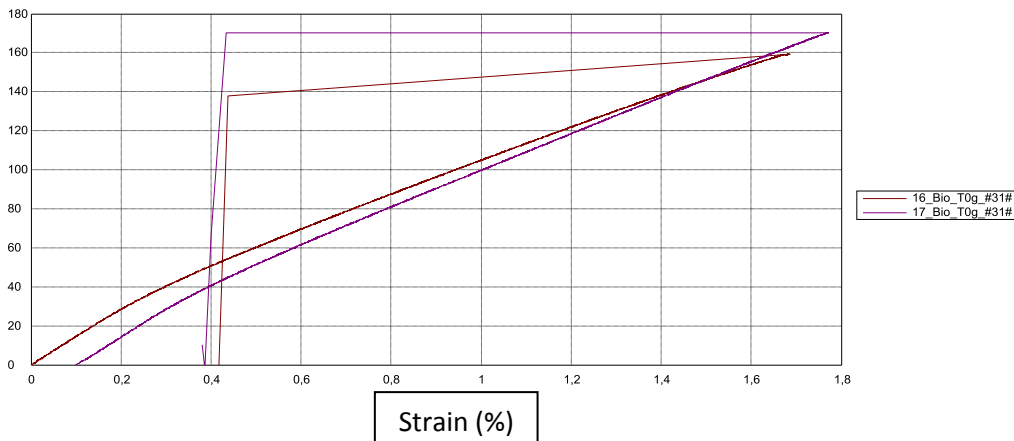
### Laminate 31 Tensile 0° test

Sample		Fm	E	Rm	Max_Disp_Ext.1(Deformacion)	I.Poisson
		kN	N/mm2	N/mm2	%	
1_Bio_TO_#31#	True	4,48	12061,50	142,88	1,45	0,39
2_Bio_TO_#31#	True	4,82	12576,90	149,83	1,61	0,41
3_Bio_TO_#31#	True	5,08	15068,80	151,07	1,47	0,84
4_Bio_TO_#31#	True	4,82	14735,50	150,17	1,28	0,45
5_Bio_TO_#31#	True	5,03	14452,90	153,63	1,43	0,22
6_Bio_TO_#31#	True	5,25	16611,40	158,46	1,54	1,78
7_Bio_TO_#31#	True	5,38	13907,20	163,85	1,62	0,48
8_Bio_TO_#31#	True	5,62	11539,10	162,78	1,64	0,18
9_Bio_TO_#31#	True	5,33	15321,40	152,63	1,37	0,51
10_Bio_TO_#31#	True	5,40	14555,50	145,98	1,42	0,60
11_Bio_TO_#31#	True	5,70	14111,70	160,94	1,61	0,45
12_Bio_TO_#31#	True	5,46	13699,00	152,07	1,49	0,51
13_Bio_TO_#31#	True	5,28	11617,00	148,62	1,56	0,30
14_Bio_TO_#31#	True	5,44	13183,90	155,60	1,57	0,23
Average		5,22	13817,30	153,47	1,50	0,53
SD		0,34	1482,99	6,23	0,11	0,40
Max		5,70	16611,40	163,85	1,64	1,78
Min		4,48	11539,10	142,88	1,28	0,18
CV		0,06	0,11	0,04	0,07	0,76



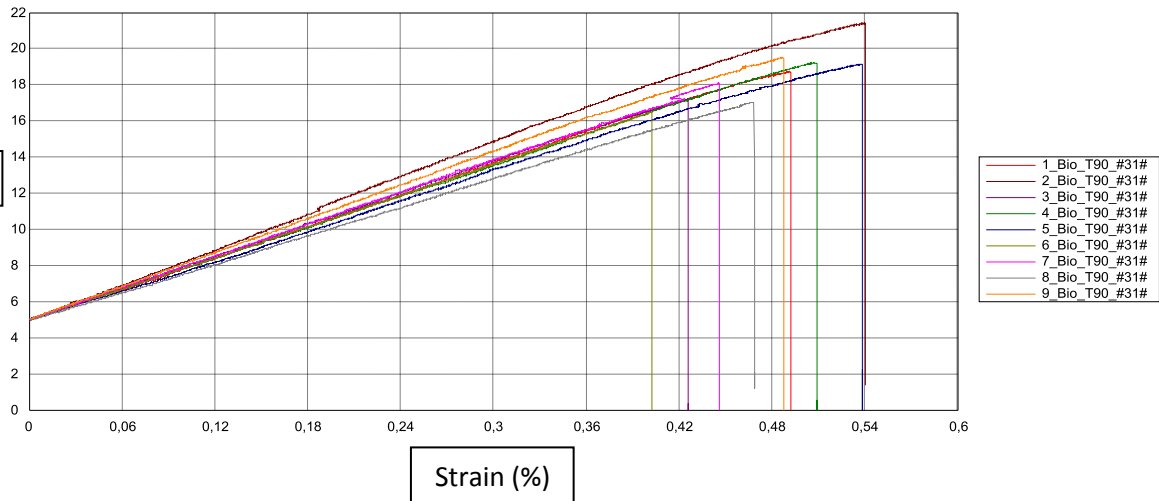
### Laminate 31 Tensile 0° test - gauges

Sample	Fm	E	Rm	Max_Disp_Ext.1(Deformacion)	I.Poisson
	kN	N/mm2	N/mm2	%	
15_Bio_TOg_#31#	5,3		160		
16_Bio_TOg_#31#	5,22	13800	159	1,7	0,46
17_Bio_TOg_#31#	5,38	14100	170	1,7	0,50



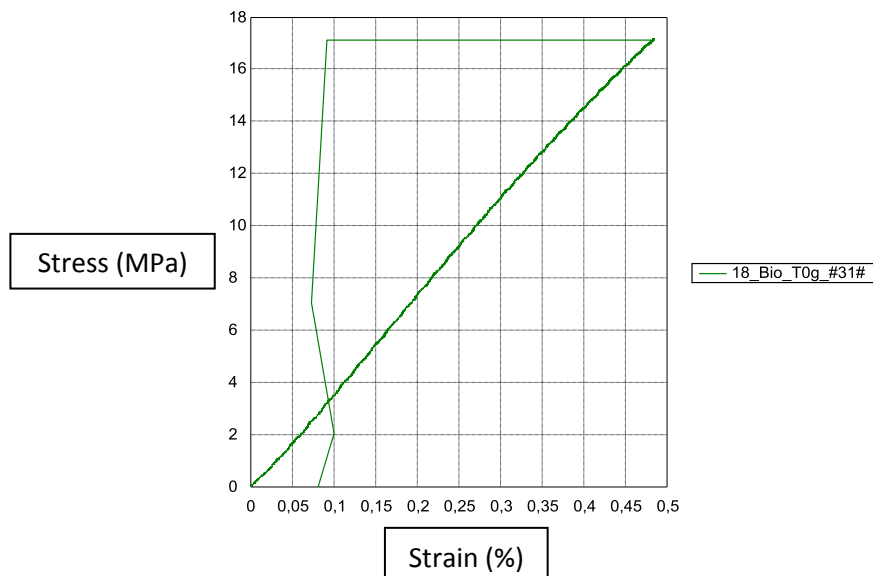
### Laminate 31 Tensile 90° test

Sample	Fm kN	E N/mm2	Rm N/mm2	Max_Disp_Ext.1 %
1_Bio_T90_#31#	1,02	2927,78	18,74	0,49
2_Bio_T90_#31#	1,14	3377,61	21,41	0,54
3_Bio_T90_#31#	0,95	2933,55	17,22	0,43
4_Bio_T90_#31#	1,03	2868,68	19,24	0,51
5_Bio_T90_#31#	1,08	2795,11	19,15	0,54
6_Bio_T90_#31#	0,92	2877,51	16,47	0,40
7_Bio_T90_#31#	0,99	2938,75	18,10	0,45
8_Bio_T90_#31#	0,96	2637,13	17,04	0,47
9_Bio_T90_#31#	1,04	3121,89	19,51	0,49
Average	1,02	2942,00	18,54	0,48
SD	0,07	208,10	1,52	0,05
Max	1,14	3377,61	21,41	0,54
Min	0,92	2637,13	16,47	0,40
Coef.Variacion	0,07	0,07	0,08	0,10



### Laminate 31 Tensile 90° test – gauge

	Fm	E	Rm	Max_Disp_Ext.1(Deformacion)	I.Poisson
18_Bio_T90g_#31#	0,956	3810	17,2	0,48	0,12

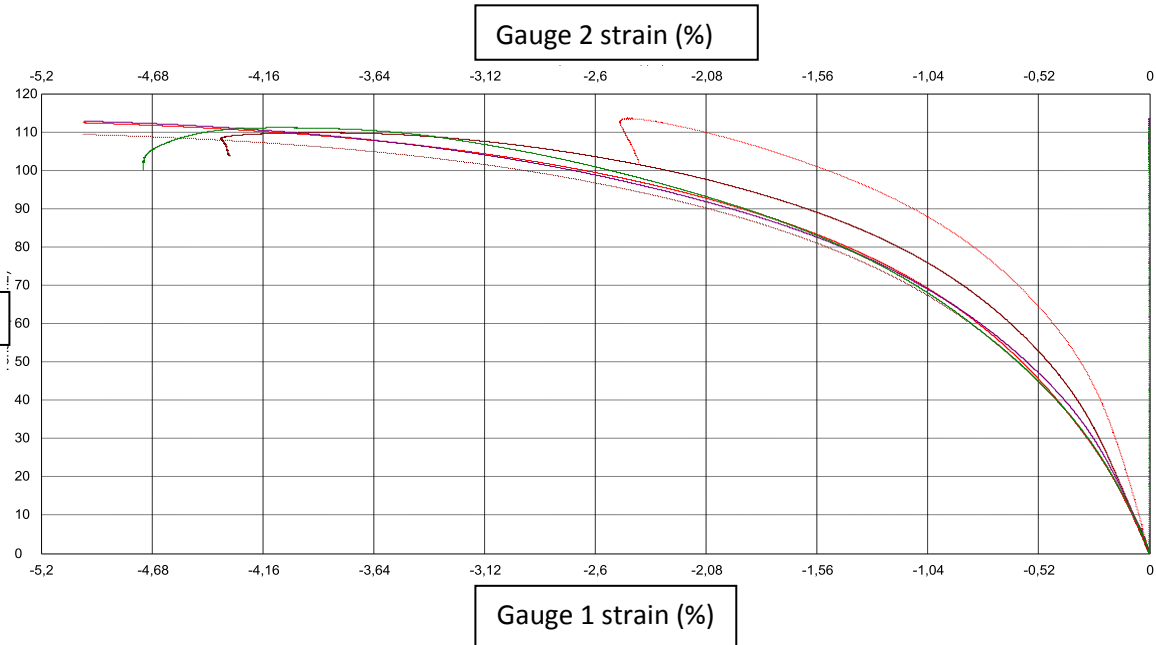


## Laminate 32 SuperSap CLR/INF (1% silane in hardener)-Biotex UD

### Laminate 32 Compression 0° test

Sample	ID	Longitudinal compression test						Vf	Mf
		a	b	F	Exc	$\sigma_{xc}$	$\epsilon_{xc}$	(%)	(%)
		mm	mm	kN	MPa	MPa	%		
1	1_Bio_CO_#32#	3,62	24,79	9820	11615,00	113	3,65	31,00	43,8
2	2_Bio_CO_#32#	3,66	24,84	10100	10635,00	110	4,25		
3	3_Bio_CO_#32#	3,40	24,90	10100	10100,00	113	5,00		
4	4_Bio_CO_#32#	3,40	25,07	10500	9250,00	111	4,70		
Average value		3,52	24,90	10130,00	<b>10400,00</b>	111,75	4,40	Parameters	Value
Standard deviation		0,14	0,12	279,76	990,61	1,50	0,59		
CV(%)				0,03	0,10	0,01	0,13		
Characteristic value					8300,03	<b>108,57</b>	<b>3,15</b>		

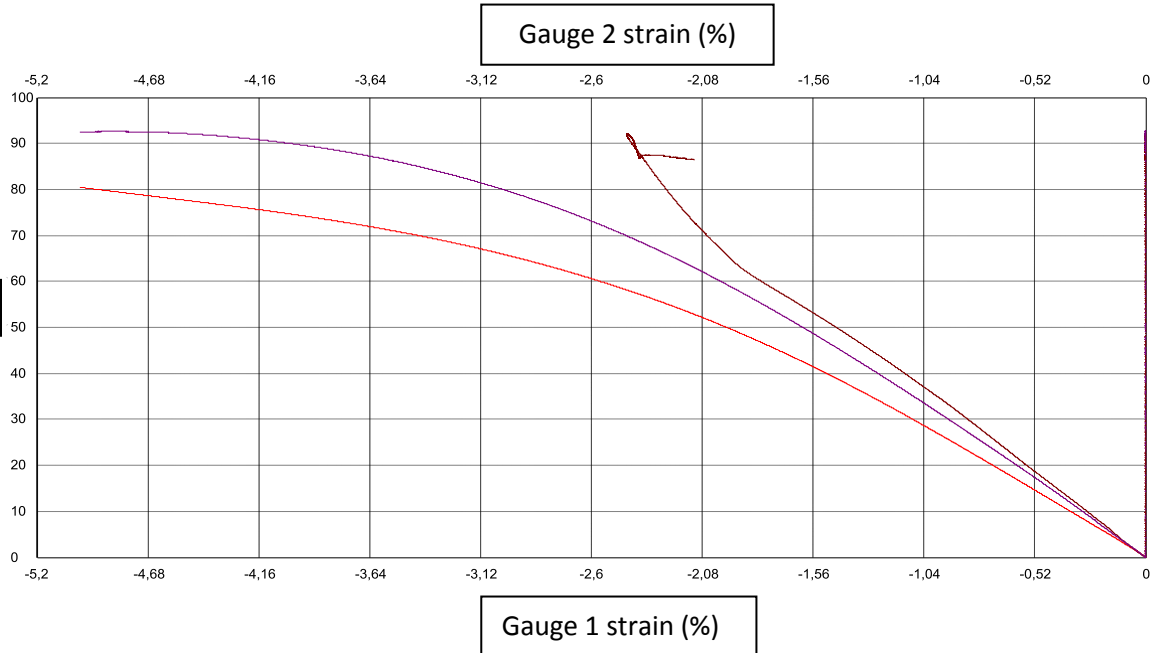
Modulus	Exc	Exc1	Gauge 1		Exc2	Gauge 2	
			$\sigma_{xc}$ 0,1	$\sigma_{xc}$ 0,3		$\sigma_{xc}$ 0,1	$\sigma_{xc}$ 0,3
1_Bio_CO_#32#	<b>11615,00</b>	<b>9335,00</b>	12,73	31,40	<b>13895,00</b>	20,26	48,05
2_Bio_CO_#32#	<b>10635,00</b>	<b>11940,00</b>	13,38	37,26	<b>9330,00</b>	12,40	31,06
3_Bio_CO_#32#	<b>10100,00</b>	<b>10100,00</b>	13,02	33,22	<b>0,00</b>		
4_Bio_CO_#32#	<b>9250,00</b>	<b>9250,00</b>	12,66	31,16	<b>0,00</b>		



### Laminate 32 Compression 90° test

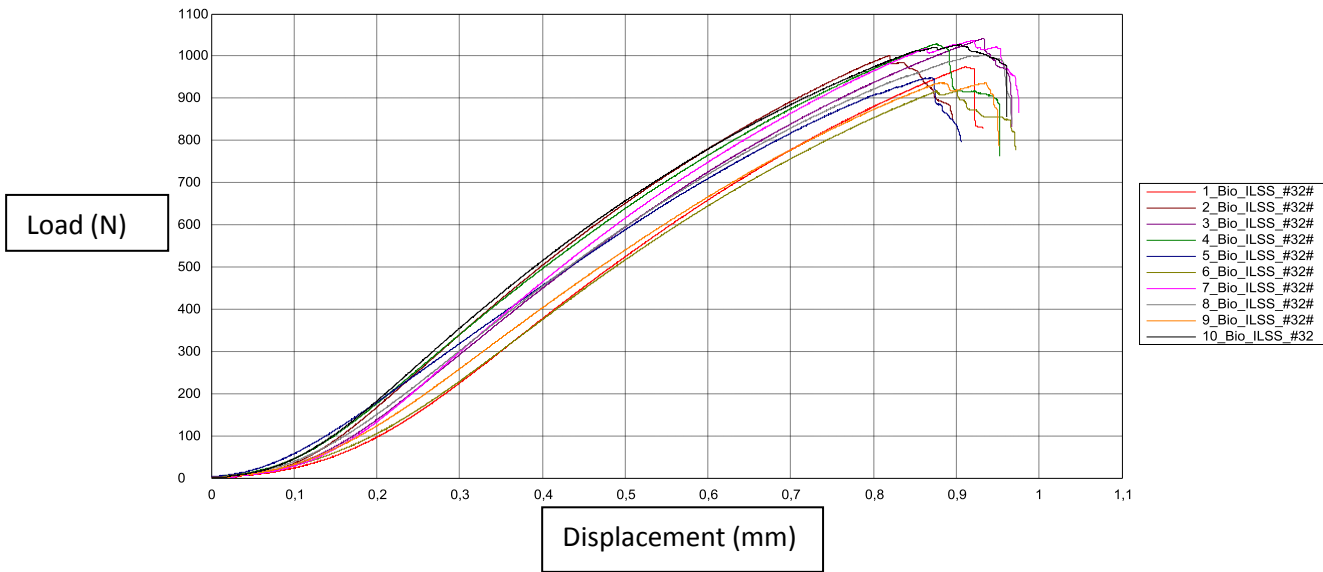
Sample	ID	Transverse compression test						Vf (%)	Mf (%)
		a mm	b mm	F kN	E <sub>yc</sub> MPa	σ <sub>yc</sub> MPa	ε <sub>yc</sub> %		
1	1_Bio_C90_#32#	3,79	24,89	7890	3307,50	83,60	3,55	0,30	42,6
2	2_Bio_C90_#32#	3,71	24,90	8500	3785,00	92,00	2,40		
3	3_Bio_C90_#32#	3,64	24,94	8410	3425,00	92,60	5,00		
4	4_Bio_C90_#32#	3,67	25,04	8420	3775,00	91,60	4,20		
Average value		3,70	24,94	8305,00	<b>3573,13</b>	89,95	3,79	Parameters	Value
Standard deviation		0,06	0,07	279,58	243,68	4,25	1,10		
CV(%)				0,03	0,07	0,05	0,29		
Characteristic value					3056,55	<b>80,93</b>	<b>1,46</b>		

Modulus	Exc	Exc1	Gauge 1		Exc2	Gauge 2	
			σ <sub>xc</sub> 0,1	σ <sub>xc</sub> 0,3		σ <sub>xc</sub> 0,1	σ <sub>xc</sub> 0,3
1_Bio_C90_#32#	<b>3307,50</b>	<b>2855,00</b>	2,96	8,67	<b>3760,00</b>	3,43	10,95
2_Bio_C90_#32#	<b>3785,00</b>	<b>3785,00</b>	3,40	10,97			
3_Bio_C90_#32#	<b>3425,00</b>	<b>3425,00</b>	3,42	10,27	<b>0,00</b>		
4_Bio_C90_#32#	<b>3775,00</b>	<b>3775,00</b>	4,55	12,10	<b>0,00</b>		



**Laminate 32 ILSS test**

	Max F	Short-beam Streghth	Max. Tension	Displacement
Sample	N	N/mm2	N/mm2	mm
1_Bio_ILSS_#32#	2010	18,84	975	0,91
2_Bio_ILSS_#32#	2170	19,85	1000	0,82
3_Bio_ILSS_#32#	2130	20,06	1040	0,93
4_Bio_ILSS_#32#	2000	19,29	1030	0,88
5_Bio_ILSS_#32#	1900	18,14	948	0,87
6_Bio_ILSS_#32#	2020	18,32	917	0,90
7_Bio_ILSS_#32#	2140	20,03	1040	0,92
8_Bio_ILSS_#32#	2040	19,26	1000	0,94
9_Bio_ILSS_#32#	1910	18,02	936	0,88
10_Bio_ILSS_#32	1980	19,27	1030	0,90
Average	2030,00	19,11	992,00	0,90
SD	92,50	0,76	45,47	0,03
Max	2170,00	20,06	1040,00	0,94
Min	1900,00	18,02	917,00	0,82
CV	0,05	0,04	0,05	0,04



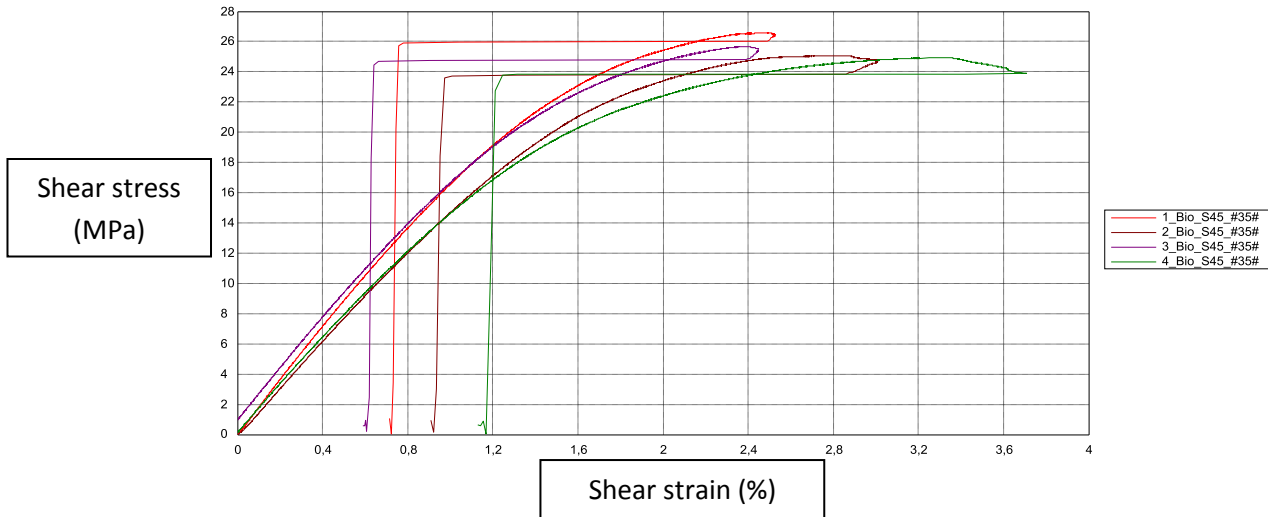
**Laminate 33 SuperSap CLR/INF (1% silane in hardener)-Biotex UD**  
**Laminate 34 SuperSap CLR/INF -Biotex UD**  
**Flexural tests**

		Initial flexural propeties		Degraded flexural properties		Percentage	
		Force (N)	Modulus (N/mm2)	Force (N)	Modulus (N/mm2)	Force (%)	Modulus (%)
Logitudinal	33-Silane in hardener	103,12	18900	65,77	7877	36,22	58,32
	34-No treated	84,47	16222	62,28	12483	26,27	23,05
Transverse	33-Silane in hardener	23,00	5720	15,03	3700	34,65	35,31
	34-No treated	21,70	5620	12,10	2985	44,24	46,89

**Laminate 35 SuperSap CLR/INF (1% silane in hardener)-Biotex UD**

**Laminate 35 In-plane shear test S45**

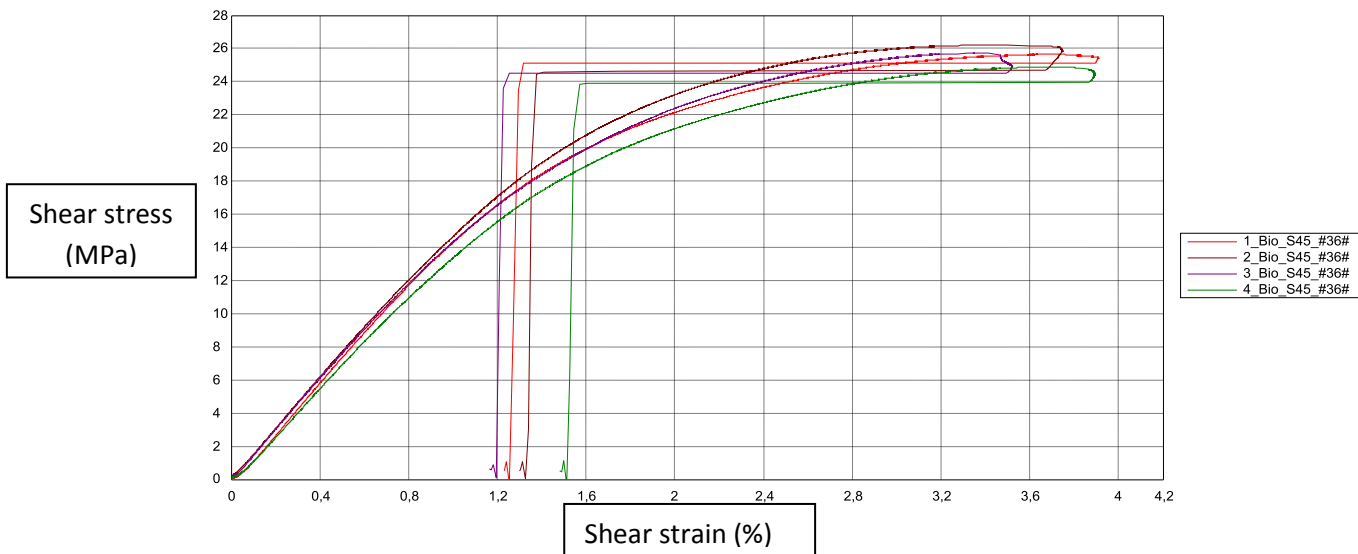
	Fmax	Shear strain	Shear strength	Modulus (0.2-0.6)
	N	%	N/mm2	N/mm2
1_Bio_S45_#35#	3010	2,5	26,6	1720
2_Bio_S45_#35#	3000	3	25,1	1540
3_Bio_S45_#35#	2870	2,4	25,7	1630
4_Bio_S45_#35#	2890	3,7	24,9	1500



**Laminate 36 SuperSap CLR/INF -Biotex UD**

**Laminate 36 In-plane shear test S45**

	Fmax	Shear strain	Shear strength	Shear modulus
Sample	N	%	N/mm2	N/mm2
1_Bio_S45_#36#	2970	3,9	25,7	1580
2_Bio_S45_#36#	2950	3,7	26,2	1560
3_Bio_S45_#36#	3000	3,5	25,7	1550
4_Bio_S45_#36#	2940	3,9	24,9	1470



# APPENDIX C



Figure D.1: Untreated flax fabric panoramic picture (left) and measurement 1(right)

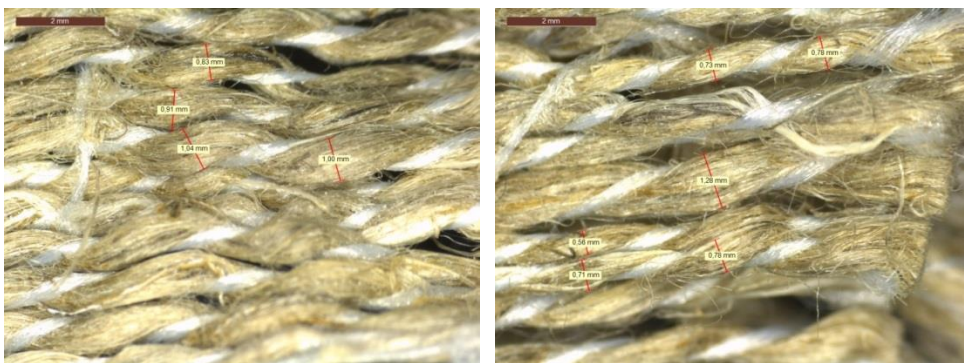


Figure D.2: Untreated flax measurement 2 (left) and 3 (right)

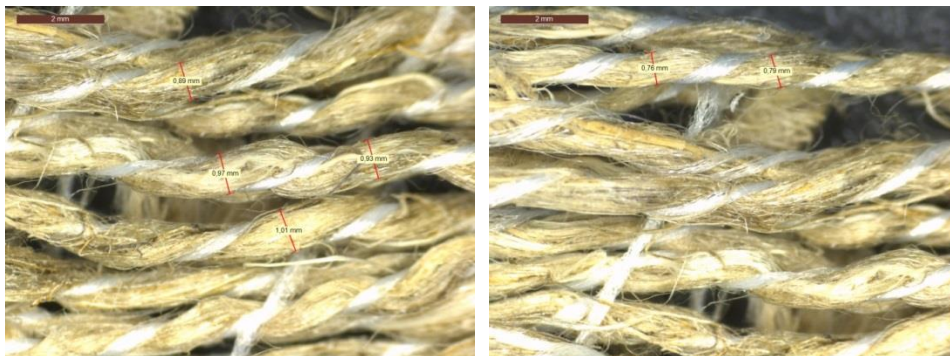


Figure D.3: Untreated flax measurement 4 (left) and 5 (right)



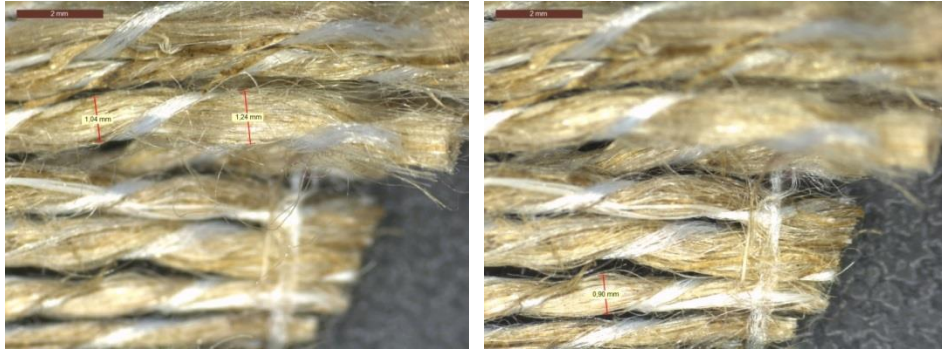


Figure D.4: 1M NaOH 3h flax treatment measurement 1 (left) and 2 (right)

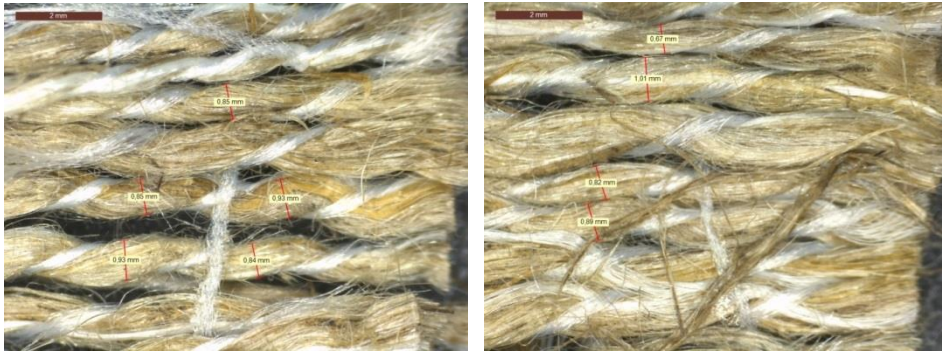


Figure D.5: 1M NaOH 3h flax treatment measurement 3 (left) and 4 (right)



Figure D. 6: 1M NaOH 3h flax treatment measurement 5

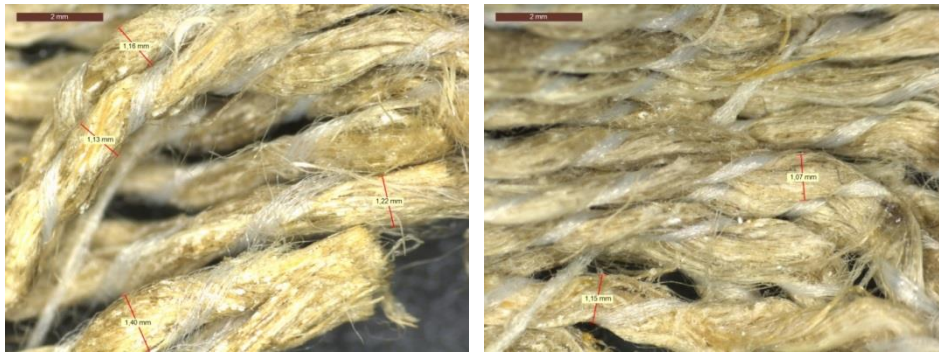


Figure D.7: 2M NaOH 72h flax treatment measurement 1(left) and 2 (right)



Figure D.8: 2M NaOH 72h flax treatment measurement 3(left) and 4 (right)

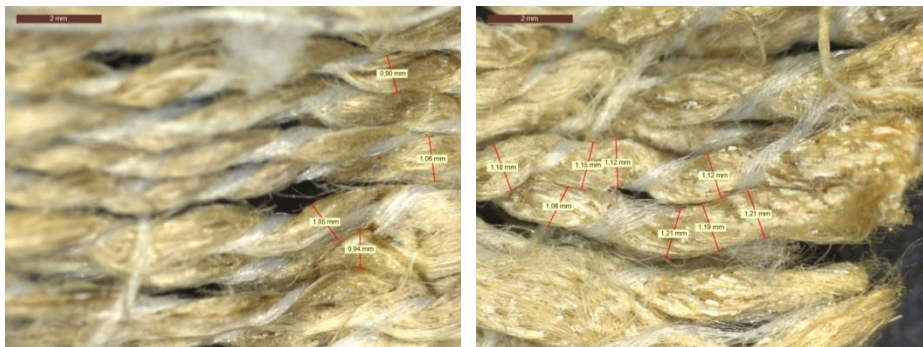


Figure D .9: 2M NaOH 72h flax treatment measurement 5 (left) and 6 (right)



Figure D.10: 2M NaOH 72h flax treatment measurement 7

# Appendix E

Immersion tests

	Date	Start	1 day			2 days			3 days			7 days			14 day			20 day			35 day			44 day			81 day			100 day-DRY		
		29-oct	30-oct			31-oct			01-nov			05-nov			12-nov			18-nov			03-dic			12-dic			18-ene			20-feb		
		Sample	g	g	%	X	g	%	X	g	%	X	g	%	X	g	%	X	g	%	X	g	%	X	g	%	X	g	%	X		
33 Silane	1	4,120	4,161	0,995	1,057	4,189	1,675	1,745	4,189	1,675	1,721	4,238	2,864	2,922	4,275	3,762	3,923	4,292	4,175	4,282	4,314	4,709	4,913	4,314	4,709	5,067	4,367	5,995	5,828	4,173	1,291	1,316
	2	3,824	3,861	0,968		3,891	1,752		3,882	1,517		3,929	2,746		3,967	3,740		3,979	4,053		4,002	4,655		4,008	4,812		4,019	5,099		3,868	1,145	
	3	3,875	3,917	1,084		3,939	1,652		3,944	1,781		3,986	2,865		4,030	4,000		4,045	4,387		4,075	5,161		4,075	5,161		4,098	5,755		3,931	1,432	
	4	3,675	3,717	1,143		3,746	1,932		3,735	1,633		3,783	2,939		3,824	4,054		3,832	4,272		3,860	5,034		3,858	4,980		3,882	5,633		3,719	1,189	
	5	4,160	4,213	1,274		4,239	1,899		4,245	2,043		4,289	3,101		4,331	4,111		4,348	4,519		4,375	5,168		4,390	5,529		4,421	6,274		4,227	1,608	
	6	4,106	4,142	0,877		4,170	1,559		4,175	1,680		4,230	3,020		4,265	3,872		4,282	4,286		4,301	4,749		4,320	5,212		4,361	6,210		4,156	1,227	
34 Untre	1	4,377	4,416	0,891	0,878	4,447	1,599	1,554	4,447	1,599	1,661	4,492	2,627	2,755	4,553	4,021	3,942	4,559	4,158	4,191	4,591	4,889	4,771	4,607	5,255	5,087	4,647	6,169	6,086	4,446	1,572	1,709
	2	4,226	4,261	0,828		4,304	1,846		4,295	1,633		4,344	2,792		4,390	3,881		4,401	4,141		4,426	4,733		4,428	4,780		4,464	5,632		4,300	1,749	
	3	4,095	4,132	0,904		4,164	1,685		4,164	1,685		4,215	2,930		4,254	3,883		4,269	4,249		4,289	4,737		4,294	4,860		4,357	6,398		4,166	1,729	
	4	4,134	4,175	0,992		4,191	1,379		4,208	1,790		4,253	2,879		4,294	3,870		4,309	4,233		4,335	4,862		4,357	5,394		4,393	6,265		4,208	1,792	
	5	4,169	4,205	0,864		4,238	1,655		4,239	1,679		4,278	2,615		4,340	4,102		4,344	4,198		4,368	4,773		4,385	5,181		4,441	6,529		4,242	1,739	
	6	4,057	4,089	0,789		4,104	1,158		4,121	1,578		4,166	2,687		4,215	3,895		4,226	4,166		4,245	4,634		4,262	5,053		4,281	5,521		4,125	1,676	

# Appendix F

## UNCERTAINTY ESTIMATION IN MECHANICAL PROPERTIES TESTS

### 1. Abstract

The current report defined Acciona Blades (AB) laboratory tests uncertainty type B values based on the ISO Guide [1]. While type A uncertainties are determined analyzing a series of independent repeated measurements, type B uncertainties are based on scientific judgment combining all available information on the possible variability of the quantity. The uncertainty data might come from properties of relevant materials, measurement instruments, manufacturer's specifications or calibration certificate data.

Most of the experimental campaign of the PhD was performed in AB laboratory, as a result the test uncertainties come from the instrumentation and machinery used in the referred laboratory.

### 2. Introduction

AB different tests uncertainties determination was performed following Lekou et al. study [2]. Based on this document the first step was to identify the parameters for which uncertainty is determined. Table 1 established the uncertainty measurands.

Table 1: Uncertainty measurands

<b>Measurand</b>	<b>Unit</b>	<b>Symbol</b>
Thickness	mm	H
Width	mm	W
Applied load	kN	F

Exhibited strain	%	$\epsilon$
Cross-sectional area	mm <sup>2</sup>	A
Elastic modulus	MPa	E
Poisson's ratio		$\nu_{21}$
Strength	MPa	$\sigma_F$
Strain at failure	%	$\epsilon_{max}$
Shear modulus	MPa	$G_{12}$
Shear strength	MPa	$T_{12F}$
Shear strain at failure	%	$\gamma_{12F}$

The following relationships are used for the measurands calculation (Equations 1-8):

$$A = H \times W \quad \text{Equation 1}$$

$$\sigma = \frac{F}{A} \quad \text{Equation 2}$$

$$E = \frac{\Delta\sigma}{\Delta\epsilon} \quad \text{Equation 3}$$

$$\nu = \frac{-\Delta\epsilon_y}{\Delta\epsilon_x} \quad \text{Equation 4}$$

$$\tau = \frac{F}{2A} \quad \text{Equation 5}$$

$$\gamma = \epsilon_x + \epsilon_y \quad \text{Equation 6}$$

$$G_{12} = \frac{\Delta\tau}{\Delta\gamma} \quad \text{Equation 7}$$

$$F^{sbs} = 0.75 \frac{F_m}{A} \quad \text{Equation 8}$$

The measurands are based in the tests performed in AB laboratory. All the tests are supported by the DNVGL-SE-0436:2016-03 Shop approval in renewable energy certificate. This certification contemplates the methods in Table 2.

Table 2: Certificated mechanical tests

Standard	Description
ISO 527-1	Plastics-Determination of tensile properties – Part 1: General principles
ISO 527-4	Plastics-Determination of tensile properties-Part 4: Test conditions for isotropic and anisotropic fibre-reinforced plastic composites
ISO 527-5	Plastics-Determination of tensile properties-Part 5: Test conditions for unidirectional fibre-reinforced plastic composites
ISO 14126	Fiber-reinforced plastic composites – Determination of compressive properties in the in-plane direction
ISO 14129	Fiber-reinforced plastic composites – Determination of the in-plane shear stress/strain response, including the in-plane shear modulus and strength, by the $\pm 45^\circ$ tension test method
ASTM D2344	Standard Test Method for Short-Beam Strength of Polymer Matrix Composite Materials and Their Laminates

### 3. Uncertainty analysis

The uncertainty type B values based in the ISO Guide were calculated for different mechanical tests measurands [1]. The combined standard uncertainty  $u_c(\gamma)$  is the positive square root of the combined variance, which is given by Equation 9.

$$u_c^2(\gamma) = \sum_{j=1}^N \left( \frac{\partial f}{\partial x_j} \right)^2 u_{x_j}^2 + 2 \sum_{j=1}^{N-1} \sum_{k=j+1}^N \frac{\partial f}{\partial x_j} \frac{\partial f}{\partial x_k} u_{x_j} u_{x_k} r(x_j, x_k)$$

Equation 9

Where  $\gamma = f(x_1, x_2, \dots, x_N)$  are the input quantities,  $u_{x_j}$  is a standard uncertainty of quantity  $x_j$  evaluated as either type A or B uncertainty and  $r(x_j, x_i)$  is the relative coefficient between  $x_j$  and  $x_k$ .

### 3.1 Uncertainty of width and thickness

Based on Equation 1 the cross section area was calculated by measuring the width and the thickness of the specimen. The use of a measuring instrument (caliper) has an associated uncertainty.

The maximum uncertainty allowed for the caliper is 0.02 mm and it assumes a rectangular distribution. When only one measurement is made, we are assuming that it is going to be the contribution of uncertainty. The type B uncertainty for measuring the thickness and width is calculated with Equation 10:

$$u_{H,instr} = \frac{0.02}{\sqrt{3}} \quad \text{Equation 10}$$

According to the ISO 527-5 standard, ISO 14129 and ASTM D2344 standard, the mean values are calculated making at least three measurements along the coupon length and such value is used to define the width and thickness of each coupon. These measurements were taken into account to define Type A total uncertainty of the thickness and width measurement. Type A uncertainty values for  $u_{W,A}$  and  $u_{H,A}$  are defined in Equations 11 and 12. The assessment of the mean value of the measured width  $W$ , and thickness  $H$ , respectively are used in Equations 11 and 12.



$$u_{W,A} = \frac{S_W}{\sqrt{n_A}} \quad \text{Equation 11}$$

$$u_{H,A} = \frac{S_H}{\sqrt{n_A}} \quad \text{Equation 12}$$

Where  $S_W$  and  $S_H$  is the standard deviation of the measurements of the width and the thickness, respectively and  $n_A$  is the number of measured for each specimen. All sourced are used in Equations 13 and 14 in order to determinate type B uncertainty of the width and thickness respectively:

$$u_W = \sqrt{u_{W,A}^2 + u_{W,instr}^2} \quad \text{Equation 13}$$

$$u_H = \sqrt{u_{H,A}^2 + u_{H,instr}^2} \quad \text{Equation 14}$$

### 3.2 Uncertainty of cross-sectional area

The measurement uncertainty of the cross-section  $u_A$  was obtained combining Equations 1 and 8, assuming thickness and width measurement are independents, see Equation 15.

$$u_A = \sqrt{\left(\frac{u_W}{W}\right)^2 + \left(\frac{u_H}{H}\right)^2} \quad \text{Equation 15}$$

### 3.3 Uncertainty of the applied force

As the calibration certificate defines the load reading device accuracy must be within  $\pm 0.5\%$  of the actual value, assuming a rectangular distribution, getting as a result Equation 16 for the  $u_F$  calculation.



$$u_F = \frac{0.5F}{100\sqrt{3}}$$

**Equation 16**

### 3.4 Uncertainty of the applied force in stress

The axial stress type B uncertainty calculation is based on Equations 1 and 2; obtaining as a result Equation 17.

$$u_\sigma = \sigma \sqrt{\left(\frac{u_F}{F}\right)^2 + \left(\frac{u_A}{A}\right)^2}$$

**Equation 17**

Where  $u_A$  was calculated using Equation 15 and  $u_F$  Equation 16.

### 3.5 Uncertainty on strain

According to the ISO standard [1] the strain gauge accuracy must be at least of  $\pm 1\%$ , because of this reason Equation 18 uncertainty might be assumed.

$$u_\varepsilon = \frac{1\varepsilon}{100\sqrt{3}}$$

**Equation 18**

### 3.6 Uncertainty of elastic modulus

The elastic modulus is calculated with Equation 19.

$$E = \frac{\sigma_2 - \sigma_1}{\varepsilon_2 - \varepsilon_1}$$

**Equation 19**

The combination for the Equation 9 and 18 leads to get the Equation 20.

$$u_E = E \sqrt{\frac{u_{\sigma_1}^2 + u_{\sigma_2}^2}{(\sigma_2 - \sigma_1)^2} + \frac{u_{\varepsilon_1}^2 + u_{\varepsilon_2}^2}{(\varepsilon_2 - \varepsilon_1)^2}} \quad \text{Equation 20}$$

If calculation the elastic modulus on the average module of both sides of the specimen, the uncertainty result as will be:

$$u_E = \sqrt{u_{E1}^2 + u_{E2}^2} \quad \text{Equation 21}$$

### 3.7 Uncertainty on Poisson's ratio

The type B Poisson's rasion uncertainty was given by the Equation 22.

$$u_{\nu} = \nu \sqrt{\frac{u_{\varepsilon_{y1}}^2 + u_{\varepsilon_{y2}}^2}{(\varepsilon_{y2} - \varepsilon_{y1})^2} + \frac{u_{\varepsilon_{x1}}^2 + u_{\varepsilon_{x2}}^2}{(\varepsilon_{x2} - \varepsilon_{x1})^2}} \quad \text{Equation 22}$$

### 3.8 Uncertainty in shear parameters: Shear strength

Equation 16 might be applied in order to calculate shear strength uncertainty, getting as a result Equation 23.

$$u_{\tau} = \frac{1}{2}\tau \sqrt{\left(\frac{u_F}{F}\right)^2 + \left(\frac{u_A}{A}\right)^2}$$

**Equation 23**

### 3.9 Uncertainty in shear parameters: Shear strain

The shear strain uncertainty was obtained applying Equation 24.

$$u_{\gamma} = \sqrt{u_{\varepsilon_x}^2 + u_{\varepsilon_y}^2}$$

**Equation 24**

### 3.10 Uncertainty in shear parameters: Shear modulus

For the shear modulus the Equation 25 was used.

$$u_G = G \sqrt{\frac{u_{\tau_1}^2 + u_{\tau_2}^2}{(\tau_2 - \tau_1)^2} + \frac{u_{\gamma_1}^2 + u_{\gamma_2}^2}{(\gamma_2 - \gamma_1)^2}}$$

**Equation 25**

### 3.11 Uncertainty in short beam strength

For the short beam strength the Equation 26 was used.

$$u_{F_{sbs}} = 0.75F^{sbs} \sqrt{\left(\frac{u_F}{F}\right)^2 + \left(\frac{u_A}{A}\right)^2}$$

**Equation 26**

The above discussed uncertainties refer to the uncertainty of the property measured by a single (individual) specimen. However, we analysed a series of test (10 specimens), whereas the test

report should also include the mean values of properties measured, along with an indication of standard deviation and Coefficient of variation (CV).

#### 4. Experimental calculation

Section 3 described the equations to apply for the type B uncertainties calculation. Section used such equations for the uncertainty values determination.

##### 4.1. ISO527 Tensile test

Longitudinal tensile test uncertainties calculation has been done using data from **3\_Bio\_T0\_#3#** and **2\_Bio\_T0g\_#29#** samples.

Measurand	Unit	Symbol	Data	Formula	Result
Thickness	mm	H	2,15/0,08/3	$u_H = \sqrt{u_{H,A}^2 + u_{H,instr}^2}$	0.047
Width	mm	W	15.24/0.92/3	$u_W = \sqrt{u_{W,A}^2 + u_{W,instr}^2}$	0,093
Cross-sectional area	mm <sup>2</sup>	A	34.19	$u_A = \sqrt{\left(\frac{u_W}{W}\right)^2 + \left(\frac{u_H}{H}\right)^2}$	0.531
Force	N	F <sub>max</sub>	5580	$u_F = \frac{0.5F}{100\sqrt{3}}$	16.11
		F <sub>0.05</sub>	457		1.32
		F <sub>0.25</sub>	1606		4.63
Applied load	N/mm <sup>2</sup>	σ <sub>max</sub>	163.23	$u_\sigma = \sigma \sqrt{\left(\frac{u_F}{F}\right)^2 + \left(\frac{u_A}{A}\right)^2}$	6.5
		σ <sub>0.05</sub>	13.46		0.54
		σ <sub>0.25</sub>	47.25		1.89
Strain	%	ε <sub>max</sub>	1.32	$u_\varepsilon = \frac{1\varepsilon}{100\sqrt{3}}$	0.0076
		ε <sub>0.05</sub>	0.05		0.00029

		$\epsilon_{0,25}$	0.25		0.0014
Elastic modulus	MPa	E	10662.60	$u_E = E \sqrt{\frac{u_{\sigma_1}^2 + u_{\sigma_2}^2}{(\sigma_2 - \sigma_1)^2} + \frac{u_{\epsilon_1}^2 + u_{\epsilon_2}^2}{(\epsilon_2 - \epsilon_1)^2}}$	620.49
Exhibited strain y	%	$\epsilon_{y0.05}$	0.021	$u_\epsilon = \frac{1\epsilon}{100\sqrt{3}}$	0.00012
		$\epsilon_{y0.25}$	0.108		0.00062
Poisson's ratio		$\nu_{21}$	0.43	$u_\vartheta = \vartheta \sqrt{\frac{u_{\epsilon_{y1}}^2 + u_{\epsilon_{y2}}^2}{(\epsilon_{y2} - \epsilon_{y1})^2} + \frac{u_{\epsilon_{x1}}^2 + u_{\epsilon_{x2}}^2}{(\epsilon_{x2} - \epsilon_{x1})^2}}$	0.0032

#### 4.2. ISO14126 Compression test

Longitudinal compression test uncertainties calculation has been done using data from samples

**1\_Bio\_C0\_#30#.**

Measurand	Unit	Symbol	Data	Formula	Result
Thickness	mm	H	0.02	$u_{H,inst} = \frac{0.02}{\sqrt{3}}$	0.012
Width	mm	W	0.02	$u_{W,inst} = \frac{0.02}{\sqrt{3}}$	0.012
Cross-sectional area	mm <sup>2</sup>	A	89.74	$u_A = \sqrt{\left(\frac{u_W}{W}\right)^2 + \left(\frac{u_H}{H}\right)^2}$	0.30
Strain in side A	%	$\epsilon_{max}$	2.50	$u_\epsilon = \frac{1\epsilon}{100\sqrt{3}}$	0.014
		$\epsilon_{0.05}$	0.05		0.00029
		$\epsilon_{0.25}$	0.25		0.0014
Strain in side B	%	$\epsilon_{max}$	3.10	$u_\epsilon = \frac{1\epsilon}{100\sqrt{3}}$	0.018

		$\epsilon_{0.05}$	0.05		0.00029
		$\epsilon_{0.25}$	0.25		0.0014
Force in side A	N	$F_{max}$	9730	$u_F = \frac{0.5F}{100\sqrt{3}}$	28.09
		$F_{0.05}$	1405		4.06
		$F_{0.25}$	3662		10.57
Applied load in side A	N/mm <sup>2</sup>	$\sigma_{max}$	108	$u_\sigma = \sigma \sqrt{\left(\frac{u_F}{F}\right)^2 + \left(\frac{u_A}{A}\right)^2}$	0.0010
		$\sigma_{0.05}$	8.87		0.00009
		$\sigma_{0.25}$	35.82		0.00034
Elastic modulus side A	MPa	E	12570	$u_E = E \sqrt{\frac{u_{\sigma_1}^2 + u_{\sigma_2}^2}{(\sigma_2 - \sigma_1)^2} + \frac{u_{\epsilon_1}^2 + u_{\epsilon_2}^2}{(\epsilon_2 - \epsilon_1)^2}}$	89.86
Force in side B	N	$F_{0.05}$	1149	$u_F = \frac{0.5F}{100\sqrt{3}}$	3.31
		$F_{0.25}$	3026		8.73
Applied load in side B	N/mm <sup>2</sup>	$\sigma_{0.05}$	6.27	$u_\sigma = \sigma \sqrt{\left(\frac{u_F}{F}\right)^2 + \left(\frac{u_A}{A}\right)^2}$	0.00006
		$\sigma_{0.25}$	29.27		0.00028
Elastic modulus in side B	MPa	E	10455	$u_E = E \sqrt{\frac{u_{\sigma_1}^2 + u_{\sigma_2}^2}{(\sigma_2 - \sigma_1)^2} + \frac{u_{\epsilon_1}^2 + u_{\epsilon_2}^2}{(\epsilon_2 - \epsilon_1)^2}}$	74.74
Elastic modulus	MPa	E	89.86 74.74	$u_E = \sqrt{u_{E_1}^2 + u_{E_2}^2}$	116.88

### 4.3. ISO 14129 In plane Shear by $\pm 45^\circ$ tensile test

In-plane shear test uncertainties calculation has been done using data from samples

**1\_Bio\_S45\_#35#.**

Measurand	Unit	Symbol	Data	Formula	Result
Thickness	mm	H	4.52/0.08/3	$u_H = \sqrt{u_{H,A}^2 + u_{H,instr}^2}$	0.047
Width	mm	W	25.05/0.1/3	$u_W = \sqrt{u_{W,A}^2 + u_{W,instr}^2}$	0.13
Cross-sectional area	mm <sup>2</sup>	A	113.22	$u_A = \sqrt{\left(\frac{u_W}{W}\right)^2 + \left(\frac{u_H}{H}\right)^2}$	1.32
Force	N	F <sub>max</sub>	3010	$u_F = \frac{0.5F}{100\sqrt{3}}$	8.69
		F <sub>0.2</sub>	212		0.61
		F <sub>0.6</sub>	999		2.88
Applied load	N/mm <sup>2</sup>	T <sub>max</sub>	40.7	$u_\tau = \frac{1}{2}\tau \sqrt{\left(\frac{u_F}{F}\right)^2 + \left(\frac{u_A}{A}\right)^2}$	0.093
		T <sub>0,1</sub>	5.0		0.012
		T <sub>0,5</sub>	18.8		0.041
Strain x	%	ε <sub>x-max</sub>	1.20	$u_\varepsilon = \frac{1\varepsilon}{100\sqrt{3}}$	0.0069
		ε <sub>x-0.2</sub>	0.07		0.0004
		ε <sub>x-0.6</sub>	0.27		0.0016
Strain y	%	ε <sub>y-max</sub>	1.30	$u_\varepsilon = \frac{1\varepsilon}{100\sqrt{3}}$	0.0075
		ε <sub>y-0.2</sub>	0.13		0.0008
		ε <sub>y-0.6</sub>	0.33		0.0019



Shear strain	%	$\gamma_{\max}$	1.5	$u_{\gamma} = \sqrt{u_{\epsilon x}^2 + u_{\epsilon y}^2}$	0.16
		$\gamma_{0.2}$	0.2		0.010
		$\gamma_{0.6}$	0.6		0.052
Elastic modulus	MPa	$G_{12}$	1720	$u_G = G \sqrt{\frac{u_{\tau_1}^2 + u_{\tau_2}^2}{(\tau_2 - \tau_1)^2} + \frac{u_{\gamma_1}^2 + u_{\gamma_2}^2}{(\gamma_2 - \gamma_1)^2}}$	18.51

#### 4.4. ASTM D2344 Short-beam test

ILSS test uncertainties calculation has been done using data from samples

**1\_Bio\_ILSS\_#32#.**

Measurand	Unit	Symbol	Data	Formula	Result
Thickness	mm	H	3.87/0.02/3	$u_H = \sqrt{u_{H,A}^2 + u_{H,instr}^2}$	0.017
Width	mm	W	13.58/0.16/3	$u_W = \sqrt{u_{W,A}^2 + u_{W,instr}^2}$	0.093
Cross-sectional area	mm <sup>2</sup>	A	32.77	$u_A = A \sqrt{\left(\frac{u_W}{W}\right)^2 + \left(\frac{u_H}{H}\right)^2}$	0.20
Force	N	$F_{\max}$	2010	$u_{Fm} = \frac{0.5F}{100\sqrt{3}}$	17.41
Applied load	N/mm <sup>2</sup>	$F_{sbs}$	18.84	$u_{F.SBS} = 0.75 \times F^{SBS} \sqrt{\left(\frac{u_F}{F}\right)^2 + \left(\frac{u_A}{A}\right)^2}$	0.15

#### 4.5. ASTM D2344 Short-beam test- Flexural tests

ILSS test uncertainties calculation has been done using data from samples

**1\_Bio\_ILSS\_#32#.**

Measurand	Unit	Symbol	Data	Formula	Result
Thickness	mm	H	3.87/0.02/3	$u_H = \sqrt{u_{H,A}^2 + u_{H,instr}^2}$	0.017
Width	mm	W	13.58/0.16/3	$u_W = \sqrt{u_{W,A}^2 + u_{W,instr}^2}$	0.093
Cross-sectional area	mm <sup>2</sup>	A	32.77	$u_A = A \sqrt{\left(\frac{u_W}{W}\right)^2 + \left(\frac{u_H}{H}\right)^2}$	0.20
Force	N	F <sub>max</sub>	2010	$u_{Fm} = \frac{0.5F}{100\sqrt{3}}$	17.41
Applied load	N/mm <sup>2</sup>	σ	18.84	$u_\sigma = \sigma \sqrt{\left(\frac{u_F}{F}\right)^2 + \left(\frac{u_A}{A}\right)^2}$	0.15

**5. References**

1. ISO (1993) Guide to the Expression of Uncertainty in Measurement. International Organization for Standardization. Geneva, Switzerland.
2. Lekou, D.J., Assimakopoulou, T.T. and Philippidis, T.P. "Estimation of the Uncertainty in Measurement of Composite Material Mechanical Properties During Static Testing". 2011. *Strain*, 47, 430–438.

## Annex 1: Tensile test uncertainties calculations

Longitudinal tensile test uncertainties calculation has been done using data from samples

**3\_Bio\_T0\_#3#** and **2\_Bio\_T0g\_#29#**.

### 1. Uncertainty of Thickness

	<b>Value 1</b>	<b>Value 2</b>	<b>Value 3</b>	<b>Average</b>	<b>SD</b>
Thickness	2.14	2.17	2.13	<b>2.15</b>	0.08

$$u_H = \sqrt{u_{H,A}^2 + u_{H,instr}^2}$$

$$u_{H,A} = \frac{s_H}{\sqrt{n_A}}$$

$$u_{H,instr} = \frac{0.02}{\sqrt{3}}$$

$$u_{H,A} = \frac{0.08}{\sqrt{3}}$$

$$u_{H,instr} = \frac{0.02}{\sqrt{3}}$$

$$u_H = \sqrt{\left(\frac{0.08}{\sqrt{3}}\right)^2 + \left(\frac{0.02}{\sqrt{3}}\right)^2} = 0.047$$

### 2. Uncertainty of Width

	<b>Value 1</b>	<b>Value 2</b>	<b>Value 3</b>	<b>Average</b>	<b>SD</b>
Width	15.33	15.22	15.16	<b>15.24</b>	0.92

$$u_W = \sqrt{u_{W,A}^2 + u_{W,instr}^2}$$

$$u_{W,inst} = \frac{0.02}{\sqrt{3}}$$

$$u_{W,A} = \frac{s_W}{\sqrt{n_A}}$$

$$u_{W,inst} = \frac{0.02}{\sqrt{3}}$$

$$u_{W,A} = \frac{0.92}{\sqrt{3}}$$

$$u_W = \sqrt{\left(\frac{0.92}{\sqrt{3}}\right)^2 + \left(\frac{0.02}{\sqrt{3}}\right)^2} = 0.093$$

### 3. Uncertainty of cross-sectional area

Specimen	H	W	A	u <sub>H</sub>	u <sub>W</sub>
	mm	mm	mm <sup>2</sup>	mm <sup>2</sup>	mm <sup>2</sup>
<b>3_Bio_T0_#3#</b>	2.20	15.54	34.19	0.047	0.531

$$u_A = \sqrt{\left(\frac{u_W}{W}\right)^2 + \left(\frac{u_H}{H}\right)^2}$$

$$u_A = 34.19 \sqrt{\left(\frac{0.531}{15.54}\right)^2 + \left(\frac{0.047}{2.20}\right)^2} = 1.38$$

### 4. Uncertainty of the applied force

Specimen	F <sub>m</sub>	F <sub>0.05</sub>	F <sub>0.25</sub>
	N	N	N
<b>3_Bio_T0_#3#</b>	5580	457	1606

$$u_F = \frac{0.5F}{100\sqrt{3}}$$

$$u_{F_m} = \frac{0.5 \times 5580}{100 \times \sqrt{3}} = 16.11$$

$$u_{F_{0.05}} = \frac{0.5 \times 457}{100 \times \sqrt{3}} = 1.32$$

$$u_{F_{0.25}} = \frac{0.5 \times 1606}{100 \times \sqrt{3}} = 4.63$$

### 5. Uncertainty on the applied load

σ <sub>max</sub>	σ <sub>0.05</sub>	σ <sub>0.25</sub>	A	u <sub>A</sub>	F <sub>m</sub>	u <sub>F<sub>m</sub></sub>	F <sub>0.05</sub>	u <sub>F<sub>0.05</sub></sub>	F <sub>0.25</sub>	u <sub>F<sub>0.25</sub></sub>
N/mm <sup>2</sup>	N/mm <sup>2</sup>	N/mm <sup>2</sup>	mm <sup>2</sup>	mm <sup>2</sup>	N	N	N	N	N	N
163.23	13.46	47.25	34.19	1.38	5580.38	16.11	457.00	1.32	1606.00	4.63

\* Sample **3\_Bio\_T0\_#3#**

$$u_{\sigma} = \sigma \sqrt{\left(\frac{u_F}{F}\right)^2 + \left(\frac{u_A}{A}\right)^2}$$

$$u_{\sigma_{max}} = 163.23 \sqrt{\left(\frac{16.11}{5580.38}\right)^2 + \left(\frac{1.38}{34.19}\right)^2} = 6.5$$

$$u_{\sigma_{0.05}} = 13.46 \sqrt{\left(\frac{1.32}{457.00}\right)^2 + \left(\frac{1.38}{34.19}\right)^2} = 0.54$$

$$u_{\sigma_{0.25}} = 47.25 \sqrt{\left(\frac{4.63}{1606.00}\right)^2 + \left(\frac{1.38}{34.19}\right)^2} = 1.89$$

## 6. Uncertainty on tensile strain in x

$\epsilon_{max}$	$\epsilon_{0.05}$	$\epsilon_{0.25}$
%	%	%
1.32	0.05	0.25

\* Sample **3\_Bio\_T0\_#3#**

$$u_{\epsilon} = \frac{1\epsilon}{100\sqrt{3}}$$

$$u_{\epsilon_m} = \frac{1 \times 1.32}{100 \times \sqrt{3}} = 0.0076$$

$$u_{\epsilon_{0.05}} = \frac{1 \times 0.05}{100 \times \sqrt{3}} = 0.00029$$

$$u_{\epsilon_{0.25}} = \frac{1 \times 0.25}{100 \times \sqrt{3}} = 0.0014$$

## 7. Uncertainty on elastic modulus

<b>E</b>	$\sigma_{1-0.05}$	$u_{\sigma 1-0.05}$	$\sigma_{2-0.25}$	$u_{\sigma 2-0.25}$	$\epsilon_{0.05}$	$u_{\epsilon 0.05}$	$\epsilon_{0.25}$	$u_{\epsilon 0.25}$
N/mm <sup>2</sup>	N/mm <sup>2</sup>	N/mm <sup>2</sup>	N/mm <sup>2</sup>	N/mm <sup>2</sup>	%	%	%	%
10662.60	13.46	0.54	47.25	1.89	0.05	0.00029	0.25	0.0014

\* Sample **3\_Bio\_T0\_#3#**

$$u_E = E \sqrt{\frac{u_{\sigma_1}^2 + u_{\sigma_2}^2}{(\sigma_2 - \sigma_1)^2} + \frac{u_{\varepsilon_1}^2 + u_{\varepsilon_2}^2}{(\varepsilon_2 - \varepsilon_1)^2}}$$

$$u_E = 10662.60 \sqrt{\frac{0.54^2 + 1.89^2}{(47.25 - 13.46)^2} + \frac{0.00029^2 + 0.00014^2}{(0.25 - 0.05)^2}} = 620.49$$

### 8. Uncertainty on tensile strain in y

$\varepsilon_{y1-0.05}$	$\varepsilon_{y2-0.25}$
%	%
0.021	0.108

\*Sample 2\_Bio\_T0g\_#29# tested with gauges

$$u_\varepsilon = \frac{1\varepsilon}{100\sqrt{3}}$$

$$u_{\varepsilon_{y1-0.05}} = \frac{1 \times 0.021}{100 \times \sqrt{3}} = 0.00012$$

$$u_{\varepsilon_{y2-0.25}} = \frac{1 \times 0.108}{100 \times \sqrt{3}} = 0.00062$$

### 9. Uncertainty on Poisson's ratio

$\nu_{21}$	$\varepsilon_{0.05}$	$u_{\varepsilon 1-0.05}$	$\varepsilon_{0.25}$	$u_{\varepsilon 2-0.25}$	$\varepsilon_{y1-0.05}$	$u_{y1-0.05}$	$\varepsilon_{y2-0.25}$	$u_{y2-0.25}$
	%	%	%	%	%	%	%	%
0.43	0.05	0.00029	0.25	0.0014	0.021	0.00012	0.108	0.00062

\*Sample 2\_Bio\_T0g\_#29# tested with gauges

$$u_\nu = \nu \sqrt{\frac{u_{\varepsilon_{y1}}^2 + u_{\varepsilon_{y2}}^2}{(\varepsilon_{y2} - \varepsilon_{y1})^2} + \frac{u_{\varepsilon_{x1}}^2 + u_{\varepsilon_{x2}}^2}{(\varepsilon_{x2} - \varepsilon_{x1})^2}}$$

$$u_\nu = 0.43 \sqrt{\frac{0.00012^2 + 0.00062^2}{(0.108 - 0.021)^2} + \frac{0.00029^2 + 0.0014^2}{(0.25 - 0.05)^2}} = 0.0032$$

## Annex 2: Compression test uncertainties calculations

Longitudinal compression test uncertainties calculation has been done using data from samples

### 1\_Bio\_C0\_#30#.

#### 1. Uncertainty of thickness

$$u_{H,inst} = \frac{0.02}{\sqrt{3}}$$
$$u_H = \frac{0.02}{\sqrt{3}} = 0.012$$

\*NOTE-For the compression samples the width has been measured in a single point, as a result  $u_{H,A}$  is equal to zero.

#### 2. Uncertainty of width

$$u_{W,inst} = \frac{0.02}{\sqrt{3}}$$
$$u_W = \frac{0.02}{\sqrt{3}} = 0.012$$

\*NOTE-For the compression samples the width has been measured in a single point, as a result  $u_{W,A}$  is equal to zero.

#### 3. Uncertainty of cross-sectional area

Specimen	H	W	A	uw	uH
	mm	mm	mm <sup>2</sup>	mm <sup>2</sup>	mm <sup>2</sup>
1_Bio_C0_#30#	3,62	24,79	89.74	0.012	0.012

$$u_A = A \sqrt{\left(\frac{u_W}{W}\right)^2 + \left(\frac{u_H}{H}\right)^2}$$

$$u_A = 89.74 \sqrt{\left(\frac{0.012}{24.79}\right)^2 + \left(\frac{0.012}{3.62}\right)^2} = 0.30$$

#### 4. Uncertainty on strain

##### 4.a. Uncertainty on strain in side A

$\epsilon_{max}$	$\epsilon_{0.05}$	$\epsilon_{0.25}$
%	%	%
2.50	0.05	0.25

\*Sample **1\_Bio\_CO\_#30#**

$$u_\epsilon = \frac{1\epsilon}{100\sqrt{3}}$$

$$u_{\epsilon_m} = \frac{1 \times 2.50}{100 \times \sqrt{3}} = 0.014$$

$$u_{\epsilon_{0.05}} = \frac{1 \times 0.05}{100 \times \sqrt{3}} = 0.00029$$

$$u_{\epsilon_{0.25}} = \frac{1 \times 0.25}{100 \times \sqrt{3}} = 0.0014$$

##### 4.b. Uncertainty on strain in side B

$\epsilon_{max}$	$\epsilon_{0.05}$	$\epsilon_{0.25}$
%	%	%
3.10	0.05	0.25

\*Sample **1\_Bio\_CO\_#30#**

$$u_\epsilon = \frac{1\epsilon}{100\sqrt{3}}$$

$$u_{\epsilon_m} = \frac{1 \times 3.10}{100 \times \sqrt{3}} = 0.018$$

$$u_{\epsilon_{0.05}} = \frac{1 \times 0.05}{100 \times \sqrt{3}} = 0.00029$$



$$u_{\varepsilon_{0.25}} = \frac{1 \times 0.25}{100 \times \sqrt{3}} = 0.0014$$

## 5. Uncertainty on applied force

### 5.a. Uncertainty of the applied force in side A

Specimen	F <sub>0.05</sub>	F <sub>0.25</sub>
	N	N
<b>1_Bio_C0_#30#</b>	1405.95	3662.10

$$u_F = \frac{0.5F}{100\sqrt{3}}$$

$$u_{F_{0.05}} = \frac{0.5 \times 1405.95}{100 \times \sqrt{3}} = 4.06$$

$$u_{F_{0.25}} = \frac{0.5 \times 3662.10}{100 \times \sqrt{3}} = 10.57$$

### 5.b. Uncertainty of the applied force in side B

Specimen	F <sub>0.05</sub>	F <sub>0.25</sub>
	N	N
<b>1_Bio_C0_#30#</b>	1149.57	3026.03

$$u_F = \frac{0.5F}{100\sqrt{3}}$$

$$u_{F_{0.05}} = \frac{0.5 \times 1149.57}{100 \times \sqrt{3}} = 3.31$$

$$u_{F_{0.25}} = \frac{0.5 \times 3026.03}{100 \times \sqrt{3}} = 8.73$$

### 5.c. Uncertainty of the maximum applied force

Specimen	F <sub>m</sub>
	N

<b>1_Bio_CO_#30#</b>	9730.00
----------------------	---------

$$u_F = \frac{0.5F}{100\sqrt{3}}$$

$$u_{F_m} = \frac{0.5 \times 9730.00}{100 \times \sqrt{3}} = 28.09$$

## 6. Uncertainty on the applied load

### 6.a. Uncertainty on the applied load in side A

<b>A</b>	<b>u<sub>A</sub></b>	<b>F<sub>0.05</sub></b>	<b>u<sub>F0.05</sub></b>	<b>σ<sub>0.05</sub></b>	<b>F<sub>0.25</sub></b>	<b>u<sub>F0.25</sub></b>	<b>σ<sub>0.25</sub></b>
mm <sup>2</sup>	mm <sup>2</sup>	N	N	N/mm <sup>2</sup>	N	N	N/mm <sup>2</sup>
89.74	0.30	1405.95	4.06	8.87	3662.10	10.57	35.82

\*Sample **1\_Bio\_CO\_#30#**

$$u_\sigma = \sigma \sqrt{\left(\frac{u_F}{F}\right)^2 + \left(\frac{u_A}{A}\right)^2}$$

$$u_{\sigma 0.05} = 8.87 \sqrt{\left(\frac{4.06}{1405.95}\right)^2 + \left(\frac{0.30}{89.74}\right)^2} = 0.00009$$

$$u_{\sigma 0.25} = 35.82 \sqrt{\left(\frac{10.57}{3662.10}\right)^2 + \left(\frac{0.30}{89.74}\right)^2} = 0.00034$$

### 6.b. Uncertainty on the applied load in side B

<b>A</b>	<b>u<sub>A</sub></b>	<b>F<sub>0.05</sub></b>	<b>u<sub>F0.05</sub></b>	<b>σ<sub>0.05</sub></b>	<b>F<sub>0.25</sub></b>	<b>u<sub>F0.25</sub></b>	<b>σ<sub>0.25</sub></b>
mm <sup>2</sup>	mm <sup>2</sup>	N	N	N/mm <sup>2</sup>	N	N	N/mm <sup>2</sup>
89.74	0.30	1149.57	3.31	6.27	3026.03	8.73	29.27

\*Sample **1\_Bio\_CO\_#30#**

$$u_\sigma = \sigma \sqrt{\left(\frac{u_F}{F}\right)^2 + \left(\frac{u_A}{A}\right)^2}$$

$$u_{\sigma 0.05} = 6.27 \sqrt{\left(\frac{3.31}{1149.57}\right)^2 + \left(\frac{0.30}{89.74}\right)^2} = 0.00006$$

$$u_{\sigma 0.25} = 29.27 \sqrt{\left(\frac{8.73}{3026.03}\right)^2 + \left(\frac{0.30}{89.74}\right)^2} = 0.00028$$

### 6.c. Uncertainty of the maximum applied load

Specimen	$F_m$	$U_{Fm}$	$\sigma_{max}$
	N	N	N/mm <sup>2</sup>
<b>1_Bio_C0_#30#</b>	9730.00	28.09	108

\*Sample **1\_Bio\_C0\_#30#**

$$u_{\sigma} = \sigma \sqrt{\left(\frac{u_F}{F}\right)^2 + \left(\frac{u_A}{A}\right)^2}$$

$$u_{\sigma max} = 108 \sqrt{\left(\frac{28.09}{9730.00}\right)^2 + \left(\frac{0.30}{89.74}\right)^2} = 0.0010$$

## 7. Uncertainty on elastic modulus

### 7. a. Uncertainty on elastic modulus in side A

$E_A$	$U_{\sigma 0.05}$	$U_{\sigma 0.25}$	$\sigma_{0.05}$	$\sigma_{0.25}$	$\epsilon_{0.05}$	$\epsilon_{0.25}$	$U_{\epsilon 0.05}$	$U_{\epsilon 0.25}$
N/mm <sup>2</sup>	N/mm <sup>2</sup>	N/mm <sup>2</sup>	N/mm <sup>2</sup>	N/mm <sup>2</sup>	%	%	%	%
12570,50	0.00009	0.00034	8.87	35.82	0.05	0.25	0.00029	0.0014

\*Sample **1\_Bio\_C0\_#30#**

$$u_{E_A} = E_A \sqrt{\frac{u_{\sigma 0.05}^2 + u_{\sigma 0.25}^2}{(\sigma_{0.05} - \sigma_{0.25})^2} + \frac{u_{\epsilon 0.05}^2 + u_{\epsilon 0.25}^2}{(\epsilon_{0.25} - \epsilon_{0.05})^2}}$$

$$u_{E_A} = 12570.50 \sqrt{\frac{0.00009^2 + 0.00034^2}{(35.82 - 8.87)^2} + \frac{0.00029^2 + 0.0014^2}{(0.25 - 0.05)^2}} = 89.86$$

### 7.b. Uncertainty on elastic modulus in side B

<b>E<sub>B</sub></b>	<b>U<sub>σ0.05</sub></b>	<b>U<sub>σ0.25</sub></b>	<b>σ<sub>0.05</sub></b>	<b>σ<sub>0.25</sub></b>	<b>ε<sub>0.05</sub></b>	<b>ε<sub>0.25</sub></b>	<b>U<sub>ε0.05</sub></b>	<b>U<sub>ε0.25</sub></b>
N/mm <sup>2</sup>	N/mm <sup>2</sup>	N/mm <sup>2</sup>	N/mm <sup>2</sup>	N/mm <sup>2</sup>	%	%	%	%
10455.00	0.00006	0.00028	6.27	29.27	0.05	0.25	0.00029	0.0014

\*Sample **1\_Bio\_C0\_#30#**

$$u_{E_B} = E_B \sqrt{\frac{u_{\sigma 0.05}^2 + u_{\sigma 0.25}^2}{(\sigma_{0.05} - \sigma_{0.25})^2} + \frac{u_{\varepsilon 0.05}^2 + u_{\varepsilon 0.25}^2}{(\varepsilon_{0.25} - \varepsilon_{0.05})^2}}$$

$$u_{E_B} = 10455.00 \sqrt{\frac{0.00006^2 + 0.00028^2}{(29.27 - 6.27)^2} + \frac{0.00029^2 + 0.0014^2}{(0.25 - 0.05)^2}} = 74.74$$

### 7.c. Uncertainty on elastic modulus

<b>Specimen</b>	<b>U<sub>EA</sub></b>	<b>U<sub>EB</sub></b>
	N/mm <sup>2</sup>	N/mm <sup>2</sup>
<b>1_Bio_C0_#30#</b>	89.86	74.74

$$u_E = \sqrt{u_{E_A}^2 + u_{E_B}^2}$$

$$u_E = \sqrt{89.86^2 + 74.74^2} = 116.88$$

### Annex 3: In-plane shear test uncertainties calculations

In-plane shear test uncertainties calculation has been done using data from samples **1\_Bio\_S45\_#35#**.

#### 1. Uncertainty of Thickness

	Value 1	Value 2	Value 3	Average	SD
Thickness	4.46	4.61	4.50	<b>4.52</b>	0.08

\*Sample **1\_Bio\_S45\_#35#**

$$u_H = \sqrt{u_{H,A}^2 + u_{H,instr}^2}$$

$$u_{H,A} = \frac{s_H}{\sqrt{n_A}}$$

$$u_{H,instr} = \frac{0.02}{\sqrt{3}}$$

$$u_{H,A} = \frac{0.08}{\sqrt{3}}$$

$$u_{H,instr} = \frac{0.02}{\sqrt{3}}$$

$$u_H = \sqrt{\left(\frac{0.08}{\sqrt{3}}\right)^2 + \left(\frac{0.02}{\sqrt{3}}\right)^2} = 0.047$$

#### 2. Uncertainty of Width

	Value 1	Value 2	Value 3	Average	SD
Width	25.02	24.96	25.16	<b>25.05</b>	0.10

\*Sample **1\_Bio\_S45\_#35#**

$$u_W = \sqrt{u_{W,A}^2 + u_{W,instr}^2}$$

$$u_{W,instr} = \frac{0.02}{\sqrt{3}}$$

$$u_{W,A} = \frac{s_W}{\sqrt{n_A}}$$

$$u_{W,instr} = \frac{0.02}{\sqrt{3}}$$

$$u_{W,A} = \frac{0.10}{\sqrt{3}}$$

$$u_W = \sqrt{\left(\frac{0.10}{\sqrt{3}}\right)^2 + \left(\frac{0.02}{\sqrt{3}}\right)^2} = 0.13$$

### 3. Uncertainty of cross-sectional area

Specimen	H	W	A	u <sub>H</sub>	u <sub>W</sub>
	mm	mm	mm <sup>2</sup>	mm <sup>2</sup>	mm <sup>2</sup>
<b>1_Bio_S45_#35#</b>	4.52	25.05	113.22	0.047	0.13

$$u_A = \sqrt{\left(\frac{u_W}{W}\right)^2 + \left(\frac{u_H}{H}\right)^2}$$

$$u_A = 113.22 \sqrt{\left(\frac{0.13}{25.05}\right)^2 + \left(\frac{0.047}{4.52}\right)^2} = 1.32$$

### 4. Uncertainty of the applied force

Specimen	F <sub>m</sub>	F <sub>0.2</sub>	F <sub>0.6</sub>
	N	N	N
<b>1_Bio_S45_#35#</b>	3010	212	999

$$u_F = \frac{0.5F}{100\sqrt{3}}$$

$$u_{F_m} = \frac{0.5 \times 3010}{100 \times \sqrt{3}} = 8.69$$

$$u_{F_{0.2}} = \frac{0.5 \times 212}{100 \times \sqrt{3}} = 0.61$$

$$u_{F_{0.6}} = \frac{0.5 \times 999}{100 \times \sqrt{3}} = 2.88$$

### 5. Uncertainty on strain in x/y

ε <sub>max-x</sub>	ε <sub>max-y</sub>	ε <sub>x-0.2</sub>	ε <sub>y-0.2</sub>	ε <sub>x-0.6</sub>	ε <sub>y-0.6</sub>
%	%	%	%	%	%

1.20	1.30	0.07	0.13	0.27	0.33
------	------	------	------	------	------

\*Sample **1\_Bio\_S45\_#35#**

$$u_{\varepsilon} = \frac{1\varepsilon}{100\sqrt{3}}$$

$$u_{\varepsilon x} = \frac{1 \times 1.20}{100 \times \sqrt{3}} = 0.0069$$

$$u_{\varepsilon y} = \frac{1 \times 1.30}{100 \times \sqrt{3}} = 0.0075$$

$$u_{\varepsilon x-0.2} = \frac{1 \times 0.07}{100 \times \sqrt{3}} = 0.0004$$

$$u_{\varepsilon y-0.2} = \frac{1 \times 0.13}{100 \times \sqrt{3}} = 0.0008$$

$$u_{\varepsilon x-0.6} = \frac{1 \times 0.27}{100 \times \sqrt{3}} = 0.0016$$

$$u_{\varepsilon y-0.6} = \frac{1 \times 0.33}{100 \times \sqrt{3}} = 0.0019$$

### 6. Uncertainty on shear strain

<b>U<sub>εmax-x</sub></b>	<b>U<sub>εmax-y</sub></b>	<b>U<sub>εx-0.2</sub></b>	<b>U<sub>εy-0.2</sub></b>	<b>U<sub>εx-0.6</sub></b>	<b>U<sub>εy-0.6</sub></b>
%	%	%	%	%	%
0.0069	0.0075	0.0004	0.0008	0.0016	0.0019

$$u_{\gamma} = \sqrt{u_{\varepsilon x}^2 + u_{\varepsilon y}^2}$$

$$u_{\gamma \max} = \sqrt{0.0069^2 + 0.0075^2} = 0.010$$

$$u_{\gamma 0.2} = \sqrt{0.0004^2 + 0.0008^2} = 0.00085$$

$$u_{\gamma 0.6} = \sqrt{0.0016^2 + 0.0019^2} = 0.0024$$

### 7. Uncertainty on the applied load

<b>A</b>	<b>U<sub>A</sub></b>	<b>F<sub>m</sub></b>	<b>U<sub>Fm</sub></b>	<b>T<sub>max</sub></b>	<b>F<sub>0.2</sub></b>	<b>U<sub>F0.2</sub></b>	<b>T<sub>0.2</sub></b>	<b>F<sub>0.6</sub></b>	<b>U<sub>F0.6</sub></b>	<b>T<sub>0.6</sub></b>
mm <sup>2</sup>	mm <sup>2</sup>	N	N	N/mm <sup>2</sup>	N	N	N/mm <sup>2</sup>	N	N	N/mm <sup>2</sup>

113.22	1.32	3010	8.69	26.6	212	0.61	1.87	999	2.88	8.82
--------	------	------	------	------	-----	------	------	-----	------	------

\*Sample **1\_Bio\_S45\_#35#**

$$u_{\tau} = \frac{1}{2} \tau \sqrt{\left(\frac{u_F}{F}\right)^2 + \left(\frac{u_A}{A}\right)^2}$$

$$u_{\tau\max} = \frac{1}{2} 26.6 \sqrt{\left(\frac{8.69}{3010}\right)^2 + \left(\frac{1.32}{113.22}\right)^2} = 0.16$$

$$u_{\tau 0.2} = \frac{1}{2} 1.87 \sqrt{\left(\frac{0.61}{212}\right)^2 + \left(\frac{1.32}{113.22}\right)^2} = 0.010$$

$$u_{\tau 0.6} = \frac{1}{2} 8.82 \sqrt{\left(\frac{2.88}{999}\right)^2 + \left(\frac{1.32}{113.22}\right)^2} = 0.052$$

### 8. Uncertainty on elastic modulus

<b>G<sub>12</sub></b>	<b>u<sub>τ0.2</sub></b>	<b>u<sub>τ0.6</sub></b>	<b>τ<sub>0.2</sub></b>	<b>τ<sub>0.6</sub></b>	<b>γ<sub>0.2</sub></b>	<b>γ<sub>0.6</sub></b>	<b>u<sub>γ0.2</sub></b>	<b>u<sub>γ0.6</sub></b>
N/mm <sup>2</sup>	N/mm <sup>2</sup>	N/mm <sup>2</sup>	N/mm <sup>2</sup>	N/mm <sup>2</sup>	%	%	%	%
1720	0.010	0.052	3.1	9.2	0.2	0.6	0.00085	0.0024

\*Sample **1\_Bio\_S45\_#35#**

$$u_{G12} = G_{12} \sqrt{\frac{u_{\tau 1}^2 + u_{\tau 2}^2}{(\tau_2 - \tau_1)^2} + \frac{u_{\gamma 1}^2 + u_{\gamma 2}^2}{(\gamma_2 - \gamma_1)^2}}$$

$$u_{G12} = 1720 \sqrt{\frac{0.010^2 + 0.052^2}{(9.2 - 3.1)^2} + \frac{0.00085^2 + 0.0024^2}{(0.60 - 0.20)^2}} = 18.51$$



## Annex 4: ILSS test uncertainties calculations

ILSS test uncertainties calculation has been done using data from samples

### 1\_Bio\_ILSS\_#32#.

#### 1. Uncertainty of thickness

	Value 1	Value 2	Value 3	Average	SD
Thickness	3.86	3.85	3.89	<b>3.87</b>	0.02

\*Sample **1\_Bio\_ILSS\_#32#**

$$u_H = \sqrt{u_{H,A}^2 + u_{H,inst}^2}$$

$$u_{H,A} = \frac{s_H}{\sqrt{n_A}} \quad u_{H,inst} = \frac{0.02}{\sqrt{3}}$$

$$u_{H,A} = \frac{0.02}{\sqrt{3}} \quad u_{H,inst} = \frac{0.02}{\sqrt{3}}$$

$$u_H = \sqrt{\left(\frac{0.02}{\sqrt{3}}\right)^2 + \left(\frac{0.02}{\sqrt{3}}\right)^2} = 0.017$$

#### 2. Uncertainty of width

	Value 1	Value 2	Value 3	Average	SD
Width	20.49	20.75	20.79	<b>13.58</b>	0.16

\*Sample **1\_Bio\_ILSS\_#32#**

$$u_W = \sqrt{u_{W,A}^2 + u_{W,inst}^2}$$

$$u_{W,A} = \frac{s_W}{\sqrt{n_A}} \quad u_{W,inst} = \frac{0.02}{\sqrt{3}}$$

$$u_{W,A} = \frac{0.16}{\sqrt{3}} \quad u_{W,inst} = \frac{0.02}{\sqrt{3}}$$

$$u_W = \sqrt{\left(\frac{0.16}{\sqrt{3}}\right)^2 + \left(\frac{0.02}{\sqrt{3}}\right)^2} = 0.093$$

### 3. Uncertainty of cross-sectional area

Specimen	H	W	A	u <sub>H</sub>	u <sub>w</sub>
	mm	mm	mm <sup>2</sup>	mm	mm
<b>1_Bio_ILSS_#32#</b>	2.15	15.24	32.77	0.017	0.093

$$u_A = A \sqrt{\left(\frac{u_W}{W}\right)^2 + \left(\frac{u_H}{H}\right)^2}$$

$$u_A = 32.77 \sqrt{\left(\frac{0.093}{15.24}\right)^2 + \left(\frac{0.017}{2.15}\right)^2} = 0.20$$

### 4. Uncertainty of force

Specimen	F <sub>sbs</sub>
	N
<b>1_Bio_ILSS_#32#</b>	2010

$$u_{Fm} = \frac{0.5F}{100\sqrt{3}}$$

$$u_{Fm} = \frac{0.5 \times 2010}{100 \times \sqrt{3}} = 17.41$$

### 5. Uncertainty on the applied load

Specimen	F <sub>max</sub>	u <sub>Fmax</sub>	A	u <sub>A</sub>
	N	N	mm <sup>2</sup>	mm <sup>2</sup>
<b>1_Bio_ILSS_#32#</b>	2010	17.41	32.77	0.20

$$u_{F^{SBS}} = 0.75 \times F^{SBS} \sqrt{\left(\frac{u_F}{F}\right)^2 + \left(\frac{u_A}{A}\right)^2}$$

$$u_{F^{sbs}} = 0.75 \times 18.84 \sqrt{\left(\frac{17.41}{2010}\right)^2 + \left(\frac{0.2}{32.77}\right)^2} = 0.15$$

# Appendix G

The two-way **ANOVA** was selected for the data study because there are two factors affecting the final property, the immersion time (A factor) and the concentration (B factor). Two-way ANOVA allows to compare population means when the populations are classified according to two (categorical) factors. Below is the outline of a two-way ANOVA table, with factors A and B, having **I** and **J** groups, respectively:

<u>Source</u>	<u>df</u>	<u>SS</u>	<u>MS</u>	<u>F</u>	<u>p-value</u>
A	$I - 1$	SSA	MSA	MSA/MSE	
B	$J - 1$	SSB	MSB	MSB/MSE	
A × B	$(I - 1)(J - 1)$	SSAB	MSAB	MSAB/MSE	
Error	$n - IJ$	SSE	MSE		
Total	$n - 1$	SST			

Where **n** is the sample size; **df** is degree of freedom; **SS** is sum of squares; **MS** is Mean Square; **F** is used for the F statistics; and **p-value** is the calculated evaluate if the null hypothesis ( $H_0$ ) or the alternate hypothesis ( $H_a$ ) are true. The hypothesis definitions are as follow:

$H_0$ : The means of all groups under consideration are equal

$H_a$ : The means are not all equal

In this particular case there are three hypotheses to prove. For the case of the null hypothesis it must be checked whether the means values of all groups are equal under immersion time, concentration and combinative effect.

I.

$H_0$ : There is no main effect due to immersion time

$H_a$ : There is a main effect due to immersion time

II.

$H_0$ : There is no main effect due to concentration

$H_a$ : There is a main effect due to concentration

### III.

$H_0$ : There is no an interaction effect between the two variables

$H_a$ : There is an interaction effect between the two variables

According to this, three different p-values are calculated and compared with the  $\alpha$  value at a determinate level of significance. In this case for a 95% level of significance the  $\alpha = 0.05$ . If the  $p\text{-value} > \alpha$ , the  $H_0$  is true, and if the  $p\text{-value} < \alpha$ , the  $H_a$  is true. Additionally if the null hypothesis is true, the F statistic has an F distribution with  $k-1$  and  $n-k$  degrees of freedom in the numerator/denominator respectively. If the alternate hypothesis is true, then F tends to be large. We reject  $H_0$  in favour of  $H_a$  if the F statistic is sufficiently large.

Once the data was analysed with ANOVA, **Fisher's F test** was used in order to determinate if the average values difference is representative or not. This procedure contemplates to rest two values in order to get a number, and the number must be compared to the LSD value: a rule was introduced in the Excel spreadsheet to colour in red the boxes where **result > LSD**. According to Fisher's method the red boxes mean that the difference between the data is significant enough. In this particular case when the boxes are unmodified means that the modification by immersion time or concentration is not significant enough to affect the mechanical property; and in the other way round, when the box is turned red, the immersion time or concentration is significantly affecting the mechanical property.

Note that for the best statistical treatment, the same amount of measurements is desired, for that reason when there is not that number, it is copied the number just above for the completion of the set of data. See the red numbers in each section first table. In the mechanical tests experimental campaigns it is very common to miss some numbers because of different reasons such as software mistake, extensometer data recording stop or load-cell data recording problems.

In the following sections the calculations resume for all the properties are shown.

# Longitudinal modulus E<sub>1</sub>

E modulus LTT		B: Concentration							
		0,25	0,5	1	1,5	2	Total Y...		
A: Immersion time	1	8961,39 10620,20 10279,60 9291,24 8935,08 9014,91 10648,80 10253,10 11093,50 10146,70	12602,70 9259,02 9191,33 10096,00 11667,90 10190,30 9419,04 9579,96 9905,71 11389,80	10581,00 9275,18 10005,20 10949,40 10150,70 9962,64 9741,82 8906,97 10578,00 9513,18	9685,35 8122,03 9049,65 6278,69 7453,10 6385,00 7358,69 7011,46 7054,89 6001,73	4301,69 5172,65 4362,05 3972,95 3947,60 3840,76 3876,28 4066,06 3758,05 4220,93		418129,98	
	3	10779,70 10384,90 11157,30 10047,80 11115,40 10032,20 10414,00 10754,10 8479,27 9282,72	10783,80 10264,30 9367,06 9371,11 8288,80 8990,58 9164,77 9529,20 10042,40 9181,88	8303,93 10729,10 8399,13 9561,48 10529,80 11246,10 10906,70 12360,80 8577,66 8267,36	8303,93 8705,80 10617,80 8261,29 9030,97 9712,83 9803,28 9587,87 9708,06 10400,10	11739,10 8705,80 10617,80 8261,29 9030,97 9712,83 9803,28 9587,87 9708,06 10400,10	2886,18 3130,49 3176,77 3257,43 3166,17 3026,69 2974,85 3119,62 3442,36 3292,76	31473,32	425353,77
	12	10291,10 10888,00 11765,40 10101,10 10025,30 9638,86 10185,40 9465,76 8618,24 8978,15	10250,70 9672,13 11265,80 10422,60 10827,80 10288,10 10740,00 8572,76 10059,60 10424,30	6358,32 6959,77 7476,57 7969,94 7351,32 6819,72 6794,41 7283,29 9987,64 9629,29	6358,32 6959,77 7476,57 7969,94 7351,32 6819,72 6794,41 7283,29 9987,64 9629,29	9015,98 10591,10 9423,22 8872,58 10723,90 12220,00 11125,00 9709,50 9747,39 9934,53	3063,85 3692,20 3641,65 3450,86 2888,33 3102,64 3065,34 3391,70 3111,82 3214,21	32622,60	413097,17
	24	9253,32 9626,97 9581,84 10214,90 9309,13 8310,75 8564,69 10950,60 8826,16 9204,06	10926,90 7605,88 8214,20 9690,30 9522,93 7544,60 9181,14 7259,32 8229,67 9958,11	7060,92 11306,20 8023,67 7021,02 8917,43 10047,90 8815,23 6907,00 8611,93 9074,64	7060,92 11306,20 8023,67 7021,02 8917,43 10047,90 8815,23 6907,00 8611,93 9074,64	6513,80 6126,86 6093,36 6647,37 6416,69 5666,63 6736,91 6385,00 8007,56 7593,09	3516,76 3483,83 3762,92 3143,20 3457,43 3328,32 3559,90 3456,91 3066,12 2848,04	33623,43	367572,11
Total Y...		395491,64	388942,5	360962,36	339518,16	139238,37	Y...	1624153,03	

Source	SS	df	MS	F <sub>0</sub>	p-value
Efecto A	40975430,51	3	13658476,84	16,08	0,0000000026535527399
Efecto B	1126725565,78	4	281681391,45	331,54	0,0000000000000000000
Efecto AB	110512596,82	12	9209383,07	10,84	0,0000000000000004499
Error	152931675,25	180	849620,42		
Total	1431145268,4	199			

n = 10  
 $t_{(0,05;180)}$  1,973  
 LSD 813,402

## Immersion time effect (A)

B <sub>1</sub> A <sub>1</sub> - B <sub>1</sub> A <sub>2</sub>	320,29	B <sub>2</sub> A <sub>1</sub> - B <sub>2</sub> A <sub>2</sub>	831,79	B <sub>3</sub> A <sub>1</sub> - B <sub>3</sub> A <sub>2</sub>	78,20	B <sub>4</sub> A <sub>1</sub> - B <sub>4</sub> A <sub>2</sub>	2316,65	B <sub>5</sub> A <sub>1</sub> - B <sub>5</sub> A <sub>2</sub>	1004,57
B <sub>1</sub> A <sub>1</sub> - B <sub>1</sub> A <sub>3</sub>	71,28	B <sub>2</sub> A <sub>1</sub> - B <sub>2</sub> A <sub>3</sub>	77,80	B <sub>3</sub> A <sub>1</sub> - B <sub>3</sub> A <sub>3</sub>	2303,38	B <sub>4</sub> A <sub>1</sub> - B <sub>4</sub> A <sub>3</sub>	2696,26	B <sub>5</sub> A <sub>1</sub> - B <sub>5</sub> A <sub>3</sub>	889,64
B <sub>1</sub> A <sub>1</sub> - B <sub>1</sub> A <sub>4</sub>	540,21	B <sub>2</sub> A <sub>1</sub> - B <sub>2</sub> A <sub>4</sub>	1516,87	B <sub>3</sub> A <sub>1</sub> - B <sub>3</sub> A <sub>4</sub>	1387,82	B <sub>4</sub> A <sub>1</sub> - B <sub>4</sub> A <sub>4</sub>	821,33	B <sub>5</sub> A <sub>1</sub> - B <sub>5</sub> A <sub>4</sub>	789,56
B <sub>1</sub> A <sub>2</sub> - B <sub>1</sub> A <sub>3</sub>	249,01	B <sub>2</sub> A <sub>2</sub> - B <sub>2</sub> A <sub>3</sub>	753,99	B <sub>3</sub> A <sub>2</sub> - B <sub>3</sub> A <sub>3</sub>	2225,18	B <sub>4</sub> A <sub>2</sub> - B <sub>4</sub> A <sub>3</sub>	379,61	B <sub>5</sub> A <sub>2</sub> - B <sub>5</sub> A <sub>3</sub>	114,93
B <sub>1</sub> A <sub>2</sub> - B <sub>1</sub> A <sub>4</sub>	860,50	B <sub>2</sub> A <sub>2</sub> - B <sub>2</sub> A <sub>4</sub>	685,09	B <sub>3</sub> A <sub>2</sub> - B <sub>3</sub> A <sub>4</sub>	1309,61	B <sub>4</sub> A <sub>2</sub> - B <sub>4</sub> A <sub>4</sub>	3137,98	B <sub>5</sub> A <sub>2</sub> - B <sub>5</sub> A <sub>4</sub>	215,01
B <sub>1</sub> A <sub>3</sub> - B <sub>1</sub> A <sub>4</sub>	611,49	B <sub>2</sub> A <sub>3</sub> - B <sub>2</sub> A <sub>4</sub>	1439,07	B <sub>3</sub> A <sub>3</sub> - B <sub>3</sub> A <sub>4</sub>	915,57	B <sub>4</sub> A <sub>3</sub> - B <sub>4</sub> A <sub>4</sub>	3517,59	B <sub>5</sub> A <sub>3</sub> - B <sub>5</sub> A <sub>4</sub>	100,08

## Concentration effect (B)

B <sub>1</sub> A <sub>1</sub> - B <sub>2</sub> A <sub>1</sub>	405,72	B <sub>1</sub> A <sub>2</sub> - B <sub>2</sub> A <sub>2</sub>	746,35	B <sub>1</sub> A <sub>3</sub> - B <sub>2</sub> A <sub>3</sub>	256,65	B <sub>1</sub> A <sub>4</sub> - B <sub>2</sub> A <sub>4</sub>	570,94
B <sub>1</sub> A <sub>1</sub> - B <sub>3</sub> A <sub>1</sub>	41,96	B <sub>1</sub> A <sub>2</sub> - B <sub>3</sub> A <sub>2</sub>	356,53	B <sub>1</sub> A <sub>3</sub> - B <sub>3</sub> A <sub>3</sub>	2332,70	B <sub>1</sub> A <sub>4</sub> - B <sub>3</sub> A <sub>4</sub>	805,65
B <sub>1</sub> A <sub>1</sub> - B <sub>4</sub> A <sub>1</sub>	2484,39	B <sub>1</sub> A <sub>2</sub> - B <sub>4</sub> A <sub>2</sub>	488,03	B <sub>1</sub> A <sub>3</sub> - B <sub>4</sub> A <sub>3</sub>	140,59	B <sub>1</sub> A <sub>4</sub> - B <sub>4</sub> A <sub>4</sub>	2765,52
B <sub>1</sub> A <sub>1</sub> - B <sub>5</sub> A <sub>1</sub>	5772,55	B <sub>1</sub> A <sub>2</sub> - B <sub>5</sub> A <sub>2</sub>	7097,41	B <sub>1</sub> A <sub>3</sub> - B <sub>5</sub> A <sub>3</sub>	6733,47	B <sub>1</sub> A <sub>4</sub> - B <sub>5</sub> A <sub>4</sub>	6021,90
B <sub>2</sub> A <sub>1</sub> - B <sub>3</sub> A <sub>1</sub>	363,77	B <sub>2</sub> A <sub>2</sub> - B <sub>3</sub> A <sub>2</sub>	389,82	B <sub>2</sub> A <sub>3</sub> - B <sub>3</sub> A <sub>3</sub>	2589,35	B <sub>2</sub> A <sub>4</sub> - B <sub>3</sub> A <sub>4</sub>	234,71
B <sub>2</sub> A <sub>1</sub> - B <sub>4</sub> A <sub>1</sub>	2890,12	B <sub>2</sub> A <sub>2</sub> - B <sub>4</sub> A <sub>2</sub>	258,32	B <sub>2</sub> A <sub>3</sub> - B <sub>4</sub> A <sub>3</sub>	116,06	B <sub>2</sub> A <sub>4</sub> - B <sub>4</sub> A <sub>4</sub>	2194,58
B <sub>2</sub> A <sub>1</sub> - B <sub>5</sub> A <sub>1</sub>	6178,27	B <sub>2</sub> A <sub>2</sub> - B <sub>5</sub> A <sub>2</sub>	6351,06	B <sub>2</sub> A <sub>3</sub> - B <sub>5</sub> A <sub>3</sub>	6990,12	B <sub>2</sub> A <sub>4</sub> - B <sub>5</sub> A <sub>4</sub>	5450,96
B <sub>3</sub> A <sub>1</sub> - B <sub>4</sub> A <sub>1</sub>	2526,35	B <sub>3</sub> A <sub>2</sub> - B <sub>4</sub> A <sub>2</sub>	131,50	B <sub>3</sub> A <sub>3</sub> - B <sub>4</sub> A <sub>3</sub>	2473,29	B <sub>3</sub> A <sub>4</sub> - B <sub>4</sub> A <sub>4</sub>	1959,87
B <sub>3</sub> A <sub>1</sub> - B <sub>5</sub> A <sub>1</sub>	5814,51	B <sub>3</sub> A <sub>2</sub> - B <sub>5</sub> A <sub>2</sub>	6740,87	B <sub>3</sub> A <sub>3</sub> - B <sub>5</sub> A <sub>3</sub>	4400,77	B <sub>3</sub> A <sub>4</sub> - B <sub>5</sub> A <sub>4</sub>	5216,25
B <sub>4</sub> A <sub>1</sub> - B <sub>5</sub> A <sub>1</sub>	3288,16	B <sub>4</sub> A <sub>2</sub> - B <sub>5</sub> A <sub>2</sub>	6609,38	B <sub>4</sub> A <sub>3</sub> - B <sub>5</sub> A <sub>3</sub>	6874,06	B <sub>4</sub> A <sub>4</sub> - B <sub>5</sub> A <sub>4</sub>	3256,38

## Longitudinal strength $\sigma_1$

Strength LTT		B: Concentration						Total $Y_{...}$	
		0,25	0,5	1	1,5	2			
A: Immersion time	1	121,40	136,10	118,18	93,84	74,66	4884,74		
		110,26	127,18	87,36	88,90	65,10			
		114,07	109,97	103,14	91,05	67,49			
		112,47	122,63	110,84	79,67	68,02			
		111,26	116,70	94,16	83,17	65,56			
		114,85	1179,91	117,02	74,63	64,80		842,03	664,49
		128,46	108,99	103,80	79,29	65,41			
		116,44	115,61	99,12	80,78	60,94			
		125,57	113,29	91,43	80,45	61,64			
		125,13	124,59	102,64	90,26	70,89			
	3	122,72	132,61	115,72	99,84	52,75	4863,15		
		127,86	114,36	113,74	92,07	53,89			
		122,85	120,63	96,03	100,05	57,85			
		114,51	113,70	111,97	93,31	49,14			
		117,99	99,62	114,86	91,66	53,14			
		107,70	1191,42	100,56	89,72	53,41		941,62	523,22
		129,00	100,67	114,26	91,21	48,90			
		114,10	114,57	108,19	86,64	53,63			
		120,83	112,50	104,11	100,56	50,81			
		113,87	104,33	106,81	96,57	49,71			
12	111,78	105,43	92,10	105,28	60,63	4808,41			
	113,39	101,35	107,19	102,43	60,56				
	112,32	113,10	92,60	97,03	56,68				
	114,03	111,41	101,66	98,82	61,51				
	105,34	108,51	96,39	103,56	56,30				
	107,64	1123,85	122,91	100,18	60,39		1007,09	579,27	
	119,26	102,02	110,12	97,46	54,37				
	121,12	99,26	100,15	97,40	55,87				
	110,93	106,35	104,96	100,53	58,11				
	108,04	119,14	106,72	104,40	54,86				
24	101,75	106,72	108,13	87,73	52,58	4485,50			
	107,18	97,84	104,73	95,68	55,41				
	111,47	108,54	92,67	86,58	55,39				
	125,58	116,41	91,88	93,00	53,23				
	105,38	1063,92	108,33	101,63	48,85		858,07	525,66	
	101,82	102,05	104,97	104,97	58,32				
	92,07	103,05	94,67	76,62	50,73				
	109,45	113,14	84,89	83,73	53,46				
	99,31	102,50	95,01	79,81	47,48				
	109,91	103,08	97,63	79,69	50,21				
Total $Y_{...}$	4559,10	4456,77	4084,49	3648,81	2292,63	$Y_{...} =$ 19041,80			

FV	SC	GDL	CM	$F_0$	p-value
Efecto A	2077,83	3	692,61	16,65	0,0001
Efecto B	84579,46	4	21144,87	508,28	0,0000
Efecto AB	3740,49	12	311,71	7,49	0,0007
Error	7488,08	180	41,60		
Total	97885,9	199			

$n = 10$

$t_{(0,05;180)} = 1,973$

LSD = 5,692

### Immersion time effect (A)

$B_1A_1 - B_1A_2$	1,15	$B_2A_1 - B_2A_2$	7,85	$B_3A_1 - B_3A_2$	8,71	$B_4A_1 - B_4A_2$	9,96	$B_5A_1 - B_5A_2$	14,13
$B_1A_1 - B_1A_3$	5,61	$B_2A_1 - B_2A_3$	10,26	$B_3A_1 - B_3A_3$	0,25	$B_4A_1 - B_4A_3$	16,51	$B_5A_1 - B_5A_3$	8,52
$B_1A_1 - B_1A_4$	11,60	$B_2A_1 - B_2A_4$	13,04	$B_3A_1 - B_3A_4$	3,00	$B_4A_1 - B_4A_4$	1,60	$B_5A_1 - B_5A_4$	13,88
$B_1A_2 - B_1A_3$	6,76	$B_2A_2 - B_2A_3$	2,41	$B_3A_2 - B_3A_3$	8,46	$B_4A_2 - B_4A_3$	6,55	$B_5A_2 - B_5A_3$	5,60
$B_1A_2 - B_1A_4$	12,75	$B_2A_2 - B_2A_4$	5,19	$B_3A_2 - B_3A_4$	11,71	$B_4A_2 - B_4A_4$	8,36	$B_5A_2 - B_5A_4$	0,24
$B_1A_3 - B_1A_4$	5,99	$B_2A_3 - B_2A_4$	2,78	$B_3A_3 - B_3A_4$	3,25	$B_4A_3 - B_4A_4$	14,90	$B_5A_3 - B_5A_4$	57,93

### Concentration effect (B)

$B_1A_1 - B_2A_1$	1,22	$B_1A_2 - B_2A_2$	7,79	$B_1A_3 - B_2A_3$	3,44	$B_1A_4 - B_2A_4$	0,23
$B_1A_1 - B_3A_1$	17,37	$B_1A_2 - B_3A_2$	9,81	$B_1A_3 - B_3A_3$	11,51	$B_1A_4 - B_3A_4$	8,77
$B_1A_1 - B_4A_1$	33,79	$B_1A_2 - B_4A_2$	24,98	$B_1A_3 - B_4A_3$	11,68	$B_1A_4 - B_4A_4$	20,58
$B_1A_1 - B_5A_1$	51,54	$B_1A_2 - B_5A_2$	66,82	$B_1A_3 - B_5A_3$	54,46	$B_1A_4 - B_5A_4$	53,83
$B_2A_1 - B_3A_1$	18,59	$B_2A_2 - B_3A_2$	2,02	$B_2A_3 - B_3A_3$	8,07	$B_2A_4 - B_3A_4$	8,55
$B_2A_1 - B_4A_1$	35,00	$B_2A_2 - B_4A_2$	17,19	$B_2A_3 - B_4A_3$	17,19	$B_2A_4 - B_4A_4$	20,36
$B_2A_1 - B_5A_1$	52,76	$B_2A_2 - B_5A_2$	59,03	$B_2A_3 - B_5A_3$	51,02	$B_2A_4 - B_5A_4$	53,60
$B_3A_1 - B_4A_1$	16,42	$B_3A_2 - B_4A_2$	15,17	$B_3A_3 - B_4A_3$	0,16	$B_3A_4 - B_4A_4$	11,81
$B_3A_1 - B_5A_1$	34,17	$B_3A_2 - B_5A_2$	57,01	$B_3A_3 - B_5A_3$	42,95	$B_3A_4 - B_5A_4$	45,05
$B_4A_1 - B_5A_1$	17,75	$B_4A_2 - B_5A_2$	41,84	$B_4A_3 - B_5A_3$	42,78	$B_4A_4 - B_5A_4$	33,24

## Longitudinal strain $\epsilon_1$

Strain LTT		B: Concentration						Total $Y_{...}$			
		0,25	0,5	1	1,5	2					
A: Immersion time	1	1,46	1,54	1,29	1,62	3,59					
		1,13	1,58	1,03	1,55	2,84					
		1,32	1,48	1,19	1,45	3,11					
		1,47	1,51	1,15	1,34	3,53					
		1,49	1,52	1,00	1,39	3,59					
		1,54	14,22	1,42	15,17	1,04	15,43	3,54	35,08		
		1,53		1,53		1,64		3,43			
		1,36		1,60		1,42		3,79			
		1,38		1,38	1,21	1,52		4,12			
		1,52		1,62	1,14	1,93			91,27		
	3	1,27	1,59	1,26	1,77	3,84					
		1,28	1,58	1,16	1,62	3,48					
		1,32	1,66	1,10	1,62	4,26					
		1,34	1,48	1,26	1,87	3,27					
		1,36	1,45	1,18	1,72	4,15					
		1,22	13,30	1,50	14,86	1,06	12,17	1,55	16,27	5,17	38,77
		1,46		1,15		1,23		1,54		3,78	
		1,30		1,54		1,12		1,32		3,78	
		1,51		1,46		1,30		1,79		3,72	
		1,24		1,44		1,50		1,47		3,31	
12	1,30	1,25	1,28	1,52	5,40						
	1,36	1,26	1,47	1,42	5,03						
	1,31	1,34	1,25	1,35	3,79						
	1,42	1,44	1,38	1,40	4,51						
	1,33	1,40	1,25	1,46	4,72						
	1,36	13,96	1,63	13,99	1,50	14,15	1,52	14,15	4,98	47,43	
	1,46		1,19		1,55		1,30		4,65		
	1,63		1,54		1,43		1,37		4,41		
	1,42		1,39		1,44		1,39		5,00		
	1,38		1,55		1,45		1,42		4,95		
24	1,19	1,34	1,32	1,68	3,32						
	1,16	1,36	1,35	2,11	3,92						
	1,23	1,34	1,46	1,66	3,60						
	1,36	1,55	2,52	1,83	4,94						
	1,24	12,70	1,52	14,73	1,43	15,00	1,76	16,58	4,25	42,25	
	1,10		1,68		1,43		1,75		5,25		
	1,13		1,52		1,40		1,16		4,11		
	1,46		1,52		1,33		1,74		4,11		
	1,36		1,51		1,34		1,40		3,86		
	1,46		1,37		1,43		1,49		4,88		
Total $Y_{...}$	54,18	58,74	52,55	62,42	163,53		$Y_{...} =$	391,43			

FV	SC	GDL	CM	$F_p$	p-value
Efecto A	1,86	3	0,62	8,81	0,0023
Efecto B	228,59	4	57,15	809,80	0,0000
Efecto AB	7,83	12	0,65	9,24	0,0003
Error	12,70	180			
Total	251,0	199	0,07		

$n = 10$

$t_{(0,05;180)}$

1,973

LSD

0,234

### Immersion time effect (A)

$B_1A_1 - B_1A_2$	0,09	$B_2A_1 - B_2A_2$	0,03	$B_3A_1 - B_3A_2$	0,08	$B_4A_1 - B_4A_2$	0,08	$B_5A_1 - B_5A_2$	0,37
$B_1A_1 - B_1A_3$	0,03	$B_2A_1 - B_2A_3$	0,12	$B_3A_1 - B_3A_3$	0,26	$B_4A_1 - B_4A_3$	0,13	$B_5A_1 - B_5A_3$	1,24
$B_1A_1 - B_1A_4$	0,15	$B_2A_1 - B_2A_4$	0,04	$B_3A_1 - B_3A_4$	0,36	$B_4A_1 - B_4A_4$	0,11	$B_5A_1 - B_5A_4$	0,72
$B_1A_2 - B_1A_3$	0,07	$B_2A_2 - B_2A_3$	0,09	$B_3A_2 - B_3A_3$	0,18	$B_4A_2 - B_4A_3$	0,21	$B_5A_2 - B_5A_3$	0,87
$B_1A_2 - B_1A_4$	0,06	$B_2A_2 - B_2A_4$	0,01	$B_3A_2 - B_3A_4$	0,28	$B_4A_2 - B_4A_4$	0,03	$B_5A_2 - B_5A_4$	0,35
$B_1A_3 - B_1A_4$	0,13	$B_2A_3 - B_2A_4$	0,07	$B_3A_3 - B_3A_4$	0,10	$B_4A_3 - B_4A_4$	0,24	$B_5A_3 - B_5A_4$	0,52

### Concentration effect (B)

$B_1A_1 - B_2A_1$	0,10	$B_1A_2 - B_2A_2$	0,16	$B_1A_3 - B_2A_3$	0,00	$B_1A_4 - B_2A_4$	0,20
$B_1A_1 - B_3A_1$	0,28	$B_1A_2 - B_3A_2$	0,11	$B_1A_3 - B_3A_3$	0,00	$B_1A_4 - B_3A_4$	0,23
$B_1A_1 - B_4A_1$	0,12	$B_1A_2 - B_4A_2$	0,30	$B_1A_3 - B_4A_3$	0,02	$B_1A_4 - B_4A_4$	0,39
$B_1A_1 - B_5A_1$	2,09	$B_1A_2 - B_5A_2$	2,55	$B_1A_3 - B_5A_3$	3,35	$B_1A_4 - B_5A_4$	2,95
$B_2A_1 - B_3A_1$	0,38	$B_2A_2 - B_3A_2$	0,27	$B_2A_3 - B_3A_3$	0,00	$B_2A_4 - B_3A_4$	0,03
$B_2A_1 - B_4A_1$	0,03	$B_2A_2 - B_4A_2$	0,14	$B_2A_3 - B_4A_3$	0,02	$B_2A_4 - B_4A_4$	0,19
$B_2A_1 - B_5A_1$	1,99	$B_2A_2 - B_5A_2$	2,39	$B_2A_3 - B_5A_3$	3,34	$B_2A_4 - B_5A_4$	2,75
$B_3A_1 - B_4A_1$	0,40	$B_3A_2 - B_4A_2$	0,41	$B_3A_3 - B_4A_3$	0,02	$B_3A_4 - B_4A_4$	0,16
$B_3A_1 - B_5A_1$	2,37	$B_3A_2 - B_5A_2$	2,66	$B_3A_3 - B_5A_3$	3,34	$B_3A_4 - B_5A_4$	2,72
$B_4A_1 - B_5A_1$	1,96	$B_4A_2 - B_5A_2$	2,25	$B_4A_3 - B_5A_3$	3,33	$B_4A_4 - B_5A_4$	2,57

## Transverse modulus E<sub>2</sub>

E modulus LTT		B: Concentration						Total Y <sub>...</sub>	
		0,25	0,5	1	1,5	2			
A: Immersion time	1	3759,37 3381,06 3409,10 3016,79 2810,50 2785,04 2652,43 2984,97 2727,53	3290,28 3091,16 3124,89 2667,47 2242,68 3252,59 2396,06 2507,79 2543,20	2839,04 2833,20 3059,49 3067,19 2826,85 3263,50 3178,15 3874,40 3535,07	3284,11 4181,58 3938,83 3697,35 3889,78 3563,20 3805,91 4102,67 4486,46		903,74 903,74 820,17 826,06 791,32 1500,50 1224,41 717,08 659,77		124416,49
	3	3299,92 3261,10 3116,33 2531,06 2155,53 2096,07 2685,28 2949,79 2487,90	2431,92 2524,89 2385,04 2483,01 2578,59 2661,60 2533,97 2418,49 2507,49	3143,40 2824,21 2596,01 3093,05 3606,11 3695,65 3791,45 3844,45 3809,36	2962,27 3204,95 3284,36 2758,34 3754,58 2923,68 2881,12 3738,90 4113,44		1040,47 1009,84 1045,03 1027,43 844,43 1028,20 1066,15 600,99 600,99		115396,83
	12	1965,90 1954,17 1995,96 2244,50 2157,22 2003,56 2391,17 2819,02 2759,98	4100,54 3132,84 2919,23 3215,11 2956,44 4109,66 2942,66 2468,98	3007,81 3736,34 3600,49 4319,40 4869,34 4466,06 3104,42 2888,68 2888,68	4303,16 4303,16 4208,54 4208,54 4337,65 4241,07 4576,94 4576,94 5636,35		1069,30 1115,82 1135,65 1032,37 1102,80 1357,83 1796,98 958,03 958,03		132879,97
	24	3163,61 3004,76 2681,53 2561,01 2116,07 2779,44 3120,60 2604,24 2553,98	2986,58 2483,84 2589,97 2879,95 2717,42 2945,75 3036,87 2855,23 3490,76	3015,66 3015,66 3090,58 3462,95 3384,38 2914,80 3282,63 3035,85 3256,58	4342,90 4632,38 5727,21 4682,86 4787,59 4658,65 4453,18 4503,68 4276,15		905,30 855,47 804,15 867,10 924,19 924,19 906,69 699,82 679,44		128661,66
Total Y <sub>...</sub>		96986,49	102415,61	120220,89	147028,48	34703,473	Y <sub>...</sub> =	501354,943	

Source	SS	df	MS	F <sub>0</sub>	p-value
Efecto A	3352082,31	3	1117360,77	3,98	0,0098888141792004200
Efecto B	32826045,12	4	8206511,28	29,23	0,0000000000000000030
Efecto AB	152318640,91	12	12693220,08	45,21	0,0000000000000000000
Error	44917828,10	160	280736,43		
Total	233414596,4	179			

n = 9

t<sub>(0,05;180)</sub>

1,975

LSD

467,961

### Immersion time effect (A)

B <sub>1</sub> A <sub>1</sub> - B <sub>1</sub> A <sub>2</sub>	294,38	B <sub>2</sub> A <sub>1</sub> - B <sub>2</sub> A <sub>2</sub>	259,11	B <sub>3</sub> A <sub>1</sub> - B <sub>3</sub> A <sub>2</sub>	192,68	B <sub>4</sub> A <sub>1</sub> - B <sub>4</sub> A <sub>2</sub>	532,83	B <sub>5</sub> A <sub>1</sub> - B <sub>5</sub> A <sub>2</sub>	8,33
B <sub>1</sub> A <sub>1</sub> - B <sub>1</sub> A <sub>3</sub>	723,53	B <sub>2</sub> A <sub>1</sub> - B <sub>2</sub> A <sub>3</sub>	367,20	B <sub>3</sub> A <sub>1</sub> - B <sub>3</sub> A <sub>3</sub>	440,43	B <sub>4</sub> A <sub>1</sub> - B <sub>4</sub> A <sub>3</sub>	544,25	B <sub>5</sub> A <sub>1</sub> - B <sub>5</sub> A <sub>3</sub>	218,00
B <sub>1</sub> A <sub>1</sub> - B <sub>1</sub> A <sub>4</sub>	294,16	B <sub>2</sub> A <sub>1</sub> - B <sub>2</sub> A <sub>4</sub>	87,03	B <sub>3</sub> A <sub>1</sub> - B <sub>3</sub> A <sub>4</sub>	1,78	B <sub>4</sub> A <sub>1</sub> - B <sub>4</sub> A <sub>4</sub>	711,47	B <sub>5</sub> A <sub>1</sub> - B <sub>5</sub> A <sub>4</sub>	78,04
B <sub>1</sub> A <sub>2</sub> - B <sub>1</sub> A <sub>3</sub>	429,15	B <sub>2</sub> A <sub>2</sub> - B <sub>2</sub> A <sub>3</sub>	626,31	B <sub>3</sub> A <sub>2</sub> - B <sub>3</sub> A <sub>3</sub>	247,75	B <sub>4</sub> A <sub>2</sub> - B <sub>4</sub> A <sub>3</sub>	1077,07	B <sub>5</sub> A <sub>2</sub> - B <sub>5</sub> A <sub>3</sub>	226,33
B <sub>1</sub> A <sub>2</sub> - B <sub>1</sub> A <sub>4</sub>	0,23	B <sub>2</sub> A <sub>2</sub> - B <sub>2</sub> A <sub>4</sub>	346,14	B <sub>3</sub> A <sub>2</sub> - B <sub>3</sub> A <sub>4</sub>	194,46	B <sub>4</sub> A <sub>2</sub> - B <sub>4</sub> A <sub>4</sub>	1244,30	B <sub>5</sub> A <sub>2</sub> - B <sub>5</sub> A <sub>4</sub>	69,72
B <sub>1</sub> A <sub>3</sub> - B <sub>1</sub> A <sub>4</sub>	429,38	B <sub>2</sub> A <sub>3</sub> - B <sub>2</sub> A <sub>4</sub>	280,18	B <sub>3</sub> A <sub>3</sub> - B <sub>3</sub> A <sub>4</sub>	442,21	B <sub>4</sub> A <sub>3</sub> - B <sub>4</sub> A <sub>4</sub>	167,23	B <sub>5</sub> A <sub>3</sub> - B <sub>5</sub> A <sub>4</sub>	296,04

### Concentration effect (B)

B <sub>1</sub> A <sub>1</sub> - B <sub>2</sub> A <sub>1</sub>	241,07	B <sub>1</sub> A <sub>2</sub> - B <sub>2</sub> A <sub>2</sub>	205,80	B <sub>1</sub> A <sub>3</sub> - B <sub>2</sub> A <sub>3</sub>	849,66	B <sub>1</sub> A <sub>4</sub> - B <sub>2</sub> A <sub>4</sub>	140,11
B <sub>1</sub> A <sub>1</sub> - B <sub>3</sub> A <sub>1</sub>	95,01	B <sub>1</sub> A <sub>2</sub> - B <sub>3</sub> A <sub>2</sub>	582,07	B <sub>1</sub> A <sub>3</sub> - B <sub>3</sub> A <sub>3</sub>	1258,97	B <sub>1</sub> A <sub>4</sub> - B <sub>3</sub> A <sub>4</sub>	387,38
B <sub>1</sub> A <sub>1</sub> - B <sub>4</sub> A <sub>1</sub>	742,31	B <sub>1</sub> A <sub>2</sub> - B <sub>4</sub> A <sub>2</sub>	503,87	B <sub>1</sub> A <sub>3</sub> - B <sub>4</sub> A <sub>3</sub>	2010,09	B <sub>1</sub> A <sub>4</sub> - B <sub>4</sub> A <sub>4</sub>	1747,94
B <sub>1</sub> A <sub>1</sub> - B <sub>5</sub> A <sub>1</sub>	1918,00	B <sub>1</sub> A <sub>2</sub> - B <sub>5</sub> A <sub>2</sub>	1631,95	B <sub>1</sub> A <sub>3</sub> - B <sub>5</sub> A <sub>3</sub>	976,47	B <sub>1</sub> A <sub>4</sub> - B <sub>5</sub> A <sub>4</sub>	1701,89
B <sub>2</sub> A <sub>1</sub> - B <sub>3</sub> A <sub>1</sub>	336,08	B <sub>2</sub> A <sub>2</sub> - B <sub>3</sub> A <sub>2</sub>	787,87	B <sub>2</sub> A <sub>3</sub> - B <sub>3</sub> A <sub>3</sub>	409,31	B <sub>2</sub> A <sub>4</sub> - B <sub>3</sub> A <sub>4</sub>	247,27
B <sub>2</sub> A <sub>1</sub> - B <sub>4</sub> A <sub>1</sub>	983,38	B <sub>2</sub> A <sub>2</sub> - B <sub>4</sub> A <sub>2</sub>	709,66	B <sub>2</sub> A <sub>3</sub> - B <sub>4</sub> A <sub>3</sub>	1160,42	B <sub>2</sub> A <sub>4</sub> - B <sub>4</sub> A <sub>4</sub>	1607,82
B <sub>2</sub> A <sub>1</sub> - B <sub>5</sub> A <sub>1</sub>	1676,93	B <sub>2</sub> A <sub>2</sub> - B <sub>5</sub> A <sub>2</sub>	1426,15	B <sub>2</sub> A <sub>3</sub> - B <sub>5</sub> A <sub>3</sub>	1826,13	B <sub>2</sub> A <sub>4</sub> - B <sub>5</sub> A <sub>4</sub>	1842,00
B <sub>3</sub> A <sub>1</sub> - B <sub>4</sub> A <sub>1</sub>	647,30	B <sub>3</sub> A <sub>2</sub> - B <sub>4</sub> A <sub>2</sub>	78,21	B <sub>3</sub> A <sub>3</sub> - B <sub>4</sub> A <sub>3</sub>	751,11	B <sub>3</sub> A <sub>4</sub> - B <sub>4</sub> A <sub>4</sub>	1360,55
B <sub>3</sub> A <sub>1</sub> - B <sub>5</sub> A <sub>1</sub>	2013,01	B <sub>3</sub> A <sub>2</sub> - B <sub>5</sub> A <sub>2</sub>	2214,02	B <sub>3</sub> A <sub>3</sub> - B <sub>5</sub> A <sub>3</sub>	2235,44	B <sub>3</sub> A <sub>4</sub> - B <sub>5</sub> A <sub>4</sub>	2089,27
B <sub>4</sub> A <sub>1</sub> - B <sub>5</sub> A <sub>1</sub>	2660,31	B <sub>4</sub> A <sub>2</sub> - B <sub>5</sub> A <sub>2</sub>	2135,81	B <sub>4</sub> A <sub>3</sub> - B <sub>5</sub> A <sub>3</sub>	2986,56	B <sub>4</sub> A <sub>4</sub> - B <sub>5</sub> A <sub>4</sub>	3449,82



## Transverse strength $\sigma_2$

E modulus LTT		B: Concentration						Total Y...
		0,25	0,5	1	1,5	2	Total Y...	
A: Immersion time	1	21,34	20,48	18,16	23,87	6,49	796,20	
		21,31	20,98	21,72	23,46	6,29		
		17,05	18,09	22,35	24,42	6,13		
		14,59	18,50	24,06	23,59	5,91		
		13,95	18,70	23,13	24,20	5,92		
		16,44	19,68	20,45	25,08	6,77		
		16,34	19,35	21,10	24,14	7,06		
		15,85	19,52	18,55	25,06	5,79		
	16,42	21,11	22,65	24,23	5,97			
	3	21,21	19,33	24,56	19,48	7,49	785,50	
		20,72	18,82	25,49	18,80	7,68		
		16,60	17,55	21,85	19,24	7,50		
		17,42	16,23	24,84	20,11	8,12		
		19,18	19,42	22,86	19,68	7,80		
		17,24	19,64	20,82	19,29	8,06		
		19,28	19,62	21,75	20,24	9,01		
		16,10	16,72	21,64	20,52	6,72		
	17,74	16,89	24,71	20,81	6,72			
	12	13,07	20,13	21,91	26,51	7,83	810,43	
		13,10	19,34	20,03	26,44	7,85		
12,51		17,44	23,88	26,98	8,19			
13,13		20,61	24,44	22,58	7,84			
12,39		19,12	27,49	25,79	8,07			
12,75		18,92	20,36	25,23	7,83			
16,83		19,08	20,36	26,21	9,99			
20,50		18,09	23,51	23,61	7,87			
19,63	18,49	23,51	23,12	7,87				
24	15,31	14,48	18,34	23,76	7,04	733,30		
	14,66	16,37	18,34	22,16	6,54			
	14,65	15,09	16,78	25,25	6,48			
	13,34	17,74	20,56	24,56	6,41			
	13,58	15,41	20,40	25,69	6,62			
	16,10	17,05	17,55	24,50	6,62			
	16,91	17,13	19,66	22,28	6,72			
	22,33	17,26	19,05	18,98	5,20			
20,54	16,35	23,65	20,49	5,36				
Total Y...	600,1102	658,7206	780,4863	830,3569	255,75934	Y... = 3125,43334		

Source	SS	df	MS	F <sub>0</sub>	p-value
Efecto A	67,84	3	22,61	3,27	0,0228149855637693000
Efecto B	315,79	4	78,95	11,41	#NUM!
Efecto AB	5688,23	12	474,02	68,53	0,0000000000000000000
Error	1106,66	160	6,92		
Total	6546,9	179			

$n = 9$

$t_{(0,05;180)}$

1,975

LSD

2,323

### Immersion time effect (A)

B <sub>1</sub> A <sub>1</sub> - B <sub>1</sub> A <sub>2</sub>	1,22	B <sub>2</sub> A <sub>1</sub> - B <sub>2</sub> A <sub>2</sub>	1,22	B <sub>3</sub> A <sub>1</sub> - B <sub>3</sub> A <sub>2</sub>	1,64	B <sub>4</sub> A <sub>1</sub> - B <sub>4</sub> A <sub>2</sub>	3,98	B <sub>5</sub> A <sub>1</sub> - B <sub>5</sub> A <sub>2</sub>	1,28
B <sub>1</sub> A <sub>1</sub> - B <sub>1</sub> A <sub>3</sub>	1,94	B <sub>2</sub> A <sub>1</sub> - B <sub>2</sub> A <sub>3</sub>	0,52	B <sub>3</sub> A <sub>1</sub> - B <sub>3</sub> A <sub>3</sub>	1,33	B <sub>4</sub> A <sub>1</sub> - B <sub>4</sub> A <sub>3</sub>	0,84	B <sub>5</sub> A <sub>1</sub> - B <sub>5</sub> A <sub>3</sub>	1,70
B <sub>1</sub> A <sub>1</sub> - B <sub>1</sub> A <sub>4</sub>	0,59	B <sub>2</sub> A <sub>1</sub> - B <sub>2</sub> A <sub>4</sub>	2,95	B <sub>3</sub> A <sub>1</sub> - B <sub>3</sub> A <sub>4</sub>	1,78	B <sub>4</sub> A <sub>1</sub> - B <sub>4</sub> A <sub>4</sub>	1,04	B <sub>5</sub> A <sub>1</sub> - B <sub>5</sub> A <sub>4</sub>	0,07
B <sub>1</sub> A <sub>2</sub> - B <sub>1</sub> A <sub>3</sub>	3,16	B <sub>2</sub> A <sub>2</sub> - B <sub>2</sub> A <sub>3</sub>	0,70	B <sub>3</sub> A <sub>2</sub> - B <sub>3</sub> A <sub>3</sub>	0,30	B <sub>4</sub> A <sub>2</sub> - B <sub>4</sub> A <sub>3</sub>	4,83	B <sub>5</sub> A <sub>2</sub> - B <sub>5</sub> A <sub>3</sub>	0,42
B <sub>1</sub> A <sub>2</sub> - B <sub>1</sub> A <sub>4</sub>	1,81	B <sub>2</sub> A <sub>2</sub> - B <sub>2</sub> A <sub>4</sub>	1,73	B <sub>3</sub> A <sub>2</sub> - B <sub>3</sub> A <sub>4</sub>	3,42	B <sub>4</sub> A <sub>2</sub> - B <sub>4</sub> A <sub>4</sub>	2,95	B <sub>5</sub> A <sub>2</sub> - B <sub>5</sub> A <sub>4</sub>	1,21
B <sub>1</sub> A <sub>3</sub> - B <sub>1</sub> A <sub>4</sub>	1,35	B <sub>2</sub> A <sub>3</sub> - B <sub>2</sub> A <sub>4</sub>	2,43	B <sub>3</sub> A <sub>3</sub> - B <sub>3</sub> A <sub>4</sub>	3,11	B <sub>4</sub> A <sub>3</sub> - B <sub>4</sub> A <sub>4</sub>	1,88	B <sub>5</sub> A <sub>3</sub> - B <sub>5</sub> A <sub>4</sub>	1,63

### Concentration effect (B)

B <sub>1</sub> A <sub>1</sub> - B <sub>2</sub> A <sub>1</sub>	2,31	B <sub>1</sub> A <sub>2</sub> - B <sub>2</sub> A <sub>2</sub>	0,13	B <sub>1</sub> A <sub>3</sub> - B <sub>2</sub> A <sub>3</sub>	3,73	B <sub>1</sub> A <sub>4</sub> - B <sub>2</sub> A <sub>4</sub>	0,05
B <sub>1</sub> A <sub>1</sub> - B <sub>3</sub> A <sub>1</sub>	3,89	B <sub>1</sub> A <sub>2</sub> - B <sub>3</sub> A <sub>2</sub>	4,30	B <sub>1</sub> A <sub>3</sub> - B <sub>3</sub> A <sub>3</sub>	7,16	B <sub>1</sub> A <sub>4</sub> - B <sub>3</sub> A <sub>4</sub>	2,69
B <sub>1</sub> A <sub>1</sub> - B <sub>4</sub> A <sub>1</sub>	6,47	B <sub>1</sub> A <sub>2</sub> - B <sub>4</sub> A <sub>2</sub>	1,27	B <sub>1</sub> A <sub>3</sub> - B <sub>4</sub> A <sub>3</sub>	9,26	B <sub>1</sub> A <sub>4</sub> - B <sub>4</sub> A <sub>4</sub>	6,02
B <sub>1</sub> A <sub>1</sub> - B <sub>5</sub> A <sub>1</sub>	9,70	B <sub>1</sub> A <sub>2</sub> - B <sub>5</sub> A <sub>2</sub>	9,64	B <sub>1</sub> A <sub>3</sub> - B <sub>5</sub> A <sub>3</sub>	6,06	B <sub>1</sub> A <sub>4</sub> - B <sub>5</sub> A <sub>4</sub>	9,04
B <sub>2</sub> A <sub>1</sub> - B <sub>3</sub> A <sub>1</sub>	1,58	B <sub>2</sub> A <sub>2</sub> - B <sub>3</sub> A <sub>2</sub>	4,43	B <sub>2</sub> A <sub>3</sub> - B <sub>3</sub> A <sub>3</sub>	3,43	B <sub>2</sub> A <sub>4</sub> - B <sub>3</sub> A <sub>4</sub>	2,75
B <sub>2</sub> A <sub>1</sub> - B <sub>4</sub> A <sub>1</sub>	4,16	B <sub>2</sub> A <sub>2</sub> - B <sub>4</sub> A <sub>2</sub>	1,40	B <sub>2</sub> A <sub>3</sub> - B <sub>4</sub> A <sub>3</sub>	5,53	B <sub>2</sub> A <sub>4</sub> - B <sub>4</sub> A <sub>4</sub>	6,08
B <sub>2</sub> A <sub>1</sub> - B <sub>5</sub> A <sub>1</sub>	12,01	B <sub>2</sub> A <sub>2</sub> - B <sub>5</sub> A <sub>2</sub>	9,51	B <sub>2</sub> A <sub>3</sub> - B <sub>5</sub> A <sub>3</sub>	9,79	B <sub>2</sub> A <sub>4</sub> - B <sub>5</sub> A <sub>4</sub>	8,99
B <sub>3</sub> A <sub>1</sub> - B <sub>4</sub> A <sub>1</sub>	2,59	B <sub>3</sub> A <sub>2</sub> - B <sub>4</sub> A <sub>2</sub>	3,03	B <sub>3</sub> A <sub>3</sub> - B <sub>4</sub> A <sub>3</sub>	2,10	B <sub>3</sub> A <sub>4</sub> - B <sub>4</sub> A <sub>4</sub>	3,33
B <sub>3</sub> A <sub>1</sub> - B <sub>5</sub> A <sub>1</sub>	13,58	B <sub>3</sub> A <sub>2</sub> - B <sub>5</sub> A <sub>2</sub>	13,94	B <sub>3</sub> A <sub>3</sub> - B <sub>5</sub> A <sub>3</sub>	13,21	B <sub>3</sub> A <sub>4</sub> - B <sub>5</sub> A <sub>4</sub>	11,73
B <sub>4</sub> A <sub>1</sub> - B <sub>5</sub> A <sub>1</sub>	16,17	B <sub>4</sub> A <sub>2</sub> - B <sub>5</sub> A <sub>2</sub>	10,91	B <sub>4</sub> A <sub>3</sub> - B <sub>5</sub> A <sub>3</sub>	15,31	B <sub>4</sub> A <sub>4</sub> - B <sub>5</sub> A <sub>4</sub>	15,07

## Transverse strain effect $\epsilon_2$

Strain TTT		B: Concentration					Total Y...
		0,25	0,5	1	1,5	2	
A: Immersion time	1	0,58 0,69 0,52 0,50 0,51 0,65 0,69 0,54 0,59	0,56 0,50 0,57 0,69 0,97 0,62 0,83 0,85 0,93	0,67 0,82 0,76 0,95 0,95 0,65 0,76 0,76 0,58	0,34 0,62 0,39 0,68 0,69 0,81 0,65 0,69 0,70	1,21 1,21 1,46 1,27 1,61 0,45 1,11 2,31 1,84	36,77
	3	0,38 0,63 0,35 0,58 0,98 0,85 0,70 0,58 0,81	0,98 0,81 0,89 0,67 0,89 0,80 0,88 0,73 0,78	0,82 0,97 0,89 0,83 0,68 0,57 0,47 0,45 0,47	0,67 0,61 0,61 0,78 0,57 0,70 0,70 0,57 0,49	1,12 1,28 1,04 1,45 1,75 1,13 0,82 1,97 1,97	37,67
	12	0,65 0,65 0,58 0,60 0,60 0,56 0,60 0,68 0,72 0,70	0,61 0,59 0,63 0,63 0,63 0,68 0,48 0,81 0,81 0,83	0,75 0,63 0,76 0,60 0,69 0,45 0,55 0,86 0,86	0,71 0,67 0,67 0,46 0,68 0,59 0,66 0,53 0,47	1,22 1,21 1,49 1,38 1,52 0,78 0,74 0,74 0,74	33,20
	24	0,47 0,50 0,52 0,48 0,68 0,58 0,53 0,84 0,77	0,47 0,64 0,60 0,64 0,54 0,62 0,58 0,60 0,50	0,51 0,42 0,51 0,48 0,45 0,48 0,47 0,60	0,61 0,53 0,66 0,66 0,70 0,68 0,53 0,39 0,44	1,43 1,40 1,71 1,58 1,28 1,28 1,73 1,18 1,87	33,66
Total Y...		22,25284	25,23722	23,63523	21,88288	48,28409	Y... = 141,29226

Source	SS	df	MS	F <sub>0</sub>	p-value
Efecto A	0,30	3	0,10	1,86	0,1387478409993170000
Efecto B	1,62	4	0,40	7,55	0,0000134737562869246
Efecto AB	12,16	12	1,01	18,94	0,0000000000000000000
Error	8,56	160	0,05		
Total	22,6	179			

$n = 9$

$t_{(0,05;180)}$

1,975

LSD

0,204

## Immersion time effect (A)

B <sub>1</sub> A <sub>1</sub> - B <sub>1</sub> A <sub>2</sub>	0,06	B <sub>2</sub> A <sub>1</sub> - B <sub>2</sub> A <sub>2</sub>	0,09	B <sub>3</sub> A <sub>1</sub> - B <sub>3</sub> A <sub>2</sub>	0,08	B <sub>4</sub> A <sub>1</sub> - B <sub>4</sub> A <sub>2</sub>	0,01	B <sub>5</sub> A <sub>1</sub> - B <sub>5</sub> A <sub>2</sub>	0,00
B <sub>1</sub> A <sub>1</sub> - B <sub>1</sub> A <sub>3</sub>	0,05	B <sub>2</sub> A <sub>1</sub> - B <sub>2</sub> A <sub>3</sub>	0,05	B <sub>3</sub> A <sub>1</sub> - B <sub>3</sub> A <sub>3</sub>	0,08	B <sub>4</sub> A <sub>1</sub> - B <sub>4</sub> A <sub>3</sub>	0,01	B <sub>5</sub> A <sub>1</sub> - B <sub>5</sub> A <sub>3</sub>	0,27
B <sub>1</sub> A <sub>1</sub> - B <sub>1</sub> A <sub>4</sub>	0,01	B <sub>2</sub> A <sub>1</sub> - B <sub>2</sub> A <sub>4</sub>	0,13	B <sub>3</sub> A <sub>1</sub> - B <sub>3</sub> A <sub>4</sub>	0,25	B <sub>4</sub> A <sub>1</sub> - B <sub>4</sub> A <sub>4</sub>	0,04	B <sub>5</sub> A <sub>1</sub> - B <sub>5</sub> A <sub>4</sub>	0,10
B <sub>1</sub> A <sub>2</sub> - B <sub>1</sub> A <sub>3</sub>	0,01	B <sub>2</sub> A <sub>2</sub> - B <sub>2</sub> A <sub>3</sub>	0,14	B <sub>3</sub> A <sub>2</sub> - B <sub>3</sub> A <sub>3</sub>	0,00	B <sub>4</sub> A <sub>2</sub> - B <sub>4</sub> A <sub>3</sub>	0,02	B <sub>5</sub> A <sub>2</sub> - B <sub>5</sub> A <sub>3</sub>	0,27
B <sub>1</sub> A <sub>2</sub> - B <sub>1</sub> A <sub>4</sub>	0,05	B <sub>2</sub> A <sub>2</sub> - B <sub>2</sub> A <sub>4</sub>	0,23	B <sub>3</sub> A <sub>2</sub> - B <sub>3</sub> A <sub>4</sub>	0,17	B <sub>4</sub> A <sub>2</sub> - B <sub>4</sub> A <sub>4</sub>	0,05	B <sub>5</sub> A <sub>2</sub> - B <sub>5</sub> A <sub>4</sub>	0,09
B <sub>1</sub> A <sub>3</sub> - B <sub>1</sub> A <sub>4</sub>	0,04	B <sub>2</sub> A <sub>3</sub> - B <sub>2</sub> A <sub>4</sub>	0,09	B <sub>3</sub> A <sub>3</sub> - B <sub>3</sub> A <sub>4</sub>	0,17	B <sub>4</sub> A <sub>3</sub> - B <sub>4</sub> A <sub>4</sub>	0,02	B <sub>5</sub> A <sub>3</sub> - B <sub>5</sub> A <sub>4</sub>	0,36

## Concentration effect (B)

B <sub>1</sub> A <sub>1</sub> - B <sub>2</sub> A <sub>1</sub>	0,13	B <sub>1</sub> A <sub>2</sub> - B <sub>2</sub> A <sub>2</sub>	0,16	B <sub>1</sub> A <sub>3</sub> - B <sub>2</sub> A <sub>3</sub>	0,03	B <sub>1</sub> A <sub>4</sub> - B <sub>2</sub> A <sub>4</sub>	0,02
B <sub>1</sub> A <sub>1</sub> - B <sub>2</sub> A <sub>1</sub>	0,16	B <sub>1</sub> A <sub>2</sub> - B <sub>2</sub> A <sub>2</sub>	0,03	B <sub>1</sub> A <sub>3</sub> - B <sub>2</sub> A <sub>3</sub>	0,04	B <sub>1</sub> A <sub>4</sub> - B <sub>2</sub> A <sub>4</sub>	0,09
B <sub>3</sub> A <sub>1</sub> - B <sub>4</sub> A <sub>1</sub>	0,03	B <sub>1</sub> A <sub>2</sub> - B <sub>4</sub> A <sub>2</sub>	0,02	B <sub>1</sub> A <sub>3</sub> - B <sub>4</sub> A <sub>3</sub>	0,03	B <sub>1</sub> A <sub>4</sub> - B <sub>4</sub> A <sub>4</sub>	0,02
B <sub>1</sub> A <sub>1</sub> - B <sub>2</sub> A <sub>1</sub>	0,72	B <sub>1</sub> A <sub>2</sub> - B <sub>2</sub> A <sub>2</sub>	0,67	B <sub>1</sub> A <sub>3</sub> - B <sub>2</sub> A <sub>3</sub>	0,41	B <sub>1</sub> A <sub>4</sub> - B <sub>2</sub> A <sub>4</sub>	0,81
B <sub>2</sub> A <sub>1</sub> - B <sub>3</sub> A <sub>1</sub>	0,04	B <sub>2</sub> A <sub>2</sub> - B <sub>3</sub> A <sub>2</sub>	0,13	B <sub>2</sub> A <sub>3</sub> - B <sub>3</sub> A <sub>3</sub>	0,01	B <sub>2</sub> A <sub>4</sub> - B <sub>3</sub> A <sub>4</sub>	0,07
B <sub>2</sub> A <sub>1</sub> - B <sub>4</sub> A <sub>1</sub>	0,10	B <sub>2</sub> A <sub>2</sub> - B <sub>4</sub> A <sub>2</sub>	0,18	B <sub>2</sub> A <sub>3</sub> - B <sub>4</sub> A <sub>3</sub>	0,06	B <sub>2</sub> A <sub>4</sub> - B <sub>4</sub> A <sub>4</sub>	0,00
B <sub>2</sub> A <sub>1</sub> - B <sub>2</sub> A <sub>1</sub>	0,60	B <sub>2</sub> A <sub>2</sub> - B <sub>2</sub> A <sub>2</sub>	0,51	B <sub>2</sub> A <sub>3</sub> - B <sub>2</sub> A <sub>3</sub>	0,37	B <sub>2</sub> A <sub>4</sub> - B <sub>2</sub> A <sub>4</sub>	0,83
B <sub>3</sub> A <sub>1</sub> - B <sub>4</sub> A <sub>1</sub>	0,13	B <sub>3</sub> A <sub>2</sub> - B <sub>4</sub> A <sub>2</sub>	0,05	B <sub>3</sub> A <sub>3</sub> - B <sub>4</sub> A <sub>3</sub>	0,07	B <sub>3</sub> A <sub>4</sub> - B <sub>4</sub> A <sub>4</sub>	0,08
B <sub>3</sub> A <sub>1</sub> - B <sub>2</sub> A <sub>1</sub>	0,56	B <sub>3</sub> A <sub>2</sub> - B <sub>2</sub> A <sub>2</sub>	0,64	B <sub>3</sub> A <sub>3</sub> - B <sub>2</sub> A <sub>3</sub>	0,37	B <sub>3</sub> A <sub>4</sub> - B <sub>2</sub> A <sub>4</sub>	0,90
B <sub>4</sub> A <sub>1</sub> - B <sub>2</sub> A <sub>1</sub>	0,69	B <sub>4</sub> A <sub>2</sub> - B <sub>2</sub> A <sub>2</sub>	0,69	B <sub>4</sub> A <sub>3</sub> - B <sub>2</sub> A <sub>3</sub>	0,44	B <sub>4</sub> A <sub>4</sub> - B <sub>2</sub> A <sub>4</sub>	0,82